SWAT 2013
Toulouse France

UNIVERSITÉ TOULOUSE III PAUL SABATIER



July 17-19, 2013

Paul Sabatier University, Toulouse, France

Conference Proceedings

Texas Water Resources Institute Technical Report – TR-471

Texas Water Resources Institute

make every drop count

The Soil and Water Assessment Tool (SWAT) is a public domain model jointly developed by USDA Agricultural Research Service (USDA-ARS) and Texas A&M AgriLife Research, part of The Texas A&M University System.

SWAT is a small watershed to river basin-scale model to simulate the quality and quantity of surface and ground water and predict the environmental impact of land use, land management practices, and climate change. SWAT is widely used in assessing soil erosion prevention and control, non-point source pollution control and regional management in watersheds.

Table of Contents

Table of Contents

Table of Contents

Table of Contents

Foreword

The organizers of the 2013 International SWAT Conference want to express their thanks to the organizations and individuals involved and their preparation and dedication to coordinate a successful conference. We would also like to thank the Scientific Committee for their support in preparing the conference agenda and allowing for scientists and researchers around the globe to participate and exchange their scientific knowledge at this conference.

We would like to give a special thank you to Paul Sabatier University and Drs. José Miguel Sánchez-Pérez and Sabine Sauvage for their countless hours and efforts to host the SWAT Community. On behalf of the SWAT Community, we extend our sincere gratitude to you and your university for the kind invitation and welcoming hospitality.

The following Conference Proceedings contains papers covering a variety of topics including but not limited to large scale applications; climate change applications; model development; database and GIS application and development; environmental applications; hydrology; best management practices (BMPs); sensitivity, calibration and uncertainty; pesticide, bacteria, metals and pharmaceuticals; sediment, nutrients, and carbon, urban processes and management; and more.

The Conference Organizers hope you enjoyed the conference and continue to view these SWAT gatherings as a positive opportunity for our international research community to share the latest innovations developed for the Soil and Water Assessment Tool.

International Organizing Committee

Dr. José Miguel SANCHEZ PEREZ
Research Director, CNRS, France

Jose Miguel Sánchez-Pérez, has a Ph.D. (1992) in Hydrogeochemistry in the University of Strasbourg (France); M.S. (1985) in Geology from University of the Basque Country in Spain. He is currently a research director assigned to ECOLAB Laboratory (CNRS - Université Paul Sabatier - Institut National Polytechnique de Toulouse) in Biogeochemical functioning of buffers zones.

José Miguel Sánchez-Pérez studies pollutant transport in hydrosystems, using extensive field data and modeling. He specializes in the functioning of wetlands, riparian zones, and groundwater systems, with particular interests in the modeling of catchment-scale pollutant transport, to predict how ecosystem functions will change under various climate change scenarios. For more details see: https://gmod.olympe.in/index.html

Dr. Sabine SAUVAGE
Research Engineer, CNRS, France

Sabine Sauvage holds a Ph.D. from the Institut National Polytechnique, Toulouse University, FRANCE. She is currently a Research Engineer at the National Center for Scientifical Research (CNRS) in the National Institute of Ecology and Environment. She is currently assigned to ECOLAB laboratory at Toulouse, and has been working on transfer modeling of contaminants in river water systems for 13 years.

Her research interests are focused on the adaptation and development of models that describe the bio-physical interactions between flows, biology and chemistry processes involved in biogenic elements and contaminants transfers in rivers at different time and space scale. More specifically, she aims to integrate by modeling the particular role of interfaces zones (ex: water/land, water/sediment) and specific buffer zones (ex: wetlands) in the dynamic of element transfer at large scale. For more details see: https://gmod.olympe.in/index.html

Organizing Committee

Dr. Claire BAFFAUT
Research Hydrologist, USDA-ARS, USA

Claire Baffaut holds an engineering degree from the School of Hydraulic Engineering in Grenoble, France and a Ph.D. from Purdue University, USA. She is currently a research hydrologist with the USDA-Agricultural Research Service (ARS) in the Cropping Systems and Water Quality Research Unit.

Her research interests include modeling watershed and landscape processes, developing practical tools to identify areas that need particular attention, and developing alternative agricultural practices for improved watershed management under changing land use, climate, and economic constraints.

Dr. Jeff ARNOLD
Agricultural Engineer, USDA-ARS, USA

Jeffrey G. Arnold has a Ph.D. (1992) in Agricultural Engineering from Purdue University; M.S. (1983) in Agricultural Engineering from University of Illinois; B.S. (1981) in Agricultural Engineering from University of Illinois. He is currently an Agricultural Engineer at the USDA-ARS, Grassland Soil and Water Research Laboratory in Temple, Texas.

Jeffrey G. Arnold develops watershed scale hydrologic and water quality process modules and integrates the processes within the SWAT model. He also actively supports application of the model for regional and national conservation and environmental assessments.

Dr. Raghavan SRINIVASAN
Professor, Texas A&M University, USA

Dr. Srinivasan has a Ph.D. (1992) degree in Agricultural Engineering from Purdue University. He is currently a professor in the departments of Ecosystem Science and Management, and Biological and Agricultural Engineering at Texas A&M University, as well as director of the Spatial Sciences Laboratory.

Dr. Srinivasan has become known and respected throughout the world for his developmental work with spatial sciences and computer-based modeling, especially the Soil and Water Assessment Tool. His research and its applications have contributed to long-lasting changes in natural resource assessments and development of management system options, currently being used in more than 90 countries.

Organizing Committee

Local Organizing Committee

Marie Ange Albouy, *Université Paul Sabatier, Toulouse, France*

Cyril Garneau, *Université de Toulouse, France*

Léonard Bernard-Jannin, *Université de Toulouse, France*

Xiaoling Sun, *Université de Toulouse, France*

Youen Grousson, *Université de Toulouse, France*

Yi Hong, *INRA, Toulouse, France*

Anne Comera-Grande, *ECOLAB, CNRS-Université de Toulouse, France*

Laurie Boithias, *ICRA, Girona, Spain*

Scientific Committee

Karim Abbaspour, *EAWAG, Switzerland*

François Anctil, *U. Laval, Canada*

Jeff Arnold, *USDA-ARS, USA*

Claire Baffaut, *USDA, USA*

Gilles Billen, *CNRS-UPMC, France*

Jose Maria Bodoque Del Pozo, *UCLM, Toledo, Spain*

Pierluigi Cau, *CRS4, Italy*

Debjani Deb, *Texas A&M University, USA*

Nicola Fohrer, *Christian-Albrechts-University, Kiel, Germany*

Josette Garnier, *CNRS-UPMC, France*

Philip Gassman, *Iowa State University, USA*

Magali Gerino, *UPS-ECOLAB, France*

A.K. Gosain, *Indian Institute of Technology, India*

Jaehak Jeong, *Texas A&M AgriLife Research, USA*

Virginia Jin, *USDA-ARS, USA*

C. Allan Jones, *Texas A&M AgriLife Research, USA*

Eric Justes, *INRA, France*

Valentina Krysanova, *PIK, Germany*

Christophe Laplanche, *INPT-ECOLAB, France*

Taesoo Lee, *Texas A&M University, USA*

Pedro Chambel Leitão, *IST-MARETEC, Portugal*

Antonio Lo Porto, *IRSA, IT*

Anne Probst, *ECOLAB, France*

Jean-Luc Probst, *CNRS-ECOLAB, France*

Ali Sadeghi, *USDA-ARS, USA*

José Miguel Sánchez-Pérez, *CNRS-ECOLAB, France*

Sabine Sauvage, *CNRS-ECOLAB, France*

R. Srinivasan, *Texas A&M University, USA*

Olivier Therond, *INRA, France*

Ann van Griensven, *UNESCO-IHE, NL*

Martin Volk, *Helmholtz Centre for Environmental Research - UFZ, Germany*

Mike White, *USDA-ARS, USA*

Estimation of Actual Evapotranspiration at Regional – Annual scale using SWAT

Azizallah Izady*
PhD student of Water Engineering Dept., College of Agriculture, Ferdowsi University of Mashhad, Mashhad, Iran (*Corresponding Author Email: az.izady@gmail.com*)

Amin Alizadeh, Kamran Davary, Ali Naghi Ziaei
Professor, Associate and Assistance Professor of Water Engineering Dept., College of Agriculture, Ferdowsi University of Mashhad, Mashhad, Iran

Samira Akhavan
Assistance Professor of Water Engineering Dept., College of Agriculture, Buali Sina University, Hamadan, Iran

Mojtaba Shafiei
PhD student of Water Engineering Dept., College of Agriculture, Ferdowsi University of Mashhad, Mashhad, Iran

Abstract

The aim of this study was to estimate actual evapotranspiration at regional – annual scale using SWAT model. For this reason, SWAT calibration and validation was done based on river discharge data from 5 gauging stations, rainfed and irrigated wheat yield data for the period Oct. 2000 to Sep. 2007 and Oct. 2007 to Sep. 2010, respectively. Because of the direct relationship between crop yield and evapotranspiration, calibration of watershed models using crop yield along with river discharge gives more confidence on the partitioning of water between soil storage, actual evapotranspiration, aquifer recharge. Results showed that SWAT provided satisfactory predictions on hydrologic budget and crop yield. Specifically, calibration (R2 = 0.82, NS=0.79) and validation (R2 = 0.71, NS=0.71) periods were quite suitable for the outlet of watershed. It also was able to predict crop yield satisfactorily for irrigated wheat in which R-factor and RMSE values were 0.97 and 0.08 ton ha^{-1}, respectively. The multi-objective calibrated model was then used to estimate and analyze the actual evapotranspiration. Mean ten-year actual evapotranspiration and precipitation was estimated 230 and 270 mm, respectively. The ten-year actual evapotranspiration to precipitation ratio at mountainous part of watershed was 99%, 80% and 77% for 2000-2001 as a dry year, 2001-2002 as a normal year and 2004-2005 as a wet year, respectively. Groundwater is an important source of water supply in the Neishaboor plain. Therefore, estimation of this ratio is not as simple as mountainous part of watershed due to uncertainties in the crop pattern data and their water requirements. It is obvious that this ratio could be more than one in some years especially dry years.

Keywords: Actual evapotranspiration, SWAT, river discharge, crop yield and Neishaboor watershed

Introduction

Much research and many applications regarding water resources, agriculture and forest management require a knowledge of ET over a range of spatial and temporal scales. The main methods (e.g. lysimeter, Bowen ratio, eddy correlation system) used conventionally to measure ET are subject to individual, field or landscape scales (Baldocchi *et al*., 2001; Brotzge and Kenneth, 2003; Yunusa *et al*., 2004; Gentine *et al*., 2007), but regional or continental ET cannot be measured directly or interpolated due to the inherent spatial heterogeneity of the land surface. Satellite provides an unprecedented spatial distribution of critical land surface variables, such as surface albedo, fractional vegetation cover, land surface temperature, so numerous physical and empirical remote sensing-based models in combination with ancillary surface and/or atmospheric data have been developed to estimate ET for clear sky days (Bastiaanssen *et al*., 1998a; Bastiaanssen, 2000; Jiang and Islam, 2001; Su, 2002; Wang *et al*., 2006). It has been proven that the remote sensing-based models could generate reasonable ET distribution across a wide range of land covers due to assimilating remotely sensed land surface temperature, which could signal the variation in evaporative fraction (Jiang and Islam, 2001; Batra *et al*., 2006), a key element affecting the variation in actual ET. However, the estimated ET amount at pixel scale have been viewed with some skepticism despite precise validation is performed on estimated ET (Su et al., 2005; Gao and Long, 2008).

The use of a hydrological approach may be an alternative way to validate ET estimates from remote sensing-based models at watershed scales (Bastiaanssen *et al*., 1998b; Kite and Droogers, 2000). ET amount can be estimated reasonably using Soil and Water Assessment Tool (SWAT) (Arnold et al. 1998) because the fundamental elements of hydrological processes, such as precipitation, runoff, can be measured directly and imported to the model (Gao and Long, 2008). SWAT is a continuous time, physically and spatially semi-distributed model developed to simulate the impact of management decisions on water, sediment and agricultural chemical yields in river basins. SWAT-based ET of the whole watershed could be used as the standard for accuracy assessment of remote sensing-based models (Gao and Long, 2008). Watershed model calibrated based on measured data at the outlet of the watershed may produce erroneous results for various landuses and subbasins within the watershed (Abbaspour et al. 2007). Therefore, calibration is required at multiple locations to improve model reliability. Moreover, calibration of a large-scale distributed hydrologic model against river discharge alone may not provide sufficient confidence for all components of the surface water balance (Faramarzi et al. 2009). For this reason, multi-criteria calibration is suggested by Abbaspour et al. (2007) for a better characterization of different components and as a way of dealing with the uncertainty problem in these regions. Because of the direct relationship between crop yield and evapotranspiration (Jensen, 1968; FAO, 1986), calibration of watershed models using crop yield along with river discharge gives more confidence on the partitioning of water between soil storage, actual evapotranspiration, aquifer recharge (Faramarzi et al. 2009; Srinivasan et al. 2010; Akhavan et al. 2010; Nair et al. 2011).

The main objective of this study was to estimate actual ET using multi-objective calibrated SWAT model in the Neishaboor watershed, Iran. For this reason, SWAT was calibrated via multi-gauge river discharge and crop yield. The SUFI-2 (Sequential Uncertainty Fitting, ver. 2) (Abbaspour 2007) tool was used to analysis uncertainty. Regard to the multi-objective calibrated model, the actual evapotranspiration was estimated at regional – annual scale.

Material and Methods

The Study Area

Neishaboor watershed is located between 35° 40′ N to 36° 39′ N latitude and 58° 17′ E to 59° 30′ E longitude with semi-arid to arid climate, in the northeast of Iran (Fig. 1). The total geographical area is 9158 km^2 that consists of 4241 km^2 mountainous terrains and about 4917 km^2 of plain. The maximum elevation is located in *Binalood* Mountains (3300 m above sea level), and the minimum elevation is at the outlet of the watershed (*Hoseinabad*) at 1050 m above sea level. The average daily discharge at *Hoseinabad station* was 0.36 cubic meter per second (CMS) for the period of 1997–2010, with a minimum value of zero and a maximum value of 89 CMS. The average annual precipitation is 265 mm, but this varies considerably from one year to another (CV = 0.13). The mean annual temperatures at *Bar* station (in the mountainous area) and *Fedisheh* station (in the plain area) are 13° C and 13.8° C, respectively. The annual potential evapotranspiration is about 2335 mm (Velayati and Tavassloi, 1991).

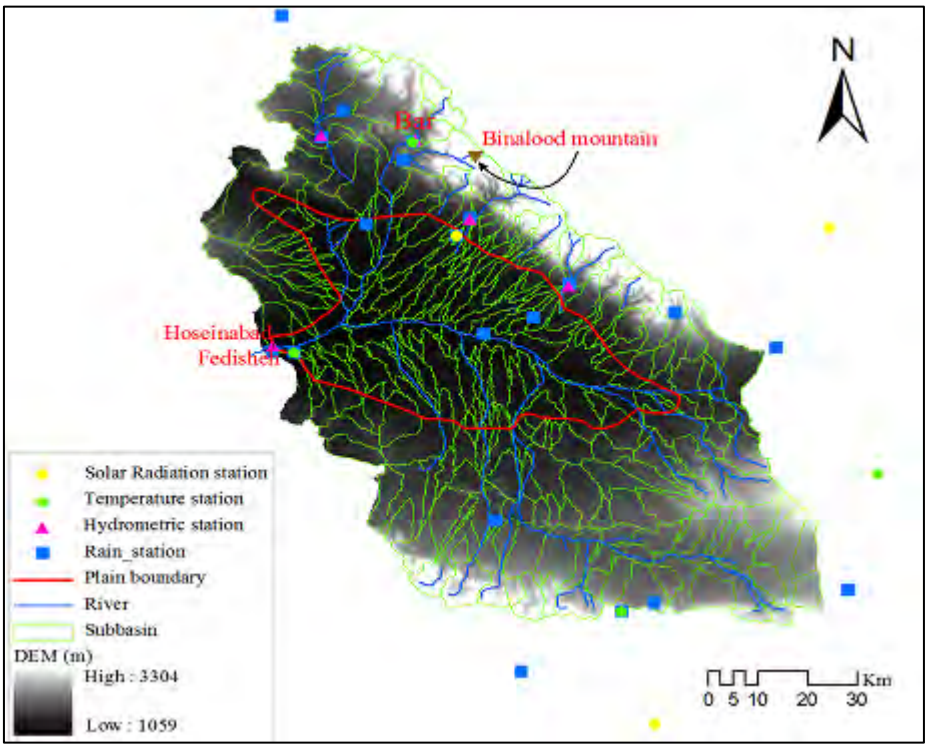

Fig. 1 Topographic map (DEM) along with meteorological stations, river network, main aquifer and SWAT delineated subbasins of the Neishaboor watershed.

SWAT Description

SWAT (Arnold et al., 1998) is a computer program that is widely used in various hydrological applications (Arnold and Allen, 1996; Vazquez-Amábile and Engel, 2005; Sun and Cornish, 2005; Narasimhan et al., 2005; Schuol and Abbaspour, 2006; Abbaspour et al., 2007; Yang et al., 2007; Akhavan et al., 2010). It is a spatially distributed, continuous river watershed scale model developed to predict the impact of land management practices on water, sediment and agricultural chemical yields in large complex watersheds with varying soils, land use and management conditions over long periods of time (Neitsch et al., 2009). Spatial parameterization of the SWAT model is performed by dividing the watershed into sub-watersheds based on topography. These are further subdivided into a series of hydrologic response units (HRU) based on unique soil, land use and slope characteristics. Main model components consist of climate, hydrology, soil temperature,

plant growth, nutrients, pesticides, land management, bacteria and water routing (Arnold etal., 1998; Gassman et al., 2007; Neitsch et al., 2009).
The model computes evaporation from soils and plants separately. Potential evapotranspiration can be modeled with the Penman–Monteith (Monteith, 1965), Priestley–Taylor (Priestley and Taylor, 1972), or Hargreaves methods (Hargreaves and Samani, 1985), depending on data availability. Potential soil water evaporation is estimated as a function of potential ET and leaf area index (LAI). Actual soil evaporation is estimated by using exponential functions of soil depth and water content. Plant water evaporation is simulated as a linear function of potential ET, LAI, and root depth, and can be limited by soil water content. The irrigation applications can be simulated for specific dates or with an auto-irrigation routine, which triggers irrigation events according to a water stress threshold. Channel routing is simulated using the variable storage or Muskingum method. A more detailed description of the model is given by Neitsch et al. (2009).

Description of datasets

Digital elevation model (DEM)

From available topographic maps, two with 1/50000 and 1/25000 scales were selected. Moreover, Shuttle Radar Topography Mission (SRTM) (http://srtm.csi.cgiar.org/SELECTION/inputCoord.asp) and Advanced Space-borne Thermal Emission and Reflection Radiometer (ASTER) (http://www.gdem.aster.ersdac.or.jp/search.jsp) DEMs were investigated. These were cross checked against each other and for conflicting points a field measurement with deferential GPS technique was performed. Finally, SRTM DEM (grid cell: 90 × 90) was selected as the base elevation model.

Digital stream network

This stream network has produced by the National Cartographic Center (NCC) at a scale of 1:25,000.

Soil map

This map has prepared by Khorasan - Razavi Regional Water Authority at a scale of 1:100,000 and soil data from watershed management and soil detailed reports. The produced map includes 41 types of soils. Soil texture along with soil gradation, rock fragment content, soil saturated hydraulic conductivity and organic carbon content were obtained from mentioned reports. Other required parameters were estimated using RetC software (van Genuchten et al., 1991).

Landuse map

This map has also prepared by Khorasan-Razavi Regional Water Authority at a scale of 1:100,000 and landuse data from watershed management detailed reports and Jihad – e – Keshavarzi office. This map consists of 14 main classes: Irrigated Cropland, Dryland Cropland, Orchard, Pasture, Range-Grasses, Range-Brush, Forest-Mixed, Forest-Evergreen, Shrubland, Bare Ground Tundra, Wetlands-Mixed, Sparsely Vegetated, Residential-Medium Density and Water. Irrigated wheat and barley, sugar beet, cotton, and alfalfa are the main crops grown in the watershed, followed by rainfed wheat.

Climate Data

Records from twenty three precipitations, four air temperature, and three solar radiation gages over a period of 14 years (1997-2010) were used in SWAT (Fig. 1). Relative humidity and wind speed was simulated using weather generator of SWAT. Data were obtained from Khorasan– Razavi Regional Water Authority and Iran Meteorological Organization. Since, SWAT is not able to represent the spatial and temporal variability of climate within the basin, precipitation lapse rate was calculated using mean annual precipitation of considered gages. SWAT allows up to 10 elevation bands to be defined in each subbasin. The solar radiation was estimated using Angstrom-Prescott equation (Angstrom, 1924). This equation has empirical coefficient that various for each location.

Fortunately, values of these empirical coefficients were available in the literature (Alizadeh and Khalili, 2009).

Crop Management Data

Neishaboor watershed is an agriculture-based watershed. Hence, the processes affecting the water balance in an agricultural watershed are highly influenced by crop management. Therefore, for the duration of simulation from 1997 to 2010, irrigated and rainfed wheat crops were examined. Typical management data such as cultivated crops, fertilizer application, tillage and harvest operations for different mentioned landuses were collected from Jihad – e – Keshavarzi office, interview with large owner farmer and local experts (field surveys) and agriculture statistical year book of local Jihad – e – Keshavarzi office. Management operations used for simulation are shown for rainfed and irrigated wheat in tables (1) and (2), respectively.

Hydrometric and Crop Yield Data

Records from five hydrometric gages (Fig. 1) and statistical year book of local Jihad – e – Keshavarzi office for crop yield over a period of 10 years (2000-2010) were used for calibration and validation.

Table 1 Management practices for irrigated wheat

Year	Operation type	Date	Descriptions
1	Tillage	September 26	Moldboard Plow
1	Tillage	September 27	Leveler
1	Planting	October 4	-
1	Fertilizer	October 5	Phosphate (18-46-00), 150 kg/ha
1	Auto-Irrigation	October 6	-
2	Fertilizer	March 15	Urea, 50 kg/ha
2	Fertilizer	April 9	Urea, 50 kg/ha
2	Fertilizer	April 30	Urea, 50 kg/ha
2	Harvest & Killing	July 13	-

Table 2 Management practices for rainfed wheat

Year	Operation type	Date	Descriptions
1	Tillage	November 23	Moldboard Plow
1	Tillage	November 24	Leveler
1	Planting	December 6	-
1	Fertilizer	December 7	Phosphate (18-46-00), 50 kg/ha
1	Fertilizer	December 7	Urea, 50 kg/ha
2	Harvest & Killing	July 17	-

Model Structure

Arc-SWAT version 2009.93.7b (Winchell et al., 2009) was used as an interface of SWAT program. The required data sets to develop the model input are: topography, soil, landuse, climatic data and crop management data.

The simulation period for the Neishaboor surface water modeling was 1997–2010; the first 3 years were used as warm-up period to mitigate the unknown initial conditions and were excluded from the analysis. Neishaboor watershed was subdivided into 248 subbasins (Fig. 1). To achieve this, watershed was first delineated using selected DEM with smallest possible threshold area (0.008%). Next, all generated outlets were removed; then, new outlets were assigned to the SWAT with regard to mountain-plain boundary, horticultural and agricultural farms border, county boundaries and available hydrometric stations limitations. It is also decided to consider one HRU for each subbasin because of facility in entering crop management data to each subbasin instead of irregularly

distributed HRUs. Therefore, another important constraint is that not only area of all subbasins is less than one percent of the watershed area but also only one soil type and landuse class is dominant in that subbasin. It should be noted that this constraint is considered for decreasing uncertainty of model because of utmost importance of HRU definition in the surface water flow prediction. Finally, new subbasins were produced regarding manually assigned outlets. This tedious and time-consuming process was done several times using trial and error with regard to mentioned constraints to obtain appropriate (landuse-class-dominant) subbasins.

The elevation band was used due to drastic variability of precipitation and temperature in the watershed, considering orographic effects. The lapse rates values were estimated 160 mm/km and 6 ^{o}C/km, respectively and 5 elevation bands were considered in each subbasin. Solar radiation was estimated using Angstrom-Prescott equation (Angstrom, 1924) in lieu of using SWAT weather generator because of its influential effect on the crop yield (Neitsch *et al*., 2009). The potential evapotranspiration was computed using the Hargreaves method in which daily precipitation, minimum and maximum temperature are the only required parameters. Also, the variable storage method is used for channel routing. Automatic irrigation method is selected for the crop management; because it is difficult to know when and how much the farmers apply irrigation during simulation periods.

Model Calibration

The SUFI-2 (Sequential Uncertainty Fitting, ver. 2) (Abbaspour, 2007) uncertainty analysis algorithm was used for calibration. In SUFI-2 parameter uncertainty represents all sources of uncertainties such as uncertainty in the driving variables (e.g. rainfall), conceptual model, parameters, and measured data. The degree to which all uncertainties are recognized is measured by an index referred to as the *P-factor*, which is the percentage of measured data bracketed by the 95% prediction uncertainty (95PPU). Another measure to quantify the strength of a calibration / uncertainty analysis is the *R-factor*, which is the average thickness of the 95PPU band divided by the standard deviation of measured data (Abbaspour, 2007).

The model calibration and validation was done based on river discharge data from 5 gauging stations, and also rainfed / irrigated wheat yield data for the period Oct. 2000 to Sep. 2007 and Oct. 2007 to Sep. 2010, respectively. SWAT was first calibrated with hydrology parameters, and then these parameters were fixed and calibrated for crop yield, in a recursive method. For this reason, hydrometric stations located in mountainous region of watershed (namely: *Andarab*, *Bar*, *Eishabad* and *Kharvm*) were calibrated separately. Next, whole watershed was calibrated by considering fixed hydrology parameters for the mentioned stations. Thereafter, subbasins with irrigated and rainfed wheat landuses were calibrated separately based on crop yield parameters. Then, entire watershed was calibrated using fixed crop parameters for mentioned subbasins. At last, calibration was rechecked by taking into consideration fixed hydrology and crop parameters for mentioned subbasins.

Different criteria were used in order to evaluate the effectiveness of the model and its ability to make predictions in the calibration and validation period. These included P-factor, R-factor, Coefficient of Determination (R2), Nash-Sutcliffe Coefficient (NS) (Nash and Sutcliffe, 1970), and Root Mean Square Error (RMSE).

Results and Discussion

Sensitivity analysis

Table (3) shows selected SWAT parameters in the calibration process and their sensitivity statistics. The sensitivity analysis showed that 21 global parameters of hydrology were sensitive to river discharge. All crop parameters also were sensitive to crop yield.

The reach transmission loss (TRNSRCH) was the most sensitive parameter for the streamflow. Due to high stream bed water losses in semi-arid and arid streams, most of the infiltration is through stream bed water losses. Therefore, runoff is controlled by the reach transmission loss in these regions (Sorman and Abdulrazzak, 1993; Scanlon et al., 2002; de Vries and Simmers, 2002; Sophocleous, 2005; Scanlon et al., 2006; Wheater, 2010; Edmunds, 2010; Yin et al., 2011). However, the curve number was found to be sensitive as much as the reach transmission loss in the Neishaboor watershed. It is worth noting that TRNSRCH parameter is calculated for the entire watershed in SWAT; therefore, it seems to be a weakness of SWAT and needs to be spatially defined at the subbasin or HRU level in order to correctly account for stream bed water losses in semi-arid and arid regions. The effective hydraulic conductivity and Manning's n value are effective parameters in the infiltration process from the stream bed. In fact, they control the loss of water through the streambed. The baseflow recession constant is a direct index of groundwater flow response to changes in recharge. The quantification of the baseflow recession constant is very important in a semi-arid watershed, where the flow and streamflow recession is low and quick, respectively (Bako and Hunt, 1988). Also, snow parameters (melt factor for snow on December 21 and snow melt base temperature) were the sensitive parameters. The reason for the sensitivities of the snow parameters is that eastern part of the Neishaboor watershed is mountainous and snowmelt controls much of the streamflows of this part.

Table 3 SWAT parameters adjusted during calibration and their sensitivity statistics and initial and final values

Parameter[a]	Physical Meaning	t-value[b]	p-value[b]	Initial range	Final range
v__TRNSRCH.bsn	Reach transmission loss	19.92	0.00	[0, 1]	[0.32, 0.57]
r__CN2.mgt	Initial SCS CN II value	18.31	0.00	[-0.5, 0.5]	[-0.42, 0.21]
v__CH_K2.rte	Effective hydraulic conductivity of channel (mm/hr)	8.24	0.00	[0, 150]	[35, 47]
v__ALPHA_BF.gw	Baseflow recession constant	3.02	0.00	[0, 1]	[0.3, 0.39]
v__CH_N2.rte	Manning's n value for the main channel	1.63	0.10	[0, 0.3]	[0.19, 0.22]
v__GW_REVAP.gw	"Revap" coefficient	1.50	0.13	[0.02, 0.2]	[0.03, 0.04]
v__SMFMN.bsn	Melt factor for snow on December 21 (mm /°C/day)	1.21	0.23	[0, 10]	[0.21, 2.47]
v__SMTMP.bsn	Snow melt base temperature (°C)	1.16	0.25	[-5, 5]	[-4.21, -2.16]
v__EPCO.hru	Plant uptake compensation factor	0.93	0.35	[0.01, 1]	[0.75, 0.81]
r__SOL_K().sol	Soil hydraulic conductivity (mm/hr)	0.90	0.37	[-0.5, 0.5]	[-0.06, 0.06]
v__SLSUBBSN.hru	Average slope length (m)	0.57	0.39	[10, 150]	[34, 43]
v__GW_DELAY.gw	Delay time for aquifer recharge (days)	0.54	0.42	[0, 500]	[471, 484]
v__RCHRG_DP.gw	Aquifer percolation coefficient	0.54	0.44	[0, 1]	[0.3, 0.47]
v__SMFMX.bsn	Melt factor for snow on June 21 (mm /°C/day)	0.45	0.65	[0, 10]	[4.87, 9.48]
r__SOL_BD().sol	Bulk Density Moist [g/cm-3]	0.42	0.67	[-0.5, 0.5]	[-0.41, -0.33]
v__SFTMP.bsn	Snowfall temperature (°C)	0.39	0.70	[-5, 5]	[0.27, 3.42]
v__ESCO.hru	Soil evaporation compensation factor	0.35	0.73	[0.01, 1]	[0.72, 0.79]
r__SOL_AWC().sol	Available water capacity	0.20	0.84	[-0.5, 0.5]	[0.23, 0.34]
v__SURLAG.bsn	Surface runoff lag coefficient	0.18	0.85	[1, 24]	[1, 7]
v__TIMP.bsn	Snow pack temperature lag factor	0.15	0.88	[0.01, 1]	[0.06, 0.67]
v__GWQMN.gw	Threshold water level in shallow aquifer for baseflow (mm)	0.14	0.89	[0, 5000]	[2388, 2812]
v__HEAT_UNITS.mgt (Irrigated wheat)	Potential heat units for plant to reach maturity	-	-	[500, 5000]	[3798, 4121]
v__HI_TARG.mgt (Irrigated wheat)	Harvest index target	-	-	[0, 1]	[0.52, 0.63]
v__AUTO_WSTRS.mgt (Irrigated wheat)	Water stress that triggers irrigation	-	-	[0, 1]	[0.86, 0.90]
v__HEAT_UNITS.mgt (Rainfed wheat)	-	-	-	[500, 5000]	[2341, 2735]
v__HI_TARG.mgt (Rainfed wheat)	-	-	-	[0, 1]	[0.13, 0.26]

[a] v: parameter value is replaced by given value or absolute change; r: parameter value is multiplied by (1 + a given value) or relative change (Abbaspour, 2007).

[b] t-value indicates parameter sensitivity: the larger the t-value, the more sensitive the parameter.

[c] p-value indicates the significance of the t-value: the smaller the p-value, the less chance of a parameter being accidentally assigned as sensitive.

Hydrology calibration and uncertainty analysis

Table (3) shows selected SWAT parameters in the calibration process and their initial and final values. These parameters were further parameterized based on the different soils, landuses and subbasins, which resulted in 66 parameters. In fact, this option in SWAT-CUP gives the analyst larger freedom in selecting the complexity of a distributed parameter scheme. By using this flexibility, a calibration process can be started with a small number of parameters that only modify a given spatial pattern, with more complexity and regional resolution added in a stepwise learning process (Abbaspour, 2007). Note that minimum and maximum range of each parameter is reported for the entire watershed, and not for each of the 66 parameters. Table 4 presents the calibration statistics for the hydrometric stations. The R-factor and P-factor is criterion for uncertainties in the conceptual model, the parameters and also the input data. The R-factor of less than 1 generally shows a good calibration result. This is obvious, in table 4, for all three stations. But, the P-factor for all stations is relatively small indicating that the actual uncertainty is likely larger.

Table 4 Model performance statistics for hydrologic calibration and validation periods

Hydrometric station	P-factor	R-factor	R2	NS	RMSE (CMS)
Andarab	0.42 (0.36)[a]	0.35 (0.41)	0.85 (0.79)	0.84 (0.79)	0.212 (0.005)
Kharvm	0.45 (0.42)	0.37 (0.61)	0.87 (0.74)	0.77 (0.66)	0.326 (0.036)
Hoseinabad (watershed outlet)	0.37 (0.42)	0.68 (0.63)	0.82 (0.71)	0.79 (0.71)	0.321 (0.004)

[a] Numbers in parentheses are validation results

The observed and simulated mean monthly river discharge in the calibration and validation periods are shown in Fig. 2. The calibration process was initiated from the upstream gauges - *Andarab*, *Bar*, *Eishabad* and *Kharvm* - located in the mountainous region of watershed as well as *Hoseinabad* which is located at the watershed outlet. In the first calibration for four mountainous hydrometric stations, SWAT could not predict the base flow except for *Andarab* station (Fig. 2a). Because, in these stations the base flow of the river is mainly comes from springs. Therefore, the springs were imported in these subbasins as point sources. But, the P-factor value increased only in the *Kharvm* station. Still, there should be some reasons for having inappropriate results in the *Bar* and *Eishabad* hydrometric stations. One reason could be severe elevation variability of these sub-basins. Having only a few precipitation gauges could not capture drastic variability of precipitation; although, the elevation band was defined in the mountainous subbasins. Inappropriate results are also for the unaccounted human activities affecting natural hydrology during the period of study. Specifically, construction of some artificial groundwater recharge sites adjacent to *Eishabad* station. Similarly, construction of a dam in *Bar* subbasin that was started in 2003 and completed in 2011. Third reason may be stated as snow cover at these two sub-basins. SWAT classifies precipitation as rain or snow based on the average daily temperature for the entire watershed and snow parameters are not spatially defined (Fontaine et al. 2002). Another reason could be shortcomings of the SCS method. This method cannot simulate runoff from melting snow and on frozen ground. It also does not consider the duration and intensity of precipitation; however, these two precipitation characteristics are necessary for semi-arid watersheds like the Neishaboor watershed (Maidment 1992). Finally, it was decided to eliminate these hydrometric stations from calibration period.

After calibrating Andarab, Eishabad and Hoseinabad separately, entire watershed was calibrated by considering fixed hydrology parameters for these stations. According to the performance indicators (R^2, *NS* and *RMSE*) SWAT predicted the streamflow well, as shown in Table 4. The correlation statistic (R^2), as a precision indicator that evaluates the linear correlation between the observed and

the simulated river discharge, is in a good range for all stations. The NS that determines the relative magnitude of the residual variance compared to the measured data variance, was in the acceptable range (> 0.5) as suggested by Moriasi et al. (2007). The *RMSE* statistic, as an accuracy indicator which is a measure of the overall error, was reasonable regarding to discharge flow range of the stations.

The validation results of streamflow are shown in Table 4 and Fig. 2. The P-factor and R-factor are similar to calibration results indicating consistency in model simulation for the calibration and validation periods.

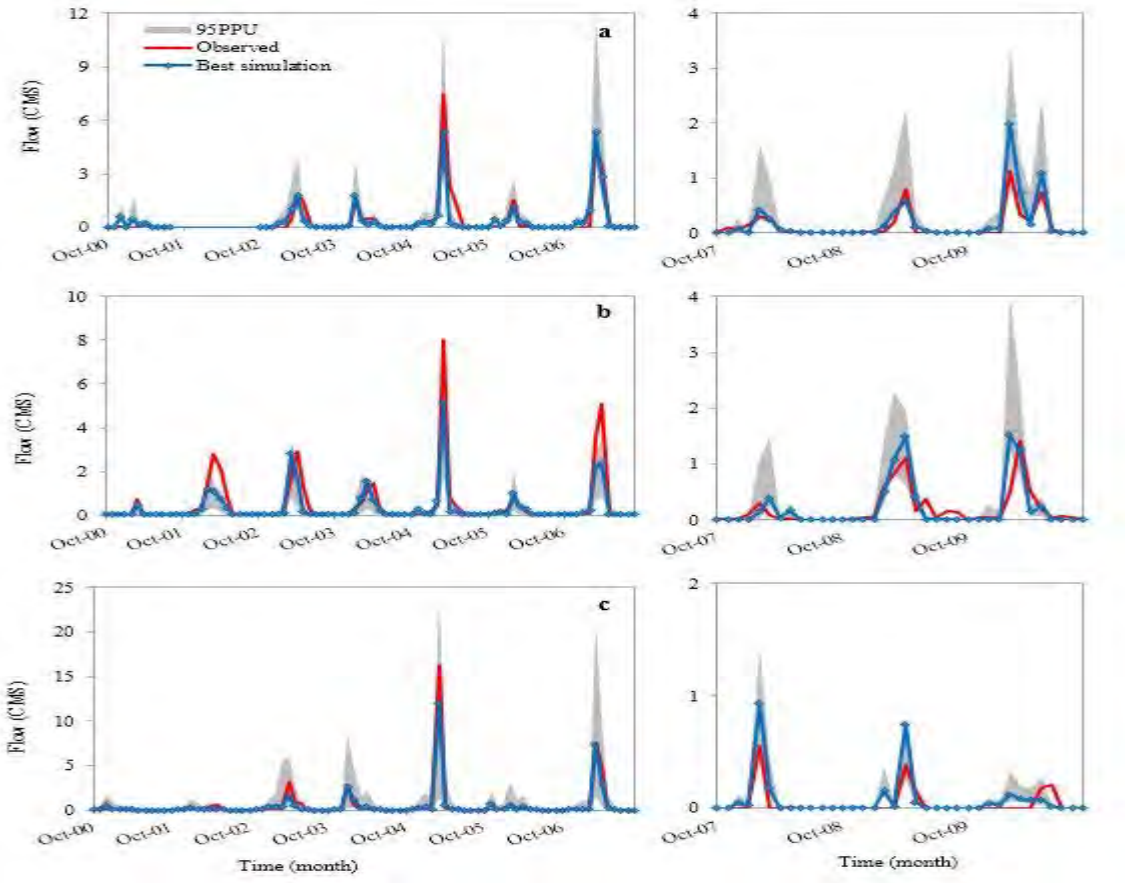

Fig. 2 Plots of observed and simulated mean monthly river discharge during calibration (left graph; Oct. 2000 to Sep. 2007) and validation (right graph; Oct. 2007 to Sep. 2010) period for **a** Andarab, **b** Kharvm, and **c** Hoseinabad hydrometric stations, respectively.

Crop yield calibration and uncertainty analysis

Calibration of a large-scale distributed hydrologic model – 9159 km^2 - against streamflow alone may not provide sufficient confidence for all components of the surface water balance. Therefore, crop yield is considered as an additional target variable in the calibration process because of the direct relationship between crop yield and evapotranspiration (Jensen, 1968; FAO, 1986). Table 3 shows a list of crop parameter ranges in the calibration results for rainfed and irrigated wheat.

Performance indicators for this part of study are RMSE and R-factor, as other indicators are not applicable due to few data available (only 7 yearly data points). Performance indicators for calibration and validation period are presented in Table 5. Regard to this table, SWAT was able to

predict crop yield satisfactorily for irrigated wheat in which R-factor and RMSE values were 0.97 and 0.08 ton ha^{-1}, respectively. While, the R-factor value for rainfed wheat is larger than irrigated wheat. One main reason of these fair results for crop yield calibration is collecting information about management practices at farm scale precisely (e.g., tillage, fertilizer and planting date). In fact, Neishaboor watershed consists of 20 counties. And, the mentioned information was collected at the counties scale via field surveys and interview with large farm owners / local experts

Figure 3 shows the observed crop yield against the simulated values. It can be seen form Fig. 3 that observed yields for irrigated and rainfed wheat are inside or very close to the predicted bands indicating good results. The validation results of crop yield are, also, shown in Table 5 and Fig. 3. Similar results were obtained for both irrigated and rainfed wheat in this period that indicates reliability of the model.

Table 5 Model performance statistics for annual crop yield calibration and validation periods

Crop	R-factor	RMSE (ton ha^{-1})
Irrigated wheat	0.97 (0.57)[a]	0.080 (0.012)
Rainfed wheat	1.16 (1.21)	0.045 (0.039)

[a] Numbers in parentheses are validation results

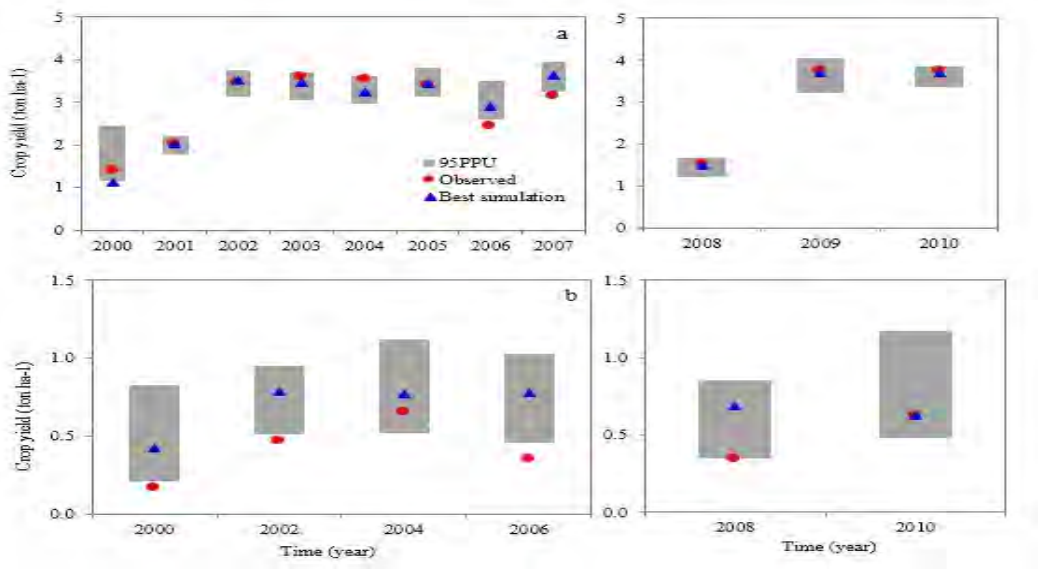

Fig. 3 Plots of observed and simulated annual crop yield during calibration (left graph; 2000 to 2007) and validation (right graph; 2008 to 2010) period for **a** irrigated and **b** rainfed wheat, respectively. Note that rainfed wheat (b) is mostly planted every other year by farmers. Therefore, it is only calibrated for years with simulated yield.

Estimation and analysis of actual evapotranspiration

The results showed that SWAT provided satisfactory predictions on hydrologic budget and crop yield. Hence, the multi-objective calibrated model was then used to estimate and analyze the actual evapotranspiration at regional-annual scale. Precipitation and actual ET are the main components of the water surface balance. Figure 4 shows the mean annual precipitation and actual ET for the Neishaboor watershed in the simulation period. Mean ten-year actual evapotranspiration and precipitation was estimated 230 and 270 mm, respectively. The ten-year actual evapotranspiration to precipitation ratio for whole watershed was 85%. For more information, this ratio is calculated for the mountainous and plain of watershed separately. This ratio was 99%, 80% and 77% for 2000-2001 at the mountainous part of the watershed as a dry year, 2001-2002 as a normal year and 2004-

2005 as a wet year, respectively. This finding clearly shows that amount of actual ET and runoff was decreased and increased, respectively due to increasing amount of precipitation. Since there is not remarkable irrigated crop at the mountainous part of the watershed, this ratio shows only the actual evapotranspiration (precipitation) to precipitation ratio. Groundwater is another source of water supply for irrigation purpose in the plain as well as precipitation. This source also effects the actual ET considerably. Therefore, this ratio shows the total actual evapotranspiration (precipitation and irrigation) to precipitation ratio. Hence, estimation of this ratio is not as simple as mountainous part of watershed due to uncertainties in the crop pattern data and their water requirements. It is obvious that this ratio could be more than one in some years especially dry years.

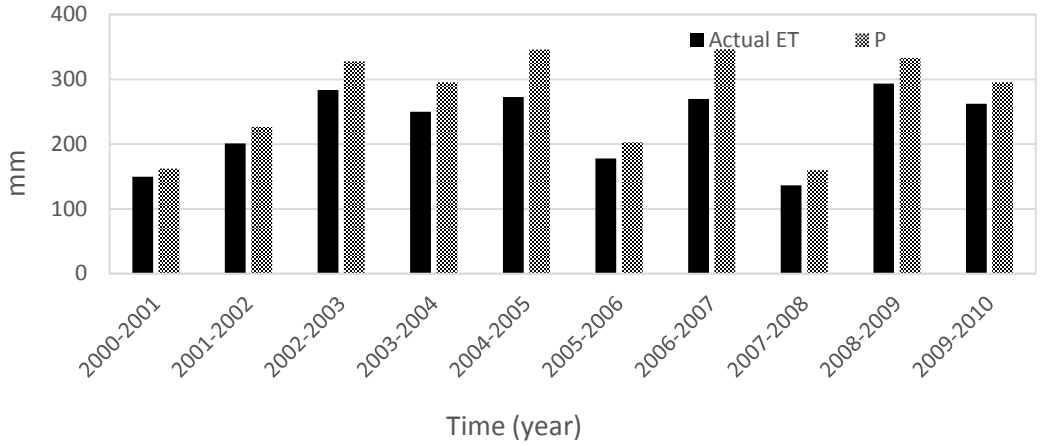

Fig. 4 Mean annual precipitation and actual ET in the simulation period.

Conclusion

In this study the importance of a thorough calibration procedure that accounts for not only the river discharge but also crop yield is investigated. The performance of the model was quite satisfactory for an arid Neishaboor watershed, where the response of flow to precipitation events is less predictable than in wetter conditions and the large number of interactive processes happening in the watershed. Gao and Long (2008) pointed out that SWAT-based ET of the whole watershed could be used as the standard for accuracy assessment of remote sensing-based models. Therefore, this study could be used to evaluate and improve the estimated actual ET using RS.

Refrences

Abbaspour, K. C., Yang, J., Maximov, I., Siber, R., Bogner, K., Mieleitner, J., Zobrist, J., Srinivasan, R., (2007) Modelling hydrology and water quality in the pre- alpine/alpine Thur watershed using SWAT. J. Hydrol. 333(2–4), 413–430

Akhavan, S., Abedi-Koupaia, J., Mousavia, S.F., Eslamiana, S.S., Abbaspourc, K.C. (2010) Application of SWAT model to investigate nitrate leaching in Hamadan–Bahar Watershed, Iran. Agriculture, Ecosystems and Environment. DOI:10.1016/j.agee.2010.10.015

Alizadeh A, Khalili N (2009) Estimation of Angstrom coefficient and developing a regression equation for solar radiation estimation (Case study: Mashhad). Journal of Water and Soil 23(1):229-238 (in Persian)

Angstrom, A. (1924) Solar and terrestrial radiation. Q. J. R. Meterol. Soc. 50:121-126

Arnold, J.G., Srinivasan, R., Muttiah, R.S., Williams, J.R., (1998) Large area hydrologic modeling and assessment—Part 1. Model development. Journal of the American water resources association (JAWRA) 34:73–89

Bako, M.D. and Hunt, D.N. (1988) Derivation of baseflow recession constant using computer and numerical analysis. Hydrological Sciences Journal, 33:(4) 357-367

Baldocchi, D., Falge, E., Gu, L., Olson, R., Hollinger, D., Running, S., et al. (2001). Fluxnet: A new tool to study the temporal and spatial variability of ecosystem-scale carbon dioxide, water vapor, and energy flux densities. Bulletin of the American Meteorological Society 82(11): 2415–2434.

Bastiaanssen, W.G.M., (2000). SEBAL-based sensible and latent heat fluxes in the irrigated Gediz Basin, Turkey. Journal of Hydrology 229: 87–1000.

Bastiaanssen, W.G.M., Menenti, M., Feddes, R.A., Holtslag, A.A.M. (1998a). A remote sensing surface energy balance algorithm for land (SEBAL): 1. Formulation. Journal of Hydrology 212–213: 198–212.

Bastiaanssen, W.G.M., Pelgrum, H.,Wang, J., Ma, Y., Moreno, J.F., Roerink, G.J., Wal TVerDer. (1998b). A remote sensing surface energy balance algorithm for land (SEBAL): 2. Validation. Journal of Hydrology 212–213: 213–229.

Batra, N., Islam, S., Venturini, V., Bisht, G., Jiang, L., (2006). Estimation and comparison of evapotranspiration from MODIS and AVHRR sensors for clear sky days over the Southern Great Plains. Remote Sensing of Environment 103: 1–15.

Brotzge, J.A., Kenneth, C.C., (2003). Examination of the surface energy budget: A comparison of eddy correlation and Bowen ration measurement systems. Journal of Hydrometeorology 4(2): 160–178.

De Vries, J.J., Simmers, I., (2002). Groundwater recharge: an overview of processes and challenges. Hydrogeology Journal 10:5–17

Edmunds, W. M., (2010). Conceptual models for recharge sequences in arid and semi-arid regions using isotopic and geochemical methods. Groundwater Modelling in Arid and Semi-Arid Areas, 1st ed. Howard S. Wheater, Simon A. Mathias and Xin Li. Published by Cambridge University Press, 21-37.

FAO, Food and Agriculture Organization (1986) Yield response to water. In: Irrigation and Drainage Paper 33. FAO, Rome, Italy

Faramarzi, M., Abbaspour, K.C., Schulin, R., Yang, H., (2009) Modelling blue and green water resources availability in Iran. Hydrological Processes 23:486–501

Fontaine, T.A., Cruickshank, T.S., Arnold, J.G. and Hotchkiss, R.H., (2002) Development of a snowfall-snowmelt routine for mountainous terrain for the soil water assessment tool (SWAT). J. Hydrol. 262(1-4): 209-223.

Gao, Y., and Long, D., (2008). Intercomparison of remote sensing-based models for estimation of evapotranspiration and accuracy assessment based on SWAT.Hydrological Processes, 22(25), 4850-4869.

Gentine, P., Entekhabi, D., Chehbouni, A., Boulet, G., Duchemin, B., (2007). Analysis of evaporative fraction diurnal behavior. Agricultural and Forest Meteorology 143: 13–29.

Hargreaves, G.H., Samani, Z.A., (1982) Estimating Potential Evapotranspiration. Journal of the Irrigation and Drainage Division 108(3):225-230

Jensen, M.E., (1968) Water Consumption by Agricultural Plants. In Water Deficits in Plant Growth (1). Academic Press, New York, pp. 1–22.

Jiang, L., Islam, S., (2001). Estimation of surface evaporation map over southern Great Plains using remote sensing data. Water Resources Research 37(2): 329–340.

Kite, G.W., Droogers, P., (2000). Comparing evapotranspiration estimates from satellites hydrological models and field data. Journal of Hydrology 229: 3–18.
Maidment, D.R., (1992) Handbook of Hydrology. McGraw-Hill, Co., New York
Monteith, J.L., (1965). Evaporation and environment. In the state and movement of water in living organisms, XIXth Symposium Society for Exp Biol, Swansea, Cambridge University Press
Nair, S.S., King, K.W., Witter, J.D., Sohngen, B.L., Fausey, N.R., (2011). importance of crop yield in calibrating watershed water quality simulation tools. Journal of the American water resources association (JAWRA) 47(6):1285–1297, DOI: 10.1111/j.1752-1688.2011.00570.x
Nash, J.E., Sutcliffe, J.V., (1970). River flow forecasting through conceptual models, part 1: A discussion of principles. Journal of Hydrology 10:282–290
Neitsch, S.L., Arnold, J.G., Kiniry, J.R., Williams, J.R., King, K.W., (2009). Soil and water assessment tool. In: Theoretical Documentation: Version 2009. TWRI TR-191, College Station, TX.
Poff, N.L., Ward J.V., (1989) Implications of streamflow variability for lotic community structure: a regional analysis of streamflow pattern. Canadian Journal of Fish and Aquatic Sciences,46:1808–1818.
Priestley, C.H.B., Taylor R.J., (1972). On the assessment of surface heat flux and evaporation using large scale parameters. Monthly weather review 100:81-92
Scanlon, B.R., Healy, R.W., Cook, P.G., (2002). Choosing appropriate techniques for quantifying groundwater recharge. Hydrogeology Journal 10:18–39, DOI: 10.1007/s10040-0010176-2
Scanlon, B.R., Keese, K.E., Flint, A.L., Flint, L.E., Gaye, C.B., Edmunds, W.M., Simmers, I., (2006) Global synthesis of groundwater recharge in semiarid and arid regions. Hydrological Processes 20(15):3335–3370
Schuol, J., Abbaspour, K.C., (2006) Calibration and uncertainty issues of a hydrological model (SWAT) applied to West Africa. Advances in Geosciences 9:137–143
Sophocleous, M.A., (2005) Groundwater recharge and sustainability in the High Plains aquifer in Kansas, USA. Hydrogeology Journal 13(2):351–365
Sorman, A.U. and Abdulrazzak, M.J., (1993) Infiltration–recharge through wadi beds in arid regions. Hydr. Sci. Jnl. 38(3), 173–186.
Srinivasan, R., Zhang, X., Arnold, J., (2010) SWAT ungauged: hydrological budget and crop yield predictions in the upper Mississippi river basin. Transactions of the ASABE 53(5): 1533-1546
Su, H., McCabe, M.F., Wood, E.F., Su, Z., Prueger, J.H., (2005). Modeling evapotranspiration during SMACEX02: Comparing two approaches for local and regional scale prediction. Journal of Hydrometeorology 6(6): 910–922.
Su, Z., (2002). The surface energy balance system (SEBS) for estimation of turbulent fluxes. Hydrology and Earth System Sciences 6(1): 85–99.
van Genuchten, M., Leij, F., Yates, S., (1991) The RETC code for quantifying the hydraulic functions of unsaturated soils. Technical Report EPA/600/2-91/065, US Environmental Protection Agency
Velayati S, Tavassloi S (1991) Resources and Problems of water in Khorasan province. Astan Ghods Razavi publisher, Mashhad, Iran (In Persian)
Walker, K., Thoms, M.C., (1993) Environmental effects of flow regulation on the lower river Murray, Australia. Regulated Rivers: Research and Management, 8:103–19.
Wang, K., Li, Z., Cribb, M., (2006). Estimation of evaporative fraction from a combination of day and night land surface temperatures and NDVI: A new method to determine the Priestley-Taylor parameter. Remote Sensing of Environment, 102: 293–305.

Wheater, H.S., (2010). Hydrological processes, groundwater recharge and surface-water/groundwater interactions in arid and semi-arid areas. Groundwater Modelling in Arid and Semi-Arid Areas, 1st ed. Howard S. Wheater, Simon A. Mathias and Xin Li. Published by Cambridge University Press, 5-37.

Winchell, M., Srinivasan, R., Di Luzio, M., Arnold, J.G., (2009) ArcSWAT Interface for SWAT2005–User's Guide. Blackland Research Center, Texas Agricultural Station and Grassland, Soil and Water Research Laboratory, USDA Agricultural Research Service, Temple, TX.

Yin, l., Hu, G., Huang, J., Wen, D., Dong, J., Wang, X., Li, H., (2011) Groundwater-recharge estimation in the Ordos Plateau, China: comparison of methods. Hydrogeology Journal 19:1563–1575, DOI: 10.1007/s10040-011-0777-3.

Yunusa, I.A.M., Walker, R.R., Lu, P., (2004) Evapotranspiration components from energy balance, sapflow and microlysimetry techniques for an irrigated vineyard in inland Australia. Agricultural and Forest Meteorology 127: 93–107.

Development of Modeling System Based On the SWAT Model as a Tool for Water Management Institution

Svajunas Plunge
Chief desk specialist at the Environmental Protection Agency of Lithuania, A. Juozapaviciaus st. 9, Vilnius LT-09311, Lithuania, email: s.plunge@aaa.am.lt

Abstract

The Soil and Water Assessment Tool (SWAT) model has been used extensively in many countries and for many different applications connected to water environment. The great majority of these applications were done on the temporary basis of scientific projects. However, for the exception of the United States, there is lack of examples on the acceptance of this model by regulatory bodies, which would invest in its application as a long term strategy to answer management questions. The Environmental Protection Agency of Lithuania (EPAL) has committed itself for such a task in order to increase its capacity in solving questions related to non-point source (NPS) water pollution problems. NPS pollution is responsible for the largest part of degradation in water ecosystems occurring in the country. Activities commenced by the EPAL included: testing the SWAT model for pilot basin, building country scale detail modeling system, the continuous collection of relevant data and the adaptation of data collection to fill the SWAT model requirements. Additionally, model applications are currently designed for many tasks such as the assessment of water quality, the assessment of pollution sources responsible for the degradation of water bodies, assessment on the effectiveness of NPS pollution abatement measures, the optimization of spatial distribution of such measures, the assessment of impacts of structural agricultural changes on water environment, etc. The aim of this article is to communicate information on the progress of the SWAT model application in Lithuania and about major encountered challenges.

Keywords: Lithuania, SWAT model, modeling system, water management.

Introduction

Application of The Soil and Water Assessment Tool (SWAT) model is widespread across the globe. There are numerous examples of model use for the different hydrological, water quality, soil, agricultural and other questions (Gassman et al., 2007). Abundant scientific articles show the great potential of the SWAT model. Currently, SWAT Literature Database for Peer-Reviewed Journal Articles holds around 1300 scientific articles (available on https://www.card.iastate.edu/swat_articles/). However, important benefits can be also delivered by SWAT outside scientific community. Water managers need such tools in many countries, which would help in decision making process. The deliverance of the SWAT model from scientific to management societies has the possibility to unlock great benefits. Such examples are available in the United States, where the model has been increasingly used for the support of Total Maximum Daily Load calculations (Borah et al., 2006). The SWAT model is also used for the evaluation of conservation practices and programs performed with multi-agency efforts and coordinated by USDA within the Conservation Effects Assessment Project (CEAP, 2013). It is hard to find reported examples of the SWAT model application in the recurring tasks of management institutions outside the United States.

There are numerous sources (Nasr et al., 2007, Barlund et al., 2007, Geza & McCray 2008, Dilks et al., 2003, EUROHARP, 2003) in the scientific literature, which examined the SWAT model's suitability for solving questions related with implementation of the European Water Framework Directive (WFD) and concluded that model can be used for such a task. However, it is hard to find examples described in the scientific literature that the SWAT model has actually been employed for such task. The model was used in many scientific projects connected with WFD implementation. RECOCA (RECOCA, 2013) and EUROHARP (EUROPARP, 2013) are examples of them. Yet, it is difficult to find examples for the application of the SWAT model for recurring tasks by water management institutions in the European Union (EU). This article is aimed to address this gap by describing the work done and results achieved in the Environmental Protection Agency of Lithuania (EPAL), where the SWAT model has been selected to aid with water management tasks. This article should be useful for water managers considering similar steps.

Early water modeling activities in the EPAL

The implementation of many requirements set by the EU water directives and the Helsinki Convention created the need for the application of water models. Initially the EPAL was considering using freely available models such as the Hydrological Simulation Program - FORTRAN (HSPF) and SWAT. However, at this stage (in the year 2003) the Danish Hydraulic Institute (DHI) offered on its part to perform study to determine the best options for the EPAL to use for water modeling tasks (DHI, 2003). This study was finished in 2004 and proposed the MIKE BASIN model. This is empirical, lumped parameters, continuous time scale, river basin model, which was primarily developed to solve water allocation problems, but has added capacity to assess nutrient loads from different sources (MIKE BASIN, 2013). MIKE BASIN was used in the first round of River Basin Management Plans (RBMPs) preparation for the whole territory of Lithuania, which ended in year the 2010. However, the main limitations of the MIKE BASIN model during the preparation projects of RBMPs greatly restricted questions on

non-point source (NPS) pollution coming from agriculture, which was responsible for the largest part of deterioration in water ecosystems. As this was the first step in the application of watershed models, such limitations were probably unavoidable. Data and expertise required for the application of more robust and physically based models, capable of answering NPS related questions, was not available during early stage. Yet, acknowledging current and future requirements coming from environmental regulations, the EPAL initiated work for preparation of complex watershed model, which would have physically based and distributed parameters characteristics and allow complex assessment of NPS and its abatement measures.

SWAT selection and testing for a pilot basin

The search of suitable solution started with the identification of criteria for the tool, which would be able to provide necessary answers to NPS water pollution questions. The main criteria for watershed model in the initial search were such as:

- Capability to assess inland water NPS pollution and its abatement measures;
- Suitable for fulfilling the WFD requirements;
- Applicability with available data;
- Good integration with GIS;
- Low cost;
- Good documentation;
- Many application examples and long development period;
- Good support.

Performed literature review was in part described in the master's thesis of Plunge (2009). The other part was described in the internal EPAL documents (EPAL, 2009b). Based on this review the SWAT model has been selected. This model was also compared against other models (MIKE BASIN, FYRIS), which were proposed to the EPAL by external consultants. Comparison criteria and methodology were based on Saloranta et al. (2003) article. This resulted in the selection of the SWAT model as the best tool for fulfilling the EPAL needs (EPAL, 2009a). However, before the final decision the SWAT model had to be tested on a pilot area in order to assess its performance and possible problems connected with its application.

As a pilot area the small catchment (14.2 km^2) of the Graisupis river was selected. This catchment is located in the middle of Lithuania, which is dominated by agricultural lands (they occupy more than 71% of catchment). It was selected, because long term monitoring program for assessing agricultural pollution was located in this area. Therefore, much of long-term important data describing water quality and agricultural activities were available for this area.

Detail model application results on the Graisupis river catchment are presented in master's thesis of Plunge (2011). Model testing in the pilot area was successful. It provided reasonable match with monitoring data. It is necessary to mention, that the stability of model, support from its community and developers, additional tools to ease SWAT application (such as ArcSWAT, SWAT-CUP and SWAT Check) and good model documentation contributed substantially in the successful SWAT model application. The prepared SWAT model on the pilot area was also used for testing different methodologies and the modeling of Best management practices (BMPs). Integration of Risk assessment framework and the assessment of NPS pollution abatement by applying the SWAT model has been presented in Plunge (2009). In

another work of Plunge (2011) is presented SWAT application for the identification of critical source areas, nitrate sensitive areas and the optimization of BMPs selection and placement in the catchment. The Graisupis river catchment also was used for the evaluation of wetlands as the BMP for NPS pollution reduction and selection for optimal sites for this measure (EPAL, 2012). These applications of the SWAT model provided good results and revealed the great potential of model to be used in the Lithuanian conditions. Results obtained from model testing allowed making the final decision for the application of the SWAT model for the whole territory of Lithuania.

SWAT model preparation for application on the country

The project for the preparation of the SWAT model for Lithuania has commenced in the spring of 2011 and ended in winter of 2012. Latvian company "Center of Processes' Analysis & Research" (PAIC) specializing in the field of hydrology, has been enlisted for this task.

The EPAL collected all necessary and available data before the beginning of project. Time series were collected up to the year 2011. Collected data included:

- GIS soil data showing spatial distribution of soils (at scales 1:10000 and 1:300000);
- GIS data on land use (CORINE data and crop declaration data);
- DEM data (10 meter raster resolution);
- River network and river basin GIS data (of different scales);
- Yearly point source data since year 2000 (loads of pollutants and coordinates of point sources);
- Daily meteorological data since year 1990 (18 stations);
- Daily flow data since year 1991 (from 64 stations);
- Monthly water quality data since year 1996 (from 139 stations);
- Fertilizer application data (collected by the Lithuanian Department of Statistics);
- Other data (various reports, statistical data, GIS and monitoring data).

The preparation of the SWAT model was done in several stages. Detail explanation of it is out of scope for this article. Yet, this information could be found in the final report of project (PAIC, 2012a). This article presents only broad overview of the main steps (see Fig. 1). Firstly data were processed into necessary form and formats. It took substantial time. Secondly, the ArcSWAT software was used for each setup to get MDB files. Later on these raw setups have been changed by applying prepared Phyton scripts in order to update default information with necessary parameters. After this the SWAT2009 rev. 477 (with some modifications done by PAIC) was used to run setups for obtaining initial results. The PAIC-SWAT program has been prepared for integration of all setups, monitoring data, editing and visualization tools into one system. This program was used for the model calibration and validation procedures. It is also important tool for working with prepared modeling system.

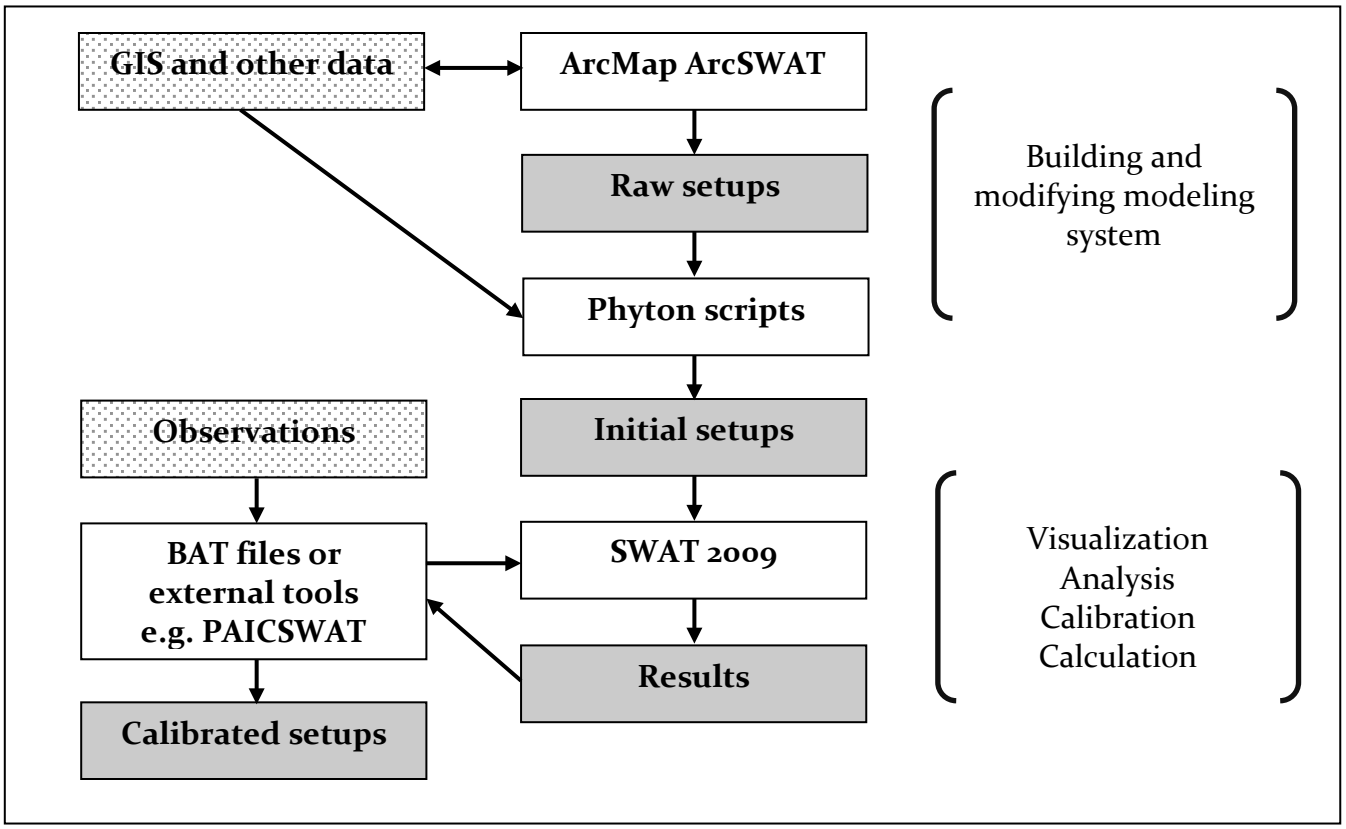

Fig. 1. Steps used in the preparation of the SWAT model setups.

Model has been prepared to be run between years 1997 to 2010. The first 3 years was used for the model warm-up. The territory of Lithuania has been divided into 129 setups (with more than 1000 SWAT model sub-basins), which in turn have been connected by 4 level hierarchical system (see Fig. 2). The first level of setups represented upstream watersheds and was designed to run first. Results from the first level were utilized by using inlets in second level watersheds. Third and fourth levels represented two largest rivers and were run in subsequent stages. Whole country model was prepared to run by using batch files to run setups in right sequence.

Model calibration requirements were set low for the project as results from it were intended to be the first step in the preparation of the SWAT model for whole country. The main reasons for this were project financial constraints and the poor quality of important data such as soil parameters and fertilization data.

As a first-step, an extensive calibration was done on the Susve river basin (1173 km^2), which was selected as the pilot basin. This basin was selected because the availability of data and the influence of multiple pressures (industrial and agricultural pollution, dams, etc). In the second step, the territory of Lithuania has been divided into 19 major regions. Each of those regions had a selected representative flow and water quality monitoring station on a main river. Initial parameters obtained from the calibration of the Susve river basin were applied for those regions. In the third step, parameters were further adjusted to fit monitoring data of selected station within each region. Finally, all setups in each of these regions were modified according to the one set of parameters obtained during calibration. This regionalization approach allowed

taking into account special hydrological characteristics of different regions while reducing substantially calibration task. The calibration on every flow and water quality station was out of the scope for this project.

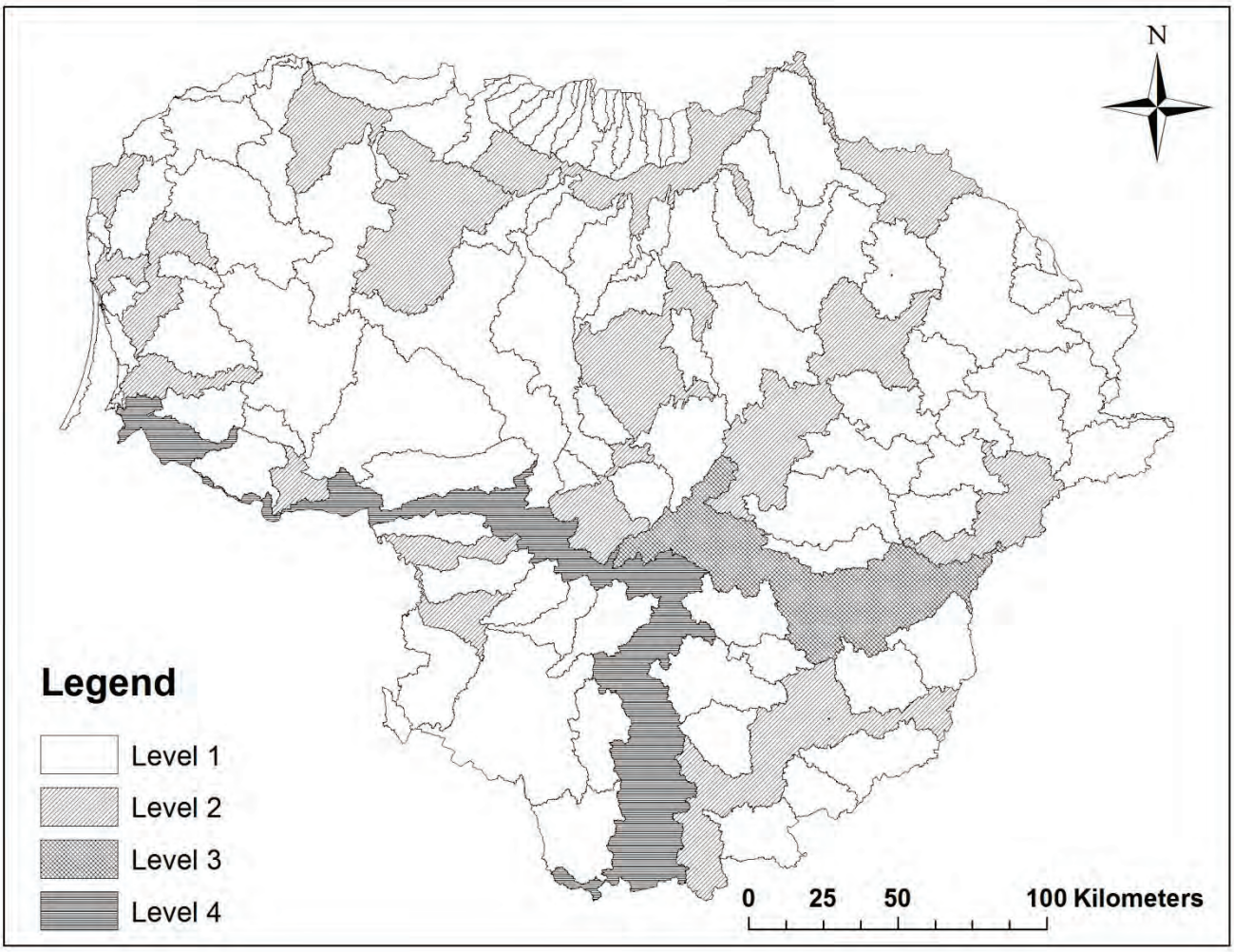

Fig. 2. Division of Lithuania's territory into watershed levels.

The results from such model calibration were satisfactory for the larger part of monitoring stations. However, for many stations results were not satisfactory, because the bigger part of data was not used for calibration and the final calibration of parameters was biased due to relation with the conditions of the Susve river basin. The data from 42 water flow stations have been used in the assessment. As the average of statistical parameters was skewed, because of the influence from extreme values, medians were calculated instead. The median of Nash-Sutcliffe values was 0.5 for daily flow modeling and 0.6 for monthly flow. The median of percent bias values for water flow modeling was around 9%. The median of Nash-Sutcliffe values for daily nitrate load values was 0.27 and a median for monthly values was 0.17 for all water quality stations (120 stations used in the assessment). For water quality stations with at least 5 full years of monitoring data (89 stations) the median of Nash-Sutcliffe values for nitrate daily values was 0.37 and for monthly - 0.26. The median of percent bias values for modeled nitrate values was

41%. Median of percent bias for modeled phosphate values was 39%. According to model evaluation guidelines given in Moriasi et al. (2007) article, model overall performance, if evaluated based on the results of medians, could be graded as satisfactory.

The main result of the SWAT model preparation project was not a fine tuned model (as this was not possible due to data limitations), but instead tools and model setups, which would enable to work further with the model. These tools include all necessary scripts and software required to manipulate input data, setup preparation, the extraction of modeling results and the integration of modeling results with monitoring data for assessment purposes. These results are vital for next steps of work on the SWAT model application. There are no possibilities to present those results in detail for this article. However, such information could be obtained from the "User manual of water quality modeling system for Lithuania" (PAIC, 2012b).

Next steps in the development of modeling system

One of the main activities, which has been initiated even before finishing the SWAT model preparation project, was continuous work on data gathering in order to collect missing data and adjust some data collection programs. The most monitoring programs are long term and designed for the implementation of certain laws or EU directives. Therefore, no quick and far-reaching changes could be made. However, discussions have been initiated by the EPAL with relevant institutions on the collection of missing data. For instance, intensive discussions are undergoing with the Ministry of Agriculture on possibilities to collect data on fertilization and agricultural practices. Moreover, some of missing data are being or have been collected within the boundaries of EPAL monitoring activities or ongoing projects. As example could be mentioned necessary parameters for the Graisupis river catchment, soil parameters for soil profiles, detail DEM, information about river channels, etc. During next steps increased collaboration between the EPAL and other relevant institutions is planned to ensure growing data availability for the SWAT model.

The EPAL also set aside resources for the project to update the RBMPs and the programmes of measures in accordance with the WFD requirements (EC, 2000). This project is planned to start in the middle of 2013 and to finish at the latest in the year 2015. Updating of the SWAT model for the territory of Lithuania and its application for running different scenarios is designated as the one of most important activities of this project. New, corrected and additionally collected data, which were previously not available, will be used in updating SWAT setups. Elaborated, extensive calibration and validation procedures are planned. The application of prepared model is planned for the evaluation of baseline scenario, which would take into account expected results from the implementation of the EU directives relevant to water environment. Additionally are planned the identification of critical source areas, the multi-objective spatial optimization of BMPs, the evaluation of impacts induced by structural changes in agriculture. One of the most important expected outcomes of planned project is the prepared reliable detailed model for the whole territory of Lithuania, which could be used for solving water management questions and providing necessary data for reporting. It is expected that the model will be used for the needs of the HELCOM Pollution load compilation data periodic reporting, the estimation of impacts of applied BMPs for National Rural support programme, the Nitrate directive, the estimation of nitrate leaching to surface and groundwater required for National reporting of greenhouse gas emissions, etc.

The EPAL also initiated collaboration with national scientific institutions (universities and institutes). For instance, lectures have been given in several universities by the EPAL specialists, which were invited as guest lecturers. These lectures were taught within relevant courses in order to attract students interested in the field of hydroinformatic to work on the SWAT model. Institutes are involved in the EPAL projects providing consultations. The EPAL freely shares results of those projects with institutes for their activities and projects and sees this as a long term strategy to attract specialists and increase benefits from investment in the SWAT model.

Main challenges

Certainly, the lack of important data is one of the main challenges for the EPAL. No usable national soil parameter data were available for the initial SWAT model preparation. For this purpose Harmonized World Soil Database was used (FAO/IIASA/ISRIC/ISSCAS/JRC, 2012). Used fertilization data were also very poor. Information about agricultural practices was not available as well as many specific model parameters. Moreover, there are also plenty problems related to data quality. The EPAL is working continuously for solving these problems.

Another, probably the most serious challenge, is attracting competent specialists required for the model development. Due to a small size of the country, there is no pool of prepared hydroinformaticians capable to work with SWAT. Even more troublesome is that payment ceilings for civil servants make it very hard to hire specialists with needed skills (especially in IT field). The EU funding is on some occasions available for hiring external consultants during different projects. However, to get long term benefits from model application, it is necessary to have competence and capacity for the model development and for its usage within the EPAL.

Lastly, it is important to mention, that despite many technical challenges connected with the application of such sophisticated tools as the SWAT model (such as the constant changes of the SWAT model revisions and versions, the lack of proper tools for model output assessment, problems related with updating input information, the lack of information about processes in the environment required for model calibration, etc), probably the most complicated are connected with the perceptions of relevant decision makers. Much of the time has to be spent in order to explain the different aspects in the development of such tools for decision makers, which have to be involved and to build trust for a process that require long term thinking.

Conclusion

The SWAT model has been selected by the EPAL as a tool to provide decision support in the field of water management. Employment of this tool is the important part of strategy for solving current and future problems connected with NPS water pollution abatement. The selection of model has been done after considering various characteristics of different models. The SWAT model has been tested on the pilot basin. Positive results were obtained for flow and water quality simulations as well as the examination of the usability of model's results for various NPS assessment methods. These results allowed making decision for starting project on the SWAT model preparation for the territory of Lithuania. Such project has finished in the end of 2012. It delivered all necessary setups and tools required to work with modeling system. The

EPAL is planning to develop further this modeling system by updating input data, improving its performance and using it in the updating of RBMPs. The development of modeling system with the long-term view is expected to provide Lithuanian water management institutions with sophisticated tools necessary for answering questions about NPS water pollution.

Acknowledgements

The author would like to thank his colleagues Jurgita Prunskyte and Martynas Pankauskas for the valuable comments, which helped to improve the quality of the manuscript.

References

Barlund, I., T. Kirkkala, O. Malve, and J. Kamari, 2007. Assessing SWAT model performance in the evaluation of management actions for the implementation of the Water Framework Directive in a Finnish catchment. *Environmental Modelling and Software* 22(5): 719-724.

Borah, D. K., G. Yagow, A. Saleh, P. L. Barnes, W. Rosenthal, E. C. Krug, and L. M. Hauck. 2006. Sediment and nutrient modeling for TMDL development and implementation. *Trans. ASABE* 49(4): 967-986.

CEAP. 2013. Conservation Effects Assessment Project. Washington, D.C.: USDA Natural Resources Conservation Service. Available at: www.nrcs.usda.gov/technical/NRI/ceap/. Accessed 6 March 2013.

DHI, 2003. Tools for groundwater and surface water analysis during implementation of the Water
Framework Directive in Lithuania. Available at:
http://www.dhigroup.com/News/2003/12/31/ToolsForGroundwaterAndSurfaceWaterAnalysisDuringImplementationOfTheWaterFrameworkDirectiveInLithuani.aspx . Accessed 5 May 2013.

Dilks, C. F., M. S. Dunn, and C. R. Ferrier, 2003. Benchmarking models for the Water Framework Directive: evaluation of SWAT for use in the Ythan catchment, UK, In: Srinivasan, R., Jacobs, J. H., jensen. R. (Eds.), 2nd International SWAT Conference Proceedings. TWRI Technical Reports, 266, 202-207. Available at: http://www.brc.tamus.edu/swat/2ndswatconf/2ndswatconfproceeding.pdf. Accessed 6 March 2013.

EC, 2000. Directive 2000/60/EC of the European Parliament and Council of 23 October 2000 establishing a framework for Community action in the field of water policy. Official Journal of the European Communities.

EPAL, 2012. Note for the application of SWAT model in the selection of suitable sites for wetlands. 02 June 2012. (In Lithuanian)

EPAL, 2009a. Note for stating problems related to water modeling services provided to the Environmental Protection Agency. 5 November 2009. (In Lithuanian)

EPAL, 2009b. Note for the assessment of opportunities, needs and required actions in regard to water modeling activities in the Environmental Protection Agency. 15 June 2012. (In Lithuanian)

Euroharp, 2013. Towards European harmonised procedures for quantification of nutrient losses from diffuse sources. Available at: http://www.wise-rtd.info/en/info/towards-european-harmonised-procedures-quantification-nutrient-losses-diffuse-sources. Accessed 6 March 2013.

Euroharp, 2003. Towards European harmonised procedures for quantification of nutrient losses from diffuse sources. Review and Literature Evaluation of Quantification tools for the Assessment of Nutrient Losses at Catchment Scale, EUROHARP1-2003.

FAO/IIASA/ISRIC/ISSCAS/JRC, 2012. Harmonized World Soil Database (version 1.2). FAO, Rome, Italy and IIASA, Laxenburg, Austria.

Gassman, W. P., M. R. Reyes, C. H. Green, and J. G. Arnold, 2007. The Soil and Water Assessment Tool: historical development, applications and future research needs. *Transactions of the ASABE* 50(4): 1211-1250.

Geza, M., and E. J. McCray, 2008. Effects of soil data resolution on SWAT model stream flow and water quality predictions. *Journal of environmental management* 88(3): 393-406.

MIKE BASIN, 2013. MIKE BASIN - integrated river basin planning. Available at: http://www.dhisoftware.com/Products/WaterResources/MIKEBASIN.aspx. Accessed 7 March 2013.

Moriasi, N. D., J. G. Arnold, M. W. Van Liew, R. L. Bingner, R. D. Harmel, and T. L. Vieth, 2007. Model Evaluation Guidelines for Systematic Quantification of Accuracy in Watershed Simulations. *American Society of Agricultural and Biological Engineers* Vol. 50(3): 885-900.

Nasr, A., M. Bruen, P. Jordan, R. Moles, G. Kiely, and P. Byrne, 2007. A comparison of SWAT, HSPF and SHETRAN/GOPC for modelling phosphorus export from three catchments in Ireland. *Water Research* 41(5): 1065-1073.

PAIC, 2012a. Development of methodics and modeling system of nitrogen and phosphorus load calculation for surface waters of Lithuania. ID Nr.100054. The Final Report by UAB „Estonian, Latvian & Lithuanian Environment" and SIA „Procesuanalīzes un izpētescentrs submitted in November 2012.

PAIC, 2012b. Water quality modeling system for Lithuania. User Manual. ID Nr.100054. SIA „Procesuanalīzes un izpētescentrs submitted in November 2012.

Plunge, S., 2011. Advanced decision support methods for solving diffuse water pollution problems. M. Sc. Thesis. Department of Earth and Ecosystem Sciences, Division of Physical Geography and Ecosystem Analysis, Centre for Geographical Information Systems, Lund University,
Sweden. Available at:
http://lup.lub.lu.se/luur/download?func=downloadFile&recordOId=3559183&fileOId=3559187
Accessed 13 March 2013.

Plunge, S., 2009. Risks versus costs: a new approach for assessment of diffuse water pollution abatement. M. Sc. Thesis. Department of Energy and Environment, Division of Environmental Systems Analysis, Chalmers University of Technology, Gothenburg, Sweden. Available at: http://publications.lib.chalmers.se/records/fulltext/125687.pdf. Accessed 13 March 2013.

RECOCA, 2013. Reduction of Baltic Sea nutrient inputs and cost allocation within the Baltic Sea catchment. Available at: http://www.balticnest.org/balticnest/research/ongoingprojects/bonus/recoca Accessed 6 March 2013.

Saloranta, T.M., J. Kamari, S. Rekolainen, O. Malve, 2003. Benchmark criteria: a tool for selecting appropriate models in the field of water management. *Environmental Management* 32 (3): 322-333.

Exploring Adaptation Options to Climate Change in Semi-Arid Watershed Using Choice of BMPs

Hamid R. Solaymani
PhD Candidate, Department of civil Engineering - IIT Delhi -New Delhi - 110016 -India
E-mail: h.solaymani@civil.iitd.ac.in or hrsolaymani@yahoo.com

A.K.Gosain
Professor of Department of civil Engineering -IIT Delhi - New Delhi -110016 -India
E-mail: gosain@civil.iitd.ac.in

Abstract

BMPs are those field operations which promote efficient use of resources, safety for stakeholders, and sustainable management of water resources. The choice of practices of the BMPs will vary from watershed to watershed due to varying characteristics. The present study has been conducted to explore adaptation options to address implications on account of climate change impact assessment in Karkheh River Basin (KRB). SWAT model has been used for impact assessment analysis. The model was calibrated using the baseline information. The results of climate change impact were obtained by using the future climate condition. It has been found that there would be explicit deficit in water and crop yield during the end century (2070-2099).

SWAT model has wide spectrum of abilities to manage the cultivation field operations. These operations are relevant to rain-fed and irrigated farming. In the KRB, such cultivated area account for about 25 percent of the total area. It has been intended to explore the adaptation options to account for the deficit in water availability through proper selection and deployment of suitable BMPs. Four of the BMPs have been selected for this study: i) Terracing, ii) Contouring, iii) Strip Cropping, and iv) Grade Stabilization Structure (GSS). These selected BMPs have been examined for the future scenarios of 'PRECIS' and 'REMO' regional climate models (RCMs) dynamically downscaled from the latest GCMs.

Keywords*:* SWAT Model; KARKHE River Basin; Best Management Practices (BMPs); Field operation; Adaptation

Introduction

Climate change enhances the water stress to states that are already battling with the issue of sustainable water resources. The water resources challenges are intensified in semi- arid and arid regions. Water resources remain as one of the most limiting factors on sustainable development due to occurrence of alternating floods and droughts. There are several application plans defined in order to combat the water resources scarcity in "2025 development vision in Iran". It has been stated, that an integrated management plan is required to prevent the negative impacts of climate change on social- economic and environment aspects. Each of these segments is expected to be strongly impacted by climate change. Therefore, impact assessment of climate change on water resources and its adaptation are of primary concern and interest.

Adaptation is response to climate change to seek possibilities and/or capabilities to impacts (IPCC, 2007). It is achieved through multi-interference and therefore needs an integrated approach. It is also required to include all the climate change vulnerability drivers to respond the impacts (Lindsey et al., 2010). Climate change adaptation can be improved by i) adjusting exposure ii) reducing sensitivity of the system to climate change impacts and iii) enhancing the system adaptive capacity (OECD, 2006). Widespread climate change impacts on water resources can be minimized by implementing management practices (USEPA 2001). Therefore, management practices can be deployed to explore the adaptation options on account of climate change impacts.

Best Management Practices (BMPs) are those field operations which promote efficient use of resources, safety for stakeholders, and sustainable management of water resources. They are often used to control the runoff, sediments and nutrients as non-point source hazards. The choice of the BMPs will vary from watershed to watershed due to varying characteristics. BMPs can be as structural and non-structural. Various BMPs are usually combined together in watershed. Harmel et al. (2008) and Webber et al. (2010) have reported various tillages with nutrient management operations and management of grazing with vegetative buffers for synergetic watershed management, respectively. When the combinations of numerous BMPs are implemented, they can effect on each others positively or negatively. Therefore it becomes important to evaluate the impacts of the selected BMPs in the watershed.

SWAT model allows using detailed management practices mainly on cultivated lands. It has wide spectrum of abilities to manage the cultivation field operations. These operations are relevant to rain-fed and irrigated farming areas. Muleta et al. (2001) used Genetic Algorithm (GA) and SWAT model to find the best landuse pattern and tillage operations to minimize the sediment yield in the basin. Arabi et al. (2006) studied application of four BMPs operations in U.S. using GA and SWAT models. They have used the BMPs operations to optimize sediment yield, Nitrogen and Phosphorus products. Tuppad et al. (2010) applied SWAT model using various BMP options in HRU, sub-basin and basin scale. SWAT was also used to simulate the intense sediment yield area by Mishra et al. (2007). From the food and water security points of view, Karkheh River Basin (KRB) has the specific situation. The

present study has been conducted to explore adaptation options to address implications on account of climate change impacts in KRB.

DATA AND METHODS

Study Area

The KRB is located in the western part of Iran, with geographical coordinates between 30° to 35° northern latitude and 46° to 49° eastern longitudes with total area of about 50800 km^2 (Fig 1). It is a sub-basin of Tigris and Euphrates River Basins in southeast portion. The population living in the basin is about 4 million (in 2002) with about one third resides in the rural areas (JAMAB 1999; Ashrafi et al. 2004). Hydrological features of the KRB are complex and heterogeneous due to its diverse topography, and natural settings of geology, climate and ecology. The water resources of the KRB comprises five major sub-basins, i.e. the Gamasiab, Qarasu, Seymareh, Kashkan and south-Karkheh as shown in Figure (1).

Fig. 1 Location of KRB in Iran with delineated of sub-basins and rivers

Basic characteristics of these five sub-basins are given in Table (1). The KRB remained largely unregulated without any large storage dam during the twentieth century. However, the first large multipurpose dam, the Karkheh dam, was completed and commissioned in 2001.

Table 1- Basic characteristics of five sub-basins of the KRB (JAMAB Consulting Co. 2006)

Sub-basins	Total area (km^2)	Average annual rainfall (mm)	Mean annual Discharge (MCM/y)	Irrigated Area (km^2)
Gamasiab	11500	465	1080	1360
Qarasu	5350	435	722	276
Kashkan	8960	390	1639	543
Seymareh	16400	350	5827	490
South-Karkheh	8590	260	5153	1110

The rain-fed farming, rangelands, forests and irrigated farming are the main land use types. The rain-fed farming and rangelands are mainly scattered throughout the mountainous region with varying degrees of coverage. Forested areas are mainly found in middle parts of the

basin. Most of the irrigated farming is concentrated in the lower region (Lower KRB) and in the upper northern regions (Gamasiab sub-basin). From the food security point of view, wheat production in KRB was 0.84 M tons and 1.4 M tons in 1996 and 2005 respectively, contributing 12.2 per cent and 10.0 per cent to the national production. In the case of barley, KRB production contributed 11.0 per cent and 16.5 per cent to the national production in 1996 and 2005 respectively. In 2005, KRB produced 0.35 M tons of maize, which contributed 17.8 percent to the national production of 1.99 M. tons (Keshavarz et al., 2012). More details of KRB are available in Solaymani and Gosain (2012).

SWAT Model Setup

The Digital Elevation Model (DEM) of 90 m resolution was used for basin and sub-basin delineation. A threshold of 500 km^2 was used for the delineation of sub-basins. This threshold was interactively devised to divide study area into a reasonable number of (50 in the present case) sub-basins (Figure 2).

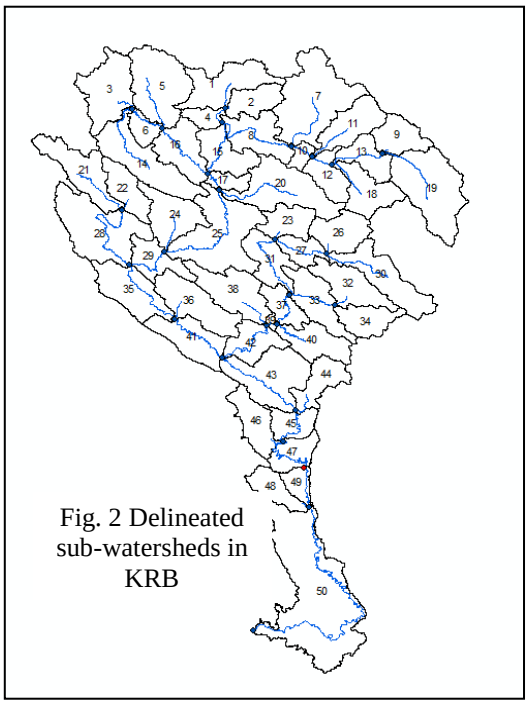

Fig. 2 Delineated sub-watersheds in KRB

The hydrological response units (HRUs) were defined based on information on landuse, soil and slope. The land use/land cover map was prepared using fine resolution Landsat ETM+ image 2002 (Mirghasemi et al, 2006). It distinguishes 18 land use/land cover classes, with rain-fed farming (33%), forest (23%), rangelands (18%), and bare lands (15%) constituting about 90% of the study area. The soil map was obtained from the global soil map of the Food and Agriculture Organization of the United Nations (FAO,1995), which provides data for 5000 soil types comprising two layers (0 –30 cm and 30 – 100 cm depth) at a spatial resolution of 10 km. The five categories of slope were defined to be used in the HRU definition, i.e., a) 0-5%; b)5-10%;c)10-20%;d) 20-30% and e) > 30%. Finally, the HRUs were defined using the land use, soil and slope information. A threshold value of 5% for land use, soil and slope was used in the HRU definition. A threshold value of 5 to 10% is commonly used in HRU definitions to avoid small HRUs, reduce total number of HRUs and thus improve the computational efficiency of the model (Starks and Moriasi 2009). Daily climatic data for the period from January 1982 to December 2005 were used for the model simulations. Precipitation and temperature data from 10 synoptic stations were available. The missing data were generated by using data of other stations.

Sensitivity Analysis

Sensitivity analysis refers to the identification of model parameters that have important effect in the specific basin. It is the step prior to model calibration. It demonstrates the impact that change to an individual input parameter has on the model response and can be performed

using a number of different methods. The method in the Arc-SWAT Interface combines the Latin Hypercube (LH) and One-factor-At-a-Time (OAT) sampling. The sensitivity analysis tool in Arc-SWAT has the capability of performing two types of analyses. The first analysis uses only modelled data to identify the impact of adjusting a parameter value on some measure of simulated output, such as average stream flow. The second analysis uses measured data to provide overall "goodness of fit" estimation between the modelled and the measured time series. Veith and Ghebremichael (2009) reported that the first type of analysis may help to identify parameters that improve a particular process or characteristic of the model, while the second type analysis identifies the parameters that are affected by the characteristics of the study watershed and those to which the given project is most sensitive. The description of parameters used for sensitivity analysis and their relative sensitivity after the analysis is presented in Table (2).

Table 2 SWAT Sensitivity analysis results for KRB

No	Parameter	Description	Initial value	Rank No. *	Rank No. **
1	ALPHA_BF	Baseflow alpha factor (Days)	0-50	2	4
2	CANMX	Maximum canopy storage (mmH_2O)	0-10	10	16
3	CH_K2	Channel Effective Hydraulic Conductivity	0-150	4	15
4	CH_N2	Manning Coefficient for Channel	0.01-0.3	6	5
5	CN2	Initial SCS Runoff Curve number for Wetting Condition-2	±20%	1	1
6	EPCO	Plant uptake compensation factor	0-1	14	20
7	ESCO	Soil Evaporation Compensation Factor	0-1	3	3
8	GW_DELAY	Ground Water Delay Time	0-50	11	10
9	GW_REVAP	Ground Water "REVAP" Coefficient	0.02-0.2	15	19
10	GWQMN	Threshold Depth for shallow aquifer for flow	0-5000	13	2
11	RCHRG_DP	Deep Aquifer Percolation Factor	0-1	7	12
12	REVAPMN	Threshold Depth of water in shallow aquifer for "REVAP"	0-500	16	18
13	SFTMP	Snowfall temperature (°C)	-5-5	20	6
14	SLOPE	Slope steepness (m/m)	0-0.6	9	13
15	SMFMN	Melt factor for snow December 21 (MM H_2O/°C-day)	0-10	20	8
16	SMFMX	Melt factor for snow June 21 (mm H_2O/°C-day)	0-10	20	11
17	SMTMP	Snow melt base (°C)	-5-5	8	7
18	SOL _AWC	Soil Available Water Capacity	0.01-0.5	20	14
19	SURLAG	Surface Runoff Lag Time	0-10	5	5
20	TIMP	Snow pack lag temperature lag factor	0-1	12	9

*without observed data - **with observed data

Model Calibration and Validation

Calibration involve in tuning of model parameters based on checking model results against observations to ensure same response over time. This involves comparing the model results, generated with the use of historic meteorological data, to recorded stream flows. In this

process, model parameters are varied until recorded flow patterns are accurately simulated. The manual calibration approach has been used for calibration in this study. The One–factor-At–a-Time (OAT) sampling has been used for manual calibration. The evaluation of calibration has been done using Graphical Procedure, Nash–Sutcliffe Efficiency (NSE), Percent Bias (PBIAS) and Root Mean Square Error (RMSE)-observations standard deviation ratio (RSR). There are more details of calibration and validation in Solaymani and Gosain. (2012).

Model Performance

Model evaluation statistics, for a daily time step, were formulated based on. As stated previously, graphical techniques provide visual model evaluation overviews and should be the first step in model evaluation. A general visual agreement between observed and simulated constituent data indicates adequate calibration and validation over the range of the constituent being simulated (Singh et al., 2004). Figure (2) demonstrate simulated and observed hydrograph from 1994 to 1999 for calibration and validation. The next step was to calculate values for NSE, PBIAS, and RMSE. Model performance can be evaluated as "satisfactory" with NSE > 0.50 and RSR < 0.70 and, for measured data of typical uncertainty, if PBIAS ± 25% for stream-flow. Moriasi et al. (2007).

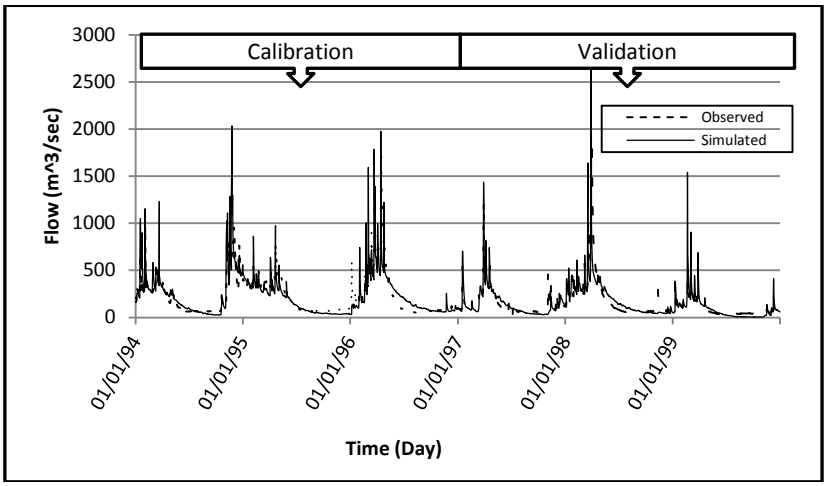

Fig. 2 Observed and simulated flow after manual calibration at Pay-e-Pol flow gauge station (Calibrated 1994 to 1996 and validated 1996 to 1999)

Table (3) summarizes the statistical results of performance for calibration and validation period using daily stream flow data with both, the manual and auto-calibration procedures. It may be observed that the performance for both calibration and validation period using manual calibration has been in general "Good" or better, whereas the performance with auto-calibration has been invariably "Unsatisfactory".

Table 3 Outputs for statistical parameters with manual calibration and auto-calibration at Pay-e-pol flow gauge station (Daily-Base data)

Approach	NSE		PBIAS		RSR	
	Calibration	Validation	Calibration	Validation	Calibration	Validation

Manual Calibration	**0.71** (Good)	**0.60** (Satisfactory)	**-0.24** (Very good)	**0.96** (Very good)	**0.6** (Good)	**0.25** (Very good)
Auto-calibration	**0.31** (Unsatisfactory)	**0.32** (Unsatisfactory)	**30.7** (Unsatisfactory)	**0.50** (Very good)	**0.71** (Unsatisfactory)	**0.78** (Unsatisfactory)

It was also decided to check the impact of the choice of interval on the performance of the model. Therefore, performance was computed again by taking the interval as monthly and the results are shown in Table (4). It may be observed that the performance has drastically improved for the monthly data under manual as well as auto-calibration. However, the manual procedure has even in this case outperformed the auto-calibration procedure.

Table 4 Outputs for statistical parameters with manual calibration and auto-calibration at Pay-e-pol flow gauge station (Using monthly data)

Approach	**NSE**		**PBIAS**		**RSR**	
	Calibration	Validation	Calibration	Validation	Calibration	Validation
Manual Calibration	**0.91** (Very good)	**0.85** (Very good)	**-0.001** (Very good)	**0.07** (Very good)	**0.31** (Very good)	**0.39** (Very good)
Auto-calibration	**0.31** (Unsatisfactory)	**0.32** (Unsatisfactory)	**0.002** Very good)	**0.77** (Very good)	**1.14** (Unsatisfactory)	**0.63** (Satisfactory)

CLIMATE CHANGE IMPACTS AND ADAPTATION

The calibrated model has then been used with climate change projections as input data. Implications of the projections have been evaluated using the SWAT model runs. Appropriate BMPs have then been identified to circumvent the effects of the climate change. Selected BMPs have been used on calibrated model to evaluate their implications on the KRB. Details of these steps are explained as follows

Climate change projections

The domains of RCM data corresponding to different climate change models are not available for all the places in the world. In this study, scenarios from REMO and PRECIS regional climate models (RCMs) have been used. The third-generation Hadley Centre's 'PRECIS' and fifth-generation of Max Planck Institute's 'REMO' are based on the latest GCMs. They have a horizontal resolution of 50x50 km with 19 levels in the atmosphere (from the surface to 30 km in the stratosphere) and four levels in the soil. The A1B emission scenario for REMO and A2 and B2 emission scenarios for PRECIS have been used.

To start with, analysis of climate change projection was made using two major parameters of temperature and precipitation influencing water resources. Monthly and annual mean daily maximum and mean daily minimum temperature for REMO (with A1B scenario) and PRECIS (with A2 and B2 scenarios) RCM models are given in Figure 3. According to Figure (3 a, b), Tmax is projected to significantly increase during summer (JJA) with changes being lower in the winter (DJF). In B2 scenario, Tmax has increased in all the months except December and January. Changes in Tmin shall have the similar trend as Tmax for A2 scenario (Figure 3d) but a lower magnitude. Change in Tmin for B2 scenario has shown

much lower increase in comparison to A2 scenario. In fact there has been a reduction in Tmin in March, April, October and November under B2 scenario (Figure 3e). As it has been observed in Figure (3 c, f), the increase in Tmax and Tmin under A1B scenario is very much less in comparison to A2 and B2 scenarios. However, maximum increase in Tmax under A1B scenario is observed in summer months and minimum in the other months. Generally, during winter and summer months, the spread of uncertainty in the temperature projections resulting from the various RCM models is higher, while it is lower during spring and autumn months.

The analysis of climate change impact on precipitation projects is show in Figure (4). The precipitation has been projected to reduce dramatically during JFM in all the scenarios of A1B, A2 and B2 in KRB. During November the average precipitation has increased slightly under A1B. Overall, the precipitation reduction has been observed under all three scenarios in KRB. These results are consistent with findings obtained from other studies in the Iran (e.g. Faramarzi et al. 2008, Abbaspour et al. 2009, Morid et al. 2008 and Massah, 2006).

SWAT has been used to simulate the crop yield under various climate change scenarios used in this study. Wheat being the main crop has been cultivated as rain-fed and irrigated in KRB. Figure (5) show the spatial distribution of the annual crop yield under present as well as various climate change projections. Rain-fed wheat is not cultivated in lower KRB that is why there is no variation. Figure (5a to d) show that the maximum reduction in crop yield is experienced in the middle KRB under B2 scenario whereas the upper KRB is impacted relatively less in comparison to the middle KRB. Similar condition is shown for irrigated wheat cultivated area in Figure (5e to h). The reduction in the crop yield is maximum for B2 scenario in upper KRB as well as lower KRB. The middle KRB can be termed as the comparatively less affected area under the irrigated wheat. The detailed result for production of the rain-fed and irrigated wheat is given as the appendix.

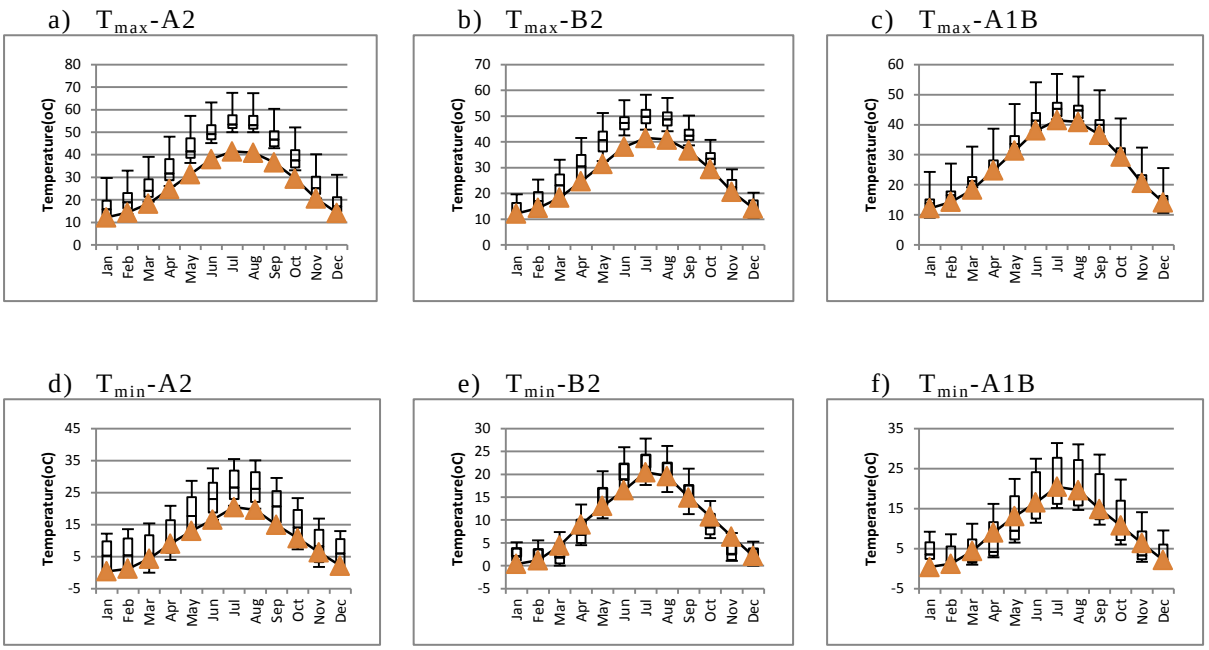

Fig. 3 Long-term monthly Temperature (average maximum and minimum daily) values for the end century (2070-2099) along with baseline (1970-1999). The box-whisker plot (median, 25th and 50th percentiles and minimum and maximum) are given for PRECIS (A2&B2) and REMO (A1B). (a), (b) and (c) show monthly values of average maximum temperature under A2, B2 and A1B emission scenarios. (d), (e) and (f) show monthly values of average minimum temperature under A2, B2 and A1B emission scenarios.

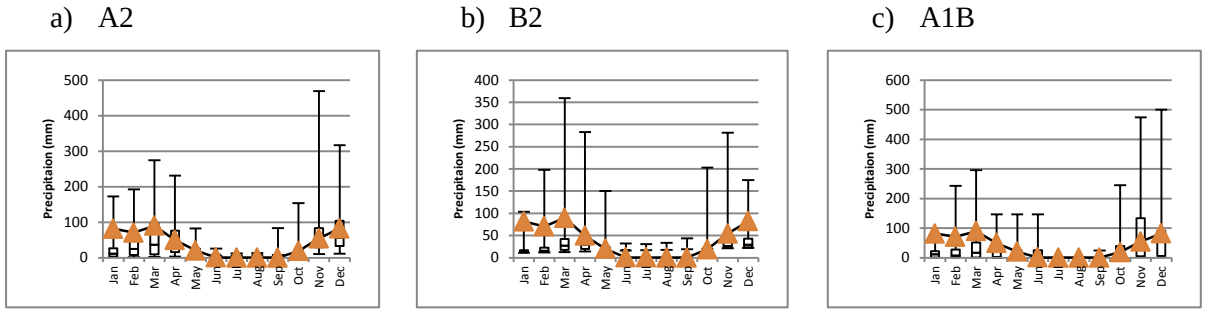

Fig. 4 Precipitation long-term values in end century (2070-2099) along with baseline (1970-1999) (triangles). The box-whisker plot (median, 25th and 50th percentiles and minimum and maximum) are given for PRECIS (A2&B2) and REMO (A1B)

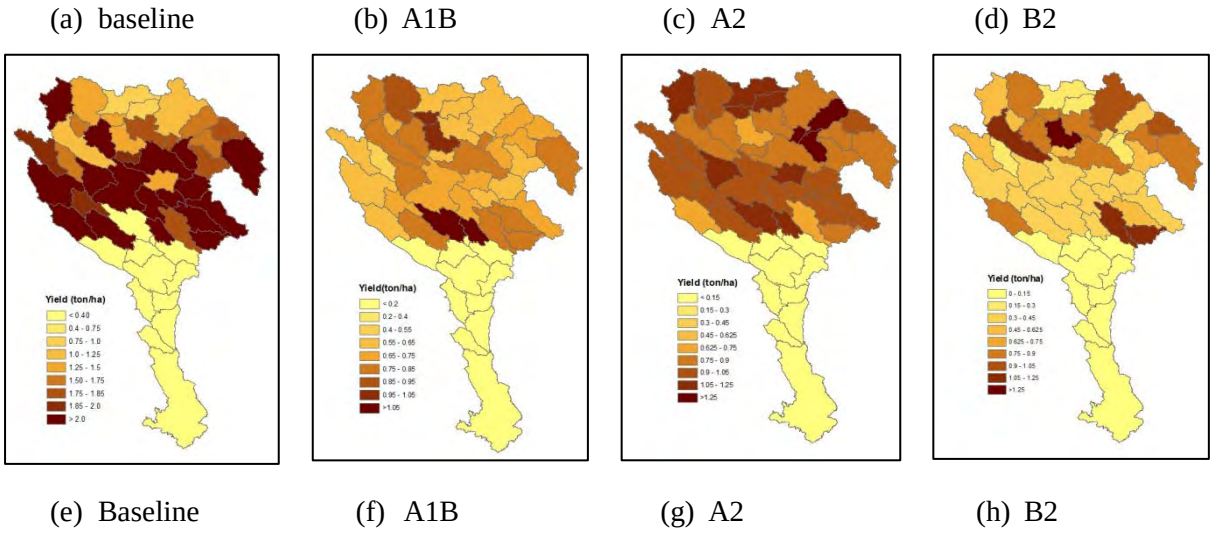

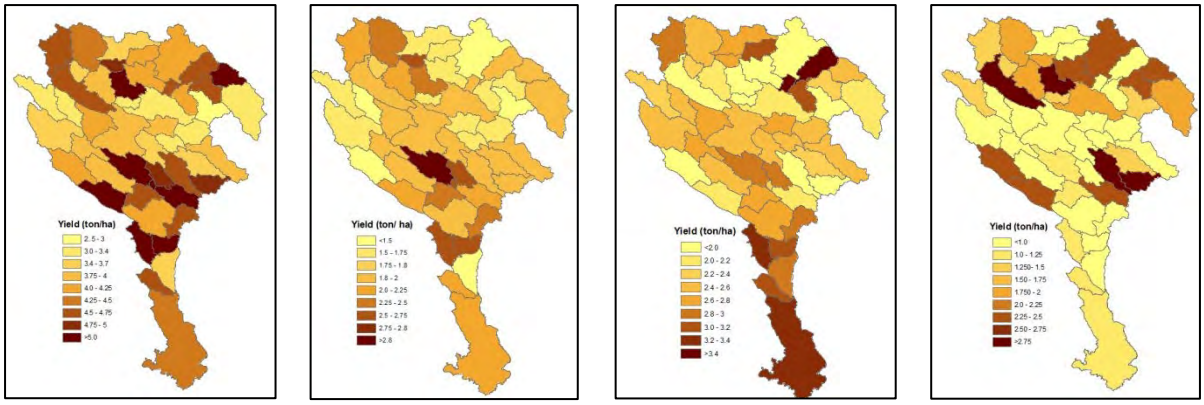

Fig. 5 Spatial distribution of climate change projections on annual rain-fed and irrigated wheat yields (ton/ha) in KRB; (a) to (d) depict the rain-fed wheat yields under baseline, A1B, A2 and B2 emission scenarios respectively, and (e) to (h) demonstrate the irrigated wheat yields under baseline, A1B, A2 and B2 emission scenarios respectively.

Selection of BMPs

Having evaluated the impacts of climate change on the crop production in the KRB, the next obvious requirement is to explore a set of options to reduce the negative climate change impact on the watershed. In the KRB, cultivated area account for about 25 percent of the total area, which comprises of rain-fed and irrigated farming areas. The selected options should comply with the specific conditions and capabilities of the cultivated land where they are to be used. The options being explored are in the form of best management practices (BMPs) that can account for the deficit in water availability through proper selection and deployment of suitable BMPs.

Four of the BMPs have been selected for this study. These are Terracing, Contouring, Strip Cropping, and Grade Stabilization Structure (GSS). Terracing is highly used to decrease the peak flow, soil surface erosion, keeping the soil moisture and water quality improvement (USEPA, 2004). Various parameters affected by terracing include CN2, SLSUBASIN (sub-basin average slope length), and USLE_P (USLE practice factor) (Bracmort et al. 2006). Contouring is the tillage practice for planting the crops aligned to terrain contours. It enhances surface detention and reduces erosion, runoff and evaporation. SWAT simulates this operation by altering CN2 to increase the surface storage and USLE_P to decrease soil surface erosion (Arnold et al., 2011). Strip cropping is a band arrangement of crops that is mainly use on steep slopes. It is incorporated by adjusting STRIP_N (Manning coefficient for overland flow), CN2, STRIP_C (USLE cropping factor) in SWAT. GSS is addressed through the structures to reduce streams and waterways slopes in natural or artificial water course. It reduces the water speed to store runoff and stabilize the grade to trap the sediments. There are some example of GSS as chutes, vertical drops, weir spillways and checkdams. They are constructed using various materials, e.g. steel sheet pile, masonry materials, reinforced concrete, wood, and earth embankments, depending on site conditions. Figure 6 shows some common GSSs that are implemented in Iran. They modify the main channel slopes (CH_S2) and the factor of channel erodibility (CH_EROD) in a sub-basin (Kaini et al. 2012). The CH_S2 parameter is reduced by 10% to facilitate GSSs simulation in SWAT.

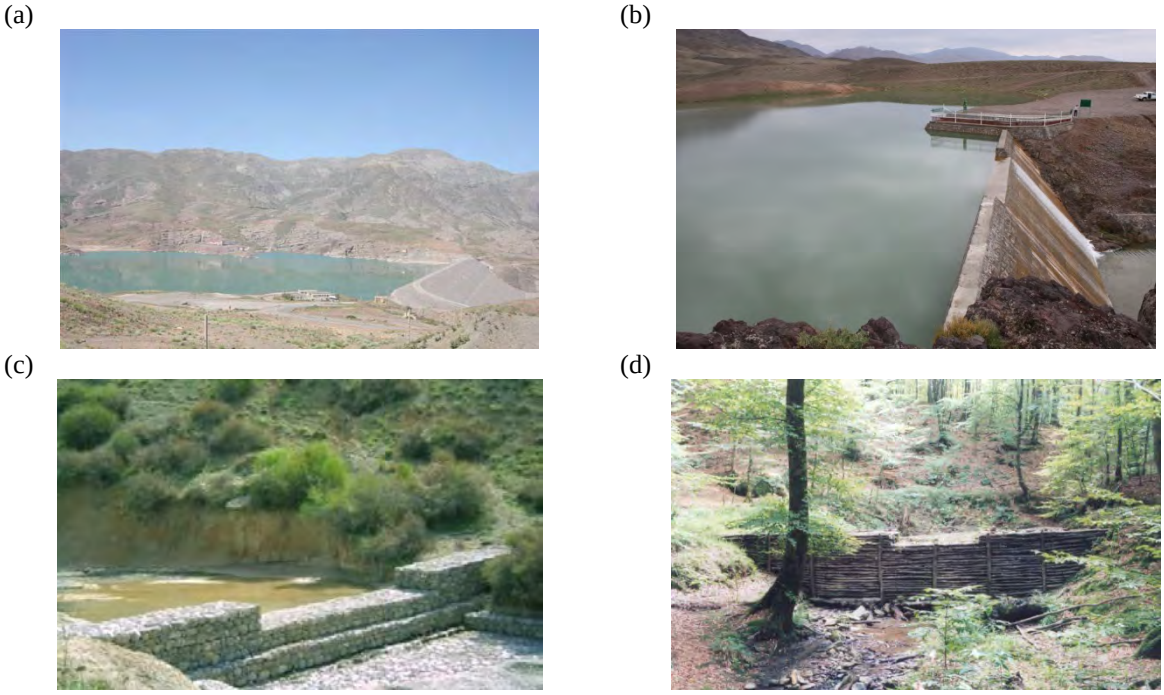

Fig. 6 Common GSSs that are implemented mainly in semi arid watersheds in Iran; (a)Earth-embankment dam, (b) Masonry check-dam, (c) Gabion check-dam, and (d) Wood check-dam that is constructed mainly in forest basins. They are constructed with various materials on different sites. (source: http://www.frw.org.ir/pageid/34/language/en-US/Default.aspx)

Performance of BMPs

Many studies have evaluated landuse change impacts on hydrological components (Alibuyong et al. 2009 and Ghaffari et al. 2009). They had assumed the landuse conversion in the entire watershed and/or some percentage changes systematically. In the present study, the selected management practices are incorporated in the cultivated portions of the watershed. The results of deployment of suitable BMPs for the deficit in water availability under different scenarios have been discussed below.

Evaluation on baseline climate condition (1970-1999)

The choice of BMPs was simulated on baseline conditions to evaluate the impacts on some major hydrologic components such as surface runoff, groundwater, and sediments yield. Terracing and strip cropping have been modelled on cultivated lands in Upper and Middle KRB due to mountainous terrain conditions. Terracing was simulated on irrigated cultivated lands due to expense of terracing in high slopes and the location of the cultivated land on the upper range in KRB. The GSS have been modelled mainly on rangelands because of their ownerships[1]. Table (5) provides the comparison of implementation of selected BMPs on the study area.

[1] In Iran, all the natural resources (rangelands, forest, and water bodies) are under the national ownership. It means all the managements and administrations are under the government.

Table 5 Comparison of selected BMPs on some hydrologic components on baseline in KRB

Basin	Management Application	Surface water (mm)	Ground water (mm)	Total sediment (ton/ha)
Upper KRB	No application	63.20	33.56	8.80
	Terracing	14.05	48.35	0.50
	Strip cropping	NCC*	NCC	NCC
	Contouring	11.8	67.83	1.93
	GSS**	53.10	9.09	-
Middle KRB	No application	125.76	62.71	18.93
	Terracing	18.98	152.03	1.76
	Strip cropping	NCC	NCC	NCC
	Contouring	23.52	127.67	2.26
	GSS	44.24	17.06	-

*NCC-No Considerable Change in compare to" No application" ** GSS-Graded Stabilization Structure

Terracing was the most effective management practices to runoff and sediment reduction in both upper and middle KRB. The surface runoff has reduced about 80% and 75% for Upper and Middle KRB respectively. There is a positive response on ground water due to surface runoff retention and penetrating. It has increased ground water by about 14mm and 90mm in upper and middle KRB respectively. Contouring has also similar impacts on the chosen hydrologic components. The surface water and total sediment erosion have reduced considerably. Total sediment was reduced by about 6 and 16 (ton/ha/year) for upper and middle KRB respectively. The GSSs are incorporated on the streams. They help in trapping the surface runoff for subsequent recharge to groundwater. Table 5 shows the reduction in surface runoff by about 16% and 65% on account of GSS in upper and middle KRB respectively. All these implementations under the present scenario have been made with respect to the prevailing interventions as per the local knowledge.

Evaluation on future climate condition (2070-2099)

Using the knowledge on the impacts due to the management practices under the present scenario, choice has been made to identify some suitable practices to circumvent the effects of the climate change. Table (6) summarizes the results of simulation on the choice of BMPs under the baseline and three climate change projections. The choice of best management practices have been made to ensure the flow reduction and increase ground water recharge in the study area. It may be seen from the Table 6 that the average surface discharge show no significant change for all climate projections from the baseline in upper as well as middle KRB. It may also be observed that the change in maximum and minimum flow is considerable; e.g. maximum flow is 718, 709.2, 33.45, and 1548 m^3/sec in baseline, A2, B2, and A1B scenarios, respectively in upper KRB with no application of BMPs. This maximum flow has reduced to 323, 490 and 1189 m^3/sec for baseline, A2, and A1B scenarios whereas it has increased to 99 m^3/sec for B2 scenario. The minimum flow in invariably increased from the present condition to the climate change scenarios. This is mainly on account of enhanced groundwater recharge. Similar trends are also observed for the middle KRB.

Therefore, implementation of appropriate BMPs can influence the local hydrology by regulating the maximum and minimum flow values range. The more import point in implementation of BMPs is their role in reducing the extreme conditions. Figure (7) provides the influence of BMPs at the monthly level for each of the climate change projections in both upper and middle KRB.

Table 6 Comparison of surface flow (m^3/sec) analysis with selected BMPs on climate change projections and baseline information in KRB

Basin	BMPs	Statistic Results	Baseline condition	Climate Scenarios		
				A2	B2	A1B
Upper KRB	No application	Mean	46.65	76.65	10.26	58.04
		Max	718	709.2	33.45	1548
		Min	0	0	1.23	0
	With application	Mean	50.63	76.44	9.44	55.20
		Max	323.1	490.7	99.29	1189
		Min	6.16	8.19	0	1.78
Middle KRB	No application	Mean	146.28	127.61	29.38	121.48
		Max	1647	1174	217.1	3476
		Min	0	0	0	0
	With application	Mean	147.67	123.19	28.34	110.81
		Max	915.20	849.6	100.4	2882
		Min	10.11	14.4	3.128	0

It may be observed from Figure (7) that the maximum flow reduction on account of the BMPs takes place during November to April under A2 and B2 scenarios in both upper and middle KRB. The management practices also cause increase in minimum, average and maximum flow during June to October under A2 and B2 scenarios. Since under A1B, duration of wet season is less, influence of BMPs is also less. The effect of BMPs on surface water under A1B is also less.

Conclusions

The SWAT model has been used on the KRB basin which has heterogeneous climatic conditions. The model has been calibrated and validated using manual and auto-calibration procedure. SWAT model allows using detailed management practices to manage the cultivation field operations. The effect of selected BMPs has been examined to circumvent the impacts of climate change under the future ‘PRECIS’ and ‘REMO’ regional climate models dynamically downscaled from the latest GCMs. The impact of selected BMPs had various effects on the major hydrological components e.g. surface runoff, groundwater and sediment erosion. Amongst the selected BMPs, terracing followed by GSS has been found to influence significantly on selected hydrologic components. Strip cropping has been found to be less effective.

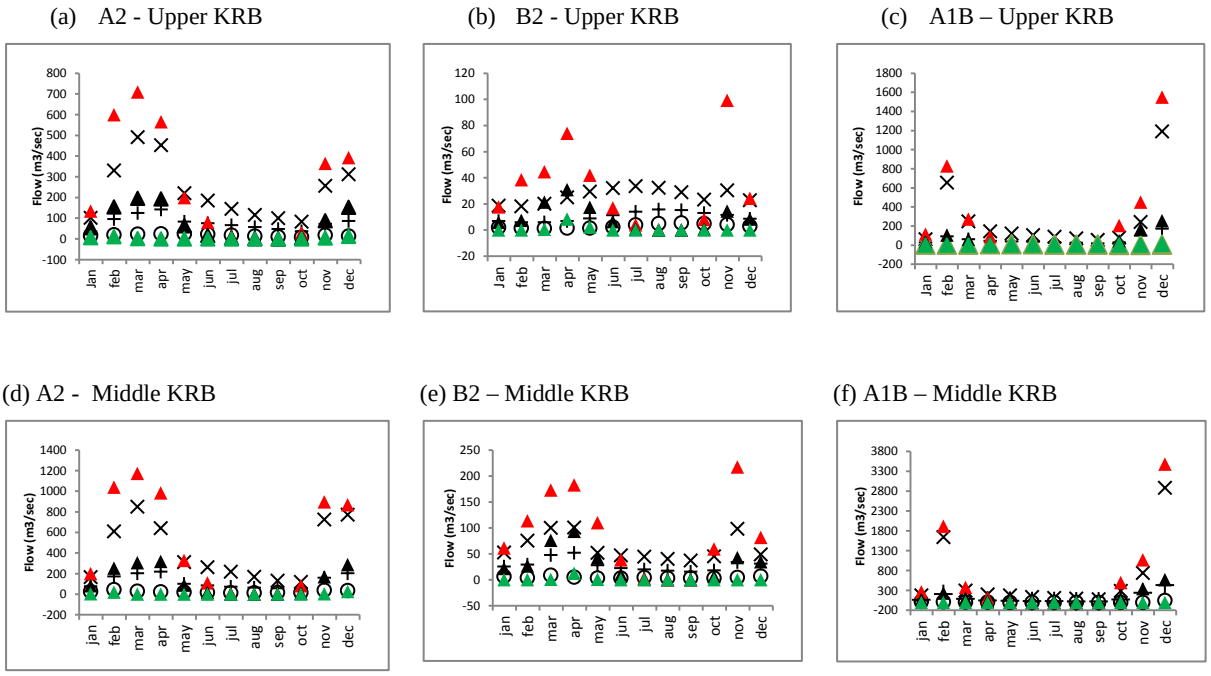

Fig. 7 Influence of choices of BMPs implementation on surface flow by various climate change projections in study area; (a)A2 scenario in upper KRB, (b) B2 scenario in upper KRB, (c) A1B scenario in upper KRB,(d) A2 scenario in middle KRB, (e) B2 scenario in middle KRB, and (f) A1B scenario in middle KRB.

Results of this study show that integrated water resources management should be used to analyse various possible BMPs comparatively.

References

Abbaspour, K. C., Faramarzi, M., Seyed Ghasemi , S., and J. Yang (2009) Assessing the impact of climate change on water resources in Iran, Water Resources Research, VOL. 45, W10434,

Alibuyong, N.R.; Ella, V.B.; Reyes, M.R.; Srinivasan, R.; Heatwole, C.; Dillaha, T. (2009) Predicting the effects of land use change on runoff and sediment yield in Manupali River subwatersheds using the SWAT model. Int. Agr. Eng. J. 18, 15–25.

Arabi, M., Govindaraju R.S., Hantush M.M., (2006) Cost-effective allocation of watershed management practices using a genetic algorithm. Water Resources Research, AGU 42:W10429. doi:10.1029/2006WR004931

Arnold J.G., J.R. Kiniry, R. Srinivasan, J.R. Williams, E.B. Haney, S.L. Neitsch, (2011) Input/Output File Documentation. (http://www.swat.tamu.edu)

Ashrafi, S.; Qureshi, A.S.; Gichuki, F., (2004) Karkheh Basin profile: Strategic research for enhancing agricultural water productivity. Draft Report. Challenge Program on Water and Food.

Bracmort K.S., Arabi M., Frankenberger J.R., Engel B.A., Arnold J.G. (2006) Modelling long term water quality impact of structural BMPs. Am Soc Agric Biol Eng 49(2):367–374

CPWF (2003) “Karkheh River Basin: Protecting dry land under environmental siege”, Karkheh Basin Brochure, Challenge Program on Water and Food (CPWF).

Faramarzi, M., Abbaspour, K., Schulin, R., Yong, H., (2008), Modelling blue and green water resources availability in Iran, Hydrol. Process. 23, 486–50.

Ghaffari, G.; Keesstra, S.; Ghodousi, J.; Ahmadi, H., (2009), SWAT- simulated hydrological impact of land-use change in the Zanjanrood Basin, Northwest Iran. Hydrol. Process., 24, 892–903.

IPCC (2001) "Climate Change 2001: Impacts, Adaptation, and Vulnerability", Contribution of Working Group II, Cambridge University Press.New York, USA.

IPCC (2007) Climate Change 2007: “Impacts, Adaptation, and Vulnerability—Contribution of Working Group II to the Third Assessment Report of the Intergovernmental Panel on Climate Change”, edited by M. L. Parry et al., Cambridge Univ. Press, Cambridge, U. K.

JAMAB Consulting Engineers, (1999) Comprehensive Assessment of National Water Resources: KARKHEH River Basin. JAMAB Consulting Engineers in association with Ministry of Energy, Iran. (In Persian)

JAMAB Consulting Engineers, (2006b), Water balance report of Karkheh River Basin area: Preliminary analysis. Tehran, Iran. (In Persian)

Kaini, P., K. Artita, J.W.Nicklow, (2012), Optimizing Structural Best Management Practices Using SWAT and Genetic Algorithm to Improve Water Quality Goals, Water Resour Manage, 26:1827–1845. DOI 10.1007/s11269-012-9989-0

Kay, A.L., H. N. Davies, V.A. Bell, R.G. Jones, (2009), Comparison of uncertainty sources for climate change impacts: Flood frequency in England. Climatic Change 2009, 92, 41–63.

Keshavarz, A., Dehghanisanij, H., Asadi, H., Oweis, T. and Abdelwahab, A.M. (Eds), (2012) Policies, Institutions and Economies of Water Resources and Management in the Karkheh River Basin of Iran, CPWF, Karkheh River Basin Research Report 10. ICARDA, Aleppo, Syria.

Lindsey J., S. Jaspars, S. Pavanello, E. Ludi, R. Slater, A. Arnall, N. Grist and S. Mtisi, (2010), "Responding to a Changing Climate: Exploring how Disaster Risk Reduction, Social Protection and Livelihoods Approaches Promote Features of Adaptive Capacity", ODI, Working Paper, No. 319.

Massah, A. R. (2006) Risk Assessment of Climate Change and it's Impacts on Water Resources;A Case Study : Zayandeh Rud Basin, Esfahan, Iran, PhD. Thesis. Faculty of Agriculture, Tarbiat Modares University, Tehran, Iran. (Farsi)

Morid, S.,Massah, A. R. (2008) Exploration of potential adaptation strategies to climate change in the ZAYANDEHRUD irrigation system, Iran, Irrig. and Drain. 59: 226–238

Mirqasemi, S.A.; Pauw, E. De. 2007. Land use change detection in the Karkheh Basin, Iran by using multi-temporal satellite images. In: Extended abstracts. International Workshop on Improving Water Productivity and Livelihood Resilience in Karkheh River Basin, ed. Ghafouri, M. Soil Conservation and Watershed Management Research Institutes (SCWNRI), Tehran, Iran. September 10-11, 2007.

Moriasis, D.N., Arnold, J. G., Van Liew, M. W., Bingner, R.L., Harmel, R. D. and Veith, T. L. 2007. Model evaluation guidelines for systematic quantification of accuracy in watershed simulation, Transactions of the ASABE. Vol. 50(3): 885-900.

Muleta M.K., Nicklow J.W., (2001), Watershed management technique to control sediment yield in agriculturally dominated areas. Water Int IWRA 26(3):435–443

Solaymani, H.R., and Gosain, A.K., (2012) SWAT Application for Snow Bound Karkheh River Basin of Iran, International SWAT Conference Proceedings-Delhi. July 16-20, 2012

Starks, P.J.; Moriasi, D.N. 2009. Spatial resolution effect of precipitation data on SWAT calibration and performance: Implications for CEAP. Transactions of the ASABE 52(4): 1171-1180.

Sutcliffe, J.V. 2004. Hydrology: A question of balance. IAHS special publication 7. Wallingford, UK: IAHS Press.

Tizro AT, Voudouris KS, Eini M (2007) Groundwater balance, safe yield and recharge feasibility in a semi-arid environment: a case study from western part of Iran. J Appl Sci 20:2967–2976.

USEPA (2001) Funding Agricultural Best Management Practices with the Clean Water State Revolving Fund (EPA 832/F-01/006).

USEPA (2004) Impact of best management practices of water quality of two small watersheds in Indiana: role of spatial scale (EPA/600/R-05/080).

Veith, T.L. and L.T. Ghebremichael. 2009. How to: applying and interpreting the SWAT Auto-calibration tools. In: Fifth International SWAT Conference Proceedings. August 5-7.

Webber, D.F.; Mickelson, S.K.; Ahmed, S.I.; Russell, J.R.; Powers, W.J.; Schultz, R.C.; Kovar, J.L., (2010), Livestock grazing and vegetative filter strip buffer effects on runoff sediment, nitrate, and phosphorus losses. *J. Soil Water Conserv. 65*, 34–41.

Appendix

Distribution of climate change projections on annual rain-fed and irrigated wheat yields (ton/ha) corresponding baseline, A1B, A2 and B2 scenarios in KRB

Subbasin	Rainfed Cultivation				Irrigated Cultivation			
	Baseline	A1B	A2	B2	Baseline	A1B	A2	B2
1	0.95	0.60	1.12	0.29	3.62	1.51	2.79	0.73
2	0.88	0.65	1.23	0.29	4.07	1.63	3.07	0.74
3	2.08	0.84	1.18	0.55	4.54	2.09	2.96	1.37
4	1.47	1.02	1.11	0.80	4.88	2.54	2.77	2.00
5	1.41	0.94	0.97	0.80	4.37	2.35	2.44	1.99
6	1.74	0.71	0.94	0.54	3.59	1.79	2.35	1.35
7	1.25	0.60	0.78	0.91	4.21	1.50	1.94	2.26
8	1.77	0.63	0.79	0.90	4.25	1.57	1.98	2.26
9	1.78	0.75	1.04	0.91	5.19	1.87	2.60	2.28
10	1.83	0.76	1.41	0.30	4.74	1.89	3.52	0.74
11	1.61	0.75	1.41	0.30	4.73	1.89	3.52	0.74
12	2.34	0.67	1.26	0.29	4.21	1.68	3.16	0.72
13	1.70	0.67	0.89	0.90	4.66	1.67	2.23	2.26
14	1.20	0.78	0.80	1.15	4.72	1.94	2.00	2.87
15	1.27	0.97	0.73	1.40	5.18	2.43	1.83	3.50
16	2.04	0.83	0.84	0.78	3.72	2.07	2.09	1.95
17	1.93	0.62	0.78	0.53	3.12	1.55	1.95	1.32
18	1.78	0.57	0.78	0.53	2.78	1.41	1.94	1.32
19	2.59	0.78	0.83	0.78	3.38	1.94	2.08	1.96
20	3.19	0.78	0.83	0.78	3.37	1.94	2.09	1.96
21	1.98	0.64	0.91	0.54	3.28	1.60	2.29	1.35
22	1.63	0.51	0.98	0.29	3.14	1.29	2.46	0.72
23	1.46	0.68	1.11	0.33	3.91	1.71	2.77	0.83
24	2.85	0.78	1.10	0.37	4.18	1.94	2.76	0.93
25	2.99	0.75	1.02	0.37	3.85	1.88	2.56	0.93
26	2.60	0.65	0.99	0.33	3.39	1.62	2.47	0.82
27	2.29	0.64	0.96	0.33	3.30	1.60	2.41	0.82
28	2.35	0.65	1.03	0.33	3.61	1.63	2.59	0.82
29	1.98	0.75	1.05	0.37	3.98	1.87	2.62	0.93
30	3.29	0.74	1.03	0.37	3.89	1.85	2.58	0.93
31	3.19	0.73	0.96	0.37	3.58	1.82	2.41	0.93
32	3.28	0.79	0.91	0.56	3.65	1.98	2.27	1.41
33	1.79	0.78	0.72	1.14	4.52	1.96	1.79	2.85
34	2.60	0.79	0.78	1.14	4.77	1.99	1.94	2.85
35	3.27	0.59	0.75	0.90	4.07	1.49	1.86	2.26
36	3.21	0.78	1.03	0.32	3.82	1.94	2.58	0.81
37	2.30	1.09	1.13	0.36	4.82	2.71	2.83	0.90
38	-	-	-	-	5.27	3.01	2.94	1.01
39	-	-	-	-	5.49	2.54	2.22	2.46
40	-	-	-	-	5.15	2.22	2.08	2.47
41	-	-	-	-	5.28	2.25	2.15	2.47
42	-	-	-	-	4.62	2.32	2.72	1.04
43	-	-	-	-	4.09	1.89	2.68	0.93
44	-	-	-	-	4.68	2.30	2.89	0.93
45	-	-	-	-	5.19	2.69	3.06	0.92
46	-	-	-	-	5.25	2.64	3.23	1.16
47	-	-	-	-	4.59	2.10	3.18	1.06
48	-	-	-	-	3.68	1.46	2.97	0.97
49	-	-	-	-	4.50	2.20	3.25	1.15

Evaluation of small watersheds inflowing Lake Shinji against the water environment

Hiroaki Somura
Faculty of Life and Environmental Science, Shimane University

Yasumichi Yone
Faculty of Life and Environmental Science, Shimane University

Yasushi Mori
Faculty of Environmental and Life Science, Okayama University

Erina Takahashi
Faculty of Life and Environmental Science, Shimane University

Abstract

In our previous study, the Hii River, where contributes approximately 80% of the discharge flowing into Lake Shinji, was selected as a target watershed with a focus on land uses such as paddy fields, upland fields, residential areas, and forestry. Then we figured out that yields per unit area of SS, TN, and TP from upland areas were the greatest, whereas yields from forests were the lowest. However, forests were the largest contributor of them in the basin, because of its dominant land area. At that time, we dealt with forest as mixed forest in the analysis because of land use GIS data set that we used. Thus, we focused on forest this time and improved the GIS data set from one category of mixed forest to six categories of natural and artificial broadleaf forests, natural and artificial coniferous forests, mixed forest, and others. Also we focused on small watersheds around the lake along with Hii River basin to evaluate its influences against the water environment. Moreover, input data sets such as DEM, Soil, the number of weather station location, point source were improved for the analysis. Parameter values were calibrated at the outlet of the Hii River basin because of no observed data in small watersheds. As a result, SWAT could simulate fluctuations of discharge following precipitation pattern relatively well. But parameter values still need to be calibrated to get more accurate results for considering influence of small watersheds, and an impact of the watershed management, especially in artificial forest, against the lake water environment.

Keywords: Hydrology, Land use, Brackish lake

Introduction

Impact assessments of land-use change, population growth/decrease and watershed development to water quantity and quality are one of the most important topics in a basin. As well, integrated managements of water environment from a river basin to downstream such as a lake are also very important for conservation and sustainable use of its resources. In recent years, water quality in a lake has been tried to improve until under environmental standard by emission control of pollutant loads to a lake and rivers through putting an adequate sewage system in place and development of laws, though water quality in a lake does not been improved well as we expected. One of the reasons is considered to be pollutant loads discharged from non-point sources such as agricultural lands. When considering watershed management and improvement of water environment in a lake, both information of a lake and rivers will be necessary.

Many researchers study about water quality targeted at Lake Shinji and Lake Nakaumi ,where is located downstream of Lake Shinji, from several perspectives (e.g. Seike et al., 2006; Sakuno et al., 2003). As well, there are some studies targeted at Hii River where is the main river basin of Lake Shinji watershed (Takeda et al., 1996; Ishitobi et al., 1988). However, few studies have been done about runoff analysis and quantitative analysis of pollutant loads by a model in Lake Shinji watershed.

Thus, we applied the Soil and Water Assessment Tool (SWAT) to Lake Shinji watershed for obtaining information related to river basin hydrology and influence of the hydrology to the lake. Especially, we focused on small watersheds around the lake along with Hii River basin to evaluate its influences against the water environment. In this stage, we tried to create stream flow of small river basins inflowing Lake Shinji as a first step of evaluation of small watersheds against the lake water environment.

Study Area

The Lake Shinji is located in the eastern part of Shimane Prefecture, Japan (Fig.1). Its watershed has an area of approximately 1,194 km^2 in this study. More than 20 rivers inflow to the lake. The largest contributor among them against ecosystems and the aquatic environment in the lake will be Hii River basin, because discharge from the Hii River contributes approximately 80 % of the discharge flowing into the lake. The length of the river from the source (Mt. Sentsu, 1,143m) to the Otsu river discharge observation station is approximately 63 km. Most of the Hii River basin is underlain by easily-weathered granite, and a large volume of sediment is provided from the upstream basin areas. In the lower reaches, the elevation of the riverbed is higher than that of the surrounding Izumo plains.

The Hii River flows into Lake Shinji and then to Lake Nakaumi, and is finally discharged into the Sea of Japan through the Sakai Channel. Lake Shinji is the third largest brackish water lake in Japan, with an area of 79.1 km^2. Lakes Shinji and Nakaumi were designated as a Wetland of International Importance by the Ramsar Convention in November 2005. The average depth of Lake Shinji is low (4.5 m), and the salinity level is only one-tenth that of sea water. Salty water sometimes flows back into Lake Shinji from Lake Nakaumi, which has a salinity half that of sea water.

Approximately 81 % of the watershed basin is forest, 13 % is occupied by paddy fields, 2 % is devoted to upland crops, and 2.0 % is residential area. According to the Ministry of Agriculture, Forestry and Fisheries (http://www.maff.go.jp/index.html), 95 % of the forest in the basin is privately owned, and of that, 48 % is artificial plantation forest. In the artificial forest, 99 % is coniferous.

During June and July, a stationary seasonal rain front forms over the district. This remains stationary for long periods, and often causes intense rain storms. Typhoons may approach the region in September, and these can cause extensive damage through strong winds and heavy rain. In winter, snow clouds form over the region and produce heavy snowfalls. In addition, winter precipitation tends to be higher than in other regions. The average annual precipitation varies from about 1,700 to 2,000 mm, and average annual maximum and minimum temperatures are 18 and 9 degrees C, respectively.

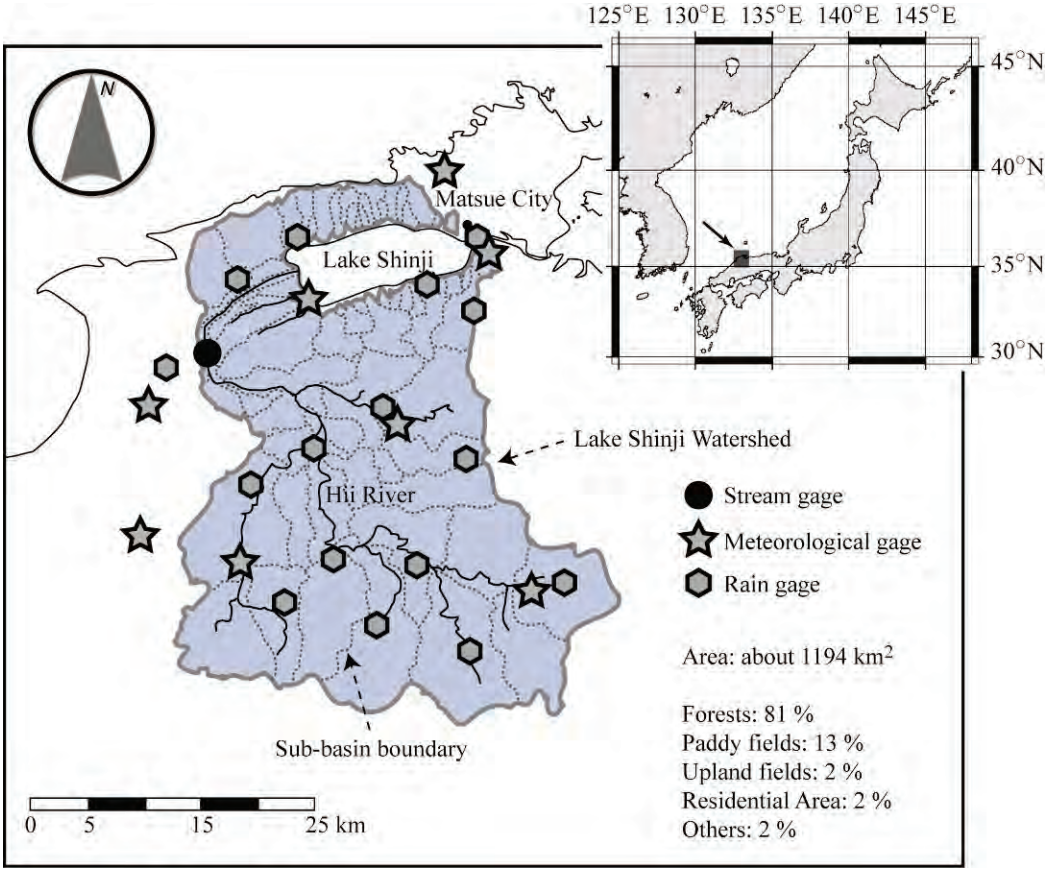

Figure 1 Study Area

Methodology

Model Description

SWAT has been widely applied for modeling watershed hydrology and simulating the movement of non-point source pollution. SWAT is a physically-based continuous time hydrologic model with an ArcView GIS interface. It was developed by the Blackland Research and Extension Center and the USDA-ARS (Arnold et al., 1998) to predict the impact of land management

practices on water, sediment, and agricultural chemical yields in large complex basins with varying soil types, land uses, and management conditions over long periods of time. The main driving force behind SWAT is the hydrological component. Hydrological processes are divided into two phases: 1) the land phase, which controls the amount of water, sediment, and nutrient loading in receiving waters; and 2) the water routing phase, which simulates movement through the channel network. SWAT delineates watersheds into sub-basins interconnected by a stream network, and each sub-basin is divided further into hydrologic response units (HRUs) based upon unique soil and land class characteristics, without any specified location in the sub-basin. Flow, sediment, and nutrient loading from each HRU in a sub-basin are summed, and the resulting loads are then routed through channels, ponds, and reservoirs to the watershed outlet (Arnold et al., 2001). The model includes a number of storage databases (i.e. soils, land cover/ plant growth, tillage, and fertilizer), which can be customized for an individual basin. A single growth model in SWAT is used for simulating all crops based on the simplification of the EPIC crop model (Williams et al., 1984). Phenological development of the crop is based on daily heat unit accumulation. The model can simulate up to 10 soil layers if sufficiently detailed information is available. SWAT provides useful information across a range of timescales (i.e. hourly, daily, monthly, and yearly time-steps; Neitsch et al., 2005).

Input data description

SWAT requires information for cropping systems, including tillage, irrigation, and the amount and timing of fertilizer application. Spatial data sets, including a digital elevation model (DEM) and GIS maps of land cover and soil, also need to be prepared. In addition, the model requires meteorological data such as daily precipitation, maximum and minimum air temperature, wind speed, relative humidity, and solar radiation data. Because there were some inconsistencies and missing climate data for the system evaluated in this study, the weather generator included in SWAT was used for filling in gaps in the measured climatic records. For the weather generator, we used climatic information statistically generated from 20 years data in and around the basin as input.

DEM data were prepared using a digital map 10-m grid (elevation) created from a 1:25,000 topographic map published by the Geographical Survey Institute (GSI). Minimum DEM data resolution should range from 30 to 300 m for flow, sediment, NO_3-N, and TP predictions (Cotter et al., 2003), and consequently the data comfortably satisfies the standard.

Land-use data were created from two data sets in this study. One is digital national information that identified categories such as paddy fields, non-paddy fields (upland fields and orchards), denuded land, forests and water. Another is prefectural information of varieties of tree species and its possession. The digital national information data was developed based on the 1:25,000 topographic map and 1:100 subdivision plat data. The data were obtained from the National Land Information Office in the MLIT (http://nlftp.mlit.go.jp/) and from Shimane prefecture. Although the percentage of agricultural lands has been changing year by year, the value was treated as constant during the simulation period.

Soil data were obtained from the 1:500,000 Fundamental Land Classification Survey soil map prepared by the MLIT (http://tochi.mlit.go.jp/tockok/index.htm). Soils were categorized into

10 groups consisting of 14 soils: dystric rhegosols, fluvic gleysols, gleysols, haplic andosols, helvic acrisols, humic cambisols, lithosols, ochric cambisols, rhodic acrisols, and vitric andosols.

Meteorological data were obtained from two organizations. One is the Japan Meteorological Agency (JMA: http://www.jma.go.jp/jma/index.html), and another is Ministry of Land, Infrastructure, Transport and Tourism (MLIT). Data from JMA such as precipitation, temperature, wind speed, and actual sunshine duration were monitored by the Automated Meteorological Data Acquisition System (AMeDAS), which consists of about 1,300 stations for precipitation and 840 stations for other weather parameters spread around Japan. These data are made available to the public in near-real time (e.g., Japan Meteorological Agency, 2011). Data from MLIT was precipitation in / around the study area, and sixteen stations were selected for this analysis. Thus, data was used from twenty one precipitation gauges and three air temperature and wind speed gauges that were located in and around the basin, and also we used relative humidity data recorded at Matsue City, which is located approximately 30 km NE of the Hii River basin. Similarly, no stations within the basin collected solar radiation data. Therefore, the solar radiation data were developed using the Angstrom formula (FAO, 1998) based on data collected by Shimane University and actual sunshine duration in the basin. The latter data was obtained from the AMeDAS data base.

Discharge data were provided by the MLIT Izumo River Office. The data were monitored at Otsu outlet.

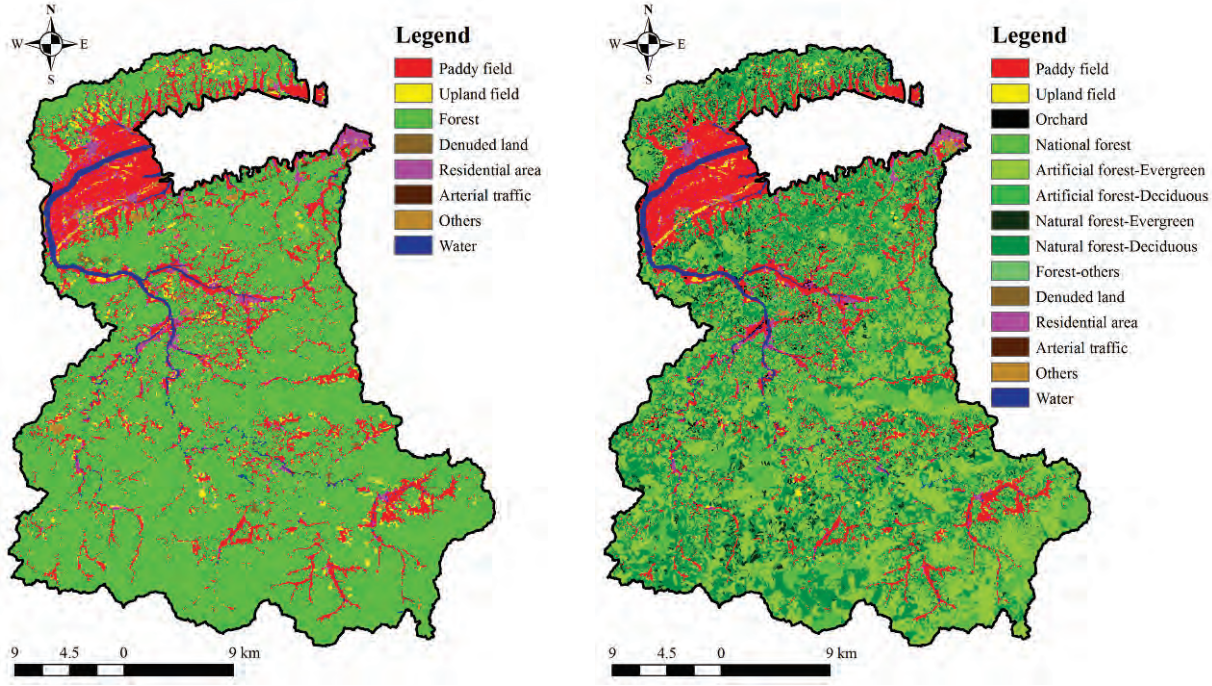

Figure 2 Original Land-use GIS data (Left side) and improved one (Right side)

Model performance evaluation

SWAT was calibrated and validated using observed data. Initial assessment of the results was performed using graphical techniques, which provide a visual comparison of simulated and

observed constituent data and preliminary overview of the model performance (ASCE, 1993). The coefficient of determination (R^2), Nash-Sutcliffe efficiency (*NSE*), root mean square error (*RMSE*) – observations standard deviation ratio (*RSR*), and percent bias (*PBIAS*) were then used to statistically evaluate the model performance.

The R^2 value is an indicator of the strength of the relationship between the observed and simulated values. R^2 ranges from zero to one, with a value of zero indicating no correlation and a value of one indicating that the predicted dispersion equals the measured dispersion (Krause et al., 2005). Gassman et al. (2007) reported that daily R^2 statistics have been used in many previous SWAT studies.

The *NSE* value (Nash and Sutcliffe, 1970) indicates how well the plot of the observed values versus the simulated values fits the unit slope line. The *NSE* values range from $-\infty$ to one, with values less than or close to zero indicating unacceptable or poor model performance, and a value of one representing a perfect match. The *NSE* value is calculated using the equation:

$$NSE = 1.0 - \left(\sum_{i=1}^{n} (Y_{obs,i} - Y_{cal,i})^2 \Big/ \sum_{i=1}^{n} (Y_{obs,i} - Y_{obs\_mean})^2 \right) \quad (1)$$

where *n* is the number of registered data, *Yobs,i* is the observed data at time *i*, *Ycal,i* is the simulated data, and *Yobs_mean* is the mean value of the observed data.

The *RSR* value is calculated as the ratio of the *RMSE* and the standard deviation of the measured data (Moriasi et al., 2007). An *RSR* value incorporates the benefits of error index statistics and includes a scaling/ normalization factor. *RSR* varies from the optimal value of zero, which indicates zero *RMSE* or residual variation, to a large positive value (Moriasi et al., 2007). *RSR* is calculated using the equation:

$$RSR = RMSE / STDEV_{obs} = \left(\sqrt{\sum_{i=1}^{n} (Y_{obs,i} - Y_{cal,i})^2} \right) \Big/ \left(\sqrt{\sum_{i=1}^{n} (Y_{obs,i} - Y_{obs\_mean})^2} \right) \quad (2)$$

where *n* is the number of registered data, *Yobs,i* is the observed data at time *i*, *Ycal,i* is the simulated data, and *Yobs_mean* is the mean value of the observed data.

The *PBIAS* is used to determine if the average tendency of the simulated data is larger or smaller than their observed counterparts (Gupta et al., 1999). The optimal value of *PBIAS* is zero, with low-magnitude values indicating accurate model simulation. Positive values indicate model underestimation bias, while negative values indicate model overestimation bias (Gupta et al., 1999). The *PBIAS* is calculated using the equation:

$$PBIAS = \left(\sum_{i=1}^{n} (Y_{obs,i} - Y_{cal,i}) \times 100 \Big/ \sum_{i=1}^{n} (Y_{obs,i}) \right) \quad (3)$$

where *n* is the number of registered data, *Yobs,i* is the observed data at time *i*, and *Ycal,i* is the simulated data.

Moriasi et al. (2007) developed model evaluation guidelines using systematic quantification of accuracy in watershed simulations, and suggested that a model simulation could be judged as "satisfactory" if NSE > 0.5, RSR $\leq$ 0.70, and the PBIAS is $\pm$ 25 % for stream flow.

Results and Discussions

Reproducibility of stream flow

In this study, SWAT was applied to Lake Shinji watershed for the period from 1985 to 2011. The watershed was divided into sixty four sub-basins in the model setup. The SWAT parameters were calibrated for 10 years from 1988 to 1997, and validated for another 14 years from 1998 to 2011, using flow data record at Otsu outlet, where is the main river basin in the watershed, and model parameters are not calibrated at other outlet of small river basins because of no observed data. The first three years (1985 to 1987) were used as a warm-up period for the model. Sensitivity analysis of model parameters was carried out as a first step of the model simulation. Parameters such as CN2, ESCO, CANMX, SOL_AWC, and BLAI had high ranking of sensitivity in the model. Alpha_BF parameter values in Hii River basin were determined by using the Baseflow Filter Program proposed by Arnold and Allen (1999). The simulated and observed statistics of flow were shown in Table 1. The calibration procedures formulated consist of finding the most appropriate parameters for hydrologic routing model component.

Table 1 Statistical evaluations of the model performance

	Calibration 1988-1997	Validation 1998-2011
NSE	0.64	0.51
R^2	0.75	0.65
RSR	0.60	0.70
PBIAS	15	18

Simulated and observed discharge on monthly time step is reported in Figure 3. The dotted line is observed flow and solid line is simulated flow. It was considered that the both results of calibration and validation were represented fluctuations of discharge relatively well, though some peaks were underestimated.

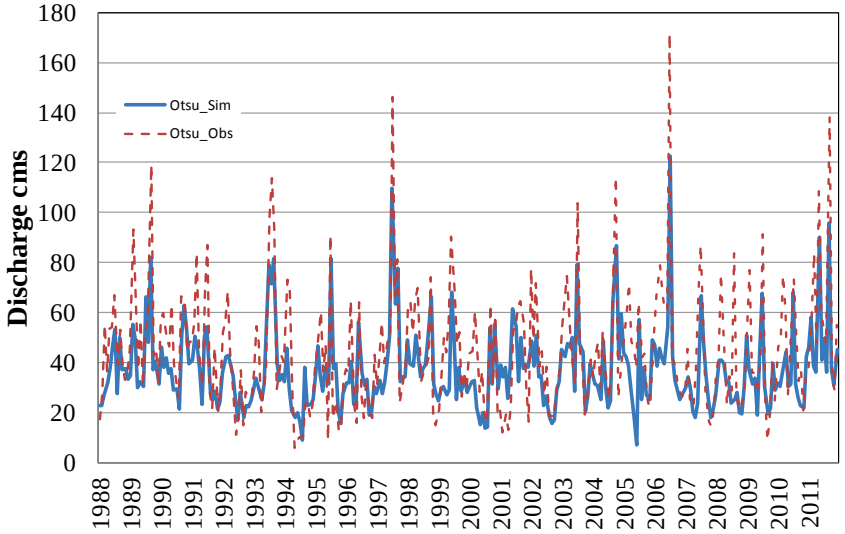

Figure 3 Simulated and observed discharges in a monthly time step

Simulated flow discharges from small river basins

After calibration and validation of the model parameter values at Otsu outlet, some of the small river basins were selected for further analysis. We have selected these small river basins from an aspect of easy access in field investigation. Observed data for flow and water quality of these small rivers have not been found yet at this moment because of no monitoring stations by city or town in the basins. The averaged annual volumes of water per area flowing Lake Shinji are of similar magnitude among the river basins which changes from 9.7 (Subbasin 14) to 15.4 (Hii River, 43), and average 12.1 m^3/km^2, though total volume of water from Hii River is the largest in the watershed. It is understandable because the volume of flow discharge is depending on the amount of precipitation in the area and it is of similar amount of precipitation in lower part of the watershed around the lake. For more accuracy, it is very important to obtain observed data to calibrate model parameter values of small river basins as a next step.

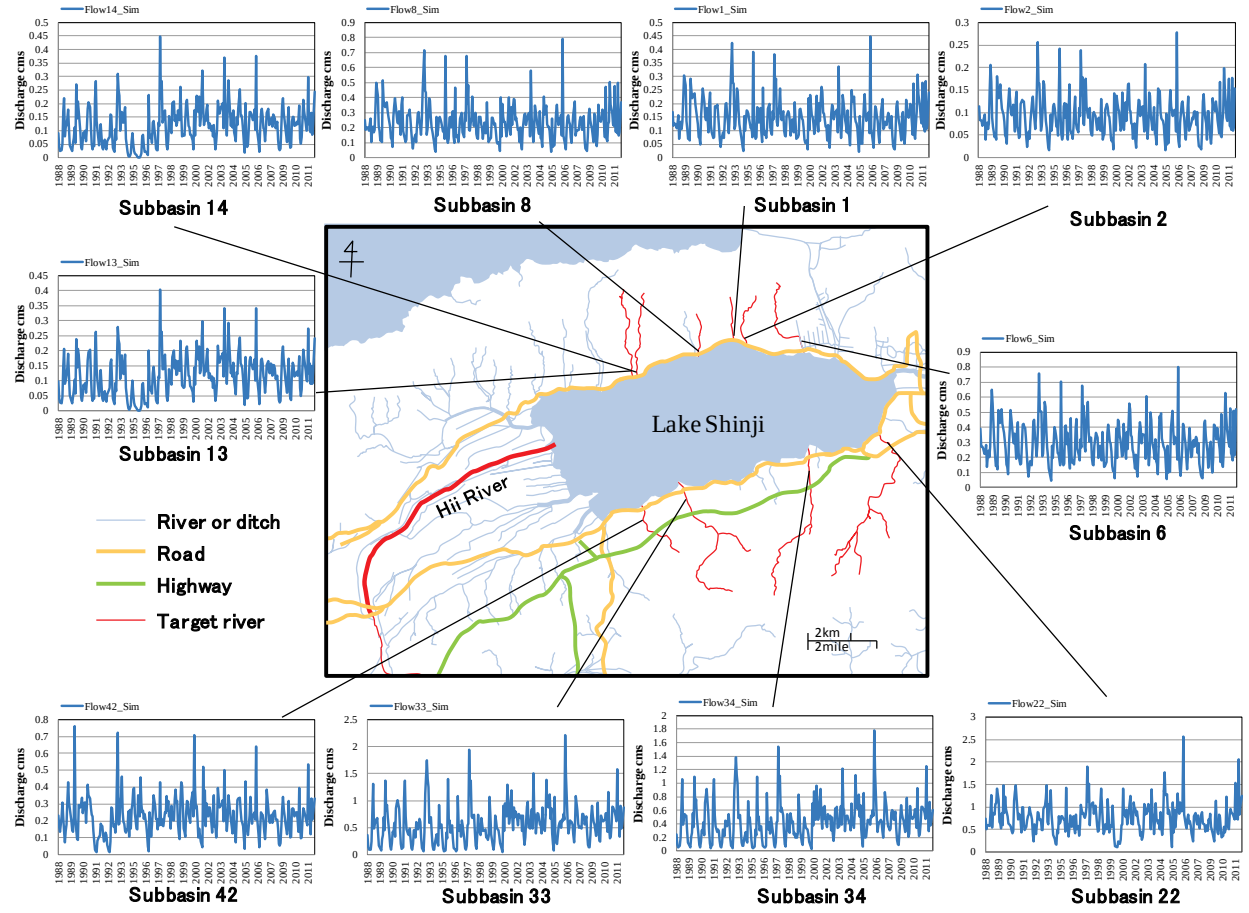

Figure 4 Simulated flow discharges from small rivers to Lake Shinji

By using these simulated flow information, preliminary calculation of averaged annual TN and TP loads from small rivers to Lake Shinji was examined (Figure 5). Water quality data were measured by our laboratory for just only eight month from May to December in 2011. From this estimation, we briefly found that averaged annual TN loads per area varied from 0.70 (Subbasin 34) to 2.2 tons /km^2 (Subbasin 6) and subbasins No. 2, 6, 8, 13 showed higher values in the watershed. As well, averaged annual TP loads per area varied from 0.043 (Hii River) to 0.33 tons /km^2 (Subbasin 6) and subbasins No. 6, 8, 13 showed higher values in the watershed.

Among the river basins, percentage of residential area is small and varied from 0.4 (Subbasin 13) to 4.9 % (Subbasin 34). Major land use is forest and varied from 70 (Subbasin 6) to 86 % (Subbasin 33). The second major land use is agriculture and varied from 11 (Subbasin 34) to 26 % (Subbasin 6). From the aspects of land use percentage and averaged annual nutrient loads, it is considered that river basins with high percentage of agricultural area shows higher load discharges per area. Also it is found that small river basins located in northern part of Lake Shinji shows higher load discharges per area than these in southern part of them.

In addition, annual total loads of TN and TP in the selected small river basins (10 subbasins except No 43) are 86 tons/year and 8 tons/year, respectively, and these values occupy about 10 % of TN and 20 % of TP of annual total loads from Hii River basin (Subbasin 43). It means that total load discharges from small river basins are relatively large though each load discharge from a small river basin is small. Thus, it is very important to evaluate an impact of small river basins against water environment of Lake Shinji along with consideration of Hii River basin.

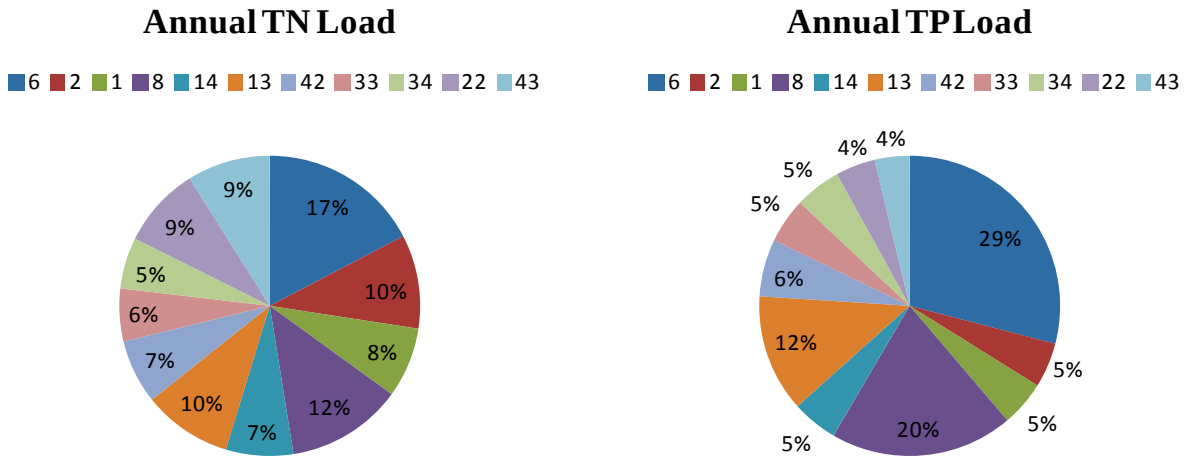

Figure 5 Preliminary calculation of averaged annual TN and TP loads from small rivers to Lake Shinji (tons/km^2)

Conclusion

Now we are trying to evaluate discharges of flow and nutrient loads from small river basins around Lake Shinji for considering conservation ways of water environment in the lake. Generally, larger rivers are paid attention for considering them because of their larger influences against water environment in the watershed, and smaller river basins are tend to be ignored because of less monitoring data and its impact. In this study, we found that total loads from small river basins may have large influences in total, though Hii River basin still has a larger impact to the lake. By accurate evaluation of impact of river basins against downstream lake water environment, it is considered that discussions for improving of water environment and sustainable use of its resources will go forward.

Acknowledgements

This study was supported by a grant-in-aid for scientific research: KAKENHI for Young Scientists (B): 24780234. The discharge and some of precipitation data were provided by the Izumo River Office of the Ministry of Land, Infrastructure, Transport and Tourism, Japan.

References

Arnold, J.G., Srinivasan, R., Muttiah, R.S., Williams, J.R., 1998. Large area hydrologic modeling and assessment part I: model development. *J. Am. Water Resour. As.* 34 (1), 73-89.

Arnold, J.G., Allen, P.M., 1999. Automated methods for estimating baseflow and ground water recharge from streamflow records. *J. Am. Water Resour. As.* 35 (2), 411-424.

Arnold, J.G., Allen, P.M., Morgan, D.S., 2001. Hydrologic model for design and constructed wetlands. *Wetlands* 21 (2), 167-178.

ASCE. 1993. Criteria for evaluation of watershed models. *J. Irrig. Drain. E.* 119 (3), 429-442.

Cotter, A.S., Chaubey, I., Costello, T.A., Soerens, T.S., Nelson, M.A., 2003. Water quality model output uncertainty as affected by spatial resolution of input data. *J. Am. Water Resour. As.* 39 (4), 977-986.

FAO, 1998. In Irrigation and Drainage Paper No.56 Crop Evapotranspiration (guidelines for computing crop water requirements), Allen RG, Pereira LS, Raes D, Smith M (eds). FAO: Rome, Italy; 290, ISBN 92-5-104219-5.

Gassman, P.W., Reyes, M.R., Green, C.H., Arnold, J.G., 2007. The soil and water assessment tool: historical development, applications, and future research directions. *T. ASABE* 50 (4), 1211-1250.

Gupta, H.V., Sorooshian, S., Yapo, P.O., 1999. Status of automatic calibration for hydrologic models: Comparison with multilevel expert calibration. *J. Hydrol. Eng.* 4 (2), 135-143.

Ishitobi, Y., Kawatsu, M., Kamiya, H., Hayashi, K. and Esumi, H. 1988. Estimation of water quality and nutrient loads in the Hii River by semi-daily sampling. *Jpn.J.Limnol.* 49(1): 11-17.

Krause, P., Boyle, D.P., Bäse, F., 2005. Comparison of different efficiency criteria for hydrological model assessment. *Adv. Geosci.* 5, 89-97.

Moriasi, D.N., Arnold, J.G., Van Liew, M.W., Binger, R.L., Harmel, R.D., Veith, T.L., 2007. Model evaluation guidelines for systematic quantification of accuracy in watershed simulations. *T. ASABE* 50 (3), 885-900.

Nash, J.E. and Sutcliffe, J.V. 1970. River flow forecasting through conceptual models. Part I - A discussion of principles -. *J. Hydrology* 10 (3), 282-290.

Neitsch, S.L., Arnold, J.G., Kiniry, J.R., Williams, J.R., 2005. Soil and water assessment tool theoretical documentation version 2005. Blackland Research Center, Temple, Texas, USA.

Seike, Y., Kondo, K., Mitamura, O., Ueda, S., Senga, Y., Fukumori, R., Fujinaga, K., Takayasu, K, and Okumura, M. 2006. Seasonal variation in nutrients and chlorophyll a in the stratified brackish lake Nakaumi, Japan. *Verh. Internat. Verein. Limnol.* 29: 1959-1965.

Sakuno, Y., Yamamoto M. and Yoshida T., 2003. Estimation of Water Temperature and Turbidity in Lake Shinji and Lake Nakaumi Using ASTER Data, 2000-2002. *Laguna* 10: 65-72.

Takeda, I., Fukushima A. and Mori Y. 1996. An estimation of runoff loads of pollutants from River Hii to Lake Shinji. *Laguna* 3: 91-96.

Williams, J.R., Jones, C.A., Dyke, P.T., 1984. A modeling approach to determining the relationship between erosion and soil productivity. *T. ASAE* 21, 129-144.

Re-conceptualizing the Soil Moisture Accounting of CN-based Runoff Estimation Method in SWAT

Mohammad Adnan Rajib
Graduate Research Assistant, School of Civil Engineering,
Purdue University, West Lafayette IN 47907, USA

Venkatesh Merwade*
Associate Professor, School of Civil Engineering,
Purdue University, West Lafayette IN 47907, USA

Cibin Raj
Post-doctoral Research Scientist, Department of Agricultural & Biological Engineering,
Purdue University, West Lafayette IN 47907, USA

Abstract

Surface runoff estimation in SWAT model is based on the SCS Curve Number (CN) method, with an option of choosing either a soil moisture-based or an evapotranspiration-based approach. The current application of CN method in SWAT does not accommodate the antecedent soil moisture storage directly into the runoff formulation, thereby leaving the implicit soil moisture accounting (SMA) of original CN method unutilized. Moreover, within a continuous watershed model, runoff estimation method should be valid not only at the end of a storm but also at any instant during the storm; again, the fraction of rainfall getting transformed into runoff should depend on the current moisture condition of soil profile along with the initial condition resulted from previous modeling time-step. Re-conceptualizing these theoretical inconsistencies, the CN method in SWAT is modified by deriving runoff volume as a derivative of time, with incorporation of four concurrent initial conditions based on a soil moisture storage threshold for runoff to occur. Both the modified and the default SWAT models are tested over two U.S. watersheds having different landuse characteristics. The HRU-level hydrologic outputs such as the surface runoff from the modified CN method are found lower compared to that from the current method invariably for landuse types, which are identified to have been attributed with an elevated soil moisture and evapotranspiration level. Consequently, total streamflow gets slightly underestimated by the modified method particularly at high flow conditions. However, pattern of these changes are reasonably consistent between both the watersheds.

Keywords: CN Method, Runoff, Soil Moisture Accounting, SWAT

* Corresponding Author. Email: vmerwade@purdue.edu

Introduction

Transformation of rainfall into surface runoff is dynamic and complex. A realistic representation of this process plays crucial role in predicting major hydrologic components under the auspices of a physically-based hydrologic model. Numerous watershed models of varying complexity exist in literature. In many of these, Soil Conservation Service Curve Number (SCS-CN) has been used as a rainfall-runoff sub-model [e.g. EPIC (USDA, 1990); HELP (Schroeder et al., 1994); L-THIA (Harbor, 1994); PRZM (Carsel et al., 1997); APEX (Williams et al. 2000); SWIM (Krysanova et al., 2000); CELTHYM (Choi et al., 2002); SWAT (Arnold et al., 2011)]. The versatility of CN method lies on its simplicity, replicable structure, and capacity of accounting several runoff producing watershed characteristics, such as soil type and antecedent moisture condition (Chung et al., 2010; Geetha et al., 2007). Despite its versatility in representing watershed characteristics, the CN method suffers from several structural inconsistencies that need to be addressed for applying in continuous hydrologic simulations.

As of its first limitation from Soil Moisture Accounting (SMA) perspective, the CN method computes surface runoff using only the total rainfall on a given day as the primary driving factor, without directly considering how much water is stored in the soil profile prior to the storm. Secondly, SCS-CN is originally designed as an event-based method having no expression of time inside its equation, which is essential for its application in a continuous hydrologic model. Accordingly, there have been limited attempts to refurbish a sound SMA procedure into CN methodology. Among the noteworthy, Williams and LaSeur (1976) were perhaps the first to attempt an SMA by computing rainfall excess using the antecedent 5-day rainfall-dependent CN values. An arbitrary fixation of maximum soil profile storage to 20 inches was the major weakness of that modified model (Williams et al. 2012; Mishra and Singh, 2004). Hawkins (1978) tried to overcome this limitation by relating evapotranspiration (ET) with CN and varying storage form 0 to ∞, with a notion that soil profile never depletes fully out of moisture. Mishra et al. (2003) differentiated between static and dynamic infiltration and incorporated the static part into the runoff equation as a loss factor along with the antecedent soil moisture amount. A different theory was given by Williams et al. (2000) who related retention parameter S with soil moisture depletion rather than available storage; later this was tested in SWAT both by Kannan et al. (2008) and Williams et al. (2012).

Out of all these modifications, the hypothesis proposed by Michel et al. (2005) is considered to be the most consistent from SMA standpoint because it counteracted both the aforesaid limitations. The SMA procedure adopted by Michel et. al. is based on a perception that the fraction of rainfall to be converted into runoff is directly proportional to the current moisture store level. Also, the runoff equations are re-derived as a function of time, validating CN to be applicable in a continuous model not only at the end of a storm but also at any instant during the storm. Some of the recent works by Jain et al. (2012), Durbude et al. (2011) and Sahu et al. (2007) mostly re-conceptualized the model proposed by Michel et al.

SWAT, as a physically-based long term hydrologic simulation model, has its own SMA procedure. The current version of SWAT computes runoff either by CN or Green-Ampt method. While using the CN method, the users have to choose from two approaches for computing S, including i) the conventional method based on soil profile water content, and ii) an alternative

method based on potential ET (Neitsch et al., 2011). In the conventional method, S is derived as a function of soil profile water content, potential maximum retention, soil's field capacity and saturation point (Williams et al., 2012; Neitsch et al., 2011; Williams et al., 1984). Thus, SWAT's underlying SMA is confined only for calculating retention parameter and thereby updating CN in every time step. In this study, the SMA-based CN approach hypothesized by Michel et al. (2005) is incorporated within SWAT's existing model-structure, with a view to identify potential changes in hydrologic components compared to SWAT's conventional CN method in a watershed scale hydrologic simulation.

Incorporating SMA-based CN Equations in SWAT

Michel's Hypothesis

SCS-CN method consists of the water balance equation and two fundamental hypotheses (Jain et al., 2012), which can be expressed, respectively, as follows:

$$P = Ia + F + Q;$$

$$\frac{Q}{P - Ia} = \frac{F}{S};\ Ia = \lambda S$$

here P = total precipitation, I_a = initial abstraction, F = cumulative infiltration, Q = direct runoff, S = potential maximum retention, and λ = abstraction coefficient (generally taken as 0.2). All the variables here except λ are dimensional [L] quantities. A combination of these equations leads to the popular form of the existing CN method:

$$Q = \frac{(P - Ia)^2}{P - Ia + S}\ if\ P > Ia \text{ or } 0 \text{ otherwise}$$

Thus, CN method calculates accumulated runoff Q corresponding to accumulated rainfall P during a rainfall event. But, in case of continuous simulations, a storm event could have ended at an earlier time or one event can get separated into several events depending on the chosen time-threshold. Accordingly, Michel et al. (2005) denoted that if the CN method is to be used within a continuous watershed model, it cannot be restricted to the accumulated storm water depths; hence, rainfall and runoff were considered as 'rate' in terms of *dP/dt* and *dQ/dt* respectively, *t* being the time.

Now, ideally a soil profile store would absorb that part of the rainfall which is not transformed into runoff (P-Q) by the basic CN equation. This can be attributed to an SMA notion that higher the moisture store level, higher the fraction of rainfall that is converted into runoff. If the moisture store level is full, all the rainfall will become runoff.

On the basis of this hypothesis, following equations were provided:

$$V - Vo = P - Q$$

$$V = Vo + P - Q$$

where V_0 = soil moisture store level at the beginning of the rainfall event (start of the simulation time-step), P = accumulated rainfall at time t along a storm, Q = accumulated runoff at time t along a storm, and V = soil moisture store level at time *t*, i.e. when the accumulated rainfall is equal to *P*. Obviously, $dV/dt = d/dt\ (P - Q)$ and with that, re-deriving the equations will lead to the following:

$$\frac{dQ}{dt} = \frac{dP}{dt}\frac{V - (Vo + Ia)}{S}\left[2 - \frac{V - (Vo + Ia)}{S}\right] if\ V > Vo + Ia$$

$$\frac{dQ}{dt} = 0 \text{ otherwise}$$

As such, the new SMA-based CN equation possesses a different threshold quantity for runoff to occur, which is $(Vo + Ia)$ other than only *Ia* as in the original equation. Michel et al. (2005) defined the new threshold $(Vo + Ia)$ as '*Sa*' and derived the following equations based on four different incident conditions:

$$If\ Vo + P \leq Sa\ , then\ Q = 0$$

$$If\ Vo < Sa \text{ and } Vo + P > Sa, then\ Q = \frac{(P + Vo - Sa)^2}{(P + Vo - Sa + S)}$$

$$If\ Sa \leq Vo < (Sa + S), then\ Q = P\left[1 - \frac{(S + Sa - Vo)^2}{S^2 + (S + Sa - Vo)P}\right]$$

$$If\ Vo = (Sa + S), then\ Q = P$$

SMA Coding in SWAT

SWAT model is available in two formats, one is in ArcGIS interface and other is the Fortran source codes. The framework of the model is divided into a sub-routine call structure within which different parts of the model are accommodated. With a view to modify the runoff estimation method based on the discussed SMA procedure, the sub-routine for computing retention parameter and curve number at individual time-steps is kept unaltered; only the specific sub-routine containing runoff equations is extracted and re-coded. Then the edited sub-routine is compiled with the rest of the SWAT code to get a new executable file. The code modification and subsequent model compilation is done over the downloaded SWAT 2009 source codes by a Visual Fortran compiler.

Study Area and Data Requirements

In order to compare between the modified and the conventional CN-based runoff estimation methods, two U.S. watersheds have been selected for inclusion in this study. These include: (i) Lake Erie basin having 270 mi^2 drainage area with outlet at Cedar Creek near Cedarville, IN (USGS gauge ID 04180000) and (ii) White river basin having 1635 mi^2 drainage area with outlet at White river in Indianapolis, IN (USGS gauge ID 03353000). Both the watersheds are mostly agricultural, though significant difference lies in the forest and developed portion. According to USGS-NLCD (2006), Cedar Creek has 15% forest and 11% developed area, for White River these proportions are 6% and 26% respectively. Figure 1 shows the study areas in relative positions within the Indiana state boundary.

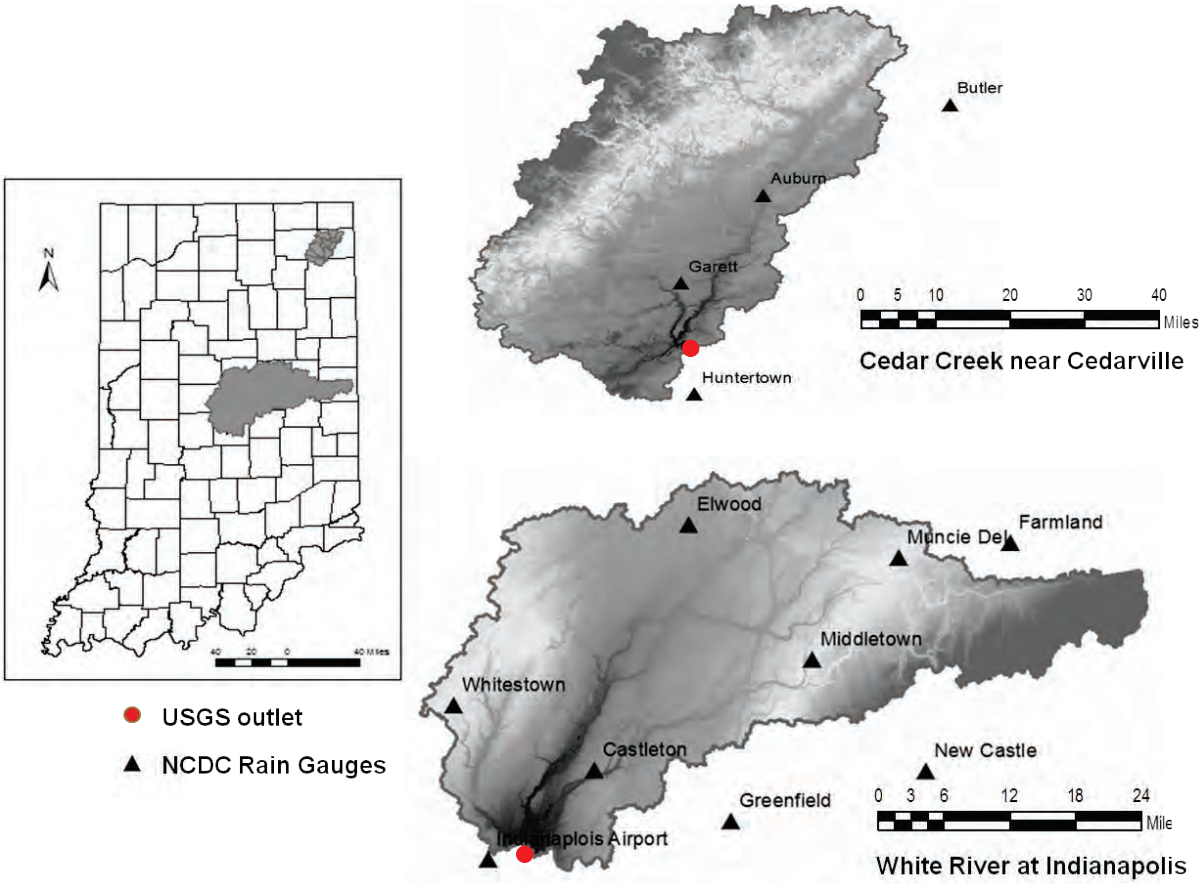

Figure 1. Study areas: Cedar Creek (top) and White River watershed (bottom) with selected rain gauges and USGS outlet locations, Indiana, USA

The geospatial data that were used in this study include: (1) 30 meter resolution 1 arc second Digital Elevation Model (DEM) from USGS National Elevation Dataset in pre-packaged arc-grid format (USGS-NED, 2013), (2) 30 meter resolution National Land Cover Dataset 2006 (USGS-NLCD, 2006), and (3) 1:250,000 scale State Soil Geographic Data (STATSGO) available in SWAT 2009 database. The time series precipitation records were obtained from National

Climatic Data Center (NCDC) available at http:// http://www.ncdc.noaa.gov/cdo-web. Temperature and other related climatic components were generated through internal weather generator within the SWAT model. The simulation period for this study is from 2009 to 2011 based on daily time-step.

Results

Watershed's hydrologic components such as the surface runoff, total streamflow, potential and actual evapotranspiration, soil profile water content etc. are compared using the uncalibrated outputs from both the SWAT's default CN based method and the newly coded SMA technique at daily time step. Except the total streamflow at the watershed outlet, all other components are analyzed at HRU level. Eventually, some significant changes have been detected out of the comparison; the extent of changes were different for different landuse types.

1. Lowered Runoff and Streamflow: In case of surface runoff (SURQ), SMA based values are mostly underestimated compared to those of original CN based method. Figure 2 shows the runoff hydrographs in case of forested and developed HRUs for Cedar Creek and White River, respectively. The hydrographs comprise area-weighted HRU-average runoff volume in individual time-steps (each day), being segregated for different landuse types. Here, the difference shown by the SMA based method is more prominent in case of urban areas (Figure 2 (b)), while for forested or agricultural areas the differences are generally quite small. The overall lowering of SURQ by the modified method is rather a desired outcome with respect to Williams et al. (2012), Neitsch et al. (2011) and Kannan et al. (2008), who noted the over-estimating tendency of SWAT's conventional CN method.

In connection with the HRU-level lower runoff responses, total streamflow simulated by the modified method is also smaller specifically at the high flow conditions (not shown here), while for low flows the difference is negligible.

2. Changes in Profile Soil Moisture Content: Figure 3 separately shows the area-weighted HRU-average daily soil profile water content (SW) for three different LU types, along with the respective difference between the two methods. Based on simulation results, following change patterns have been identified:

i) SW can be higher for the SMA based CN method; the difference being quite prominent in agricultural HRUs (Figure 3(a)).

ii) A specific temporal trend is detected from HRU-level analysis of SW profile in both the study watersheds. For all three landuse cases, the calculated difference between the conventional and newly coded SMA method becomes considerably larger in summer (5-10 mm). For agricultural areas, this difference is found to have exceeded 20 mm when the results are compared separately at individual HRU-scale. Such variation in the predicted daily SW value is very significant considering the amount of average daily rainfall over the watersheds. In case of forested and developed HRUs (Figure 3(b) and (c)), both the methods mostly exhibit identical SW profile (i.e. minimal difference) except in summer. Generally, this particular temporal pattern is consistent in the watershed-average SW profile as a whole (not shown here).

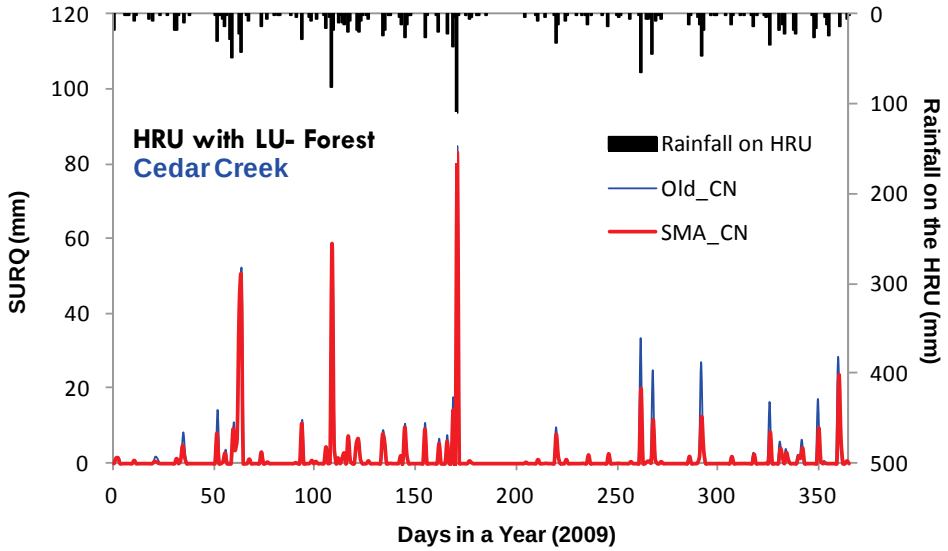

(a)

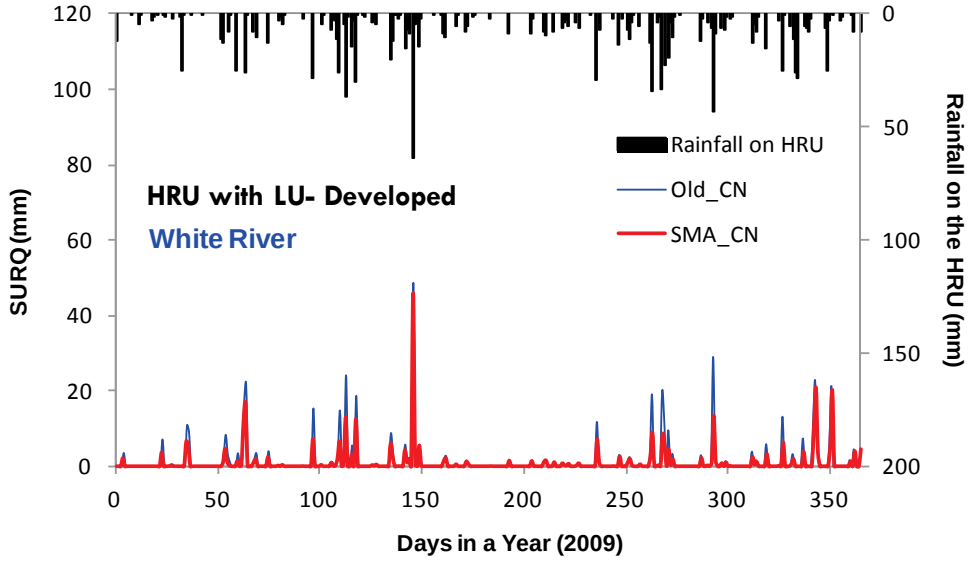

(b)

Figure 2. Comparison of uncalibrated HRU-level surface runoff between SMA and Original CN-based methods: (a) forested landuse (Cedar Creek), (b) developed landuse (White River).

3. Increased ET and Conservation of Daily Water Balance: The reduced surface runoff and streamflow simulated by the modified method should have increased the sub-surface components including SW. Figure 4 shows the HRU-averaged actual ET for Cedar Creek watershed, showing higher amounts by the modified method particularly in summer days. The scenario is similar for White River as well. Therefore, the lesser SW as shown in Figure 3 is resulted from the increased ET in the SMA technique. However, Total Potential Evapotranspiration (PET) remains the same in both methods.

Subsequently, the ground water components, e.g. percolation, shallow aquifer storage and baseflow contribution get lowered in the modified method. As a validation step, the daily water balance is calculated in individual HRU-level following: *SW (end of day) = SW (start of day) + Rainfall + Snow Melt – ET – Surface Runoff - Percolation*; the net balance produces nearly perfect correlation between the two methods having $R^2 \approx 1$ for all HRUs.

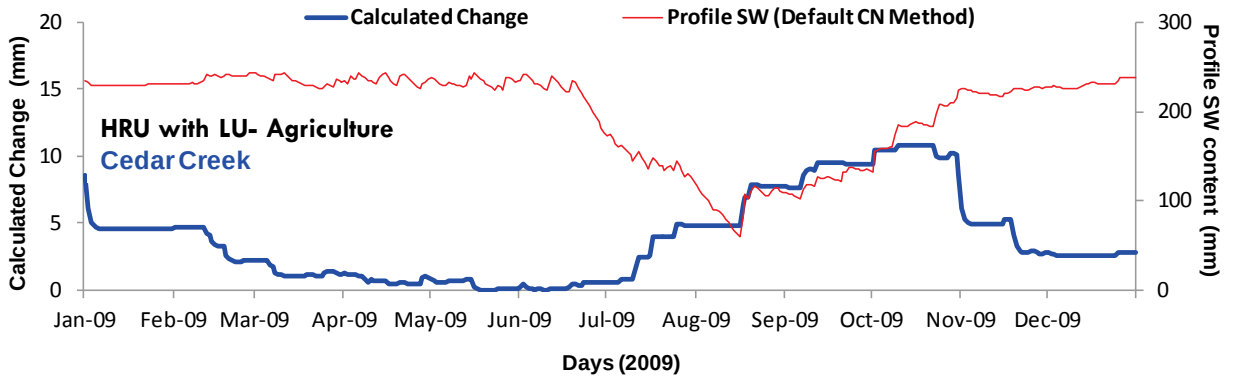

(a)

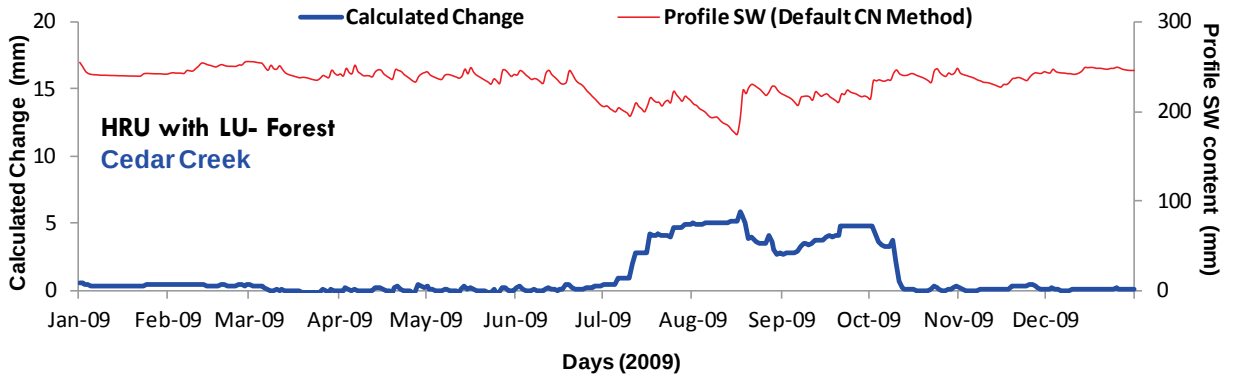

(b)

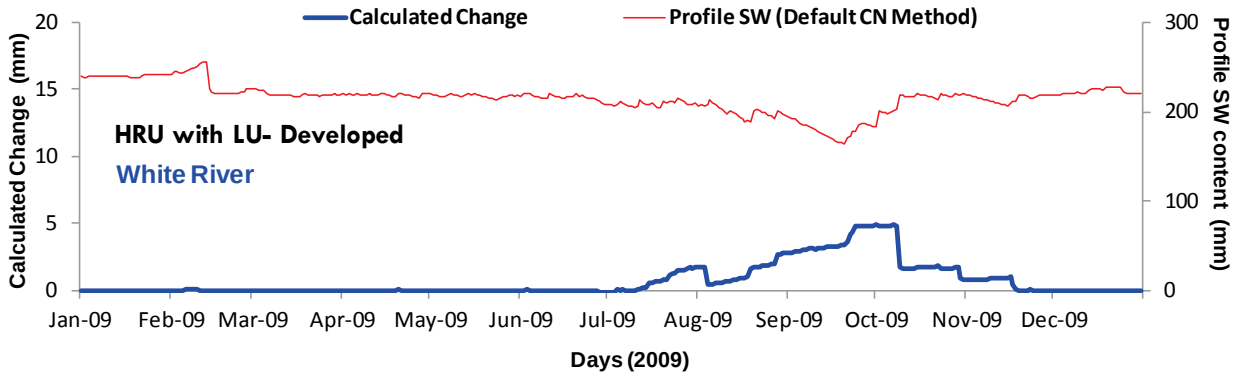

(c)

Figure 3. Area-weighted HRU-average soil profile water content with respective calculated difference (change = SMA method - Conventional Method): (a) agricultural landuse (Cedar Creek), (b) forested landuse (Cedar Creek), (c) developed landuse (White River). Patterns shown here are consistent in individual HRUs of particular LU types, as well as in watershed-scale.

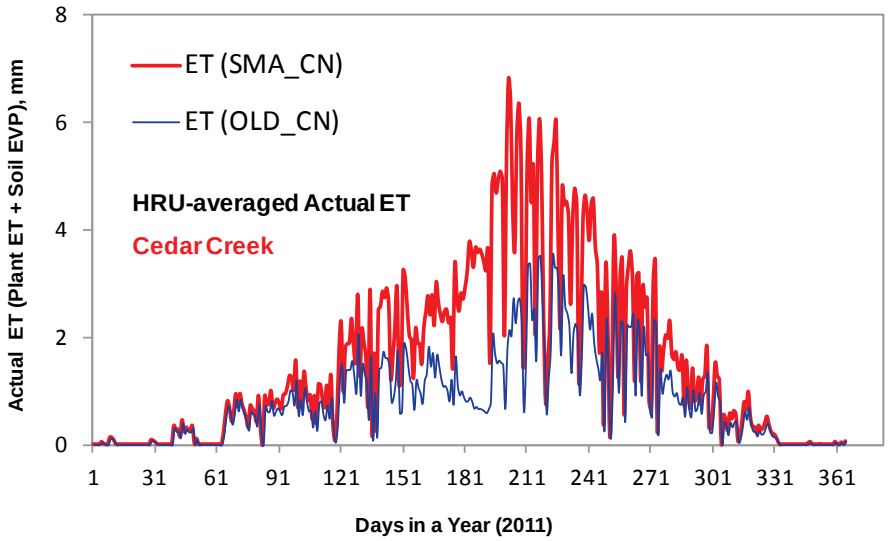

Figure 4. Comparison of HRU-averaged Actual ET by original and SMA-based CN method in Cedar Creek watershed.

Summary and Future Work

In this study, a modified CN method is incorporated into existing SWAT source code which is more realistic from soil moisture accounting standpoint. Some of the structural inconsistencies of the original CN method have also been highlighted focusing onto its application in continuous hydrologic models. Simulation results for individual HRUs reveal lowering of surface runoff with higher soil moisture by the SMA technique compared to the conventional model. The increase in soil moisture along with other related ground water components as resulted from the modified model has found to have been attributed with a higher ET. Importantly, the calculated HRU-level daily net water balance has turned out to be almost same in both cases.

In addition to the major hydrologic components discussed in this study, tracking of additional variables can lead to a better understanding of the underlying processes that are causing the newly incorporated SMA technique to produce different results from SWAT's default CN method. Variables like the canopy storage, potential maximum moisture retention, and actual soil evaporation are likely to become decisive at this stage. Furthermore, vigorous experimentations are necessary for validating the modified SWAT model under heterogeneous scenarios of diverse landuse and soil characteristics, irrigation and tile drainage, cropping pattern, water quality perspective, and climatic change.

References

Carsel, R., J. Imhoff, P. Hummel, J. Cheplick, and A. Donigan. 1997. PRZM 3.1 Users Manual: National Exposure Research Lab, Office of Research and Development, U.S. Environmental Protection Agency: Athens, Georgia.

Choi, J. Y., B. A. Engel, and H. W. Chung. 2002. Daily stream flow modeling and assessment based on the curve number technique. *Hydrological Processes* 16: 3131–3150.

Chung, W. H., I. T. Wang, and R. Y. Wang. 2010. Theory-based SCS-CN method and its applications. *Journal of Hydrologic Engineering* 15(12): 1045-1058.

Durbude, D. G., M. K. Jain, and S. K. Mishra. 2011. Long-term hydrologic simulation using SCS-CN-based improved soil moisture accounting procedure. *Hydrological Processes* 25: 561-579.

Geetha, K., S. K. Mishra, T. I. Eldho, A. K. Rastogi, and R. P. Pandey. 2007. Modification to SCS-CN method for long-term hydrologic simulation. *Journal of Irrigation and Drainage Engineering* 133(5): 475–489.

Harbor, J. M. 1994. A practical method for estimating the impact of land use change on surface runoff, ground water recharge, and wet land hydrology. *Journal of American Planning Association* 60: 95–108.

Hawkins, R. H. 1978. Runoff curve number with varying site moisture. *Journal of Irrigation and Drainage Engineering* 104: 389–398.

Jain, M. K., D. G. Durbude, and S. K. Mishra. 2012. Improved CN-Based Long-Term Hydrologic Simulation Model. *Journal of Hydrologic Engineering* 17(11), 1204–1220.

Kannan, N., C. Santhi, J. R. Williams, and J. G. Arnold. 2008. Development of a continuous soil moisture accounting procedure for curve number methodology and its behaviour with different evapotranspiration methods. *Hydrological Processes* 22: 2114-2121.

Krysanova, V., F. Wechsung, and J. G. Arnold. 2000. SWIM User Manual. Potsdam Institute for Climate Impact Research: Potsdam, Germany.

Michel, C., A. Vazken, and C. Perrin. 2005. Soil conservation service curve number method: how to mend a wrong soil moisture accounting procedure?. *Water Resources Research* 41(2): 1–6.

Mishra, S. K., and V. P. Singh. 2004. Long-term hydrological simulation based on the soil conservation service curve number. *Hydrological Processes* 18: 1291–1313.

Mishra, S. K., V. P. Singh., J. J. Sansalone, and V. Aravamuthan. 2004. A modified SCS-CN method: characterization and testing. *Water Resources Management* 17: 37-68.

Neitsch, S. L., J. G. Arnold, J. R. Kiniry, and J. R. Williams. 2011. Soil and Water Assessment Tool: theoretical documentation, version 2009. Texas Water Resources Institute Technical Report No. 406: Texas A&M University System, College Station, TX, USA.

Sahu, R. K., S. K. Mishra, T. I. Eldho, and M. K. Jain. 2007. An advanced soil moisture accounting procedure for SCS curve number method. *Hydrological Processes* 21: 2827–2881.

Schroeder, P. R, T. S. Dozier, P. A. Zappi, B. M. McEnroe, J. W. Sjostrom, and R. L. Peyton. 1994. *The Hydrologic Evaluation of Landfill Performance (HELP) Model: engineering documentation for version 3*. EPA/600/R- 94/168b, September 1994: U.S. Environmental Protection Agency, Office of Research and Development, Washington, DC.

USDA. 1990. EPIC-Erosion Productivity Impact Calculator 1: model documentation. United States Department of Agriculture (USDA) Technical Bulletin No. 1768: Washington, DC.

USGS-NED. 2013. National Elevation Dataset: United States Geological Survey National Map Viewer. Available at: http://viewer.nationalmap.gov/viewer/. Accessed 10 March, 2013.

USGS-NLCD. 2006. National Land Cover Data Set, 2006: United States Geological Survey National Map Viewer. Available at: http://viewer.nationalmap.gov/viewer/. Accessed 10 March, 2013.

Williams, J. R., N. Kannan, X. Wang, C. Santhi, and J. G. Arnold. 2012. Evolution of the SCS runoff curve number method and its application to continuous runoff simulation. *Journal of Hydrologic Engineering* 17(11), 1221–1229.

Williams, J. R., J. G. Arnold., and R. Srinivasan 2000. The APEX model. BRC report No. 00-06: Texas A & M University System, Temple, TX.

Williams, J. R., C. A. Jones, and P. T. Dyke. 1984. A modeling approach to determining the relationship between erosion and soil productivity. *Trans. ASAE* 27(1), 129–144.

Williams J. R, and V. LaSeur. 1976. Water yield model using SCS curve numbers. *Journal of Hydraulic Engineering* 102: 1241–1253.

Usage of Biofuel to Mitigate the Current Environmental Impact of Aviation

Shine Jude Hamilton Antony
Ecole Nationale De L' Aviation Civile, Toulouse France

Abstract

Aviation biofuel is a biofuel used for aircraft. Aviation biofuel is widely considered by the aviation industry to be one of the primary means by which the industry can reduce its carbon footprint. To Overcome the problems of fuel scarce and rapid increase in fuel cost and also to reduce increasing air pollution due to larger number of Civilian Aircrafts, more improvements have been made by using Bio-fuel blend 20 i.e., purified Jatropha seed oil 20% by volume and Jet A 80%-(HIGHLY PURIFIED KEROSENSE) by volume mixture) for Turbine powered Engines; and the results obtained were good due to significant environmental and economical benefits.

The fuel mixture blend 24 reduces the emissions by Carbon dioxide(80% compared to Jet A), Water Vapour(H_2O),Nitric Oxide(NO) and Nitrogen Oxide(NO_2). It can extend the life of Turbine engine and also be used as a fuel lubricity, additive in Jet A fuel. It results in a slight drop in fuel economy. It can be used in any turbine engines of aircraft and no modification to the engine and fuel system. It is an alternative fuel and provides a domestic renewable energy supply. Jatropha, one source of Potential biofuels, estimated using it could reduce green house gas emissions by up to 85%. The most effective way to decrease a carbon footprint is to decrease the dependence on carbon emitting fuels and to increase the dependence on biofuels. It is found that renewable energy supply fuels is responsible for less Co_2 than fossil fuel generation.

Keywords: Alternative fuels, Biofuel, Biofuel Blend(B_{20}), Jatropha Seed Oil, Jatropha seed oil, Special Pretreatment technology, Methanol, Free fatty acids, emissions, renewable energy, fuel lubricity additive fuel economy.

Environmental Impacts

The contribution of civil air craft – in flights to global Co_2 emissions has been estimated at around 2%. Like all human activities involving combustion, most forms of aviation release carbon dioxide (CO_2) and other greenhouse gases into the Earth's atmosphere, contributing to the acceleration of global warming and (in the case of CO_2) ocean acidification However, in the case of high altitude airlines frequent by the near stratosphere, non-CO_2 altitude-sensitive effects may increase the total impact on anthropogenic (human-made) climate change significantly.

Pollutants Affecting the Atmosphere:

Subsonic aircraft-in-flight contribute to climate change in four ways:

Carbon dioxide (CO_2)

CO_2 emissions from aircraft-in-flight are the most significant and best understood element of aviation's total contribution to climate change. The level and effects of CO_2 emissions are currently believed to be broadly the same regardless of altitude (i.e. they have the same atmospheric effects as ground based emissions). In 1992, emissions of CO_2 from aircraft were estimated at around 2% of all such anthropogenic emissions, and that year the atmospheric concentration of CO_2 attributable to aviation was around 1% of the total anthropogenic increase since the industrial revolution, having accumulated primarily over just the last 50 years.

Oxides of Nitrogen (NO_x)

At the high altitudes flown by large jet airliners around the tropopause, emissions of NO_x are particularly effective in forming ozone (O_3) in the upper troposphere. High altitude (8-13km) NO_x emissions result in greater concentrations of O_3 than surface NO_x emissions, and these in turn have a greater global warming effect. The effect of O_3 concentrations are regional and local (as opposed to CO_2 emissions, which are global).

NO_x emissions also reduce ambient levels of methane, another greenhouse gas, resulting in a climate cooling effect. But this effect does not offset the O_3 forming effect of NO_x

emissions. It is now believed that aircraft sulfur and water emissions in the stratosphere tend to deplete O_3, partially offsetting the NO_x-induced O_3 increases. These effects have not been quantified. This problem does not apply to aircraft that fly lower in the troposphere, such as light aircraft or many commuter aircraft.

Water Vapour (H_2O)

One of the products of burning hydrocarbons in oxygen is water vapour, a greenhouse gas. Water vapour produced by aircraft engines at high altitude, under certain atmospheric conditions, condenses into droplets to form Condensation trails, or contrails. Contrails are visible line clouds that form in cold, humid atmospheres and are thought to have a global warming effect (though one less significant than either CO_2 emissions or NO_x induced effects) SPM-2. Contrails are extremely rare from lower-altitude aircraft, or from propeller-driven aircraft or rotorcraft.

Cirrus clouds have been observed to develop after the persistent formation of contrails and have been found to have a global warming effect over-and-above that of contrail formation alone. There is a degree of scientific uncertainty about the contribution of contrail and cirrus cloud formation to global warming and attempts to estimate aviation's overall climate change contribution do not tend to include its effects on cirrus cloud enhancement.

Particulates

Least significant is the release of soot and sulfate particles. Soot absorbs heat and has a warming effect; sulfate particles reflect radiation and have a small cooling effect. In addition, they can influence the formation and properties of clouds. All aircraft powered by combustion will release some amount of soot.

Reducing Environmental Impact of Aviation

Aviation biofuel is widely considered by the aviation industry to be one of the primary means by which the industry can reduce its carbon foot print.

Currently aviation represents 2% of global emissions, but is expected to grow to 3% by 2050.

Jatropha, one source of Potential biofuels, estimated using its could reduce green house gas emissions by up to 85%. Biofuel do not contain sulfur compounds and thus do not emit sulfur dioxide.

The most effective way to decrease a carbon footprint is to decrease the dependence on carbon emitting fuels and to increase the dependence on biofuels. It is found that renewable energy supply fuels is responsible for less Co_2 than fossil fuel generation.

In addition to increase market advantage and differentiation eco efficiency can also help to reduce costs where alternative energy system.

By developing technological solutions to reduce carbon emissions such as innovative air craft design or commercially viable and truly sustainable alternative fuels.

By using a biofuel demonstration with boeing during 2008 and this was a world first flight using biofuel by a commercial airline.

Year	Airline	Aircraft	Biofuel	Blend
Dec 2008	Air New Zealand	Boeing 747	Jatropha	successfully completed on 30 December 2008. The engine was then removed to be scrutinised and studied to identify any differences between the Jatropha blend and regular Jet

				A1. No effects to performances were found.
Nov 2010	TAM	Airbus 320	Jatropha	A 50⁄50 biofuel blend of conventional and jatropha oil
Oct 2011	Air China	Boeing 747-400	Jatropha	Air China flew China's first flight using aviationbiofuels. The flight was conducted using Chinese grown jatropha oil from PetroChina.
Jul 2011	Interjet	Airbus A 321	Jatropha	Flight was powered by 27% jatropha between Mexico City and Tuxtla
Aug 2011	Air Mexico	Boeing 777-200	Jatropha	Air mexico flew the world's first trans-Atlantic revenue flight, from Mexico City to Madrid with passengers

Materials and Methods

It is significant to point out that, the non-edible vegetable oil of Jatrophacarcus has the requisite potential of providing a commercially viable alternative to Jet A fuel, since it has desirable physio chemical and performance characteristics comparable to Jet A. The comparison of properties of Jatropha oil and standard specifications of Jet A are shown in Table I

Table I

Specification	Standard specification of Jatropha oil	Standard specification of Jet Fuel A
Specific gravity	0.91	0.74-0.84
Flashpoint	110°c	>60°c
Carbon residue	0.64	0.1 to over 30%
Cetane value	51	40-50
Distillation point	295°c	176°c
Kinematic Viscosity	50.73 cs	7.9 cs
Sulphur %	0.13%	0.25%
Calorific Value	9470 kcal/kg	10400 kcal/kg
Fuel Freezing Point for Jet A	2°c	-40°c

Experiments were conducted using the above blend on different Aero engines and finally the result obtained by using the blend mixture B20 was some what good due to significant environmental benefits and also results in a slight drop in fuel economy.

JATROPHA PLANT WITH FRUITS

JATROPHA SEED AND OIL

Analysis of the Jatropha seed shown following chemical composition

TABLE II

Moisture	6.20%
Protein	18.00%
Fat	38.00%
Carbohydrates	17.00%
Fiber	15.50%
Ash	5.30%
Oil Content	33-40%
Saponification Value	Very High

The Jatropha seeds are dried thoroughly and then by using Rotary oil extractor, the oil is being extracted, then the oils and fats are filtered and pre-processed to remove water and contaminants. If free fatty acids are present, they can be removed in to bio fuel using special pretreatment technologies, for every 3 kg of seeds, 1kg of oil will be extracted. The pretreated oils and fats are

then mixed with methanol and NaOH used as a catalyst. The Oil molecules are broken reformed in to methylesters and glycerol, which are then separated from each and purified.

The purified oil named as Biofuel refers to the pure fuel before blending with Jet A fuel. Finally 20% of volume of pure fuel of Biofuel mixed with 80% by volume of Jet A fuel and named as biofuel blend B20.

Results and Discussions

Jatropha, one source of Potential biofuels, estimated using it could reduce green house gas emissions by up to 85%. The most effective way to decrease a carbon footprint is to decrease the dependence on carbon emitting fuels and to increase the dependence on biofuels. It is found that renewable energy supply fuels is responsible for less Co_2 than fossil fuel generation.

Using Biofuel mixed as blend with Jet A fuel and bio fuel blends are denoted as 'BXX' with 'XX' representing the percentage of biofuel contained in the blend as follows

Name of Blend	% of Biofuel(Purified Jatropha seed oil) by volume	% of Jet A by volume
B_{10}	10	90
B_{15}	15	85
B_{20}	20	80
B_{25}	25	75
B_{30}	30	70

Conclusion

To overcome the problems of fuel scarce and rapid increase in fuel cost and also to reduce increasing air pollution due to large number of aircraft, more improvements have been made by using Biofuel blend 20 purified Jatropha seed oil 20% by volume and Jet A 80% by volume mixture for Turbine engines; and the results obtained were good due to significant environmental and economic benefits.

The fuel mixture blend 20 reduces the emissions by carbon monoxide, carbon dioxide (75% compared to Jet A fuel), Nitrous Oxide and Sulphur dioxide.

It can extend the life of turbine engines and also it results in a slight drop in fuel economy.

It can be used in any turbine engines of aircraft and no modification to the engine and fuel systems.

It is an alternative fuel and provides a domestic renewable energy supply.

References

1. IPCC Special Report on Aviation Global Emissions
2. "Renewable and Alternative Energy Fact Sheet". *Agricultural Research and Cooperative Extension*. Penn State College of Agricultural Science. Retrieved March 7, 2012.
3. "Technical Report: Near-Term Feasibility of Alternative Jet Fuels". Sponsored by the FAA. Authored by MIT staff. Published by RAND Corporation. Retrieved August 22, 2012.
4. "Biodiesel FAQ". University of Kentucky College of Agriculture. 2006. Retrieved August 22, 2012.
5. IATA Fact Sheet: Alternative Fuels
6. Morris, John (2010-06-07). "EADS Sets First Public Algae-Biofuel Flight At ILA Berlin". Aviation Week. Retrieved 2010-07-12.
7. Hilkevitch, Jon (November 11, 2011). "Continental Airlines flight is first in U.S. to use biofuel". *LA Times*. Retrieved April 16, 2012.
8. "Alaska Airlines Launching Biofuel-Powered Commercial Service In The United States"

SWATing your APEX model: a how-to from the trenches

Claire Baffaut, PhD*

USDA-ARS-CSWQRU, 241 Agricultural Engineering Building, University of Missouri, Columbia, MO 65211, USA, claire.baffaut@ars.usda.gov.

Carl Bolster, PhD

USDA-ARS-AWMRU, 230 Bennett Lane, Bowling Green, KY 42104, USA.

Nathan Nelson, PhD

Kansas State University, Agronomy Department, 2708 Throckmorton Plant Sciences Center, Manhattan, KS 66506-5501, USA.

Mike van Liew, PhD

University of Nebraska, 229 L.W. Chase Hall, PO Box 830726, Lincoln, NE 68583-0726, USA.

Jeff Arnold, PhD

USDA-ARS-GSWRL, 808 East Blackland Road, Temple, TX 76502, USA.

Jimmy Williams, PhD

Temple Research and Extension Center (Texas A&M AgriLife Research), 720 East Blackland Road, Temple, TX 76502, USA.

Abstract

Methodologies to link edge-of-field observations to stream loadings need to be developed to integrate what we know of soil and water quality at the field scale to watersheds and river basins. The Soil and Water Assessment Tool (SWAT) can be used to scale up results obtained at the field scale with the Agricultural Policy Environmental eXtender (APEX). The APEX and SWAT models are particularly well adapted to this integration because they belong to the same family of models and have many common input parameters. However, they are not identical and the differences need to be recognized before both models can be used jointly. For example, while runoff can be calculated with the Curve Number method in both models, calculation of the soil water retention parameter is different and leads to different curve numbers, and thus runoff. Similarly, both models can use the MUSLE equation to calculate sediment loss but the equations used to calculate peak runoff rate differ. This paper reviews some differences in algorithm and parameterization between APEX and SWAT. Since APEX parameterization is more flexible, we define how it can be parameterized so that it becomes equivalent to SWAT, whenever possible. Differences were identified in how APEX and SWAT calculate runoff, potential evapotranspiration, peak runoff rate, harvest index, and transfer between the phosphorus pools. When parameterization does not take these differences into account, the models do result in different values of output variables. This analysis will help model users separate the model effects from true scale effects when parameterizing these models, and interpreting their results.

Keywords: APEX, SWAT, parameterization.

Introduction

Methodologies to link edge-of-field observations to stream loadings need to be developed to integrate what we know of soil and water quality at the field scale to watersheds and river basins. The Soil and Water Assessment Tool (SWAT, Gassman et al., 2007) can be used to scale up results obtained at the field scale with the Agricultural Policy Environmental eXtender (APEX, Gassman et al., 2010). The APEX and SWAT models are particularly well adapted to this integration because they belong to the same family of models and have many common input parameters. APEX provides a higher degree of computation, and the ability to simulate processes that are not so well simulated in SWAT. For example, APEX can be used to assess the effect of management practices for which landscape position is an important factor or the effect of climate change on weed competition. SWAT can then be used to upscale these results to a larger scale, taking into account other land uses in the watershed, and the transport processes that occur in the stream network.

This combination of models was used to estimate the effects of farm level conservation practices simulated with APEX to watershed scale and ultimately for the Mississippi River Basin (Wang et al., 2006, 2011) for the Conservation Effects Assessment Program (USDA-NRCS, 2012). In these studies, APEX was validated separately for cropland before being incorporated into the SWAT model, with SWAT parameters then calibrated independently without further adjustment of the APEX parameters. Given the similarities between both models, model users may be tempted to link and calibrate them together with watershed scale data, especially when field scale data are not available. Doing so requires consistency in the processes and the parameterization of APEX and SWAT so that all subareas (APEX) and hydrologic response units (HRU) are treated in the same way. Essentially, parameterization is needed to produce similar results. If not, a bias between land simulated with APEX and with SWAT will be introduced, which may affect model calibration and interpretation of the results.

The objectives of this paper were to 1) review how primary processes are simulated with SWAT and APEX and identify significant differences, 2) describe how to parameterize APEX to make it as consistent as possible with SWAT, and 3) describe the impact of differences in process equations on output variables. We examined the equations and parameters for selected processes: runoff generation, snowmelt, potential evapotranspiration, peak runoff rate and phosphorus transformations in the soil. Sources of information included the SWAT2009 (Neitsch et al., 2011) and APEX0806 (Williams et al., 2012) theoretical documentations as well as the respective Fortran codes. Equation numbers indicated herein are the same as in these documentations. Whenever possible, we provided suggestions for parameterizing APEX and make it equivalent to SWAT. When equations were taken out of the code instead of the manual, independent equation numbers were given.

Runoff generation

Both APEX and SWAT provide the same two options for calculating surface runoff: the SCS curve number method and the Green and Ampt infiltration equation. With the curve number method, both models use the same equation for calculating runoff volume and for calculating the curve number (CN) for dry (CN1) and wet (CN3) conditions based on CN2 values. APEX

provides the option of deterministically estimating CN as a function land use, soil hydrologic group, soil water content or potential evapotranspiration (PET), and possible frozen conditions. Alternatively, the model provides the option of stochastically varying this deterministic value within ± 5 units using a triangular distribution to represent factors that can affect runoff but are not taken into account by the model. The first option (deterministic value) should be selected to be equivalent to the adjustments of CN in SWAT. One should refer to the table of land use numbers in the APEX theoretical documentation to assign a value in the SWAT model.

Both models have an option for allowing the soil water retention parameter to vary with accumulated plant evapotranspiration or with soil water content. With the plant evapotranspiration method, the APEX curve number index coefficient (*parm 42)* and the SWAT plant ET curve number coefficient *(cncoef)* should have the same value. With the soil water content method, the assumptions to calculate the two coefficients of the S-curve that calculate retention as a function of soil water content are slightly different. While APEX uses average moisture conditions (CN2) and wet conditions (CN3) as the two points that define the curve, SWAT uses wet conditions and saturation. In addition, the wet conditions status is defined by field capacity in SWAT and by the user in APEX. As a result, the curves that define retention as a function of soil water content can be close but not identical (fig. 1). Finally, APEX and SWAT use two different dependent variables to calculate the retention parameter: SWAT uses the plant available water, i.e., the soil water of the soil profile excluding water held at the wilting point and APEX uses the ratio of plant available water by water held at field capacity excluding water held at the wilting point (FCC, table 1).

Table 1. Differences in how SWAT and APEX calculate soil water retention using soil water content.

	SWAT	*APEX*
Variable used to calculate retention	Soil water – wilting point	FCC = $\frac{soil\ water - wilting\ point}{Field\ capacity - wilting\ point}$
Points used to define the S-shape curve	Wet conditions Saturation	Average conditions (CN2) Wet conditions (CN3)
Definition of wet conditions	Field capacity (CN3)	A user-defined point between field capacity and saturation

The two soil water contents defined in the APEX parameter file, corresponding to average and wet moisture conditions, give the flexibility to match the SWAT definition of the curve. However, the values of these two water contents vary with the curve number, and with field capacity and saturation level, which are functions of clay content and bulk density and have to be determined on a case-by-case basis. Since a complete match is impossible, the user may have to choose between a good match at low or high water contents (fig. 1). Given these discrepancies, users who want similar calculations of soil water retention in SWAT and APEX should select the accumulated plant evapotranspiration method and ensure that *parm42* in APEX and *cncoef* in SWAT are the same.

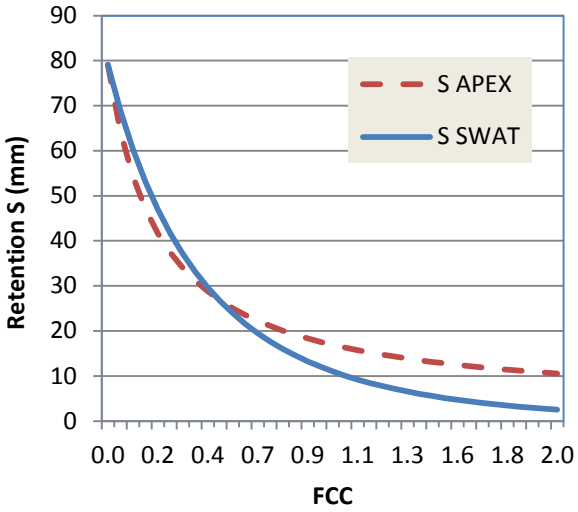

Figure 1. Retention parameter as a function of FCC, as calculated by SWAT and APEX for a hypothetical soil with CN2 = 89, a bulk density of 1.4 g cm^{-3}, and 20% clay content. FCC is the ratio of available water to field capacity excluding water held at wilting point.

Finally, APEX adjusts CN to account for slopes greater or less than 5%. SWAT does not make this modification and the adjustment must be made prior to specifying the CN value. It should be noted that the equation presented in the SWAT manual for adjusting CN for slope is not the same as the equation used in APEX. In order to make APEX and SWAT parameterization equivalent, one should use the equation used in APEX to manually adjust the retention parameter with slope before entering its value as a SWAT input.

Runoff during frozen conditions

Equations used to modify the retention parameter S for frozen slopes are different for the two models. Frozen conditions exist when the first soil layer is frozen, i.e. temperature less than -1.0 ^{o}C in the soil layer below the top 10 mm. In these conditions:

- APEX calculates the retention as a fraction of that calculated during unfrozen conditions. The fraction is specified by the user in the parameter file (*parm 22*) and has a default value of 0.1.
- SWAT calculates the frozen soil retention parameter as:

$$S_{frz} = S_{max}[1 - \exp(-cnfroz\_bsn * S)] \quad [2:1.1.10]$$

where S_{frz} is the retention parameter adjusted from frozen soils, S_{max} is the maximum possible retention on any given day, cnfroz_bsn is a user-specified coefficient with a default value of 0.000862, and S is the retention parameter calculated as a function of soil water content or PET.

Both reduce retention by a considerable amount in the range of values typical of crop land. When the fraction is one tenth (the default fraction in APEX) and for CN2 in the 75-85 range, these equations result in comparable retention amounts; for lower values of CN typical of well drained crop land and forest or range landuse, SWAT produces higher retention values than APEX. Conversely, APEX produces slightly higher retention values when CN2 is above 90. By

adjusting both the fraction of retention in APEX and the frozen soil coefficient in SWAT as proposed in table 2, one can obtain similar results for a limited range of CN values.

Table 2. Adjustment of the APEX fraction of retention and the SWAT frozen soil coefficient to obtain similar values of retention reduction as a function of the curve number.

CN	*APEX fraction of retention*	*SWAT cnfroz_bsn*
35	0.5	0.00040
40	0.5	0.00060
50	0.4	0.00740
60	0.3	0.00862
70	0.2	0.00862
80	0.1	0.00862
90	0.05	0.00862

With the Green and Ampt method, each model uses a different equation. APEX uses a form that utilizes the CN retention parameter and the saturated hydraulic conductivity whereas SWAT uses a form that includes wetting front matric potential, change in volumetric moisture content across the wetting front, and effective hydraulic conductivity calculated from the saturated hydraulic conductivity and CN. Impacts of these differences would depend on all these parameters and have not been investigated.

Potential evapotranspiration

SWAT provides three options for calculating potential evapotranspiration (Hargreaves, Priestly-Taylor, and Penman-Monteith), whereas APEX offers five options (Hargreaves, Penman, Penman-Monteith, Priestley-Taylor, and Bair-Robertson). Although the Hargreaves, Penman-Monteith, and Priestly-Taylor methods are available in both SWAT and APEX for calculating PET, some important differences exist in how these methods are implemented. We describe below the differences for Hargreaves and Priestley-Taylor.

Hargreaves Method

SWAT uses an unmodified version of the 1985 Hargreaves PET equation:

$$PET = 0.0023 * \frac{H_0}{\lambda} * (T_{av} + 17.8) * (T_{mx} - T_{mn})^{0.5} \quad [2:2.2.24]$$

$$\lambda = 2.501 - 0.00236 * T_{av} \quad [1:2.3.6]$$

where PET is in mm/day, λ is latent heat of vaporization (MJ kg^{-1}), H_0 is extraterrestrial radiation (MJ m^{-2} day^{-1}), T_{av} is average daily air temperature (ºC), T_{mx} is maximum daily air temperature (ºC), and T_{mn} is minimum daily air temperature (ºC). H_0 is calculated as:

$$H_0 = 37.59 E_0 [\omega T_{sr} sin\delta\ sin\phi + cosin\delta\ cosin\phi \sin(\omega T_{sr})] \quad [1:1.2.6]$$

$$E_0 = 1 + 0.033 \cos\left(\frac{2\pi d_n}{365}\right) \quad [1:1.1.1]$$

$$\delta = sin^{-1}\left\{0.4 sin\left[\frac{2\pi}{365}(d_n - 82)\right]\right\} \quad [1:1.1.2]$$

$$T_{sr} = \frac{cos^{-1}(-tan\delta\ tan\phi)}{\omega} \quad [1:1.1.4]$$

where E_0 is the eccentricity correction factor of the earth's orbit, ω is the angular velocity of the earth's rotation (0.2618 rad h^{-1}), T_{sr} is the hour of sunrise, δ is the solar declination in radians, ϕ is the geographic latitude in radians, and d_n is day of year (starting on 1 January). Equation 1:1.1.4 is only used for latitudes between 66.5° and -66.5°. For extreme latitudes, there is no sunrise in winter (Tsr = 0) and Tsr = π/ω in summer.

APEX uses a modified version of the 1985 Hargreaves equation in which the exponent and the coefficient are 0.0032 and 0.6 instead of 0.0023 and 0.5, though these coefficients can be adjusted back setting *parm* 23 to 0.0023 and *parm* 34 to 0.5. However, APEX uses the maximum daily radiation at the earth's surface H_{mx} (Eq. 15 in APEX and 1:1.2.7 in SWAT, see below) instead of the extraterrestrial radiation H_0 (Eq. 97), and the latent heat of vaporization λ is slightly different (Eqs[1:2.3.6] and 93c).

$$PET = 0.0032 * \left(\frac{H_{mx}}{\lambda}\right) * (T_{av} + 17.8) * (T_{mx} - T_{mn})^{0.6} \quad [97]$$

$$\lambda = 2.501 - 0.0022 * T_{av} \quad [93c]$$

$$H_{mx} = 30 * E_0[\omega T_{sr} sin\delta\ sin\phi + cos\delta\ cos\phi \sin(\omega T_{sr})] \quad [15]$$

Differences in how SWAT and APEX calculate PET using the Hargreaves method were investigated by calculating PET using temperature data collected from the Kentucky Mesonet site located at Western Kentucky University's experimental farm located in Bowling Green, KY (latitude of 36.93°, fig. 2).

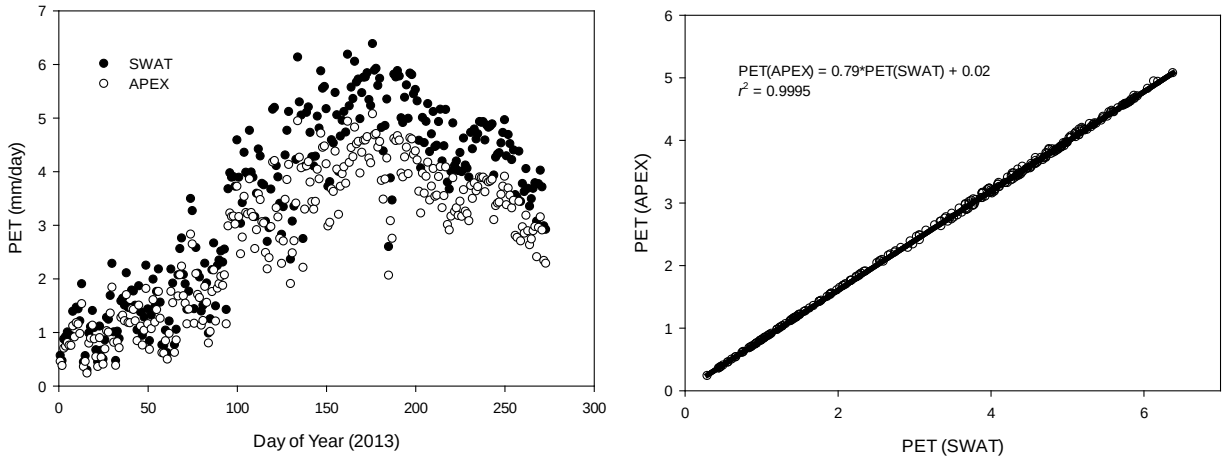

Figure 2. Potential evapotranspiration rates calculated by the Hargreaves method using the equations used in the SWAT and APEX models for Bowling Green, KY from 1 January 2013 to 30 September 2013. APEX *parm 23* was set to 0.0023 and *parm 34* was set to 0.5.

When the coefficient and exponent in the Hargreaves equation are set to 0.0023 and 0.5, respectively, PET calculated by SWAT was about 20% higher than with APEX. Under these conditions the only difference is the different radiation used by the two models. If we use H_{mx} (eq. 1:1.2.7, see below) instead of H_0 (eq. 1:1.2.6) when calculating PET in SWAT (eq. 2:2.2.24), the two models produce essentially identical PET values. If the coefficient and exponents were set to 0.0032 and 0.6, Hargreaves PET values calculated with APEX would be 40 % higher than with SWAT.

Priestley-Taylor Method

For calculating PET using the Priestly-Taylor method, SWAT uses the following equations:

$$PET = \frac{1.28}{\lambda} * \frac{\Delta}{\Delta+\gamma}(H_{net} - G) \quad [2:2.2.23]$$

$$\Delta = \frac{4098*e^0}{(T_{av}+237.3)^2} \quad [1:2.3.4]$$

$$e^0 = exp\left[\frac{16.78*T_{av}-116.9}{T_{av}+237.3}\right] \quad [1:2.3.2]$$

$$\gamma = \frac{c_p*P}{0.622*\lambda} \quad [1:2.3.7]$$

$$P = 101.3 - 0.01152 * EL + 0.544 * 10^{-6} * EL^2 \quad [1:2.3.8]$$

$$H_{net} = (1-\alpha) * H_{day} + H_b \quad [1:1.2.12]$$

$$H_b = -\left[a * \frac{H_{day}}{H_{mx}} - b\right] * \left[a_1 + b_1\sqrt{R_h * e^0}\right] * \sigma * T_K^4 \quad [1:1.2.22]$$

$$H_{mx} = 30 * E_0[\omega T_{sr} sin\delta\ sin\phi + cos\delta\ cos\phi \sin(\omega T_{sr})] \quad [1:1.2.7]$$

where Δ is the slope of the saturation vapor pressure-temperature curve (kPa C^{-1}), e^0 is the daily saturation vapor pressure (kPa), γ is the psychrometric constant (kPa C^{-1}), c_p is the specific heat of moist air at constant pressure ($1.013*10^{-3}$ MJ kg^{-1} C^{-1}), *P* is atmospheric pressure (kPa), *EL* is elevation (m), H_{net} is net radiation (MJ m^{-2} d^{-1}), *G* is the heat flux density to the ground surface (MJ m^{-2} d^{-1}) and is set to zero for daily heat flux calculations, H_{day} is short-wave solar radiation reaching the ground surface (MJ m^{-2} d^{-1}), H_b is net incoming long-wave radiation (MJ m^{-2} d^{-1}), α is albedo, H_{mx} is maximum possible solar radiation reaching the ground surface (MJ m^{-2} d^{-1}), R_h is relative humidity, σ is the Stefan-Boltzmann constant (4.903×10^{-9} MJ m^{-2} K^{-4} d^{-1}) and *a*, *b*, a_1, and b_1 are constants with default values of 0.9, -0.1, 0.34, and -0.139, respectively.

The APEX model uses the following equations:

$$PET = \frac{1.28}{\lambda} * \frac{\Delta}{\Delta+\gamma} * H_{net} * (1 - AB) \quad [96]$$

$$H_{net} = H_{day} * (1 - AB) - RBO * (0.9 * \frac{H_{day}}{H_{mx}} + 0.1) \quad [93a]$$

$$\Delta = \frac{e^0}{TK} * (\frac{6790.5}{TK} - 5.029) \quad [93b]$$

$$\gamma = 6.595 * 10^{-4} * P \quad [93d]$$

$$P = 101.3 * EL * (0.01152 - 5.44 * 10^{-7} * EL) \quad [93e]$$

$$RBO = \left(0.34 - 0.14 * \sqrt{e^0 * R_h}\right) * 4.9 * 10^{-9} * TK^4 \quad [93g]$$

$$e^0 = 0.1 * exp * \left(54.879 - 5.029 * \ln(TK) - \frac{6790.5}{TK}\right) \quad [93i]$$

where *AB* is albedo, TK is mean daily air temperature (K), and *RBO* is net outgoing long-wave radiation (MJ m^{-2} d^{-1}).

Rearranging the above equations shows more clearly their similarities and differences. The Priestly-Taylor method in SWAT can be simplified to the following:

$$PET = \frac{1.28}{\lambda} * \frac{\Delta}{\Delta + \gamma} * H_{net}$$

$$H_{net} = (1 - \alpha) * H_{day} - (0.34 - 0.14 * \sqrt{e^0 * R_h}) * \left(0.9 * \frac{H_{day}}{H_{mx}} + 0.1\right) * 4.9x10^{-9} * TK^4$$

Rearranging the Priestly-Taylor method in APEX and using the same variables used in SWAT yields:

$$PET = \frac{1.28}{\lambda} * \frac{\Delta}{\Delta + \gamma} * H_{net} * (1 - \alpha)$$

$$H_{net} = (1 - \alpha) * H_{day} - (0.34 - 0.14 * \sqrt{e^0 * R_h}) * \left(0.9 * \frac{H_{day}}{H_{mx}} + 0.1\right) * 4.9x10^{-9} * TK^4$$

Minor differences exist in calculating most of the variables. The models do calculate the psychrometric constant γ differently. With SWAT, γ explicitly includes the latent heat of vaporization λ in its calculation (Eq. 1:2.3.7), and therefore varies with temperature whereas it is temperature independent in APEX (Eq. 93d). This can lead to slight differences between the models depending on air temperature, typically less than 5% for air temperatures below 40 ^{o}C. The major difference between the two models is that the APEX model accounts for albedo twice by including it in Eq. 96 when calculating PET and in Eq. 93a to calculate net radiation. As a result, APEX PET values are 80 % of the values calculated with SWAT when albedo is set to 0.2 (fig. 3). Important differences also exist in how the two models calculate albedo.

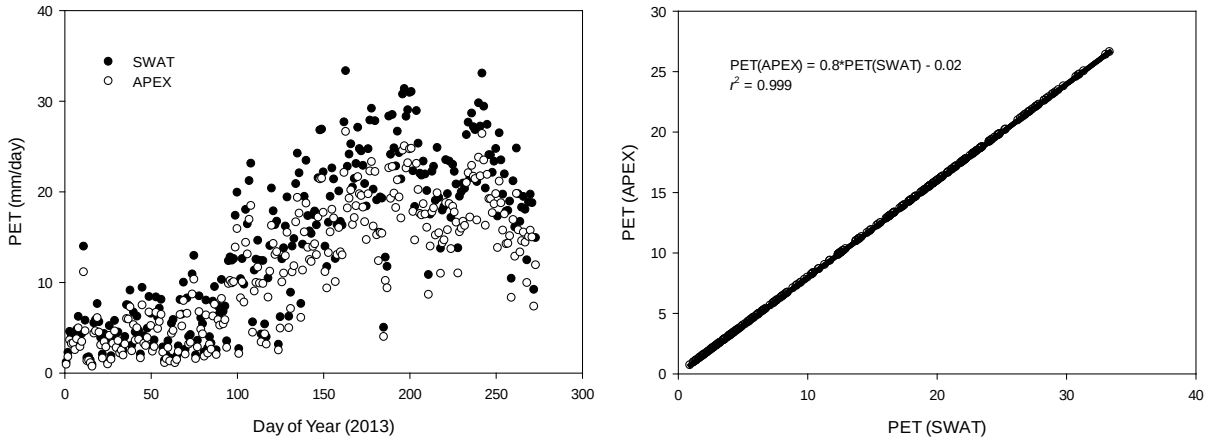

Figure 3. Potential evapotranspiration rates calculated by the Priestley-Taylor method using the SWAT and APEX models for Bowling Green, KY from 1 January 2013 to 30 September 2013. Albedo was set at 0.2.

Determination of peak flow rate

The common method for sediment loss calculation is to use MUSLE, with the peak flow rate being estimated with the modified rational formula and a stochastic element. While other choices are possible with APEX, this is the method that APEX and SWAT have in common. It requires estimation of the time of concentration and of the event ½ hour rainfall. Regarding time of concentration, the overland flow time of concentration is similar. For the channel flow time of

concentration, APEX and SWAT use the same equation, albeit with different coefficients (0.62 for SWAT and 1.75 for APEX). We have neither investigated the reason for these different values nor their impact.

Half-hour rainfall amounts are a function of the maximum monthly half-hour rainfall, included in the climate file and defined in both cases by the user. There is a difference in how SWAT and APEX estimate the average monthly ½ hour fraction of rainfall. APEX uses Eq. 1:

$$alp_{.5,mon}=APM\left(\frac{-RFV_{.5u,mon}}{\mu_{month}*\ln\left(\frac{0.5}{NY*NWD_{month}}\right)}\right) \quad (1)$$

where APM is an adjustment factor specified in the site file, $RFV_{.5u,mon}$ is the maximum ½ hour rainfall for the month (user input), μ_{month} is the mean event rainfall amount for the month, NY is the number of years in the rainfall record used to estimate the maximum ½ hour rainfall, and NWD_{month} is the average number of wet days for the month.

On the other hand, SWAT uses Eq.1:3.2.2:

$$alp_{.5,mon}= adj_{0.5\propto}\left(1-exp\left[\frac{R_{0.5\ sm(mon)}}{\mu_{month}*ln\left(\frac{0.5}{NY*NWD_{month}}\right)}\right]\right) \quad [1:3.2.2]$$

where $adj_{0.5\alpha}$ is a user specified adjustment factor for the peak runoff rate and $R_{0.5\ sm(mon)}$ is the smoothed maximum ½ hour rainfall for the specified month. The smoothed maximum ½ hour rainfall is the arithmetic average of the extreme maximum ½ hour rainfall (user input) for the specified month, the preceding one and the following one. These two different equations, as well as the use of a smoothed maximum ½ hour rainfall in SWAT result in significant differences in the mean value of the ½ hour rainfall.

Harvest index adjustment as a function of water stress

When plants are stressed by a lack of water, both models calculate the corresponding reduction on crop yield by adjusting the harvest index. Both SWAT and APEX use a similar equation to calculate the adjustment: Eq. 5:3.3.1 (SWAT) and 282 (APEX).

$$HI_{act} = (HI - HI_{min}) \cdot F + HI_{min} \quad [5:3.3.1 \text{ and } 282]$$

However in SWAT, F is calculated as a function of the water deficiency factor γ_{wu}: ratio of accumulated actual evapotranspiration to accumulated PET (Eq. 5:3.3.1b]. In APEX, the theoretical documentation and the code show that it is calculated as a function of the accumulated plant water use between heat unit index of 0.5 and 1 (SWH).

$$F = \frac{\gamma_{wu}}{\gamma_{wu}+\exp[6.13-0.883\cdot\gamma_{wu}]} \quad [5:3.3.1b]$$

$$F = \frac{SWH}{SWH+\exp[5.563-0.03155\cdot SWH]} \quad [282a]$$

Fluxes between the phosphorus pools

Both APEX and SWAT use the three-pool model developed by Jones et al. (1984) to track inorganic (mineral) phosphorus in the soil: the labile or soluble pool contains P that can be readily absorbed by plants; the active pool is in relatively fast equilibrium with the soluble pool; and the stable pool is in a slow equilibrium with the active pool. In both models, the

concentration of soluble P in runoff is directly proportional to the soluble pool and the P fluxes between the pools are functions of soil parameters and P content. However, the equations are again slightly different and not completely reconcilable.

Soluble P in runoff

SWAT computes dissolved P losses in runoff as a function of the soluble P pool and a linear partitioning coefficient (*PHOSKD*). APEX provides the option of a linear partitioning coefficient similar to SWAT or the Langmuir equation. To set APEX equivalent to SWAT, select the linear partitioning method and set *parm* 8 = PHOSKD.

Flux between the soluble and active pools

In SWAT, the rate of transfer between the soluble and active mineral pools is a function of the phosphorus sorption coefficient (*psp*), also called the P availability index:

$$rto = psp / (1.- psp) \quad (2)$$

$$rmn = (sol\_solp - sol\_actp * rto) \quad (3)$$

if ($rmn > 0.$) $f = rmn * 0.1$ [3:2.3.2]

if ($rmn < 0.$) $f = rmn * 0.6$ [3:2.3.3]

where *rto* determines the size of the soluble pool (*sol_solp*) relative to the active P pool (*sol_actp*) at equilibrium, *rmn* is the difference between the soluble pool at any given time and the soluble pool at equilibrium (or imbalance in *sol_solp*), and *f* is daily flux, or P amount transferred from soluble to active, *f* is added to active P and subtracted from soluble P. As shown from these equations, the rate of flow from active to soluble is six times faster than it is from solution to active. Finally, the rate of flow has a maximum value set to the amount of P in the soluble pool.

In APEX, the APEX0806 code shows that the rate of flow between the soluble and active pools is the same for each transfer direction. In addition, that rate is a function of *rmn* and a user input parameter, *parm 84*.

$$f= rmn * parm\ 84 \quad (4)$$

In order to make APEX similar to SWAT, we recommend setting *parm 84* to 0.1. This makes equation (4) similar to equation (3:2.3.2), and is what was recommended in the original paper on phosphorus cycling and transport by Jones et al. (1984). This translates to a rate of P fixation similar to that in SWAT when fertilizer is added, but slower release of phosphorus from the active pool for plant uptake or after P has been removed by runoff.

However, APEX defines *rto* slightly differently: the size of the soluble pool at equilibrium has an upper bound of 80% of the active pool (equation 5).

$$rto = \min [0.8, psp / (1.- psp)] \quad (5)$$

Although *psp* can be a user input in APEX, equation (5) effectively limits *psp* to 0.44. Thus, if *psp* is greater than 0.44, phosphorus transport calculated with SWAT is likely to be greater than with APEX. For values of *psp* equal or less than 0.44, results will be more similar as the only difference rests with the coefficient used to adjust the rate of transfer from labile to active.

Flux between the stable and active pools

In both models, the rate of transfer from active to stable is based on the assumption that the two pools are in slow equilibrium and that the stable mineral pool is 4 times the size of the active pool. In SWAT, the movement of phosphorus between these two pools is governed by:

$$roc = bk * (4.*sol\_actp - sol\_stap) \quad [3:2.3.4]$$

In APEX, the equation is slightly different:

$$roc = parm\ 85 * bk * (4.*sol\_actp - sol\_stap) \quad (6)$$

Differences emerge in the definition of *bk*. In APEX, *bk* is based on the calcareous and weathering characteristics of the soil, including *psp*. It will range from 0.0002 to 0.0008. In SWAT, *bk* changes only with the direction of the transfer. When the flux is from the active to the stable pool, *bk* is set to 0.0006. When the flux goes from the stable to the active pool, *bk* is $1/10^{th}$ of that. Thus, it is not possible to reconcile the two formulations. Setting *parm 85* to 1 is consistent with the original expression of the equation by Jones et al. (1984). With *parm 85* set to 1, differences in P flux between stable and active pools will likely have negligible impacts on P loss due to the very slow rates of transfer between these pools.

The recommendations for *parm 84* (0.1) and *parm 85* (1) produce equivalent equations when P additions are greater than P removal (e.g., manure applications or P fertilization system). The soluble pool is then larger than at equilibrium and there is P transfer from soluble to active. The active pool is then greater than at equilibrium and there is P transfer active to stable. The caveat is that *psp* in APEX is effectively limited to 0.44. Additionally, these recommended settings are greater than the APEX range for these parameters (0.0001 to 0.001). It is not clear why the APEX documentation has such low ranges.

Conclusion

The use of APEX and SWAT in combination is appealing to study scaling problems between field and watershed. Both models are based on similar theoretical concepts and equations but subtle differences exist in how the equations were implemented in each. These differences can result in discrepancies in model output and different parameterizations. One should be aware of these differences and the need to calibrate each model separately using separate data sets. This paper constitutes the beginning of an inventory of the differences that exist between these two commonly used models. In some cases, these differences can be resolved by careful parameterization of the selected options and model parameters. In others, the differences cannot be resolved and may result in significant discrepancies in the values of output variables calculated by each model.

Significant differences were identified in how APEX and SWAT calculate components of the water balance, namely runoff and potential evapotranspiration (PET), peak runoff rate used to calculate sediment yields, and transfer between the phosphorus pools. When parameterization does not take these differences into account, the models do result in different values of output variables. We caution the reader that this review is not exhaustive but it highlights important differences in how the models handle runoff, PET, or nutrient cycling. These differences need to be accounted for when comparing sediment, nutrient, or pesticide loss calculated from these two models.

Not all these differences are relevant or important for all simulation studies. However, anyone who is considering using both SWAT and APEX to assess the impact of climatic, land use, or management factors on productivity, flow, or water quality should be aware of them and how they might affect results interpretation. For example, the differences in how the harvest index is reduced as a function of water stress is important to assess productivity and associated water balance in arid regions or in relation to climate change, but may be less important in regions where precipitation is abundant. We would like to encourage users of SWAT and APEX to further investigate these differences and add to this document.

References

Gassman, P. W., M. R. Reyes, C. H. Green, and J. G. Arnold. 2007. The Soil and Water Assessment Tool: Historical Development, Applications, and Future Research Directions. *Trans. ASABE* 50(4):1211-1250.

Gassman, P. W., J. R. Williams, X. Wang, A. Saleh, E. Osei, L. M. Hauck, R. C. Izaurralde, and J. D. Flowers. 2010. Invited Review Article: The Agricultural Policy/Environmental eXtender (APEX) Model: An Emerging Tool for Landscape and Watershed Environmental Analyses. *Trans. ASABE* 53(3):711-740.

Jones, C. A., C. V. Cole, A. N. Sharpley, and J. R. Williams. 1984. A Simplified Soil and Plant Phosphorus Model: I. Documentation. *Soil Sci Soc Am J* 48:800-805.

Neitsch, S. L., J.G. Arnold, J.R. Kiniry, and J. R. Williams. 2011. Soil and Water Assessment Tool Theoretical Documentation Version 2009. TWRI Technical Report No. 406. College Station, Texas: T. W. R. Institute.

USDA-NRCS. 2012. Assessment of the effects of conservation practices on cultivated cropland in the upper Mississippi River basin. July 2012. Washington, D.C.: USDA Natural Resources Conservation Service. Available at: http://www.nrcs.usda.gov/Internet/FSE_DOCUMENTS/stelprdb1042093.pdf. Accessed 5 June 2013.

Wang, X., S. R. Potter, J. R. Williams, J. D. Atwood, and T. Pitts. 2006. Sensitivity analysis of APEX for national assessment. *Trans. ASABE* 49(3): 679-688.

Wang, X., N. Kannan, C. Santhi, S. R. Potter, J. R. Williams, and J. G. Arnold. 2011. Integrating APEX output for cultivated cropland with SWAT simulation for regional modeling. *Trans. ASABE* 54(4): 1281-1298.

Williams, J. R., R. C. Izaurralde, and E. M. Steglich. 2012. Agricultural Policy/Environmental Extender model: theoretical documentation, version 0806. Temple, Texas: Blackland Research and Extension Center.

`

Adapting SWAT model for the evaluation of water harvesting systems in an arid environment: a case from Jordan

Lubna Al-Mahasneh*

National Center for Agricultural Research and Extension (NCARE), Research engineer, Amman, Jordan, Lmahasneh@ncare.gov.jo

Feras Ziadat

International Center for Agricultural Research in the Dry Areas (ICARDA), Amman, Jordan, f.ziadat@cgiar.org

Raghavan Srinivasan

Spatial Science laboratory, Texas A&M University, Texas, Agricultural Experimental Station, College Station, Texas, USA, r-srinivasan@tamu.edu

Khaldoun Shatanawi

Assistant Professor, Civil Engineering Department, Faculty of Engineering and Technology, The University of Jordan, Amman, Jordan, kshatanawi@ju.edu.jo

Abstract:

Water scarcity and land degradation are widespread problems that affect agricultural productivity, food security and environmental quality in several parts of the world, particularly in the dry areas. Sustainable management of soil and water is necessary to optimize the use of limited rainwater for crop production and to decrease soil erosion. One management option is utilizing rainfall more efficiently through water harvesting. In arid areas, different types of water harvesting techniques (WHT) are being developed by researchers and used by farmers to utilize runoff water and to enhance plant growth. However, the effect of water harvesting on the reduction of soil erosion and runoff is not adequately known. This study aims at adapting the SWAT model to predict the impacts of selected water harvesting interventions on the bio-physical and hydrological processes and to evaluate their application in arid environments. Four sites, representing small sub-watersheds (hill slopes) were selected for modeling purposes in Al-Majidyya village 40 km south-east of Amman, which represents an arid area of Jordan (known locally as Al-Badia). The average annual rainfall in this area is less than 150 mm. Two small sub-watersheds (paired swales) were selected to measure runoff and

erosion, using flow meters and ISCO automatic samplers. One of these swales has been treated using Vallerani plough to form intermittent pits to collect and store runoff water. This swale was planted by Salsola vermiculata shrubs and the other swale has been left without any intervention (control representing the natural rangelands in the area). The other two small sub-watersheds (paired swales) were selected to measure sediment yield only using geo-textile trap. One of these paired swales contains continuous contour ridges as water harvesting measure and was planted with Atriplex halimus shrubs while the other sub-watershed was left without intervention and planted with Barley (Hordeum vulgare), representing the farmer practices. The model input parameters were derived using the SWAT ArcGIS Interface. Some parameters (Leaf Area Index and Harvest Index) for plant growth were modified to suit the prevailing arid conditions in the watersheds. Many iterations were carried out by introducing different management options in SWAT databases taking into account the subbasin, HRU and curve number values. The model overestimated the runoff and sediment yield from the water harvesting sites and to large extent accurately estimated for the sites without interventions. For example, the sediment yield predicted for the continuous contour ridges for a selected storm was 0.09 t/ha whereas no sediments were observed in the field. The predicted sediment yield for the barley site was 0.55 t/ha and the observed value was 0.34 t/ha. Manual calibration/comparisons for measured and observed results are needed to adapt the model for this arid environment and to accurately estimate the effect of water harvesting interventions. In addition the comparison of biomass and crop yield will also be analyzed between observed and SWAT predicted outputs.

Keywords: soil and water losses, soil conservation, land degradation, rangelands

Introduction

Accelerated soil erosion and water scarcity are widespread problems that affect agricultural productivity, food security and environmental quality in many countries of the world. Jordan is one of the countries that are suffering from water shortage and land degradation. Arid environments, such as Al-Badia, in Jordan are characterized by sporadic, low average annual rainfall and very high rainfall intensities that may cause runoff and erosion. Runoff causes erosion of the fertile topsoil which results in land degradation on site and increasing the risk of flooding towards the wadis.

Sustainable natural resources for both soil and water are required in order to optimize the benefit of available rainwater for crop production and to decrease the soil erosion and enhance soil fertility. Therefore, several types of water harvesting techniques (WHT) have been developed. For thousands of years, inhabitants of the dry areas have constructed water-harvesting systems that helped them cope with water scarcity (El Amami, 1984; Boers, 1994; Oweis et al., 2004) and support their livelihood.

The benefits of water harvesting in arid areas are not only to secure runoff water and recharge aquifers tapped for irrigation but also to increase crop production as well as decrease soil erosion. However, the effect of water harvesting on the reduction of soil erosion and runoff is not adequately known.

This study aims at adapting the SWAT model to predict the impacts of selected water harvesting interventions on the soil erosion and runoff. Therefore, the use of models to simulate the process at watershed scale has become a crucial and an important tool for estimating runoff and sediment yield and for quantifying the impacts of water harvesting interventions at various spatial and temporal scales. In this respect, SWAT (Soil and Water Assessment Tool) arises as a well-known useful model for quantifying soil erosion, sediment yield and runoff water (Arnold et al., 1998). Many studies that utilize SWAT to simulate soil erosion and sediment yield have been conducted. However; none specifically addressed the impact of water harvesting interventions in quantifying runoff and sediment yield. Therefore, SWAT is needed to simulate the

spatial and temporal variation of runoff, sediments and productivity in arid watersheds and the impact of the implemented water-harvesting interventions.

Materials and Methods:

Study area description:

Four sites, representing small sub-watersheds (hill slopes) were selected for modeling purposes in Al-Majidyya village 40 km south-east of Amman, which represents an arid area of Jordan (known locally as Al-Badia, Figure1).

Two small sub-watersheds (paired swales) were selected to measure sediment yield only, using geo-textile trap (silt fences), which is a low-cost technique used to measure onsite hillslope erosion. Such a technique is easy to install by making the sediment trap face the upslope. The geotextile trap is folded to form a pocket for the sediment to settle on and reduce the possibility of sediment undermining. One of these paired swales (Contour Ridge site) contains continuous contour ridges as water harvesting measures and was planted with `Atriplex halimus shrubs, while the other sub-watershed (Barley site) was left as control site without intervention and planted with Barley (Hordeum vulgare), representing the farmer practices (Figure1).

The other two small sub-watersheds (paired swales) were selected to measure runoff and erosion, using flow meters and ISCO automatic samplers by establishing a weir as a control section at each outlet. One of these swales (Vallerani site) has been treated using Vallerani plough to form intermittent pits to collect and store runoff water. This swale was planted by Salsola vermiculata shrubs and the other swale has been left without any interventions (control representing the natural rangelands in the area). Each (paired swales) is located in close proximity to each other to minimize differences in climate, soils, vegetation, topography (elevation, aspect, and slope).

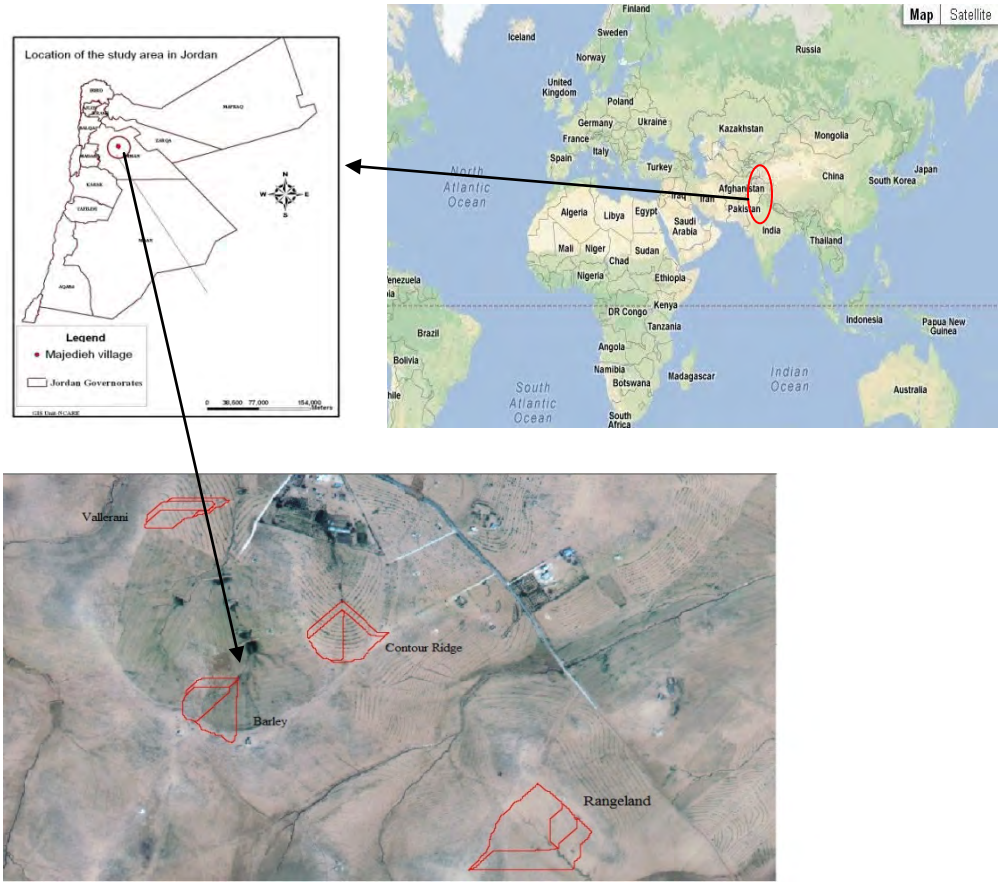

Figure 1: location of the study area in Jordan and four modeling watersheds that represent Al-Badia.

SWAT model:

Soil and Water Assessment Tool (SWAT) is a physically based continuous event watershed hydrologic simulator that estimates the impact of land management practices on surface and subsurface water movement, sediment, and agricultural chemical yields in large, complex watersheds with different soils, land use, and management conditions over 100 years of time (Arnold et al., 1998). The SWAT program is supported with an interface in ArcGIS (ARCSWAT 2009, Di Luzio et al., 2002) for the characterization of watershed hydrologic features and storage, as well as the organization and manipulation associated spatial and temporal data.

SWAT2012 version with its interface of ARCGIS 10.0 (Di Luzio et al., 2002) was used to execute this study.

The basic data required to develop the model input parameters were: topography, soil, landuse and climatic data. The unique portion of the watershed determined by the hydrological response units (HRU) based on soil, landuse and slope in addition to physical processes and crops operations and management (irrigation, tillage, harvesting, and fertilizer). The model input information were prepared in the following pattern:

Catchment configurations: derivation of DEM (Digital Elevation Model) was extracted using ArcGIS for each site by the information provided from the executed topographic survey using total station at 50 cm resolution.

Soil map: Sampling grids were taken for each soil observation location using Global Positioning Systems (GPS). A bio-physical characterization surveys were conducted for each observation location based on the soil data collection form. Soil Samples for surface and subsurface at each observation location were taken for physical and chemical Laboratory analyses. Some of physiochemical soil properties were measured such as bulk density, organic matter, stone content and texture, and some of soil parameters were estimated such as hydraulic conductivity, available water holding capacity using soil parameters estimate (SOILPAR v2.00) and the other soil parameters were estimated from input/output documentation of SWAT model such as erodibility K factor and Albedo. Soil map was produced with Thiessen polygon method with unique name using ArcGIS. A user soil database was developed with all relevant soil parameters required to input to SWAT2012.

Landuse map: Recent and high resolution satellite imagery for the site (type world view 60 cm, spring 2011) was used for identifying and digitizing the existing landuse/landcover classes using ArcGIS. The classes of landuse were those that are used by SWAT model with some modification for selected landuse classes. As a result, new SWAT landuse codes were created in term of changing the parameters of plant growth and other conditions that may characterize the sites.

Climate data: historic records for the metrological data (rainfall, temperature, solar radiation, relative humidity/or dew point, wind speed) from Queen Alia International

Airport station and Muaqqer station that belongs to the University of Jordan are the nearest stations of the sites which were used to run the weather generator file. In addition to an automatic rain gage was installed in the site to measure the rainfall intensities during the rainy seasons.

Hydrological and sediment data:

The required information of eroded sediment yields on the geotextile traps was estimated. In addition, to the information and samples of generated runoff at the weirs edge were recorded using flow meter probes and ISCO automatic samplers. Moreover, the rainfall intensities from rain gauge were used.

Results and discussion:

Sediment yield prediction using SWAT:

This presented study focuses to discuss the application of SWAT model to study the impact of water harvesting interventions on the soil erosion. SWAT utilizes the Modified Universal Soil Loss Equation (MUSLE) to estimate soil losses. This equation developed by Williams (1975) uses the amount of runoff generated in each HRU to simulate sediment yield for each HRU in each sub basin. Then, they are added to compute the contribution of sediment yield for whole basin. As a result, sediment yield predictions are improved, the accuracy of the prediction is increased and sediment yields on individual rainfall events (storms) can be estimated (Neitsch et al., 2002). The SWAT model was simulated to the site implemented by continuous contour ridges and the control site without water harvesting intervention. The model outputs determined daily and monthly sediment yields (kg/ha) based on some modifications that suit the existing arid conditions in both sites.

The application of the SWAT in arid regions requires modifications of the existing SWAT databases and parameters. Therefore the existing land cover/plant parameters are not suitable for arid environment in Al-Badia of Jordan conditions. One of the limitations, in this study, was the little or no data or available literature for the crops planted in the study area (Atriplex, Salsola shrubs and winter barley). Another challenge was how to

consider the continuous contour ridges as certain type of water harvesting interventions (Figure 2) implemented in the site. This consideration was involved in both model setup and simulation processes. Also, this challenge not only to consider it as soil conservation management practices but also as intervention measures that optimize the benefit of the rain water and increase plant productivity and reduce soil erosion.

Figure 2: Continuous contour ridges as one type of the water harvesting interventions implemented in the site.

The measured data from the field for sediment yields for the site implemented by water harvesting interventions type continuous contour ridges were totally different for the control site

The traditional procedure adopted by farmers in the control site in plantation and management of winter barley usually contributes to the soil erosion. The land is tilled in up and down slopes. This way makes the soil very loose and become weak especially that the soil texture in the site contains a high percent of silt. As a result, the traditional farmer practices contribute in a direct way to the sediment amounts transported and eroded on the site, where also the amount and pattern of rainfall intensity in that area can easily washe off the top soil and nutrients which is cause soil erosion by water (Figure 3).

Figure 3: control site planted by Barley as farmer practices and the problem of soil erosion and transported sediment yields at the geotextile traps.

As a result, one of the considerations is including the established contour ridges planted with Atriplex in the produced HRUs by adding a new landuse class and modifying the crop database which contains SWAT plant growth parameters. Therefore, new SWAT landuse codes were created with the appropriate modifications (contour ridges and barely). The modified parameters are Harvest Index (HVI), Leaf Area Index (LAI) parameters and identifying the landuse conditions that affect the Curve number values corresponding to each hydrological soil group in the basin for both sites. In addition to modifying the management and operations for each site. The operations are the plant/begin growing season, harvest and kill and applying fertilizers. Change the heat units' parameter according to the management type and existing operation for each landuse class for each site as summarized in the Table (1).

Furthermore, the physical processes were considered in the model setup and in the SWAT management practices options for selected produced HRUs in the basin for each site.

Table1: Some parameters values changed in the SWAT landuse code*

Site	Parameter	
	HVI	LAI
Continuous Contour Ridges	0.9	1.5
Winter Barley	0.54	4

(* these values were modified by Dr. Srinivasan, R., April,2012)

Simulation of the SWAT model periods was identified. The whole period was Nov. 2005 to Dec. 2012. A period of 2005 till 2010 was used to warm up the model. However, Two years of measured data for soil erosion were collected during winter seasons of Nov. 2011/ May 2012 and Nov. 2012/ May 2013. Furthermore, these will be used for calibration and verification the model outputs.

Figure (4) illustrates the obtained results without calibration. It is shown that the magnitude and temporal variation of simulated monthly sediment yield for the selected storms in January does not match the observed sediment loads. Timings of occurrence of the peaks for observed and simulated sediment yield as well. However, they look in the same pattern but the model over-predicted sediment amounts during the January 2012 and it was also over estimated some peak values except the storm happened at December 2012. Although, the simulated and observed are closely match in magnitude and temporal variations at the end of the season in March 2012, Unlike, the contour ridges site that contains a (Continuous Contour Ridges as certain type of water harvesting measures), no sediments were observed in the field during all storms within the same period. But the model simulation output without calibration for monthly sediment yield was over estimated as illustrated the in figure (5) comparing with the measured one. The model with this result maybe requires fine-tuning to the input model parameters to include the established continuous contour ridges as water harvesting interventions in the site and its impacts that reduce the soil erosion. So, calibration and verification analysis is required.

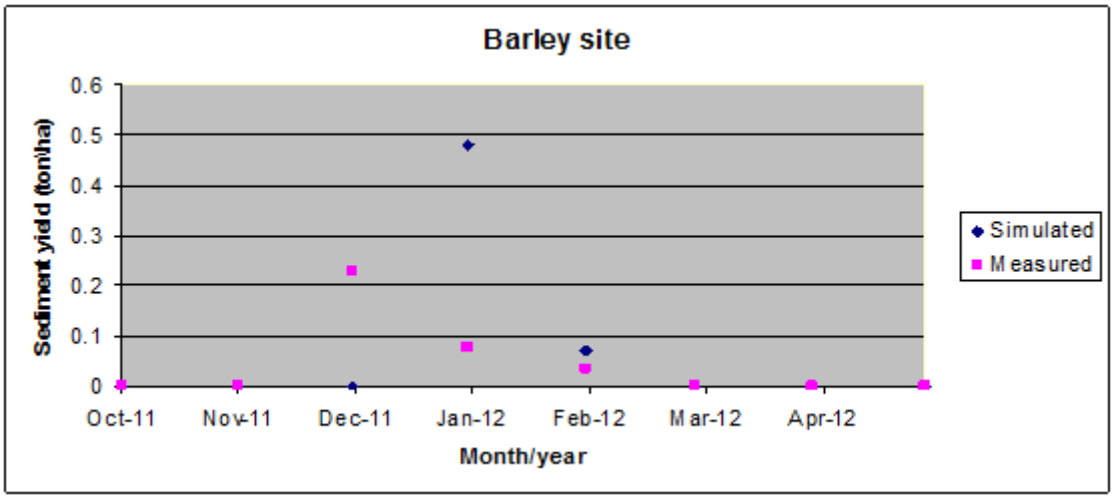

Figure 4: comparison of sediment yields (ton/ha) between SWAT simulation output and measured in the field for barley site.

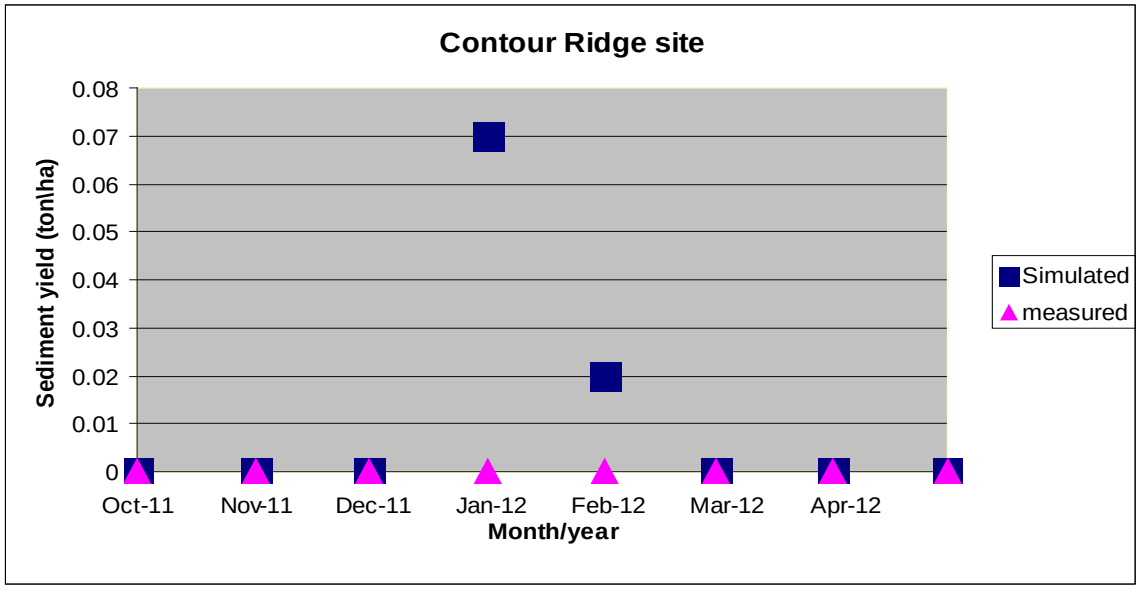

Figure 5: comparison of sediment yields (ton/ha) between SWAT simulation output and measured in the field for Continuous Contour Ridges site.

Biomass predictions using SWAT:

The SWAT model was used to simulate total biomass yield throughout barley, contour ridges and vallerani sites. The parameters which affect the biomass production are Leaf Area Index (LAI), soil evaporation and evapotranspiration. LAI values is estimated for each HRU by changing some plant growth parameters build in the model to suit existing

condition in the study area. So the LAI was changed as mentioned in Table1. SWAT calculates the potential growth of plant for each day of simulation as a function of energy where the plant intercepts the efficiency of its conversion into biomass. Actual growth and actual LAI are dependent on stress factors like water, temperatures and nutrients. Optimal leaf area index is related with crop stage which in turn depends on the crop heat units. These heat units are defined in the SWAT database for each crop. The SWAT model was used to simulate total biomass yield. The model is under predicted the biomass production for the sites implemented by water harvesting interventions. In the contrast, the model is well matched with measured by assumption of applying fertilizers of 10 k/ha N for barley site (Figure 6).

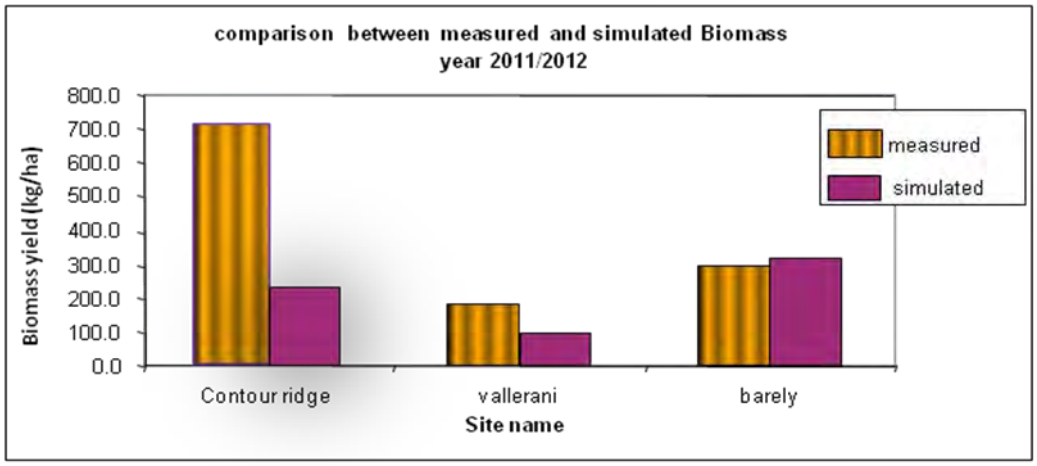

Figure 6: comparison between measured and simulated biomass for the sites.

Figure 7 illustrates that different scenarios were applied to the barley site that assume applying of the natural and chemical fertilizers will improve the crop biomass and yields

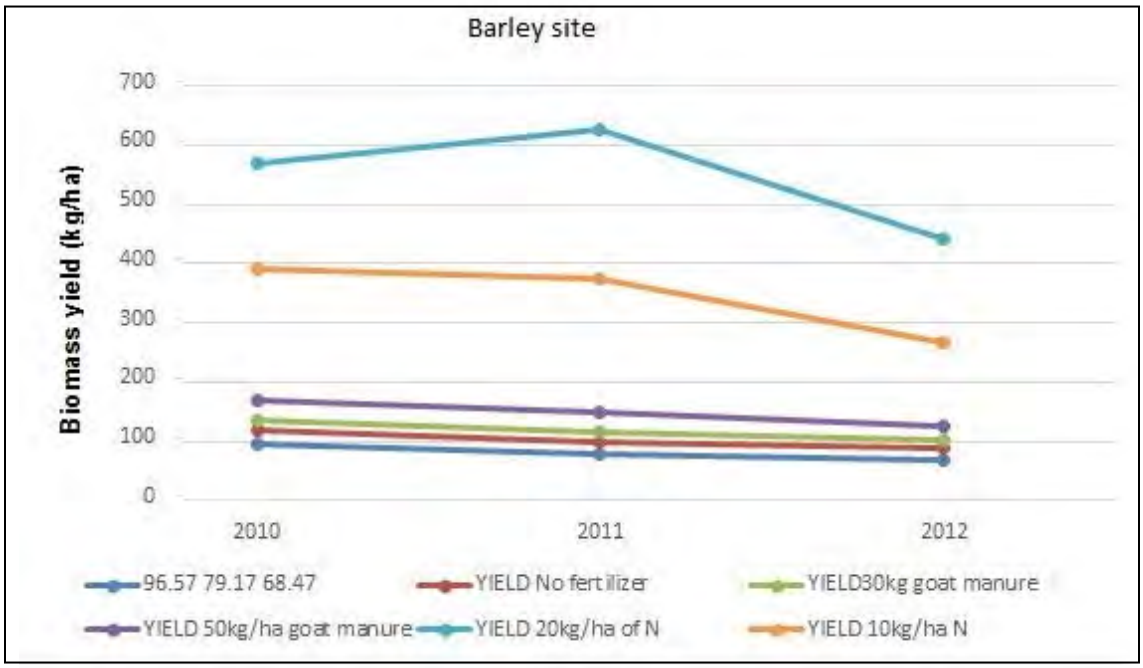

Figure 7: comparison of different scenarios applied to the barley site for the model biomass outputs. (Source: Dr. Srinivasan, R., April, 2012)

Conclusions:

This study focuses on simulation of SWAT model to predict the sediment yields for the sites that measure the soil erosion only. These are barley and contour ridges. In addition to simulate the model to predict the biomass productions for the sites of Barley, Contour ridges and Vallerani. The most important input data include meteorology, topography, soil data, landuse, water harvesting interventions and the applied agricultural practices. This study modeled the sediment yield from the site implemented by contour ridges water harvesting interventions and control site for the rainy season of 2011/2012.

SWAT outputs were evaluated by comparing simulated sediment yields with the measured sediment loads from the two sites.

Soil erosion from watersheds contributes a large amount of top soil and nutrients each year. The measured data presents evidence that the water harvesting interventions

reduce the soil erosion and can aid in reducing losses and thereby have the potential to optimize the benefit of rainfall especially in the arid environment.

The biomass results can be significant for the farmers to adopt the water harvesting interventions which maximize the productivity.

References

Journal article

Bingner, R. L., Garbrecht, J., Arnold, J. G., and Srinivasan, R.: Effect of watershed division on simulation of runoff and fine sediment yield, *Transactions of the American Society of Civil Engineers, 40(5), 1329–1335.*

Ouessar M., Sghaier M., Mahdhi N., Abdelli F., De graaff J., Cchaieb H., Yahyaoui H. and Gabriel D. (2004). An integrated approach for impact assessment of water harvesting techniques in dry areas: the case of oued oum zessar watershed (Tunisia). Environmental Monitoring and Assessment (99) : 127–140.

Ouessar, M., Bruggeman A., Abdelli, F., Mohtar, R. H., Gabriels D., and Cornelis, W. M. (2008). Modelling water-harvesting systems in the arid south of Tunisia using SWAT. Hydrology and Earth System Sciences Discussions, (5), 1863–1902.

Robichaud, P.R.; McCool, D.K.; Pannkuk, C.D.; Brown, R.E.; Mutch, P.W. 2001. Trap Efficiency of Silt Fences Used in Hillslope Erosion Studies. Soil erosion for the 21st century: proceedings of the international symposium. St. Joseph, MI: ASAE. 541-543. ASAE Pub. No. 701P0007.

Hessel, R. and Tenge, A. (2008). A pragmatic approach to modelling soil and water conservation measures with a catchment scale erosion model. CATENA, 74(2), 119-126.

Robichaud, Peter R.; Brown, Robert E. 2002. Silt fences: an economical technique for measuring hillslope soil erosion. Gen. Tech. Rep. RMRS-GTR-94. 24 p.

Published paper

Almeida, C., Chambel-Leitao, P. Jauch, E. And Neves. R.(2011)SWAT LAI calibration with local LAI measurements. : Proceedings, 2011 International SWAT Conference. June15-17, 2011. University of Castilla La Mancha at Toledo, Spain.

Guevara, B., Casanova, M. and Ramos, M. 2011. Soil erosion modelling in agro-forested catchment of NE Spain affected by gullying using SWAT: Proceedings, 2011 International SWAT Conference. June15-17, 2011. University of Castilla La Mancha at Toledo, Spain.

Kuwajima, J., Crestano, S., Zuquette, L., Mauad, F.)2011). Challenges and difficulties in sediment modeling applied to sedimentation study of the Lobo reservoir in Brazil. : Proceedings, 2011 International SWAT Conference. June15-17, 2011. University of Castilla La Mancha at Toledo, Spain.

Oweis, T., D. Prinz and A. Hachum. 2001. Water Harvesting: Indigenous Knowledge for the Future of the Drier Environments. ICARDA, Aleppo, Syria. 40 pages.

Tue, V., Srinivasan, R., Shie-Yui, L. and Adri, V. 2011. Quantifying SWAT runoff using grided observations and reanalysis data for Dakbla river basin, Vietnam. : Proceedings, 2011 International SWAT Conference. June15-17, 2011. University of Castilla La Mancha at Toledo, Spain.

Dissertation or thesis

Ziadat, F. (1995). Effect of management practices on soil losses in arid to semi arid area in Jordan. Unpublished Ms Dissertation. University of Jordan.

Swat Owl: A New Tool for Quicker Visualisation of SWAT Outputs and Calibration

Philip Selby, Catchment Modeller
Mott MacDonald, Integrated Water Resources Management
Cambridge CB1 2RS, UK, philip.selby@mottmac.com

Abstract

Swat Owl is a new suite of tools which has been developed to allow SWAT modellers to see snapshots of model outputs. The tool runs as a stand-alone executable file and speedily produces graphical outputs, summaries of water balance data, and calibration statistics. The user can switch between saved model runs to compare the effect of changes to parameters on the water balances and calibrations. The tools have been developed as part of an ongoing project to model 23 surface water catchments for Anglian Water (East of England).

Swat Owl comprises the following tools (i) snapshot of average annual water balance (ii) average monthly water balance charts for entire model (iii) graphs showing a wide selection of parameters output at HRU level (iv) graphical output of flow data for all the reaches and subbasins on one page (v) graphical output of observed and modelled flows with built-in baseflow calculation, Nash Sutcliffe calculations, and other statistics. (vi) a scripting tool to automatically run SQL 'Update' queries, re-write SWAT input files, run the model, save the results and statistics, and log the changes.

The aim of the paper is to demonstrate the tool to a wider audience and to demonstrate how rapid visualisation of water balance outputs can lead to better understanding of how parameters influence the flow paths within SWAT leading to faster calibration and better representation of catchment flows. Feedback on the usefulness of the tool will be invited.

Keywords: SWAT, Postprocessor, Calibration Statistics, Water Balance Summary, SQL Updates, Graphical Output, Baseflow Calculation.

Introduction

Various efficiency tools have been developed which have helped to speed up the SWAT modelling process and analyse SWAT model outputs. Swat Owl is an effort to bring these tools together in one package. Two main objectives have driven the development of Swat Owl, these are to:

- Provide a quick and easy way to read and visualise model outputs.
- Provide a quick and easy way to automate the changing of parameters followed by the running of SWAT.

As the SWAT model develops and the SWAT community widens, tools for processing SWAT data, running scenarios, and processing results will continue to be developed. It is important that this knowledge is shared. This paper gives an overview of the tools and methods in the Swat Owl package and the thinking behind its development.

The Swat Owl tools have been developed in the context of a major programme at Anglian Water (in Cambridge, UK) to model 23 of their surface water catchments in SWAT and use them to assess catchment management issues. This work involves the equivalent of two full-time SWAT modellers over a two-year period and for a project of this scale efficiencies are important.

This paper sets out the rationale for Swat Owl and gives an overview of the tools and their development. A Swat Owl user guide is presented in Appendix A.

Rationale for Swat Owl

Review of other SWAT Tools

Before the tools in Swat Owl were developed, an evaluation of other useful SWAT tools was completed. SWAT Error Checker and SWAT-CUP stand out as adding most value to the modelling process. These two tools have both been used in the Anglian Water modelling programme and the Swat Owl tool is considered to be complementary to them. An overview of the SWAT Error Checker and SWAT-CUP is given below.

SWAT Error Checker

SWAT Error Checker provides a useful overview of the output files in SWAT. It concentrates on high-level outputs, providing overviews of the catchment hydrology, sediment loading, nitrogen cycle, plant growth, reservoir balances etc. It performs simple checks to identify potential model issues and generates warnings if any are found.

The strengths of SWAT Error Checker lie in its presentation of many different high-level overviews, much of the information is diagrammatically shown, and it can quickly and easily screen model issues.

SWAT-CUP

SWAT-CUP (Abbaspour, 2007) is a sophisticated tool for setting up and running calibration scenarios. It uses a bespoke script to define ranges, over which input parameters can be tested, making it a very powerful tool for calibration and uncertainty analysis. SWAT-CUP calibrates time-series datasets, using metrics such as Nash-Sutcliffe, and produces graphs with simulation results showing uncertainty ranges.

The strengths of SWAT-CUP lie in its ability assist with understanding the sensitivities of each parameter and optimize model calibrations.

The Purpose of Swat Owl

Swat Owl has been built with the ability to run a series of SWAT models after changing a particular parameter, and then quickly visualise and compare the outputs of each model after each change.

SWAT Error Checker provides some of the required functionality but it is unable to rapidly step through a number of different SWAT model runs to compare the results. In addition, it only compares results at a high level, with no time-series data. Likewise SWAT-CUP provides some of the required functionality through analysis of flow series data. However, model results are not saved between runs so the user can only compare the impact of the most recent model parameter changes on the current model output – understanding of the model changes is limited without being able to interrogate the output of each model run.

Swat Owl is intended to be complementary to SWAT Error Checker and SWAT-CUP, filling the gap between the very effective high-level checks SWAT Error Checker provides and the powerful calibration and sensitivity analysis engine of SWAT-CUP.

Use of Swat Owl for SWAT Modelling

Model calibration is more than simply matching modelled and observed flow (or water quality) using parameters to give a good statistical correlation; it also requires good representation of the various hydrological pathways. Swat Owl provides the means to understand the effect of parameterisation and calibration by displaying time series data for the key hydrological pathways at watershed, subbasin, and HRU level, and provides calibration analysis for time-series flow data.

Since the outputs of model runs are saved it is easy to review the effects of model changes. Through automation of model runs a large amount of valuable data can be generated, avoiding the slow process of making changes to the model database tables and then updating the text files. This adds value to the modelling process by:

- Speeding up parameterisation and calibration actions
- Widening the scope for completing additional model runs to aid understanding of the model parameters.

The Swat Owl Tools

Overview

The tools in Swat Owl are broadly categorized as follows:

- A scripting tool allowing SWAT runs to be automated
- Graphical outputs of key hydrological parameters:
  - Average annual water balance.
  - Monthly water balance.
  - Subbasin outputs
- HRU outputs.
- Correlation analysis of modelled and observed flows.

SWAT Run Automation Tool

A SWAT-run automation tool enables the user to automatically (and in sequence):

- make changes to the model database files;
- update the SWAT text input files from these tables;
- run the SWAT model; and then,
- save key model outputs to a new folder.

This is the 'engine' room of Swat Owl, allowing the user to set up multiple runs, let SWAT run, and then inspect the results files and compare the runs with other Swat Owl tools. Model changes are made using a script which integrates SQL (Structured Query Language) 'UPDATE' commands. The SQL commands make changes to the model database tables and Swat Owl keeps track of which tables have been changed and then updates the text input files (in the TxtInOut directory). Figure 1 illustrates this process.

After each run the following SWAT output files are copied to the new directory.

- output.hru
- output.mgt
- output.pst
- output.rch
- output.rsv
- output.sed
- output.std
- output.sub
- output.wtr
- basins.bsn
- input.std

Figure 1: SWAT Model Automation

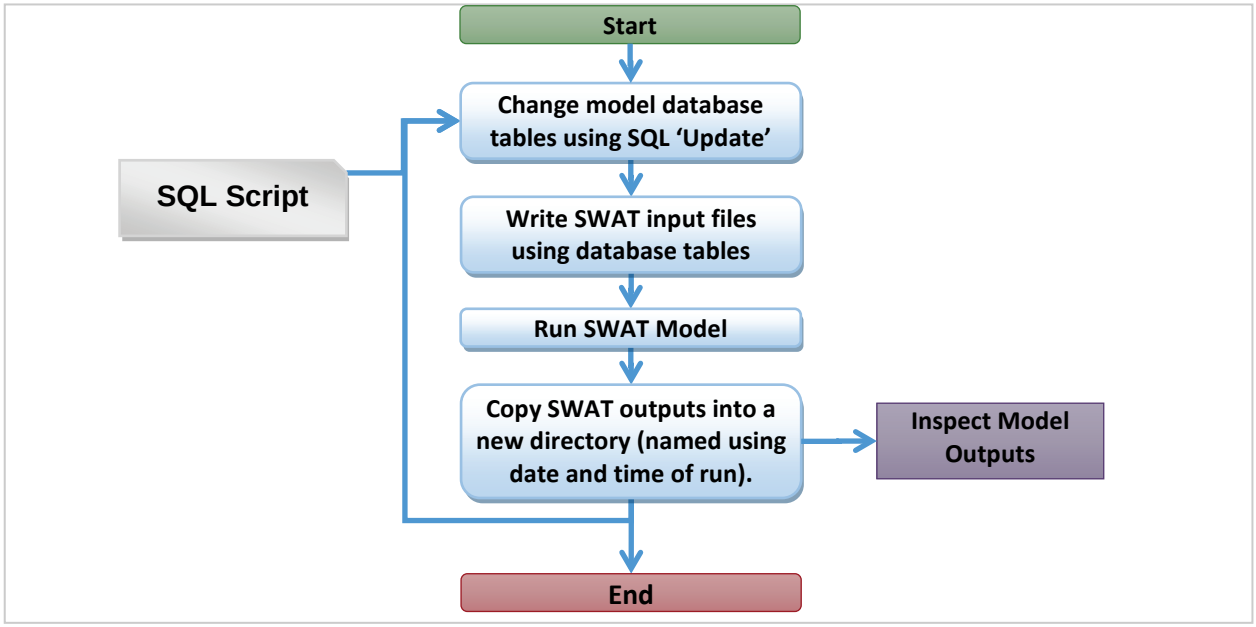

Annual Water Balance

The annual water balance tool reads outputs from the 'output.std' file and presents them on a hydrological cross-section (borrowed from the SWAT theoretical documentation (Arnold Et Al, 2012). It also provides the water balance numbers in a text box.

The concept of the cross-section populated with the water balance values is borrowed from SWAT Error Checker. As an addition, Swat Owl includes the Tile Flow water balance component.

The annual water balance is an important output of the SWAT model. When building a hydrological model typically the average annual water balance provides a first check of hydrological water balance components. The modeller will want to see whether the ratios of various water balance parameters are within expected ranges and whether they fit with their conceptual understanding of the catchment. The average annual water balance will be reviewed as the model calibration develops, especially after major changes are made, and when watershed parameters are changed.

Appendix A5 provides a guide to using of the Average Annual Water Balance tool.

Monthly Water Balance

The monthly water balance tool reads the monthly values from the 'output.std' file for key hydrological components and provides an overview of the changes to the hydrological components over the duration of the model run time. Each component is displayed as a separate chart and a summary chart showing the breakdown of the components contributing to overall yield is shown.

Water balance components are given in millimeters. Typically the monthly water balance will be used to understand the key changes that take place in the model when basin wide parameters are changed and when any substantive change is made to hydrological or crop growth parameters. It helps provide an understanding of how hydrological components vary in proportion to one another (most often driven by seasonal changes). It is also used to diagnose any fundamental problems in the model – for instance if a component fails to reach a steady state, disappears, or doesn't appear in a certain timeframe, it could indicate model issues.

Appendix A6 provides a guide to using of the Monthly Water Balance tool.

Subbasin Outputs

The subbasin outputs tool reads monthly values from the 'output.sub' file and the 'output.rch' file. It provides a chart, for each subbasin, showing the main water balance components and shows the soluble pesticide exiting each subbasin.

All the subbasins are plotted on the same scale so that the magnitude of flow out of each subbasin can be compared. The tool provides the opportunity to compare between the relative components of stream flow in each subbasin – this enables the user to check whether the hydrological pathways and water quality dynamics have been modelled in each subbasin (or a sample of subbasins) is in line with the conceptual understanding of the catchment.

Appendix A7 provides a guide to using of the Subbasin Output tool.

HRU Output (and Crop Growth) Tool

The HRU output tool reads monthly hydrological parameters from the 'output.hru' file. Up to three HRUs can be compared side-by-side with each water balance component presented in a different chart over a selected period.

When a particular change has been made to a model parameter at HRU level it is useful to see the impact on the particular HRUs in question as well as the impact on the calibration. The HRU tool also allows the user to drill down on issues limiting the hydrological calibration, usually once they have assessed the watershed balance and the subbasin outputs. Although a detailed analysis of what is happening at the HRU is often not appropriate, understanding the output of selected HRUs can help diagnose model issues.

The growth output tool is an extension of the HRU tool and reads key crop growth parameters from the 'output.hru' file. The output shows whether particular crops in particular soils are growing and what is constraining any growth, providing an easy first check of what is happening in each HRU.

Appendix A8 provides a guide to using of the HRU Output tool.

Calibration Analysis Tool

The calibration analysis tool reads flows from the reach files (reach.dat) specified when the SWAT model is configured (see fig.fig file). For each of these reach files it looks for a corresponding file, created by the user, which contains the observed flows for the same reach.

Observed and modelled flows are read in, processed, and then presented graphically along with key calibration statistics for a model period specified by the user. Built-in algorithms filter the data to exclude periods where there is no observed data or where it is erroneous.

Analysis is completed for every pair set of data (observed and modelled flows) that is found in the SWAT output directory (TxtInOut) with the plotted data shown for consecutive days of recorded (and validated) data.

The graphical outputs of the tool include:

- A plot of observed and modelled flows on over the select period (the modelling period by default)
- A plot of cumulative observed and modelled flows over the selected period.
- A plot of rank modelled and observed flows over the selected period.
- A plot of observed and modelled flows excluding any periods where observed flows was missing and plotted against number of days from the model start (only counting days with valid data).

The statistical outputs of the tool compare modelled and observed flows over the selected period and include:

- NSE (Nash Sutcliffe Efficiency)
- RSR (the ratio of the root-mean-square error of simulated streamflow to the standard deviation of the measured data)
- PBIAS (Percentage bias)

Appendix A10 provides a guide to using of the Calibration Analysis tool.

Technical Development of Swat Owl

Overview

The technical development of Swat Owl described below relates to Swat Owl version 1.0.

It is beyond the scope of this paper to document the code behind the tools. However, below is a summary of the important procedures, methods and code libraries which Swat Owl uses:

- The Swat Owl code language is VB.net
- ZedGraph plug-in was used as the main graphing component.
- ADODB connection was used to read and write data to the model database.
- General Expressions were used to parse text files.
- LINQ was used to summarise and filter SWAT data.

Limitations and Planned Development

A more complete review of Swat Owl is planned along with more thorough debugging. Table 1 show a list of the limitations and issues, which have been identified to date, and the proposed action to address them.

Table 1: Swat Owl Limitations and Issues and Proposed Action.

Item	Limitation / Issue	Proposed Action
1	Only reads monthly data from Subbasins, reaches and HRUs files	Reading daily data is not currently a requirement
2	Automated changes to SWAT parameters is restricted to a few tables (bsn, gw, hru, mgt, sol, pest)	Other tables are being added as required and prioritized by current Swat Owl use.
3	May not work with every version of the SWAT and ArcSWAT executable.	Should be tested with all versions of SWAT. Minor changes to text parsing routines may be required.
4	It is not fully tested outside of Windows 7 (64bit) or on slower computers.	Further tests planned.
5	Swat Owl was designed using a screen resolution of 1680 by 1050.	Further tests planned. It could be optimised for different resolutions.
6	Multicore threading could be used to speed when batch running SWAT.	This would speed up calibration by allowing model runs to be done in parallel – not a priority at present.

Conclusion

Swat Owl provides a rapid way of comparing the results of several SWAT model runs following changes to parameters and allows the user to assess the effects the parameters have on the hydrological and chemical pathways, and crop growth. The user can step through and easily see the results after changing each parameter. In this way Swat Owl is a useful aid to model parameterisation and calibration.

References

Abbaspour, K.C. 2007. User Manual for SWAT-CUP, Swat Calibration and Uncertainty Analysis Programs. Swiss Federal Institute of Aquatic Science and Technology, Eawag, Dübendorf, Switzerland.

SWAT Error Checker – Version 1.0, September 28, 2011.

Arnold J.G, Kiniry J.R, Srinivasan R, Williams J.R, Haney E.B, Neitsch S.L. 2012. Soil and Water Assessment Tool. Input/Output Documentation, Version 2012. Texas Water Resources Institute. TR-439.

Appendix A – Swat Owl User Guide

Introduction

This user guide relates to version 1.0 of the Swat Owl packages. Each of the tools within Swat Owl is presented with simple instructions for their use.

Overview of Swat Owl Window

Figure A1 gives an overview of the main Swat Owl window highlighting the main areas for, model run selection, tool selection, and the output window.

Figure A1: Overview of Swat Owl Tool

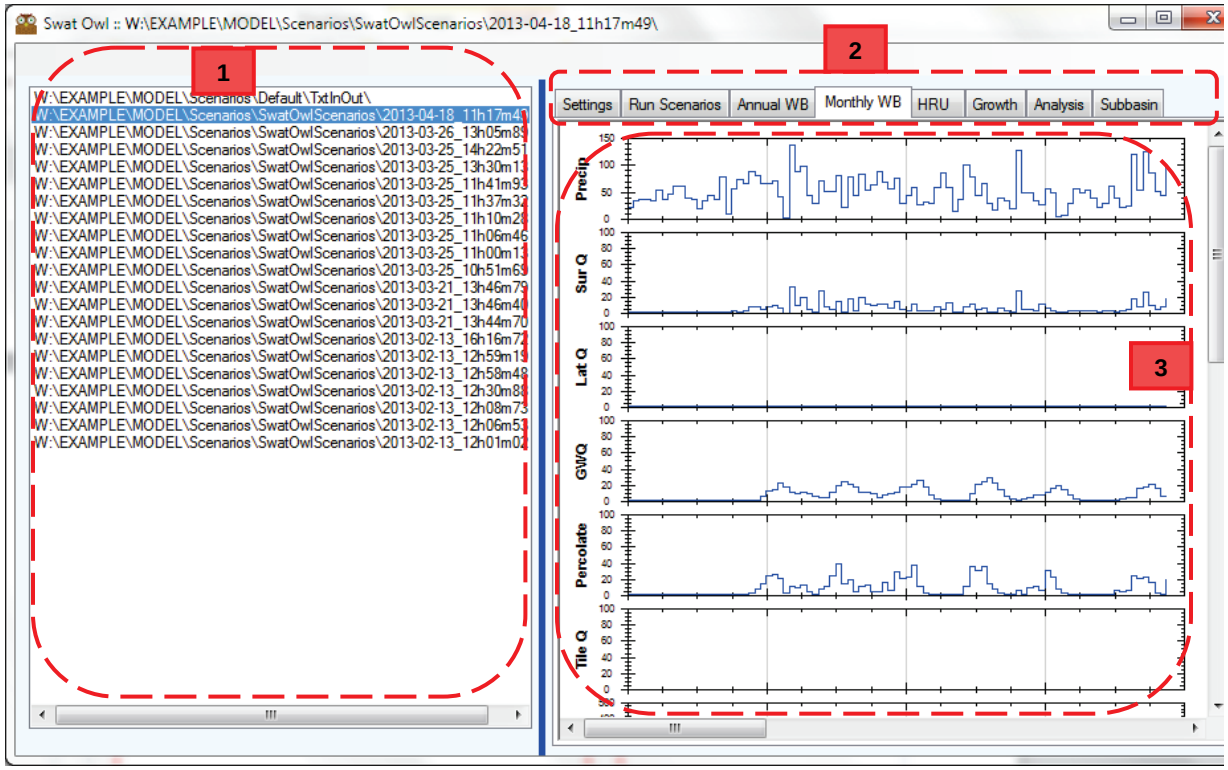

1. Model run selection panel.
2. Tool/settings selection tab.
3. Main input/output window.

Selection of Model Run Files

Figure A2 shows the model run selection panel which allows the user to select which set of SWAT model results to display based on the directory where the output files are stored. The panel lists all the subdirectories which lie within the folder called specified by the user setting 'SCENARIODIR'.

Figure A2: SWAT Model Run Selection Panel

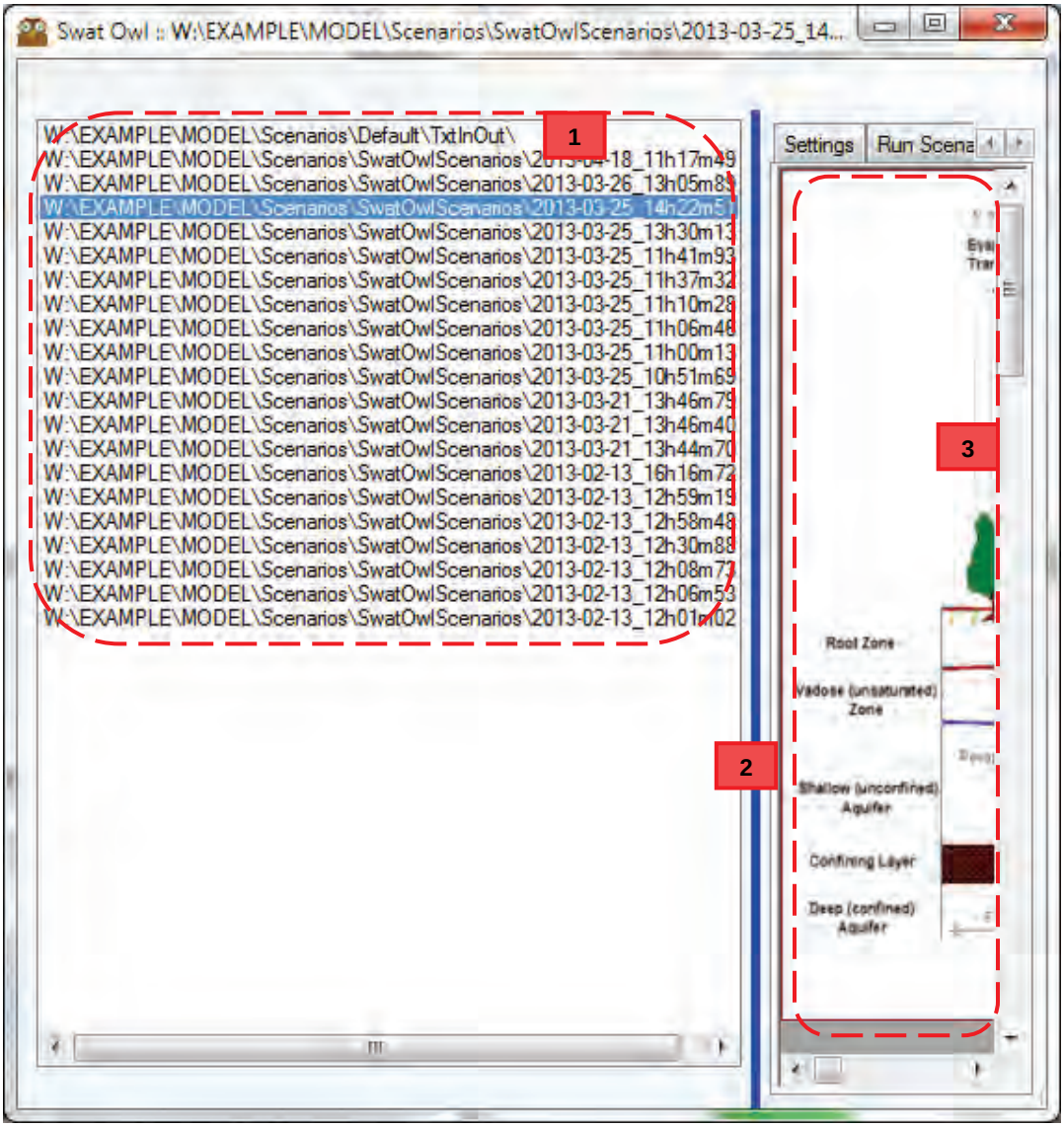

1. Click on results directory (or use up/down keys) to select SWAT run from directory list.
2. Double-click on the blue bar to show or hide directory selection panel. Drag left/right to resize panel.
3. The data and charts in the model output window is updated when the directory is changed.

Swat Owl Settings

Figure A3 shows the settings tab where the key model parameters are established. The settings file 'C:\Users\%USERNAME%\AppData\Local\SwatOwl\SwatOwlSettings.txt' is used to instruct Swat Owl which files to load on start-up along with the locations of the model files etc.

Figure A3: Swat Owl Settings

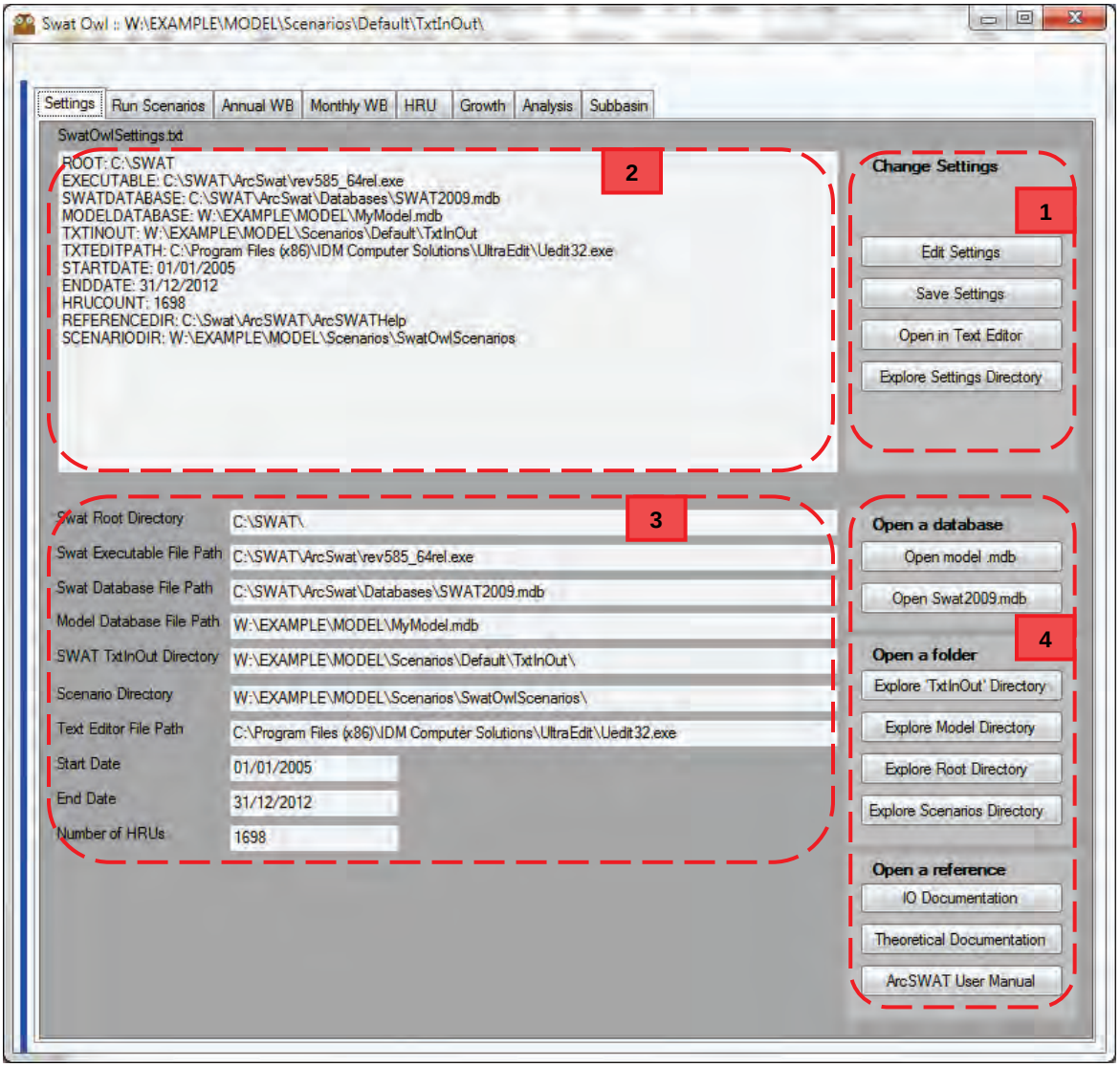

1. Click 'Edit Settings' (or Open in Text Editor) to edit the 'SwatOwlSettings.txt' file.
2. Edit the settings in this text box using the example format.(and then click 'Save Settings')
3. On 'Save Sttings' the settings bed replicated here, where they can be checked.
4. Use the buttons here as convenient links to open model files and directories.

Note: If Swat Owl is not functioning properly after changes to the settings, it may be that some of the settings needed to take effect at start-up. Closing and reopening Swat Owl should resolve this.

Automation of SWAT Runs

Figure A4 shows the 'Run Scenarios' tab containing a tool for automatically making changes to SWAT and running scenarios. A script can be entered to batch run SWAT, making model changes between each run. Model runs are logged and their outputs are saved.

Figure A4: Automated Parameter Changing and Model Runs

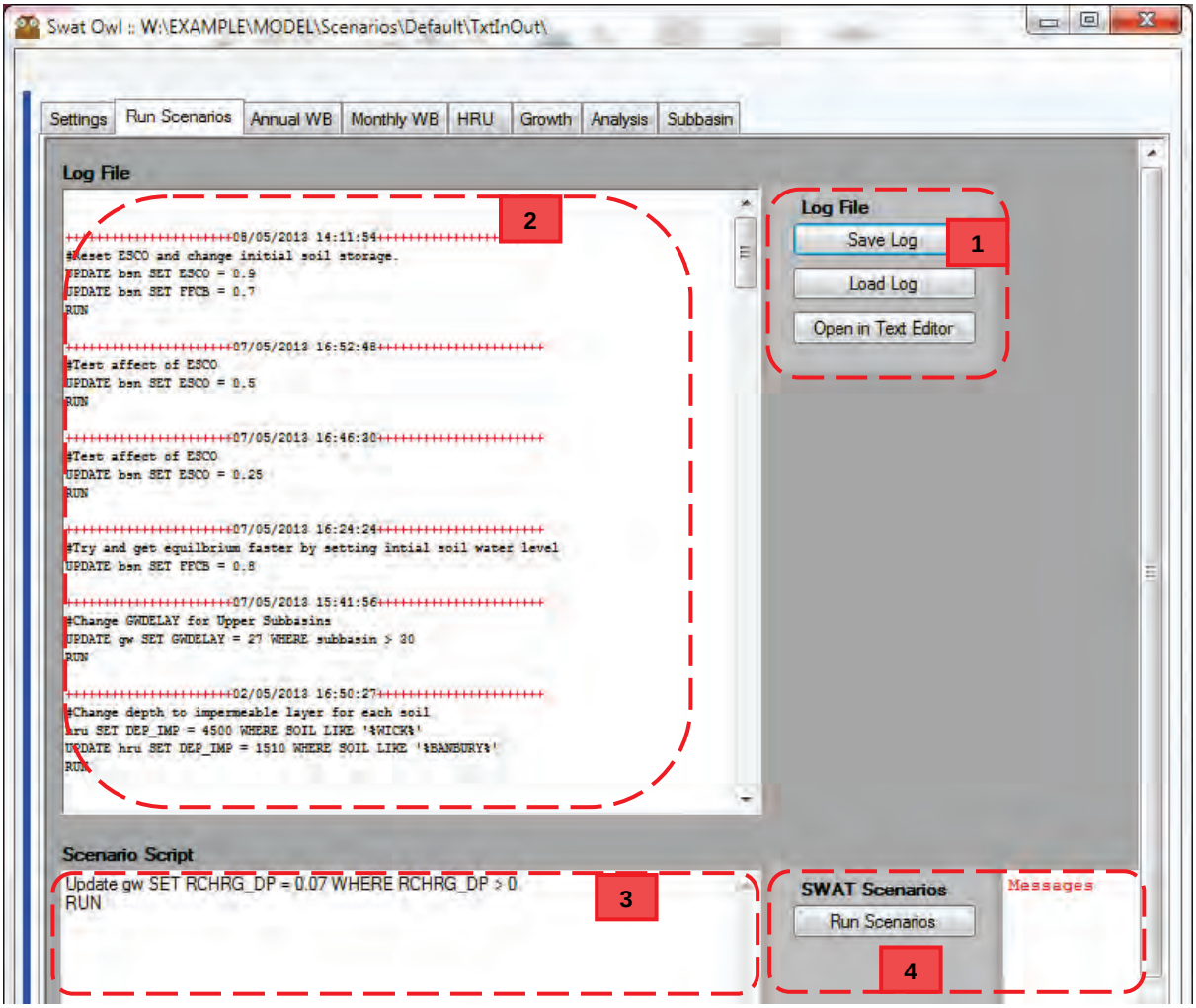

1. Click on 'Load log'. This loads the 'SwatRunLog.txt' file which is stored in the TxtInOut directory. (After first use the log file should automatically load).
2. Enter Swat Owl SQL scripts, followed by 'RUN' after each set of changes. Each line must contain a complete SQL statement, a comment or a RUN command. A comment is marked with the '#' symbol. The model is run with the 'RUN' command (must be in capital letters).
3. Click on "Run Scenarios" to RUN the script. Messages (including any run-time errors) will be written into the text box to the right of this button.
4. The log file is updated by Swat Owl after each run, however it can be updated manually, for instance to include additional notes, and then saved.

Writing a Script

The tool recognises SQL ‘update’ queries. Each line must contain a complete SQL statement, a comment or a RUN command. A comment is marked with the ‘#’ symbol. The model is run with the ‘RUN’ command (must be in capital letters).

Example1:

```
#Scenario 1a: ESCO and EPCO
UPDATE bsn SET ESCO = 0.25
UPDATE bsn SET EPCO = 0.5
RUN
#Scenario 1b: ESCO and EPCO
UPDATE bsn SET ESCO = 0.5
UPDATE bsn SET EPCO = 0.1
RUN
#Scenario 1c: ESCO and EPCO
UPDATE bsn SET ESCO = 0.75
UPDATE bsn SET EPCO = 0.3
RUN
```

Three SWAT model runs are completed based with different values of ESCO and EPCO

Example2:

```
#Scenario 1a: Update ESCO
UPDATE hru SET DEP_IMP = 4500 WHERE SOIL LIKE '%WICK%'
UPDATE hru SET DEP_IMP = 1510 WHERE SOIL LIKE
'%BANBURY%'
RUN
```

One SWAT model runs is completed, after altering the value of DEP_IMP for two different soils

N.B: The wildcard in VB.NET is ‘%’ whereas in access VBA it is ‘’.*

Note: At present Swat Owl is only capable of writing the following mdb tables to text files:
In the model mdb:

- bsn, gw, hru, mgt, sol

In SWAT2009.mdb

- pest

ArcSWAT or SWAT Editor should be used to update other files.

Annual Water Balance

The 'Annual WB' tab provides an overview of the model annual average water balance, as shown in Figure A5. The values are updated from the 'output.std' file when the selection is changed in the Model Run Selection Panel.

Figure A5: Annual Water Balance

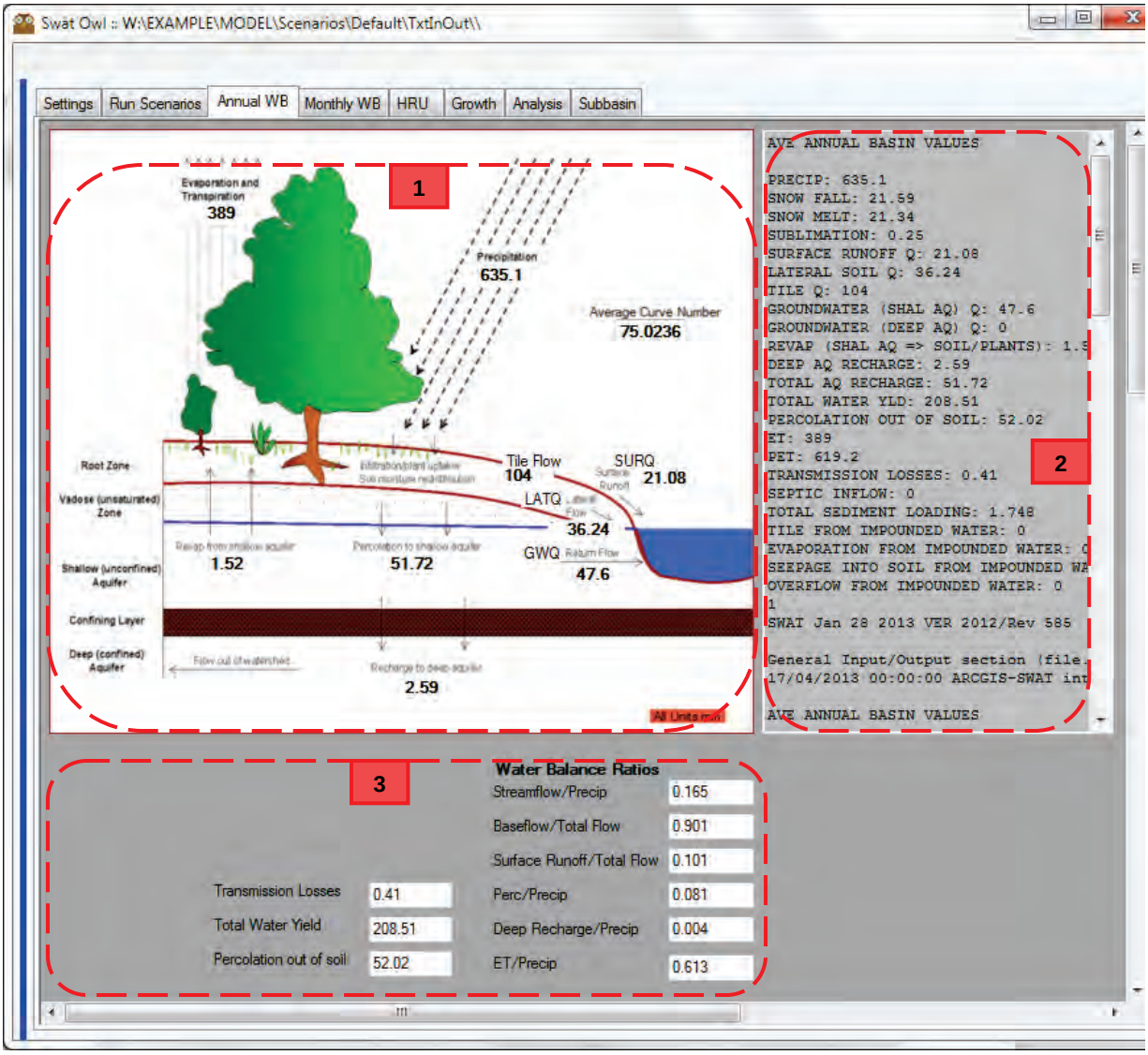

1. This area summarises the key water balance components on a hydrological cross-section.
2. The average annual basin values, taken from the output.std file are displayed here.
3. A summary of calculated water balance ratios is provided.

Monthly Water Balance

The 'Monthly WB' tab provides an overview of the model monthly water balance, as shown in Figure A6. The values are updated from the 'output.std' file when the selection is changed in the Model Run Selection Panel.

Figure A6: Monthly Water Balance

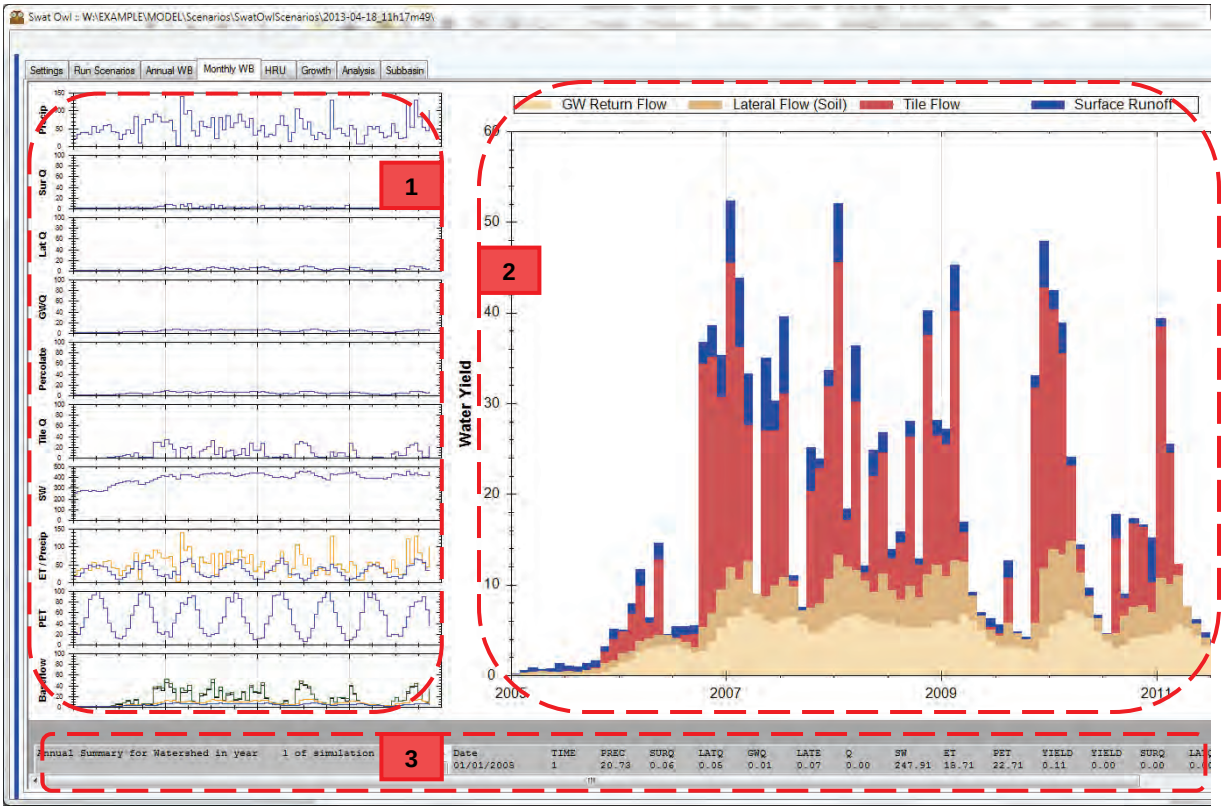

1. Individual monthly water balance components from the output.std file are shown here for the selected period, including: Precipitation, SurQ, LatQ, GWC, Percolate, Tile Q, SW, ET, PET (please refer to the SWAT Input/output manual for definitions of these parameters).
2. A stacked graph showing the breakdown of the components contributing to the total yield (contribution to catchment stream flow) is shown here.
3. These text boxes show the monthly values from the output.std file before and after processing them into a tabular format.

Subbasin Outputs

The ‘Monthly WB’ tab provides an overview of the components contributing to the total yield (contribution to catchment stream flow) for each basin as shown in Figure A7. The values are updated from the ‘output.sub’ and ‘output.rch’ files when the selection is changed in the Model Run Selection Panel. In order to use this tool the SWAT model should be run with model outputs set to a monthly time-step.

Figure A7: Subbasin Outputs

1. Outputs are charted for every subbasin in the model. Subbasin graphs are added top to bottom, followed by left to right.

HRU Outputs

The 'HRU' tab provides an overview of the hydrological outputs for selected HRUs as shown in Figure A8. The data is taken from the 'output.hru'. The values are updated when the selection is changed in the Model Run Selection Panel or when a new HRU is selected. In order to use this tool the SWAT model should be run with model outputs set to a monthly time-step and to write the full set of HRU values.

Figure A8: HRU Outputs

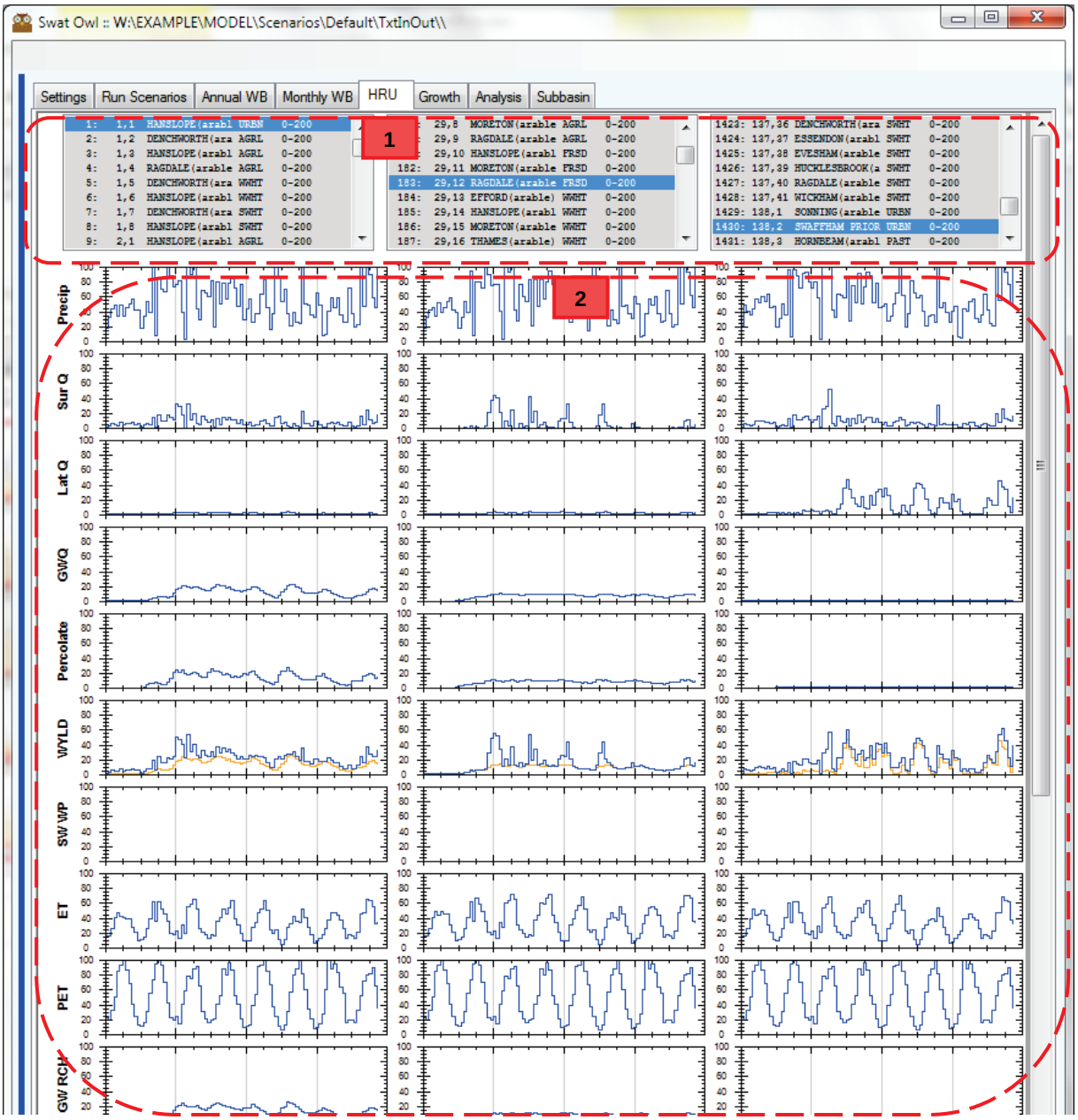

1. Select up to three HRUs to be compared from the full list of HRUs.
2. Key hydrological parameters are displayed for each HRU. (Scroll down in the tool to see more parameters).

Outputs for the HRUs are extended onto the ‘Growth’ tab which shows key crop growth parameters for the plants in each HRU, as shown in Figure A9.

Figure A9: Subbasin Outputs

1. Selected HRUs are shown here. (To make a new selection refer to the HRU tab)
2. Crop growth parameters for selected HRUs.

Analysis Outputs

The 'Analysis' tab, as shown in Figure A10, provides outputs showing statistical and graphical analysis of the calibration between observed and modelled flows for selected model reaches. The values are updated when the selection is changed in the Model Run Selection Panel or when a new HRU is selected.

Figure A10: Reach Calibration Analysis

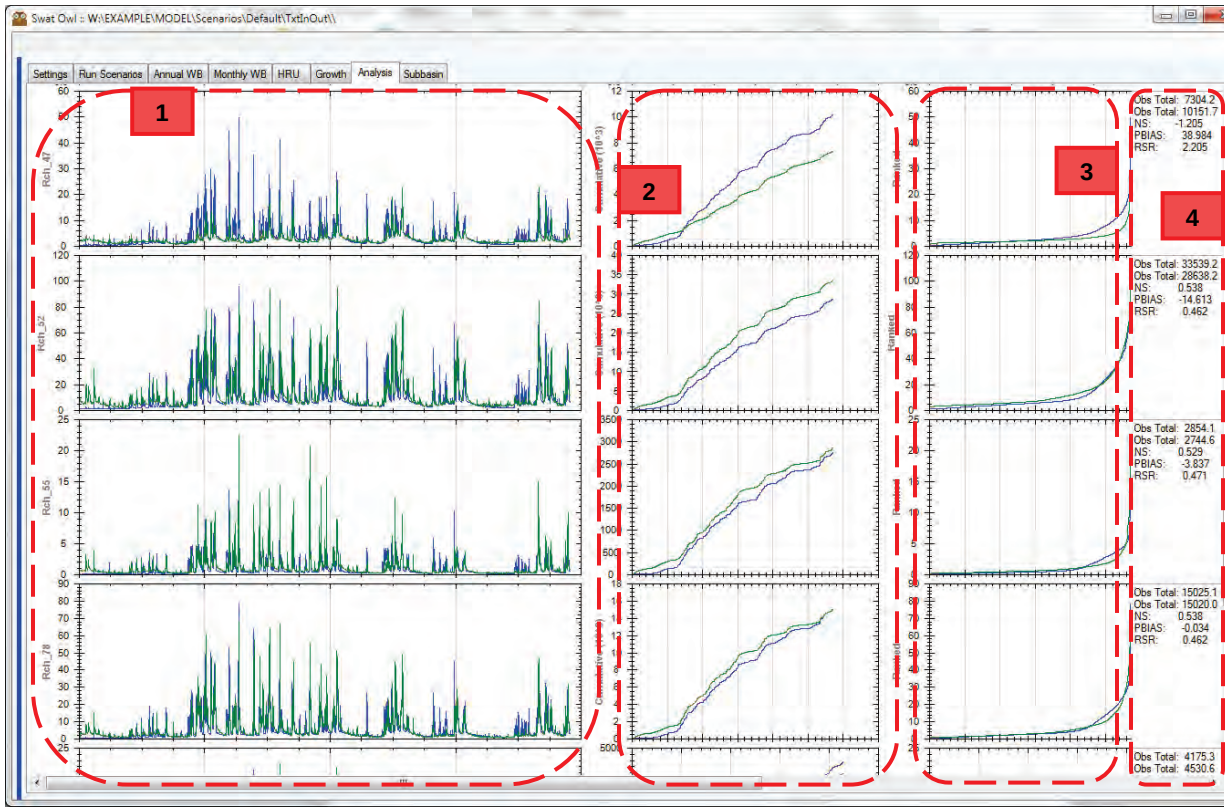

1. The observed and modelled flow series for the selected period.
2. Cumulative observed and modelled flows for each modelled day with valid observation data.
3. Modelled and observed flow (ranked by magnitude of observed flows) for each modelled day with valid observation data.
4. Correlation analysis for observed and modelled flow series showing:
   - NS (Nash-Sutcliffe) value
   - PBIAS (Percentage Bias)
   - RSR (ratio of root-mean-square error of simulated streamflow to the standard deviation of the measured data)

Calibration Input File Formats

Modelled data is read from the reach files which should be specified in fig.fig file, using the following filename format:

- reach?.dat (where ? is the number of each modelled reach to be analysed

Observed data is read from text file prepared by the modeller. A file corresponding to each reach?.dat file should be prepared are placed in the model 'TxtInOut' folder using the following filename format:

- ObsFlow?.csv (where ? is the number of each modelled reach to be analysed

Each CSV should start on the same date as the model outputs and should be formatted following the example given below:

Date,Q[m3/s]
01/01/2005, 0.020
02/01/2005, 0.023
03/01/2005, 0.032
04/01/2005, 0.07
05/01/2005, 0.075
etc.

Graph Functionality

The graphs within Swat Owl contain a number of different features. Figure A11 gives and overview of some of the graph features that accessed by the user.

Figure A11: Graph Functions in Swat Owl

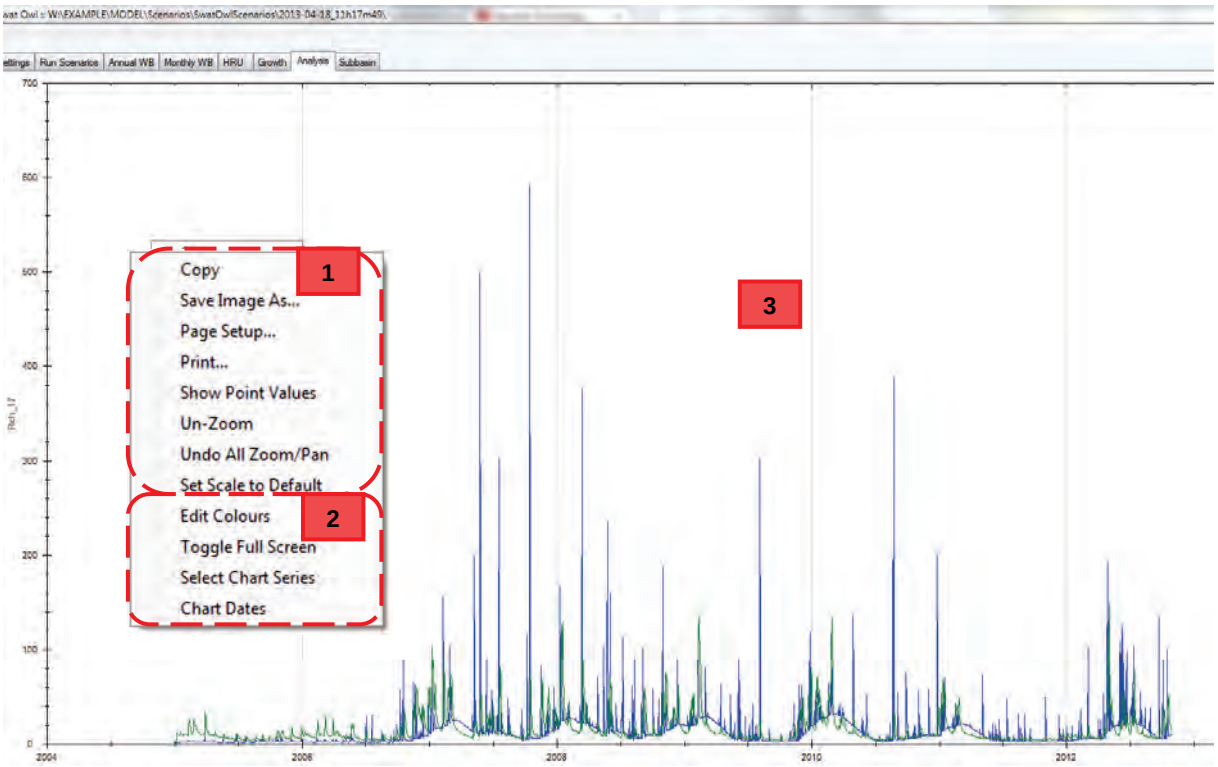

A context menu can be activated by right-clicking on the charts within Swat Owl. The context menu contains two sets of menu items.

1. Generic methods included in ZedGraph (the graphing module used). See http://zedgraph.sourceforge.net.
2. Custom menu items added for Swat Owl, including:
   - Edit Colours – Allows the colour of plotted data series to be changed.
   - Toggle Full Screen – Shows a larger version of the selected graph.
   - Select Chart Series – Shows or hides chart series as per selection.
   - Alters the chart start and end dates.

Additional graph features are available using the mouse buttons:

3. Use the mouse buttons with the graph background selected:
   - Draw a box whilst click and holding the left mouse button to zoom in/out.
   - Use the scroll button to zoom in or out.
   - Click and hold the scroll button to pan in any direction.

New insight into pesticide partition coefficient K_d for modelling pesticide fluvial transport with the SWAT model

Laurie Boithias*

University of Toulouse; INPT, UPS; Laboratoire Ecologie Fonctionnelle et Environnement (EcoLab), Avenue de l'Agrobiopole, 31326 Castanet Tolosan Cedex, France;

CNRS, EcoLab, 31326 Castanet Tolosan Cedex, France.

* l.boithias@gmail.com

Sabine Sauvage

University of Toulouse; INPT, UPS; Laboratoire Ecologie Fonctionnelle et Environnement (EcoLab), Avenue de l'Agrobiopole, 31326 Castanet Tolosan Cedex, France;

CNRS, EcoLab, 31326 Castanet Tolosan Cedex, France.

Georges Merlina

University of Toulouse; INPT, UPS; Laboratoire Ecologie Fonctionnelle et Environnement (EcoLab), Avenue de l'Agrobiopole, 31326 Castanet Tolosan Cedex, France;

CNRS, EcoLab, 31326 Castanet Tolosan Cedex, France.

Séverine Jean

University of Toulouse; INPT, UPS; Laboratoire Ecologie Fonctionnelle et Environnement (EcoLab), Avenue de l'Agrobiopole, 31326 Castanet Tolosan Cedex, France;

CNRS, EcoLab, 31326 Castanet Tolosan Cedex, France.

Jean-Luc Probst

University of Toulouse; INPT, UPS; Laboratoire Ecologie Fonctionnelle et Environnement (EcoLab), Avenue de l'Agrobiopole, 31326 Castanet Tolosan Cedex, France;

CNRS, EcoLab, 31326 Castanet Tolosan Cedex, France.

José-Miguel Sánchez-Pèrez

University of Toulouse; INPT, UPS; Laboratoire Ecologie Fonctionnelle et Environnement (EcoLab), Avenue de l'Agrobiopole, 31326 Castanet Tolosan Cedex, France;

CNRS, EcoLab, 31326 Castanet Tolosan Cedex, France.

Raghavan Srinivasan

Grassland, Soil & Water Research Laboratory, Texas A&M University, Temple, Texas 76502 USA

Jeff Arnold

Grassland, Soil & Water Research Laboratory, USDA-ARS, Temple, Texas 76502 USA

Abstract

Pesticides used for crop protection are leached with rainfall events to groundwater and surface water. The bioavailable dissolved fraction threatens the fluvial ecosystems. Pesticide partitioning in the environment is therefore one of the key pesticide fate processes that should be properly formalized for risk assessment. In modelling approaches, the partition coefficient K_d is usually estimated from different empirical models based on laboratory batch studies, such as Karickhoff equation. We first showed that the partition parameter in SWAT was more sensitive in the river network than in the soil. Therefore we sought a new relationship for K_d in rivers, relating K_d to the octanol/water distribution coefficient K_{ow} and to the Total Suspended Matter (TSM) concentration. This relationship was obtained from in-stream measurements of TSM and of Particulate Organic Carbon (POC) sampled from 2007 to 2010 at the outlet of the 1110 km² Save catchment. We also calculated the K_d values of 7 pesticide molecules for both high flow and low flow periods (2009-2010). We sought a relationship between TSM and the percentage of POC in TSM. We related the organic carbon normalized partition coefficient K_{oc} to K_{ow}. We showed a bias of 0.5 between in-stream observed K_{oc} average values and K_{oc} values calculated with Karickhoff's equation. Thus, we expressed K_d depending on the widely literature-related variable K_{ow} and on the commonly observed and simulated TSM concentration: K_d became a variable in time and space depending on simulated TSM concentration. The novel equation can be implemented in the SWAT model.

Keywords: Sorption, Flood, SWAT model, Save river.

Introduction

Intensive agriculture is known to have a detrimental effect on soils, on surface water and on groundwater quality. Organic pollutants, such as excessive pesticides loading from cultivated land, are transferred to surrounding surface water either dissolved or sorbed to particles, and may be harmful to aquatic ecosystems (Betekov et al., 2013; Polard et al., 2011; Proia et al., 2013). Pesticides loads may also render stream water and groundwater unfit for drinking water provision (EC, 1998). Recent studies in the south-western France area showed the role of intense rainfall events such as floods on pesticides fate and transport (Boithias et al., 2011, 2014; Taghavi et al., 2010, 2011). Understanding pesticide dynamics during storm events is actually of major importance to assess surface water quality degradation risk and models, such as SWAT (Arnold et al., 1998), are useful for large-scale assessments. However, Boithias et al. (2011, 2012) showed that the partition of pesticide modeled with SWAT could be not realistic (see the inversion of partition during the beginning of May 2010 flood in Fig. 1).

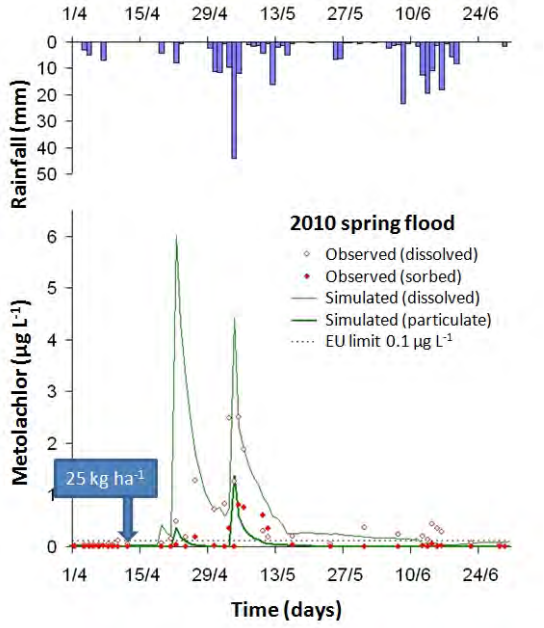

Fig. 1. Simulated and observed metolachlor concentrations at the outlet of the Save catchment during the 2010 April-June high flow period (adapted from Boithias et al., 2011, 2012).

Adsorption of pesticides to the solid phase (organic matter and clay content) is a key process driving the transport and fate of pesticides in the environment that is usually quantified by the partition coefficient K_d. To parameterize K_d in the SWAT model, Neitsh et al. (2009) suggest to use both the relationship of Karickhoff et al. (1979) between the organic carbon normalized partition coefficient (K_{oc}) and the octanol/water distribution coefficient (K_{ow}), together with the assumption of Chapra (1997) regarding a constant organic matter content (f_{oc}). Thus, K_d is defined for each molecule as a constant value in time and space for a whole drainage network.

In this study, we handle the hypothesis that K_d varies over time and space following the dynamics of suspended matters and specifically the dynamics of organic fraction, and that this dynamics should be more accurately included within the SWAT model for its further use as a large scale pesticide fate model. The aims of this study were therefore (1) to check to which extent the K_d depends on the hydrological regime, (2) to check which parameters in the SWAT model are mostly driving the pesticide partition, and (3) to establish a relationship between K_d, K_{ow} and TSM. Thus the pesticide-specific K_d parameter could become a variable in time and space, implementable in the SWAT model.

Material and methods

Study area

The river Save is located in south-western France and drains an area of 1110 km² (Fig. 2). Calcic soils stem from molasses and represent 61% of the whole catchment area with a clay content ranging from 35% to 50%. They are located on the top of the hills and on their slopes. Non-

calcic silty soils represent 30% of the soil in this area (40–60% silt). They are mainly located downstream, close to the Garonne alluvial plain. Alluvial deposits are found along the streams and represent 9% of the catchment area (Boithias et al., 2013). Top soil organic matter content is about 2% (Veyssy et al., 1999).

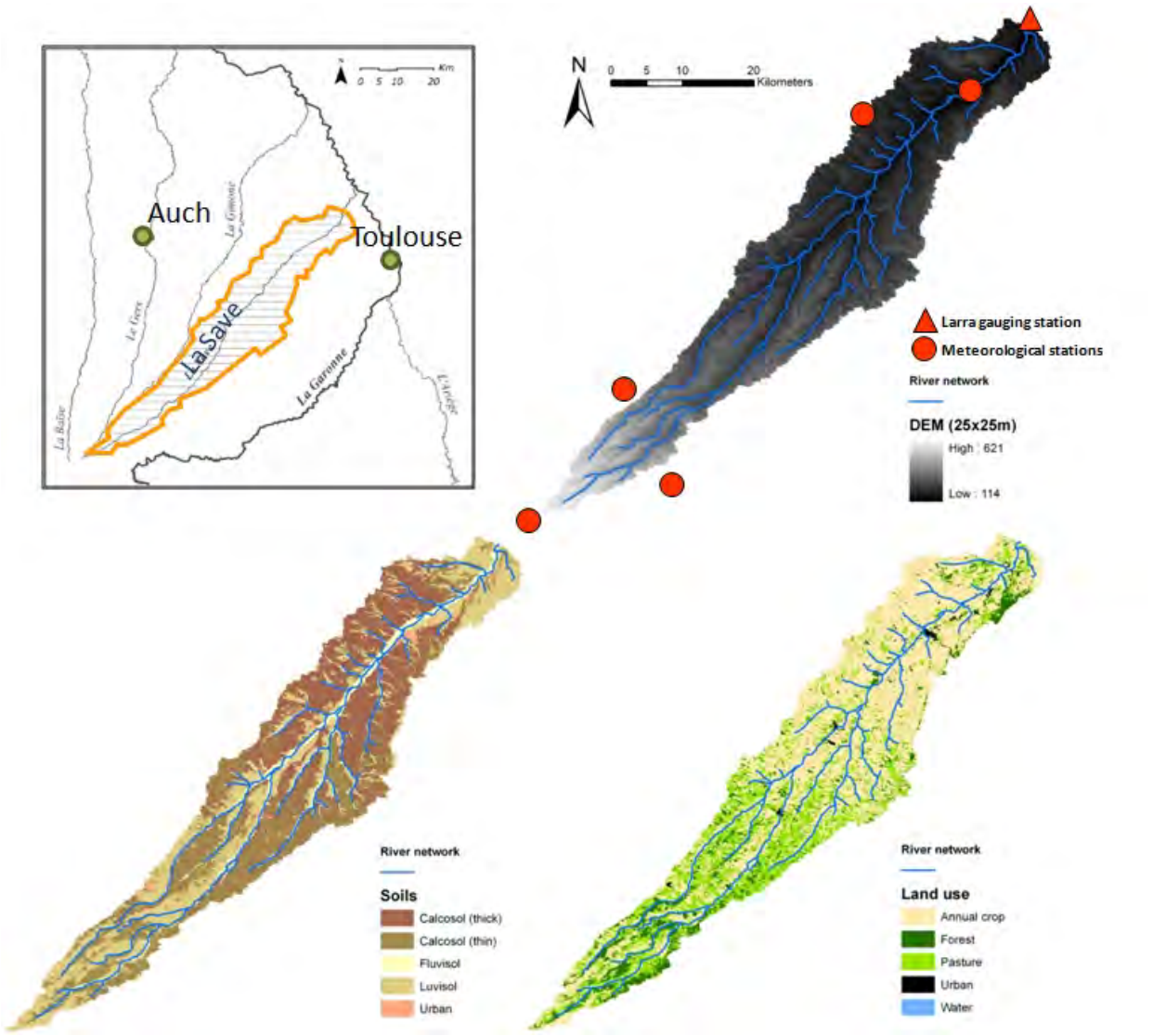

Fig. 2. The Save river catchment (localization, altitudes, soils and land uses).

The climate is temperate oceanic. The river Save hydrological regime is mainly pluvial with a maximum discharge in May and low flows during the summer (July–September). The annual precipitation is of 600 to 900 mm with an annual evapotranspiration of 500–600 mm (1998–2010). Mean annual discharge measured by the hydrometric station at the catchment outlet is about 6.1 $m^3 s^{-1}$ (1998–2010). During low flows, the river flow is sustained upstream by the Neste canal (about 1 $m^3 s^{-1}$) that derives water from a Pyrenean river for irrigation purpose (data from Compagnie d'Aménagement des Coteaux de Gascogne – CACG).

Approximately 90% of the catchment surface is devoted to agriculture. The upstream part of the catchment is a hilly agricultural area mainly covered with pasture and forest associated to cereals and corn on small plateaus (Macary et al., 2013). The downstream part is devoted to intensive

agriculture with mainly both corn grown as monoculture and a 4–year crop rotation alternating winter wheat with sunflower and corn, sorghum or soybean. The 110 km^2 of corn are irrigated with 210 mm yr^{-1} of water from July to September (Boithias et al., 2013).

Observed data

The river Save discharge was monitored continuously from 2007 to 2010 at the catchment outlet gauging station (Fig. 2) by the CACG. Also at the catchment outlet, Total Suspended Matter (TSM) and Particulate Organic Carbon (POC) were monitored from July 2009 to October 2010, both manually and automatically, as described in previous studies on the same catchment (Oeurng et al., 2011). An automatic water sampler, connected to a probe, was programmed to activate pumping water for 30 cm water level variations during high flows, for the rising and falling stages, thus providing 1 to 29 river water samples per stormflow event depending on its intensity. Grab sampling was also undertaken near the probe position at weekly intervals during low flow. TSM and POC laboratory analysis were performed as described in Oeurng et al. (2011). Additional POC and TSM concentrations measured from January 2007 to March 2009 (Oeurng et al., 2011) were used in this study. The pesticide laboratory analysis of the 170 collected samples was performed as described by Taghavi et al. (2010, 2011) on both filtered and unfiltered extracts of the same sample of water with a limit of detection ranging between 0.001 to 0.003 µg L^{-1} depending on the molecule. A total of 7 non-charged molecules with log(K_{ow}) values ranging from 1.5 to 4.8 (mean = 3±1) were considered in this study (alachlor, atrazine, deethylatrazine (DEA – metabolite of atrazine), isoproturon, metolachlor, tebuconazole and trifluralin).

Values of TSM, POC and pesticides concentrations were aggregated at hydrological event scale in order to avoid the bias stemming from the data sampling frequency. K_d (L mg^{-1} or m^3 g^{-1}) at hydrological event scale were then calculated based on the measured pesticides concentrations in raw and filtered water samples:

$$K_d = \frac{C_{sorbed}}{C_{soluble}}$$

where C_{sorbed} (µg mg^{-1} or mg g^{-1}) and $C_{soluble}$ (µg L^{-1}) are the observed pesticide concentrations in sorbed and dissolved phases respectively. K_{oc} ((mg gC^{-1}) / (mg m^{-3})) at hydrological event scale were calculated following:

$$K_{oc} = \frac{K_d}{f_{oc}}$$

where f_{oc} is the organic matter content included in TSM (gC g^{-1}).

Sensitivity analysis

In the SWAT model, the partition of pesticides is differently expressed depending on the modeled compartment (Neitsch et al., 2009) (Table 1).

Table 1. Partition coefficients in the SWAT model.

Partition in soil (K_p)	Partition in river (F_d)
$K_p = f_{oc} \cdot SK_{oc}$	$F_d = \frac{1}{1 + CK_{oc} \cdot TSM}$

The sensitivity of the inputs SK_{oc} and CK_{oc} driving the partition in SWAT was assessed for both metolachlor and aclonifen at catchment outlet. It was calculated as the average (S) of 10 relative sensitivity indices (S_i) (Melching and Yoon, 1996):

$$S_i = \frac{\partial P}{\partial I} \cdot \frac{I}{P(I)}$$

With P the prediction (the 1998−2010 average ratio between sorbed and dissolved pesticide loads in the soil and at the catchment outlet, respectively) and I the input value (SK_{oc} or CK_{oc}, respectively). The sensitivity analysis was performed on a previously calibrated SWAT project regarding hydrology, suspended sediments, nitrate and pesticides (Boithias et al., 2012, 2013). Both the SK_{oc} and CK_{oc} were changed within a [−50%;+50%] range with regard to the calibrated values of SK_{oc} and CK_{oc}.

Results from the field

The data set allowed segregating 11 high flow periods and 5 low flow periods. The K_d values (Fig. 3) calculated at the outlet of the Save catchment are in the range of the K_d value reported by other studies in the environment by Maillard et al. (2011), Taghavi et al. (2010) and Tomlin et al. (2009). A dominant trend for all molecules is that K_d changes depending on the hydrological regime: (1) the minimal K_d value is observed during high flows and (2) the median K_d value increases during low flows.

In addition, strong correlations are found between POC and TSM (R^2 = 0.97) and between POC and maximal discharge (R^2 = 0.92), suggesting that K_d strongly depends on the discharge (Boithias et al., 2014).

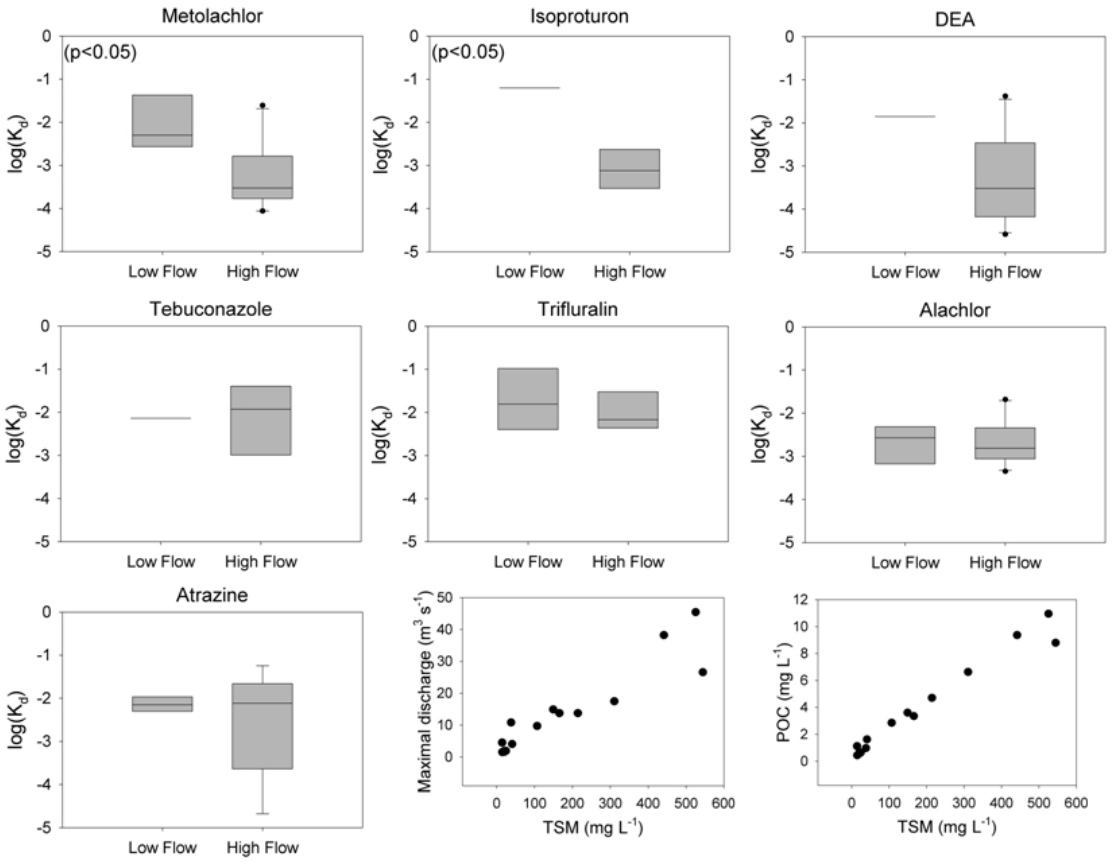

Fig. 3. K_d values of 7 pesticide molecules at the outlet of the Save catchment during high flow and low flow (2009-2010) (Boithias et al., 2014).

Results from the SWAT model

The sensitivity analysis shows that the parameter driving the partition in the river is three times more sensitive than the parameter driving the partition in the soil for both pesticides modeled with SWAT (Table 2). Therefore, we focus on the SWAT parameter driving the partition in the river (CK_{oc}).

Table 2. Sensitivity indices of partition coefficients in both soil and river (outlet) within the SWAT model for both metolachlor and aclonifen pesticides.

	S_i mean	
	Metolachlor	**Aclonifen**
Partition in the soil (SK_{oc})	-0,44	-0,30
Partition in the river (CK_{oc})	-1,17	-0,95

A novel equation to be implemented in the SWAT model

Using the $K_d = f_{oc} \cdot K_{oc}$ equation, we sought a relationship between f_{oc} and the TSM concentration, that is easily measurable and simulated in the SWAT models, and between K_{oc} and the widely literature-related variable K_{ow}.

Relationship between f_{oc} and TSM

The Fig. 4 shows that f_{oc} (-) decreases when TSM (mg L^{-1}) increases, following a hyperbolic equation (please see Boithias et al. 2014 for full details):

$$f_{oc} = \frac{0.09}{TSM - 5} + 0.02$$

The vertical asymptote is the minimal TSM concentration at catchment outlet, whereas the horizontal asymptote is the rate of organic matter reported for south-western France top soils.

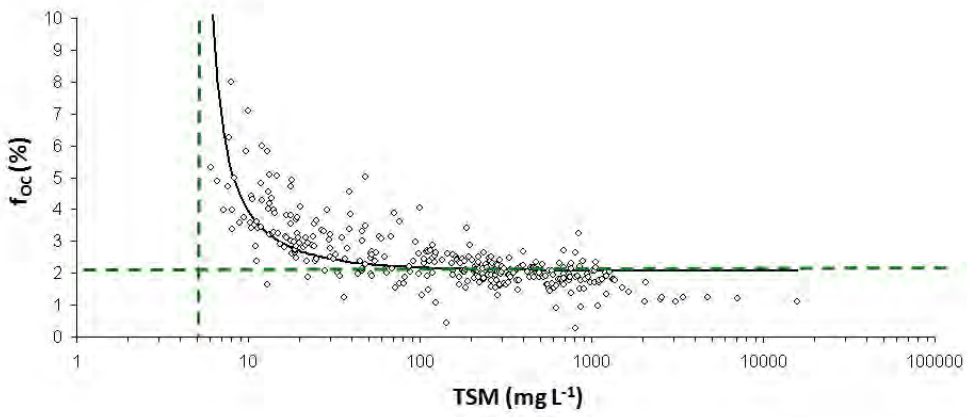

Fig. 4. Relationship between the measured total suspended matter (TSM) and the measured organic carbon content in TSM (f_{oc}) at the outlet of the Save catchment (data collected from 2007 to 2010) (Boithias et al., 2014).

Relationship between K_{oc} and K_{ow}

The Fig. 5 shows that K_{oc} and K_{ow} are related by the following equation (please see Boithias et al. 2014 for full details):

$$K_{oc} = 0.01 \cdot K_{ow}^{0.4}$$

Where K_{oc} is in ((mg gC^{-1}) / (mg m^{-3})) and K_{ow} is in ((mg $m_{octanol}^{-3}$) / (mg m_{water}^{-3})). It is worth noting that in the case of the Save catchment, the slope of the equation is about two times lower than the slope calculated from the equation published by Karickhoff et al. (1979). The conditions of experiments described in Karickhoff et al. (1979) were different to ours in the Save river catchment. Karickhoff et al. (1979) worked in batch laboratory conditions, using sediments of homogeneous silt fractions and dilution rates that are not the ones reported in the Save river water. Also, the average log(K_{ow}) value of the molecules they studied is two logarithmic units higher than the average log(K_{ow}) value of the molecules we analyzed. Please see Boithias et al. (2014) for full details.

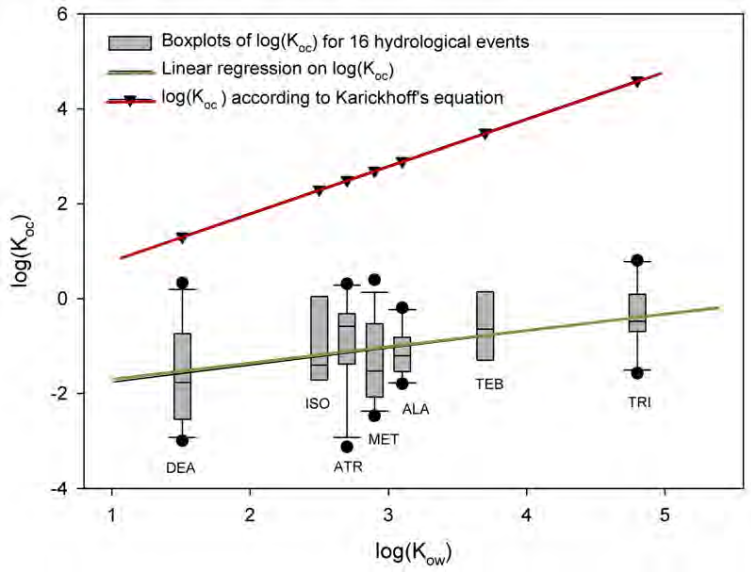

Fig. 5. Relationship between K_{oc} and K_{ow} at river Save catchment outlet for 7 pesticide molecules (alachlor, atrazine, deethylatrazine, isoproturon, metolachlor, tebuconazole and trifluralin) (data collected from 2009 to 2010) (Boithias et al., 2014).

Conclusion

This study provided a K_d (L mg^{-1} or m^3 g^{-1}) calculation method based on the easily measurable and easily SWAT modeled TSM concentration, and on the widely literature-related variable K_{ow}:

$$K_d = \left(\frac{0.09}{TSM - 5} + 0.02 \right) \cdot (0.01 \cdot K_{ow}^{0.4})$$

This study also highlighted that:

1. The sensitivity of the partition coefficient parameter in the SWAT model is three times stronger for the river than for the soil.
2. The hyperbolic relationship between TSM and f_{oc} allows predicting K_d for each hydrological condition through the simple measure or the easy simulation of TSM. K_d is expressed for each molecule through its specific K_{ow}.
3. The use of the equation of Karickhoff et al. (1979) for pesticide partition in river may not be suitable to parameterize the SWAT model, as such K_{oc} values do not include the full variability depending on the hydrological conditions.
4. The parameters of the latter equation are easily understandable, and few data of discharge, TSM, POC and corresponding pesticides concentrations are needed to properly calibrate its parameters.

At last, the here-suggested equation can be applied to a wide range of catchments and organic contaminants.

Acknowledgements

This work was performed as part of the EU Interreg SUDOE IVB program (SOE1/P2/F146 AguaFlash project, http://www.aguaflash-sudoe.eu) and funded by ERDF and the Midi-Pyrénées Region. We sincerely thank the CACG for discharge data and Ecolab staff for field and laboratory support.

References

Arnold, J.G., R. Srinivasan, R.S. Muttiah, and J.R. Williams. 1998. Large area hydrologic modeling and assessment. I. Model development. *J. Am. Water Resour. Assoc.* 34(1):73–89.

Beketov, M.A., B.J. Kefford, R.B. Schafer, and M. Liess. 2013. Pesticides reduce regional biodiversity of stream invertebrates. *PNAS* 110:11039–11043.

Boithias, L., S. Sauvage, L. Taghavi, G. Merlina, J.L. Probst, and J.M. Sánchez Pérez. 2011. Occurrence of metolachlor and trifluralin losses in the Save river agricultural catchment during floods. *J. Hazard. Mater.* 196:210–219.

Boithias, L., S. Sauvage, G. Merlina, S. Jean, J.L. Probst, and J.M. Sánchez-Pérez. 2014. New insight into pesticide partition coefficient K_d for modelling pesticide fluvial transport: application to an agricultural catchment in south-western France. *Chemosphere* In press DOI: 10.1016/j.chemosphere.2013.10.050.

Boithias, L., S. Sauvage, R. Srinivasan, F. Macary, and J.M. Sánchez-Pérez. 2012. Sensitivity of the pesticide application date for pesticide fate modelling during floods using the SWAT model. 2012 International SWAT Conference, July 18-20, Delhi, India.

Boithias, L., R. Srinivasan, S. Sauvage, F. Macary, and J.M. Sánchez-Pérez. 2013. Daily nitrate losses: implication on long term river quality in an intensive agricultural catchment (south-western France). *J. Environ. Qual.* In press DOI: 10.2134/jeq2011.0367.

Chapra, S.C. 1997. *Surface water-quality modeling*. McGrawHill, Boston, USA.

EC, 1998. Directive 98/83/EC of 3 November 1998 on the quality of water intended for human consumption. Off. J. Eur. Communities L330, Off. J. Eur. Communities L330.

Karickhoff, S.W., D.S. Brown, and T.A. Scott. 1979. Sorption of hydrophobic pollutants on natural sediments. *Water Res.* 13(3):241–248.

Macary, F., O. Leccia, J. Almeida Dias, S. Morin, and J.M. Sánchez-Pérez. 2013. Agro-environmental risk evaluation by a spatialised multi-criteria modelling combined with the PIXAL method. *Int. J. Geomatics Spatial Anal.* 23 :39–70.

Maillard, E., S. Payraudeau, E. Faivre, C. Grégoire, S. Gangloff, and G. Imfeld. 2011. Removal of pesticide mixtures in a stormwater wetland collecting runoff from a vineyard catchment. Sci. *Total Environ.* 409:2317–2324.

Melching, C.S., and C.G. Yoon. 1996. Key Sources of Uncertainty in QUAL2E Model of Passaic River. *J. Water Resour. Plann. Manage.* 122:105–113.

Neitsch, S.L., J.G. Arnold, J.R. Kiniry, and J.R. Williams. 2009. Soil and Water Assessment Tool theoretical documentation - version 2009 (TR406).

Oeurng, C., S. Sauvage, A. Coynel, E. Maneux, H. Etcheber, and J.M. Sánchez-Pérez. 2011. Fluvial transport of suspended sediment and organic carbon during flood events in a large agricultural catchment in southwest France. *Hydrol. Process.* 25(15):2365–2378.

Polard, T., S. Jean, L. Gauthier, C. Laplanche, G. Merlina, J.M. Sánchez-Pérez, and E. Pinelli. 2011. Mutagenic impact on fish of runoff events in agricultural areas in south-west France. *Aquat. Toxicol.* 101(1):126–134.

Proia, L., V. Osorio, S. Soley, M. Köck-Schulmeyer, S. Pérez, D. Barceló, A.M. Romaní, and S. Sabater. 2013. Effects of pesticides and pharmaceuticals on biofilms in a highly impacted river. *Environ. Pollut.* 178:220–228.

Taghavi, L., G. Merlina, and J.L. Probst. 2011. The role of storm flows in concentration of pesticides associated with particulate and dissolved fractions as a threat to aquatic ecosystems. Case study: the agricultural watershed of Save river (Southwest of France). Knowl. Manage. *Aquat. Ecosyst.* 400(06):11.

Taghavi, L., J.L. Probst, G. Merlina, A.L. Marchand, G. Durbe, and A. Probst. 2010. Flood event impact on pesticide transfer in a small agricultural catchment (Montousse at Aurade, south west France). *Int. J. Environ. Anal. Chem.* 90(3):390–405.

Tomlin, E. 2009. *The Pesticide Manual*, Fifteenth ed, A World Compendium. C.D.S. Tomlin.

Veyssy, E., H. Etcheber, R.G. Lin, P. Buat-Menard, and E. Maneux. 1999. Seasonal variation and origin of particulate organic carbon in the lower Garonne River at La Reole (southwestern France). *Hydrobiologia* 391:113–126.

Using SWAT Models to Inform Catchment Management Approaches to Pesticide Control – A UK Water Industry Case Study.

Philip Selby, Catchment Modeller
Mott MacDonald, Integrated Water Resources Management
Cambridge CB1 2RS, UK, philip.selby@mottmac.com

Dr Frances Elwell, Water Quality Scientist
Mott MacDonald, Integrated Water Resources Management
Mott MacDonald, Cambridge CB1 2RS, UK.

Jenny Sandberg, Catchment Modeller
Anglian Water, Water Resources Management Team
Milton House, Cowley Road, Cambridge, CB4 0AP

Abstract

The UK Water Industry is concerned about metaldehyde (used in some molluscicides*) which is being found in surface water and groundwater. A regulatory limit of 0.1µg/l of any pesticide is in place for drinking water. Concentrations above this limit have been recorded in raw water and metaldehyde is difficult and expensive to remove through water treatment. Anglian Water, the largest UK water company by area, is exploring the potential benefits of working with the agricultural sector to change how, where and when metaldehyde is used – work which falls under their catchment management programme.*

The potential effectiveness of catchment management in reducing diffuse metaldehyde pollution is being investigated using SWAT. In total, 23 surface water catchments are being modelled. The models are being calibrated using measured stream flows and metaldehyde concentrations. Catchment management scenarios are then modelled by changing the land use and management operations in SWAT.

New approaches and tools have been developed to apportion arable crop types based on historic percentages of arable land and assuming typical crop rotations. Stochastic techniques have been used to select subbasins/HRUs to implement catchment management scenarios by changing land use and reducing metaldehyde applications, and/or using alternative pesticides. The results of these scenarios are informing Anglian Water's business planning for catchment management.

This paper describes how SWAT is being used to test catchment management scenarios; sets out the methods that have been developed to implement the scenarios; and, shows how the results are being compared and interpreted.

Keywords: SWAT, catchment management, pesticide, metaldehyde, diffuse pollution, water quality, land use, management operations.

Introduction

Anglian Water is assessing the feasibility of using catchment management solutions to improve raw water quality at their drinking water abstractions. The primary driver is the existing regulatory standard of 0.1 µg/l for individual pesticides in drinking water (EU Drinking Water Directive 98/83/EC) and Article 7 of the Water Framework Directive (2000/60/EC). Metaldehyde is a pesticide used in some molluscicides, which are applied to the soil to protect crops from slug damage during their early development – most typically, in East Anglia, to protect winter wheat and winter oil seed rape, which are sown in early autumn. Metaldehyde is primarily carried into water courses during rainfall-runoff events through direct run off, through field drains and through lateral flow through the soils.

The objective of this project is to assess the feasibility of using catchment management measures to manage risk from metaldehyde to drinking water abstractions (river intakes, raw water reservoirs with natural catchments or pumped storage). Measures considered include:

- Promoting best practice as to how, where and when metaldehyde is used,
- Encouraging reductions in the amount of metaldehyde that is applied to fields, and
- Promoting use of alternative pesticides.

Numerical models are being built using SWAT for 23 surface water catchments to assess the effectiveness of using catchment management measures to reduce in-stream metaldehyde concentrations and help to enhance understanding of how metaldehyde enters the watercourse. This is enabling a more targeted approach to catchment management to be developed. Alongside the numerical modelling stakeholder liaison is taking place (for example, with Catchment Sensitive Farming (CSF) groups and the UK Environment Agency. Figure 1, outlines this process.

Figure 1: Overview of Anglian Water's Surface Water Catchment Modelling Process

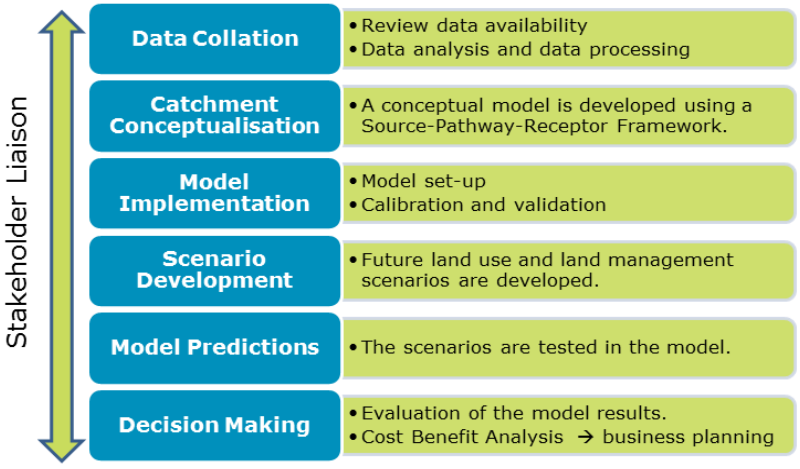

This paper reports on how the approach to modelling the catchments has been developed since the modelling was initiated, building on approaches outlined in Sandberg & Elwell (2011). Methods have been developed to build the SWAT models in a way that allows Anglian Water to

explore catchment management issues. A selection of these methods has been presented in this paper, falling into the following categories:

- Catchment conceptualisation.
- Model set-up and development of tools
- Calibration of in-stream metaldehyde concentrations.
- Implementation of catchment management scenarios.

Catchment Conceptualisation

Significant efforts have been made to develop sound conceptual models of the modeled catchments in relation to available data and spatial scale. This includes identifying the principal pathways of metaldehyde in relation to soil type and land use. A generic conceptual model was developed which can be refined for each catchment during the calibration process.

Metaldehyde Pathways

Given that metaldehyde was first detected in drinking water in 2007, there is relatively little information available on fate and behavior of the substance in the environment. However, a number of (unpublished) small-scale field studies indicate that the primary pathways of metaldehyde are via surface runoff and field drains in the autumn and winter. Bypass flow though soils cracks is also thought to be important, particularly where cracks are connected to underlying drains. Other possible pathways for metaldehyde from source into stream will include:

- Direct application to water, ditches or drainage channels, and point sources from poor application and spillages
- Lateral flow through soil matrix
- Lateral flow via groundwater

Additionally, upstream reservoirs, storage lakes, ponds and other areas of standing water may accumulate or attenuate metaldehyde, either increasing its concentration through evaporation or diluting it where mixing takes place, also influencing metaldehyde concentrations in upstream storage. Finally metaldehyde can enters a water supply reservoir where it is influenced by rainfall, evaporation, abstraction for water supplies and irrigation, reservoir sediment levels and bedrock permeability.

Metaldehyde can be transferred through the catchments in three forms:

- Dissolved chemical;
- Pellet Fragments; and
- Chemical sorbed to mobilised sediments.

Table 1 and Figure 5 summarise the potential diffuse pathways and their relevance to the various forms of metaldehyde.

Figure 5: Generic conceptual model of metaldehyde pathways and degradation.

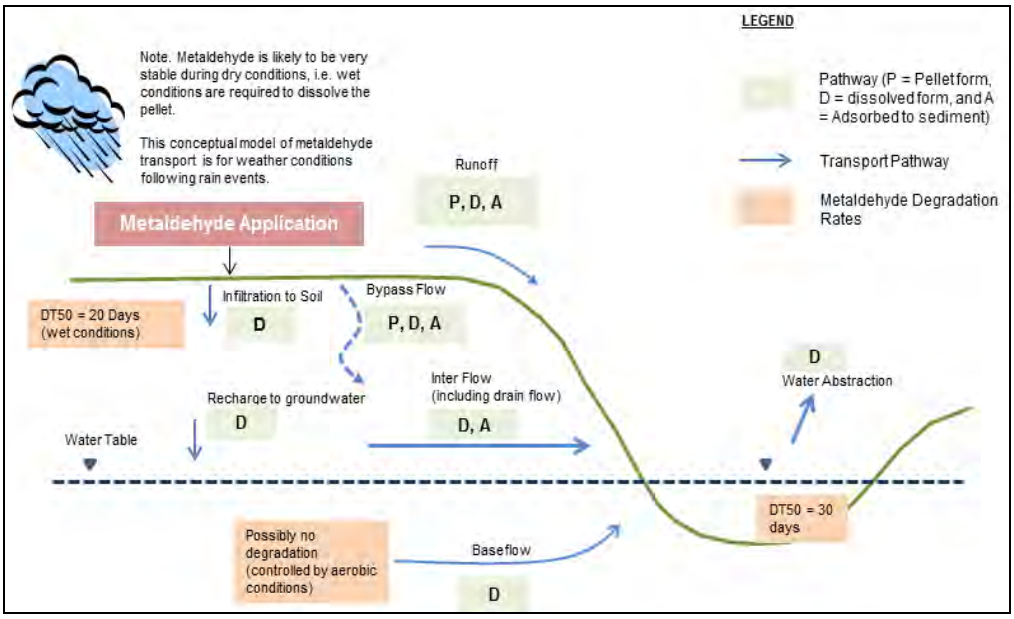

Table 1: Relevance of pathways for different forms of metaldehyde.

Pathway	Pellet	Dissolved in Water	Sorbed to Sediment
Surface Runoff	X	X	X
Infiltration through soil profile		X	
Underdrainage		X	X
Bypass Flow	X	X	X

Land use

As metaldehyde usage is associated with particular crops it is important to establish an understanding of the cropping patterns within the catchments. Field scale data is not available for this study; hence a simplified set of possible rotations is defined for the catchments using generic information about rotation patterns on different types of soils within the Anglian region.

To incorporate this to the SWAT models, a stochastic Excel tool was developed and is further explained below, in the 'Assigning Crop Types and Rotations' section.

Model Set-up and Development of Tools

The models have been set-up with a view of an easy implementation of catchment scenarios. This includes ensuring that the delineation of Hydrological Response Units (HRUs) takes into account the key features identified in the conceptual models, such as the role of soil type on metaldehyde pathways. A number of pre-processing tools have been developed to simplify model set-up and to reduce the risk of error. One of these (the crop rotation tool) is described in this section.

Spatial Representation of Catchments

The HRU definition splits subbasins into HRUs according to threshold percentages (by area) of soil, land use, and slope. For the catchment management scenarios the most important of these categories is land use, as the quantities of metaldehyde applied to arable land depend on crop types, followed by soil type.

Catchment management scenarios differentiate between arable land use next to the main streams and further away and a method of differencing these areas, which can be employed in scenario testing, has been defined:

- Buffer strips were drawn around the streams (as polygons in ArcGIS). As an example, in the Grafham catchment, which represents a large catchment covering approximately 2600 km^2 buffer strips were drawn at a distance of 1000 m and 2000 m around the stream lines.
- The buffer strip polygons were used to intersect the land use layer creating a number of subcategories for each arable land use according to its maximum distance from the stream.
- Further GIS processing was carried out to combine any polygons less than a threshold area into adjacent polygons.
- The land use layer was reclassified according to these sub categories using three surrogate land use types (crop types are assigned to each HRU in the management operations set up).

The sub-categorisation of the arable land increased the number of HRUs. To limit the number of HRUs the slope was defined as a single category as it was found that there was sufficient spatial distribution of the HRUs without using it (i.e. to accurately represent model domains and to run land management scenarios). Thresholds of 5% for land use and soils were used in the HRU definition.

A flow chart showing the framework that was used to set up the HRUs is shown in Figure 3.

Figure 3: Implementation of HRUs for Catchment Management Model

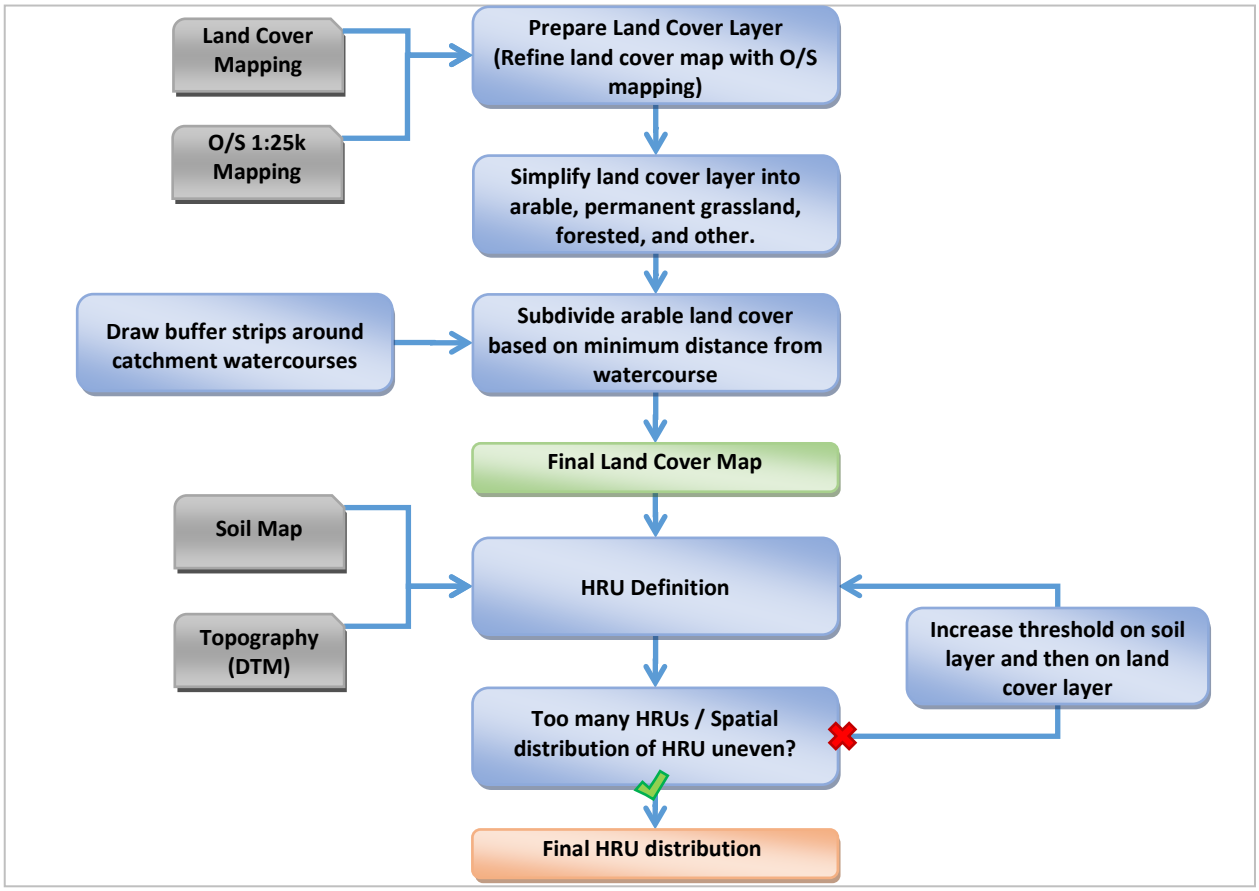

Assigning Crop Types and Rotations

Crop rotations were included by assigning appropriate crop types to the HRUs for each model. For the catchment models, whilst detailed mapping showing arable land cover is available, there is insufficient data to accurately assign particular crop rotations to the HRUs. Instead, general knowledge of cropping patterns and information on the proportions of crops planted in each year was assumed to synthesise a crop planting schedule for each HRU.

To match the percentages of each crop type in the catchment as closely as possible, a stochastic process was used. Crop rotations are randomly picked from a list of probable rotation sequences and the resulting proportion of crop types is compared with target crop proportions. The process iterates until the solution with the lowest residual error is found between simulated and observed land use proportions. A percentage tolerance, for which calculated and target levels should match, was allocated to each crop. The process is illustrated in Figure 4.

The entire process is implemented in Microsoft Excel. The outcome is a matrix giving the complete list of HRUs with crop types for each year of the rotation sequence. Visual basic routines are then used to write the management tables for each based on this information and generic operations for each type of crop.

Figure 4: Stochastic Assignment of Land Use According to Target %

Subbasin	HRU*	Area	Selected Rotation	Year 1	Year 2	Year 3	Year 4	Year 5	Year 6
1	1	1.01	15	WWHT	GRBN	WWHT	WWHT	CANA	WWHT
1	2	3.58	7	WWHT	WWHT	WWHT	WWHT	WWHT	WWHT
1	3	3.01	2	WWHT	CANA	WWHT	WWHT	WWHT	WWHT
2	4	2.23	5	WWHT	WWHT	WWHT	WWHT	CANA	WWHT
2	5	1.20	6	WWHT	WWHT	WWHT	WWHT	WWHT	CANA
2	6	1.76	9	WWHT	CANA	WWHT	WWHT	CANA	WWHT
3	7	0.97	14	GRBN	WWHT	WWHT	CANA	WWHT	WWHT
3	8	0.02	8	CANA	WWHT	WWHT	CANA	WWHT	WWHT
3	9	0.89	11	CANA	WWHT	WWHT	GRBN	WWHT	WWHT
3	10	2.89	5	WWHT	WWHT	WWHT	WWHT	CANA	WWHT
4	11	3.68	10	WWHT	WWHT	CANA	WWHT	WWHT	CANA
4	12	4.45	5	WWHT	WWHT	WWHT	WWHT	CANA	WWHT
4	13	1.82	11	CANA	WWHT	WWHT	GRBN	WWHT	WWHT
5	14	2.68	7	WWHT	WWHT	WWHT	WWHT	WWHT	WWHT
5	15	4.60	11	CANA	WWHT	WWHT	GRBN	WWHT	WWHT
5	16	1.59	6	WWHT	WWHT	WWHT	WWHT	WWHT	CANA
5	17	2.20	9	WWHT	CANA	WWHT	WWHT	CANA	WWHT
5	18	3.46	16	WWHT	WWHT	GRBN	WWHT	WWHT	CANA
6	19	3.06	11	CANA	WWHT	WWHT	GRBN	WWHT	WWHT
6	20	4.62	2	WWHT	CANA	WWHT	WWHT	WWHT	WWHT

etc..

Randomly generated number corresponding to a rotation pattern

Typical Rotations Patterns

Rotation	Year 1	Year 2	Year 3	etc
1	CANA	WWHT	WWHT	CANA
2	WWHT	CANA	WWHT	WWHT
3	WWHT	WWHT	CANA	WWHT
4	CANA	WWHT	WWHT	GRBN
5	WWHT	CANA	WWHT	WWHT
etc	WWHT	WWHT	CANA	WWHT

CANA: Winter Oil Seed Rape
WWHT: Winter Wheat
GRBN: Green Beans

CALCULATED %	WWHT	78%	83%	82%	80%	69%	83%
	CANA	20%	15%	12%	2%	31%	17%
	GRBN	2%	2%	6%	18%	0%	0%
TARGET % (Tolerance = ±5%)	WWHT	80%	85%	80%	75%	75%	75%
	CANA	15%	10%	15%	15%	20%	20%
	GRBN	5%	5%	5%	10%	5%	5%

An acceptable solution is found when the calculated and target percentages are within the specified tolerance.

Implementation of Metaldehyde Modelling in SWAT

Metaldehyde was added to the SWAT pesticide database for each catchment model, it is assumed to be applied to each arable HRU at a loading appropriate to its crop type, based on typical application rates for each crop.

Chemical and Physical Characteristics of Metaldehyde

Chemical and physical characteristics of metaldehyde were added to the SWAT pesticide database and to the . The initial values were based on the values found in a literature search as summarized in Table 2. The SWAT pesticide database includes parameters which allow SWAT to model how the pesticide interacts with the plants and their foliage. Since metaldehyde is applied in pellet form around the time of planting when foliage is minimal, it was assumed that it by-passes any interactions with plant and is applied directly to the soil.

Table 2: Metaldehyde Parameters used in SWAT

Description	SWAT Parameter	Initial Value
Soil adsorption coefficient normalized for soil organic carbon content	SKOC (mg/kg)(mg/L)	120
Wash-off fraction (fraction of pesticide on the plant canopy that may be dislodged)	WOF	0.7
Degradation half-life of the chemical on the foliage	HLIFE_F (days)	5
Degradation half-life of the chemical in the soil	HLIFE_S (days)	10
Solubility of the chemical in water	WSOL (mg/L or ppm)	200
Application efficiency	AP_EF	0.5
Pesticide reaction coefficient (in reaches)	CHPST_REA	0.007

Metaldehyde Application

Metaldehyde application was defined by loading (kg/ha) base on FERA data (FERA, 2010) and is associated with crop type defined for each HRU (in the mgt1 table). Historical application dates were estimated based on a generic crop calendar for the Anglian region, assuming that the first application occur at out close to the drilling date and, where available, on farm survey data and advice from an agronomist.

Metaldehyde Transport

When looking at the pathways of metaldehyde, particular consideration has been given to crack flow and tile drainage as conceptually these provide fast pathways to the catchment streams.

Crack Flow

Crack flow is a phenomena associated with the drying of clay soils. Cracks on the surface of dry clay soils provide preferential pathways for overland flow during rainfall-runoff events for the first rain after a dry period. As the soil is wetted these cracks reduce and crack flow becomes insignificant during sustained wet periods. Crack flow provides a potential fast pathway for metaldehyde and there is a significant proportion of clayey soils within the modeled catchments so conceptually crack flow is of importance.

SWAT is able to simulate crack flow, however to-date the necessary routines to route pesticide with crack flow have not been included. Therefore, to avoid underestimating metaldehyde, these catchment models do not use the crack flow option in SWAT. This presents a limitation to the catchment models.

Tile Drainage

Tile drains have typically been installed on arable land to encourage drainage in heavy soils which would regularly reach field capacity. Tile drains are thought to act as a fast pathway through which metaldehyde enters the catchment streams. No actual data about the presence of tile drainage in these catchments was available, instead tile drains have been assumed to be present within certain HRUs according to their soil types and land use based on information from

the UK National Soil Resources Institute (NSRI)) and Corine land cover map 2000 (EEA, 2000). A method for categorising the likely presence of land drainage from standard data sets has been defined (Sandberg & Elwell, 2011).

It was important to include tile flow within the catchments in sensible proportions in order to capture the associated metaldehyde load. The tile flow calculated by SWAT is controlled by the parameterisation of an impervious layer, specified by its depth, the depth of the drains and the drainage design (time to drain to field capacity). It is important to calibrate this at a HRU level (i.e. adjusting DEP_IMP, DDRAIN, GDRAIN and TDRAIN) differentiating between clayey soils and other soils.

It is not possible to accurately represent mole drainage systems using the current specification of SWAT. Mole drains are unlined channels and in UK these are commonly installed on heavy clay soils to remove excess water as it enters from the top soil. The mole channels are of often connected to a collector pipe system. These are often backfilled with permeable material and could potentially provide a rapid metaldehyde pathway.

Degradation of Metaldehyde in Streams

Our knowledge of the processes of metaldehyde in streams is limited and therefore we have represented all the physical and chemical effects in a single metaldehyde degradation rate (CHPST_REA) which was calculated using the aqueous half-life of metaldehyde in water. Results from an unpublished study indicates that metaldehyde is relatively stable in water environments, with a half life around 60 days in flowing water and around 250 days in pond systems. However since the half-life is partly influenced by catchment characteristics it has been treated as a calibration parameter in this modeling study.

Metaldehyde Calibration

Hydrological Influence

In terms of drinking water compliance, it is particularly important to reduce metaldehyde peaks. These are heavily influenced by hydrological flow peaks, so it is important to match these peaks during calibration. Hydrological calibration is based on matching daily observed and modelled stream flows and takes place before the water quality calibration. It was also important that proportions of flow routed through each hydrological pathway fitted with the conceptual understanding, even if this was at some expense to the calibration of stream flows, since some flow pathways are disproportionately important in terms of metaldehyde loading.

Water Quality Calibration Methodology

Observed metaldehyde concentrations, usually sampled at the abstraction point or at the inflow to a raw water storage reservoir, were used to calibrate the models. Historical metaldehyde observations have typically been weekly spot samples, which presents a challenge when calibrating a SWAT model with a daily time step and attempting to reproduce metaldehyde peaks, which may only last a few hours.

A methodology to standardise the water quality calibration across the catchments has been established. However, a wide range of uncertainties will be inherent to the calibrations, so comparing the impact of catchment scenarios with the same impact in another catchments is not possible since their uncertainties will differ. Instead the calibrations provide baselines, for individual catchments, against which catchment management scenarios can be assessed.

The following approach to calibration was adopted:

- Ensure metaldehyde is applied to crops before the observed in-stream peaks in metaldehyde concentration.
- Prioritise the timing and shape of the peaks over the magnitude of the peaks. Given the high degree of uncertainty with regards to application quantities and management practices, it is very difficult to replicate the exact magnitude of the peaks and the magnitude is uncertain because it is a spot sample compared with the daily average.
- Adjust the timing of metaldehyde application so that the modelled and observed peak timings are as closely matched as possible, whilst accounting for the fact that observed data is not available for every modelled peak.
- Adjust the application efficiency and/or wash-off fraction so that the modelled peak values are within ±50% of the observed. Alternatively, only apply metaldehyde to a pre-defined proportion of winter wheat and oilseed rape crops (randomly selected).
- Adjust the metaldehyde degradation parameters (half-life in soil) and/or tile drainage parameters so that the recession curve passes through the measured data points, and so that the tail of the modelled metaldehyde peak reaches equilibrium levels at the same time as the observed (but not necessarily the same value).

Calibration Example

A recently modelled catchment has been chosen to illustrate the approach to water quality calibration. The catchment chosen supplies Ravensthorpe reservoir and is situated in Northamptonshire (UK). The metaldehyde calibration for the Ravensthorpe catchment is shown in Figure 6.

Figure 6: Metaldehyde Calibration (Ravensthorpe Catchment)

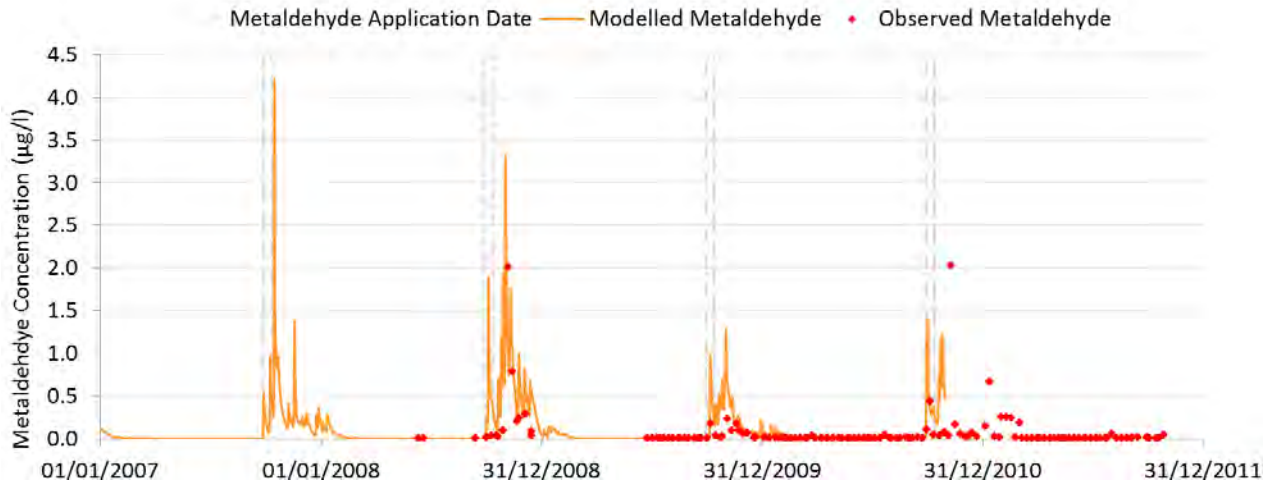

Table 3 gives an overview of the calibration actions which were required to produce this calibration and provides some interpretation of the reason for the changes.

Table 3: Water Quality Calibration Actions for Ravensthorpe Catchment

SWAT Parameter	Calibration Actions	Interpretation
Application Efficiency (AP_EF) Initial: 0.5 Calibrated: 0.25	Reduced to decrease the magnitude of the modelled metaldehyde peak concentrations to more realistic levels.	Actual application quantities compared with those quoted in surveys or literature may be less overall (although it may be greater for particular fields) and farmers may apply fewer slug pellets to fields where there is there is less risk of slug damage. Buffer strips and other non-productive land may be included in our estimated area of arable land leading to an overestimation of the area over which metaldehyde is applied. Anecdotally, reported metaldehyde application can be much higher than actual application and typically less metaldehyde is applied to the lighter soils.
Degradation Half-Life in Soil (HLIFE_S) Initial: 10 Calibrated: 40	Increased to model a more rapid recession in metaldehyde concentrations.	This parameter had the most significant effect in controlling the modelled metaldehyde concentrations over the first few days after rainfall. The parameter represents the chemical degradation within soil and also includes other mechanisms whereby the pathway of metaldehyde is inhibited, such as the physical degradation of the pellet, including lodging of pellets within the soil.
Soil Adsorption Coefficient (SKOC) Initial: 120 Calibrated: 210	Increased to increase the proportion of metaldehyde adsorbed by the soil.	The in stream concentrations are more influenced by the half-life of metaldehyde in soil if the adsorption coefficient is increased. This parameter is changed in tandem with the degradation half-life in soil so that more metaldehyde is degraded in the soil.
Pesticide Reaction Coefficient (CHPST_REA) Initial: 0.007 Calibrated: 0.1	Increased to reduce background concentrations.	This parameter is important to control the background concentrations of metaldehyde in the catchment streams.

Catchment Management Scenarios

Rationale

Catchment management scenarios can be established by changing the management operations tables within SWAT. The impact on the concentrations of metaldehyde compared with the calibrated baselines can then be studied.

Scenarios

The modelled scenarios include implementing one or more of the following catchment management interventions:

- Preventing metaldehyde application over some areas of the catchment (e.g. land use change or alternative product)
- Limiting metaldehyde application rates
- Limiting the number of applications per season

Scenarios are applied to selected proportions of arable land across the catchment:

- At random
- Targeting conceptually high-risk areas, such as:
    - Areas next to watercourses
    - The downstream end of the catchment
    - Soils with high run-off potential

Implementation in SWAT

To implement the catchment management scenarios, subbasins or HRUs are selected, according to the scenario criteria. A scenario implementation tool, set up in Microsoft Excel, was used to select appropriate areas in the catchment for each scenario, and automatically generates an "SQL" script, to run in Microsoft Access, to make the necessary changes to the SWAT model database.

The scenario implementation tool was set up to select areas of the catchment by specifying selection criteria for subbasins or HRUs based on their land use (which includes the subcategories defined by the buffer strips), soil type, and distance from the catchment outlet (e.g. a downstream proportion of the catchment could be selected). For each of these categories a target proportion of catchment subbasins or HRUs meeting each criteria can be selected or a completely random subbasin selection can be made.

Random selections based on target percentages are found using a similar methodology to that described in the 'HRU Crop Types and Rotations' section above. A stochastic process is followed whereby subbasins' or HRUs' metaldehyde applications are randomly switched on or off. The selected area is compared to the target value until the percentages are within a defined tolerance. The process iterates until the lowest percentage difference is found within the maximum number of iterations. This process is implemented in Microsoft Excel and is illustrated for an example catchment (Ravensthorpe) in Figure 7.

For each scenario, the SQL scripts generated for each catchment makes changes to the metaldehyde application rates defined in the management table either removing the application or reducing the rate.

Figure 7: Random Selection of 50% of Land (by Subbasin) for Example Catchment

Subbasin	Area	Selected On/Off
1	38.06	1
2	145.49	1
3	24.21	1
4	0.35	0
5	78.51	0
6	25.45	0
7	35.00	1
8	31.77	1
9	54.56	0
10	123.22	0
11	30.53	1
12	79.89	1
13	43.65	0
14	6.78	1
15	61.33	1
16	12.35	0
17	35.46	0
18	3.37	0
19	41.68	1
20	34.20	0
21	6.26	0
22	31.34	1
23	58.34	0
24	18.14	1
25	0.52	1
26	0.02	0
27	99.88	0
28	59.10	0
29	27.28	1
30	41.66	0
….	….	….
51	3.30	1
CALCULATED %		48%
TARGET % (+/- 5%)		50%

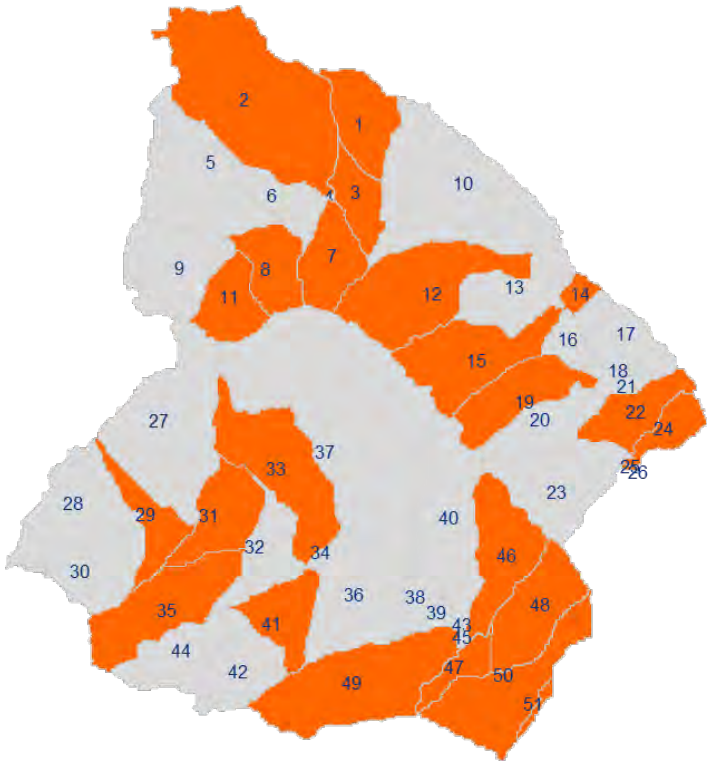

Subbasins are randomly selected as being on or off (i.e. included as part of the selection or not)

Iterates until matches target % within specified tolerance

Comparison of Scenario Results

An approach has been established to analyse the scenario outcomes. The scenario metaldehyde concentrations are compared with the calibrated baseline metaldehyde concentrations.

Statistical analysis of the model results was carried out using the total, mean and standard deviation of metaldehyde concentrations. Anglian Water is interested in reducing the number of peaks that exceed a threshold value (0.1µg/l) so supplementary statistical analysis (using the same statistics) was completed excluding all data points with values beneath the threshold value defined limit. Also, the RMSE (Root Mean Square Error) of the highest recoded metaldehyde

peaks, compared to the corresponding modeled values, was calculated. RMSE was calculated for the top 3, 6, 9, 12, and 15 peaks

The change in the maximum metaldehyde peak provided a quick way to compare the scenarios with the baseline. The number of modeled peaks exceeding the defined limit was also used as a comparison. Figure 8 and Figure 9 show examples of these analyses, for the Ravensthorpe catchment, with a range of compared against the baseline calibration (Scenario 0). Scenarios 1 to 4 represent specific catchment management scenarios, where metaldehyde applications are removed from targeted or randomly selected proportions of arable land, and/or metaldehyde applications rates are limited.

Figure 8: Maximum metaldehyde concentration (as a percentage of baseline)

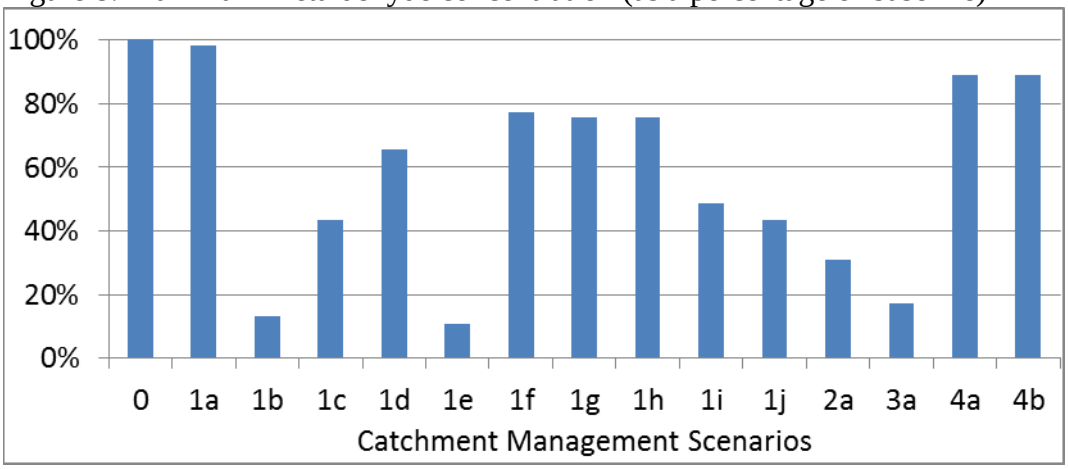

Figure 9: Modelled peaks exceeding 0.1µg/l (as a percentage of baseline)

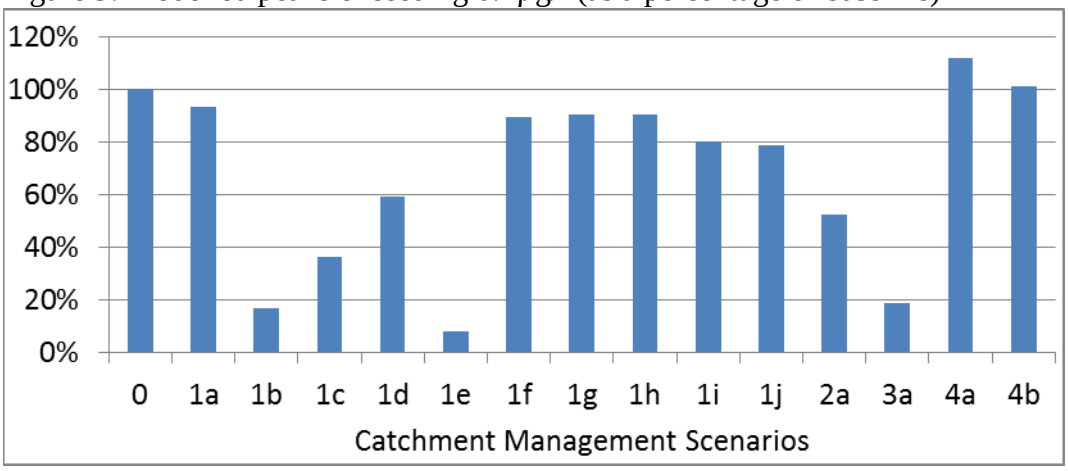

Analysis of Subbasin Contributions

Additional analysis of concentrations of metaldehyde contributed by each subbasin provided better understanding of the scenarios. SWAT subbasin outputs show the total metaldehyde concentration in stream flow entering and exiting each catchment but due to the decay rate and changes in phases (i.e. to and from sorbed/dissolved metaldehyde) simply subtracting one from the other did not provide a clear understanding of subbasin contributions, so an alternative method was devised.

The scenario tool was set up to set up a series of models runs where:

- Metaldehyde application was 'switched on' in only one basin at a time.
- Metaldehyde application was 'switched off' in one basin at a time; and the

Following this analysis, the metaldehyde concentrations in each reach were plotted to get a better understanding of the impact of each subbasin. Spatial representation of this information in terms of average annual and maximum loadings of metaldehyde for each subbasin provided an overview of subbasin outputs. The analysis of all the model runs was incorporated into a single map showing the data. Figure 10 shows an example of total metaldehyde contributed by each subbasin for a selected scenario, normalized by subbasin area. This indicates which subbasins are high-risk, in terms of the amount of metaldehyde reaching catchment streams.

Figure 10: Total Contribution of Metaldehyde by Subbasin for Grafham Catchment

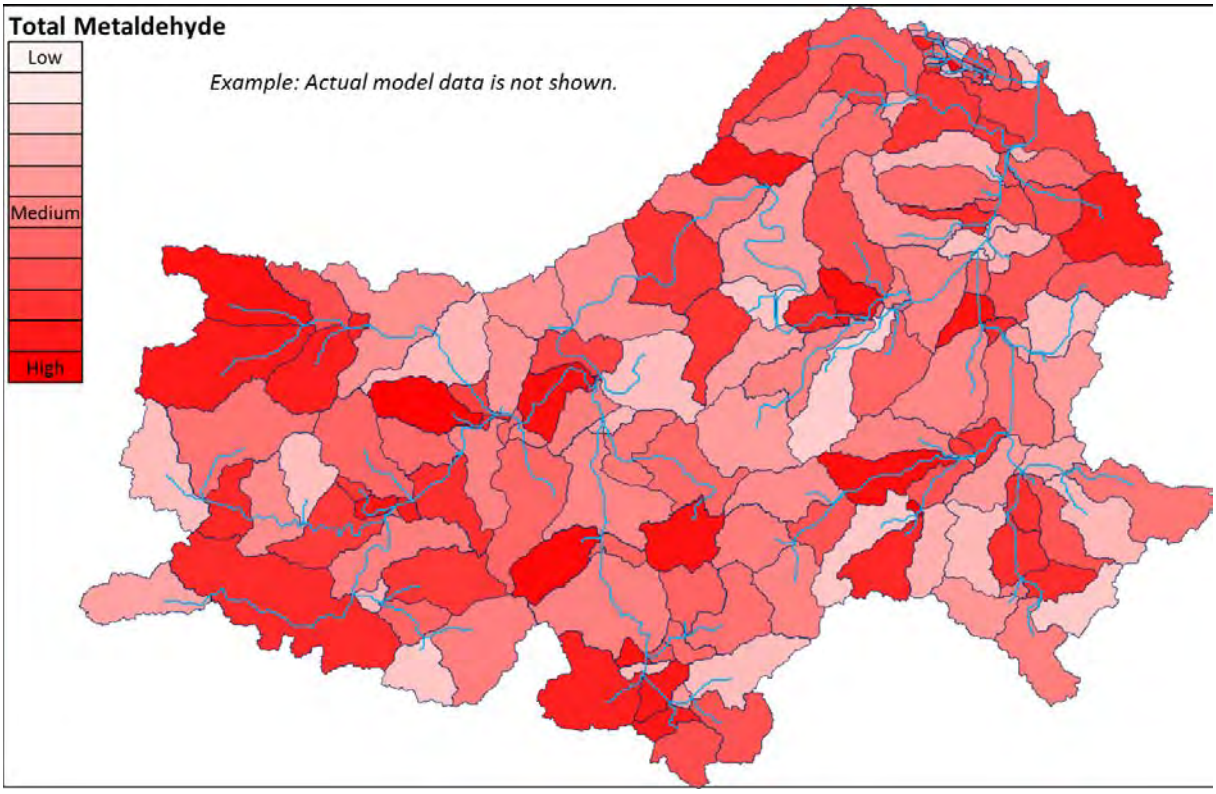

Conclusion

SWAT models are being developed to simulate metaldehyde transport in 23 surface water catchments in East Anglia (UK) and to assess the impact of catchment management scenarios.

Results from the first completed models show that good calibration can be achieved but there is scope for improvements in some areas. Whilst the calibrations have a degree of uncertainty, provided they are used as baselines against which to compare (for a particular catchment) the relative impact of scenarios, they can provide a useful assessment of catchment management interventions.

As in most large-scale studies the lack of data has proved to be the most significant contributor to model uncertainty. In particular the lack of information on application dates, rates and locations. However, the available data is sufficient to develop a robust understanding of the type of catchment management solutions that would be required to achieve raw water concentrations below 0.1 µg/l and where such solutions should be targeted. The output from this study provides a robust basis for potential future more targeted catchment activities and has been useful in the decision making process in terms of allowing the assessment of the impact of various actions.

A generic approach has been developed for conceptualization of catchments, model implementation and calibration. Such approach ensures transparency in the modeling process. To effectively allow implementation of catchment management scenarios to the calibrated model, the nature of the scenarios should be considered before the model build starts so that the subbasin delineations and HRU definition provide sufficient spatial definition. In this case if has proved to be important to distinguish between arable land close to the main stream, and soil types.

Where detailed land use data is unavailable, a stochastic approach can be used to assign crop types based on assumed or target percentages, and probable crop rotation sequences. The result is a matrix representing the crop type in each HRU for each year in the rotation period. A tool has been designed to write the management operations table using this matrix.

A large proportion of the modeled catchments are having some form of under drainage installed, and it is thought that this could be a major pathway of metaldehyde. The current specification of the SWAT model does not allow an accurate representation of mole drains which differs from standard pipe drains; in particular the potential direct pathway between the top soil and the permeable backfill above the collector pipes. Similarly, the model does not include pesticide loading is bypass flow, although it can be included as a hydrological component in the model. The result from these model deficiencies is that the proportional distribution of hydrological pathways may be less well represented in modeled clay rich HRUs, where both bypass flow and mole drains occur. It is recommended that changes to the source code are made:

1. include pesticide loadings in bypass flow (adopt a similar approach to nitrate in tile drains).
2. include a function where a fraction of bypass flow and associated pesticide loadings is directly added to the drain flow and pesticide loading in the drain (similar to the approach adopted by Fox et al. 2004).

Acknowledgements

The authors wish to acknowledge: Anglian Water, who have funded this project; the Environment Agency who have provided various data for the model; Cranfield University for their technical support and model reviews; colleagues at Anglian Water and Mott MacDonald for their support and advice.

References

Sandberg, J., Elwell F.C., 2011. The Impact of Land Management on Drinking Water Quality: a Water Industry Application, East of England. (International Swat Conference, 2011).

Edinburgh University, 2010. Edina AgCensus Service, http://edina.ac.uk/agcensus

FERA (Food and Environment Research Agency), 2010. Regional Breakdown of Metaldehyde Use for 2008-2010

European Environment Agency, 2000. Corine Land Cover Map. Raster (130 m grid cells).

NSRI (National Soil Resources Institute), NatMap Vector - spatial distribution of soil associations (1: 250 000 scale)

Fox, G.A., Nalone, R., Sabbagh, G.J., & Rojas, K. 2004. Interrelationship of macropores and subsurface drainage for conservative tracer and pesticide transport. Journal of Environmental Quality, 33, 2281-2289

Development of a grid-based version of the SWAT landscape model

Hendrik Rathjens*
Department of Geography, Kiel University, Kiel, Germany
*E-mail: rathjens@geographie.uni-kiel.de

Natascha Oppelt
Department of Geography, Kiel University, Kiel,Germany

Martin Volk
Department of Computational Landscape Ecology, UFZ Helmholtz Centre for Environmental Research, Leipzig, Germany

Jeffrey G. Arnold
USDA-ARS Grassland, Soil and Water Research Laboratory, Temple, Texas, USA

Abstract

Integrated river basin models should provide a spatially distributed representation of basin hydrology and transport processes. However, until recently the conventional sub-watershed discretization in SWAT is unable to account for spatial variability within a sub-basin and to simulate runoff and infiltration processes in landscape units.

To overcome these shortcomings, SWAT is currently being modified by the integration of a landscape routing model to enhance its spatial representation of hydrology and transport processes within a watershed. The modified model enables a distributed simulation of runoff, sediment and nutrients between sub-watersheds, grid cells, or routing units in the land-phase of the hydrologic cycle. The combination of this landscape routing and SWATgrid, an interface preparing the input data for setting up SWAT based on grid cells, promises a spatially fully distributed model that includes surface, lateral, and groundwater fluxes in each grid cell of the watershed.

Hence, this paper presents the development of such a grid-based version of the SWAT landscape model. Water balance simulations as well the spatial distribution of surface runoff, subsurface flow and evapotranspiration and the simulation of the hydrograph at the watershed outlet are examined. The results are promising and satisfactory output was obtained with the grid-based landscape model: Nash-Sutcliffe model efficiencies for daily stream flow were 0.59 and 0.61 for calibration and validation period. Finally, present developments, existing problems and next steps are pointed out.

Keywords: grid cell, grid-based simulation, discretization scheme, SWATgrid, landscape routing

Introduction

River basin models are valuable tools for investigating the impact of land use and management on landscape hydrology, sediment transport and water quality. SWAT has proven to be a suitable tool under many landscape conditions around the world. In most applications SWAT prediction accuracy was satisfactory to obtain knowledge of the hydrologic system and the watershed processes (Arnold and Fohrer, 2005; Gassman et al., 2007). However, previous studies showed that the assessment of the effects of conservation practices on watershed-scale water quality relies strongly on flow and transport models used (Mausbach and Dedrick, 2004). In this context, the inability to model flow and transport from one landscape position to another prior to the entry into the stream turned out to be one of the shortcomings of SWAT (e.g., Gassman et al., 2007; Bosch et al., 2010). The SWAT model utilizes a hydrologic response unit (HRU) approach. The watershed is divided here into sub-watersheds which are further subdivided into HRUs; individual areas of similar soil, topography and land-use are lumped together within a sub-watershed to form a HRU. That means that the HRUs represent percentages of the sub-watershed area and are not spatially related within a simulation. Transported water and matter from HRUs are currently routed directly into the stream channel. Therefore, the impact of an upslope HRU on a downslope HRU cannot be assessed and the model is unable to simulate sufficiently the effects of conservation practices, catch crops or crop rotations undertaken in certain landscape units (Arnold et al., 2010). The non-spatial aspect of the HRUs and the inability to model flow and sediment in the land-phase of the hydrological cycle (Neitsch et al. 2011) have been identified as key weaknesses of the model (e.g., Gassman et al., 2007). To fulfill the requirements in river basin management, integrated models should provide a spatially distributed representation of basin hydrology and transport processes (Arnold et al., 2010; Bosch et al., 2010). The incorporation of greater spatial detail into SWAT has therefore been investigated with the focus on (1) developing routing capabilities between landscape units (Volk et al., 2007; Arnold et al., 2010) and (2) developing a grid-based SWAT model setup (Rathjens and Oppelt, 2012).

The newly developed SWAT landscape is able to route surface runoff, lateral subsurface flow, and shallow groundwater flow between defined routing units. The model was tested by Arnold et al. (2010) and Bosch et al. (2010). Both studies concluded that additional development and testing of the SWAT landscape model is necessary to confirm model operation. The results are, however, “encouraging” (Bosch et al., 2010) and show a realistic representation of landscape flow and transport processes in a watershed. A detailed description of the landscape routing model is given by Arnold et al. (2010).

The combination of the landscape routing model and a grid-based setup results in a spatially fully distributed model that includes surface, lateral, and groundwater fluxes in each grid cell of the watershed. The aims of this study are (1) to present the development of the grid-based version of landscape model and (2) to test the hydrologic components of the SWAT landscape model at the grid-scale. The model is evaluated by using daily discharge at the catchment outlet and analyzing the spatial distribution of simulated surface runoff, subsurface flow and evapotranspiration. The Little River Watershed (LRW), a coastal plain watershed near Tifton (Georgia, USA), served as a test site to evaluate the methodology.

Materials and Methods

Study Area

The study area is the Little River Watershed (LRW) located in Central South Georgia (USA), near Tifton in the South Atlantic Coastal Plain (see Figure 1). Hydrology and water quality of the LRW have been monitored since 1967 (Sheridan, 1997). The area was focus of many research projects investigating water quantity and quality aspects (see Bosch et al., 2010). Furthermore, the LRW served as a test site for several SWAT related studies (e.g., Bosch et al., 2004; Feyereisen et al., 2007; Cho et al., 2009; Cho et al., 2012). Bosch et al. (2010) tested the SWAT landscape model in a sub-basin of the LRW.

The LRW covers an area of 334 km² and shows a relatively flat topography. It is characterized by a dense stream network (1.54 km^{-1}). The channels are surrounded by broad, flat alluvial floodplains, river terraces and gently sloping uplands. Half of the area has upland surface slopes less than 2 % and the remaining slopes lie in the 2 to 5 % range; the stream network channel slopes range between 0.1 and 0.5 % (Sheridan, 1997). Figure 1 gives an overview of the LRW stream network, topography, and land use and soil type distributions. The LRW is a mixed land use watershed and contains row crop agriculture, pasture and forage, upland forest, riparian forest, urban land and water areas (see Figure 1). Riparian forest wetlands dominate the landscape

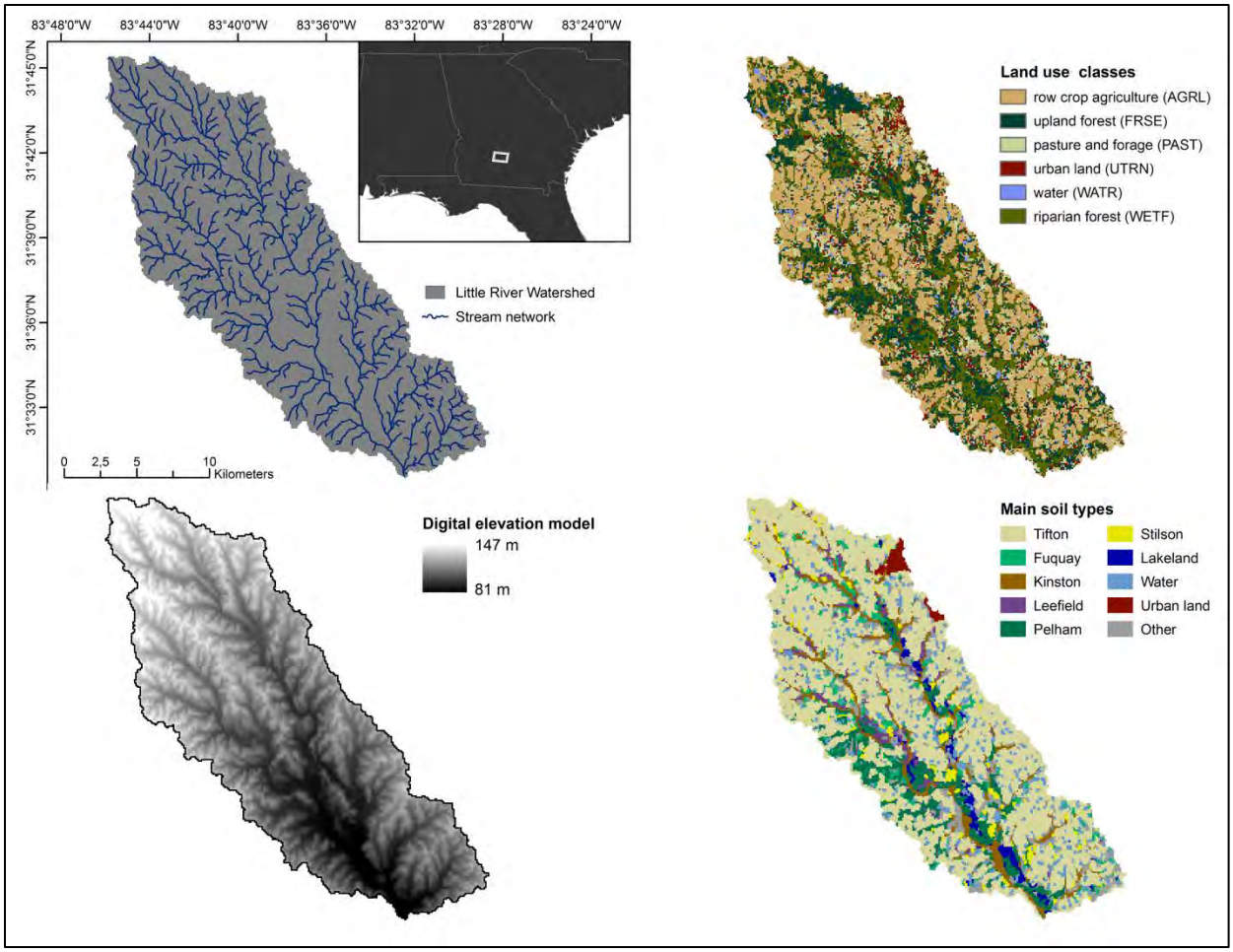

Figure 1. Location of the Little River Watershed in Georgia (USA) and its stream network, topography and land use and soil type coverages.

around the dense network of stream channels, while upland areas are mostly characterized by agricultural use (Bosch et al., 2004). The surface soil textures are generally sands and sandy loams with high infiltration rates, which are underlain by the shallow, impermeable clay-rich Hawthorne formation. This formation restricts downward movement of infiltrated precipitation and promotes lateral movement of water from uplands downslope as shallow groundwater flow to the stream channels (Sheridan, 1997; Cho et al., 2012). The climate of the LRW is humid subtropical (Cho et al., 2012); from 2004 to 2008 the mean annual temperature is 19 °C and the mean annual precipitation is 1059 mm. Rainfall is unevenly distributed and often occurs as short-duration, high-intensity convective thunderstorms during midsummer and winter months (Bosch et al., 1999).

SWAT and SWAT Landscape Model

SWAT (Arnold et al., 1998) is a catchment-scale model developed to simulate the water cycle, the corresponding fluxes of energy and matter (e.g. sediment, nutrients, pesticides and bacteria) as well as the impact of management practices on these fluxes. The simulated hydrological processes include surface runoff (SCS (Soil Conservation Services) curve number or Green and Ampt infiltration equation), percolation, lateral flow, groundwater flow from shallow aquifers to streams, evapotranspiration (Hargreaves, Priestley-Taylor or Penman-Monteith method), snowmelt, transmission losses from streams, channel routing (variable storage routing or muskingum routing method) and water storage and losses from ponds. A detailed description of all components can be found in Arnold et al. (1998) and Neitsch et al. (2011). In this study the SCS curve number method was used to calculate surface runoff; Penman-Monteith method was applied to estimate evapotranspiration; variable storage method was selected for channel routing.

SWAT divides the hydrology of a watershed into two major phases: (1) the land phase of the hydrologic cycle controls the quantitative flow of water entering the reach. (2) The routing phase determines the movement of water through the channel network to its outlet (Neitsch et al., 2010). The current SWAT version does not allow runoff to distribute between routing units in the land phase of the hydrological cycle. Thus**,** SWAT is not able to simulate runoff and infiltration processes that typically occur in a landscape. To overcome this shortcoming Arnold et al. (2010) developed a landscape routing method that enables surface, lateral and groundwater runoff interaction within the landscape. A detailed description of the landscape routing processes implemented in a SWAT prototype can be found in Arnold et al. (2010). This paper presents the development of the SWAT landscape routing model to a grid-based version that includes surface, lateral, and groundwater fluxes in each grid cell.

Estimating the partitioning ratio of landscape and channelized flow

The SWAT landscape routing model enables the distribution of runoff between grid cells in the land-phase of the hydrologic cycle. This raises the question which part of the flow is routed as channelized flow and which part is routed through the landscape. In this context, channel heads represent the major boundary between landscape and channel flow processes. Thus, the channel head location is a crucial parameter to realistically represent flow and transport processes in a watershed. The concept of Hydrological Sensitive Areas (HSAs, e.g., Walter et al., 2000; Agnew

et al., 2006) and the detection of channel heads by average source areas (Jaeger et al., 2007) were selected as useful methods to develop an index that can be used to partition landscape and channel flow in a watershed. HSAs can be characterized by the probability that a particular location in a watershed will generate runoff. Agnew et al. (2006) used a topographic index (λ) to detect HSAs. They found that the general patterns of high hydrological sensitivity are similar to those with high λ values. The topographic index they used takes the form

$$\lambda_i = \ln\left(\frac{A_i}{\tan(\beta_i) K_{sat\,i} Z_i}\right) \in \mathbb{R}_{\geq 0}, i = 1, \dots, n,$$

where n is number of grids in the watershed and i is the number of a particular grid cell. λ_i is the topographic (or wetness) index [ln(d m^{-1})], A_i is the upslope contributing area per unit contour length [m], β_i is the local surface topographic slope angle, $K_{sat\,i}$ is the mean saturated hydraulic conductivity of the soil [m d^{-1}] and $Z_i$is the soil depth [m]. λ can be easily calculated for each grid cell in a watershed and solely requires a DEM and soil data that are necessary for SWAT modeling anyway (see also Agnew et al., 2006). Grids with high λ_i values are expected to have a high probability to generate runoff; channelized flow processes are expected to be dominant towards landscape flow processes in these grids.

The original λ index is modified to obtain an index that spatially represents the partitioning ratio of channel and landscape flow processes. First, λ is transformed to a normalized index:

$$\lambda_{norm,i} = \frac{\lambda_i}{\max_{i=1,\dots,n}\{\lambda_i\}} \in [0,1], \; i = 1, \dots, n.$$

Second, λ_{norm} is adjusted to realistically represent the position of channel head locations in the watershed. No channel routing processes should be hold where no channels exist. Jaeger et al. (2007) stated that an average source area size based on field surveys may provide the most practical method for identifying channel head source areas. Thus, the drainage density (DD [km^{-1}]) of the watershed is used to adjust λ_{norm} values. The drainage density is defined by the length [km] of all channels in the watershed divided by the total drainage area (DA [km²]) of the watershed. Therefore, the smallest λ_{norm} values are set to zero (i.e. no channel flow) until the sum of all $\lambda_{norm,i}$ values multiplied with the unit contour length of the current grid cell matches the drainage density of the watershed. The resulting normalized index can be stated as

$$\lambda_{DD,i} \in [0,1], i = 1, \dots, n, \text{ satisfying } DD \approx \frac{\sum_{i=1}^{n} \lambda_{DD,i}\, l_i}{DA},$$

where l_i [km] is the unit contour length of the current grid cell. $\lambda_{DD,i}$ represents the fraction of channelized flow and $1 - \lambda_{DD,i}$ represents the fraction of landscape flow for grid cell i.

Modeling Framework

The interface SWATgrid (Rathjens and Oppelt, 2012) was used for developing grid-based SWAT model input using weather data and spatially distributed geographic datasets. Table 1 gives an overview on the data used for model input. Differences between the weather stations may dominate the spatial model output. To spatially analyze the output of the SWAT landscape model, values of all weather stations were aggregated to one data set and integrated in the simulation.

Table 1. SWAT input data sources for the LRW (downloadable at: ftp://www.tiftonars.org/).

Data type	Scale / Resolution	Source	Data description
Topography	30 m	Georgia GIS Data Clearinghouse	Digital Elevation Model (DEM)
Land use	30 m	Sullivan et al. (2007)	Land use classification based on Landsat 7 imagery (20 Jul 2003)
Soils	1 : 12 000	Soil Survey Geographic Database (SSURGO)	Soil physical properties
Weather	25 Stations (rainfall) 2 Stations (temperature, wind speed, relative humidity, solar radiation)	Bosch et al. (2007)	Daily weather data (1 Jan 2004 to 31 Dec 2008)

SWATgrid divides the watershed into linked grids. Runoff from a grid cell flows to one of the eight adjacent cells. The topographic index λ_{DD} is used to determine the share of channelized and landscape flow in the watershed. As a compromise between an accurate spatial representation and a manageable model, DEM, soil and land use data were resampled to a resolution of 100 m (1 ha). Grid-based simulations with the SWAT landscape model were conducted for a five-year period from 2004 to 2008, excluding two years of model warm-up. The accuracy of the simulated streamflow and water balance was examined for this period. To evaluate model performance four quantitative statistics were applied, i.e. the coefficient of determination (R^2), Nash-Sutcliffe efficiency (NSE; Nash and Sutcliffe, 1970) and percent bias (PBIAS; Gupta et al., 1999). The grid-based LRW model takes approximate 1 hour per simulated year on a single 2.67 GHz processor. As a consequence manual calibration was performed by comparing simulated and observed discharge at the watershed outlet solely for the year 2004. The calibrated parameter set was validated using the time period from 2005 to 2008. Based on previous studies (Bosch et al., 2004; Cho et al., 2012) and a manual sensitivity analysis five parameters were included in model calibration (see Table 2): soil evaporation compensation factor (ESCO), groundwater parameters (GW_DELAY, ALPHA_BF and GWQMN), and surface runoff lag coefficient (SURLAG). A detailed description of each parameter is provided by Neitsch et al. (2011).

Table 2. SWAT input parameters chosen for hydrologic calibration and final calibrated values.

Parameters	Default	Lower limit	Upper limit	Value
ESCO.bsn	0.95	0	1	1.00
SURLAG.bsn	4	0.05	24	0.15
GW_DELAY.gw	31	0	500	0.75
ALPHA_BF.gw	0.048	0	1	0.96
GWQMN.gw	0	0	5000	50.0

Results and Discussion

Partitioning Ratio of landscape and channelized Flow

In this study the topographic index λ that has been commonly used to identify runoff generating areas was modified to obtain estimates of this partitioning ratio (λ_{DD}). Figure 2 shows the spatial distribution of λ_{DD}values in the LRW. Patterns of both indices suggest a stream network (Figure 2a and b) similar to the mapped network (see Figure 1). The method selected for normalization results in a discontinuous distribution of channelized flow fractions λ_{DD}, which leads to abrupt channel heads in the in the λ_{DD} map (see Figure 2b). Previous channel initiation related studies by Montgomery and Dietrich (1988 and 1989) assessed that abrupt channel heads occur more frequently than gradual channel heads in basins with gentle slopes and infiltration excess overland flow, which applies for the LRW. Thus, the λ_{DD} seems to represent the spatial distribution of flow and transport processes realistically. However, both abrupt as well as gradual channel heads are likely to occur in the LRW. Future studies should focus on the question on which type of channel head is dominant in the LRW. Variations of the λ_{DD} index will be tested to represent flow processes and channel head locations as plausible as possible.

Simulation of daily discharge at the watershed outlet

One aim of this research was to assess how well the new grid-based landscape configuration performs. Simulations were carried out for the period from 2004 to 2008. Measures of model performance including PBIAS, R^2 and NSE values are listed in Table 3. The measures indicate that model calibration and validation performance ratings for total, monthly and daily streamflows are within a satisfactory range. Monthly NSE and R^2 values are better than daily values, a result that is often observed in model applications (e.g., Moriasi et al., 2007).

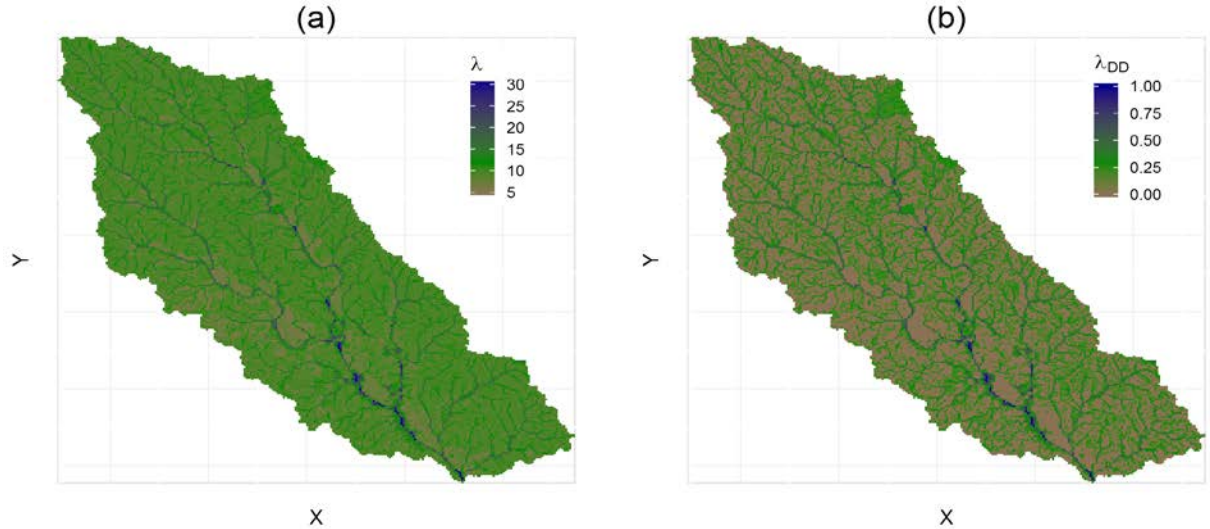

Figure 2. Spatial distribution of the topographic index (a) λ and the partitioning ratio (b) λ_{DD} used for channelized and landscape flow separation in the LRW.

Table 3. Summary of performance measures of grid-based SWAT simulations for the LRW from 2004 (calibration period) and from 2005 to 2008 (validation period).

Periods	Streamflow [mm/a]		PBIAS	R^2		NSE	
	Observed	Simulated	[%]	Daily	Monthly	Daily	Monthly
Calibration	297	245	17.39	0.59	0.93	0.59	0.90
Validation	212	172	18.99	0.66	0.84	0.61	0.76

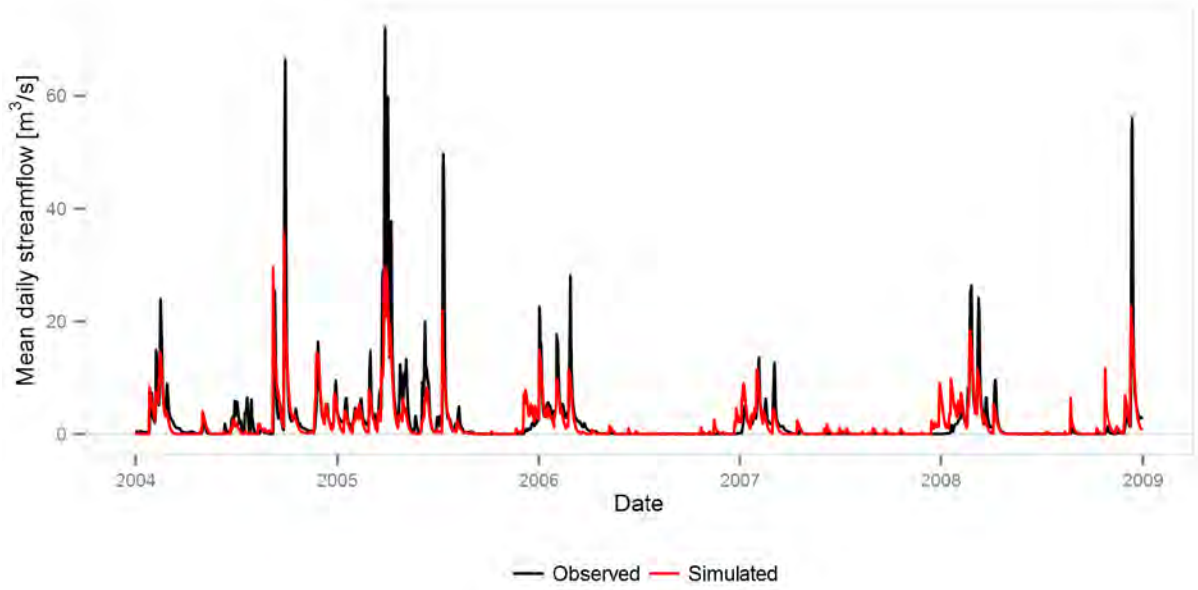

Figure 3. Observed and simulated daily streamflow for the LRW from 2004 to 2008.

A hydrograph of daily streamflow for the 5-year period (see Figure 3) indicates that the grid-based SWAT model simulated daily streamflow satisfactory in both low and high flow conditions. The model, however, tends to underpredict discharge peaks during the entire period. Discharge values show a different behavior between the years of the simulation period. In 2004 and 2005 measured discharge values are comparatively high (297 mm and 433 mm) while from 2006 to 2008 discharge values are lower (139 mm in average). Zero-flow conditions were observed during each of the dry years. The model in general predicts the trends in observed data and the previously reported tendency of over-predicting streamflow during zero-flow conditions (Bosch et al., 2004; Feyereisen et al., 2007) does not occur (see also Cho et al., 2012).

Spatial analysis

The spatial distribution of the model output parameters shows the impact of topography, landscape position, land use classes and soil types on model output. To evaluate the landscape grid approach, spatial distributions of surface runoff (SURQ, see Figure 4a), lateral flow (LATQ, see Figure 4b), groundwater runoff (GWQ, see Figure 4c) and evapotranspiration (ET, see Figure 4d) were analyzed. At this stage, the model is not spatially calibrated; thus, the spatial output could not be evaluated quantitatively but have been analyzed qualitatively. Spatial characteristics of each output parameter and the effects of the landscape routing model and the flow partitioning ratio are further explained below.

Highest SURQ values occur as expected on urban land areas. The model simulates more surface runoff in the upland areas than in the floodplain areas around the channel network. This can be explained by the steeper slopes in the upland areas (which are dominated by agricultural land use), while the valley areas are mainly forested. Higher slope angles and higher curve number values on agricultural land lead to this larger amount of surface runoff. However, sands and sandy loams with high infiltration rates dominate and thus, most of the water infiltrates and is not routed through the landscape as surface runoff.

Increasing lateral flow is accurately simulated at steeper slopes in the upland; spatial patterns of LATQ and slope values show similarity, and the spatial distribution of LATQ values is reasonable. The highest LATQ values occur at the steepest slopes and almost no lateral flow occurs in the valley bottoms. In the steeper areas the model routes the lateral flow through the landscape, whereas in the flat parts water seeps and feeds shallow groundwater.

Unlike the SURQ and LATQ results, GWQ patterns indicate a routing scheme. That means the main part of flow routed through the landscape is groundwater runoff. Due to the high infiltration rates most water infiltrates until it reaches the soil that is underlain by the nearly impermeable Hawthorne formation. From there it is routed through the landscape as shallow groundwater. The model depicts groundwater flow reasonable; ground water runoff increases and concentrates as the water moves down the landscape from the upland area to the valley. The amount of groundwater sudden decreases at a certain position in the landscape when the slope decreases and the model forces the water to flow into a stream channel. The topographic index λ_{DD} determines the position in the landscape where the water is passed from the land-phase into the routing phase; GWQ and λ_{DD} (see Figure 4c and 2d) patterns look similar. The spatial GWQ patterns indicate abrupt channel initiation processes caused by seepage erosion on gentler slopes. This confirms results given by Montgomery and Dietrich (1989), who concluded that abrupt channel heads mainly occur in landscapes with gentler slopes and high infiltration capacity.

Considering inflow from higher landscape positions, the model simulates more ET in the valley bottoms than in the upland areas. Highest ET values occur in the water and forested wetland areas around the channel network, while the urban land and agricultural areas on higher landscape positions produce less ET (see Figure 4d).

Conclusions and outlook

In this study, a grid-based version of the SWAT landscape model was developed to simulate processes across grid cells in the land-phase of the hydrological cycle. The fully distributed model includes surface, lateral, and groundwater fluxes in each grid cell of the watershed. The landscape model requires a spatial partition of landscape and channelized flow processes. The flow separation ratio turned out to be a crucial parameter for the plausible representation of flow and transport processes in a watershed. The estimation of the partition ratio was based on a topographic index that considers soil properties, topography and the drainage density of the watershed. The resulting index has shown the capability to plausibly represent the spatial distribution of flow and transport processes in a watershed. However, additional research of the partitioning

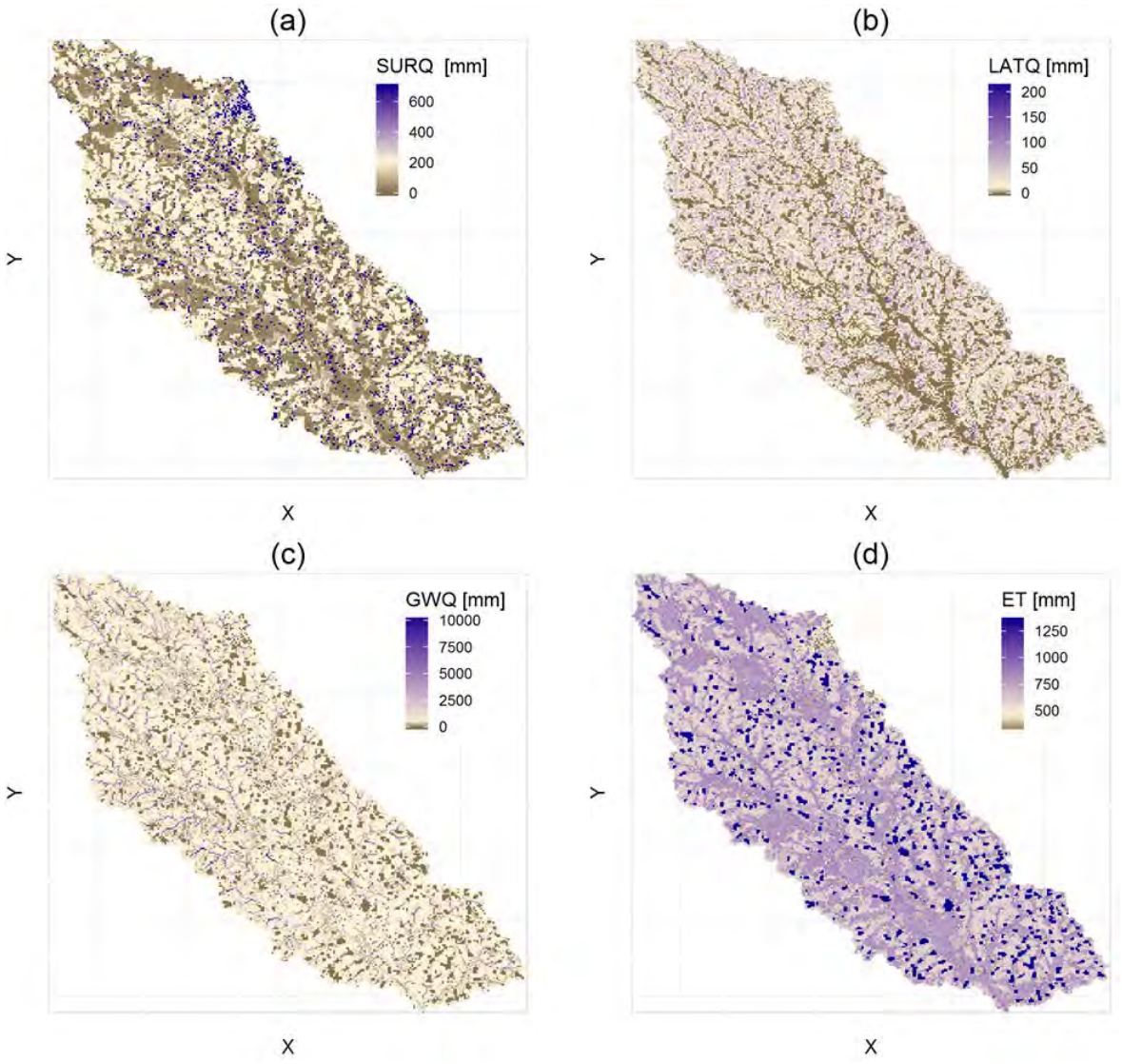

Figure 4. Average annual (a) surface runoff [mm], (b) lateral runoff [mm], (c) groundwater runoff [mm] and (d) evapotranspiration [mm] in the LRW from 2004 to 2008.

ratio parameter is necessary. In the future, different estimations of the flow separation ratio will be tested and proven by field surveys.

The model was calibrated and validated for the Little River Watershed (LRW, 334 km²) near Tifton, Georgia. The results suggest that the grid-based landscape model simulated satisfactory the streamflow hydrograph at the outlet of the LRW (daily NSE > 0.59) and that both the grid-based model as well as the commonly used HRU approach can be calibrated (e.g., Bosch et al., 2004; Cho et al., 2012). However, model calibration can still be improved. A challenge is that the grid based approach results in a considerable increase of computation time, which impedes the time-consuming manual or auto-calibration procedure. A second aim of the study was to spatially analyze the hydrologic components of the landscape model; the availability of spatially distributed model output is a major advantage of the grid-based model. Spatial LRW model results showed that the grid-based landscape model is able to reasonably simulate the impact of the landscape position on evapotranspiration, and surface, lateral and groundwater runoff. All results

presented are, however, limited to the study area. Additional calibration and testing of the grid-based SWAT landscape model is necessary. Further studies in larger watersheds with different hydrological and landscape characteristics are required to confirm the study's findings.

With the results from this study we can conclude that the presented model could provide a more plausible basis for water quantity and quality simulations that require a detailed spatial analysis. Geographic information systems and remote sensing techniques develop rapidly and an increasing amount of spatial and temporal high-resolution data becomes available. The integration of these data into the SWAT landscape model seems to be very promising for enhanced spatial analysis of environmental issues within a watershed and therefore justifies the challenges inherent to the grid-based approach.

References

Agnew, L. J., S. Lyon, P. Gerard-Marchant, V. B. Collins, A. J. Lembo, T. S. Steenhuis, and M. T. Walter. 2006. Identifying hydrologically sensitive areas: Bridging the gap between science and application. *J. Environ. Manage.* 78(1): 63–76.

Arnold, J. G., P. M. Allen, J. R. Williams, and D. D. Bosch. 2010. Assessment of different representations of spatial variability on SWAT model performance. *Trans. ASABE* 53(5): 1433-1443.

Arnold, J. G., and N. Fohrer. 2005. SWAT2000: current capabilities and research opportunities in applied watershed modelling. *Hydrol. Process.* 19(3): 563–572.

Arnold, J. G., R. Srinivasan, R. S. Muttiah, and J. R. Williams. 1998. Large area hydrologic modeling and assessment part I: model development. *JAWRA* 34(1): 73–89.

Bosch, D.D., J. G. Arnold, M. Volk, P. M. Allen. 2010. Simulation of a low-gradient coastal plain watershed using the SWAT landscape model. *Trans. ASABE 53*(5): 1445-1456.

Bosch, D. D., H. L. Batten, and J. G. Arnold. 2004. Evaluation of the SWAT model on a coastal plain agricultural watershed. *Trans. ASAE* 47(5): 1493–1506.

Bosch, D. D. J. M. Sheridan, and F. M. Davis. 1999. Rainfall characteristics and spatial correlation for the Georgia Coastal Plain. *Trans. ASABE* 42(6): 1637–1644.

Bosch, D. D., J. M. Sheridan, and L. K. Marshall. 2007. Precipitation, soil moisture, and climate database, Little River Experimental Watershed, Georgia, United States. *Water Resour. Res.* 43(1): 1-5

Cho, J., D. D. Bosch, R. Lowrance, T. Strickland, and G. Vellidis. 2009. Effect of spatial distribution of rainfall on temporal and spatial uncertainty of SWAT output. *Trans. ASABE* 52(5): 1545–1555.

Cho, J., D. D. Bosch, G. Vellidis, R. Lowrance, and T. Strickland. 2012. Multi-site evaluation of hydrology component of SWAT in the coastal plain of southwest Georgia. *Hydrol. Process* . In press.

Feyereisen, G., T.C. Strickland, D. D. Bosch, and D. G. Sullivan. 2007. Evaluation of SWAT manual calibration and input parameter sensitivity in the Little River Watershed. *Trans. ASABE* 50(3): 843–855.

Gassman, P. W., M. R. Reyes, C. H. Green, and J. G. Arnold. 2007. The Soil and Water Assessment Tool: historical development, applications, and future research directions. *Trans. ASABE* 50(4): 1211–1250.

Gupta, H. V., S. Sorooshian, and P. O. Yapo. 1999. Status of Automatic Calibration for Hydrologic Models: Comparison with Multilevel Expert Calibration. *J. Hydrol. Eng.* 4(2): 135–143.

Jaeger, K. L., D. R. Montgomery, and S. M. Bolton. 2007. Channel and perennial flow initiation in headwater streams: management implications of variability in source-area size. *Environ. Manage.* 40(5): 775–786.

Mausbach, M. J., and A. R. Dedrick. 2004. The length we go: Measuring environmental benefits of conservation practices. *J. Soil Water Conserv.* 59(5): 96-103.

Montgomery, D. R., and W. E. Dietrich. 1988. Where do channels begin? *Nature* 336(1): 232–234.

Montgomery, D. R., and W. E. Dietrich. 1989. Source areas, drainage density, and channel initiation. *Water Resour. Res.* 25(8): 1907–1918.

Moriasi, D. N., J. G. Arnold, M. W. Van Liew, R. L. Bingner, R. D. Harmel, and T. L. Veith. 2007. Model evaluation guidelines for systematic quantification of accuracy in watershed simulations. *Trans. ASABE* 50(3): 885–900.

Nash, J.E., and J.V. Sutcliffe. 1970. River flow forecasting through conceptual models part 1 - A discussion of principles. *J. Hydrol.* 10(3): 282–290.

Neitsch, S. L., J. G. Arnold, J. R. Kiniry, R. Srinivasan, and J. R. Williams. 2011. Soil and Water Assessment Tool Input/Output File Documentation: Version 2009. Texas Water Ressources Institute Technical Report No. 365. College Statation, Tx.

Rathjens, H., and N. Oppelt. 2012. SWATgrid: An interface for setting up SWAT in a grid-based discretization scheme. *Comp. & Geosci.* 45(1): 161-167.

Sheridan, J. M. 1997. Rainfall-streamflow relations for Coastal Plain watersheds. *Appl. Eng. Agric.* 13(3): 333-344.

Sullivan, D. G., H. L. Batten, D. D. Bosch, J. Sheridan, and T. Strickland. 2007. Little River Experimental Watershed, Tifton, Georgia, United States: A geographic database. *Water Resour. Res.* 43(1): 1–4.

Volk, M., J. G. Arnold, D. D. Bosch, P. M. Allen, and C. H. Green. 2007. Watershed configuration and simulation of landscape processes with the SWAT model. In *MODSIM 2007 International Congress on Modelling and Simulation*, 2383–2389. L. Oxley and D. Kulasiri, eds. Modeling and Simulation Society of Australia and New Zealand.

Walter, M. T., M. F. Walter, E. S. Brooks, T. S. Steenhuis, J. Boll, and K. Weiler. 2000. Hydrologically sensitive areas: Variable source area hydrology implications for water quality risk assessment. *J. Soil Water Conserv.* 55(3): 277–284.

Application of the SWAT Model to assess climate change impacts on water balances and crop yields in the West Seti River Basin

Pabitra Gurung
International Water Management Institute (IWMI), Kathmandu, Nepal
(p.gurung@cgiar.org),

Luna Bharati
International Water Management Institute (IWMI), Kathmandu, Nepal

Saroj Karki
Institute of Engineering, Pulchowk Campus, Tribhuvan University, Kathmandu, Nepal

Abstract

The West Seti River basin is located in the far western region of Nepal and has a catchment area of 7,438 km^2 and annual rainfall of approximately 1921 mm. According to Siddiqui et al., (2012) this basin is one of the most vulnerable in Nepal. The average elevation of the basin is 2505 m but can vary from 314 m to 7043 m in the Api and Nampa high mountain ranges. Agricultural land in this basin is categorized into three types: level terraces; slope terraces; and, valleys. The major summer cereal crops in the basin are rice, maize and millet and the major winter cereal crops are wheat and barley.

The Soil and Water Assessment Tool (SWAT) is used to simulate water balances in different cropping patterns under current and future climates. The results show that total precipitation over rice, maize, millet, wheat and barley fields are 1002 mm, 818 mm, 788 mm, 186 mm and 169 mm respectively whereas total simulated actual evapotranspiration (ET) are 534 mm, 452 mm, 322 mm, 138 mm and 177 mm respectively under current climate. Actual ET will change by +0.7% in rice, +3.4% in maize, -3.4% in millet, +41.2% in wheat and +36.2% in barley under future climate projections. Results show that yield of rice, maize and millet will decrease by 10%, 7.9% and 26.1% whereas yield of wheat and barley will increase by 7.8% and 5.8% respectively. Therefore, the impact of climate change shows that summer crop yields will decrease and winter crop yields will increase.

Key Words: Water Balance, Hydrological Modeling, Climate Change, Crop Yields, SWAT

Introduction

The Himalayan region is considered sensitive to climate change (CC), and developing countries, such as Nepal, are more vulnerable to CC because they have limited capacity to adapt to it (IPCC 2001). The Fourth Assessment of the Intergovernmental Panel on CC (IPCC 2007) states that due to increasing concentration of greenhouse gases in the atmosphere, a warming of about 0.2°C per decade is projected for the next two decades for a range of Special Report on Emissions Scenarios (SRES). The mountain regions of Nepal are the major source of water storage in the form of ice and snow. Between 1977 and 2000, the mean maximum temperature of Nepal increased by 0.06°C per year (Hua, 2009). The rise in temperature will affect the hydrological cycle, which in turn will have an impact on water availability, evapotranspiration, runoff and the discharge regime of rivers (Sayari et al., 2011).

Water has been identified as the key resource for development and economic growth of Nepal (WECS, 2011), therefore managing spatial and temporal water resources variability is critical in river basins that are vulnerable to climate change. In Nepal, most of the agricultural land in the hills and middle mountains depends on the rainfall and only few lands have irrigation access from local streams. The irrigation water management should be balanced with soil fertility management to increase the monsoonal crop yields and increasing soil fertility without considering the irrigation could result in crop failure (Shrestha et al., 2013). Consequently, agricultural production depends on the water availability in the local streams; and on the amount and timing of rainfall. Therefore, the central idea of this paper is to evaluate the impact of climate change on the soil water balance in the agricultural lands of the West Seti River sub-basins and subsequently to measure change in the yields of cereal crops. The spatially distributed agro-hydrological models are widely used to simulate hydrological parameters and crop yields in the river basin scale. Thus Soil and Water Assessment Tool (SWAT) is used to simulate water balance and crop yields in this study.

STUDY AREA: the West River Sub-basin

According to a study on climate change vulnerability in the middle and high mountain regions of Nepal (Siddiqui et al., 2012), the West Seti sub-basin was identified as one of the most vulnerable sub-basins in relation to climate change. The West Seti River Sub-basin is located in the far western region of Nepal (Figure 1) and has a catchment area of 7,438 km^2 and has confluence point with the Karnali River as the basin outlet. The sub-basin originates from the snow fields and glaciers around the twin peaks of Api and Nampa in the south facing slopes of the main Himalayas. The average elevation of the sub-basin is 2505 m but it varies from 314 m at sub-basin outlet, to 7043 m of Api and Nampa high mountain ranges. The West Seti River is one of the major tributaries of Sapta Karnali River (the longest river of Nepal). In the period of 1981 to 2010, the average annual rainfall within the sub-basin was 1921 mm whereas seasonal precipitation was 137 mm in the winter; 261 mm in the pre-monsoon; 1449 mm in the monsoon; and, 74 mm in the post-monsoon seasons. Therefore, in this sub-basin almost 75% of annual rainfall occurred during the monsoon season. In the period 1981-2010, the daily maximum temperature varied from -17.3°C to +46.7°C and minimum temperature varied from -23.4°C to +31.3°C. The projected climate result shows that the average daily maximum temperature will change by -0.62°C to +0.66°C per decade and minimum temperature will change by -1.14°C to +0.03°C per decade in this study area. This shows an average day becomes hotter and night becomes colder.

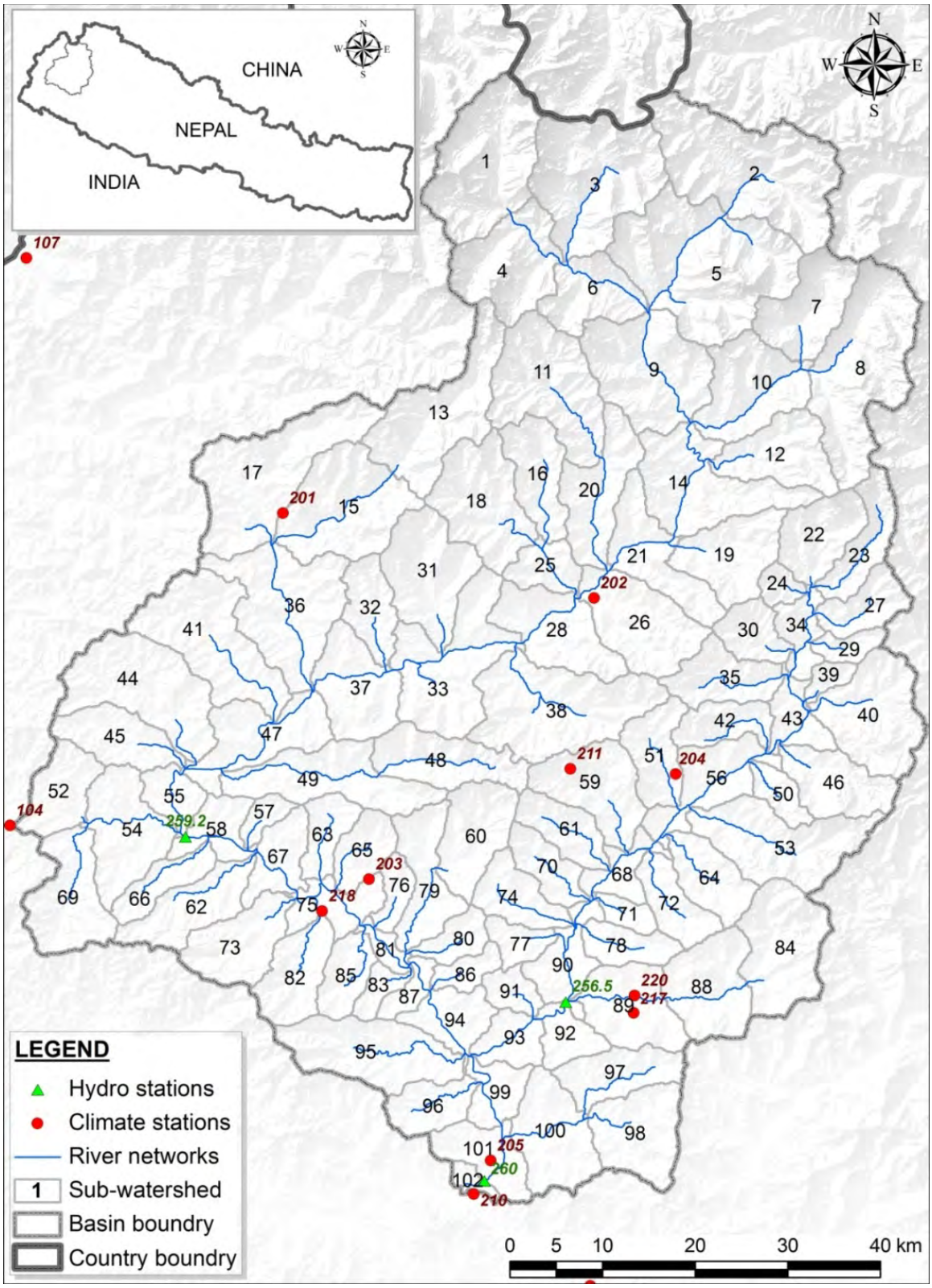

Figure 1: West Set River Sub-basin/Sub-watersheds with location of hydro meteorological stations

DATA AND SOURCES

Hydro-Meteorological Data

SWAT requires time series of observed climate data i.e. rainfall, minimum and maximum temperature, solar radiation, wind speed and relative humidity. In this study, time series climate data from 1981to 2010 from Department of Hydrology and Meteorological (DHM) of Nepal was used for model input. In addition, daily observed hydrological data obtained from DHM was used to calibrate and validate the model output. Altogether, data from 15 climate stations and 3 hydro stations was used for this study.

In this study, projected climate data from DHM (downscaled from PRECIS, and WRF regional climate models) were used to model future scenarios. The downscaled climate variables were based on the five global climate models (GCMs): ECHAM5, and HadCM3 in PRECIS; and, Era40, CCSM, ECHAM5, GFDL, and HadCM3 in WRF. The average of projected climate data from these seven projections, under A1B scenario, was used to assess climate change impacts. The projected climate time series data covered the periods from 1971 to 2000 as base line and 2031 to 2060 as the future projection.

Spatial Data

SWAT requires three basic files for delineating the basin into sub-basins and hydrologic response units: Digital Elevation Model (DEM); Soil map; and, Land Use/Land Cover (LULC) map. The Advanced Space borne Thermal Emission and Reflection Radiometer (ASTER) Global Digital Elevation Model Version 2 (GDEM V2) with 1-arc second (approximately 30 m at the equator) resolution is used for the DEM in this study. This ASTER GDEM was jointly developed by the Ministry of Economy, Trade, and Industry (METI) of Japan and the United States National Aeronautics and Space Administration (NASA). The sources of the land cover map and soil map are from National Land Use Project (NLUP), Ministry of Land Reform and Management (MoLRM), Nepal.

Agricultural Data

Based on MoAC (2005), the crops considered in this study are: rice, maize, wheat, barley, millet, potato, oilseed, sugarcane and vegetables. Agricultural fields in level terraces are classified into

rice (19%), millet (16%), sugarcane (1%) and vegetables (64%) whereas agricultural fields in slope terraces are classified into maize (36%), oilseeds (6%), potato (8%) and vegetables (50%). All the agricultural fields in river valleys are classified as rice fields. Wheat and barley are considered as winter crops in rotation with summer crops such as rice, maize, millet, oilseeds and vegetables; whereas sugarcane and potato do not contain a second crop.

METHODS

Soil and Water Assessment Tool (SWAT)

SWAT is a process-based continuous hydrological model that predicts the impact of land management practices on water, sediment and agricultural chemical yields in complex sub-basins with varying soils, land use and management conditions (Arnold et al., 1998; Neitsch et al., 2011; Srinivasan et al., 1998). The main components of the model include: climate, hydrology, erosion, soil temperature, plant growth, nutrients, pesticides, land management, and, channel and reservoir routing. Conceptually SWAT divides a basin into sub-basins. Each sub-basin is connected through a stream channel and further divided in to Hydrologic Response Unit (HRU). HRUs are a unique combination of a soil and a vegetation type in a sub watershed, and SWAT simulates hydrology, vegetation growth, and management practices at the HRU level.

The hydrologic cycle as simulated by SWAT is based on the water balance equation:

$$SW_t = SW_o + \sum_{i=1}^{n} (R_{day} - Q_{surf} - E_a - w_{seep} - Q_{gw}) \qquad (1)$$

Where,

SW_t : Final soil water content (mm)

SW_o : Initial soil water content (mm)

t : Time (day)

R_{day} : Amount of precipitation on day i (mm)

Q_{surf} : Amount of surface runoff on day i (mm)

E_a : Amount of actual evapotranspiration on day i (mm)

w_{seep} : Amount of percolation on day i (mm)

Q_{gw} : Amount of return flow on day i (mm)

Since the model maintains a continuous water balance, the subdivision of the basin enables the model to reflect differences in ET for various crops and soils. Thus, runoff is predicted separately for each sub-basin and routed to obtain the total runoff for the basin. This increases the accuracy and gives a much better physical description of the water balance. More detailed descriptions of the model can be found in Arnold et al. (2011) and Neitsch et al. (2011).

The SWAT model partitions crop yield from the total biomass on a daily basis (Arnold et al., 2011). The partitioning is based on the fraction of the above-ground plant dry biomass removed as dry economic yield and this fraction is known as harvest index (Neitsch et al., 2011). The harvest and kill operation is enabled to evaluate the crop yields in the modeling. The equations for the crop yield are;

$$YLD = bio_{ag} \times HI, \quad \text{when } HI \le 1 \tag{2}$$

$$YLD = bio \times \left(1 - \frac{1}{1 + HI}\right), \quad \text{when } HI > 1 \tag{3}$$

Where,

YLD = Crop yield (kg/ha),

bio_{ag} = Above-ground biomass on the day of harvest (kg/ha),

HI = Harvest index on the day of harvest, and

bio = Total plant biomass on the day of harvest (kg/ha)

In this study, the harvest index considered for optimal growing conditions are: rice, 0.50; maize, 0.50; millet, 0.25; wheat, 0.40; and, barley, 0.54. Whereas the harvest index considered under highly stressed growing conditions are 0.25, 0.30, 0.10, 0.20, and 0.20 for rice, maize, millet, wheat and barley respectively. The potential harvest index for a given day is depend of the

harvest index for the plant at maturity given ideal growing conditions and the fraction of potential heat units accumulated for the plant (Neitsch et al., 2011). Thus SWAT takes into account the change in harvest index for the crops when there is water stress at certain phases of the crops. The equation for the actual harvest index in water stress condition is;

$$HI_{act} = (HI - HI_{\min}) \frac{\gamma_{wu}}{\gamma_{wu} + \exp[6.13 - 0.883\gamma_{wu}]} + HI_{\min} \quad (4)$$

$$\gamma_{wu} = 100 \frac{\sum_{i=1}^{m} E_a}{\sum_{i=1}^{m} E_o} \quad (5)$$

Where,

HI_{act} = Actual harvest index,

$HI_{\min}$ = Harvest index for the plant in drought conditions,

γ_{wu} = Water deficiency factor,

E_a = Amount of actual ET on day i (mm),

E_o = Amount of potential ET on day i (mm),

i = Day in the plant growing season, and

m = Day in harvest

Model Calibration and Validation

The stations and period considered for model calibration and validation are described in Table 1. The model performance is determined by Nash-Sutcliffe Efficiency (NSE) with respect to the daily and monthly observed flow data (Karki, 2012). The performance (Table 1) is acceptable as described by Liu and De Smedt (2004); and, Moriasi et al. (2007). Whereas, the simulated crop yields are not validated due to lack of data therefore only changes in crop yields are presented in this study.

Table 1: Hydrological Stations in the West Seti River Sub-basin and Model Performance (Karki, 2012)

Station	Period		Model Performance (%)			
	Calibration	Validation	Calibration		Validation	
			Daily	Monthly	Daily	Monthly
Budhi Ganga, Chitreghat	2001-2003	2004-2006	73	90	60	78
Seti River, Gopaghat	1986-1990	1991-1995	67	86	54	90
West Seti, Banga	1981-1985	1986-1990	74	93	68	85

RESULTS AND DISCUSSIONS

Trend of Actual Evapotranspiration (ET) and Crop Yields

Figure 2 represents the correlation between simulated annual actual ET and crop yields for the period from 1981 to 2010. This study considers three scenarios of crop rotations in a year. They are;

a) Rice-Wheat-Vegetables rotation scenario,
b) Millet-Wheat rotation scenario, and
c) Maize-Barley rotation scenario

The study shows a positive correlation between actual ET and crop yields however, the correlation coefficients are less than 0.50 in all crop rotation scenarios. In scenarios (a) and (b), crop yields gradually increase with respect to increase in actual ET. Linear trend lines show that the ratios of actual ET by crop yields are 0.95 and 0.84 in scenarios (a) and (b) respectively. In contrary, the scenario (c) shows crop yields increase slightly with respect to an abrupt increase in actual ET. Hence, the linear trend line shows that the ratio of actual ET by crop yields is 3.52 in scenario (c).

Figure 3 illustrates the trend of change in actual ET and crop yields under the selected crop rotation scenarios in the period from 1981 to 2010. Results show a declining trend of both actual ET and crop yields in the simulation period. The trend of changes in crop yields is following the trend of change in actual ET in all crop rotation scenarios.

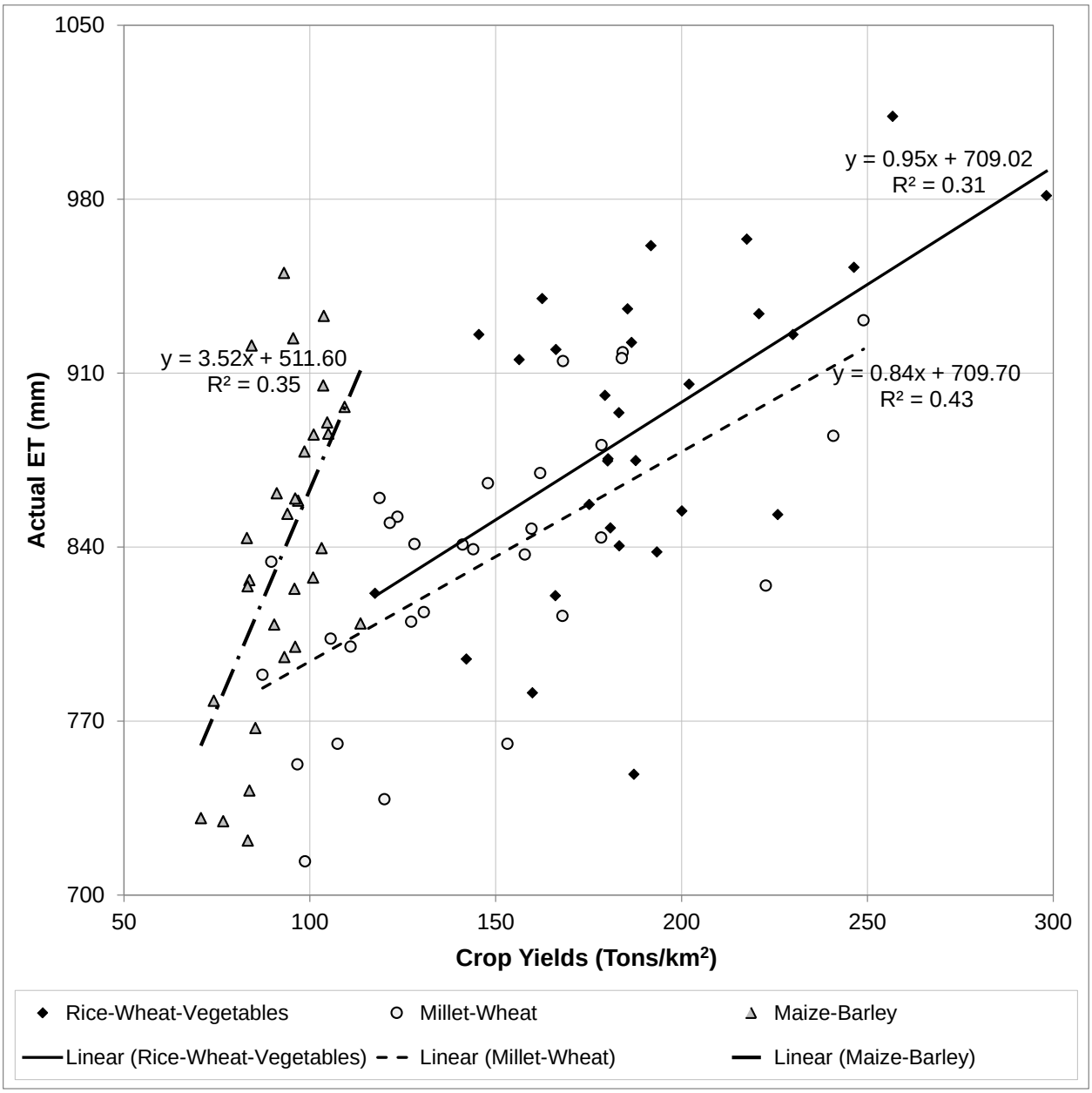

Figure 2: Correlation between Simulated Annual Actual Evapotranspiration (ET) and Crop Yields under Selected Crop Rotation Scenarios for 1981-2010 Periods

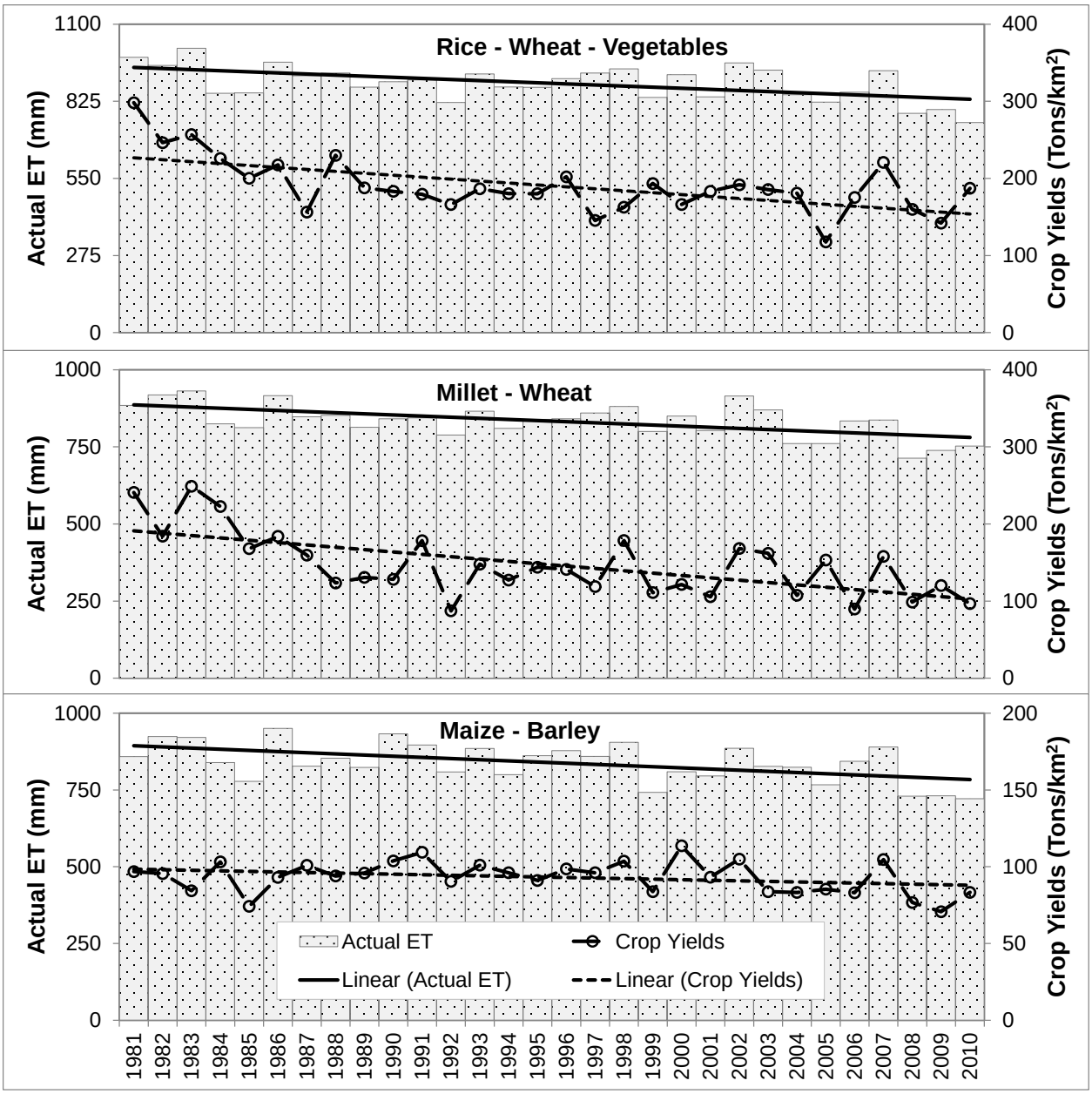

Figure 3: Actual Evapotranspiration (ET) and Crop Yields Trend under Selected Crop Rotation Scenarios for 1981-2010 Periods

Water Balance and Crop Yields

As afore mentioned, the model runs from 1981 to 2010 with daily climate data and the outcome of this study represents average results over a 30 year period as a current climate scenario. The model result shows that total precipitation over rice, maize, millet, wheat and barley fields are 1002 mm, 818 mm, 788 mm, 186 mm and 169 mm respectively whereas total simulated actual

ET are 534 mm, 452 mm, 322 mm, 138 mm and 177 mm respectively under the current climate (Table 2). Similarly, simulated surface runoff from the crop fields and crop yields are presented in the Table 2. In the study, the total surface water yields are validated with the observed river flows however the simulated crop yields are not validated as there are no available data which spatially covers over the study area. All the crops are considered as rain-fed and the auto-irrigation option of model is enabled in the simulation. In auto-irrigation option, the model will automatically apply water up to a maximum amount whenever there is water stress in crops (Neitsch et al., 2011). Hence this study only looked into how climate change will impact on the crop yields with default parameters of the model and by auto-application of irrigation.

Table 2: Simulated Water Balance and Crop Yields under Current Climate

Variables	**Summer Crop**			**Winter Crop**	
	Rice	**Maize**	**Millet**	**Wheat**	**Barley**
Precipitation (mm)	1002	818	788	186	169
Actual ET (mm)	534	452	322	138	177
Surface Runoff (mm)	235	175	170	7	10
Crop Yields (Tons/km^2)	54	83	15	45	29

Impact of Climate Change on Water Balance and Crop Yields

The climate change impact study is assessed by comparing between the model results of baseline (from 1971 to 2000) and future projections (from 2031 to 2060). The model results show that the total precipitation will change by -4.4% in rice, +0.5% in maize, -9.5% in millet, +37.3% in wheat, and +30.6% in barley fields. Similarly, actual ET will change by +0.7% in rice, +3.4% in maize, -3.4% in millet, +41.2% in wheat, and +36.2% in barley, under future climate projections. Actual ET will increase in all crops except in millet because water availability will decrease in the millet fields. The linear correlation will occur in the percentage change between precipitation and actual ET; and, between crops yield and actual ET (Figure 4). However, the correlation equations between actual ET and crop yields are different between summer and winter crop (Figure 4). The change in surface runoff on the crop fields is presented in the Table 3. Whereas the impact of climate change results show that crop yields from rice, maize and millet will decrease by 10%, 7.9% and 26.1% respectively, the yield of wheat and barley will increase by

7.8% and 5.8% respectively under future climate. The precipitation on the summer crops will decrease, except in maize which will impact negatively on the crop yields (Table 3). Whereas, precipitation on the winter crops will increase and this will lead to an increase in crop yields. Hence, the impact of climate change shows that summer crop yields will decrease and winter crop yields will increase. Therefore, the changes in amount of precipitation will impact on the actual ET, and then on the crop yields.

Table 3: Percentage Change in Simulated Water Balance and Crop Yields under Future Climate

Variables	**Summer Crop**			**Winter Crop**	
	Rice	**Maize**	**Millet**	**Wheat**	**Barley**
Precipitation	-4.4%	+0.5%	-9.5%	+37.3%	+30.6%
Actual ET	+0.7%	+3.4%	-3.4%	+41.2%	+36.2%
Surface Runoff	-12.6%	-6.3%	-16.9%	+21.9%	+18.1%
Crop Yields	-10.0%	-7.9%	-26.1%	+7.8%	+5.8%

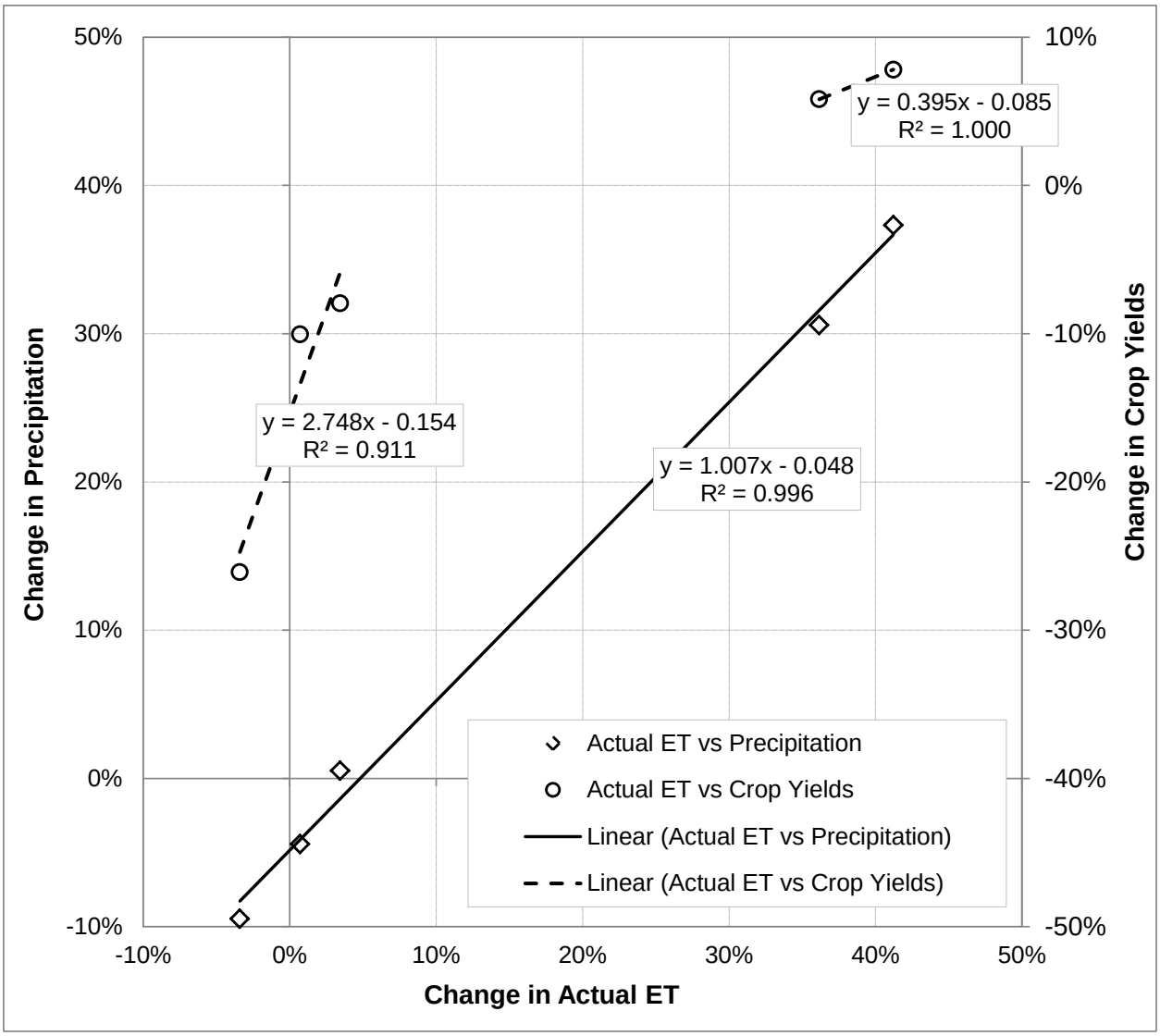

Figure 4: Correlation of Percentage Change between Precipitation and Actual ET, and between Crop Yields and Actual ET under Future Climate Scenario

Conclusion

The result of the model simulation under current climate conditions shows declining trends of actual ET and crop yields in this study area. The projected model results show that summer precipitation will decrease except on the maize fields and winter precipitation will increase; whereas actual ET will increase for all crops except in millet under future climate scenario. As a result, summer crop yields will decrease and winter crop yields will increase under projected climate change scenarios. However, there is large degree of uncertainty in the simulated results

due to disagreement among the projected future climate scenarios (Bharati et al., 2012) and this uncertainty can reliably be reduced by using only a selection of GCMs that shows high inter-model similarity for the current and future climate (Sperna Weiland et al., 2012).

The SWAT model is found to be a good tool to simulate the water balances and crop yields under current and future climate scenarios. However, the model's performance will depend on the model inputs and availability of observed data to validate output. In this study, simulated water balance components are more precise due to the availability of observed river flow data. Whereas, due to unavailability of spatially coverage of crop yields data, the study is confident to present only changes in crop yields under future climate scenario.

References

Arnold, J. G., Kiniry, J. R., Srinivasan, R., Williams, J. R., Haney, E. B., and Neitsch, S. L. 2011. *Soil and Water Assessment Tool Input/Output File Documentation Version 2009*. Texas Water Resources Institute Technical Report No. 365, Texas A&M University System, College Station, Texas.

Arnold, J. G., R. Srinivasan, R. S. Muttiah, and J. R. Williams. 1998. Large area hydrologic modeling and assessment, Part I: Model development. *Journal of the American Water Resources Association.* 34(1): 73 – 89.

Bharati, L., P. Gurung, and P. Jayakody. 2012. Hydrologic Characterization of the Koshi Basin and the Impact of Climate Change. *Hydro Nepal: Journal of Water, Energy and Environment. Special issue on "Proceedings of National Conference on Water, Food Security and Climate Change in Nepal"*. 23 – 29.

Hua, O. 2009. The Himalayas - water storage under threat. Water Storage - A strategy for climate change adaptation in the Himalayas. *Sustainable Mountain Development No. 56, ICIMOD.* 3 - 5.

IPCC. 2007. Climate Change 2007: Impacts, Adaptation and Vulnerability, Contribution of Working Group II to the Fourth Assessment Report of the Intergovernmental Panel on Climate Change. Cambridge, UK: Cambridge University Press.

IPCC. 2001. J. McCarthy; O. Canziani ; N. Leary ; D. Dokken and K. White (eds) in Cimate Change 2001: Impacts, Adaptation and Vulnareability. Cambridge: Cambridge University Press.

Karki, S. 2012. Application of uncertainty analysis techniques to SWAT model: a case study of West Seti River basin, Nepal. MSc thesis. Department of Civil Engineering, Institute of Engineering, Pulchowk Campus, Tribhuvan University, Nepal.

Liu, Y.B., and F. De Smedt. 2004. *WetSpa Extension, Documentation and User Manual.* Department of Hydrology and Hydraulic Engineering, Vrije Universiteit Brussel, Belgium. 108p.

Moriasi, D.N., J. G. Arnold, M. W. van Liew, R. L. Bingner, R. D. Harmel, and T. L. Veith. 2007. Model Evaluation Guidelines for Systematic Quantification of Accuracy in Watershed Simulations. *American Society of Agricultural and Biological Engineers.* 50(3): 885-900.

MoAC. 2005. Statistical Information on Nepalese Agriculture (Time Series Information). Agri Statistics Section, Agri-Business Promotion and Statistics Division, Ministry of Agriculture and Co-operatives (MoAC), Government of Nepal.

Neitsch, S.L., J. G. Arnold, J. R. Kiniry, and J. R. Williams. 2011. *Soil and Water Assessment Tool Theoretical Documentation Version 2009.* Texas Water Resources Institute Technical Report No. 406, Texas A&M University System, College Station, Texas.

Sayari, N., M. Bannayan, A. Farid, A. Alizadeh, and M. R. H. Kermani. 2011. Crop Water Consumption and Crop Yield Prediction under Climate Change Conditions at Northest of Iran. *International Conference on Environmental and Computer Science. IACSIT Press, Singapore. IPCBEE.* 19: 112 – 117.

Shrestha, N., D. Raes, E. Vanuytrecht, and S. K. Sah, S.K. 2013. Cereal yield stabilization in Terai (Nepal) by water and soil fertility management modeling. *Agricultural Water Management.* 122: 53 – 62.

Siddiqui, S., L. Bharati, M. Panta, P. Gurung, B. Rakhal, and L. D. Maharjan. 2012. *Nepal: Building Climate Resilience in Watersheds in Mountain Eco-Regions.* Technical Assistance Consultant's Report for Department of Soil Conservation and Watershed Management (DSCWM), Government of Nepal. International Water Management Institute (IWMI).

Sperna Weiland, F. C., L. P. H. van Beek, A. H. Weerts, and M. F. P. Bierkens. 2012. Extracting information from an ensemble of GCMs to reliably assess future global runoff change. *Journal of Hydrology*. 412-413: 66 – 75.

Srinivasan, R., T. S. Ramanarayanan, J. G. Arnold, and S. T. Bednarz. 1998. Large area hydrologic modeling and assessment Part II: Model application. *Journal of the American Water Resources Association.* 34(1): 91 – 101.

WECS. 2011. Water resources of Nepal in the context of climate change. Water and Energy Commission Secretariat, Government of Nepal, Kathmandu, Nepal.

Assessing the impact of Climate Change Scenarios on water resources in the Bhima River Basin in India

B. D. Kulkanri
Indian Institute of Tropical Meteorology, Pune 411008
bdkul@tropmet.res.in

N. R. Deshpande

S. D. Bansod

Abstract

*In this study, impacts of climate change on water balance components in the Bhima river basin in are investigated. A distributed hydrological model namely Soil and Water Assessment Tool (SWAT) has been used for study. Using outputs from RCM, viz. PRECIS ("**P**roviding **RE**gional **C**limates for **I**mpacts **S**tudies") are applied to generate daily monthly time series of precipitation, surface flow, water yield, ET and PET. Monthly calibration and validation of the SWAT model for stream flow were performed after conducting sensitivity analysis. Manual and automatic calibration methods were used for calibration. Thirty one (1970- 1990) years of meteorological and measured stream flow data were used for calibration and validation. The periods 1970-1986 and 1987-1990 were used for calibration and validation respectively including two years of warm-up period (1970 and 1971). The R^2 value during the calibration period shows a good correlation between observed and simulated values of stream flow. The R^2 and NSE values were found to be as 0.72 and 0.80 respectively. The R^2 value during the validation period shows a good correlation between observed and simulated values of stream flow. The R^2 and NSE values were found to be as 0.69 and 0.81 respectively.*

Using the calibrated model simulation at 29 sub-basins of the Bhima basin has been conducted 30 years of data belonging to control (present) and the reaming the remaining 60 years data (2011-2040) & (2041-2070) were corresponding to CHG (future) climate scenario. Quantification of climate change impact analysis has revealed that increase in precipitation has been predicted in almost half of the month of the year , while in the remaining months decrease in precipitation has been predicted. The magnitude of this increase/decrease in precipitation over the Bhima basin has been variable over various months.

Keywords: PRECIS, SWAT-Model, Soil, Land-use-land cover , Water Balance

INTRODUCTION

Climate change is mainly characterized by long-term trends in the temperature, sea level, precipitation changes and frequencies of droughts and floods etc. It is now well-established that the Earth's climate system has clearly changed, on global as well as regional scale, since the pre-industrial era. Some of these changes are attributed to human activities. Human activities have increased the atmospheric concentration of greenhouse gases and aerosols and these constituents have actively helped to increase temperature in recent few decades.

The general impacts of climate change on water resources have been brought out by the Third Assessment Report of the Intergovernmental Panel of Climate Change (IPCC), 2001). Observed warming over several decades has been linked to changes in the large-scale hydrological cycle such as, increasing atmospheric water vapor content; changing precipitation patterns, intensity and extremes; reduced snow cover and widespread melting of ice; and changes in soil moisture and runoff. Precipitation changes show substantial spatial and temporal variability.. The frequency of heavy precipitation events (or proportion of total rainfall from heavy falls) has increased over most areas.

(Goswami et. al. 2006). Changes in the total amount of precipitation as well as in its frequency and intensity have been predicted which shall in turn affect eh magnitude and timing of runoff and soil moisture status. The impacts of climate change are also predicted to be dependent on the baseline condition of the water supply system and ability of water resource managers to respond not only to climate change but also to population growth and changes in demands technology, as well as economic, social and legislative conditions. The coping capacity of the societies shall vary with respect to their preparedness. Courtiers with integrated water management systems may protect water users from climate change at minimal cost, whereas others may have to bear substantial economic, social and environmental costs to do the same.

Thus, impact of climate change is going to be most severe in the developing countries, because of their poor capacity to cope with and adapt to climate variability. This paper presents detailed results of predicted water balance components in the Bhima river basin of the country on account of climate change.

Keeping the importance of the subject , an attempt has been made in this study to quantify the impact of climate change on the water resources of the Bhima river basin using hydrological model. The study uses the **PRECIS** ("**P**roviding **RE**gional **C**limates for **I**mpacts **S**tudies") daily weather data to determine the control or present and GHG (Green house Gas) or future Water availability in space and time. **PRECIS** (pronounced as in the French **précis** - "PRAY-sea") is based on the Hadley Centre's regional climate modeling system.

STUDY AREA

This study was carried out in the Bhima river basin, a major sub-basin of the Krishna river basin in India. (Figure 1). The study basin is shared mainly by the Maharashtra , Karnataka and Andhra Pradesh states. The main channel of the river has a total length of 725 km and drains a total land area of about 48,631 km^2. Ujjani Dam, is one of the major water resources project of the basin.

Materials and Methods

SWAT (Soil and Water Assessment Tool) is a physically based, continuous-time model, developed by Dr. Jeff Arnold for UDSA-ARS (Agricultural Research Service; Arnold and Fohrer, 2005). It is used in many countries (Rosenberg et al. 1999). In China, the model has been used to simulate or predict runoff of different basins, e.g. the Yangtze River (Huang and Zhang, 2004; Zhu and Zhang 2005), Sanchuanhe River (Luo et al. 2008). In India also this model has been extensively used for climate change study of Indian River basins by IIT Delhi (Gosian et al 2006). The model has capability of being used for watersheds as well as the major river basin systems. It is distributed continuous, daily time interval hydrological model with an ArcGIS interface for pre and post processing of the input and output data. The study determines the present water availability in space and time without incorporating any man made changes like dams, diversions etc. The same framework then used to predict the impact to climatic change on the availability of water resources (future) by using the predicted data of a PRECIS with assumption that the land use shall not change over time.

DATA INPUTS FOR HYDROLOGICAL MODELING

The SWAT model requires data on terrain, land use, soil weather for the assessment of water-resources availability at desired locations of the drainage basin. To create a SWAT dataset, the interface needs to access ARC GIS with spatial analyst extension and data set files , which provide certain types of information about the watershed. The following maps and database files were prepared prior to making the simulation runs.

Digital Elevation Model (DEM)

DEM represents a topographic surface in terms of a set of elevation values measured at a finite number of points. DEM for study area have downloaded from ASTER GDM., ASTER Global Digital Elevation Model (ASTER GDEM) .The Ministry of Economy, Trade and Industry of Japan (METI) and the National Aeronautics and Space Administration (NASA) are collaborating on a project to develop ASTER Global Digital Elevation Model (ASTER GDEM), a DEM data which is acquired by a satellite-borne sensor "ASTER" to cover all the land on earth . The resolution of data is 30 seconds and it is downloaded in degree tiles and then mosaic using ARC GIS tool box. The stream layer and watershed layer have been generated using above mentioned data set.

Soil Data

The published paper maps of soil layer have been procured from the National Bureau of Soil Survey and Land Use Planning (NBSS&LUP, 2002), Nagpur, a premier Institute of the Indian Council of Agriculture Research (ICAR). These soil maps were first digitized and various soil properties viz .Hydrological Group, Maximum routing Depth (mm), Depth of soil at various layers, Water holding capacity of the soil, Texture of the soil, Bulk Density, Moist soil Albedo, Erosion factor of the soil have been worked out.

Land Cover/Land Use Layer

Classified land cover data produced using remote sensing by the University of Maryland Global Land cover Facility (13 categories) with resolution of 1 km grid cell size has been used (Hansen et al., 1999).

Delineation of the River Basin

Automatic delineation of the Bhima river basin is done by using the DEM as input and the final outflow point on the river basin as the final drainage point . Fig. 1 depicts the modeled river basin (automatically delineated using ARCGIS). The river basin has been further divided into sub-basins depending on the selection of the threshold value.

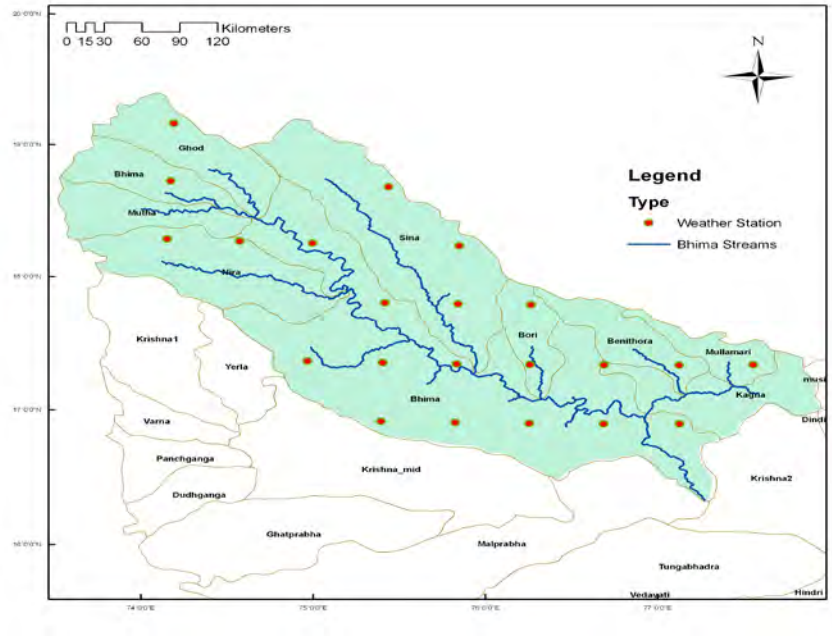

Fig. 1: Bhima river basin along with Weather stations

Weather Data

Weather Generator Data

SWAT requires daily values of precipitation, maximum and minimum temperature, solar radiation, relative humidity and wind speed. For generating this data, daily grided observed precipitation and temperature values published by India Meteorological Department (IMD) for the period 1901-2005 and 1950-2000 respectively have been used. Climatic data for solar radiation, wind and humidity published by IMD has also been used. Weather monitoring stations are also shown in Fig. 1.

Weather Data (Climate Model Data)

The data generated in transient experiments PRECIS (("**P**roviding **RE**gional **C**limates for **I**mpacts **S**tudies"), at a resolution 0.44°x 0.44°latitue by longitude RCM grid points has

been obtained from Indian Institute of Tropical Meteorology (IITM),Pune, India. PRECIS is an atmospheric and land surface model of limited area and high resolution which is locatable over any part of the globe. PRECIS is forced at its lateral boundaries by the simulations of high resolution global model (HadAM3H).

The daily weather data on temperature (maximum and minimum), rainfall, solar radiation, wind speed and relative humidity at all the grid locations were processed. The centroid of each grid point is then taken as the location of weather station to be used in the SWAT model. The procedure has been used for processing the control/present (representing series (1960-1990) and the GHG (Green House Gas) A1B scenarios, (representing series 2011-2040 and 2041-2070) .

HYDROLOGICAL MODELING OF THE BHIMA RIVER BASIN

The ArcSWAT distributed hydrologic model has been used. The basin has been sub-divided in to 29 sub-basins using threshold values adapted to divide the basin into a reasonable number of sub-basins so as to account for the spatial variability. After mapping the basins for terrain, land use and soil, each of the basins has been simulated imposing the weather conditions predicted for control and GHG climate.

Model calibration and validation for simulation

Monthly calibration and validation of the SWAT model for stream flow were performed after conducting sensitivity analysis. Manual and automatic calibration methods were used for calibration. The sensitivity analysis and calibration currently available in the SWAT-CUP , Sequential Uncertainty Fitting (SUFI 2 method) were performed to determine optimal parameter values for output variable based upon observed data collected at a single gauge outlet of the Nira river watershed at Sarati (17^0 54' 00 N, 75^0 02' 00 E). Twenty one (1970- 1990) years of meteorological and measured stream flow data were used for calibration and validation. The periods 1970-1986 and 1987- 1990 were used for calibration and validation respectively including two years of warm-up period (1970 and 1971). The warm-up period minimizes the effect of the simulated initial state variable such as soil water content and surface residue. After each parameter adjustment, the simulation and measured stream flow was compared to judge the improvement in the model prediction. The performance of the model in simulating hydrologic variables was evaluated with the help of statistical parameters such as coefficient of determination (R^2) and Nash-Suttcliffe Simulation Efficiency (NSE). The R^2 value indicates the relationship between the observed and simulated values. NSE indicates how well the plot of observed verses simulated values fits the 1:1 line, mean absolute error (MAE) and Root Mean Square Error (RMSE) indicates the error between observed and simulated values. Model prediction is considered unacceptable if the R^2 and NSE values less than or very close to 0 while perfect if the values are 1. While MAE and RMSE have has a lower limit, the value of 0 which is the optimal value for each of them. Statistical parameters for model evaluation are given in Table 1.

Table 1 Statistical parameters for Model evaluation

Statistics	Calibration Period	Validation Period
R^2	0.72	0.69
NSC	0.82	0.77
RMSC	1.08	1.14

The scatter plots of the observed and simulated monthly stream flow for the calibration period during June to September as been shown in Fig 2 (a) .

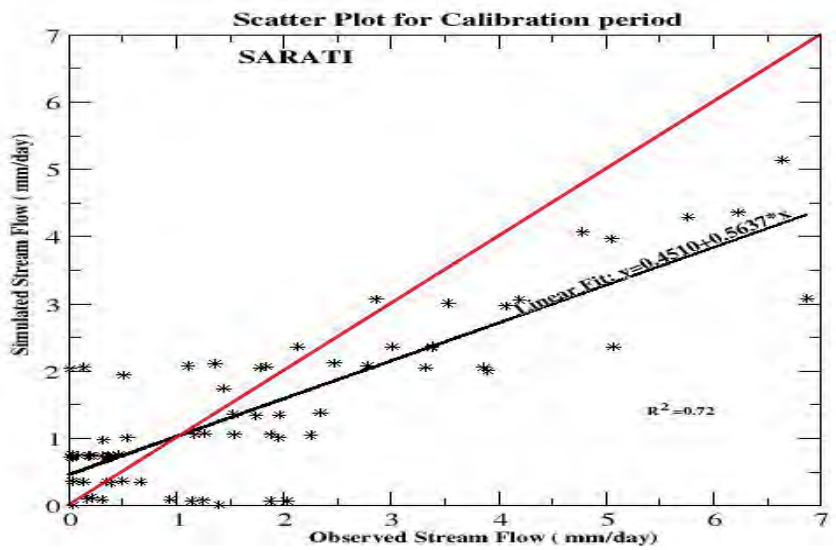

Fig 2 (a**)** Scatter plot for calibration period (1970-1986)

The major portion of the scatter plot is well distributed about the regression line indicating the model capability of estimating stream flow for well-distributed normal rainfall events. The R^2 and NSE values were found to be as 0.72 and 0.82 respectively.
The R^2 value during the calibration period shows a good correlation between observed and simulated values of stream flow. The scatter plots of the observed and simulated monthly stream flow for validation period (1987-1990) during June to September has been show in the Fig.2 (b). It has been also found that major portion of the scatter plot is well distributed about the regression line. The R^2 and NSE values were found to be as 0.69 and 0.77 respectively during the validation period. Though R^2 value during the validation period is comparatively low, it shows a good correlation between observed and simulated values of stream flow.

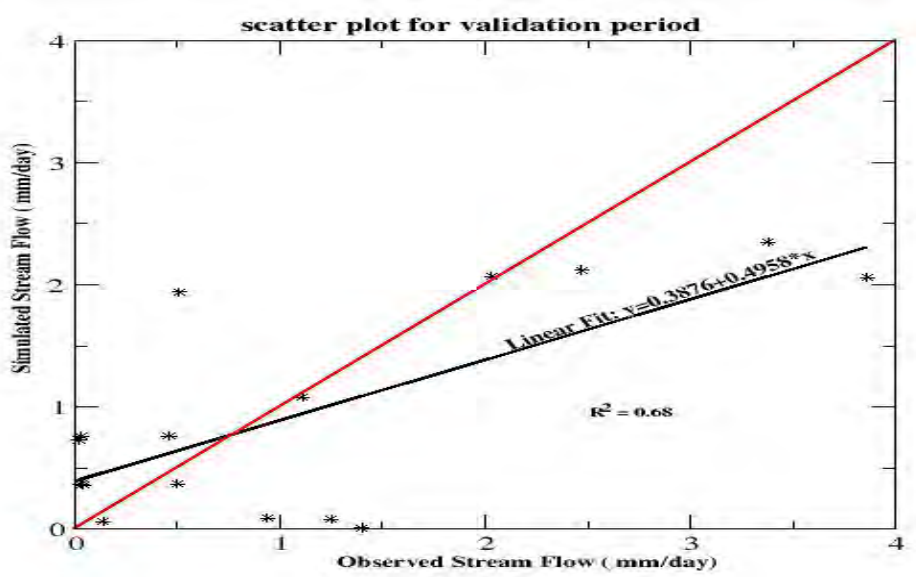

Fig 2 (b) Scatter plot for validation period (1987-1990)

The simulated monthly monsoon streamflow values have been compared with the observed stream flow values and shown in Figure 3. It has been found that the magnitudes of the simulated stream flow are lower than that of observed stream flow for most of the years during high rainfall events. In case of normal rainfall events the prediction matches with the measured values. As initially the soil was dry and major portion of rainfall was retained in the cultivable land, the runoff was generated less in the beginning of the monsoon season. It is observed that the stream flow mainly depends on the nature of rainfall. Heavy and continuous rainfall in short span of time produces more runoff. The observed as well as simulated high runoff during July, August and September months of high rainfall are ascribed to slower recharge process.

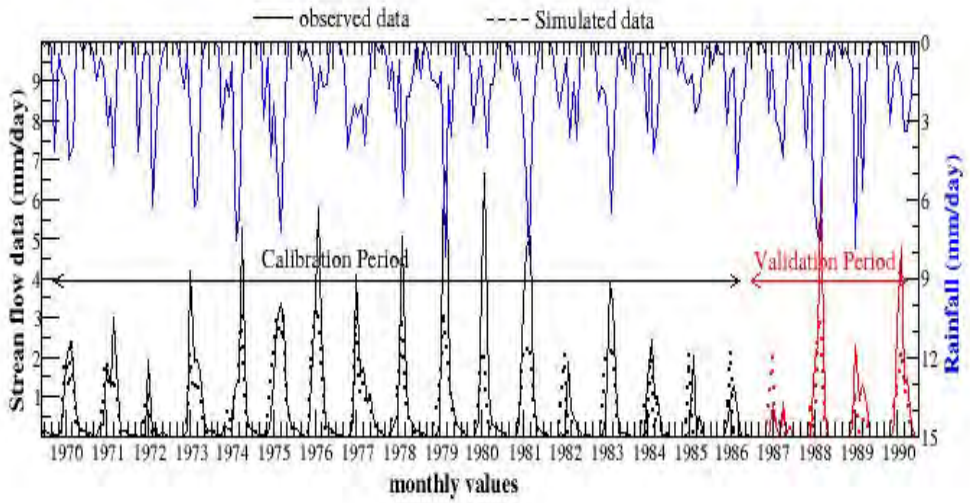

Fig 3Comparison between the simulated and observed monthly monsoon streamflow during calibration and validation period

After validating the hydrologic models with the historical record , the next step to simulate the hydrologic parameter using PRECIS data corresponding to different scenarios used in this study The details of different projections for different periods are given in succeeding sections.

CONTROL CLIMATE SCENARIO

The Bhima river basin has been simulated using the ArcSWAT model firstly by using generated daily weather data of the PRECIS, A1B control climate scenario (1960-1990). Although the SWAT model does not require elaborate calibration, yet in the present case, any calibration was not meaningful since the simulated weather data is being used for the control period which is not the historical data corresponding to the recorded runoff (Gosain & Sandhya Rao, 2007). An evaluation of the PRECIS model, skills and biases is well comparable with observed precipitation and temperature patterns with those in the baseline simulation. (Rup Kumar et al., 2006). The SWAT model has been used on various Indian catchments of varied sizes and it has been observed that the model performs very well without much calibration (Gosain et al., 2006). Presently, the model has been used with the assumption that every river basin is a virgin area without any manmade change incorporated, which was reasonable for making the initial study.

The model generates detailed outputs on flow at sub-basin outflow points, actual evapotranspiration and soil moisture status at daily interval. Further sub-divisions of the total flow into components such as surface and subsurface runoff, recharge to the ground water can be made on daily basis. The monthly average precipitation, actual evapotranspiration and water yield as simulated by the model over the Bhima basin as whole for control scenario as well as for two A1B have been computed.

PRECIS Climate Scenario

The model has been then run on the Bhima river basin using GHG climate scenarios (for the years, 2011-2040 & 2041- 2070) data but without changing the land use. The outputs of these two scenarios have been made available at sub-basin levels for the Bhima river basin. Detailed analyses have been performed on the problem basin to demonstrate the impacts at the sub-basin level. All annual water balance components have been normalized, by using mean and standard deviation of respective water balance components for the base line period (fig.4). The variation in mean annual water balance components from current to GHG scenarios shows that there has been increase in the annual precipitation. The increase in precipitation has been found more prominent for the period 2041-2070. For the period 2011-2040 there is slight decrease in surface runoff, where as for the period 2041-2070 surface runoff as well as annual water yield & actual evapotranspiration also likely to be increased. However, there is a decrease in soil moisture storage.

CHANGES IN WATER BALANCE COMPONENTS

As mentioned above the monthly average precipitation, actual evapotranspiration, potential evapotranspiration, surface flow and water yield as simulated over the Bhima

basin as a whole for control and two Scenarios(A1B PRECIS) has been obtained. Fig 5 the variation in mean monthly water balance components from control to GHG scenario, both in terms of change in individual values of these components as well as percentage of change over control It may be observed from the above figures that increase in precipitation has been predicted in almost more than half of the months the year, while remaining months decrease in precipitation has been predicted. The magnitude of this increase/decrease in precipitation over the Bhima basin has been variable over various months. The monthly average precipitation, actual evapotranspiration and water yield as simulated by the model over the basin is increased during the period 2041-2070.

.

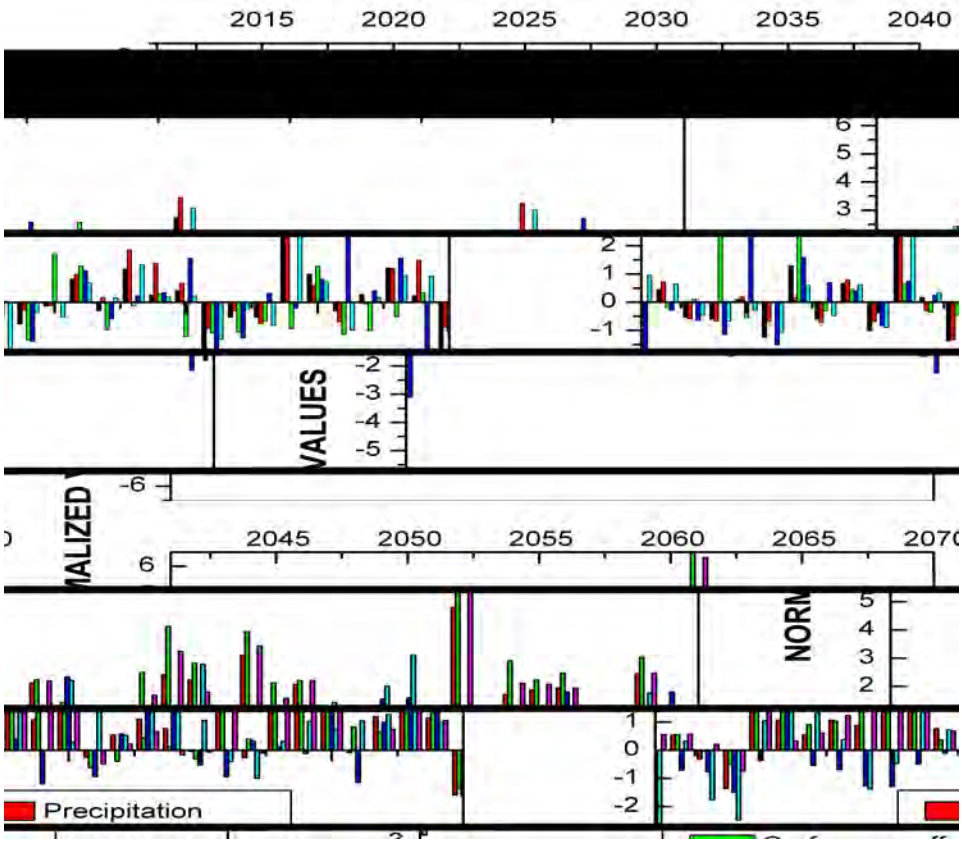

Fig.4 Mean monthly water balance components for A1B Scenarios (2011-2040 & 2041-2070)

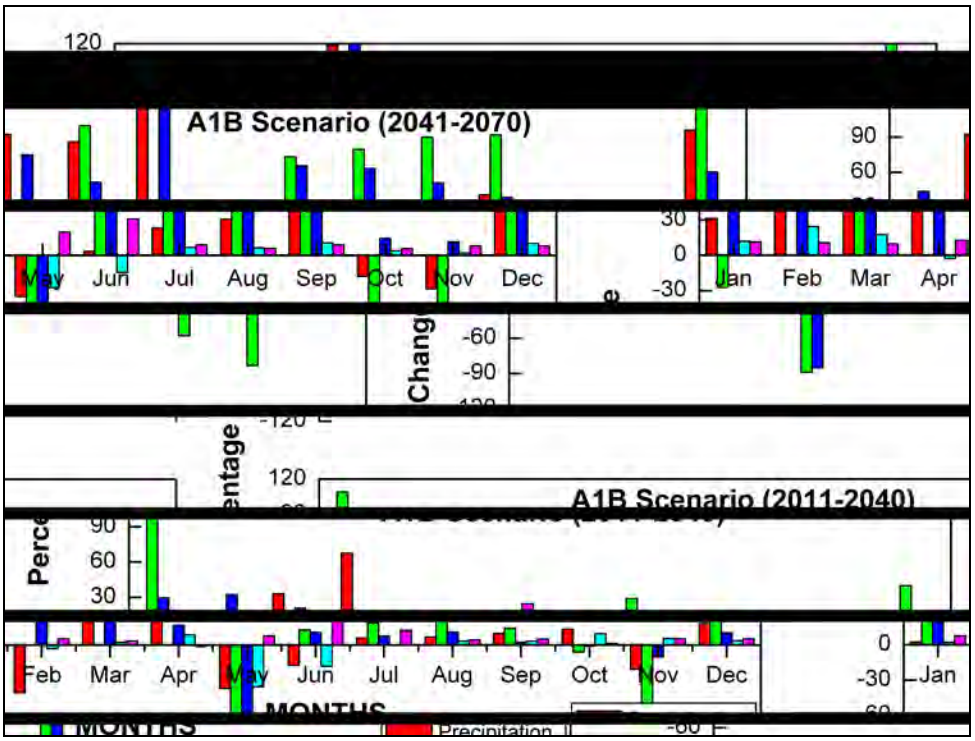

Fig. 5 Difference in mean monthly water balance components from control to A1B Scenario

Limitations of the Study

It also should be noted that future flow conditions cannot be projected exactly due to uncertainty in climate change scenarios and GCM outputs. However, the general results of this analysis should be identified and incorporated into water resources management plans in order to promote more sustainable water use in the study area.

Climate change impact assessment on water availability, the study watershed consider two model analyses and out puts, which are depends on simplified assumptions. Hence, it is unquestionable that the uncertainties presented in each of the models and model outputs kept on cumulating while progressing towards the final output. These Uncertainties include: Uncertainty Linked to Data quality, General circulation Model (GCMs), Emission scenarios.

The model simulations considered only future climate change scenarios assuming all other things constant. But change in land use scenarios, soil, management activities and other climate variables will also contribute some impacts on water availability and crop production.

CONCLUSION

In this study projections of precipitation and evaporation change and their impacts on stream flow were investigated in the Bhima river basin for the 21st century. This study attempts to quantify the climate change impacts on soil water availability and surface runoff using PRECIS model output and water balance simulation modelling approach of SWAT model. In doing so this study reached to the following summaries.

1. The result of hydrological model calibration and validation indicated that the SWAT model simulates the stream flow appreciably well for the study area. The model performance criterion which is used to evaluate the model result, the coefficient of determination and the Nash-Sutcliffe simulation efficiency values obtained proved this fact.

2. Hydrological impact of future climate change scenarios indicated that there will be variation in mean annual water balance components from current to GHG scenarios shows that there has been increase in the annual precipitation. The increase in precipitation has been found more prominent for the period 2041-2070. For the period 2011-2040 there is slight decrease in surface runoff, where as for the period 2041-2070 surface runoff as well as annual water yield and actual evapotranspiration also likely to be increased. However, there is a decrease in soil moisture storage.

3. This study used future climate series for one of the RCM, PRECIS for the impact analysis. Due to uncertainties in climate forecasting, the use of climate model ensembles and multiple scenarios will be useful for understanding the range of climate change impact that can be expected on the water resources in the Bhima river basin.

Acknowledgments

Authors are thankful to Prof. B. N. Goswami, Director, IITM, Pune, Dr. R. Krishnan, Scientist-G and Head Centre for Climate Change Research, for their keen interest and encouragement for carrying out this study.

REFERENCES

Arnold, J.G., Fohrer, N., (2005) SWAT2000 current capabilities and research opportunities in applied watershed modelling. Hydrological Processes 19, pp. 563-572.

Gosain, A. K. Sandhya Rao and Debajit Basuray (2006) Climate change impact assessment on hydrology of Indian river basins Current Sciences Vol. 90 No. 3, pp. 346-353

Gosain, A. K. & Sandhya Rao (2007) Impact Assessment of Climate Changes on Water Resources of two River systems of India. Jalvigyan Sameeksha, Vol22, 2007, pp. 1-19

Goswami B.N**.,** Venugopal V., Sengupta D., Madhusoodanan M.S., Xavier Prince K., (2006) Increasing trend of Extreme Rain Events over India in a Warming Environment, Science, 314, 5804, 1 December, 1442-1445

Hansen. M. C., DeFries, R. S., Townshend, J. R. G. and Sohlberg, R. (2009) *1 km Global Land Cover Data Set Derived from AVHRR.* Global Land Cover Facility, University of Maryland institute for Advanced Computer Studies, College Park, Maryland, USA, 1999.

Huang, Q.H., Zhang, W.C., (2004) Improvement and application of GIS-based distributed SWAT hydrological modelling on high altitude, cold, Semi-arid catchment of Heihe River Basin, China. Journal of Nanjing Forestry University (Natural Sciences Edition) 28 (2), pp. 22-26.

IPCC 2001: Climate Change (2000) – The science of climate change. Assessment report of the IPCC (Intergovernmental Panel for Climate Change) Working Group I (Eds J. T. Houghton et al) and WMO/UNEP, Cambridge University Press, Cambridge.

Luo, R., Xu, Z.X., Cheng, L., (2008) Application of SWAT model in the Sanchuan River catchment. Journal of Water Resources & Water Engineering 19 (5), pp. 28-33

NBSS &LUP (2002) : National Bureau of Soil & Land use Planning , Nagpur Soils of India NBSS Publ. No. 94 pp. 1-129

Rosenberg, N.J., Epstein, D.J., Wang, D., (1999) Possible impacts of global warming on the hydrological of the Ogallala aquifer region. Climatic Change 42 (4), pp. 677-692

Rupa Kumar, K., Sahai, A. K., Krishna Kumar, K. , Patwardhan, S. K., Mishra, P. K., Revadekar, J. V., Kamala, K. & Pant, G. B. (2006) High- resolution climate change scenarios for India for the 21st century. Current Science. Vol. 90 No. 3 Feb. 2006 pp.334-345

Zhu, L., Zhang, W.C., (2005) Responses of water resources to climatic changes in the upper stream of the Hanjiang River basin based on rainfall-runoff simulations. Resources Science 27 (2), pp. 16-22.

Comparing the Changes in Hydrology due to Different Development Regulations using Sub-Daily SWAT

Roger H. Glick, P.E., Ph.D.
Watershed Protection Department
City of Austin, Texas
PO Box 1088
Austin, TX 78767
Roger.Glick@austintexas.gov

Leila Gosselink, P.E.
Watershed Protection Department
City of Austin, Texas
PO Box 1088
Austin, TX 78767
Leila.Gosselink@austintexas.gov

Abstract

The City of Austin, Texas is in the process of updating its land development regulations and requested that the hydrologic impacts of the new regulations be compared to existing regulations. The authors increased the scope of the project in order to determine the overall effectiveness of land development regulations with respect to changes in hydrology. Four development scenarios were modeled using SWAT. These models represented conditions from pre-1970s through the proposed regulations and a baseline undeveloped scenario. Scenarios were compared based on impacts on flooding, erosion and aquatic life potential. Early regulations with narrow stream buffers and detention basins addressed infrequent flood events but increased the peak flows associated with return periods less than 25 years, increased excess shear and changed hydrologic metrics indicating a probable decrease in aquatic life potential. Later regulations, including the proposed regulation, which include more extensive creek buffers, detention and water quality controls, controlled the infrequent flood events and decreased the peaks flows for different return periods to near undeveloped conditions, reduced excess shear and maintained hydrologic metrics for aquatic life potential.

Keywords: Hydrology, development, flooding, erosion, aquatic life

Introduction

Over the past forty years the City of Austin (COA), Texas has implemented various rules and ordinances in order to protect the public, property and the natural environment from the changes in hydrology associated with urbanization. The initial ordinance, the Waterways Ordinance (WO) was passed in 1974 and focused primarily on flooding. The Comprehensive Watershed Ordinance (CWO) was passed in 1986 and included creek buffers and addressed water quality and erosion concerns in addition to flooding. The City is in the process of adopting the Watershed Protection Ordinance (WPO) which will build on the CWO. A rigorous evaluation of the effectiveness of these ordinances was not possible using field data due to multiple ordinances applied to a given watershed over time and the length of time for natural processes like erosion to occur.

This study evaluates effectiveness of these ordinances with respect to flooding, erosion and aquatic life potential using the sub-daily and urban BMP options in the latest version of AcrSWAT (2012.10.17) (Arnold et al, 2013).

Study Site and Model Development

The study site is a 4.99 km^2 tributary of Gilleland Creek located east of Austin, TX (30°17'45"N, 97°33'12"W) in the Blackland Prairie eco-region (Fig. 1). The watershed is currently undeveloped and dominated by unimproved pasture and scattered honey mesquite (*Prosopis glandulosa*) and eastern red cedar (*Juniperus viginiana*). In addition to modeling the undeveloped condition, four models were developed for this watershed based on the different regulations. All five models used the same SSURGO soils data and 3-m DEM developed from LIDAR data collected by COA in 2003.

The land use maps for the different development scenarios were created by the COA Watershed Protection Department's (WPD) Policy and Planning staff. Initially, a 'wallpaper' was created containing the various land uses in proportions found throughout the city. Buffers and easements were them applied to the stream in accordance to the different regulations. Prior to the implementation of WO, the only requirement was a limited easement of 9 m from the centerline of the creek along the channel with drainage areas >130 ha (320 ac). The WO required a wider easement (30 m) to the same extent. CWO required a wider buffer (45 m) which could include no development and an additional water quality transition zone of 60 m which could have limited development. The proposed WPO required a wider buffer (90m) but does away with the water quality transition zone. WPO also extends smaller buffers (30m) to areas with drainage >25 ha (64 ac). Precipitation was based 15-min rainfall from two gauges that are part of the COA Flood Early Warning System. Daily temperature data were from the NWS Robert Mueller Airport station. Other weather inputs were generated using the WGEN_US_COOP_1960_2010 database in ArcSWAT. Since the watershed is ungaged, model parameters were adjusted based on local knowledge and used for all scenarios. The adjusted parameters are in Table 1.

In addition to different land use requirements, the ordinances also had different requirements for stormwater control measures (SCMs). The WO was focused primarily on flooding generated by larger storm events and only required detention to control the peak flow from the 2-, 10-, 25- and 100-yr 24-hr design rainfall (Type III) (COA, 2013a). This was accomplished by placing an on-

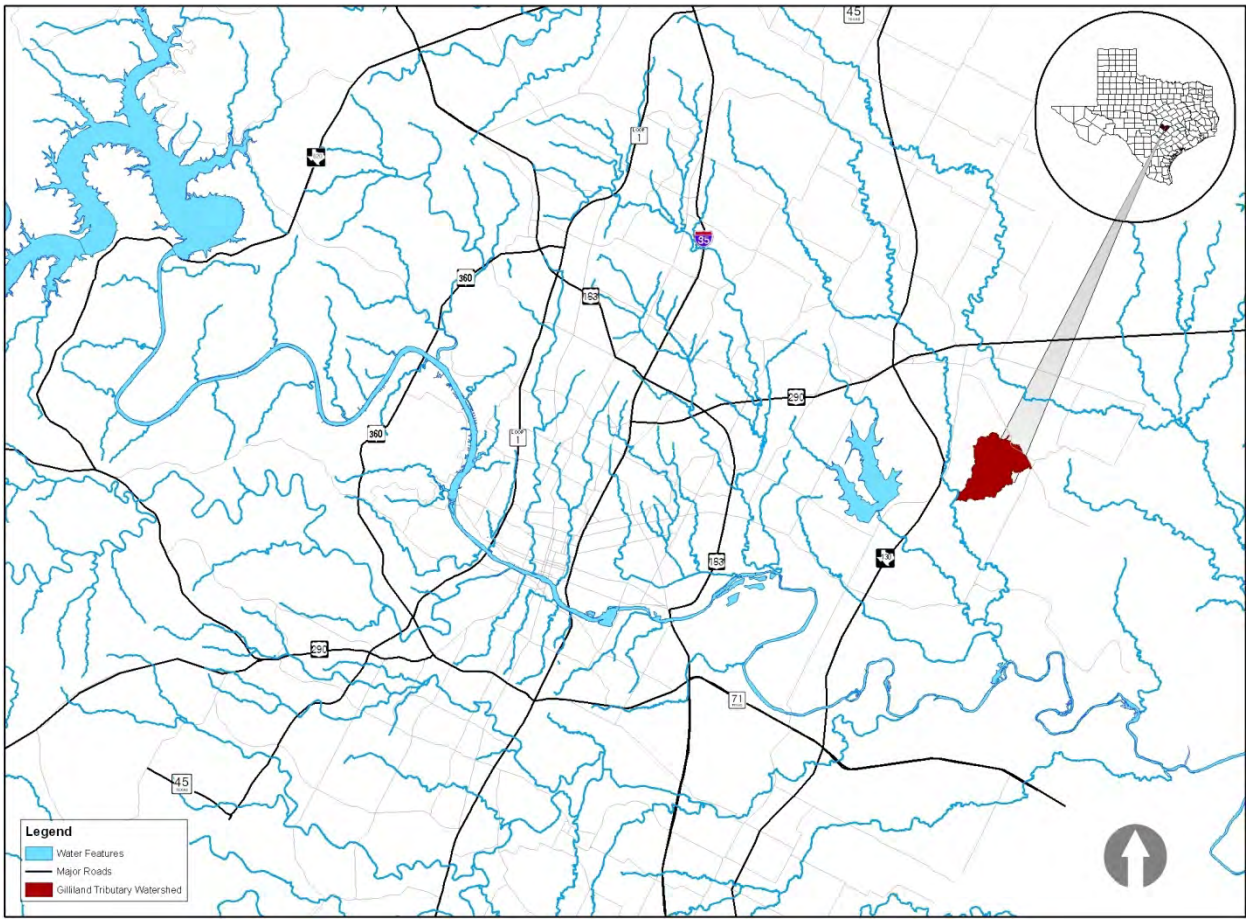

Figure 1. Gilleland tributary study area.

line detention basin at the outlet of reach 9 (see Figure 2). The peak discharges from the developed conditions for the design rainfalls matched the undeveloped peaks after passing through the detention basin. This detention basin design was also used for the CWO and WPO models.

In addition to detention, CWO and WPO require water quality controls, typically accomplished with sedimentation-filtration basins (SF). The typical COA SF is designed to capture a specified volume of upland runoff from urban areas in a sedimentation basin. The outlet of the sedimentation basin is usually controlled by an orifice designed to allow water to pass to the sand filter basin at a rate that would allow the entire volume to be drained in 48 hours. Effluent from the sand filter is discharged into the creek. The volume of the sedimentation basin is determined by the impervious cover of the contributing area: for 20% impervious cover, the volume is 1.27 cm; for every additional 10% of impervious cover, the capture volume increases by 0.254 cm. If the volume of the sedimentation basin is exceeded, additional flow bypasses the system and is discharged into the creek (COA, 2013b). In ArcSWAT 2012.10.7 SF basins are applied to runoff from specified urban HRUs, the runoff is then combined with runoff from other HRUs before being routed through the reach.

The five models were run for twenty-five years 1987-2012 based on the valid 15-minute rainfall dataset. The first two years were used as a warm up period and not used for analyses.

Table 1. Calibration parameters for Gilleland scenarios

Parameter	Value	File
CH_N2	0.035	.RTE
CH_K2	5	.RTE
ALPHA_BNK	0.25	.RTE
ALPHA_BF	0.1	.GW
GW-DELAY	10	.GW
BFLO_DIST	0.25	.BSN
IUH	2	.BSN
UHALPHA	4	.BSN
SURLAG	1	.BSN
IRTE	1	.BSN
CH_N1*	0.035	.SUB
CH_K1*	5	.SUB
CN for PAST*	-4	MGT

* for undeveloped case only

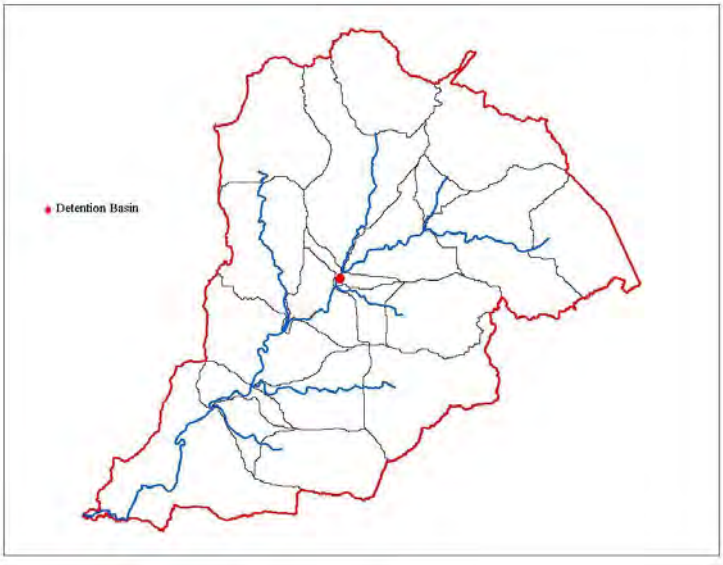

Figure 2. Detention basin location in WO, CWO and WPO models.

Data Analyses

Data from each scenario were analyzed based on the three different missions for WPD, flooding erosion and water quality & aquatic health. Flooding was assessed through peak flow rates for different return periods. Erosion was assessed by an evaluation of annual average cumulative excess shear. Water quality was not addressed in this study but the potential impacts of hydrologic modification on aquatic life were assessed.

Table 2. Peak flow rate recurrence intervals for development scenarios on Gilleland tributary.

Recurrence Interval (yr)	UND (cms)	PRE (cms)	WO (cms)	CWO (cms)	WPO (cms)
24.00	39.4	65.2	50.7	39.3	39.7
12.00	37.8	62.7	47.6	32.9	38.6
8.00	36.1	52.7	43.1	31.2	32.8
6.00	34.8	50.1	41.2	31.1	31.9
4.00	32.1	49.3	39.3	29.1	29.9
3.00	30.6	45.9	37.5	26.4	29.7
2.00	25.7	40.7	33.1	22.8	25.3
1.50	21.7	38.3	29.9	18.4	22.2
1.00	18.8	32.8	27.9	12.6	15.2
0.75	16.4	29.5	24.2	10.4	12.8
0.50	11.4	23.8	20.3	3.87	4.96
0.25	5.59	17.6	14.4	0.616	0.681

Flood Impacts

Typical flood analyses examine large and infrequent flood events based on design rainfall events to protect lives and property. However, less frequent events may also cause problems with low water crossings or inundation of the floodplain. While detention basins may limit peak discharge, the recurrence of that discharge may be more frequent than previously experienced. Frequent flood peaks were assessed in this study by comparing the peaks at given return periods to the same return period peaks. This was accomplished by ranking the storm peaks in descending order for the 23 year period of analysis. Then, assuming a Weibull distribution, average recurrence interval was determined by,

$$T = \frac{N+1}{m} \quad [1]$$

where T is the average recurrence interval in years, N is the number of years in the record and m is the rank of the event (Gordon, et al., 1994). Recurrence events for the five development scenarios on Gilleland are presented in Table 2.

Based on the modeling study, pre-ordinance development (PRE) exhibited much higher peaks for every recurrence interval. The 1-yr recurrence for undeveloped (UND) would be expected approximately every 3 months while the UND 24-yr recurrence would occur approximately every 18 months. Adding the detention basin at the end of Reach 9 in the WO scenario had some impact but not as much as planned. It was hoped that by placing the detention basin in this location the downstream flood peak would pass before the upstream peak arrived. This worked to some extent but all of the peak flows were higher for every recurrence interval. This was more pronounced at the more frequent events (<2-yr) because the smallest storm the detention basin was designed to control was the 2-yr rainfall event. The addition of SF controls in the CWO and WPO scenarios significantly reduced the peak discharges across all recurrence intervals, nearly matching the undeveloped condition for recurrence intervals between 2 and 24

years. For more frequent recurrence intervals the SF controls removed almost the entire peak, such that the 3-month peak was almost non-existent.

Erosion Impacts

The impacts of development on erosion potential were assessed using average annual excess shear (ES). Excess shear occurs when the shear stress exceeds the critical shear for the stream bed and bank. When the flow exceeds the channel capacity and spills into the floodplain, average velocities drop and total shear decreases while shear in the channel will continue to increase. To account for this, this study only examined shear in the main channel.

Shear and critical shear were computed using the following equations:

$$\tau = \gamma_w \cdot D_H \cdot S_w \quad [2]$$

and

$$\tau_c = \Theta_c(S_g - 1) \cdot \gamma_w \cdot d_{50} \quad [3]$$

where,

τ = shear (Pa)
τ_c = critical shear (Pa)
γ_w = density of water (kg/m^3)
D_H = depth of water (m)
S_w = channel slope (m/m)
S_g = specific gravity of soil, 2.65
d_{50} = median particle diameter (m)
θ_c = critical Shield's parameter, 0.047

ES was defined as:

$$ES = \sum(\tau - \tau_c) \text{ for all } \tau > \tau_c \quad [4]$$

Hydraulic properties at the watershed outlet were estimated using WinXSPRO 3.0 (Hardy, et al., 2005). This program uses the channel cross-section and slope (estimated from the DEM) to develop a stage-discharge relationship based on Manning's equation. The program allows the user to treat the floodplain differently than the main channel to separate total flow from flow in the main channel. A Manning's n of 0.035 was used in the channel while 0.1 was used in the floodplain. WinXSPRO computed shear discharge as a function of stage for both the total cross-section and the main channel. A table relating channel ES to discharge, assuming a 19 mm median particle diameter, was developed and loaded into Hydstra version 10.3.2 (Kisters, 2011). The HYCRSUM routine in Hydstra was used to compute cumulative excess shear for the 23 year study period based on flow generated by the sub-daily SWAT models. Average annual excess shear for the five scenarios is presented in Figure 3.

With the 19 mm median particle diameter, ES increased by 181% without any regulations compared to the undeveloped scenario. When detention was added as part of the WO scenario ES increased by 196%. The increase in ES with the added detention is a result of the detention basin maintaining flows above the flow associated with τ_c for a longer period of time. The CWO

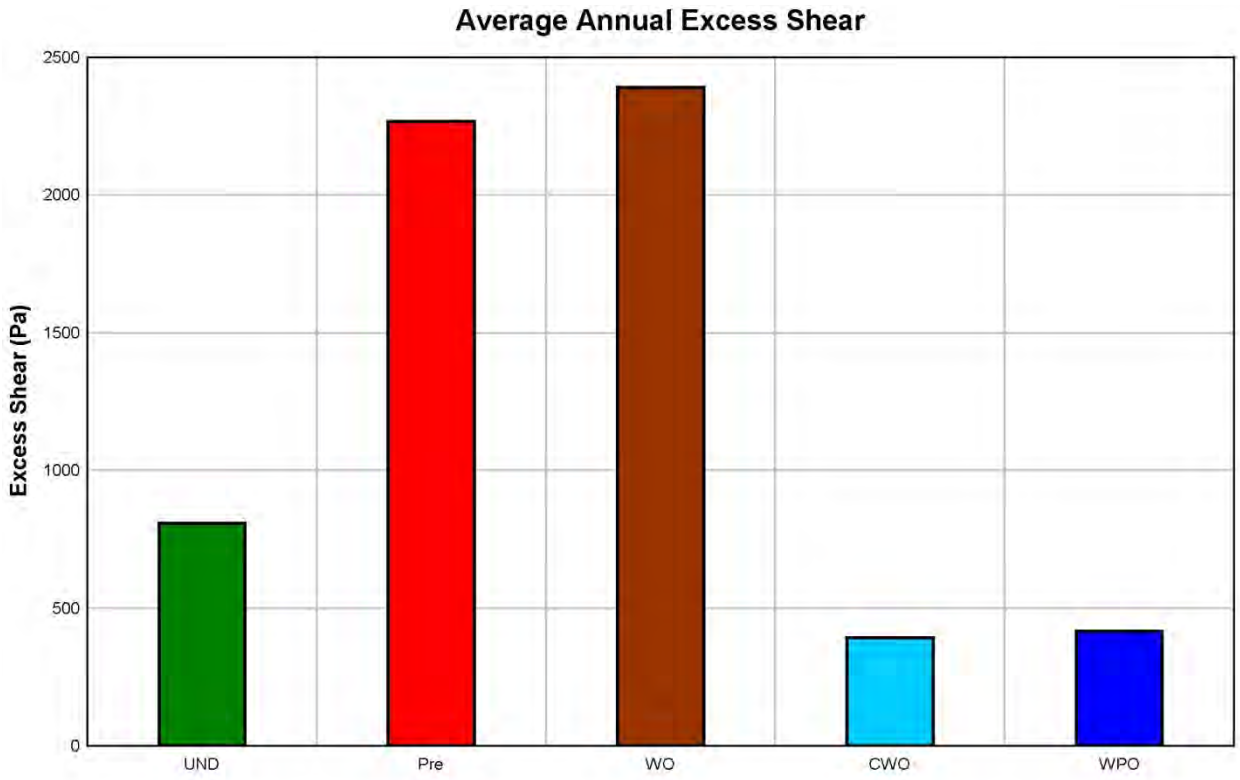

Figure 3. Average annual excess shear for five different development scenarios in the Gilliland tributary assuming a 19 mm median particle diameter.

and WPO scenarios resulted in a reduction of ES by approximately 50% compared to undeveloped. This may result in some aggrading of the stream under this condition until equilibrium is reached with a new median particle size is reached.

Another study by COA (Glick and Gosselink, 2013) indicates that these trends hold for other particle sizes. However, for median particle diameters less than 19 mm, there will be degradation of the channels even with the inclusion of SF basins given this channel cross-section. This is due to the long drawdown time of the SF basins resulting flows above the critical flow associated with τ_c for smaller particle sizes. This will be of most concern in areas like the one where the study watershed is located with deep clay soils. While the increased buffers associated with the proposed WPO may not address this directly, the wider buffer will provide an area for the processes to occur without threatening structures.

Aquatic Life

The potential impacts on aquatic life were evaluated based on various hydrologic metrics identified by Glick and Gosselink (2009; 2011; 2012) and Glick, et al. (2010) which correlated well with COA Environmental Integrity Index (EII) aquatic life scores. These metrics measure the presence/absence of flow, the ratio of baseflow to total flow and the variability of the flow regime. These metrics are not absolute; some changes in the metrics might indicate a 'better' flow regime. However, it would be a change to regime in which the naturally occurring organisms developed. Use of these metrics should be based on local background conditions.

Table 3. Hydrologic flow metrics associated with aquatic life potential in the Austin, TX area for different development scenarios.

	UND	PRE	WO	CWO	WPO
T_{dry}	0.524	0.244	0.256	0.010	0.099
BFR	0.3734	0.1491	0.1534	0.6382	0.6328
F_{Ln}	15.78	27.04	28.83	10.87	8.65
F_{Ld} (day)	16.41	4.88	4.63	4.13	4.39
Q_{Peak} (cms)	39.4	65.2	50.7	39.3	39.1
SD	0.391	0.713	0.658	0.322	0.332
F_{Hn}	16.83	84.09	79.22	26.65	23.91
F_{Hn} (day)	2.30	0.16	0.19	4.61	5.19
$+_{mean}$ (cms)	0.100	0.246	0.244	0.113	0.106
$-_{mean}$ (cms)	0.047	0.076	0.077	0.026	0.026

Ten hydrologic metrics which correlate well with EII aquatic life score were computed for the different scenarios (Table 3). These metrics fall into two broad categories: stream flow and flow variability. The first four metrics, T_{dry} (dry fraction, >0.003 cms), BFR (baseflow ratio), F_{Ld} (average length of low flow/dry events, >0.003 cms), and F_{Ln} (annual number of low flow/dry events), are indicators of flow, primarily non-storm flows. As watersheds urbanize, creeks in arid and semi-arid areas tend to be dry more frequently; the ratio of baseflow to stream flow decreases; and the number of wet-dry cycles increases. Alteration of these may affect life cycles of the naturally occurring aquatic species. Of particular concern may be F_{Ln}; as the number of low-flow cycles increases the species may not be able to complete their life cycle, reducing species diversity. The stream flow metrics in Table 3 indicate that the aquatic life potential would tend to decline without regulations (PRE) and if detention alone is the only SCM strategy employed. The stream would be dry more often and BFR is reduced by more than 50%. In addition, the number of dry cycles increased (F_{Ln}) where increases indicate the potential interruption of the normal life cycles for some of the aquatic species. These numbers correspond well to other Austin area creeks with measured flow that were developed under these regulations (Glick, et al., 2010). With the addition of SF as an SCM in the CWO and WPO scenarios the stream appears to have more baseflow and be dry less frequently than in the undeveloped condition. This would be beneficial to the aquatic community but may shift the biological community composition from its natural state. As yet there are no gauged watersheds fully developed under CWO regulations so it is difficult to assess if this would actually be the case but it does appear that the addition of SF is beneficial to aquatic health with respect to low flow conditions.

The remaining metrics measure flow variability. These are more important to habitat stability. Q_{peak} (peak flow rate) and SD (standard deviation) provide an indication of the overall peak and variability. The combination of detention and SF used in the CWO and WPO scenarios appear to produce flows that are similar to the undeveloped condition while PRE and WO scenarios have higher peaks and more variability. This can also be seen in the mean daily flow duration curve (Figure 4) and the flood analyses in Table 2. F_{Hd} (duration of high-pulse events) and F_{Hn} (number of high-pulse events) are indicators of flow in excess of the 75^{th} percentile of the undeveloped condition; typically duration of high pulses decrease with development but the

Figure 4. Mean daily flow duration curves for different development scenarios of the Gilliland tributary.

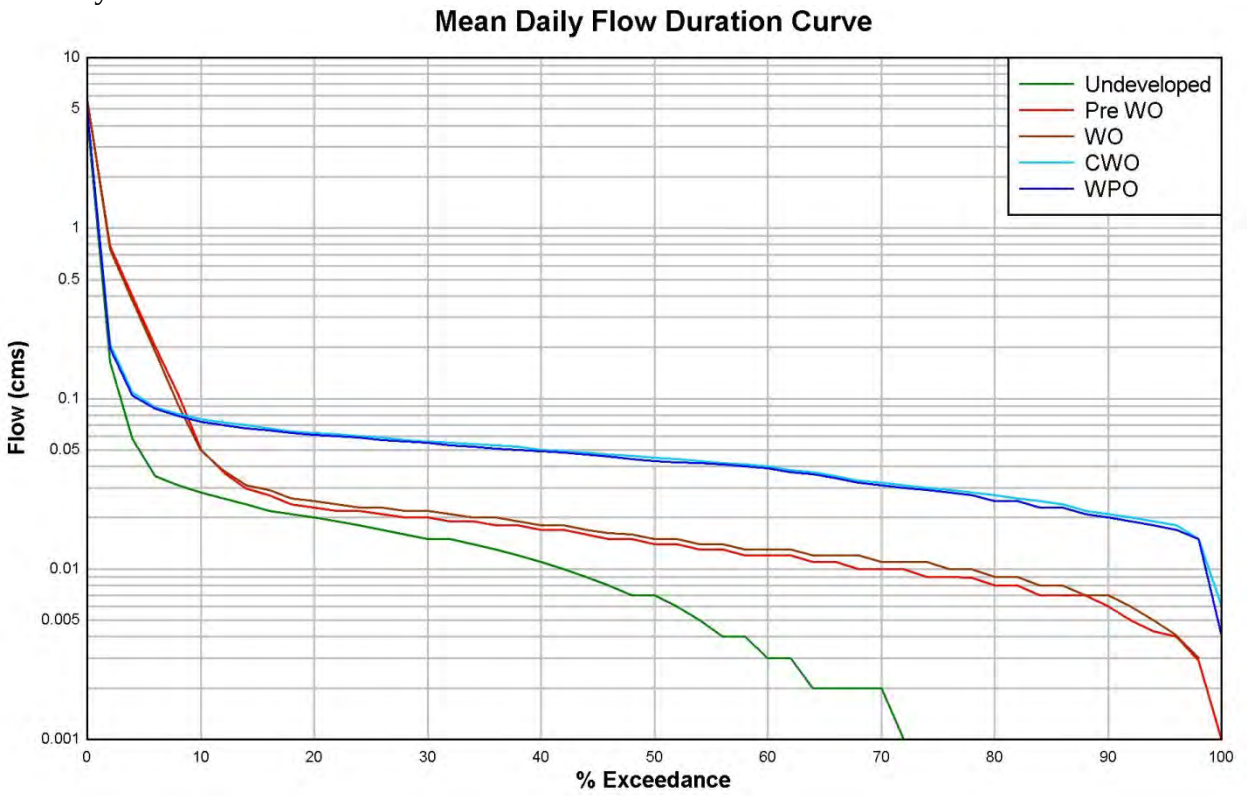

numbers increases. The change in these metrics without SCMs and detention only is dramatic, indicating a very flashy stream. The addition of SFs to the system under the CWO and WPO scenarios mitigate these changes to some extent, however the long drawdown of the SF controls results in extended high flow condition based on the undeveloped 75th percentile flow rate. Since the 75th percentile flow for the undeveloped condition was low, the increase in F_{Hd} may be outweighed by extending baseflow. The final measures of flow variability, $+_{mean}$ and $-_{mean}$, are the average rates of rise and fall in the daily mean flow rate. These typically increase with development. The use of detention alone has little impact on these variables but it appears the use of SF will address the changes in average rise to a large extent but reduces the average fall, once again due to the long drawdown times associated with SF.

There appears to be a slight improvement in the hydrologic metrics comparing CWO and WPO which may be a result of the increased buffers. This improvement is modest compared to the incorporation of SF as SCMs in the CWO.

Conclusions

Four scenarios based on different development regulations and an undeveloped condition were simulated for twenty-three years using the sub-hourly version of SWAT and urban BMP routines. The scenarios represented pre regulation development, development under the Waterways Ordinance in the 1970s, the Comprehensive Watershed Ordinance of the 1980s and a proposed Watershed Protection Ordinance. These scenarios were compared to the undeveloped

condition and the changes in hydrology were evaluated on impacts on flooding, erosion and aquatic life potential.

Changes in hydrology associated with development prior to regulations indicated increased flood frequencies, increased erosion and degradation of aquatic life potential. The Waterways Ordinance focused primarily on flooding from larger rainfall events by incorporating detention basins. The changes in hydrology still indicated more frequent high flow events, increased erosion and degradation of aquatic life potential. The Comprehensive Watershed Ordinance included requirements for water quality control in addition to wider stream buffers and detention. The CWO reduced flood frequencies and erosion to near the undeveloped condition and maintained flow metrics in ranges associated with good aquatic life potential. The primary difference between the CWO and the proposed Watershed Protection Ordinance is extending stream buffer into the headwaters of creeks. The SWAT model was not able to significantly differentiate these changes; however, the WPO, like the CWO, significantly reduced the hydrologic impact of development.

Acknowledgements

The authors would like to acknowledge the financial support of the citizens of the City of Austin and the technical support of the staff of the Watershed Protection Department, especially the Water Quality Monitoring Section. Without this support, this study would not have been possible.

References

Arnold, J., J. Kiniry, R. Srinivasan, J. Williams, E. Haney and S. Neitsch. 2013. Soil & water assessment tool input/output documentation version 2012. Texas Water Resources Institute, TR-439. College Station, TX.

City of Austin. 2013a. City of Austin Drainage Criteria Manual. American Legal Publishing.

City of Austin. 2013b. City of Austin Environmental Criteria Manual. American Legal Publishing.

Glick, R.H., L. Gosselink, B. Bai, and C. Herrington. 2010. Relating hydrologic metrics to in-stream aquatic life in semi-arid areas. In *Proceedings of the 2010 Watershed Technology Conference*. Earth University, Costa Rica.

Glick, R.H. and L. Gosselink. 2009. Predicting aquatic life potential under various development scenarios in urban streams using SWAT. In *Proceedings of the 2009 International SWAT Conference*. Boulder CO, USA.

Glick, R.H. and L. Gosselink. 2011. Applying the sub-daily SWAT model to assess aquativ life potential under different development scenarios in the Austin Texas area. In *Proceedings of the 2011 International SWAT Conference*. Toledo, Spain.

Glick, R.H. and L. Gosselink. 2012. Using SWAT to predict pre- and post-development hydrologic regimes. In *Proceedings of the 2012 21st Century Watershed Technology Conference: Improving Water Quality and the Environment.* Bari, Italy.

Glick, R.H. and L. Gosselink. 2013. Simulating the impacts of retention basins on erosion potential in urban streams using SWAT. In *Proceedings of the 2013 International SWAT Conference*. Toulouse, France.

Gordon, N.D., T.A. McMahon and B.L. Finlayson. 1994. *Stream Hydrology: An Introduction for Ecologists.* John Wiley & Sons New York.

Hardy, T., P. Panja and D Mathias. 2005. *WinXSPRO, a channel cross section analyzer, user's manual, version 3.0.* United States Department of Agriculture, Forest Service. General Technical Report RMRS-GRT-147.

Kisters, Pty, Ltd. 2011. Hydstra, V.10.3.2. Weston Creek, Canberra, Australia.

Simulating the Impacts of Retention Basins on Erosion Potential in Urban Streams using SWAT

Roger H. Glick, P.E., Ph.D.
Watershed Protection Department
City of Austin, Texas
PO Box 1088
Austin, TX 78767
Roger.Glick@austintexas.gov

Leila Gosselink, P.E.
Watershed Protection Department
City of Austin, Texas
PO Box 1088
Austin, TX 78767
Leila.Gosselink@austintexas.gov

Abstract

Urbanization typically has detrimental impacts on stream bank stability due to increased erosion potential. Studies have indicated that detention facilities designed to control large runoff events do little to address this problem and may exacerbate the problem. Recent studies by the City of Austin, Texas have shown that smaller retention facilities designed to address water quality concerns may have the added benefit of reducing the erosion potential associated with development. This study employs the new urban BMP routines in SWAT to examine the effects of retention volume and draw-down rate on excess shear. Three different levels of development intensity were simulated for 23 years with differing retention volumes and drawdown rates. Excess shear was computed for each model run based on four different median particle sizes, 12.5, 19, 25.4 and 38 mm and compared to excess shear in an undeveloped, stable channel.

Increased retention volumes reduced excess shear for 19, 25.4 and 38 mm median particle sizes but increased excess shear for 12.5 mm median particle size because the flow rate associated with draining retention basins was greater that the flow rate associated with the critical shear. Increasing drawdown duration decreased excess shear for 12.5, 19, 25.4 mm median particle sizes but increased excess shear for the 38 mm median particle size because the retention basins were full more often, creating bypass flow with rates exceeding the critical shear for this particle size.

Keywords: Erosion control, modeling urban development

Introduction

Many municipalities in the United States require stormwater quality controls in addition to detention controls for extreme flood events. These water quality controls fall into two broad classes; flow-through devices where the flow rate into the device is approximately the same as the flow rate out or retention devices that capture a design volume of runoff and release it at a slower rate. Several studies (HDR Engineering, 2007; 2011; Glick and Gosselink, 2012; 2013) indicate that the use of retention type water quality controls provide an additional benefit of reducing erosion potential of stream bed and banks.

This study evaluated the effects of varying retention volumes and drawdown rates on excess shear in three hypothetical watersheds of varying impervious cover. These results were compared to the excess shear in an undeveloped watershed. Four watershed models were developed using the sub-daily and urban BMP options in the latest version of AcrSWAT (2012.10.17) (Arnold et al, 2013).

Study Site and Model Development

The study site is a 4.99 km^2 tributary of Gilleland Creek located east of Austin, TX (30°17'45"N, 97°33'12"W) in the Blackland Prairie eco-region (Fig. 1). The watershed is currently undeveloped and dominated by unimproved pasture and scattered honey mesquite (*Prosopis glandulosa*) and eastern red cedar (*Juniperus viginiana*). In addition to modeling the undeveloped condition, three models were developed for this watershed based on the differing development density. The low density cover model corresponded to the entire catchment being developed as low density single-family residential under current regulations resulting in an aggregate impervious of 34.9%. The medium density model represented a mixed use scenario and had 51.2% impervious cover while the high density model assumed all commercial development and an impervious cover of 64.4%. All five models used the same SSURGO soils data and 3-m DEM developed from LIDAR data collected by COA in 2003.

Precipitation was based on 15-min rainfall from two gauges that are part of the COA Flood Early Warning System. Daily temperature data were from the NWS Robert Mueller Airport station. Other weather inputs were generated using the WGEN_US_COOP_1960_2010 database in ArcSWAT. Since the watershed is ungaged, model parameters were adjusted based on local knowledge and used for all scenarios. The adjusted parameters are in Table 1.

To better match existing regulations, a detention basin designed to control the peak flow from the 2-, 10-, 25- and 100-yr 24-hr design rainfall (Type III) runoff events was placed at the outlet of reach 9 (see Figure 2). The peak discharges from the developed conditions for the design rainfalls matched the undeveloped peaks after passing through the detention basin.

The four capture volumes used in the study were based on current and historical capture volume requirements. The first capture volume was 12.7 mm (0.5 in.) of runoff, regardless of impervious cover. This was a historical design standard and is no longer used. The second capture volume is the current City of Austin (COA) standard; for impervious cover equal to or

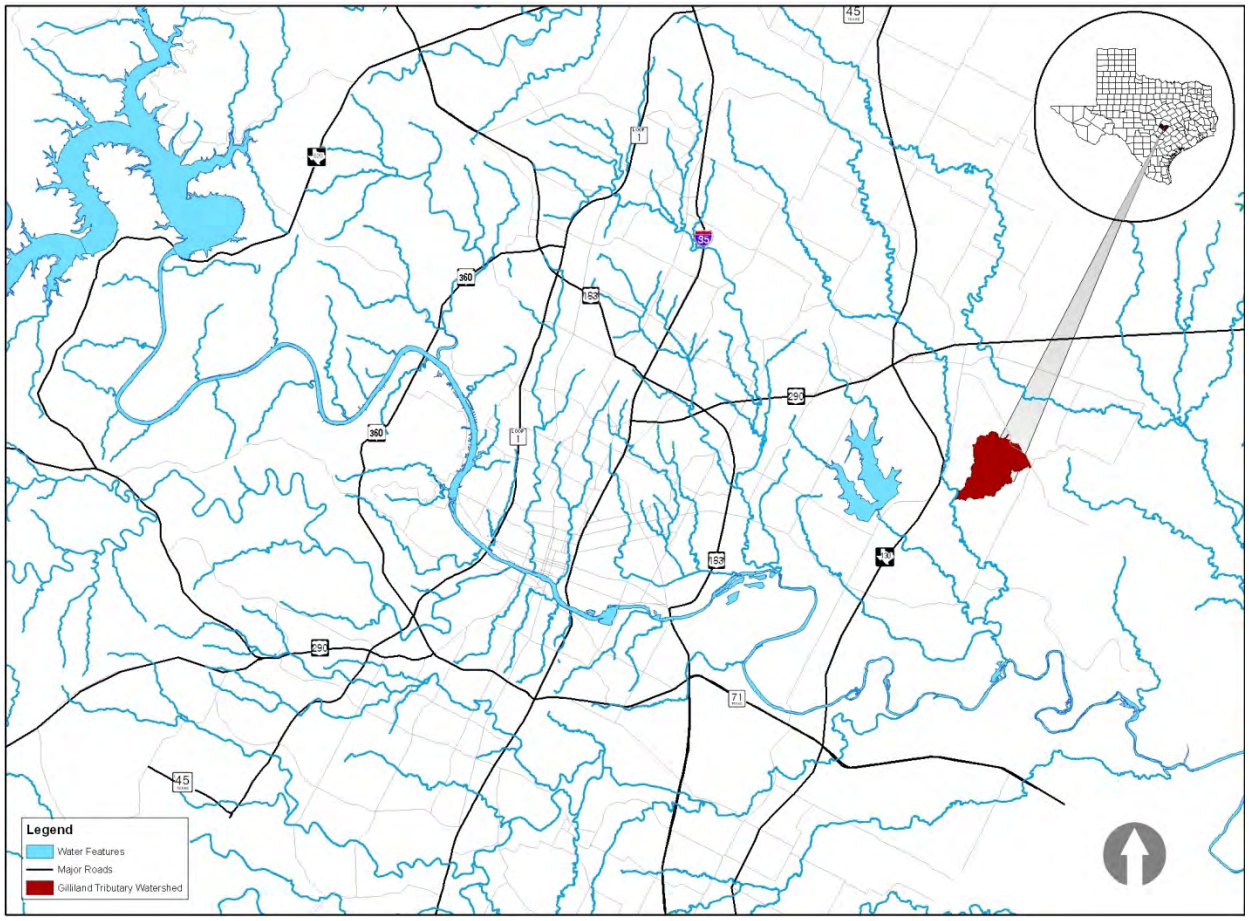

Figure 1. Gilleland tributary study area.

Table 1. Calibration parameters for Gilleland scenarios

Parameter	Value	File
CH_N2	0.035	.RTE
CH_K2	5	.RTE
ALPHA_BNK	0.25	.RTE
ALPHA_BF	0.1	.GW
GW-DELAY	10	.GW
BFLO_DIST	0.25	.BSN
IUH	2	.BSN
UHALPHA	4	.BSN
SURLAG	1	.BSN
IRTE	1	.BSN
CH_N1*	0.035	.SUB
CH_K1*	5	.SUB
CN for PAST*	-4	MGT

* for undeveloped case only

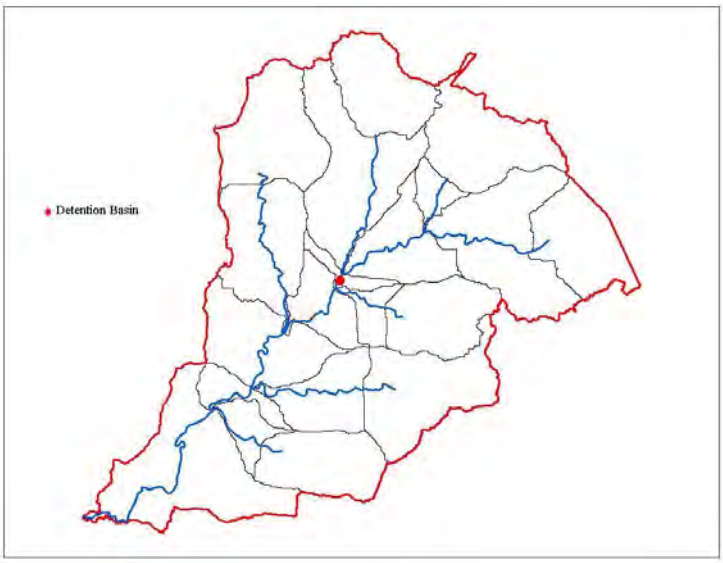

Figure 2. Detention basin location in WO, CWO and WPO models.

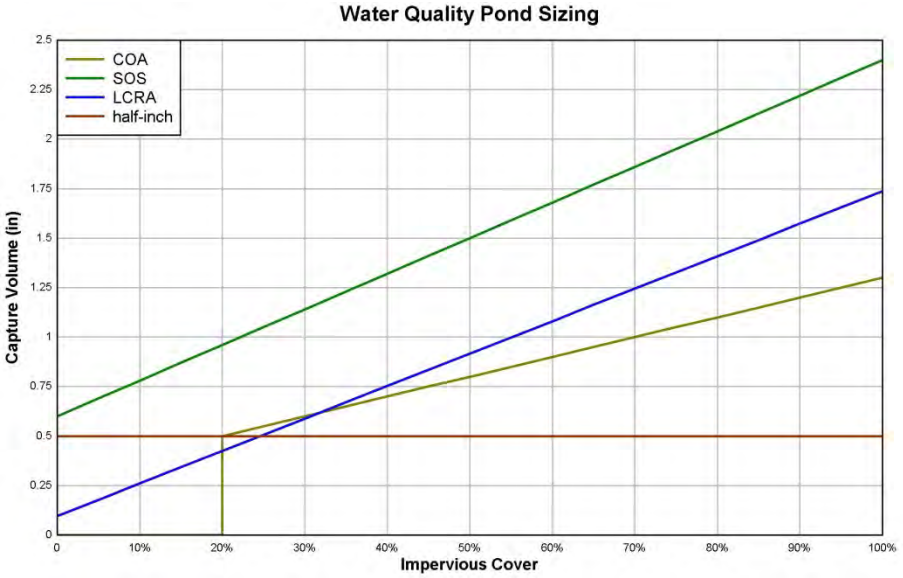

Figure 3. Capture volume vs. impervious cover for four different retention SCM designs.

greater than 20% impervious cover, 12.7 mm of runoff plus 2.54 mm (0.1 in) for every 10% impervious cover greater than 20% (COA, 2013). The third capture volume was based on the Lower Colorado River Authority's (LCRA) design standard capturing the runoff generated by the 1-yr, 3-hr rainfall event (LCRA, 2007). The last and largest capture volume was based on the requirements in the COA Barton Springs Zone (SOS) to capture the runoff from the 2-yr, 3-hr rainfall event (COA, 2013). Examples of these are shown in Figure 3.

Data Analyses

The erosion potential for each scenario was assessed using average annual excess shear as the bench mark. Excess shear occurs when the shear stress exceeds the critical shear for the stream bed and bank. Shear and critical shear were computed using the following equations:

$$\tau = \gamma_w \cdot D_H \cdot S_w \quad [1]$$

and

$$\tau_c = \Theta_c(S_g - 1) \cdot \gamma_w \cdot d_{50} \quad [2]$$

where,

τ = shear (Pa)
τ_c = critical shear (Pa)
γ_w = density of water (kg/m^3)
D_H = depth of water (m)
S_w = channel slope (m/m)
S_g = specific gravity of soil, 2.65
d_{50} = median particle diameter (m)
θ_c = critical Shield's parameter, 0.047

ES was defined as:

$$ES = \sum(\tau - \tau_c) \text{ for all } \tau > \tau_c \quad [3]$$

Hydraulic properties of the watershed outlet were estimated using WinXSPRO 3.0 (Hardy, et al., 2005). This program uses the channel cross-section and slope (estimated from the DEM) to develop a stage-discharge relationship based on Manning's equation. The channel cross-section at the end of the watershed with delineated floodplain is in Figure 4. The program allows the user to treat the floodplain differently than the main channel to separate total flow from flow in the main channel. This is necessary because as water spills into the floodplain, the average velocity drops, resulting in a decrease in total shear at that discharge. However, velocity in the main channel increases and the shear on the channel bed and bank also increases.

Assuming a Manning's n of 0.035 in the channel and 0.1 in the floodplain, WinXSPRO was used to compute shear and discharge as a function of stage for both the total cross-section and the main channel. Figure 5 shows the difference in total (based on average velocity) and channel shear at different flow rates. Tables relating channel excess shear to total discharge for four different median particle diameters, 12.5, 19.0, 25.4 and 38.0 mm were developed and loaded into Hydstra version 10.3.2 (Kisters, 2011). The HYCRSUM routine in Hydstra was used to compute cumulative excess shear for the 23 year study period based on flow generated by the sub-daily SWAT models.

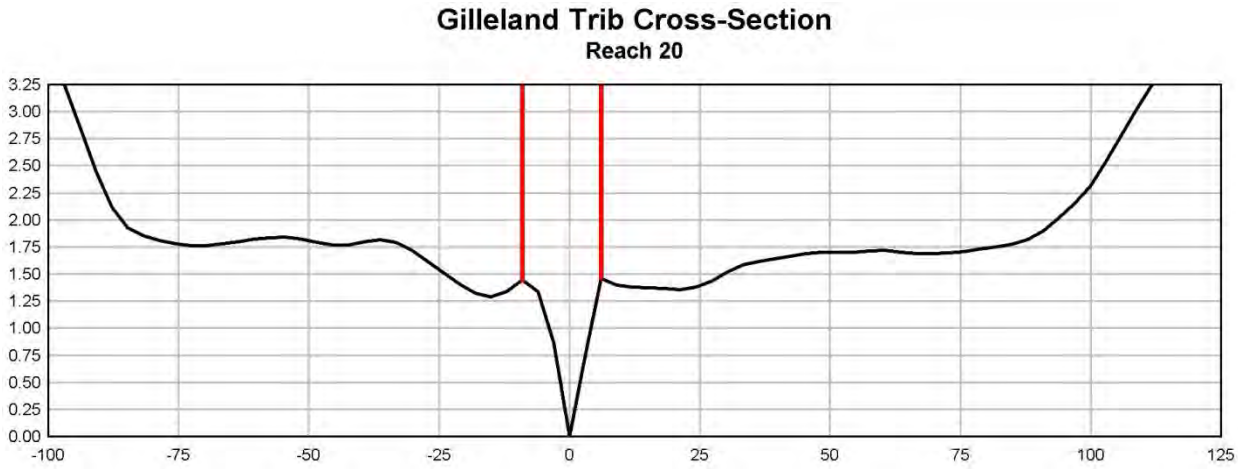

Figure 4. Gilleland tributary channel cross-section at the mouth of the watershed. Floodplain delineated by red lines.

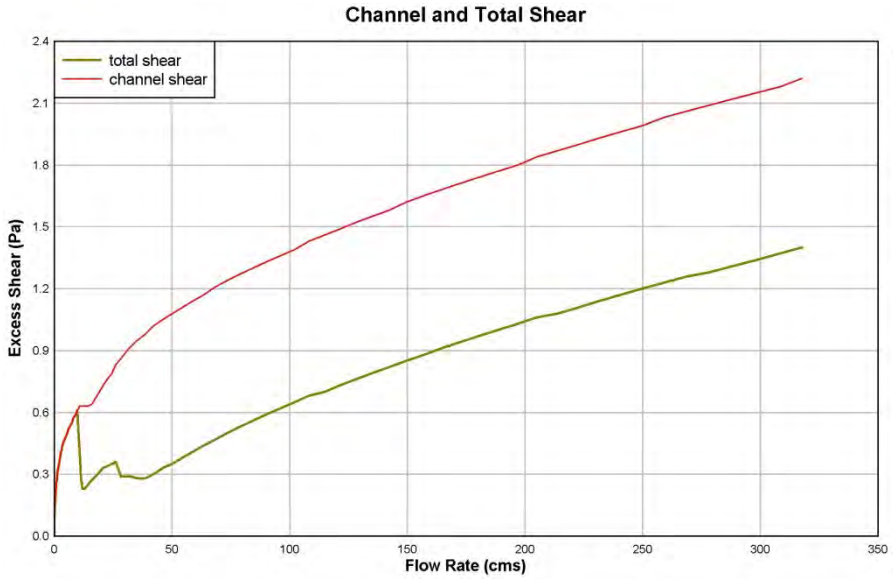

Figure 5. Total and channel shear for the Gilleland tributary channel.

The flow rate associated with τ_c, Q_c, increases exponentially as the median particle size increases (Figure 6). The critical flow rate for small median particle diameters is in the range that it may be exceeded by controlled releases from retention structures if not correctly designed. As the median particle diameter increases, only large runoff events create enough shear to generate erosion in this watershed. In a watershed with a steeper slope or different channel configuration, lower flow rates may be associated with the critical shear.

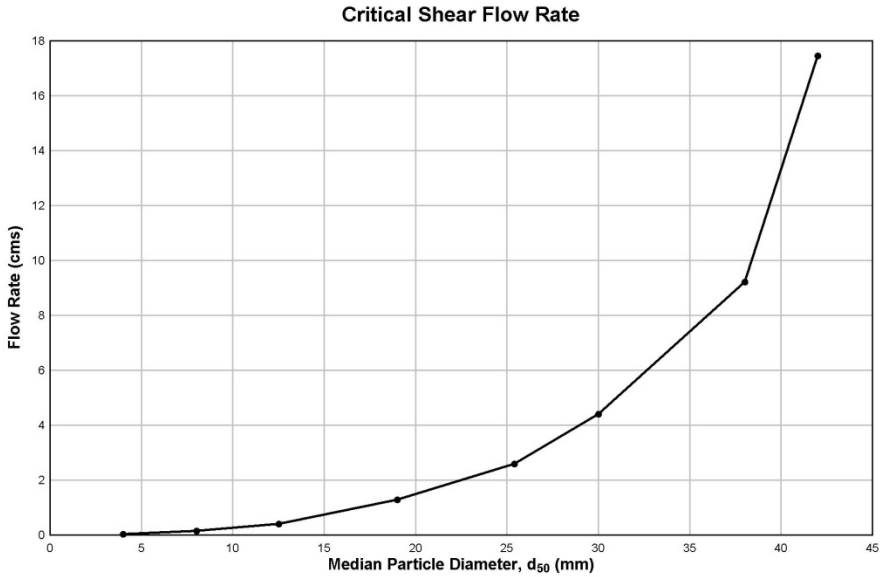

Figure 6. Relationship between critical flow rate for erosion and median particle diameter.

Results and Discussion

Results of the analyses grouped by drawdown rate are presented in Table 2. For ease of comparison, the results are the average of the different capture volumes for that drawdown rate and median particle diameter. Compared to the undeveloped condition, not using retention controls increased average annual excess shear by approximately 200% for the low impervious cover scenario to over 300% for the high impervious cover scenario regardless of particle size. This increase in excess shear would create channel widening and/or down cutting, especially for smaller median particle sizes. The cost to mitigate these changes is typically on the order of $1,000,000 US per 300 linear meters, assuming no structures are threatened.

Incorporating retention controls reduced annual average excess shear for all cases. For particle sizes less than 38mm, increasing drawdown time reduced excess shear. For particle sizes greater than 19 mm, the reduction in excess shear was sufficient to account for all of the increases associated with increased development intensity. While excess shear was reduced in all cases for the 12.5 mm median particle size, the reduction was lower than that for the larger particle sizes and the excess shear exceeded the undeveloped case except for the longest drawdown rate on the medium and low impervious cover scenarios. This was a result of the flow rate in the channel during the drawdown of the retention basins still exceeding Q_c for that particle size (see Figure 7). This will be the case for smaller particle sizes as well (Figure 6). This should be taken into account when designing retention basins for erosion control and longer drawdown times may be required.

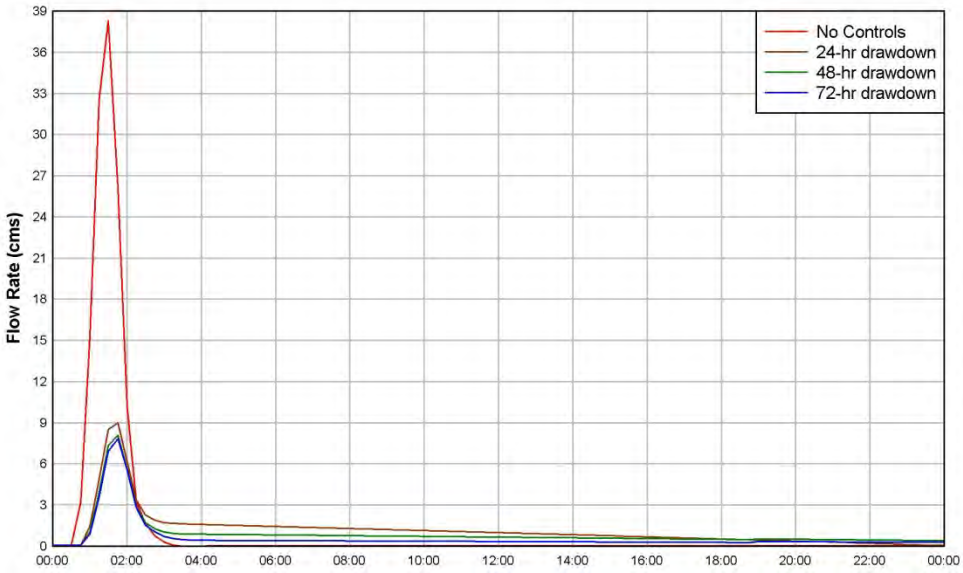

Figure 7. Hydrograph for Gilleland Tributary demonstrating the effects of varying drawdown time.

Table 2. Average-annual cumulative excess shear (Pa) for the Gilleland tributary grouped by particle size and drawdown duration. Different basin sizes have been averaged.

Particle Diameter	Drawdown Duration	Impervious Cover		
		High	Med	Low
12.5 mm	UND		1466	
	None	4597	3894	3055
	24-hr	4128	3277	2365
	48-hr	3383	2384	1656
	72-hr	1964	1329	952
19.0 mm	UND		808	
	None	2564	2111	1602
	24-hr	672	550	451
	48-hr	547	449	398
	72-hr	485	422	402
25.4 mm	UND		407	
	None	1318	1054	783
	24-hr	231	200	194
	48-hr	240	211	202
	72-hr	267	232	220
38.0 mm	UND		61.3	
	None	252	183	129
	24-hr	58.9	49.0	44.1
	48-hr	61.1	51.7	46.1
	72-hr	67.1	56.5	50.5

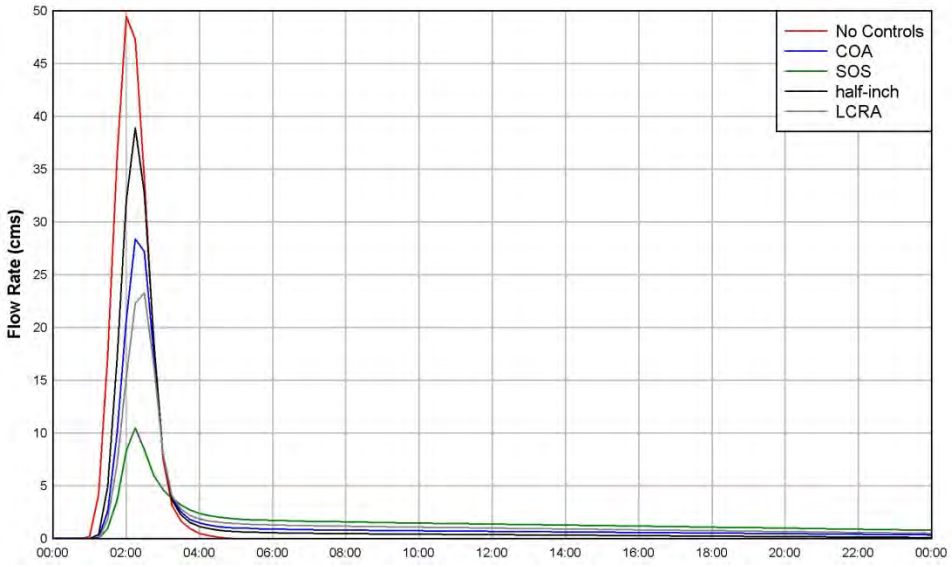

Figure 8. Hydrograph for Gilleland Tributary demonstrating the effects of varying capture volume.

Average annual excess shear for the 38 mm median particle size increased with longer drawdown times. For this channel, Q_c for the 38 mm particle size was associated with near bank-full flows. By incorporating retention controls, the only times these flow rates occurred were when the retention basins were full and runoff bypassed the retention basin uncontrolled. By increasing the drawdown time, the capture volume was exceeded more frequently, thus increasing the excess shear for the 38 mm particle size. While the shear did increase, it was still less than the uncontrolled shear and two orders of magnitude less that the excess shear for the 12.5 mm particle size.

Increasing the capture volume reduced excess shear for median particle sizes of 19 mm and greater (see Table 3). For particle sizes of 12.5 mm, increasing the capture volume increased the excess shear. Increasing the capture volume and holding the drawdown time constant results in higher discharge rates (see Figure 8), exceeding Q_c for the 12.5 mm particle size in this channel. For larger median particle sizes, increasing the capture volume reduces the flow rate of the direct runoff which exceeds Q_c and reduces excess shear.

These results indicate that if the primary objective of including retention controls is to reduce excess shear and erosion, channels with smaller median particle sizes will be most problematic. These will require larger retention basins with longer drawdown times. The designs for these retention basins would need to ensure that the cumulative discharges into the channel not exceed Q_c for the target particle size

One of the primary objectives of this study was to determine if existing COA sizing criteria for water quality retention controls were sufficient to address erosion concerns. Table 4 contains the ratios of developed to undeveloped average annual excess shear using existing COA sizing regulations and 48-hr drawdown requirements. Values less than one indicate excess shear is less than the undeveloped scenario.

Table 3. Average-annual cumulative excess shear (Pa) for the Gilleland tributary grouped by particle size and design basin size. Different drawdown durations have been averaged.

Particle Diameter	Control Sizing	Impervious Cover		
		High	Med	Low
12.5 mm	UND		1466	
	None	4597	3894	3055
	Half-Inch	2332	1805	1373
	COA	3128	2138	1558
	LCRA	3416	2480	1592
	SOS	3757	2898	2106
19.0 mm	UND		808	
	None	2564	2111	1602
	Half-Inch	912	694	531
	COA	508	449	421
	LCRA	466	414	408
	SOS	387	338	309
25.4 mm	UND		407	
	None	1318	1054	783
	Half-Inch	497	375	290
	COA	229	219	222
	LCRA	174	180	212
	SOS	83.1	83.4	97.5
38.0 mm	UND		61.3	
	None	252	183	129
	Half-Inch	120	90.9	66.9
	COA	64.7	56.7	51.8
	LCRA	46.4	44.9	49.3
	SOS	18.1	17.0	19.6

Table 4. Ratio of developed to undeveloped excess shear using existing COA design requirements.

Scenario	12.5mm	19mm	25.4mm	38mm
High IC	2.41	0.51	0.55	1.03
Med IC	1.36	0.48	0.54	0.93
Low IC	1.03	0.49	0.54	0.83

Existing COA design requirements mitigate increases in annual average excess shear for median particle sizes for 19 mm and greater and for 12.5 mm in the low impervious cover scenario. As impervious cover increased the performance of COA decreased for the 12.5 mm particle size. Even though the excess shear is greater than the undeveloped scenario, excess shear was reduced

by 25% and 50% for medium and high impervious cover scenarios compared no controls. If the drawdown duration were extended to 72-hr instead of 48-hr using the existing basin sizing, the increase in excess shear would be mitigated for the medium and high impervious cover scenarios using a 12.5 mm median particle size. Since these basins are primarily designed for water quality, not erosion mitigation, changes in pond bypass would need to be evaluated prior to making any changes.

Conclusion

The use of retention based water quality controls in many cases provides an additional benefit of reducing the increase in excess shear in the stream channel associated with development. The reduction of excess shear should help maintain equilibrium in the channel, reduce erosion and the expenses of repairing erosion problems.

Increasing the retention volume will reduce excess shear given the discharge from the basin is less than the flow rate associated with the critical shear in the channel. Extending the drawdown time for the retention basin will reduce excess shear given the retention volume is sufficient to prevent excess bypass of the retention basin.

In channels with small median particle diameters (≤12 mm) balancing retention volume and drawdown time is required. A large retention volume with a short drawdown time may increase excess shear because the discharge may be above the critical flow rate. Smaller retention volumes with longer drawdown rates may produce excess bypass.

Acknowledgements

The authors would like to acknowledge the financial support of the citizens of the City of Austin and the technical support of the staff of the Watershed Protection Department, especially the Water Quality Monitoring Section. Without this support, this study would not have been possible.

References

Arnold, J., J. Kiniry, R. Srinivasan, J. Williams, E. Haney and S. Neitsch. 2013. Soil & water assessment tool input/output documentation version 2012. Texas Water Resources Institute, TR-439. College Station, TX.

City of Austin. 2013. City of Austin Environmental Criteria Manual. American Legal Publishing.

Glick, R.H. and L. Gosselink. 2012. Using SWAT to predict pre- and post-development hydrologic regimes. In *Proceedings of the 2012 21st Century Watershed Technology Conference: Improving Water Quality and the Environment.* Bari, Italy.

Glick, R.H. and L. Gosselink. 2013. Comparing the Changes in Hydrology due to Different Development Regulations using Sub-Daily SWAT. In *Proceedings of the 2013 International SWAT Conference*. Toulouse, France.

Hardy, T., P. Panja and D Mathias. 2005. *WinXSPRO, a channel cross section analyzer, user's manual, version 3.0.* United States Department of Agriculture, Forest Service. General Technical Report RMRS-GRT-147.

HDR Engineering. 2011. Quantification of long-term benefits of on-site erosion detention for developing Austin watersheds: stream protection curve. Technical report prepared for the City of Austin.

HDR Engineering. 2007. Quantification of long-term benefits of on-site erosion detention for developing Austin watersheds. Technical report prepared for the City of Austin.

Kisters, Pty, Ltd. 2011. Hydstra, V.10.3.2. Weston Creek, Canberra, Australia.

Lower Colorado River Authority. 2007. Highland Lakes Watershed Ordinance, Water Quality Management Technical Manual. Available at www.LCRA.org. Austin, TX

Using SWAT model to evaluate the impact of community-based soil and water conservation interventions for an Ethiopian watershed

Hailu Kendie Addis*
Amhara Regional Agricultural Research Institute, Bahir Dar, Ethiopia

Stefan Strohmeier
Institute of Hydraulics and Rural Water Management, University of Natural Resources and Life Sciences, Vienna, Austria

Raghavan Srinivasan
Spatial Sciences Laboratory, Texas A&M University, College Station, USA

Feras Ziadat
International Center for Agricultural Research in the Dry Areas, Amman, Jordan

Andreas Klik
Institute of Hydraulics and Rural Water Management, University of Natural Resources and Life Sciences, Vienna, Austria

Abstract

Extensive land degradation in the Ethiopian highlands forces the rural communities to prevent further soil erosion to ensure sustainable land management in the endangered regions. Soil conservation measures are continuously being established in some areas by research and/or development projects but the effects at field and watershed level are unclear.
The objective of this study is to model runoff and sediment yield in the Gumara-Maksegnit watershed in the northern Amhara region, to assess the impact of selected soil and water conservation interventions. SWAT was used to simulate the 54 km² large watershed, locally treated by stone bunds and water retention ponds, based on SRTM-DEM data, soil data derived from 234 observations, a land-use map based on supervised satellite-image classification and weather data from four different rain gauges. Runoff and sediment concentration was monitored at three gauging stations to provide a reliable model calibration. Comprehensive field monitoring was undertaken to assess upland and channel processes and thus to consolidate the model performance. By means of the calibrated model mean annual runoff (271 mm) and soil loss (22.6 t ha^{-1}) was calculated and the highly endangered regions concerning land degradation were located. The achieved NSE of modeled and observed daily runoff of 0.777 indicates that the SWAT model can be properly used for the assessment of the on-site watershed characteristics and based on this, various scenarios can be simulated to identify efficient soil conservation strategies for the study area.

Keywords: Soil conservation, gully erosion, Ethiopian highlands, sediment concentration.

Introduction

In Ethiopia, soil erosion by water contributes significantly to food insecurity and constitutes a serious threat to sustainability of the existing subsistence agriculture (Hurni, 1993; Sutcliffe, 1993; Sonneveld, 2002). FAO (1984) and Hurni (1993) estimated that in the Ethiopian highlands annual soil loss reaches up to 200 to 300 tons per hectare.
The extensive famine of 1973 and 1974 initiated a first governmental rethinking concerning rural land management and consequently large-scale soil conservation and rehabilitation programs were undertaken (Hurni, 1985). Kruger et al. (1996) reported that between 1975 and 1989, 980000 hectares of cropland were protected by terraces and 310000 hectares of denuded lands were re-vegetated in highly degraded areas. However, the achievements of several soil conservation projects remained below the expectations and considerable efforts in soil conservation failed to prevent ongoing land degradation.
In the Gumara-Maksegnit watershed in the Ethiopian highlands a study was carried out to 1.) localize the hot-spots of surface runoff and soil erosion and 2.) to evaluate the effects of different soil conservation techniques. SWAT was used to model the 54 km² large watershed, locally treated by soil conservation measures, to be used as a basis for future watershed planning to combine agricultural and socio-economic demands with soil conservation requirements according to the spatially variable conditions of this region.

Materials and Methods

Study area

The Gumara-Maksegnit watershed is located in the Lake Tana basin in the northwestern Amhara region, Ethiopia between 12° 24’ and 12° 31’ North and between 37° 33’ and 37° 37’ East. The 54 km² large watershed drains into the Gumara River, which ultimately reaches Lake Tana. The climate in the northwestern Amhara region is characterized by heavy rainfall events during the rainy season from May to October and a dry spell from November to April. Mean annual rainfall is about 1170 mm at which more than 90 % of the rainfall occurs during the rainy season. The average monthly maximum and minimum temperatures are 28.5°C respectively 13.6°C. The elevation of the watershed ranges from 1920 m to 2860 m above sea level.
In the watershed five different soil types were determined: sandy clay loam, sandy loam, clay loam, loam, and clay. Shallow loam soils (rooting depth < 15 cm) were found in the upper part of the watershed whereas clay soils with rooting depth > 100 cm were found in the lower areas near the outlet of the catchment.
The watershed is mainly covered by agricultural land (74%) followed by forest (23%), pasture (2%) and villages. The major crops of the agricultural lands include sorghum, teff, faba bean, lentil, wheat, chick pea, linseed, fenugreek, and barley. Teff and sorghum are the main staple crops whereas chick pea is grown in the lower regions and cannot be grown as a crop in the higher altitude.

Figure 1. Overview of the project area in the northwest Amhara region, Ethiopia.

SWAT model

SWAT 2009 (Neitsch et al., 2009) and ArcGIS 9.3 was used to simulate hydrologic and sediment transport processes in daily time step resolution. Surface runoff was calculated by SCS CN method to user-friendly assess land management, soil, climate and vegetation effects (Hjemfeldt, 1991; Arnold and Allen, 1998; Baker and Miller, 2013) on runoff. Soil conservation measures were considered by modification of the cover and management factor (CUSLE) and the support practice factor (PUSLE) of the Modified Universal Soil Loss Equation (MUSLE) (Williams, 1995).

SWAT input and calibration data

A DEM of the watershed was prepared using SRTM (Shuttle Radar Topography Mission) data with 90 m grid resolution. Land use input was prepared based on supervised SPOT satellite image classification using Erdas Imagine 9.1. A soil map was created based on 234 soil samples

taken in 500 m grid across the entire watershed. Climate data was available from four different rainfall, four temperature, one solar radiation, one relative humidity, and one wind speed gauge within respectively close to the catchment. The available climate data ranges from 1997 to 2011.

Figure 2. SWAT input data: left figure shows elevation data and the locations of the gauging stations, the central figure shows land use data and the right figure shows the soil map.

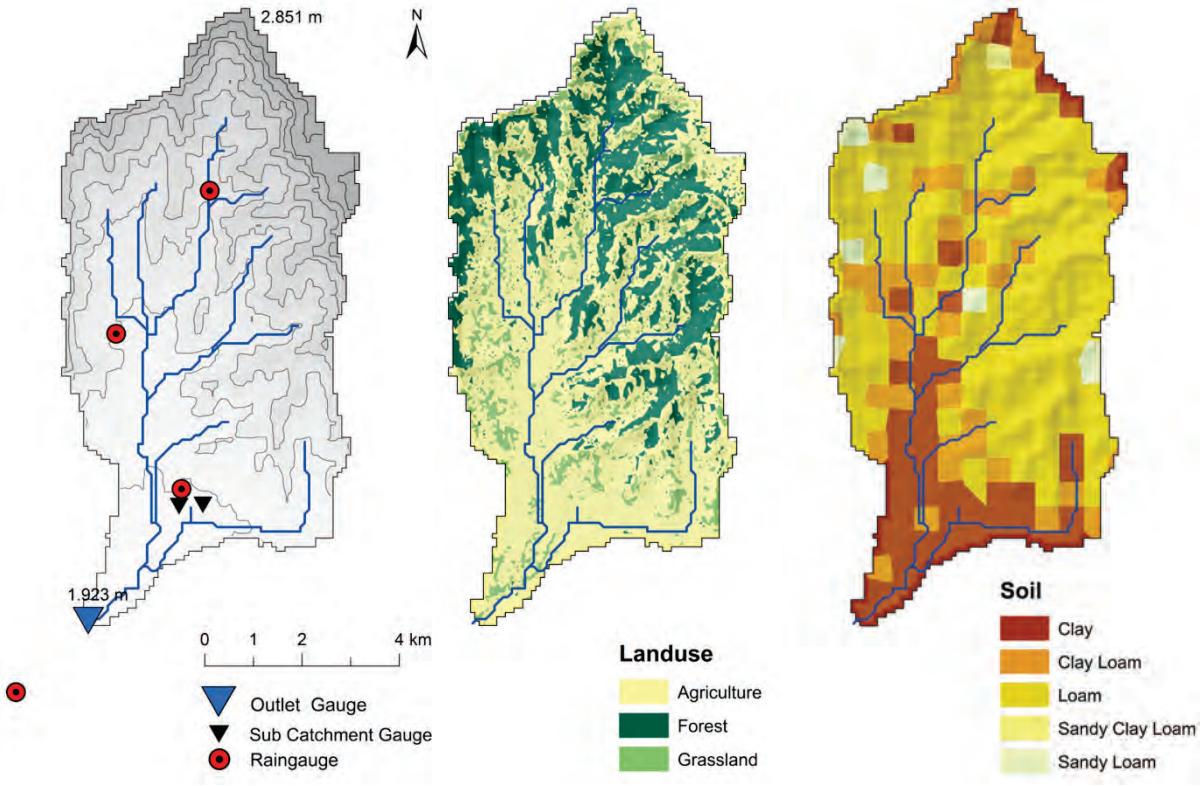

In the catchment a dense gully network cuts through the upland which strongly affects the drainage and translation processes of runoff and therefore proper delineation of the watershed is crucial. In this study, the drainage density of a representative sub-catchment was analyzed by hand-held GPS survey which indicated the average drainage area between 2 and 10 ha.
The model was calibrated based on daily runoff data at the outlet gauging station of the watershed, from 4th of July, 2011 to the 12th of July, 2011 and from 23rd of July, 2011 to 20th September, 2011. The fixed outlet cross section is equipped by a continuously logging water level sensor to calculate discharge by a rating curve established based on water level and manual flow velocity measurements using a 1D flow velocity device. Continuous discharge data was transferred into daily runoff for daily time step SWAT calibration.

Figure 3. Hydrograph at the main outlet and precipitation data from the nearest rain gauge (Outlet).

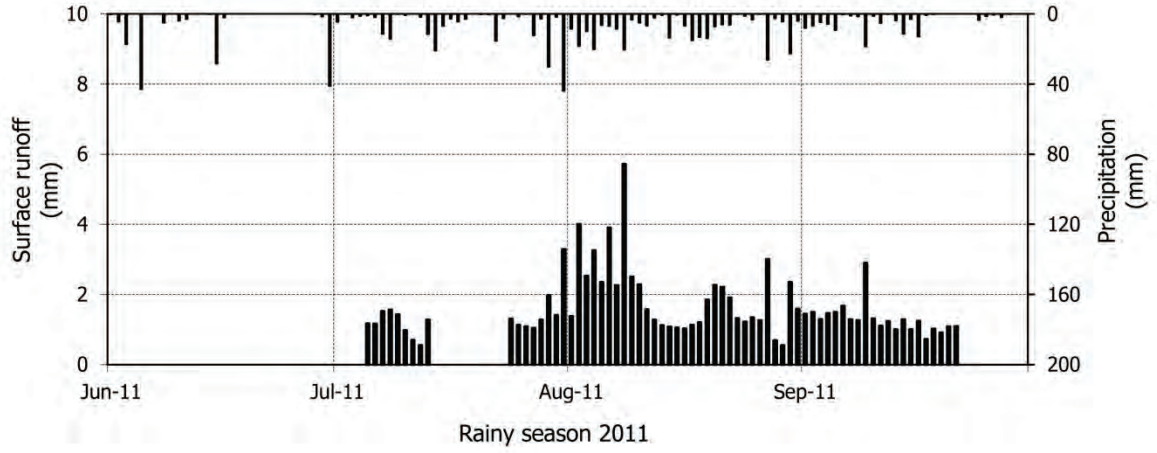

Sediment concentration was manually sampled at three stages of various flood events. As selectively sampled sediment data may not be suitable for daily based model calibration, sediment data was used to establish a relation between runoff and sediment concentration (Figure 4). Based on the manual sampling upper and lower boundaries of potential sediment concentration for certain discharge was defined.

Figure 4. Scatter plot of discharge and sediment concentration of the manual bottle sampling at the main outlet. Dashed lines indicate the lower and upper defined limit of the expected relation between discharge and sediment concentration.

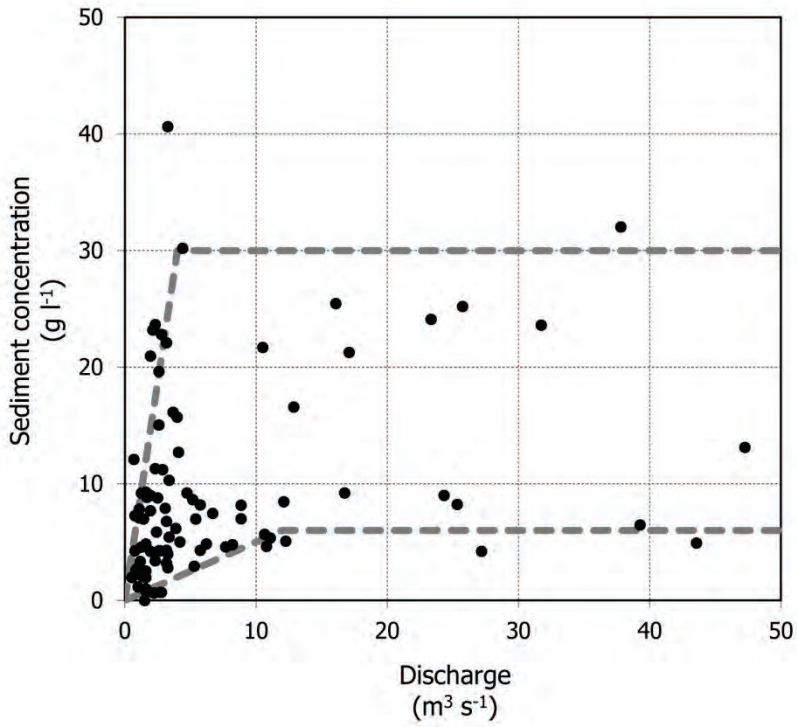

Calibration and sensitivity analyses

For model calibration most affective parameters on runoff were selected based on a sensitivity analyses. Therefore auto-calibration and sensitivity-analysis of SWAT was used alternatingly to iteratively locate the controlling parameters on simulated runoff. For the sensitivity analysis each of the chosen parameter was varied in 5% steps between -20% and +20% of the expected value. After ranking the ten most sensitive parameters a manual calibration was performed and soil conservation treatments such as stone bunds and small water retention ponds were implemented in the model.

To simulate soil conservation effects of the stone bunds the curve number (CN) and practice factor (P) of HRU`s located in the central part of the watershed were manually adjusted. In this study, CN of stone bund treated HRU`s was reduced by three units, also reported by Lanckriet et al. (2012) for a watershed study in the northwestern Amhara region. For the adjustment of the P-factor different recommendations exist in the literature - for example Nyssen et al. (2007) estimated a P-factor of 0.32 for stone bund practices in a North-Ethiopian catchment and Hessel and Tenge (2008) used a P-factor of 0.50 for a watershed in Kenya. In the Gumara-Maksegnit watershed an erosion plot monitoring was carried out to evaluate on-site conditions of the stone bund measures. The monitoring indicated highly variable soil loss rates on treated and untreated field plots as soil loss was heavily affected by spatially variable stone and crop cover. Entirely, the erosion plot monitoring suggested a minor soil conservation effect of the stone bunds compared to studies of Nyssen et al. (2007) and Hessel and Tenge (2008) and consequently we

decided to set the P-factor for stone bund treated fields to 0.85. Additionally, five retention ponds of 125 m³ volume were integrated in the SWAT model, even though the effect on surface runoff might be negligible for watershed level output.

Figure 5. Stone bund treated fields (left image) and the small channel above the stone bund (right image).

Nash-Sutcliffe coefficient (NSE; Nash and Sutcliffe, 1970) was used to evaluate the model performance. The Nash-Sutcliffe coefficient (NSE) is calculated by following equation:

$$NSE = 1 - \frac{\sum_{i=1}^{n}(Q_o - Q_s)^2}{\sum_{i=1}^{n}(Q_o - Q_{O,mean})^2} \qquad (1)$$

where Q_O is the observed discharge, Q_S is the simulated discharge and $Q_{O,mean}$ is the mean observed discharge.

Results

The sensitivity analysis indicated curve number (CN) as most descriptive parameter concerning runoff, followed by the base flow parameters APLHA_BF and GW_DELAY. Figure 6 illustrates observed and simulated runoff data of the calibrated model on a daily basis for the rainy season 2011. It can be seen that the peak flows are properly described and also the lower flows during short dry periods fit well to the outlet-hydrograph. The well described peak flows (Figure 6) indicate that the SCS CN procedure can be properly used for the translation of the rainwater in this watershed. Low flows are controlled by base- and interflow processes and hence APLHA_BF and GW_DELAY were most effective parameters. The calibrated model predicts ca. 2 to 5 mm mean daily runoff (ca. 0.05 to 0.10 $m^3 s^{-1}$ mean daily discharge) at the end of the dry spell (from February to April) which confirms to our field prospection. The calculated NSE (Equation 1) of observed and simulated runoff is 0.777, which indicates a “very good” model performance according to the ratings of Saleh et al. (2000) for daily runoff data using SWAT.

However, it should be noted that the model is not yet validated and the processing of recorded data of the rainy season 2012 is still in progress.

Figure 6. Comparison of observed and simulated runoff data at the main outlet.

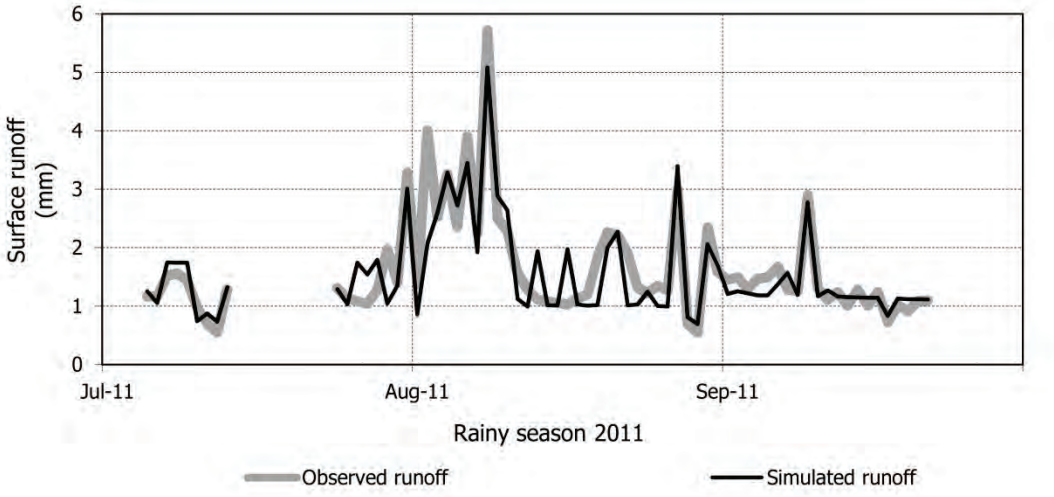

Simulated sediment yield was compared to the expected sediment yield based on manual bottle sampling (Figure 7), three times a runoff event at the outlet gauging station of the watershed. The expected sediment yield ranges between 2.9 and 27.6 t ha^{-1} whereas the model predicts 10.0 t ha^{-1} sediment yield for the observed period in 2011.

Figure 7. Comparison of the expected range of sediment yield (manual bottle sampling) and the simulated sediment yield (SWAT) at the main outlet.

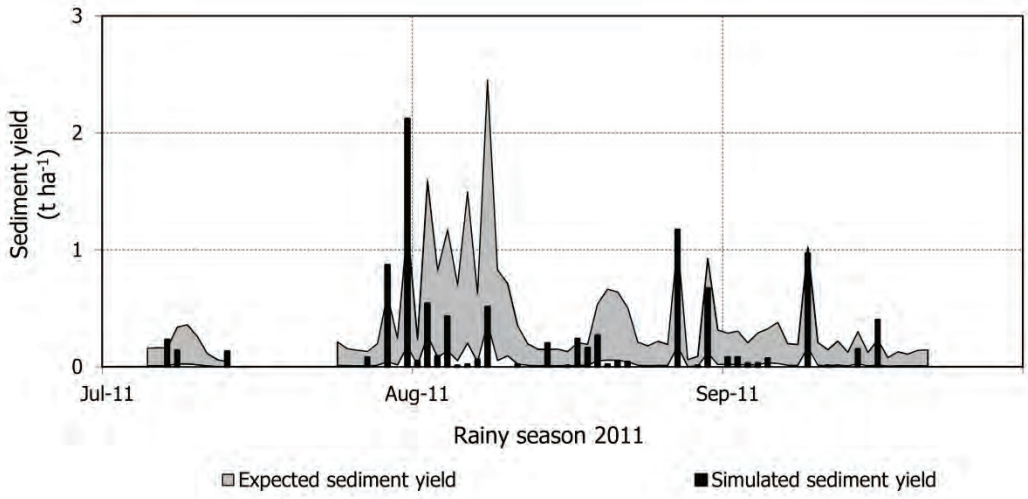

To localize the hot-spot areas of surface runoff and soil loss mean annual values were calculated using climate data from 1997 to 2011. Simulated mean annual surface runoff ranges from < 250 mm in the northern watershed to > 350 mm in the southern part of the watershed (Figure 8). This might refer to the higher forest-cover in the northern areas but also to the applied stone bunds in the central part and the heavy clay soils in the southern part of the watershed. Hence, the runoff map in Figure 8 indicates a high potential for water harvesting strategies in the near outlet regions. Contrarily the soil loss map indicates highly endangered regions in the northern parts of the watershed which might refer to the remarkable steepness of the relative sub basins. Comparatively low mean annual soil loss (< 20 t ha^{-1}) occurs in the central sub basins which indicates the positive effect of local soil conservation measures already applied.

Figure 8. Mean annual runoff and soil loss predicted by SWAT.

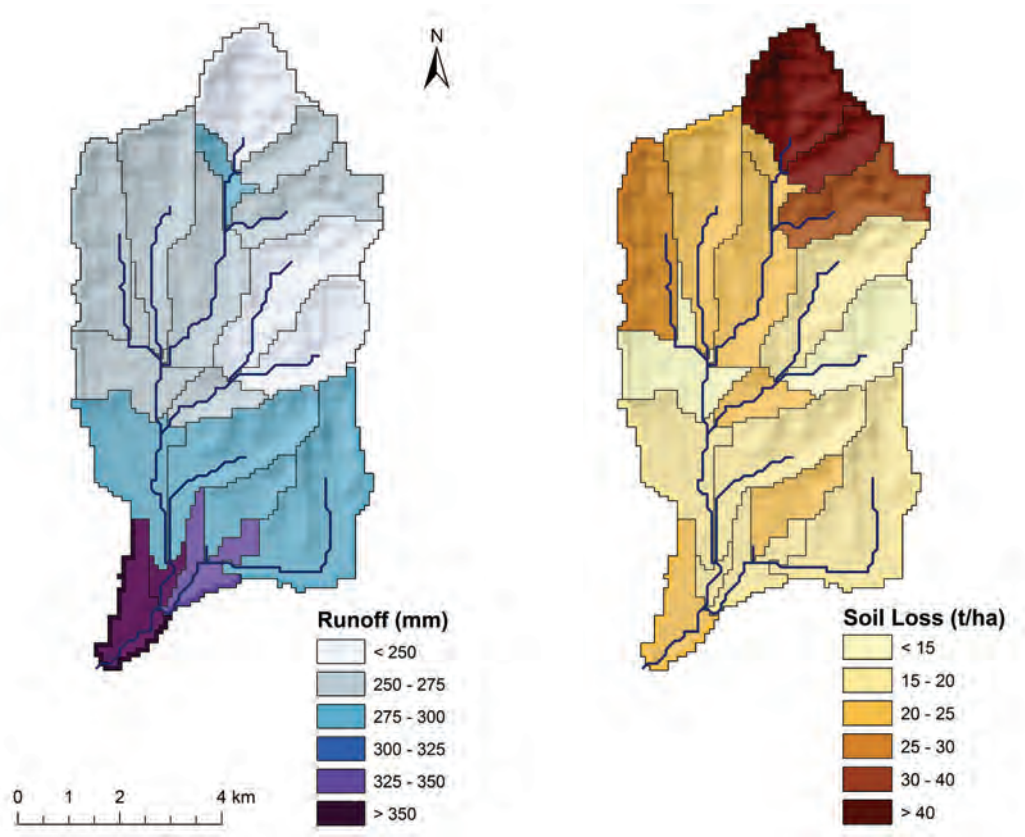

Discussion

The hydrograph at the outlet of the watershed is dominated by the short-period peak flows, occurring several times weekly, which interrupt mean base flow of ca. 1 $m^3 s^{-1}$ during the rainy season. Intense rainfall events correspond to peak flows in daily temporal scale (Figure 3) which states that rainwater is routed through the watershed in sub-daily time intervals. This refers to the steep sloped and small sized catchment (54 km^2) and the convective rainfall characteristics in the Ethiopian highlands. At the outlet, peak discharges of about 30 $m^3 s^{-1}$ have been observed during field works in 2012 whereas extreme floods are expected to exceed this amount several times. Controversially, the SWAT model derives maximum mean daily discharges of less than 10 $m^3 s^{-1}$ for whole calibration period 2011 which is a consequence of the daily based runoff computation. Thus, the erosional force of the flowing water in the channel is accordingly underestimated. Based on the fact that bottle samples at the watershed outlet provide lumped information of upland and channel sediment sources, the unclear sediment contribution of the gullies negatively affects the evaluation of upland erosion as well. In the watershed various field studies are still in progress to evaluate the seasonal gully growth and ongoing monitoring of upland erosion on a plot level is planned. However, up to now reliable determination of the proportion of upland and

channel erosion is not yet available and therefore the expectations concerning soil loss have to be considered cautiously.
Spatially variable rainfalls can harm the entire watershed model as local rainfall data recorded by any rain gauge is transferred to the nearest neighboring sub basins by the model. From our observations, on the 29th of June 2011, 90 mm of rainfall was recorded in a time period less than two hours and 124 mm of rainfall was recorded in less than five hours at the northern rain gauge in the watershed, whereas the central rain gauge recorded < 5 mm precipitation on similar day. The negative effect of up-scaling of local rainfall data is shown by some peaks in the simulated runoff in the hydrograph at which the observed runoff stagnates (and vice versa). However, based on the overall "very good" model performance according to the ratings of Saleh et al. (2000) we assume that the model assigns the sources of upland runoff - and accordingly upland soil erosion - in proper spatial distribution within the 18 sub basins, even though the magnitudes of the declared runoff and erosion rates are uncertain.

Conclusions

This study showed that SWAT can be used to simulate hydrology and sediment transport characteristics of a small and steep sloped watershed in the Ethiopian highlands on a daily basis. Moreover it was shown that SWAT allows reliable consideration of local soil conservation effects of stone bunds and small scale retention ponds.
Referring to the daily time step resolution, sub-daily watershed processes like flash floods and consequential peaks in discharge and gully erosion might be systematically underestimated by our model. This negatively affects the assignment of sediment sources (upland and channel) as the modeled sediment yield is verified by lumped sediment data monitored at the outlet of the watershed. However, predicted sediment yield fits to the expectations based on manual bottle sampling. Thus, we conclude that the calibrated model can be used to locate potential hot-spot areas concerning surface runoff and soil erosion in the uplands.
Based on the calibrated SWAT model, advanced soil conservation scenarios can be simulated to spatially optimize soil conservation and hence to support sustainable land management in the future.

Acknowledgements
The authors thank the Gondar Agricultural Research Centre, the Gondar Soil Laboratory and the local watershed community for their active cooperation and for providing a peaceful working environment. We also like to thank the Austrian Development Agency for financial support.

References
Arnold, J. G., and P. M. Allen. 1998. Estimating hydrologic budgets for three Illinois watersheds. *Journal of Hydrol*ogy 176: 57–77.

Baker, J. T., and S. N. Miller. 2013. Using the Soil and Water Assessment Tool (SWAT) to assess land use impact on water resources in an East African watershed. *Journal of Hydrology* 486: 100-111.

FAO.1984. Ethiopian Highland reclamation Study (EHRS). Final Report, Vol. 1-2. Rome, Italy.

Hessel, R., and A. Tenge. 2008. A pragmatic approach to modelling soil and water conservation measures with a catchment scale erosion model. *CATENA* 74(2): 119-126.

Hjelmfelt, A. T. 1991. Investigation of curve number procedure. *J. Hydrol. Eng.* 17(6): 725–735.

Hurni, H. 1985. Erosion - Productivity - Conservation Systems in Ethiopia. *In Proc. 4th International Conference on Soil Conservation* 654-674. Maracay, Venezuela.

Hurni, H. 1993. Land degradation, famine and land resource scenarios in Ethiopia. *In: D. Pimentel (ed.) world soil erosion and conservation* 27-62. Cambridge Univ. Press, Cambridge, UK.

Kruger, H., F. Berhanu, G. Yohannes, and K. Kefeni. 1996. Creating an inventory of indigenous soil and water conservation measures in Ethiopia. In: *Sustaining the Soil Indigenous Soil and Water Conservation in Africa International*. Institute for Environment and Development, Earthscan, London.

Lanckriet, S., T. Araya, W. Cornelis, E. Verfaillie, J. Poesen, B. Govaerts, H. Bauer, J. Deckers, M. Haile, and J. Nyssen. 2012. Impact of conservation agriculture on catchment runoff and soil loss under changing climate conditions in May Zeg-zeg (Ethiopia).
Journal of Hydrology 475: 336-349.

Nash, J. E., and J. V. Sutcliffe. 1970. River flow forecasting through conceptual models.
Part I – A discussion of principles. *J. Hydrol*. 10(3): 282–290.

Neitsch, S. L., J. G. Arnold, J. R. Kiniry R. Srinivasan, and J. R. Williams. 2009. Soil and Water Assessment Tool input/output documentation version 2009.

Nyssen, J., J. Poesen, D. Gebremichael, K. Vancampenhout, M. D'aes, G. Yihdego, G. Govers, H. Leirs, J. Moeyersons, J. Naudts, N. Haregeweyn, M. Haile, and J. Deckers. 2007.
Interdisciplinary on-site evaluation of stone bunds to control soil erosion on cropland in Northern Ethiopia. *Soil and Tillage Research* 94(1): 151-163.

Saleh, A. J., J. G. Arnold, P. W. Gassman, L. M. Hauk, W. D. Rosenthal, J. R. Williams and A. M. S. MacFarland. 2000. Application of SWAT for the upper Bosque River watershed. *Trans. ASAE* 43(5): 1077-1087.

Sonneveld, B. 2002. Land under pressure: the impact of water erosion on food production in Ethiopia. Shaker publishing, Maastricht, Netherlands.

Sutcliffe, J. P. 1993. Economic assessment of land degradation in the Ethiopian highlands: a case study. National Conservation Strategy Secretariat, Ministry of Planning and Economic Development, Addis Ababa, Ethiopia.

Williams, J. R. 1995. Sediment-yield prediction with universal equation using runoff energy factor. *In: Present and prospective technology for predicting sediment yield and sources: Proceedings of the sediment-yield workshop*, USDA Sedimentation Lab., Oxford, MS, November 28-30, 1972. ARS-S-40.

Evaluating the simulation of evapotranspiration and groundwater-surface water interaction using SWAT: the river Zenne (Belgium) case study

Olkeba Tolessa Leta

Department of Hydrology and Hydraulic Engineering, Vrije Universiteit Brussel, Pleinlaan 2, 1050 Brussels, Belgium

Aklilu Dinkneh

Department of Hydrology and Hydraulic Engineering, Vrije Universiteit Brussel, Pleinlaan 2, 1050 Brussels, Belgium

Ann van Griensven

Department of Hydrology and Hydraulic Engineering, Vrije Universiteit Brussel, Pleinlaan 2, 1050 Brussels, Belgium

UNESCO-IHE Institute for Water Education, Core of Hydrology and Water Resources, The Netherlands

Christian Anibas

Department of Hydrology and Hydraulic Engineering, Vrije Universiteit Brussel, Pleinlaan 2, 1050 Brussels, Belgium

Willy Bauwens

Department of Hydrology and Hydraulic Engineering, Vrije Universiteit Brussel, Pleinlaan 2,

1050 Brussels, Belgium

Abstract

Spatially distributed hydrologic simulators, such as the Soil and Water Assessment Tool (SWAT), are important tool for integrated river basin management, as they represent different spatial processes- like evapotranspiration (ET), interception, infiltration, groundwater-surface water interaction (GWSW)- at river reach or basin scale. SWAT calculates evaporation from interception, based on the amount of water stored on the canopy. A close look at the estimated ET for forested areas in the Zenne basin indicates that the actual implementation of this process in SWAT potentially underestimates the forest ET, namely when the maximum canopy storage is activated by the CANMX parameter and increased from zero. Consequently, we corrected the SWAT codes, in order to improve the intercept ET estimation. Another issue in SWAT is related to the GWSW interaction. In the actual version of SWAT, either seepage from the river bed or groundwater flow to the river take place. It is hence not possible to simulate both gaining and losing processes, e.g. when rivers seasonally alternate from losing streams to gaining streams and back. Therefore, we also modified the codes to allow either gaining or losing, depending on the groundwater discharge from the sub-basin. The objective of this study is to evaluate how the modified SWAT simulates the intercept ET and the GWSW interaction. It is shown that the

modified SWAT substantially improves the variability of the intercept ET with land cover and gives similar water balance of the basin. Incorporating the gaining or losing streams option also improved the performance of the model. Our findings confirm the applicability of the modified SWAT, but further research on the use of remotely sensed data and environmental tracing techniques (temperature sensors or isotopes) are needed to support the results.

Keywords: Evapotranspiration, intercept, groundwater-surface water interactions, SWAT, river Zenne

Introduction

Distributed or semi-distributed hydrologic simulators can be used for representing the different spatial processes (precipitation, evapotranspiration, interception, infiltration, percolation, surface runoff, lateral flow, groundwater flow, groundwater-surface water interaction, etc) at river reach or basin scale by using physically-based mathematical equations. Additionally, such models are useful for integrated river basin management and decision making. For example, the Soil and Water Assessment Tool (SWAT) (Arnold et al., 1998) represents the different processes based on the water balance equation in a soil profile. Hereby, the evapotranspiration (ET) process is the primary mechanism through which water is removed from a catchment. As a consequence, the adequate estimation of ET plays a critical role in the water balance calculations. SWAT offers three options to estimate the potential evapotranspiration (PET) from climatic data: the Penman-Monteith method (Monteith, 1995), the Hargreaves method (Hargreaves et al., 1985) and the Priestley-Taylor method (Priestley & Taylor, 1972).

SWAT also account for the evaporation of intercepted precipitation. However, a close look at the source codes showed that this ET estimation can be erroneous when the maximum canopy interception is activated by the CANMX parameter. Hereby, ET can be substantially underestimated when CANMX is increased from zero, especially for forested areas. For this, we allowed the plant evapotranspiration to go beyond PET as computed for alfalfa in SWAT.

We also noted an error in the calculation of the evaporation from open water bodies, such as lakes and reservoirs. In the actual code, the latter is calculated as 60% of the sub-basin PET, while obviously the PET should be about 60% of the open water evaporation. In our version of SWAT, we used the Penman method for the calculation of the evaporation of the open water bodies.

The groundwater-surface water (GWSW) interaction refers to the processes whereby surface water is recharged to the groundwater through seepage from the river and/or whereby groundwater is discharged towards the river. In streams, the interaction takes place in one of three ways, as discussed by Sophocleous (2002): streams can be gaining, losing or disconnected. For hydraulically connected systems, streams are considered as gaining when they receive groundwater. This commonly occurs in humid climates (Sophocleous, 2002, Winter, 1999). Oppositely, streams can be categorized as losing streams, when the streams recharge the underlying groundwater body. Disconnected streams do not have hydraulic contact with groundwater system (Winter, 1999). Both the losing and hydraulically disconnected streams are common in arid climates. Other scenarios exist when a stream changes from gaining (and vice versa) as a function of time or even when gaining and losing occur simultaneously, but in different reaches of the river (Anibas et al., 2011).

The GWSW processes are governed by a difference in water elevation between the river and the shallow aquifer in the riparian zone. While these processes vary in space and time, our catchment scale simulators are often poor in representing the temporal variability of these interactions. For example, in SWAT, the water elevations are not computed, but the groundwater discharge is simulated by means of the hydrological processes in the river basin, while seepage in the river bed is governed by a parameter – the channel transmission loss (Ch_K2) – that represents the hydraulic conductivity of the river bed. In the current SWAT simulator, it is hence not possible to simulate processes (gaining and losing) where rivers seasonally alternate from losing rivers to gaining rivers and vice versa. In addition, both processes cannot be simulated simultaneously.

In this study, we analyze how SWAT is simulating the different processes and how these processes can be improved in order to better represent the dynamics of the processes in space and time. Therefore, the objective of the paper is to better represent the intercept ET estimation and the GWSW interaction by modified SWAT codes. We developed a SWAT model for the river Zenne basin (Belgium).

Materials and methods

The SWAT simulator

SWAT is a physically-based, semi-distributed, hydrologic simulator that operates on different time steps at a basin scale. It was originally developed to predict the impact of watershed management on water, sediment, nutrients and agricultural and chemical yields at basin scale (Arnold et al., 1998). Additionally, SWAT can integrate complex watersheds with varying land use, weather, soils, topography and management conditions over a long period of time. The model is interfaced with a geographic information system (GIS) to integrate the various spatial and hydro-meteorological data (Winchell et al., 2010). A watershed is divided into a number of sub-basins that have homogeneous climatic conditions (Van Liew et al., 2005). Sub-basins are further subdivided into hydrological response units (HRUs) based on a homogenous combination of land use, soil type and slope (Arnold et al., 2011). The water balance equation of the model includes precipitation, surface runoff, actual evapotranspiration, interflow and return flow components (Neitsch et al., 2011). The simulator uses a modification of the Soil Conservation Service Curve Number (SCS-CN) method (USDA-SCS, 1986), which determines the surface runoff based on the antecedent moisture content for each HRU or, alternatively, it uses the Green and Ampt method as modified by Mein and Larson (Mein & Larson, 1973) if sub-daily precipitation data are provided. The percolation through each soil layer is estimated using a storage routing technique (Arnold et al., 1995). River routing can be performed by the variable storage method (Williams, 1969) or by the Muskingum method (Chow, 1959). In this study, the CN and Muskingum methods are used.

The Zenne basin

The river Zenne drains an area of 1162 km² and flows through the three administrative regions of Belgium (Fig.1): the Walloon region (574 km²), the Brussels-Capital region (162 km²) and the Flemish region (426 km²). After a length of about 103 km, it finally meets the river Dijle, where it is subject to the tidal influence of the river Scheldt. Upstream from Brussels, the river follows a natural meandering course. The river basin is crossed by a canal. In the Walloon region, the canal is fed by former tributaries of the river (Leta et al., 2012). The canal also receives water from the river through overflow structures, to prevent flooding in the Brussels-Capital region.

This study is limited to the upper part of the basin, upstream of the Brussels-Capital region. The upstream basin has an area of ca. 747 km² and a population density of 470 inhabitants per km². The elevation ranges from 18 to 171m.a.s.l. The land use within the basin is dominated by agricultural land use (56%), followed by pasture (22%) and mixed forest (11%). The remaining areas are covered by urban land, rangeland and water bodies. The major soil type is loam (79%), while the other soils (anthropogenic, sandy loam, sand, loamy sand and clay) account for 21%.

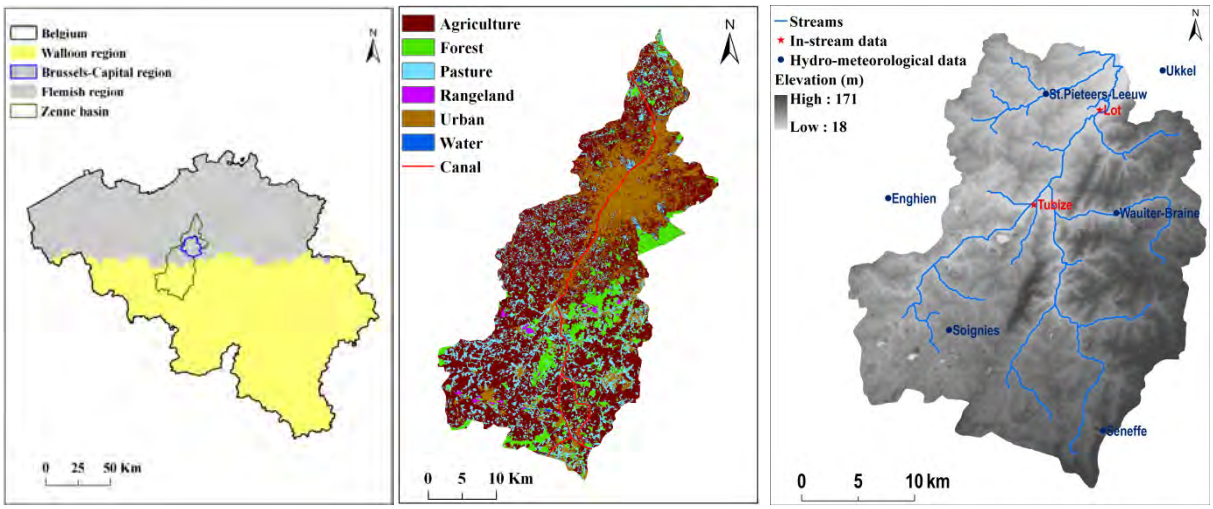

Figure 1: The location of the Zenne basin in Belgium (left), the land use map of the basin with its canal (middle) and the upstream basin DEM with its hydro-meteorological stations (right).

The data

We developed the SWAT model based on 30x30m Digital Elevation Models obtained from OC GIS-Vlaanderen and ASTER GDEM, on 20x20m soil and land use maps from OC GIS Vlaanderen and the Carte Numérique des Sols de Wallonie, and on Corrine land cover data from Ministère de la Région Wallonne- Générale de I'Aménagement du Territoire, du Logement et du Patrimoine. We obtained daily precipitation data for the station of Ukkel of the Royal Meteorological Institute of Belgium, for the stations of Enghien, Soignies, Seneffe and Wautier-Braine of the Direction Générale opérationnelle de la Mobilité et des Voies Hydrauliques (DVGH) and for the station of St.Pieters-Leeuw of the Vlaamse Milieu Maatschappij (VMM). Daily maximum and minimum temperatures, wind speed, solar radiation and relative humidity were also available for the Ukkel station. For model parameter optimization and groundwater-surface water interaction analysis, we used the daily stream flow data of Tubize, obtained from DGVH, and of Lot, as obtained from VMM. The locations of the hydro-meteorological station are given in Fig.1.

The methods

As mentioned in the introduction, the SWAT simulator has shortcomings regarding the simulation of the evapotranspiration and the groundwater-surface water interaction processes. To this purpose, two adaptations have been made and analyzed:

(1) **Modification 1**: the first adaptation is related to the evapotranspiration processes, whereby we allowed the plant evapotranspiration to go beyond PET (in SWAT computed for alfalfa). Such a change mainly effects forest that can have evapotransiration that can be substantially bigger than the PET of alfalfa.

(2) **Modification 2**: as SWAT only considers losing streams, the second adaptation was done to improve the in-stream groundwater-surface water interaction, whereby a river reach can be either gaining or losing at a certain moment of time, depending on whether there is discharge of groundwater from the sub-basin. We also allowed the seepage from the river bed (Ch_K2) to be negative, to represent the upwelling of groundwater towards the river, by implementing the following conditions for a river reach *i* located in sub-basin *i*:

a. In the case of gaining river, (i.e., when sub-basin groundwater, gw_sub(i) > 0), then the channel seep, Ch_K2 (i) can only be negative, representing a positive flux
b. In the case of loosing river, (i.e., when sub-basin groundwater, gw_sub(i) = 0), then the Ch_K2 parameter can also be positive, representing negative flux

Rivers reaches can, depending on the daily gw_sub(i) values, switch temporally from gaining to loosing and vice versa.

The model setup, calibration and validation

Considering the watershed outlet at Lot, we built the SWAT2009 (revision 488) model based on the geospatial data –the DEM, the land use map and the soil map (Fig.1 and Fig.2) and on hydro-meteorological data for the period 1985-2008. Using the DEM, we divided the upstream part of the basin into sub-basins. Further, in order to consider the sub-catchments that are draining to the canal and the overflow from the river to the canal at Lembeek, we manually added additional outlets at those locations. In total we defined 26 sub-basins. Sub-basins 10, 15, 20, 22 and 26 drain to the canal whereas the overflow occurs at the outlet of sub-basin 6 (Fig.2). A total of 194 HRUs were defined based on a user defined threshold value of 5% for the land uses, 15% for the soils and 35% for the slopes. Since all the necessary meteorological data are available, we used the Penman-Monteith method option for the PET estimation.

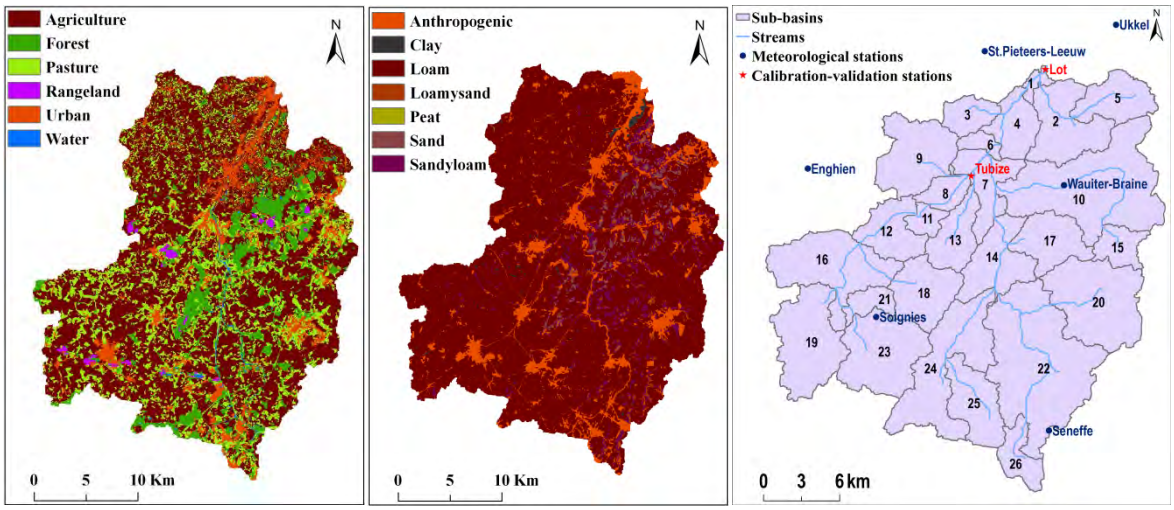

Figure 2: The upstream basin land use (left), soil type (middle) and the delineated sub-basins with the used hydro-meteorological data (right)

We split the data into a warm up period (1985-1987) - to initialize the initial state variables of the system such as the soil moisture content, a calibration period (1998-2008) and a validation period (1988-1997). Before calibration, we carried out a sensitivity analysis (SA) in order to screen the most important parameters for the model calibration. For this, we used the Latin hypercube One-factor-At-a-Time (LH-OAT), as implemented in SWAT (van Griensven et al., 2002). For model parameter calibration, we used the automatic model optimization procedure, the Shuffled Complex Evolution (SCE-UA) algorithm (Duan et al., 1994), as implemented in SWAT (van Griensven et al., 2002). Due to the high variability in catchment characteristics of the case study, we used a simultaneous multi-site calibration technique. Finally, we manually fine tuned the calibrated parameters particularly to obtain a reasonable discrepancy in mass balance components.

For model performance evaluation, we consistently used four statistical metrics: the Nash-Sutcliffe efficiency (NSE), the percent bias (PBIAS), the root mean square error (RMSE), and the ratio between the RMSE and the standard deviation of the observations (RSR). The latter metrics are combined to assess a global performance, as suggested by Moriasi et al (2007).

Results and discussion

Due to the high number of parameters of SWAT, we first performed a sensitivity analysis (SA) to identify the most sensitive parameters. The most sensitive parameters for the Zenne model are given in Table 1. Consequently, we considered these parameters for model calibration. The optimal parameter values are shown in Table 1. The table also shows the optimal parameter values for the adapted version of the simulator. It is clearly noticed that even though there are some differences in optimal parameter values between the original and adapted version of SWAT, the major differences relate to those parameters that are related to the evapotranspiration processes. For example, the soil evaporation compensation factor (ESCO) and the maximum canopy storage (Canmx) are noticeably changed. It shows how these parameters are important in ET estimation.

Table 1: The optimized parameter values of the SWAT model using the original and adapted ET calculations

Parameter	Description	Unit	Range	Calibrated (original)		Calibrated (Adapted)	
				Tubize	Lot	Tubize	Lot
Alpha_Bf	Baseflow alpha factor	day^{-1}	0-1	0.974	0.001	0.973	0.001
Canmx	Maximum canopy storage*	mm	0-10	2.0-9.0	2.5-10.0	1.5-7.0	1.5-7.0
Ch_N2	Manning's rougness coefficient		0-1	0.048	0.023	0.034	0.025
CN2	Curve number at moisture condition II**		35-98	71-94	49-65	71-94	50-67
ESCO	Soil evaporation compensation factor		0-1	0.446	0.014	0.606	0.554
Gw_Delay	Groundwater delay	day	0-100	6.247	18.091	4.900	12.750
Gw_Revap	Groundwater revap coefficient		0.02-0.2	0.178	0.050	0.113	0.081
Gwqmn	Minimum depth for groundwater flow ocurrence	mm	0-5000	29.549	6.056	19.164	3.139
Revapmn	Minimum depth for groundwater revap ocurrence	mm	0-500	6.287	2.178	1.262	9.376
Sol_Awc	Soil water available capacity***		0-1	0.14-0.34	0.14-0.30	0.14-0.34	0.14-0.30
Surlag	Surface runoff lag coefficient	day	0-10	1.330	1.330	0.964	0.964

* varies with land use type; ** varies with land use, soil & slope; *** varies with soil type

As it can be noticed from Table 1, when the two observations were used simultaneously, some of the optimized surface water and the groundwater parameters show large difference within the catchment. For example, for both versions of SWAT, the optimized groundwater delay (Gw_delay) value for Lot observation is approximately 3 fold of Tubize. Also the groundwater recession constant (Alpha_bf) of Lot is nearly zero while it is close to the upper bound value for the Tubize observations. The low value of Gw_delay and high value of Alpha_bf at Tubize can result in quick groundwater response to recharge in the western part of the basin. In addition, the calibrated CN2 values of Lot observation are relatively low as compared to the values obtained for the Tubize.

The differences in the optimized parameter values show that the relationship between stream flow, topography, land use, soil and precipitation is different for the two stations. One possible reasonable could be related to the heterogeneity in the geological formations of the basin (Meyus et al., 2004, Peeters, 2010). The latter might impact the hydrological processes (e.g., recharge, infiltration) of the basin. For instance, from the reported recharge map of the Flemish region (that includes our case study) by Meyus et al (2004), we noted that the western part of the basin is dominated by discharge zones (recharge close to 0) while the eastern part of the river show

high recharge zones. It turns out that the eastern part of the basin (Lot outlet) get low CN2 due to the high infiltration and recharge processes, which in turn reduces the surface runoff processes.

The ET effects on the mass balance

In order to see the effect of the intercept ET on the water balance components, the water balance was analyzed for the original version of SWAT as well as for the adapted version (Table 2). We assigned different interception values (Canmx) according to the different land use classes of the basin, so that forest will get high Canmx. In general, one can notice from Table 2 that the calibrated original and recalibrated adapted SWAT models of the river Zenne provide similar water balance components except for lateral flow. In the case of adapted version, the lateral flow component is increased. This could be related to the ESCO parameter that received higher values after calibration. As a consequence, less water is extracted from the lower levels and the lateral flow increases. However, when the calibrated parameter values of the original SWAT were used, some differences in water balance values are observed. Further, the water balance components are lowered due to the ET increase by 17mm. Globally, the annual ET of the basin approximately accounts 60% of the annual precipitation.

Table 2: The average yearly water balance components of SWAT for original and adapted versions for ET Calculations (WYLD = water yield; SR= surface runoff; BF= base flow; LF= lateral flow; Revap= aquifer evaporation; DL= deep aquifer losses; ET= evapotranspiration; Delta= balance error)

Water components (mm/y)	**Precipitation**	**WYLD**	**SR**	**BF**	**LF**	**Revap**	**DL**	**ET**	**delta**
Observed	901.2	310	76	234					
Original SWAT		330	76	221	33	33	10	523	**6**
Adapted SWAT (uncalib.)		313	75	207	32	33	9	540	**5**
Adapted SWAT (recalib.)		333	72	212	49	35	10	519	**5**

Table 3 shows the ET values for different land uses. For the original SWAT, one notices that the ET for forests is lower than the ET for agriculture, which is counter-intuitive. The adapted version shows that the highest ET occurs in the forests, as expected. The impact of the adaptation can also clearly be seen on Fig.3. The figure also reveals that for the other land uses, the pattern of ET pattern values are similar both for the original and adapted versions.

Table 3: The estimated ET for the different land use classes of the basin

Land use class	**Agriculture**	**Forest**	**Pasture**	**Rangeland**	**Urban**
Preciptation (mm/y)	900	907	901	893	901
Original SWAT (mm/y)	566	544	465	459	361
Adapted SWAT without recalib. (mm/y)	572	612	470	464	413
Adapted SWAT with recalib. (mm/y)	549	585	454	449	399

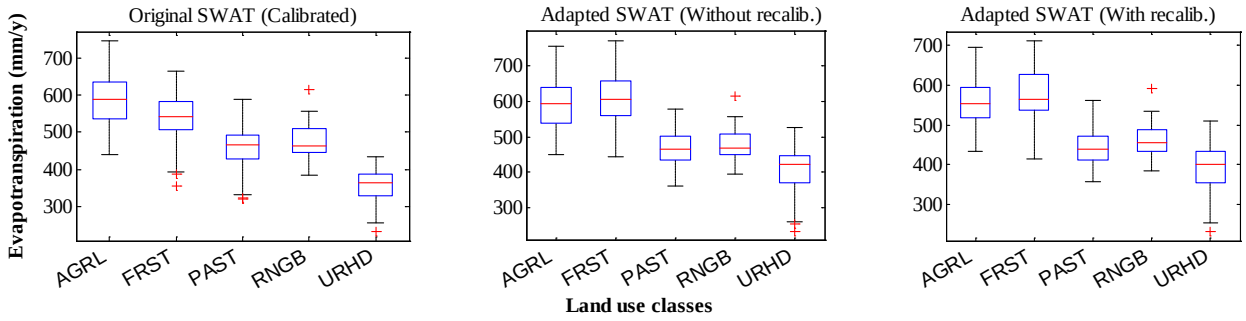

Figure 3: The box and whiskers plots of yearly ET values for the different land use classes (AGRL: agriculture, FRST: forest, PAST: pasture, RNGB: rangeland and URHD: urban) of the basin obtained with the original ET estimator (left) and adapted version (middle & right) of SWAT.

Figure 4 shows the yearly observed and simulated water yield with the average yearly precipitation of the basin. Results indicate that the two versions simulate similar water yield. A PBIAS of 6.5% for the original SWAT and 7.5% for the adapted SWAT are obtained, showing very good model performance but overestimation bias during calibration. Similarly, a model overestimation bias of 12.2% (original SWAT) and 12.3% (adapted SWAT) achieved during validation period, indicating good model performance.

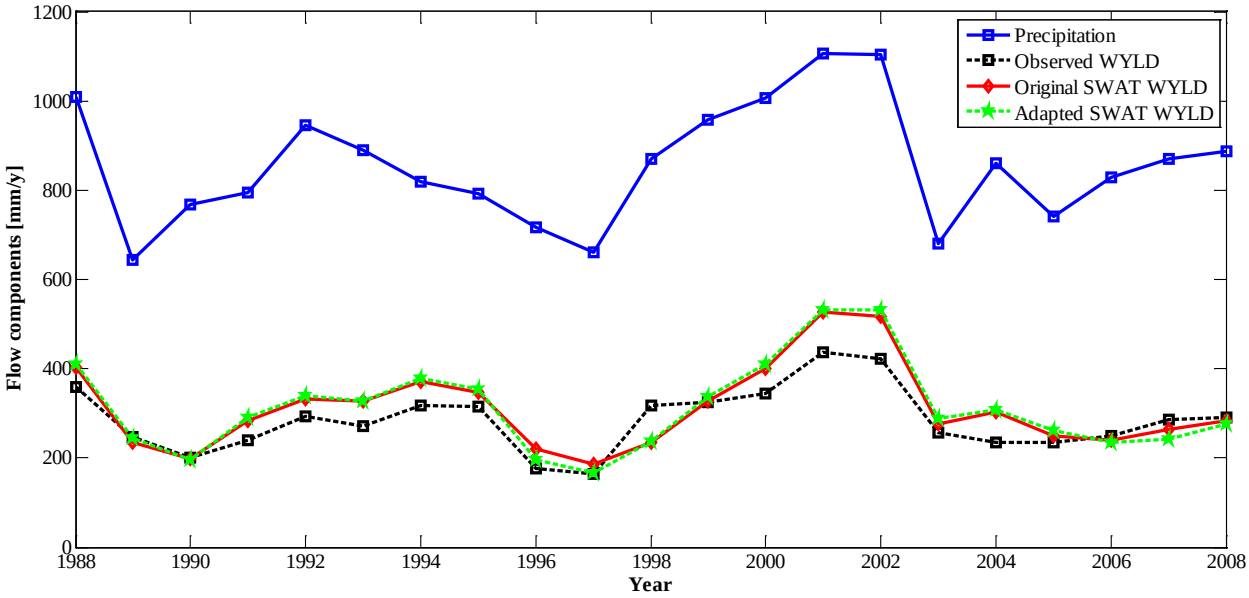

Figure 4: Observed and simulated yearly water yield of the basin for the calibration (1998-2008) and validation (1988-1997), using the original and adapted SWAT

Though the adapted version shows similar model performance for yearly water yield, the ET of forest is still higher than the other land use classes (Fig.3), which shows its superiority over the original SWAT. In both versions, if daily stream flow prediction is considered, the performance of the models is very good (Moriasi et al., 2007) as given in Table 4.

Table 4: Summary of the model performance evaluation for daily stream flow simulations at Tubize and Lot

Metrics	Original SWAT		Adapted SWAT without recalib.		Adapted SWAT with recalib.	
	Tubize	Lot	Tubize	Lot	Tubize	Lot
RMSE (m^3/s)	1.29	1.57	1.35	1.83	1.36	1.64
RSR	0.46	0.46	0.48	0.53	0.49	0.48
PBIAS (%)	5.8	-1.6	-23.5	-19.1	13.3	2.4
NSE	0.78	0.79	0.77	0.72	0.76	0.77

The groundwater-surface water interaction

Since the original version of SWAT allows only downward movement of water from streams to groundwater bodies (losing streams), we adapted the model in order to represent both upwelling of water to streams and seepage from streams. In the Zenne basin, there are some reaches (reach 1-7, 14, 17, 24 & 25; see Fig.2 for further information) that are running parallel to the canal and that gain some additional water fluxes through leakage from the canal towards these river reaches. To represent this process, we allowed in these river reaches to obtain a negative value for the channel transmission parameter (Ch_K2) in the calibration processes. The calibrated result indeed reveals a negative channel transmission that indicates an upward movement of water from the groundwater bodies to the streams (Table 5). This is an interesting result that indicates the interactions between the canal and the streams, whereby water leaks from the canal to the streams.

Table 5: The optimal parameter values for the original and the adapted SWAT version, considering GWSW interaction

Parameter	Description	Unit	Range	Calibrated (original)		Calibrated (Adapted)	
				Tubize	Lot	Tubize	Lot
Alpha_Bf	Baseflow alpha factor	day^{-1}	0-1	0.974	0.001	0.986	0.000
Canmx	Maximum canopy storage*	mm	0-10	2.0-9.0	2.0-9.0	2.0-7.0	2.0-7.0
Ch_N2	Manning's rougness coefficient		0-1	0.048	0.023	0.043	0.022
Ch_K2	Channel transmission parameter	mmh^{-1}	0-150	0.00	0.00	0.00	-10.79
CN2	Curve number at moisture condition II**		35-98	71-94	49-65	70-93.5	45-61
ESCO	Soil evaporation compensation factor		0-1	0.45	0.01	0.84	0.58
Gw_Delay	Groundwater delay	day	0-100	6.25	18.09	3.47	8.05
Gw_Revap	Groundwater revap coefficient		0.02-0.2	0.18	0.05	0.09	0.06
Gwqmn	Minimum depth for groundwater flow ocurrence	mm	0-5000	29.55	6.06	99.25	15.94
Revapmn	Minimum depth for groundwater revap ocurrence	mm	0-500	6.29	2.18	85.80	16.33
Sol_Awc	Soil water available capacity***		0-1	0.14-0.34	0.14-0.30	0.14-0.34	0.14-0.30
Surlag	Surface runoff lag coefficient	day	0-10	1.33	1.33	1.26	1.26

* varies with land use type; ** varies with land use, soil & slope; *** varies with soil type

Additional information that can be drawn from Table 5 is where a small decrement of CN2 can be seen, which could be related to an increased discharge from the groundwater system. As a consequence, less surface runoff might be expected in the eastern part of the basin. Again, this might be related to the heterogeneity in geological formations and the recharge processes of the basin. This is also supported by a higher groundwater contribution that accounts for 77% of the total water yield (Table 6). This is consistent with the results obtained from a base flow filtering program (Arnold & Allen, 1999) that indicates a base flow of 76%.

Table 6: Summary of the annual average water balance

Period	Method	Precipitation	WYLD	SR	BF	LF	Revap	DL	ET	Delta
Calibration	Observed (mm/y)	901	310	76	234					
	Original SWAT (mm/y)		330	76	221	33	33	10	523	**6**
	Adapted SWAT (mm/y)		342	69	220	55	27	10	517	**3**
Validation	Observed (mm/y)	804	258	60	199					
	Original SWAT (mm/y)		290	65	195	30	33	8	483	**-10**
	Adapted SWAT (mm/y)		300	59	193	50	27	8	481	**-14**

Finally, incorporating the losing and gaining options in to the SWAT simulator improved the performance of the model for daily stream flow simulation (Table 7). The performance statistics show a very good model performance (Moriasi et al., 2007) but a lower NSE is noticed for the validation at Tubize. The latter is suspected to be caused by stream flow measurement errors.

Table 7: Summary of model performance evaluation statistics for daily stream flow simulations

		Calibration (1998-2008)				Validation (1988-1997)			
	Station	RMSE (m^3/s)	RSR	PBIAS (%)	NSE	RMSE (m^3/s)	RSR	PBIAS (%)	NSE
Original SWAT	Tubize	1.29	0.46	5.8	0.78	1.64	0.77	18.14	0.41 (0.64)*
Adapted SWAT		1.28	0.46	0.12	0.80	1.72	0.80	11.45	0.35 (0.61)*
Original SWAT	Lot	1.57	0.46	-1.6	0.79	1.38	0.43	11.92	0.85
Adapted SWAT		1.52	0.44	-1.93	0.82	1.44	0.45	10.44	0.85

* inside bracket NSE for 1994-1997 from validation period

The daily stream flow hydrograph as shown in Fig.5 reveals that the adapted version has a tendency to better mimic the flows, especially for the medium to low flows and recession curves.

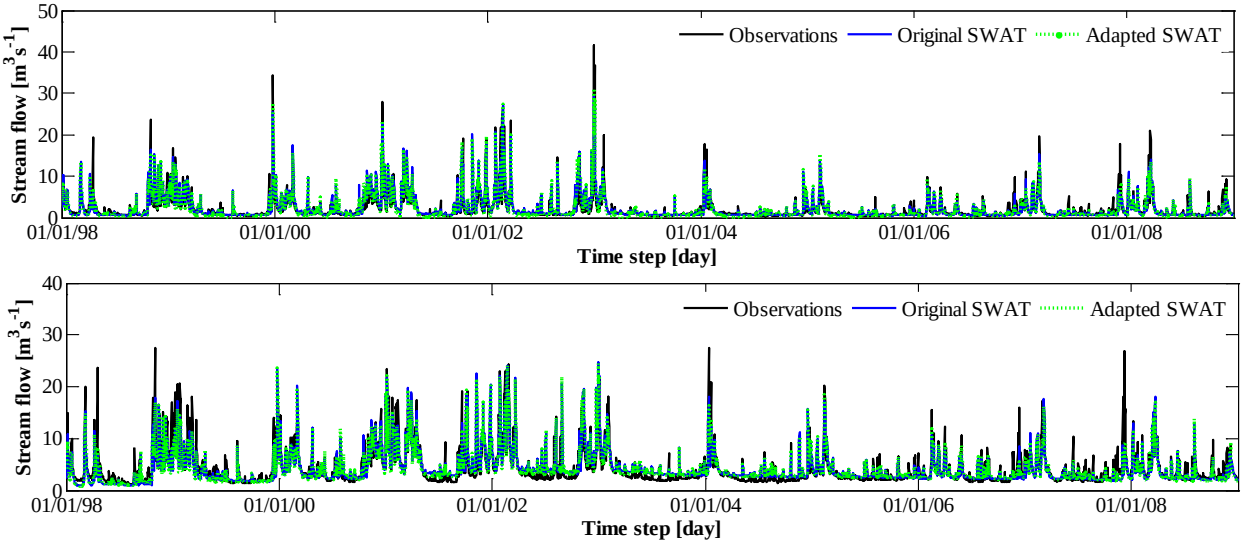

Figure 5: The observed and simulated daily stream flow at Tubize (top) and Lot (bottom) for the calibration (1998-2008) period

Conclusions

A SWAT model has been developed and calibrated for the upstream part of the river Zenne basin. Realizing the underestimation of the evapotranspiration (ET) from forest areas and the limitation of a uni-directional representation of the groundwater-surface water (GWSW)

interactions in SWAT, we modified the original source codes in view of mending these problems. The results indicate that the modified ET method provides a better representation of the ET, both spatially and temporally. Further, we found that by allowing for both losing and gaining conditions regarding the GWSW interactions in SWAT, the performance of the model was improved. For the river Zenne, we obtained a negative channel transmission parameter, indicating on average a gaining stream, as it is expected due to water leaks from the canal to the river. Our findings confirm the applicability of the modified SWAT but further research on the use of remotely sensed data and environmental tracing techniques (e.g. temperature sensors or isotopes) are needed to support the results.

Acknowledgements

The authors would like to thank INNOVIRIS (Environment Impulse Programme of the Brussels Capital Region) for supporting the GESZ research project. We are indebted to the Royal Meteorological Institute of Belgium (KMI), the Flemish Environmental Agency (VMM), and the Walloon Region (DGVH and DGARNE) for providing data.

References

Anibas C., Buis K., Verhoeven R., Meire P.& Batelaan O. (2011). A simple thermal mapping method for seasonal spatial patterns of groundwater–surface water interaction. J. Hydrol. **397**(1–2), 93-104

Arnold J. G., Williams J. R.& Maidment D. R. (1995). Continuous-time water and sediment-routing model for large basins. J. Hydraul. Eng. **121**(2), 171-183

Arnold J. G., Srinivasan R., Mukundan R. S.& Williams J. R. (1998). Large area hydrologic modeling and assessment part I: model development. J. Am. Water Resour. Assoc. **34**(1), 73-78

Arnold J. G.& Allen P. M. (1999). Automated methods for estimating baseflow and ground water recharge from streamflow records. Journal of the American Water Resources Association **35**(2), 411-424

Arnold J. G., Kiniry J. R., Srinivasan R., Williams J. R., Haney E. B.& Neitsch S. L. (2011). Soil and Water Assessment Tool. Input/output file documentation, Version 2009. Agrilife Blackland Research Center, Temple, Texas 76502

Chow V. T. (1959). Open channel hydraulics. McGraw-Hill Book Company, New York

Duan Q., Sorooshian S.& Gupta V. K. (1994). Optimal use of the SCE-UA global optimization method for calibrating watershed models. J. Hydrol. **158**(3–4), 265-284

Hargreaves G. L., Hargreaves G. H.& Riley J. P. (1985). Agricultural benefits for Senegal River basin. J. Irrig. Drainage Eng. **111**(2), 113-124

Leta O. T., Shrestha N. K., De Fraine B., van Griensven A.& Bauwens W. (2012). OpenMI based flow and water quality modelling of the River Zenne. In: SHF (Hrsg.), Proc. SimHydro 2012, 2nd International conference, 12th -14th September, Nice-Sophia Antipolis, Nice, France

Mein R. G.& Larson C. L. (1973). Modeling infiltration during a steady rain. Water Resour. Res. **9**(2), 384-394

Meyus Y., Woldeamlak S. T., Batelaan O.& De Smedt F. 2004. Opbouw van een Vlaams groundwatervoedingsmodel: Deelrapport 2, totaal Vlaams groundwater model (VGM)-karteergebied en vlaanderen, Vrije Universiteit Brussel, Brussels

Monteith J. L. (1995). Evaporation and environment, Symp. Soc. Exp. Biol., pp. 205-234

Moriasi D. N., Arnold J. G., Van Liew M. W., Bingner R. L., Harmel R. D.& Veith T. L. (2007). Model evaluation guidelines for systematic quantification of accuracy in watershed simulations. Tansactions of the ASABE **50**(3), 885-900

Neitsch S. L., Arnold J. G., Kiniry J. R.& Williams J. R. (2011). Soil & Water Assessment Tool. Theoretical documentation, Version 2009. Grassland, Soil and Water Research Laboratory, Agricultural Rsearch Service Blackland Research Center-Texas AgriLife Research

Peeters L. 2010. Groundwater and geochemical modelling of the unconfined Brussels aquifer, Belgium. PhD dissertation Thesis, KU Leuven, Leuven
Priestley C. H. B.& Taylor R. J. (1972). On the assessment of surface heat flux and evaporation using large-scale parameters. Mon. Weather Rev. **100**(2), 81-92
Sophocleous M. (2002). Interactions between groundwater and surface water: the state of the science. Hydrogeol. J. **10**(1), 52-67
USDA-SCS (1986). US Department of Agriculture-Soil Conservation Service (USDA-SCS): Urban hydrology for small watersheds. USDA, Washington, DC
van Griensven A., Francos A.& Bauwens W. (2002). Sensitivity analysis and auto-calibration of an integral dynamic model for river water quality. Water Sci. Technol. **45**(9), 325-332
Van Liew M. W., Arnold J. G.& Bosch D. D. (2005). Problems and potential of autocalibrating a hydrologic model. Trans. ASABE **48**(3), 1025-1040
Williams J. R. (1969). Flood routing with variable travel time or variable storage coefficients. Trans. ASABE **12**(1), 0100-0103
Winchell M., Srinivasan R.& Luzio M. D. (2010). ArcSWAT interface for SWAT2009 user's guide. Soil and Water Research Laboratory, Agricultural Research Service, Blackland, Texas
Winter T. C. (1999). Relation of streams, lakes, and wetlands to groundwater flow systems. Hydrogeol. J. **7**(1), 28-45

SWAT Application in Low-Gradient Coastal Plain Landscapes[1,2]

D.D. Bosch, Research Hydrologist
USDA-ARS Southeast Watershed Research Laboratory, Tifton, Georgia USA;
david.bosch@ars.usda.gov
J.G. Arnold, Research Agricultural Engineer
USDA-ARS Grassland, Soil and Water Research Laboratory, Temple, Texas
M. Volk, Research Scientist
UFZ – Helmholtz Centre for Environmental Research, Leipzig, Germany
P.M. Allen, Professor
Department of Geology, Baylor University, Waco, Texas

Abstract

Low-gradient coastal plain watersheds present unique challenges for watershed modeling. Broad low-gradient floodplains with considerable in-stream vegetation contribute to low-velocity streamflow. In addition, direct interaction between streamflow and surficial aquifers must also be considered. Here we examine several efforts that have involved application of the Soil and Water Assessment Tool (SWAT) to the Little River Experimental Watershed (LREW) in South-central Georgia within the Coastal Plain region of the US. Specific objectives include: 1) Examine prior attempts to model the hydrology and water quality of the LREW; 2) Summarize the outcomes of prior SWAT modeling attempts; 3) Identify consistent weaknesses in the computer simulations; and 4) Propose guidance for future applications. Climatic and hydrologic data from the LREW were used. Results indicate streamflow timing and groundwater contributions can be managed through parameter adjustment. While calibrated SWAT simulations provide acceptable water balances, discrepancies remain between simulated and observed streamflow for periods where large rainfall events occur during seasonably dry summer conditions. SWAT revisions, including the grid version of SWAT, better landscape differentiation, parameter variation throughout the year, differentiation of slow-return and fast-return groundwater flow, and sub-daily time steps, should yield improved representation of hydrology within Coastal Plain watersheds.

Keywords: groundwater, streamflow, hydrology, watersheds

[1] Contribution from the USDA-ARS, Southeast Watershed Research Laboratory, 2316 Rainwater Road, PO Box 748, Tifton, GA 31793, in cooperation with Univ. of Georgia Tifton Campus

[2] Trade names and company names are included for the benefit of the reader and do not imply any endorsement or preferential treatment of the products listed by the USDA. All programs and services of the USDA are offered on a nondiscriminatory basis without regard to race, color, national origin, religion, sex, age, marital status, or handicap.

Introduction

The Coastal Plain (CP) region of the United States (US) extends 3500 km from the state of New Jersey in the Northeast to Texas in the South-central. The CP is generally wet and includes many rivers, marshes, and swamps. The area is composed primarily of sedimentary rock and unlithified sediments and is used primarily for agriculture.

The most notable feature of the CP is its flat terrain. Much of the region also contains shallow surficial aquifers. The terrain, in combination with high groundwater tables, increases the interaction between surface water and groundwater. Soils in the CP tend to be either very sandy or poorly drained. In addition, the CP receives some of the highest annual rainfall of the US, often occurring in high intensity events associated with tropical storms and hurricanes. These characteristics have large implications on hydrology and pollutant transport. It is these same features which make modeling of CP watersheds challenging.

Here we examine several efforts that have involved application of the Soil and Water Assessment Tool (SWAT) to the Little River Experimental Watershed (LREW) in South-central Georgia within the CP (Figure 1). The LREW is considered to be fairly typical of many watersheds within the CP. Specific objectives include: 1) Examine prior attempts to model the hydrology and water quality of the LREW; 2) Summarize the outcomes of prior SWAT modeling attempts; 3) Identify consistent weaknesses in the computer simulations; and 4) Propose guidance for future applications.

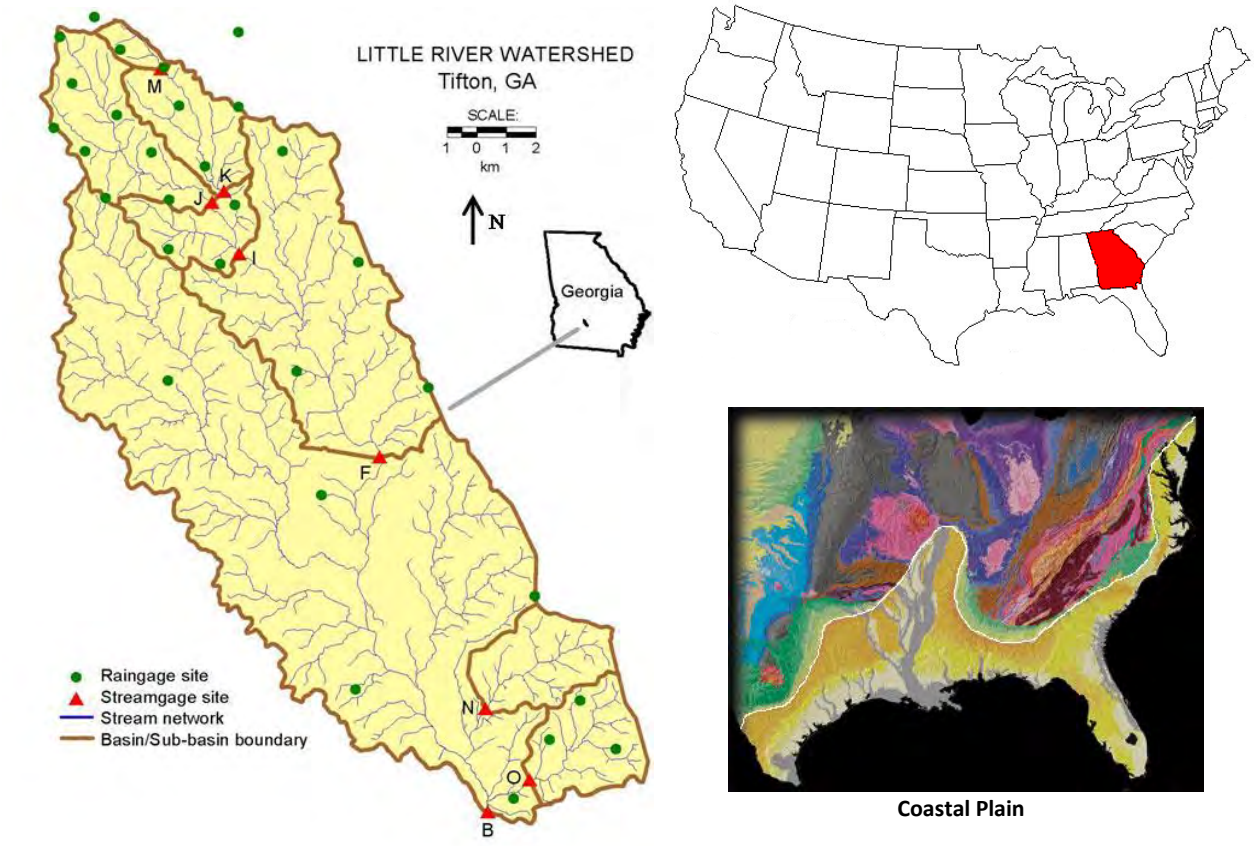

Figure 1. Little River Experimental Watersheds.

Methods

The LREW (31º28'54" N, 83º35'03" W) is located in the headwaters area of the Suwannee River Basin, a major U.S. interstate basin that originates in Georgia and empties into the Gulf of Mexico in the Big Bend region of Florida (Fig. 1) (Bosch et al., 2007). Streamflow data have been collected from the LREW since late 1967 (Bosch et al., 2007). The LREW is currently instrumented to measure streamflow for the 334 km^2 primary drainage area (Watershed B) and seven subwatersheds that range from approximately 2.6 km^2 to 114.9 km^2 (Fig. 1, Table 1).

Table 1. Little River Experimental Watershed subwatershed areas.

Station Name	Latitude	Longitude	Drainage Area (km^2)	Stream Order	Data Record
B	31º28'54"N	83º35'03"W	334.3	5	Oct. 14, 1971 to present
F	31º36'17"N	83º37'52"W	114.9	4	Nov. 29, 1968 to present
I	31º40'28"N	83º41'26"W	49.9	4	Dec. 08, 1967 to present
J	31º41'33"N	83º42'08"W	22.1	3	Dec. 01, 1967 to present
K	31º28'54"N	83º35'03"W	16.7	3	Dec. 06, 1967 to present
M	31º44'19"N	83º43'27"W	2.6	2	Dec. 06, 1967 to Dec. 31, 1988; Nov. 1, 2002 to present
N	31º31'04"N	83º35'11"W	15.7	4	Oct. 3, 1970 to Jan. 31, 1982; Aug. 01, 2002 to present
O	31º29'36"N	83º34'03"W	15.9	4	Nov. 29, 1968 to Jan. 31, 1982; Jan. 01, 1993 to present

The LREW is located on sands, silts, and clays underlain by limestones that form the Floridian aquifer which is confined in this region. Upland slopes within the watershed are 0 to 8% while channel slopes are on the order of 0.1 to 0.5%. Precipitation occurs almost exclusively as rainfall, with an annual mean of 1200 mm. Distribution of rainfall within the year is highly variable, although the fall months are typically dry. Water balance studies on the watershed indicate streamflow is around 27% of annual rainfall, ET is 73%, and percolation to regional deep groundwater is negligible due to the presence of plinthite and a geologic aquiclude at depth (the Hawthorne Formation) promoting lateral movement of excess water from uplands down slope as shallow return flow to surface drainage. Observed streamflow is composed of direct surface runoff (5% of annual rainfall) and return flow from the shallow surficial aquifer (22% of annual rainfall). Row crop, pasture, and forest areas cover approximately 41%, 7%, and 47% of the LREW, respectively. The watershed is typical of the heavily vegetated, slow-moving stream systems in the CP of the U.S. Discharge is highly variable. Streamflow in the upper reaches of the LREW typically ceases during late summer and fall. The relatively impermeable Hawthorne formation separates surface water from the underlying aquifer, uncoupling river discharge from the deeper Floridan aquifer system (Sheridan, 1997).

Prior SWAT Modeling Results

Since 2004, SWAT (Arnold et al., 1998; Arnold and Fohrer, 2005) has been used to simulate the hydrologic characteristics of the LREW. An overview of these studies is presented in Table 2.

Table 2. Nash Suttcliffe Simulation Efficiencies (NSE) reported from studies on Little River Experimental Watersheds.

Reference	Simulated Watershed	Simulated Years	Hydrology	Water Quality	Daily		Monthly	
					NSE* - calibration	NSE* - validation	NSE* - calibration	NSE* - validation
Bosch et al., (2004)	J	1997-2002	Yes	No	-0.03	NA	0.80	NA
Cho et al., (2009)	J, K, I	1985-1994	Yes	Yes	0.78-0.79	NA	0.95	NA
Cho et al., (2010a)	N	2003-2006	Yes	Yes	NA	NA	0.86	NA
Cho et al., (2010b)	K and B	1996-2004	Yes	Yes	0.77 (LRK)	NA	0.94 (LRK)	0.89
Cho et al., (2012)	K, J, O, I. F, and B	1996-1999 cal.; 2000-2004 val.	Yes	No	0.78 (LRK)	0.62-0.80	0.96 (LRK)	0.84-0.94
Feyereisen et al., (2007)	K	1995-2004	Yes	No	0.56	NA	0.88	NA
Joseph et al., (2012)	I	2002-2004 cal; 2005-2006 val.	Yes	No	0.92-0.76	0.78	NA	NA
Muleta (2012a)	F, I, J, K, and M	2000-2003 cal.; 2004-2006 val.	Yes	No	0.38-0.79 Seasonal Variables	0.37-0.61 Seasonal Variables	NA	NA
Muleta (2012b)	F and J	2000-2003 cal.; 2004-2006 val.	Yes	No	NA	NA	0.71-0.73	0.13-0.60
Van Liew et al. (2005)	F and B	1997-2002 cal; 1972-1996 val.	Yes	No	-0.36-0.78	-0.25-0.68	0.44-0.92	0.47-0.90
Van Liew et al. (2007)	F and B	1997-2002 cal; 1972-1996 val.	Yes	No	0.64-0.71	0.66-0.68	0.83-0.90	0.88-0.89
Veith et al. (2010)	B	1997-2002	Yes	No	NA	NA	0.90	NA
White et al. (2009)	K	1995-2004	Yes	No	0.66-0.78 Seasonal Variables	NA	NA	NA
Zhang et al. (2009a)	B	1999-2001	Yes	No	0.79	0.84	NA	NA
Zhang et al. (2011)	B	1991-2002	Yes	No	0.52-0.78	NA	NA	NA
Zhang et al. (2012)	F and B	1998-2005	Yes	No	0.64-0.68	NA	NA	NA

*for hydrology, for cases of multiple runs the range is reported

Bosch et al. (2004) conducted simulations of LRJ and reported Nash Sutcliffe Efficiency (NSE) values for monthly total streamflow (NSE_m) of 0.80. While satisfactory monthly and annual simulations were obtained, Bosch et al. (2004) reported discrepancies between observed and simulated hydrograph peaks, time to peak, and hydrograph durations (Fig. 2). In particular, simulations of flow events occurring during the summer period when evapotranspiration rates were high and the shallow water table was low yielded underestimates of peak discharge and overestimates of hydrograph durations. These characteristics indicated difficulty in adequately representing baseflow and storage characteristics of the shallow aquifer. During dry summer conditions, the model underpredicted direct surface runoff as well as the amount of available storage in the surficial aquifer.

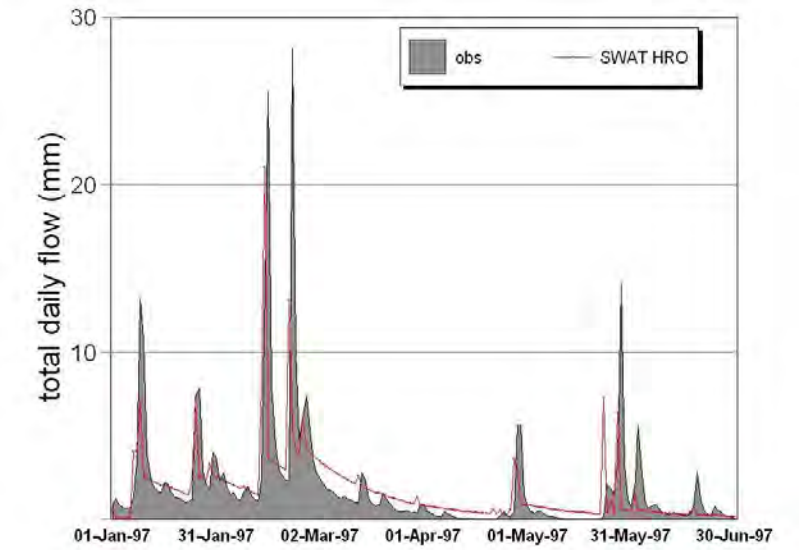

Figure 2. SWAT simulation results for Little River Watershed J (Bosch et al., 2004)

Similar to the findings of Bosch et al. (2004), Van Liew et al. (2005, 2007) also reported estimating the time to peak on many events one day too early. Feyereisen et al. (2007), Van Liew et al. (2005, 2007), and Joseph et al. (2012) also report overestimation of summer low flows, a phenomena that was first reported for the SWRRB model by Arnold and Williams (1987) for LRB. This is likely a reflection of an inability to adequately describe the wide seasonal variations in streamflow in the LREW with a single parameter set.

Additional simulations with no variation in parameter sets by season (Cho et al. 2012; Veith et al., 2010; Zhang et al., 2009a, 2009b, 2011, 2012) yielded improvements in the model simulations (Table 2). However, each of these studies still reported difficulty fitting both the winter and summer streamflow conditions adequately. As illustrated by the cumulative probability distribution reported by Cho et al. (2012) there remained a model tendency to predict too many small events (primarily during late summer and early winter) and too few large events (Fig. 3). Results were improved for the smaller watershed LRK which was used for model calibration (Cho et al., 2012).

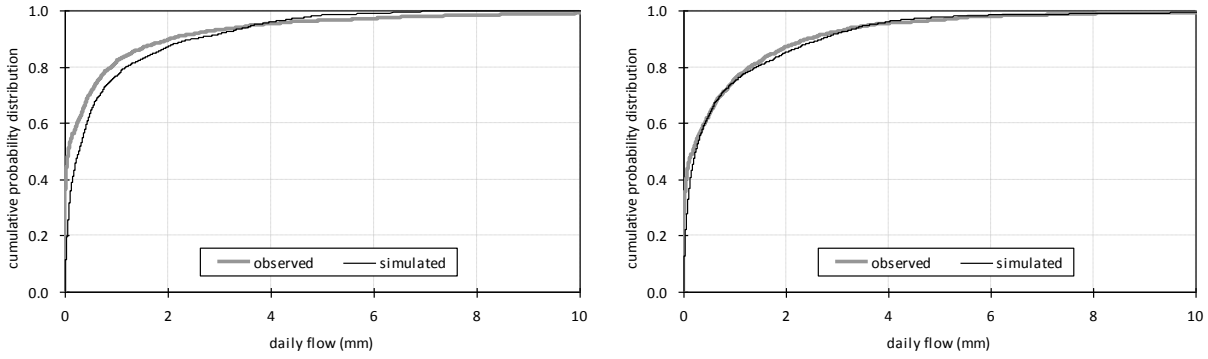

Figure 3. Cumulative probability distribution curve for the observed and simulated daily flow for (a) LRB and (b) LRK watersheds 1996-2004 (Cho et al., 2012).

Joseph et al. (2012) also reported difficulty fitting simulated recession curves for late summer and early winter events (Fig. 4). They attributed the poor fit during these periods to the effects of the surficial aquifer and an inability to adequately model storage within the aquifer, in particular the aquifer storage below the broad dendritic channel itself. Each of these results illustrates the difficulty of accurately simulating the dynamic conditions of low-gradient watersheds with considerable storage within the surficial aquifer. As described by Bosch et al. (2003), during periods of low evapotranspiration and high rainfall saturated conditions exist with little remaining available aquifer storage. During these conditions surface runoff is high and rapid. During periods of high evapotranspiration the aquifer rapidly drops and available aquifer storage increases, leading to less groundwater contributions to streamflow and greater opportunity for infiltration. In some cases, as the aquifer drops streamflow can be lost to the surficial aquifer (Bosch et al., 1996). As seen from the observed data, while the surface runoff component can remain high during these dryer conditions the baseflow component is short-lived.

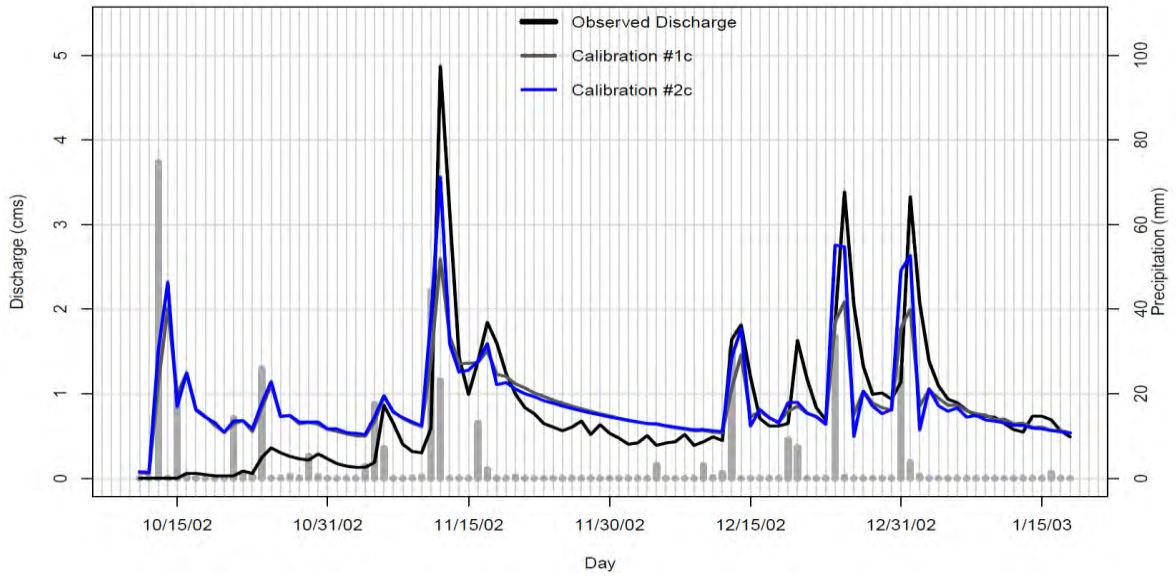

Figure 4. Simulation results for Little River Watershed I obtained by Joseph et al. (2012).

More recently, researchers have explored the possibility of varying different parameters by season in order to better fit the wide variety of aquifer storage encountered in the watershed. White et al. (2009) varied CN values between growing (May-November) and dormant (December-April) seasons for all agricultural row-crops. Their simulations resulted in better model performance during the dry seasons but an underprediciton of streamflow during wet seasons (White et al., 2009). These results indicate the model performance may be a result of seasonal differences in both surface runoff and subsurface storage.

Mueleta (2012a) performed a parameter optimization routine whereby different parameters were developed for December through April and June through October periods. These were characterized as periods with streamflow to rainfall ratios greater than 0.1 (December-April) and those with ratios less than 0.1 (June-October). Their results indicated considerable differences in the optimized parameters for the two seasonal divisions. The parameters exhibiting the greatest changes by season were ESCO (the soil evaporation compensation factor), Ch_K2 (the effective hydraulic conductivity of the main channel alluvium), and Sol_K (soil hydraulic conductivity). The importance of CN in the model predictions remained high for both seasons. Mueleta (2012a) found less significance in ESCO for dry season calibration, indicating that soil evaporation played less of a role in estimating streamflow during dry months because soil

moisture was generally low to begin with. Furthermore, the greater importance in Sol_K found for the dry season indicated infiltration played a greater role during the dry period than during the wet period. During wet periods in this watershed surface runoff is largely controlled by saturation excess, decreasing the importance of Sol_K in the winter season. Interestingly, Ch_K2 was found more important for the summer season, indicating that infiltration into the surficial aquifer below the channel was more important during this season. Each of these findings illustrates the importance of accurately simulating available storage in the surficial aquifer.

While the results of Mueleta (2012a) improved the dry season performance of the model, problems remained accurately simulating the time to peak (Fig. 5). This is likely related to the daily time step typically used in the simulation. For all of the Little River sub-watersheds other than B, the time to peak is less than 1 day (Sheridan, 1994). Thus, using daily rainfall and daily time steps it would be impossible for the model to accurately estimate the time to peak correctly.

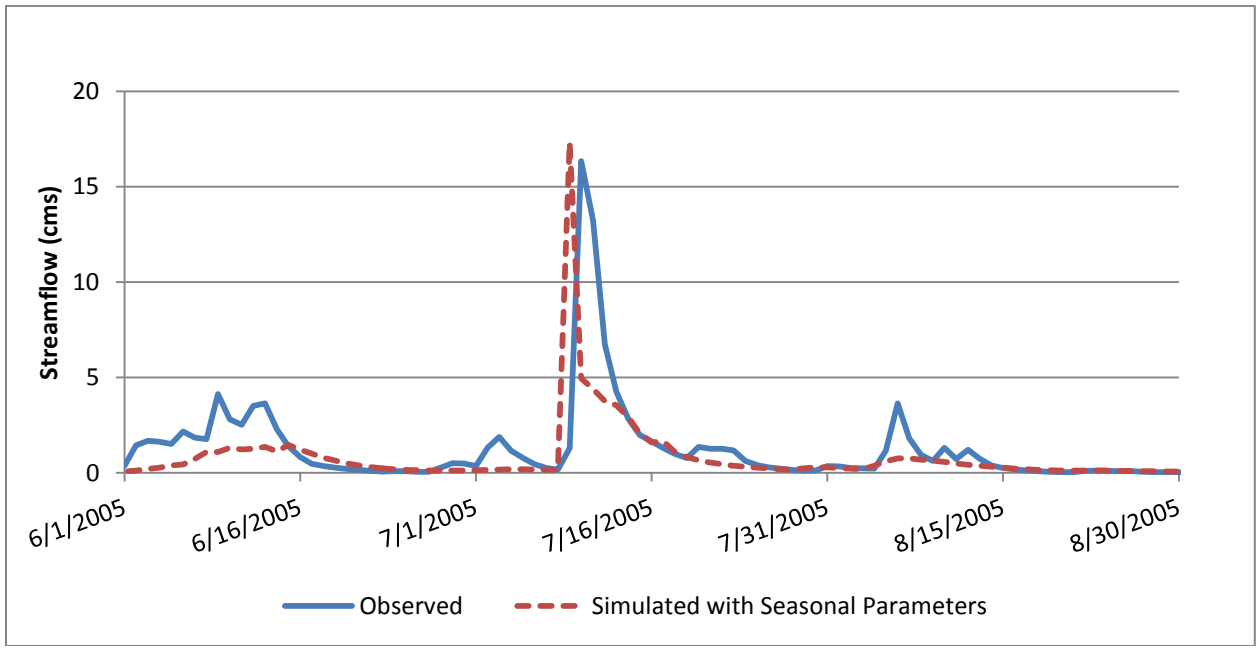

Figure 5. Simulation of watershed F for a dry season period from June 1, 2005 through August 30, 2005 utilizing seasonal parameters (Mueleta, 2012a).

Results of Zhang et al. (2011) support using different parameter sets to address different hydraulic conditions within the watershed. In their study, Zhang et al. (2011) developed a SWAT version to simultaneously calibrate the model for surface flow dominated conditions or for baseflow dominated conditions. In the case of the LREW watersheds, high water table conditions generally experienced in the winter generate high volumes of baseflow in addition to event based surface runoff. Summer streamflow responses tend to be surface runoff dominated due to low water table conditions that generate little baseflow in addition to rapid surface runoff. Zhang et al. (2011) results indicated a large difference in the derived parameter sets, in particular in the parameters Surlag (surface runoff lag coefficient), Ch_K2 (effective hydraulic conductivity in the main channel alluvium), GWQMN (threshold depth of water in the shallow aquifer required for return flow to occur), and REVAPMN (threshold depth of water in the shallow aquifer for re-evaporation to occur). This set of parameters points to the need to represent aquifer storage during conditions driven by baseflow differently from when they would

be driven by surface flow. As pointed out by Zhang et al. (2011), depending on the modeler's interest, i.e. representing surface runoff dominated events or subsurface runoff dominated total flow, different optimization routines could be used.

Discussion and Conclusions

This review illustrates the difficulty associated with simulating the low-gradient streams of the CP region which are heavily influenced by available storage within the surficial aquifer. Prior studies have illustrated that overall water balance results (annual and monthly) provided by the SWAT model for the LREW have been very good (Table 2). Manual and automated calibrations have yielded good approximations of peak flows during high flow winter events. During typically years, it is these events that will transport the majority of the water volume and contaminants. However, a widely varying shallow water table makes simulation of the watershed with a single parameter set challenging.

Results varying the parameters by season (White et al., 2009; Mueleta, 2012a) have been encouraging and present one possible avenue of improved simulations. Luo et al. (2012) incorporated a slow-reacting groundwater reservoir to SWAT to account for seasonal differences in baseflow, resulting in significant improvements in the representation of baseflow throughout the year. This technique, differentiating between more rapid lateral flow within the vadose zone and slower shallow groundwater flow, may offer a method for improving simulation of these characteristics within the LREW. Sub-daily time steps have recently been used with the SWAT model to improve hydrograph representations for urban watersheds (Jeong et al., 2010; Jeong et al., 2011). Sub-daily simulation should also yield better representations of hydrograph timing for smaller watersheds.

Subsequent improvements will likely involve expanding the spatial capabilities of the model to more dynamically simulate actual water table conditions throughout the landscape and other geographic features, both in the upland and the stream channel. It is anticipated that landscape revisions of the SWAT model along these lines will lead to significant improvement of simulation of this phenomena. One possible route for incorporating these revisions into the SWAT model was presented by Arnold et al. (2010) and tested on a small CP Watershed by Bosch et al. (2010). A grid based SWAT model may also allow closer representations of the landscape physical features and in particular the spatial variation of the surficial aquifer (Rathjens et al., 2013). Simulations of the LREW using the SWAT grid based model are particularly encouraging regarding yielding better hydrograph representations (Rathjens et al., 2013). Utilizing the current model capabilities (landscape routing, grid based, sub-daily time steps, and variable aquifer characteristics) will likely lead to superior model performance in estimating hydrograph time to peak.

References

Arnold, J.G., P.M. Allen, M. Volk, J.R. Williams, and D.D. Bosch. 2010. Assessment of different representations of spatial variability on SWAT model performance. Trans. of the Am. Soc. Agr. and Bio. Eng. 53(5):1433-1443.

Arnold, J.G. and J.R. Williams. 1987. Validation of SWRRB-Simulator for Water Resources in Rural Basins. ASCE Water Res. Plann. and Manage. 113(2):243-256.

Arnold, J.G., R. Srinivasan, R.S. Muttiah, and J.R. Williams. 1998. Large-area hydrologic modeling and assessment: Part I. Model development. J. American Water Resources Assoc. 34(1):73-89.

Arnold, J.G. and N. Fohrer. 2005. SWAT2000: Current capabilities and research opportunities in applied watershed modeling. Hydrol. Proc. 19(3):563-572.

Bosch, D.D., J.G. Arnold, M. Volk, P.M. Allen. 2010. Simulation of a Low-Gradient Coastal Plain Watershed using the SWAT Landscape Model. Trans. of the Am. Soc. of Agr. and Bio. Eng. 53(5):1445-1456.

Bosch, D.D., R.R. Lowrance, J.M. Sheridan, and R.G. Williams. 2003. Groundwater storage effect on streamflow for a Southeastern Coastal Plain Watershed. Ground Water. 41(7):903-912.

Bosch, D.D., J.M. Sheridan, and R.R. Lowrance. 1996. Hydraulic gradients and flow rates of a shallow coastal plain aquifer in a forested riparian buffer. Trans. Am. Soc. Agr. Eng. 39(3):865-871.

Bosch, D.D., J.M. Sheridan, H.L. Batten, and J.G. Arnold. 2004. Evaluation of the SWAT Model on a Coastal Plain Agricultural Watershed. Trans. Am. Soc. of Agr. Eng. 47(5):1493-1506.

Bosch, D. D., and J. M. Sheridan. 2007. Stream discharge database, Little River Experimental Watershed, Georgia, United States. Water Resour. Res. 43(9). W09473.

Cho, J., D. Bosch, R. Lowrance, T. Strickland, and G. Vellidis. 2009. Effect of spatial distribution of rainfall on temporal and spatial uncertainty of SWAT output. Trans. of the Am. Soc. of Agr. and Bio. Eng. 52(5):1545-1555.

Cho, J., D.D. Bosch, G. Vellidis, R. Lowrance, and T.C. Strickland. 2012. Multi-site Evaluation of Hydrology Component of SWAT in the Coastal Plain of Southwest Georgia. Hydrological Processes. Doi:10.1002/hyp.9341.

Cho, J., R. R. Lowrance, D.D. Bosch, T.C. Strickland, Y.G. Her, and G. Vellidis. 2010a. Effect of watershed subdivision and filter width on SWAT simulation of a Coastal Plain Watershed. J. of Am. Water Res. Assoc. 46(3): 586-602.

Cho, J., G. Vellidis, D.D. Bosch, R.R. Lowrance, and T.C. Strickland. 2010b. Water quality effects of simulated conservation practice scenarios in the Little River Experimental Watershed. J. of Soil and Water Conservation Society. 65(6):463-473.

Feyereisen, G.W., T.C. Strickland, D.D. Bosch, and D.G. Sullivan. 2007. Evaluation of SWAT Manual Calibration and Input Parameter Sensitivity in the Little River Watershed. Trans. Am. Soc. of Agr. and Bio. Eng. 50(3):843-855.

Jeong, J., N. Kannan, J. Arnold, R. Glick, L. Gosselink, and R. Srinivasan. 2010. Evelopment and integration of sub-hourly rainfall-runoff modeling capability within a watershed model. Water Resources Mgmt. 24(15):4504-4527.

Jeong, J., N. Kannan, J.G. Arnold, L. Gosselink, R. Glick, and R. Srinivasan. 2011. Development of sub-daily erosion and sediment transport algorithms for SWAT. Trans. of the

Am. Soc. of Agr. and Bio. Eng. 54(5):1685-1691.

Joseph, J.F., H.O. Sharif, J.G. Arnold, and D.D. Bosch. 2012. The impact of asynchronicity on event-flow estimation in basin scale hydrologic model calibration. J. of the American Water Resources Assoc. Doi: 10.1111/jawr.12011.

Luo, Y., Arnold, J.G., and Allen, P.M. 2012. Baseflow simulation of SWAT in an inland river basin in Tianshan Mountains, Northwest China. Hydrology and Earth System Sciences. 16:1259-1267.

Muleta, M. 2012a. Improving model performance using season-based evaluation. J. of Hydrologic Engineering. 17(1):191-200.

Muleta, M. 2012b. Model performance sensitivity to objective function during automated calibrations. J. of Hydrologic Engineering. 17(6): 756-767.

Rathjens, H. N. Oppelt, and M. Volk. 2013. Development of a grid-based version of the SWAT landscape model. In Proceedings of the 2013 International SWAT Conference. Toulouse, France. July 15-19, 2013.

Sheridan, J.M. 1994. Hydrograph time parameters for flatland watersheds. Trans. of the Am. Soc. of Agr. Eng. 37:103-113.

Sheridan, J.M. 1997. Rainfall-streamflow relationships for Coastal Plain watersheds. Applied Eng. in Agr. 13:333-344.

Veith, T.L., M.W. VanLiew, D.D. Bosch, and J.G. Arnold. 2010. Parameter sensitivity and uncertainty in SWAT: A comparison across 5 USDA-ARS watersheds. Trans. of the Am. Soc. of Agr. and Bio. Eng. 53(5):1477-1486.

Van Liew, M.W., J.G. Arnold, and D.D. Bosch. 2005. Problems and potential of autocalibrating a hydrologic model. Trans. Am. Soc. of Agr. Eng. 48(3):1025-1040.

Van Liew, M.W., T.L. Veith, D.D. Bosch, and J.G. Arnold. 2007. Suitability of SWAT for the Conservation Effects Assessment Project: Comparison on USDA Agricultural Research Service Watersheds. J. Hydrologic Engineering. 12(2):173-189.

White, E.D., G.W. Feyereisen, T.L. Veith, and D.D. Bosch. 2009. Improving daily water yield estimates in the Little River Watershed: SWAT adjustments. Trans. of the Am. Soc. of Agr. and Bio. Eng. 52(1):69-79.

Zhang, X., R.C. Izaurralde, Z. Zong, K. Zhao, and A.M. Thomson. 2012. Evaluating the efficiency of a multi-core aware multi-objective optimization tool for calibrating the SWAT model. Trans. of the Am. Soc. of Agr. and Bio. Eng. 55(5):1723-1731.

Zhang, X., R. Srinivasan, J.G. Arnold, R.C. Izaurradale, and D.D. Bosch. 2011. Simultaneous calibration of surface flow and baseflow simulations: A revisit of the SWAT model calibration framework. Hydrological Processes. 25(14):2313-2320.

Zhang, X., R. Srinivasan, and D. Bosch. 2009a. Calibration and uncertainty analysis of the SWAT model using genetic algorithms and Bayesian model averaging. J. of Hydrology. 374(2009): 307-317.

Zhang, X., R. Srinivasan, and M. Van Liew. 2009b. On the use of multi-algorithm, genetically adaptive multi-objective method for multi-site calibration of the SWAT model. Hydrol. Process. DOI: 10.1002/hyp.

Spatial Integration of SWAT, MODFLOW, and RT3D for Simulation of Hydrologic and Water Quality Processes in Irrigated Agricultural Watersheds

Tyler Wible

Dept. Civil-Env. Eng., Colorado State University, Fort Collins, CO, United States.

Jeff Ditty

Dept. Civil-Env. Eng., Colorado State University, Fort Collins, CO, United States.

Dr. Ryan Bailey

Dept. Civil-Env. Eng., Colorado State University, Fort Collins, CO, United States.

Dr. Mazdak Arabi

Dept. Civil-Env. Eng., Colorado State University, Fort Collins, CO, United States.

Abstract

Watershed models are valuable tools in assessing surface and subsurface water quantity and quality impacts due to land management practices in watersheds of varying scale and complexity. However, surface water models typically lack sufficient detail in groundwater systems to accurately describe heavily irrigated agricultural or groundwater driven watersheds. Similarly, groundwater models typically lack important land surface processes like plant growth, nutrient cycling, and overland flow to stream networks. In this study, we present a model that is capable of simulating both land surface and subsurface flow and nutrient transport through the coupling of SWAT with the variably-saturated groundwater flow model, MODFLOW-UZF, and a variably-saturated groundwater solute reactive transport model, UZF-RT3D. Overland flow and stream routing are handled by the SWAT subroutines, while fluxes of water and chemical species within the subsurface and associated loadings to and from surface water are handled through the subroutines of MODFLOW-UZF and UZF-RT3D. Also, secondary SWAT pre-processing algorithms are used to distribute spatially disaggregated HRUs to improve representation of watershed heterogeneity. The accuracy and usefulness of the SWAT-MODFLOW-RT3D model is illustrated through application to a study basin within the United States wherein groundwater is a significant contributing factor to surface water processes.

Keywords: SWAT, MODFLOW, watershed modeling, groundwater, groundwater solute transport, irrigated agriculture

Introduction

Watershed models have become the standard in assessing changes in surface and subsurface water quality due to changes in land management, land use, and climate. Most of these models are able to account for varying levels of scale and complexity depending on the availability of data. However, current popular watershed models typically lack sufficient detail in simulating spatially-variable groundwater processes. Consequently, the accuracy of the model is reduced when streamflow is influenced by groundwater flow. For example, basins with heavy irrigation often experience high water tables, which increase subsurface hydraulic gradients and consequently yield high volumes of groundwater discharge to the stream network. On the other hand, groundwater models typically lack important land surface processes such as plant growth, nutrient cycling, and overland flow transport. Additionally groundwater models do not implement and test various best-management practices (BMPs), a key requirement for watershed water quality analysis. To combine the benefits of both current watershed and groundwater models, this study presents a linkage between SWAT (Arnold et al., 1998) , MODFLOW-NWT-UZF (Niswonger et al., 2006 and Niswonger et al., 2011), and UZF-RT3D (Bailey et al., 2012) to provide a modeling framework that accounts for land surface processes, in-stream processes, the assessment of BMPs, as well as subsurface flow, spatially variable hydrogeologic features, and reactive transport of nutrients at the watershed scale.

Model Development

To create the comprehensive hydrologic and water quality watershed model, the Soil and Water Assessment Tool (SWAT) is modified and coupled with MODFLOW-NWT-UZF and UZF-RT3D. MODFLOW-NWT-UZF (Niswonger et al., 2006 and Niswonger et al., 2011) is a fully distributed finite-difference grid-based subsurface flow model which allows for spatially varying groundwater parameters (i.e. hydraulic conductivity, bedrock elevation). UZF-RT3D is based on the original solute reactive transport modeling code RT3D (Clement, 1997), and accounts for reactive transport and interaction of multiple chemical species in variably-saturated porous media, with variably saturated flow supplied by MODFLOW simulations using the Unsaturated Zone Flow (UZF1) package (Niswonger et al., 2006). These models were combined to retain their respective strengths so that SWAT handles land surface, in-stream, shallow subsurface hydrologic, biological, and nutrient processes, MODFLOW-NWT-UZF handles variably-saturated subsurface flow and interaction with the stream network, and UZF-RT3D handles the transport of chemically reactive solutes in variably-saturated subsurface flow systems and mass loadings to/from the stream network.

SWAT currently handles water and chemical transport by dividing a watershed into two different categories: subbasins, and landscapes. Within each subbasin, 3 landscape zones, designated as the divide, hill slope, and floodplain (Arnold et al., 2010) are established. Within a given subbasin and given landscape, unique combinations of soil type, land use, slope, and management practices are intersected to define hydrologic response units (HRUs). Calculations are then performed for each HRU to account for processes such as plant growth, snow accumulation, snow melt, infiltration, evapotranspiration, and precipitation. SWAT's groundwater subroutines were deactivated in order to allow MODFLOW-NWT-UZF to calculate groundwater movment. SWAT and MODFLOW-NWT-UZF determines the direction and amount of flow through the watershed's aquifer and critical zone so that RT3D can simulate the

reactive transport of solute in the subsurface. Figure 1 outlines the processes or concepts handled by each model (SWAT, MODFLOW-NWT-UZF, UZF-RT3D), which is also outlined below in a bulleted format.

SWAT handles the following processes:

- Infiltration
- Evapotranspiration
- Plant growth and root zone processes
- Overland flow and transport
- Lateral subsurface flow in SWAT's "soil zone"
- Stream flow and transport

MODFLOW-NWT-UZF handles the following processes :

- Vadose zone percolation below the soil profile, via the UZF1 package of MODFLOW
- Recharge to the water table, via the RCH package of MODFLOW
- Water table elevation
- Saturated groundwater flow
- Groundwater pumping, via the WEL package of MODFLOW
- Groundwater discharge to streams (baseflow), stream seepage to groundwater, via the RIVR package of MODFLOW

UZF-RT3D handles the following processes:

- Saturated and unsaturated (vadose zone) transport of chemical species
- Chemical species interaction with geologic formations (e.g., autotrophic denitrification in the presence of marine shale)
- Mass fluxes of nitrogen and phosphorus pumped from groundwater
- Mass loadings of nitrogen and phosphorus from the aquifer to the stream network (via groundwater discharge)
- Mass loadings of nitrogen and phosphorus from the stream network to the aquifer (via stream seepage)

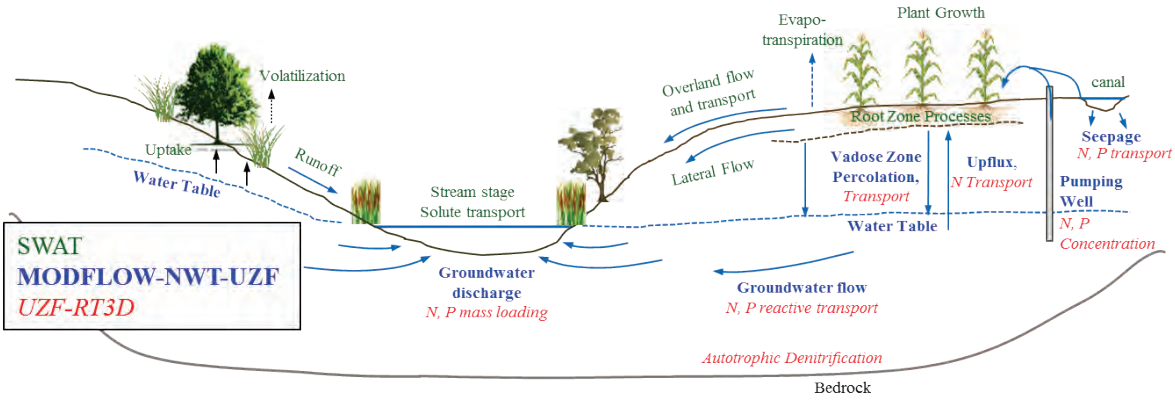

Figure 1: Breakdown of watershed processes simulated by SWAT (green), MODFLOW-NWT-UZF (bolded blue), and UZF-RT3D (italicized red)

Passing information (as shown in Figure 2) between the models occurs on a daily time step. The combined SWAT, MODFLOW-NWT-UZF, and UZF-RT3D begins executing SWAT's overland flow and "soil zone" process calculations for every HRU within the watershed. The outputs of these calculations are then mapped to MODFLOW's grid cells (explained below). MODFLOW-NWT-UZF then calculates variably-saturated subsurface processes, whereupon flow results are provided to UZF-RT3D for subsurface reactive solute transport. Once UZF-RT3D finishes, the resulting water table elevation, seepage/groundwater discharge to rivers and nutrient loadings to/from rivers is mapped back to SWAT HRUs. SWAT then proceeds to route surface and subsurface contributions to river segments, down the river segments to subbasin outlets, and through the watershed network.

RIVER (RIV) (Harbaugh et al., 2000), a MODFLOW package, determines whether return flow or seepage occurs for each river segment. The RIV package utilizes two inputs, the stream stage (outputted by SWAT from the current day) and the simulated water table elevation. Locations of MODFLOW river cells are determined during pre-processing, and the inputs for the grid cells are river parameters (channel width, channel bottom elevation, hydraulic conductivity) as supplied to or calculated by SWAT. The seepage and return flows are then used by UZF-RT3D to calculate mass loadings to/from the stream network. This allows SWAT to perform in-stream routing for the current time step. In the case of groundwater upflux from a shallow water table elevation, the method used by Sophocleous and Perkins (2000) and Kim et al. (2008) is adopted. Groundwater upflux volumes, as calculated by MODFLOW, are distributed over SWAT's soil profile layers, beginning with the bottom layer and limited by the saturated water content of each layer. Nitrogen and Phosphorus associated with groundwater upflux is distributed among the layers of the soil profile in a similar manner.

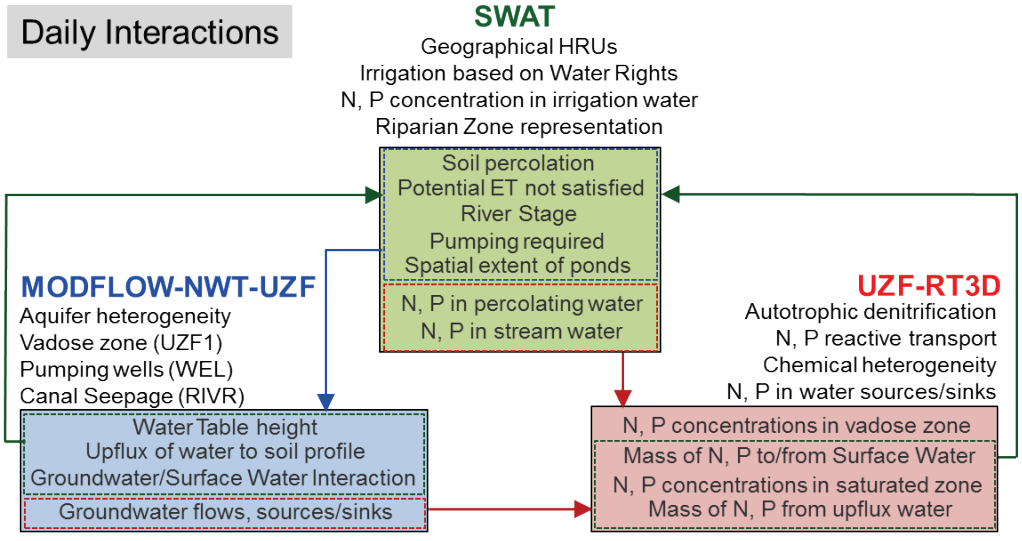

Figure 2: Flow of information between SWAT, MODFLOW-NWT-UZF, and UZF-RT3D

Spatial Integration

To facilitate the linkage between the spatially discontinuous HRU-based SWAT model and the spatially continuous grid-based MODFLOW model, a series of mapping functions have been developed. Using the contributing areas of HRUs within grid cells, and vice versa, as weights, various parameters are mapped from SWAT HRUs to the MODFLOW grid and back (illustrated in Figure 3). This interaction between HRUs and grid cells also creates a general format that can be utilized for SWAT to any finite difference model utilizing grid-based schemes.

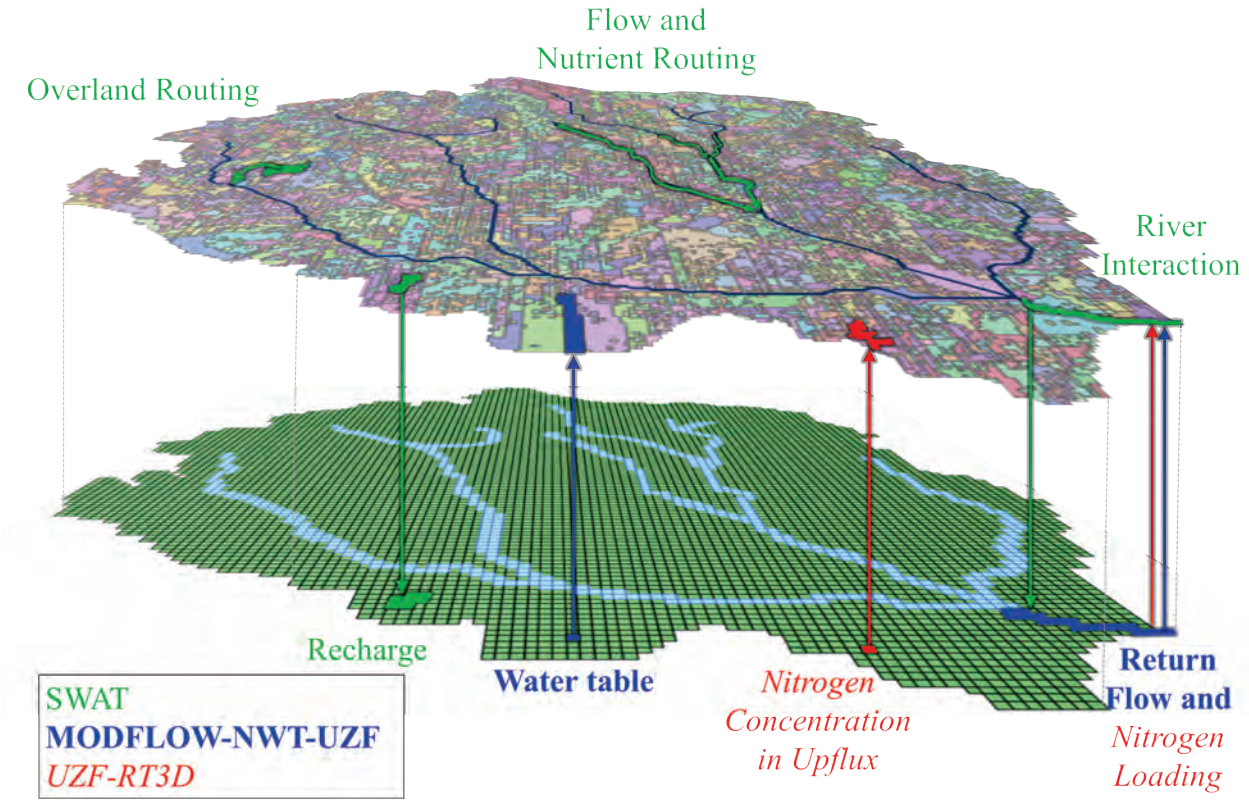

Figure 3: Spatial interaction between SWAT (green text), MODFLOW-NWT-UZF (bolded blue text), and UZF-RT3D (italicized red text)

Application to Upper Klamath Basin

The SWAT-MODFLOW-RT3D model will be demonstrated through an application to the Upper Klamath Basin, located in northern California and southern Oregon (Figure 4). The Upper Klamath Basin has water quantity and quality problems due to significant stream flow contribution from groundwater and specifically natural springs (Gannett et al., 2010). The MODFLOW model developed by Gannett et al (2012) illustrates the locations and complexity of the various agricultural drains, wells, and reservoir extents within the Upper Klamath Basin (Figure 5). It is due to this complex agricultural water drainage and well pumping combined with the porous volcanic nature of the geology of the Upper Klamath Basin which makes it particularly difficult to simulate using available surface-only or subsurface-only watershed models.

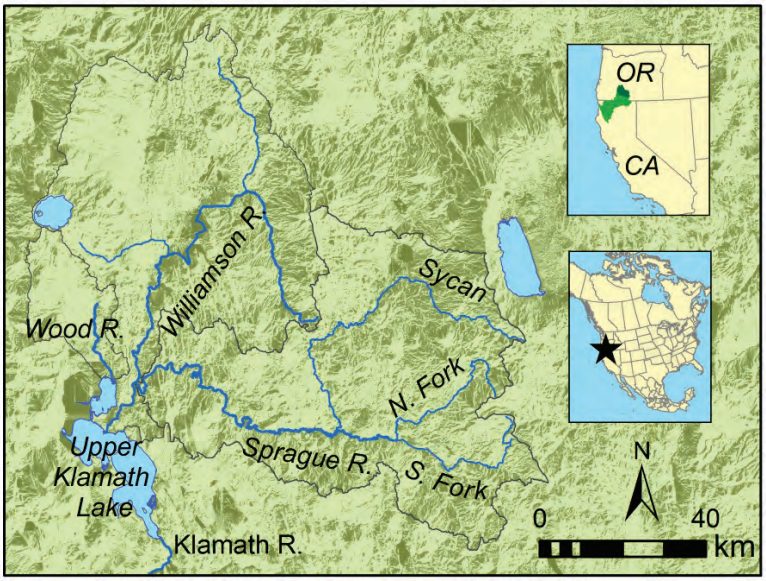

Figure 4: Upper Klamath Basin, in northern California and southern Oregon

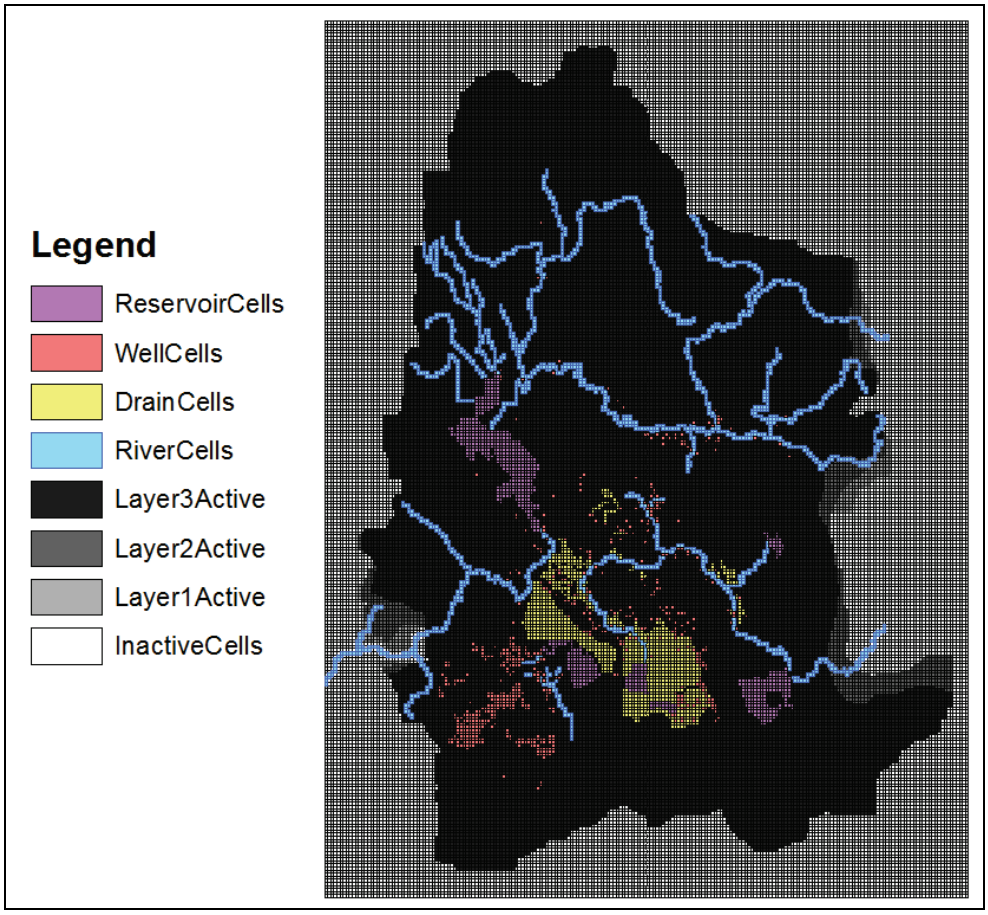

Figure 5: Upper Klamath MODFLOW Model Features

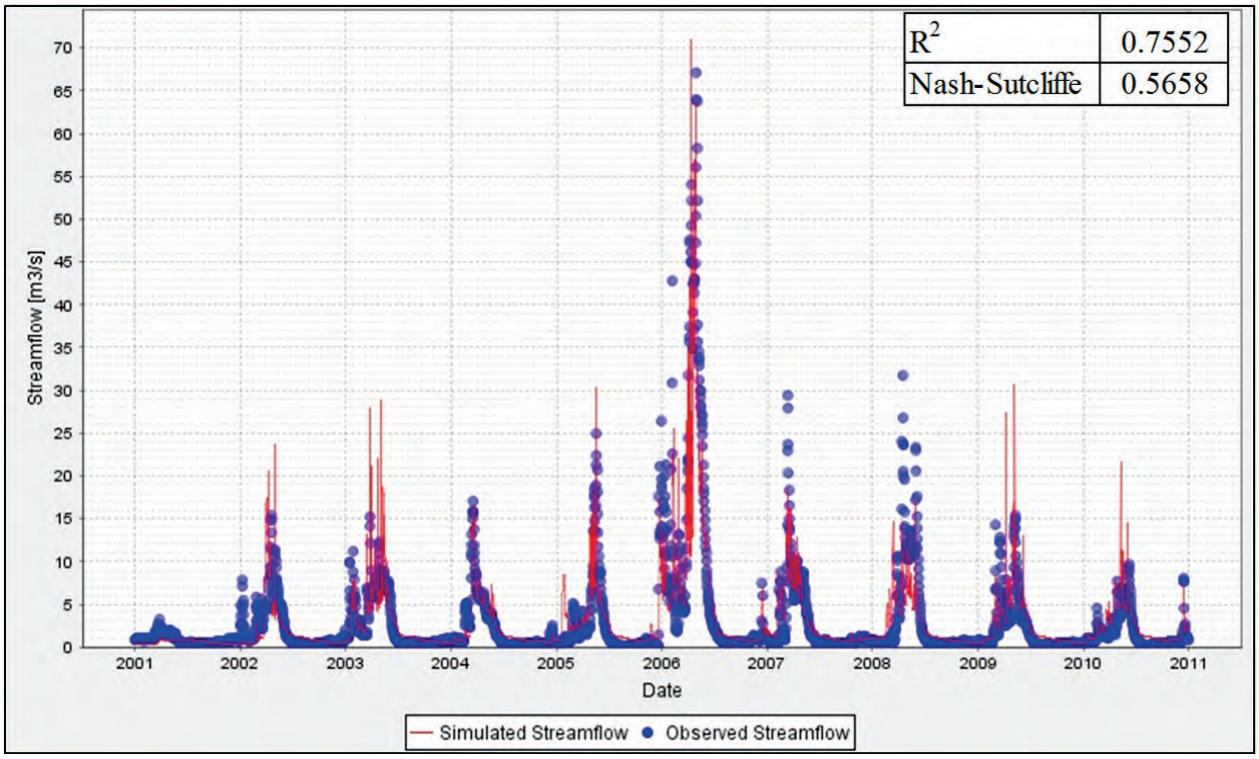

Figure 6: Sycan River, Post-Calibration Results

Preliminary results (SWAT only) on the Sprague River in the Upper Klamath Basin show good results for surface-runoff driven tributaries (minimal baseflow levels) like the Sycan River (Figure 6). These post-calibration results have high correlation coefficients to observed data. Conversely, rivers in this system which are groundwater driven, such as the North Fork of the Sprague River (as seen by its elevated baseflow level), show poor results before combined manual and auto-calibration using dynamically dimensioned search algorithms (Figure 7). While, post-calibration results from the SWAT simulations still do not accurately reflect the significant baseflow contribution to stream discharge (Figure 8). The low R^2 value and the low Nash-Sutcliffe coefficient both indicate that the model does not accurately reflect observed data. Closer observation of Figure 7 reveals an increase in baseflow on an annual basis, which is not feasible or represented in the observed data.

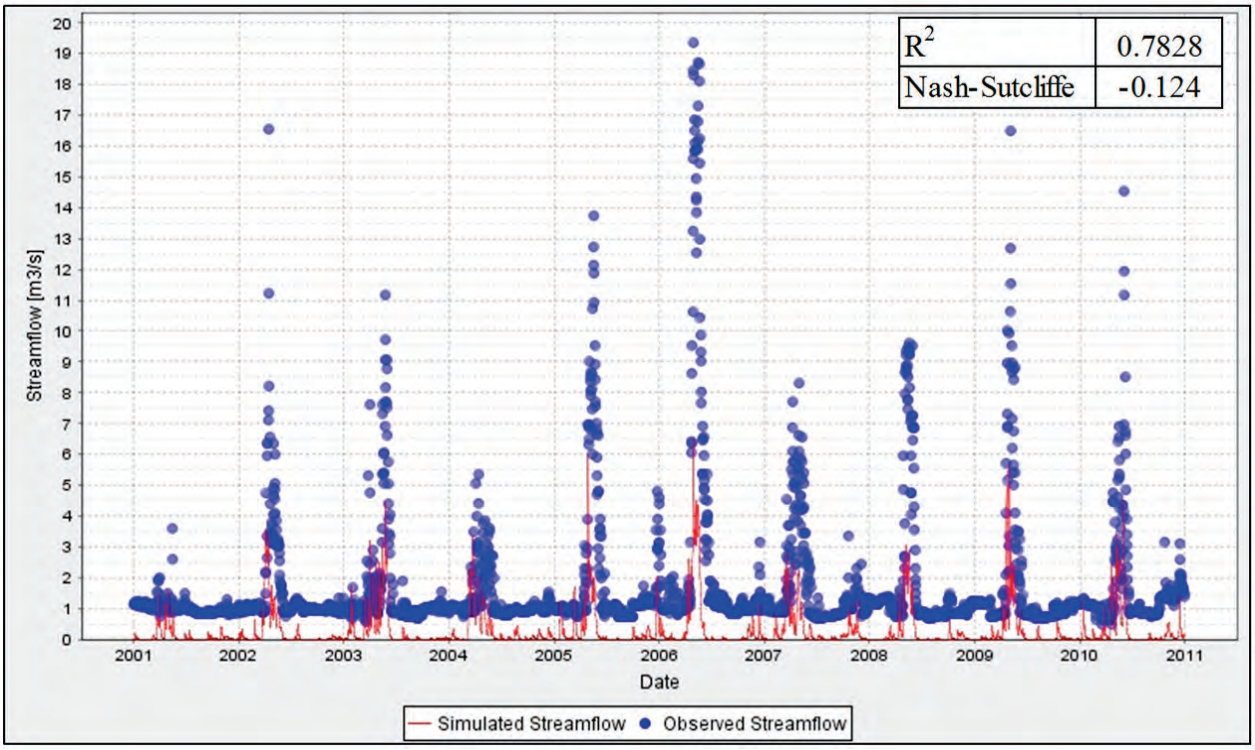

Figure 7: N. Fork Sprague River, Pre-Calibration

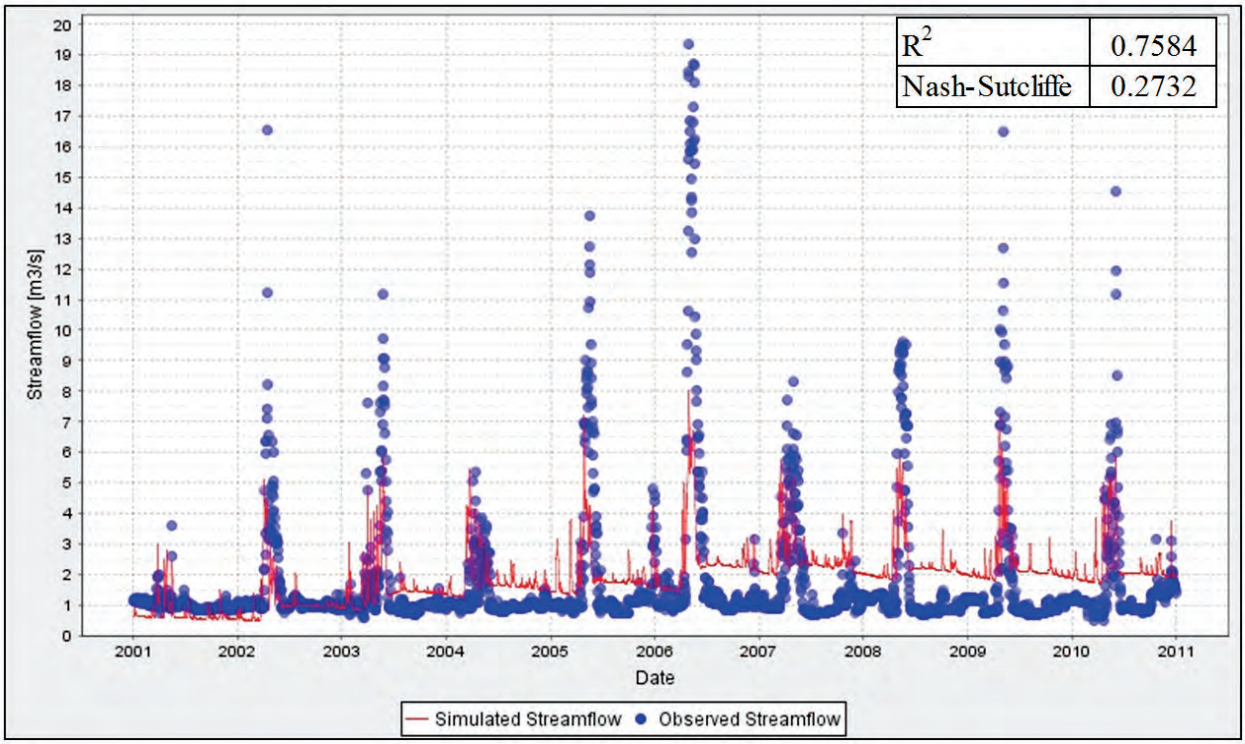

Figure 8: N. Fork Sprague River, Post-Calibration

Conclusion

Retaining the strengths of each of the respective models, namely land surface processes in SWAT, variably saturated groundwater computation in MODFLOW-NWT-UZF, and reactive solute transport within variably saturated groundwater systems in UZF-RT3D, a comprehensive hydrologic model is accomplished. A comprehensive model, like SWAT-MODFLOW-RT3D, will enable accurate simulations of stream flow and nutrient mass loading in watersheds for which stream flow can be either surface water driven or groundwater driven due to a complex combination of surface water allocations, historic agriculture and diversions, and geologic features. From SWAT, surface water infiltration is passed to MODFLOW-NWT-UZF based on the contributing areas of the HRUs to the groundwater grid. Return flows and mass loadings are then calculated and passed back to SWAT. The comprehensive model includes the subsurface flow and reactive processes, while still retaining the land surface computations and BMP assessments of SWAT. The need for such a model is highlighted by the North Fork of the Sprague River in the Upper Klamath River basin, where stream flow heavily influenced by groundwater hydrology. The Upper Klamath River basin will be the subject of testing the model to determine the benefit gained by coupling SWAT with a physically-based distributed groundwater flow and reactive transport model.

Acknowledgements
This study is funded by the U.S. Department of Agriculture-National Institute of Food and Agriculture (NIFA) Grant Number 2012-67003-19904.

References

Arnold, J.G., Srinivasan, R., Muttiah, R.S., Williams, J.R. 1998. Large area hydrologic modeling and assessment Part I Model development. *Journal of American Water Resources Association. (JAWRA),* 34(1): 73-89.

Arnold, J.G., Allen, P.M., Volk, M., Williams, J.R., Bosch, D.D. 2010. Assessment of Different Representations of Spatial Variability on SWAT Model Performance. SWAT. 2010 American Society of Agricultural and Biological Engineers. 53(s): 1433-1443.

Bailey, R.T., Morway, E.D., Niswonger, R., and T.K. Gates. 2013. Modeling variably saturated multispecies reactive groundwater solute transport with MODFLOW-UZF and RT3D. *Groundwater*, 51(5), 752-761.

Clement, T.P. 1997. RT3D – A modular computer code for simulating reactive multi-species transport in 3-dimensional groundwater aquifer. Draft report. PNNL-SA-28967. Richland, Washington: PNNL.

Gannett, M.W., Lite, K.E., Jr., La Marche, J.L., Fisher, B.J., and D.J. Polette. 2010. Groundwater hydrology of the Upper Klamath Basin, Oregon and California. U.S. Geological Survey Scientific Investigations Report 2007-5050, Version 1.1.

Gannett, M.W., B.J. Wagner, and K.E. Lite, Jr. 2012. Groundwater simulation and management models for the Upper Klamath Basin, Oregon and California. U.S. Geological Survey Scientific Investigations Report 2012-5062.

Harbaugh, A.W., Banta, E.R., Hill, M.C., and M.G. McDonald. 2000. MODFLOW-2000, The U.S. Geological Survey modular ground-water model – User guide to modularization concepts and the ground-water flow process. USGS Open-File Report: 2000-92.

Kim, N.W., Chung, I.M., Won, Y.S., and J.G. Arnold. 2008. Development and application of the integrated SWAT-MODFLOW model. *Journal of Hydrology*, 356:1-16.

Niswonger, R.G., Prudic, D.E., and R.S. Regan. 2006. Documentation of the unsaturated-zone flow (UZF1) package for modeling unsaturated flow between the land surface and the water table with MODFLOW-2005, USGS Techniques and Methods 6-A19.

Niswonger, R.G., Panday, S., and M. Ibaraki. 2011. MODFLOW-NWT, A Newton formulation for MODFLOW-2005: USGS Survey Techniques and Methods 6–A37.

Sophocleous, M., and S.P. Perkins. 2000. Methodology and application of combined watershed and ground-water models in Kansas. *Journal of Hydrology*, 236:185-201.

Spatial representation of evapotranspiration in the Mara basin: results derived from the SWAT model and remote sensing products

Tadesse Alemayehu*

Vrije Universiteit Brussel, Department of Hydrology and Hydraulic Engineering, Pleinlaan 2, 1050

tabiew@vub.ac.be

Ann van Griensven

Fidelis Kilonz

Vrije Universiteit Brussel, Department of Hydrology and Hydraulic Engineering, Pleinlaan 2, 1050

UNESCO-IHE Institute for Water Education, Department of Water Science and Engineering, Delft, the Netherlands

Willy Bauwens

Vrije Universiteit Brussel, Department of Hydrology and Hydraulic Engineering, Pleinlaan 2, 1050

Abstract

Next to precipitation, evapotranspiration (ET) is a crucial as well as dominant component in a river basin water balance. Hence, it is vital to explore the spatial variability of ET across different cover types in a basin. However, the measurement of ET is often described as time and labor consuming and thus, hydrological models are considered as an alternative. Physically based and process-oriented models simulate a series of physical and plant physiological processes controlling ET. Therefore, we applied the Soil and Water Assessment Tool (SWAT, version 2012) to simulate hydrological process in the Upper Mara basin. Firstly, the SWAT model was built and then calibrated and validated in this data scarce tropical watershed for the period of 1980-1992. Secondly, the SWAT estimated ET fluxes were analyzed at various spatial scales. In addition, the ET spatial variability was evaluated using remote sensing products from MODerate Resolution Imaging Spectroradiometer (MODIS). As noted in the analysis, the SWAT model often did not give realistic spatial patterns of ET at the HRU level that is consistent with the landcover types. In contrast, the results from MODIS ET showed spatially consistent ET variability which reflected the landscape heterogeneity. In conclusion, the reasonable SWAT model's skills in simulating discharges with calibrated parameters, might not guarantee similar performance for other water balance components such as ET. Thus, the use of spatially distributed ET estimates from remote sensing data during calibration and validation processes

could potentially improve the prediction abilities of hydrological models in the data scarce Upper Mara basin.

Keywords*:* Mara basin, SWAT, Evapotranspiration, MODIS, spatial variabili

Introduction

Evapotranspiration (ET) is a crucial as well as dominant component in a river basin water balance, and it accounts for 60% of the outgoing flux from the input precipitation in a catchment (Brutsaert, 1986). Information on the amount of ET flux over a range of spatial and temporal scales for a specific locality is an essential component in the design, development and monitoring of hydrological, agricultural and environmental systems (Senay et al., 2011).

One of the classic approaches to compute ET in a basin is ultimately using the water balance concept (Droogers, 2000; Senay et al., 2011). Most often precipitation and runoff data can be readily obtained from hydrometeorological stations. Therefore, a calibrated model forced by these dataset could be used to estimate the ET fluxes from the system and the measured primary hydrology elements helps to logically constrain the ET estimates (Gao and Liu, 2012). By the same token, the physically based Soil and Water Assessment Tool version 2012 version 2012 (SWAT) simulator was applied to compute the ET flux in the Mara basin. Intuitively, the accuracy of ET amount estimates of each HRU and their aggregated values for the whole watershed simulated by SWAT would be reliable because this simulator has a strong physical basis which is essential to represent hydrological processes realistically. Furthermore, Liu et al.(2003) outlined the advantages of process based models when used for ET mapping: (1) each component of ET that make up the total ET is taken into consideration and explicitly quantified; (2) the strong correlation between vegetation and ET are accounted for using spatially distributed vegetation index (i.e. leaf area index) and vegetation functional parameters such as stomatal conductance; (3) the interaction between soil moisture and ET can be explicitly described, among others.

However, most often distributed hydrological models are calibrated against the observed discharge time series from one or more gauging stations. Apparently, these models show reasonable skills to simulate discharges based on the calibrated parameters; however, this does not guaranty a good performance on the simulated ET (Muthuwatta et al., 2009). A river basin surface characteristics, by its very nature, varies spatially and their combination with a large number of model parameters inhabits the identification of one set of parameters describing the natural system (Immerzeel and Droogers, 2008). Consequently, more than one parameter combination could provide the same result. The problem of equifinality has been widely discussed in literatures (Seibert and McDonnell, 2002; Beven, 2006; Immerzeel and Droogers, 2008). Hence, the question if our models can represent the hydrological processes such as the ET flux in a proper way so that they are able to do what they are aimed for remains as a key issue.

In the last few decades satellite data have been ideally suited for deriving spatially continuous fields of ET using energy balance techniques (Bastiaanssen et al., 2002; Allen et al., 2011). Mu et al. (2011) computed ET flux globally using remote sensing data for land surface characteristics. This global MODIS data have been evaluated for various climatic conditions and locations (Mu et al., 2011; Kim et al., 2012) and the studies concluded the importance of this ET product for hydrological applications. Owing to this, the ET for the study area were mapped using data from this global dataset.

In this study, we modeled the data scarce Upper Mara river basin using SWAT simulator (Arnold et al., 1998). Subsequently, the model was calibrated and validated using Sequential Uncertainty Fitting (SUFI-2) (Abbaspour et al., 2004). Therefore, the aim of this paper is to analyze the spatial variability of the simulated ET fluxes derived from two sources: from the calibrated semi-distributed SWAT model and MODIS 16 ET data from 2000 to 2010.

Description of the Upper Mara basin

The Mara River basin is shared between Kenya and Tanzania and has an area of about 13,750 km^2. The Upper Mara River basin, which forms the recharge area for the Mara River basin, covers an area of about 3,000 km^2 (Fig. 1). This part of the basin is drained by two main rivers originating from the Mau forest-the Amala and the Nyangores, which merge at the midsection to form the Mara River. The rainfall distribution in this area is by bimodal ranging from 700 mm in the lower areas to 1800 mm in the mid and upper sections (Kilonzo et al., 2012). Furthermore, the basin is characterized by mountainous topography ranging from 1563 to 3063 meters above the sea level (Fig. 1).

Kilonzo et al. (2010) mentioned that the main socio-economic activities (which define land use types) are determined by the hydro-climatic and ecological zonations with pasture and herding restricted to the lowlands, commercial mechanized agriculture (mostly large scale maize and wheat cultivation) in the floodplains, subsistence maize production in the midsection, tea and forestry in the high rainfall areas and vegetable production in the upper sections. The main soil types in the Upper Mara basin include loams and clay loams.

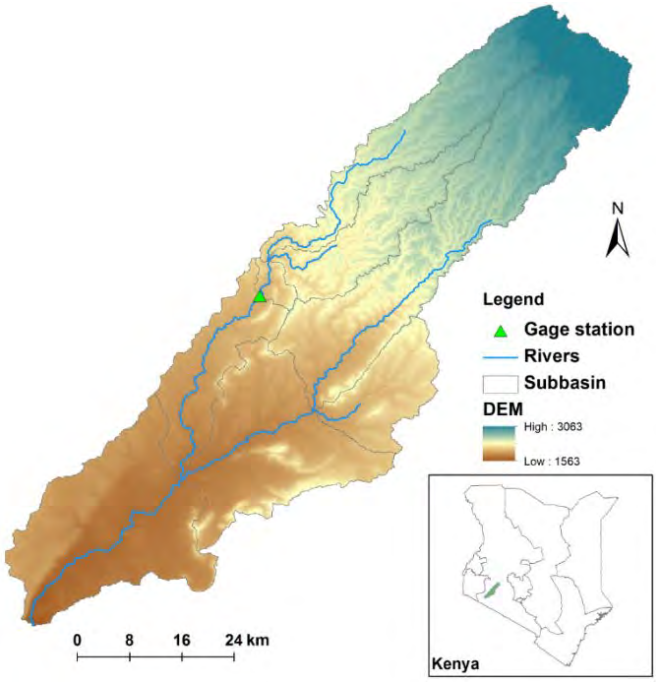

Fig. 1 Map of the Upper Mara basin with an inset map of Kenya

Methodology

Firstly, the hydrological processes in the study area were modeled using the SWAT (Arnold et al., 1998) simulator, and subsequently the preliminary results of the simulated ET estimates were analyzed at different spatial scales. Furthermore, the MODIS ET products were adopted to investigate the spatial variability of ET across various land use types. The descriptions of each method are explained briefly in the following sections.

SWAT model

The SWAT simulator (Arnold et al., 1998) is a semi-distributed physically-based hydrological model that simulates flow and nutrient transport and transformations at river basin or catchment scale. It uses a GIS based interface that allows to use topography maps (DEM), landuse maps and soil maps and hence create sub-basins which are further subdivided in hydrological response units (HRUs). HRUs are areas with similar land use, soil and slope classes in the sub-basin. For each HRU, hydrological, soil, crop and chemical processes are computed on a daily time step to provide the inputs into the river network. A very interesting feature of SWAT is that it enables to compute crop growth processes and land use management practices and their effects on hydrology and water balance (Neitsch et al., 2011).

The Penman–Monteith method is used to calculate daily reference evapotranspiration (ET_{ref}) and eventually used to simulate ET, in which evaporation from the soil surface and transpiration from vegetation are simulated separately. Soil water evaporation is estimated as an exponential function of soil depth and water content, based on ET_{ref} and a soil cover index calculated by aboveground biomass, confined to the upper limit of 80% of plant available water on a given day.

In this study, we applied five procedures for SWAT application to the study area: i) climatic and spatial data preparation, ii) watershed delineation and discretization, iii) HRU definition, iv) calibration and validation, and v) output analysis. The Upper Mara River basin was divided into eight subbasins and 144 HRUs in the SWAT model.

SWAT inputs

Daily climatic data such as rainfall, temperature, humidity and wind speed are required by the SWAT model. Daily rainfall measurements from Olegurone, Bomet Water Supply and Tenwek Mission were used to force the SWAT model. Since there is no meteorological station in the catchment which measures maximum and minimum temperature, wind speed and relative humidity, a weather generator prepared for this region by Kilonzo et al. (2012) were used. Besides, the missing data from the aforementioned rainfall stations were filled using the weather generator.

SWAT requires three spatial dataset to characterize a watershed, namely soil type, land cover/use and digital elevation model (DEM). Obviously, these groups of data determine the factors that shape the various processes in a watershed, such as surface runoff, recharge and evapotranspiration and among others. The soil classification data was extracted from the 1:2 000

000 Soil Terrain Database of East Africa (SOTER) and the dominant soil class in the basin is composed of 42% clay, 42% silt, and 16% sand. The land use/cover classifications for 1986 and 2006 for the Upper Mara basin were obtained from Kilonzo et al. (2010). This study used the 30 meters resolution Landsat Thematic Mapper images acquired for year 1986 and 2006.

Model calibration and validation

The calibration and validation of the SWAT model was carried out using the observed daily discharge data of the Nyangores River at Bomet Water Supply gauging station from 1980 to 1992. The calibration and validation were carried out using the data from 1985 - 1992, and 1980 – 1982, respectively. The first three years from the calibration period were used to warm up the model.

SUFI-2 (Abbaspour et al., 2004) auto-calibration algorithm in SWAT-CUP 2012 package was employed to calibrate the model. In SUFI-2, parameter uncertainty accounts for all sources of uncertainties such as uncertainty in forcing rainfall data, parameters, and observed flow. The performance of the model was then evaluated using the popular Nash-Sutcliffe Efficiency (NSE) and the coefficient of determination (R^2), and among others.

Remote sensing products

Global MODIS evapotranspiration product (MOD16A2), hereafter MODIS ET, provides ET for vegetated surface at a regular 1 km^2 spatial resolution (http://www.ntsg.umt.edu/project/mod16). This ET product is computed based on the Penman–Monteith logic (Eq.1) using MODIS global data (MODIS land cover and FPAR/LAI data) and global surface meteorology data from the Global Modeling and Assimilation Office (Mu et al., 2011).

$$\lambda E = \frac{S \times A \times \rho \times C_p \times (e_{sat} - e)/r_a}{s + \gamma \times (1 + {}^{r_s}/_{r_a})}$$

where λE is the latent heat flux and λ is the latent heat of evaporation; s=d(e_{sat})/dT, the slope of the curve relating saturated water vapor pressure (e_{sat}) to temperature; A is available energy partitioned between sensible heat, latent heat and soil heat fluxes on land surface; ρ is air density; C_p is the specific heat capacity of air; and r_a is the aerodynamic resistance.

The ET computation in this product accounts for the ET fluxes from transpiration and interception by vegetation and moist soil during day and night time (Mu et al., 2011). This product has been evaluated across different climates and locations using observed ET measurements from flux towers (Mu et al., 2011; Kim et al., 2012) and the studies concluded the potential use of this global data for scientific applications. In this study, we used the MODIS ET at the annual scale to investigate the spatial variability of ET across the Upper Mara basin.

Results and Discussion

Given the scarcity of hydrometeorological data in the study area, the results observed from the calibrated and validated SWAT model are encouraging to carry out further analysis from the simulation outputs. However, while interpreting the results, the uncertainty associated with the input data should be taken to an account. As observed from the MODIS ET, ET varies spatially in the Upper Mara basin within various landcover types. In the next sections, results from the SWAT model and MODIS ET products are presented back-to-back.

Calibration and Validation Results

On the basis of the three rainfall stations used in this study, the basin wide average annual rainfall from 1988-1992 as computed in the SWAT model was about 1360 mm. This figure is comparable with the range of areal rainfall estimates from previous studies by NBI (2008) and Kilonzo et al. (2012). The visual comparison of the simulated and observed discharges at Bomet Water Supply gaging station showed a fair fitness for the calibration period (Fig. 2). In addition, as the statistical evaluation criteria showed, the calibrated SWAT model performed satisfactorily with NSE and R^2 of 0.57 and 0.58, respectively for daily flows. The performance of the model also further improved when compared at a monthly time step. Apparently, one of the likely reasons for lower performance of the model could be attributed to the low density of rainfall stations used in the model.

The fair representation of the hydrological processes in the SWAT model for the Upper Mara River based on the range of parameters set found during the calibration process was conformed by implementing the validation procedure. As shown in Fig. 3, the SWAT model performs fairly for the validation period as well. The NSE and R^2 for this period were 0.61 and 0.72, respectively.

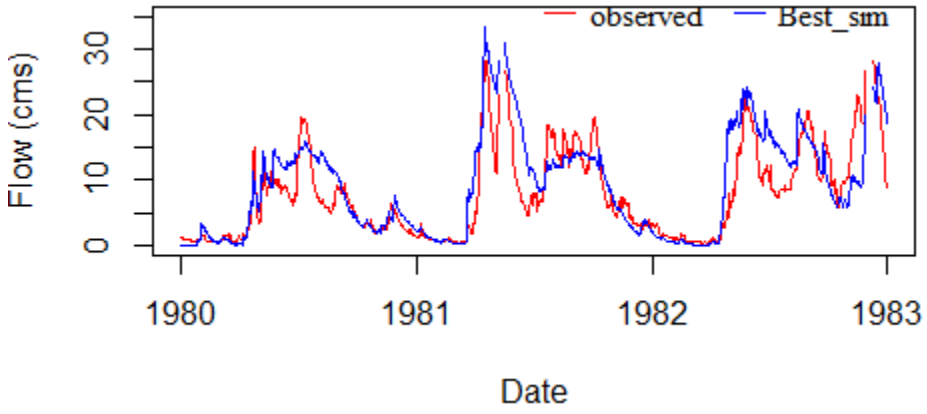

Fig. 2 Satisfactory comparison of observed and simulated flow during the calibration period

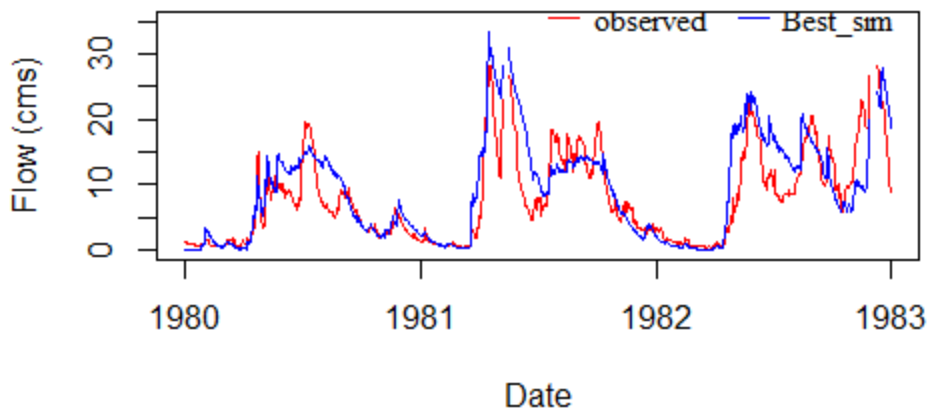

Fig. 3 Satisfactory comparison of observed and simulated flow during the validation period

SWAT simulated evapotranspiration

Since the performance of the SWAT model for Upper Mara basin was fairly good, it was worthy to analyse the model's simulation on the largest outgoing flux (i.e. ET) of the water balance. Yet, we used average mean annual values for the analysis because the goal of the study was to investigate the spatial variability. As noted in the water balance analysis from 1988 to 1992, ET accounts for the loss of about 60% of the mean annual precipitation in the basin. Besides, the SWAT model estimated about 814 mm mean annual ET over the area of interest.

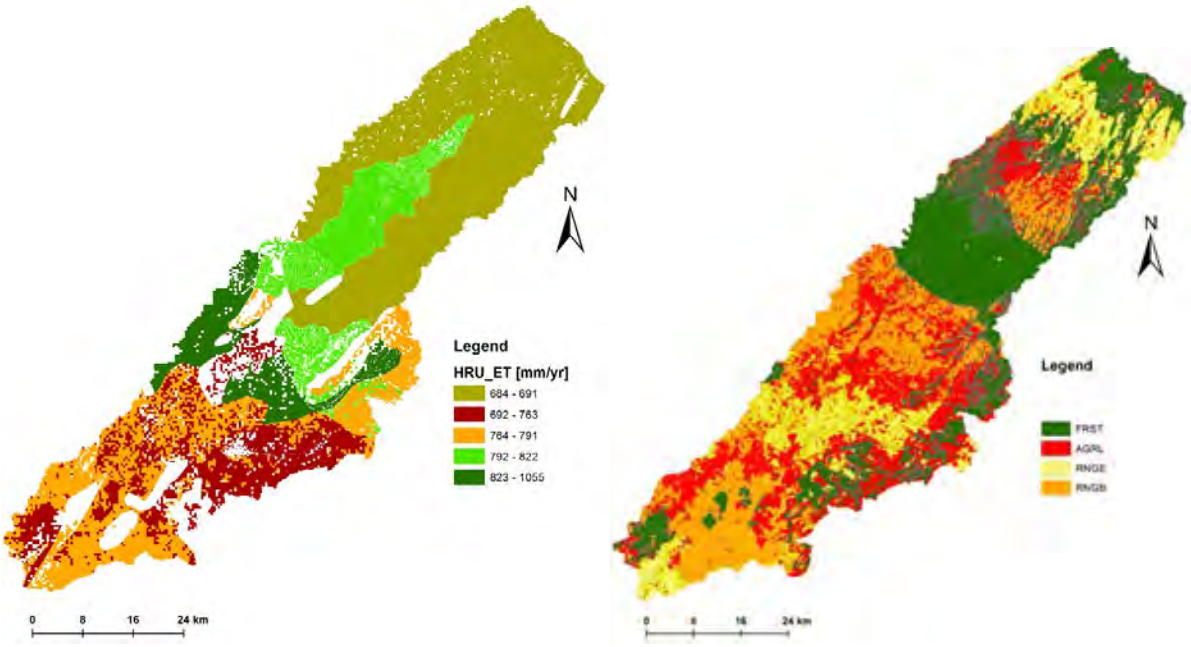

Fig. 4 Spatial variability of SWAT simulated mean annual ET at HRUs level (left) and landcover types in 1986 (Kilonzo et al. 2010) (right)

The land surface physical characteristics such as vegetation cover, soil, elevation and among others vary spatially in the Upper Mara basin. Consequently, it is worth to investigate the simulated mean annual ET at the HRU level. As depicted in Fig. 4, the mean annual ET varies at the HRU level and ranges from 684-1055 mm yr^{-1}. Despite the domination of forest cover in the upstearm part of the basin, the HRUs in this part observed to have lower ET fluxes. In contrast, the highest mean annual ET fluxes were observed in the midsection of the basin where agricultural landuse type is common.

We analyzed the SWAT simulated ET per landuse class in the study area. Areas covered by range land with bush have a slightly higher mean annual ET flux than areas covered by forest (Table 1). On the other hand, agricultural landuse type revealed the lowest ET flux.

Table 1 Mean annual ET flux for different land cover types in the Upper Mara basin

Landuse type	Area (km^2)	% of Area	ET [mm yr^{-1}]
FRST	988	33.5	820
AGRL	818	27.7	797
RNGE	526	17.8	812
RNGB	612	20.7	832

In general, as it turned out from the results, the simulated ET spatial variability showed inconsistencies compared to the landcover types at the HRU level. Nevertheless, at a coarser spatial scale (i.e. per landuse class) the estimated ET revealed a better consistency, meaning the vegetated areas tends to have a higher ET than agricultural areas. However, the differences in the computed ET among the landuse types were not significant. Theoretically the LAI and canopy storage (CANMX) are the two important vegetated surface characteristics needed in ET flux computations in SWAT. As would be expected, in the calibrated SWAT model the LAI and CANMX values are larger for forested areas and smaller for agricultural area. However, we noted discrepancies at the estimated ET at the HRU level. One of the likely reasons is the less sensitivity of the model to these parameters. We observed from the global sensitivity analysis in SUFI-2 that soil water holding capacity (sol_awc), the curve number (CN2) and soil evaporation compensation factor (ESCO) were the top sensitive parameters.

Evapotranspiration from MODIS

Fig. 5 presents the mean of annual ET from 2000 to 2010 together with the land cover classifications for year 2006. The mean annual ET at 1 km pixel resolution showed significant spatial variability and the averaged ET over the entire basin was about 1103 mm yr^{-1}. The downstream part of the basin had a lower ET flux which is covered by agriculture and range land mixed with grasses. In the middle section of the basin, where the Mau forest complex located, a higher ET values were observed. In this part of the basin the mean annual ET fluxes reached up to 1500 mm in some pixels. Even though there is no available in situ observed ET flux in the

study area, compared to long term averaged rainfall in the upper of the basin (i.e. 1400 mm yr^{-1}) (NBI, 2008) the MODIS ET estimate seems to some extent overestimated.

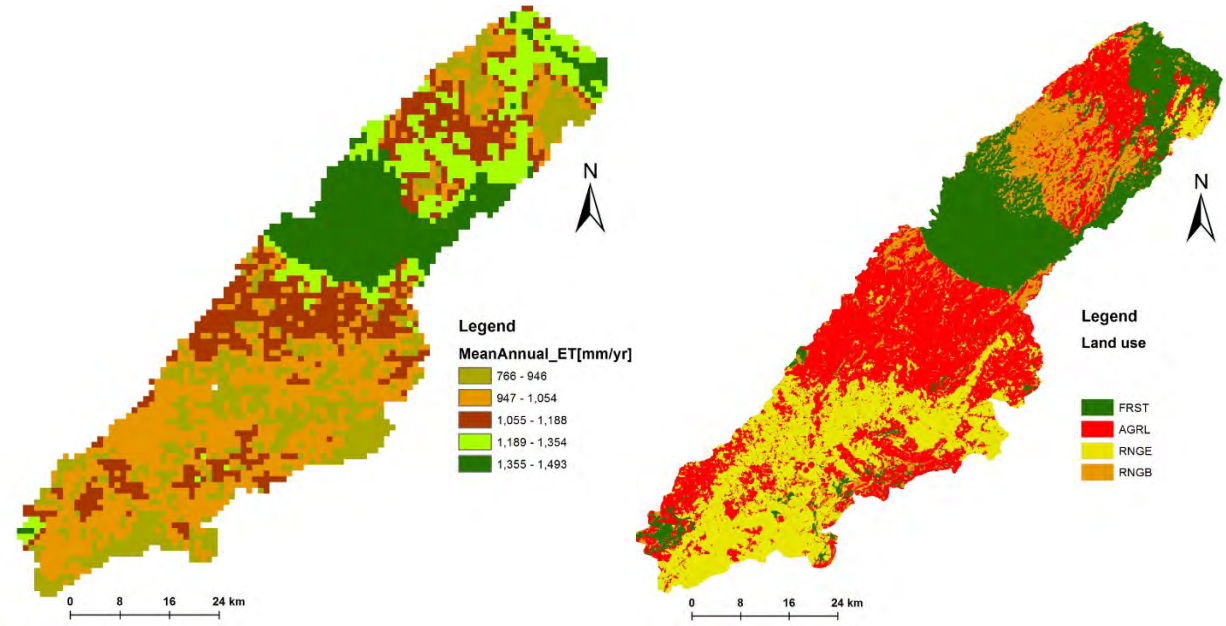

Fig. 5 Spatial variability of mean annual ET for Upper Mara basin (left) and landcover class for 2006 (Kilonzo et al. 2010) (right).

As depicted in Fig. 6, part of the basin covered by forest showed a higher mean annual ET while areas covered by grasses and agricultural crops revealed relatively a lower mean annual ET flux. We used the standard deviation of the mean annual values to further scrutinize the ET spatial variability within each landcover type. As a result, we observed a substantial ET variability within each cover types (Fig. 6). The maximum variability was in forest cover (185 mm) whereas the lower variation was noted in range land mixed with grass cover (92 mm).

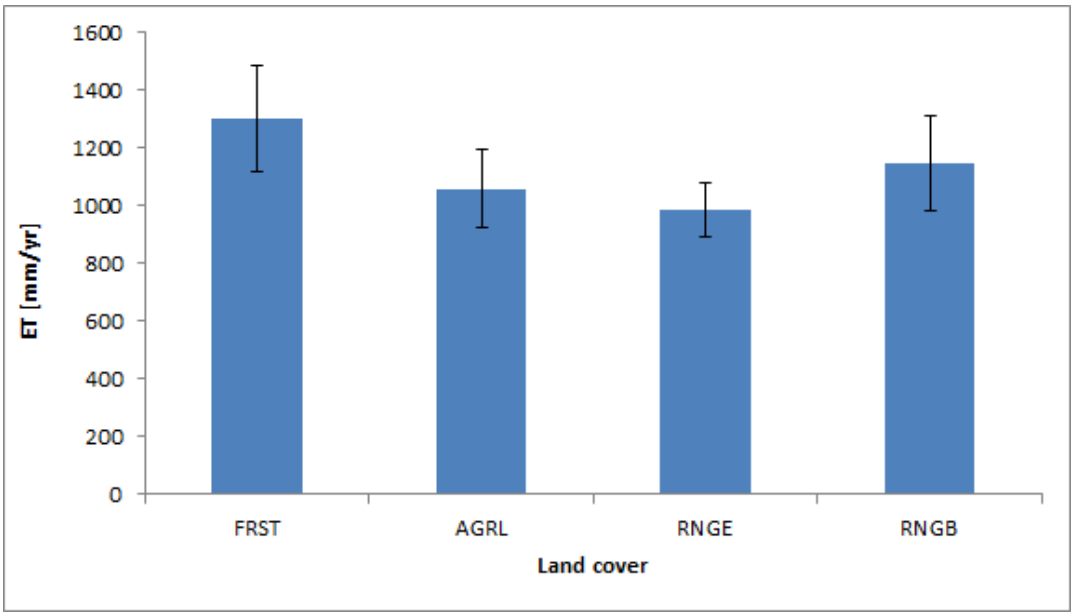

Fig. 6 The average annual ET per landcover class for Upper Mara basin. The standard deviation is represented by the solid vertical lines.

Overall, the spatial variability of ET from MODIS reflected well the heterogeneity in the Upper Mara basin. In addition, the ET estimates are consistent with the land cover type from year 2006. At this point it should be noted that the spectral signatures used for the land cover classification and MODIS ET are from independent sensors. The ET mapping using MODIS products from remote sensing techniques might be less reliable at a finer resolution; however, it provides consistent estimates for watershed average response (McCabe and Wood, 2006)

Conclusion

In this study, we analyzed the spatial variability of ET flux over the Upper Mara basin using mean annual ET from two sources: i) SWAT simulated ET, and ii) MODIS ET product. Given the data scarcity in the region and its consequent uncertainty on the model simulations, we used mean annual average values to assess the spatial variability of ET. Therefore, the following preliminary conclusions were drawn from the study.

The SWAT simulated ET at the HRU level was inconsistent with the landcover type used as the model's input. In addition, the differences in mean annual ET flux per landuse class were insignificant. On the other hand, the ET flux from remote sensing captured well the variation in surface vegetation cover, yet the amount of ET fluxes in some pixels deemed to be overestimated compared to the long term mean annual rainfall. Thus, apply the remote sensing ET during model calibration and validation processes could benefit hydrological modeling efforts in a data scarce river basin.

References

Abbaspour, K.C., Johnson, C. a., Van Genuchten, M.T., 2004. Estimating Uncertain Flow and Transport Parameters Using a Sequential Uncertainty Fitting Procedure. Vadose Zone Journal 3 (4), 1340–1352.

Allen, R., Irmak, A., Trezza, R., Hendrickx, J.M.H., Bastiaanssen, W., Kjaersgaard, J., 2011. Satellite-based ET estimation in agriculture using SEBAL and METRIC 4027, 4011–4027.

Arnold, J.G., Srinivasan, R., Muttiah, R.S., Williams, J.R., 1998. Large area hydrologic modeling and assessment part i: model development. Journal of the American Water Resources Association 34 (1), 73–89.

Bastiaanssen, W.G.M., Ahmad, M.-D., Chemin, Y., 2002. Satellite surveillance of evaporative depletion across the Indus Basin. Water Resources Research 38 (12), 1273.

Beven, K., 2006. A manifesto for the equifinality thesis. Journal of Hydrology 320 (1-2), 18–36.

Brutsaert, W., 1986. Catchment-scale evaporation and the atmospheric boundary layer. Water Resources Research 22 (9S), 39S–45S.

Droogers, P., 2000. Estimating actual evapotranspiration using a detailed agro-hydrological model. Journal of Hydrology 229 (1-2), 50–58.

Gao, Y.C., Liu, M.F., 2012. Evaluation of high-resolution satellite precipitation products using rain gauge observations over the Tibetan Plateau. Hydrology and Earth System Sciences Discussions 9 (8), 9503–9532.

Immerzeel, W.W., Droogers, P., 2008. Calibration of a distributed hydrological model based on satellite evapotranspiration. Journal of Hydrology 349 (3-4), 411–424.

Kilonzo, F., Obando, J., A, V.G., Bauwens, W., 2012. Improving model performance in poorly gauged catchments. Centre International Capacity Development (CICD) Series (1868-8578), 1–14.

Kim, H.W., Hwang, K., Mu, Q., Lee, S.O., Choi, M., 2012. Validation of MODIS 16 Global Terrestrial Evapotranspiration Products in Various Climates and Land Cover Types in Asia 16, 229–238.

Liu, J., Chen, J.M., Cihlar, J., 2003. Mapping evapotranspiration based on remote sensing: An application to Canada's landmass. Water Resources Research 39 (7).

McCabe, M.F., Wood, E.F., 2006. Scale influences on the remote estimation of evapotranspiration using multiple satellite sensors. Remote Sensing of Environment 105 (4), 271–285.

Mu, Q., Zhao, M., Running, S.W., 2011. Improvements to a MODIS global terrestrial evapotranspiration algorithm. Remote Sensing of Environment 115 (8), 1781–1800.

Muthuwatta, L.A.L.P., Booij, M.J., Rientjes, T.O.M.H.M., 2009. Calibration of a semi-distributed hydrological model using discharge and remote sensing data. In: New Approaches to Hydrological Prediction in Data-sparse Regions.

NBI, 2008. Mara River Basin Transboundary Integrated Water Resources Management and Development Project Mara River Basin Monograph Final Report Water Resources and Energy Management (WREM).

Neitsch, S.L., Arnold, J.G., Kiniry, J.R., Williams, J.R., 2011. Soil & Water Assessment Tool Theoretical Documentation Version 2009.

Seibert, J., McDonnell, J.J., 2002. On the dialog between experimentalist and modeler in catchment hydrology: Use of soft data for multicriteria model calibration. Water Resources Research 38 (11), 23–1–23–14.

Senay, G.B., Leake, S., Nagler, P.L., Artan, G., Dickinson, J., Cordova, J.T., Glenn, E.P., 2011. Estimating basin scale evapotranspiration (ET) by water balance and remote sensing methods. Hydrological Processes 25 (26), 4037–4049.

Predicting the Impacts of Agricultural Management Practices on Water, Sediments and Phosphorus Loads

N.B. Bonumá
Department of Sanitary and Environmental Engineering, Federal University of Santa Catarina, Brazil, nadia.bonuma@ufsc.br

P.R. Zanin
MS.student, Environmental Engineering Graduate Program, Federal University of Santa Catarina, Brazil

J.P.G. Minella
Department of Soils, Federal University of Santa Maria, Brazil

J.M. Reichert
Department of Soils, Federal University of Santa Maria, Brazil

Abstract

Shallow soils of Southern Brazil under tobacco cropping are generally potential for degradation environmental contamination, because they are based on inadequate agricultural operations and excessive fertilizer rates application. Changes in management practices may affect water balance, sediment and nutrient loads of agricultural areas. This paper evaluates by a modeling approach the impact of farming practices on runoff, sediment and phosphorus loads at Arroio Lino watershed, located in Southern Brazil. This watershed is cropped with tobacco under conventional management system and high fertilizer rates application. The SWAT model was used to generate a 30-year simulation period. Three scenarios of management practices were tested: conventional tillage (CT), minimum tillage (MT) and no-tillage cultivation (NT) with reduction of 50% of fertilizer rate application. Surface flow decreased when decreasing tillage intensity, but the baseflow increased following the same order of magnitude. Hence, the percentage deviation in the water yield is only 6%. The highest decrease in sediment yield was between conventional tillage scenarios and no-tillage scenarios (66%). The phosphorus loads major change (60%) was due to the decrease (-50%) in the fertilizer rate application instead of due to the change in management practices. No-tillage practices did not significantly affect the water yield, but greatly affected sediment due to reduction of soil erosion. The soluble P losses increased mainly when the fertilised doses increased. In conclusion it can be stated that conventional tillage practices need to be replaced by less intensive tillage practices in order to minimize environmental impacts caused by a particular land use.

Keywords: Soil erosion, Nutrients, Land use scenarios, SWAT model

Introduction

The combination of inadequate soil use (cultivation on sloping lands and near to water courses) and inadequate management (intensive revolving of soil and low cover levels) with high available phosphorus rates renders the cultivated areas as a great source of sediments (Minella et al. 2007) and phosphorus to the water courses (Pellegrini et al. 2009).

Fertilizer P application together with cropping practices can have a lasting effect on soil fertility and can result in water pollution. Moreover, for the same return period, phosphorus losses were generally greater from plots cultivated up and down the slope than from those cultivated across the slope (Quinton et al., 2001).

The cultivation of tobacco in agricultural highland, involving intensive soil preparation, leads to a great soil erosion and phosphorus transferred to superficial water bodies (Pellegrini et al. 2009).

Incompatible agricultural practices with the land use capability of these regions and the application of high fertilizer and pesticide rates make tobacco cultivation an activity with a high contamination risk for water resources in watersheds (Kaiser et al., 2010).

The effect of management systems on soil attributes, sediment movement and organic carbon exportation was evaluated by Mello (2006) in a rural watershed under tobacco crop in Southern Brazil. The most degraded soils were those under conventional tillage. These areas presented the highest soil losses, and also presented the largest sediments movement on the hillslope. Whereas, the conversion to minimum tillage and no tillage systems increased soil quality and reduced sediment delivery.

The main tillage systems of the tobacco crops in Southern Brazil were studied by Pellegrini (2006). The author concluded that soil management systems that include oats as cover crop in winter, using ridge (*camalhão*) and involve minimal soil tillage maintain higher productivity in tobacco reducing losses being more sustainable in the long term.

Water quality models have proven to be a reliable tool for decision making and scenario analysis. The Soil and Water Assessment Tool (SWAT) model (Arnold et al., 1998) was developed to predict the impact of land management practices on water, sediment and agricultural chemical yields in watersheds with varying soils, land use and management conditions (Neitsch et al., 2005). Applications of SWAT model for modeling land use changes and management practices have been expanded worldwide, such as Chaplot et al. (2003); Behera and Panda (2006); Bormann et al. (2007); Ullrich and Volk (2009) and Uzeika et al. (2012).

The main objective of this study was to make realistic predictions of the impacts of agricultural management changes on the water balance, sediments and phosphorus loads at the Arroio Lino watershed using the SWAT model.

Materials and Methods

Study area description

The Arroio Lino watershed covers 4.8 km^2 and is located in Agudo County, in the state of Rio Grande do Sul, Brazil (Figure 1). Almost 30% of the Arroio Lino watershed area is occupied by annual crops and more than 50% by native forest cover. Approximately 90% of the crop areas are devoted to tobacco production (Pellegrini et al., 2009).

Most of the tobacco crops are cultivated under conventional tillage with intense agricultural exploration which have increased surface runoff and hillslope erosion due to the removal of vegetation. These affects have contributed to excessive sediment and nutrient loads inputs to the streams.

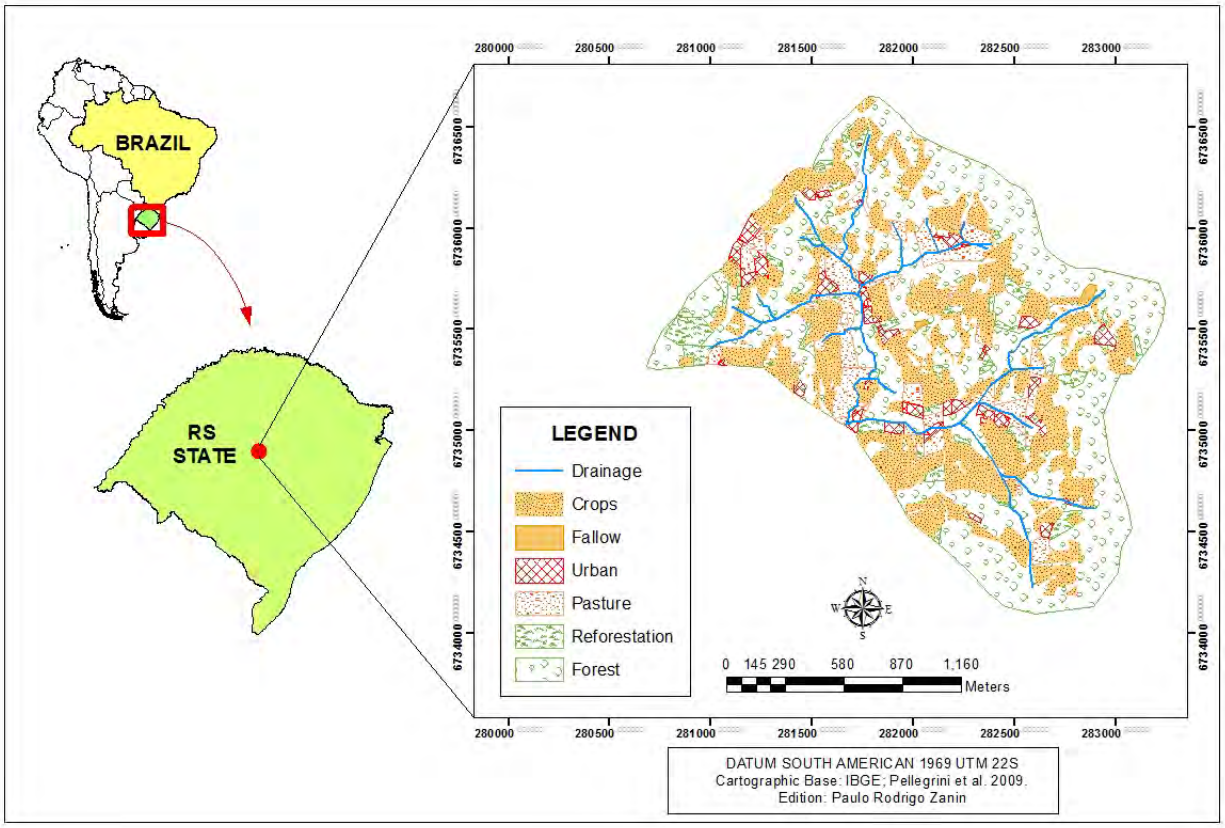

Figure 1 – Land use in the Arroio Lino watershed, Brazil

SWAT Model and input data

The SWAT model requires topography, land use, management, soil parameters input, and weather data. The digital maps (topography, land use and soil types) were processed with a GIS preprocessing interface to create the required model input files.

SWAT simulates a watershed by dividing it into multiple subbasins, which are further divided into hydrologic response units (HRU's). These HRU's are the product of overlaying soils, land use and slope classes.

According to Neitsch *et al*. (2005) a set of parameters is directly related to the simulations of management practices, such as the biological mixing efficiency (BIOMIX), mixing efficiency of tillage operation (EFFMIX), depth of mixing caused by the tillage operation (DEPTIL), initial SCS runoff curve number for moisture condition II (CN2), Manning's "n" value for overland flow (OV_N), and USLE equation support practice factor (USLE_P).

The biological mixing efficiency (BIOMIX) is the redistribution of soil constituents as a result of the activity of biota in the soil. Studies have shown that biological mixing can be significant in systems where the soil is only infrequently disturbed. In general, as a management system shifts from conventional tillage to conservation tillage to no-till there will be an increase in biological mixing. The efficiency of biological mixing is defined by the user and is conceptually the same as the mixing efficiency of a tillage implement. The redistribution of nutrients by biological mixing is calculated using the same methodology as that used for a tillage operation. If no value for BIOMIX is entered, the model will set BIOMIX = 0.20.

The mixing efficiency of tillage operation (EFFMIX) specifies the fraction of materials (residue, nutrients and pesticides) on the soil surface which are mixed uniformly throughout the soil depth of mixing caused by the tillage operation (DEPTIL). The remaining fraction of residue and nutrients is left in the original location (soil surface or layer).

Initial SCS runoff curve number for moisture condition II (CN2) is a function of the soil's permeability, land use and antecedent soil water. CN2 may be updated in plant, tillage, harvest and kill operations.

USLE equation support practice factor (USLE_P) is defined as the ratio of soil loss with a specific support practice to the corresponding loss with up-and-down slope culture. Support practices include contour tillage, strip cropping on the contour, and terrace systems (Neitsch *et al*., 2005).

Results and Discussion

Climatic Characteristics of the 30 Years Simulated Period

Simulated rainfall (PREC), potential evapotranspiration (PET) and evapotranspiration (ET) over the simulated period are presented in Figure 1. Annual rainfall ranged between 1145 and 2196 mm year^{-1} with a median and standard deviation of 1686 and 257 mm, respectively.

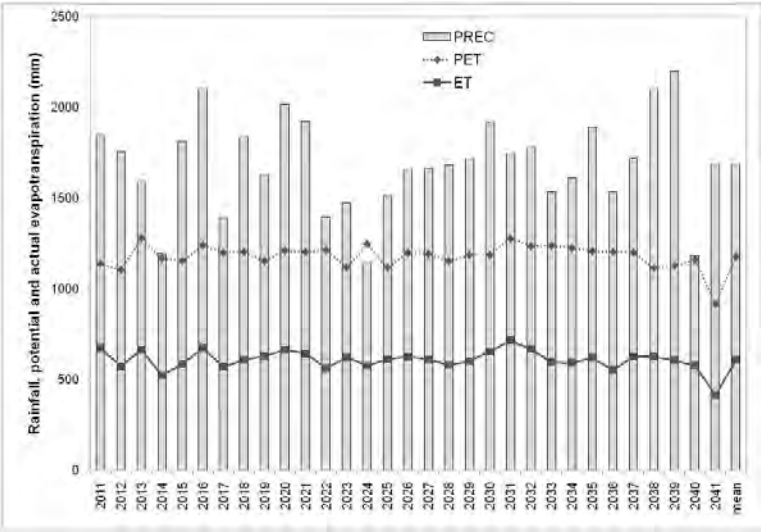

Figure 2 – Simulated rainfall, potential evapotranspiration and evapotranspiration over the thirty years period.

Land use change and crop management scenarios

After calibration and verification of SWAT model for stream flow (Bonumá et al., 2013), sediments (Bonumá et al., 2012) and phosphorus (Bonumá, 2011) different management scenarios were simulated in Arroio Lino watershed.

Three different management systems were considered for the generation of these scenarios: conventional tillage (CT), minimum tillage or conservation tillage (MT) and no-tillage cultivation (NT). The model output parameters investigated are surface runoff, baseflow, total water yield, total sediment loading, organic phosphorus, soluble phosphorus, and total phosphorus. Tables 1, 2 and 3 list the schedule management operations and table 4 lists the tillage treatments parameters.

Table 1 - Schedule management operations for conventional tillage (CT).

Year	Month	Day	Crop	Operation	Description
2	1	29	Tobacco	Harvest and kill operation	
1	7	1		Tillage	Plow and Harrow
1	9	10		Tillage	Ridging plow
1	9	12	Tobacco	Planting	
1	9	12	Tobacco	Fertilizer application	10-18-20, 850 Kg ha^{-1}
1	10	21	Tobacco	Fertilizer application	14-00-14, 200 kg ha^{-1}
1	10	21	Tobacco	Tillage	Plow
1	11	11	Tobacco	Fertilizer application	14-00-14, 200 kg ha^{-1}
1	11	11	Tobacco	Tillage	Plow
1	12	10	Tobacco	Harvest	

Table 2 - Schedule management operations for minimum tillage (MT).

Year	Month	Date	Land Use	Operation type	Description
1	1	29	Tobacco	Harvest and kill operation	
1	2	1	Corn	Planting	
1	5	6	Corn	Harvest and kill operation	
1	5	7		Tillage	Plow
1	5	8	Oat	Planting	
1	8	31	Oat	End of growing season	
1	9	1		Tillage	Plow and Harrow
1	9	11		Tillage	Ridging plow
1	9	12	Tobacco	Planting	
1	9	12	Tobacco	Fertilizer application	10-18-20, 850 Kg ha^{-1}
1	10	21	Tobacco	Fertilizer application	14-00-14, 200 kg ha^{-1}
1	10	21	Tobacco	Tillage	Plow
1	11	11	Tobacco	Fertilizer application	14-00-14, 200 kg ha^{-1}
1	11	11	Tobacco	Tillage	Plow
1	12	1	Tobacco	Harvest	

Table 3 - Schedule management operations for no-tillage cultivation (NT).

Year	Month	Date	Land Use	Operation type	Description
1	1	29	Tobacco	Harvest and kill operation	
1	2	1	Corn	Planting	
1	5	6	Corn	Harvest and kill operation	
1	5	7		Tillage	Plow and Harrow
1	5	8	Oat	Planting	
1	8	31	Oat	End of growing season	
1	9	12	Tobacco	Planting	
1	9	12	Tobacco	Fertilizer application	10-18-20, 425 kg ha^{-1}
1	10	21	Tobacco	Fertilizer application	14-00-14, 200 kg ha^{-1}
1	10	21	Tobacco	Tillage	Plow
1	12	10	Tobacco	Harvest	

Table 4 - Schedule management operations.

Scenario	DEPTIL(mm)[a,b]	EFFMIX[b,c]	BIOMIX[d]	OV_N[b]	CN2[b,d]
CT	300	0.95	0.1	0.09	default
MT	300	0.55	0.3	0.13	-4%
NT	25	0.05	0.4	0.30	-6%

DEPTIL = Depth of mixing caused by the tillage operation; EFFMIX = Mixing efficiency of tillage operation; BIOMIX = Biological mixing efficiency; OV_N = Manning's "n" value for overland flow; CN2 = Initial SCS runoff curve number for moisture condition II; [a] Pellegrini (2006); [b] Neitsch et al., (2005); [c] Behera and Panda, (2006); [d] Ullrich and Volk, (2009).

Effect of tillage and fertilizer on runoff, sediment and on nutrient losses

Figure 3 illustrate the percentage deviation of modeling results regarding to application of management scenarios on water balance components, nutrients and sediment loading. In general the largest differences were between conventional tillage scenarios and no-tillage scenarios.

The surface runoff (SR) decreased when changing from conventional tillage to minimum tillage (CT-MT), minimum tillage to no tillage (MT-NT) and conventional tillage to no tillage (CT-NT). However, the baseflow (BF) increased when decreasing tillage intensity following almost the same order of magnitude that the increase in surface flow. Hence, the percentage deviation in the water yield (WY) is only 6% due to change from conventional tillage to no-tillage management practice.

The highest decrease in sediment yield (SY) was between conventional tillage scenarios and no-tillage scenarios (CT-NT, 66%), followed by conventional tillage to no tillage (CT-MT, 39%) and minimum tillage to no tillage (MT-NT, 28%). Pellegrini (2006) analyzing different management scenarios in plot field scale in Arroio Lino watershed found the same range of variation.

In relation to the soluble phosphorus (Psol), organic phosphorus (Porg) and total phosphorus (Ptot) loads the major change was due to the decrease (-50%) in the fertilizer rate application (CT-NT) than due to the change in management practices (MT-NT and CT-MT). Lessening the P rate by 50% in tobacco fields decreased mean P annual loads by 60%.

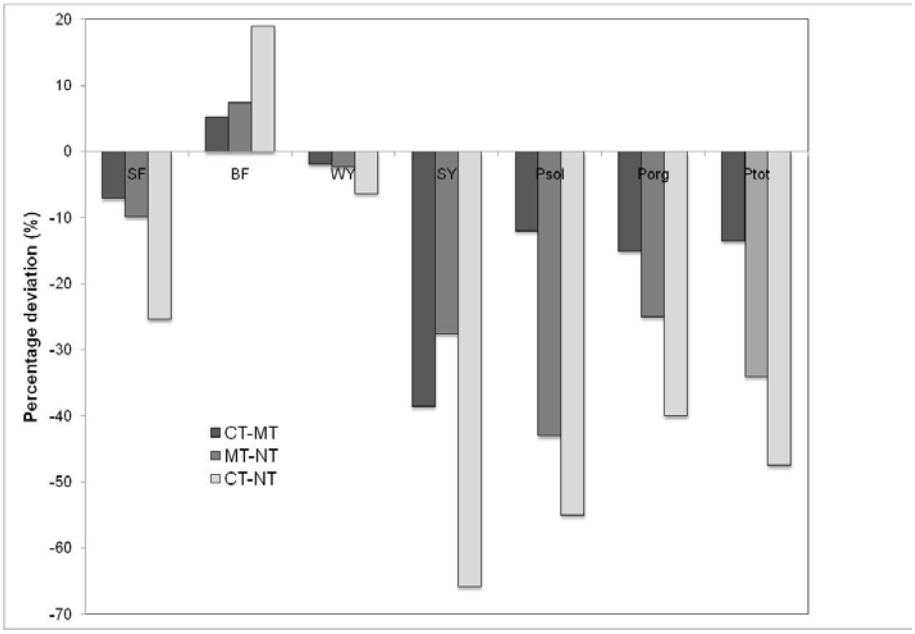

Figure 3 – Percentage deviation of modeling results regarding to application of management scenarios on water balance components, nutrients and sediment loading.

Conclusion

Three different management scenarios were tested in the Arroio Lino watershed, in Southern Brazil using the calibrated SWAT model were tested over a 30 years simulated period.

The scenarios were conventional tillage (CT), minimum tillage or conservation tillage (MT) and no-tillage cultivation (NT) with reduction of 50% of fertilizer rate application. The results suggested that decreasing tillage intensity resulted in an increase of baseflow while surface runoff and total water yield decreased. At the same time sediment and phosphorus loads decreased regarding to the decrease of overland flow and soil erosion.

Data generated with this study, along with the existing ones, support the idea that conventional tillage practices need to be replaced by less intensive tillage practices in order to minimize the sediment yield and phosphorus losses in order to minimize social environmental impacts caused by a particular usage of the land.

References

Arnold, J.G.; Srinivasan, R.; Muttiah, R.S.; Williams, J.R. 1998. Large area hydrologic modeling and assessment part I: model development. *J. Am. Water Resour. Assoc.***,** v. 34, p. 73–89.

Arnold, J.G.; Fohrer, N. 2005. SWAT2000: current capabilities and research opportunities in applied watershed modeling. *Hydrological Processes*, v. 19, p. 563-572.

Behera, S.; Panda, R.K. 2006. Evaluation of management alternatives for an agricultural watershed in a sub-humid subtropical region using a physical process based model. *Agriculture, Ecosystems and Environment***,** v. 113, p. 62–72.

Bonumá, N. B. 2011. Modeling of water, sediment and phosphorus loads in an agricultural watershed in southern Brazil. PhD diss. Federal University of Santa Maria, Santa Maria, Brazil.

Bonumá, N. B., Rossi, C.G., Arnold, J. G., Reichert, J.M., Paiva, E. M. C. D. 2013. Hydrology evaluation of the Soil and Water Assessment Tool considering measurement uncertainty for a small watershed in Southern Brazil. *Applied Engineering in Agriculture*, v. 29, p. 189-200.

Bonumá, N.B.; Rossi, C.H.G. ; Arnold, J.G. ; Reichert, J.M.; Minella, J.P.; Allen, P. M. ; Volk, M. 2012. Simulating Landscape Sediment Transport Capacity by Using a Modified SWAT Model. *Journal of Environmental Quality*.

Bormann, H.; Breuer, L.; Graff, T.; Huisman, J. 2007. Analysing the effects of soil properties changes associated with land use changes on the simulated water balance: A comparison of three hydrological catchment models for scenario analysis. *Ecological modeling***,** v. 209, p. 29–40.

Chaplot, V.; Saleh, A.; Jaynes, D.B.; Arnold, J. 2007. Predicting water, sediment and NO_3-N loads under scenarios of land-use and management practices in a flat watershed. *Water, Air, and Soil Pollution*, v. 154, p. 271–293.

Gassman, P.W.; Reyes, M.R.; Green, C.H.; Arnold, J.G. 2007. The Soil and Water Assessment Tool: Historical development, applications, and future research directions. *Transactions of the American Society of Agricultural and Biological Engineers*, v. 50, n. 4, p. 1211-1250.

Kaiser, D. R. et al. A. 2010. Nitrate and Ammonium in soil solution in tobacco management systems. *Brazilian J. Soil Sci.*, v. 34, n. 2, p. 379-388.

Mello, N. A. 2006. Efeito do sistema de manejo nos atributos do solo, movimentação de sedimentos e exportação de carbono orgânico numa microbacia rural sob cultura do fumo**.** 2006. 273f. Tese (Doutorado em Ciência do Solo) – UFRGS, Porto Alegre.

Minella, J.P.G.; Merten, G.H.; Reichert, J.M.; Rheinheimer, D.S. 2007. Identificação e implicações para a conservação do solo das fontes de sedimentos em bacias hidrográficas. *Brazilian J. Soil Sci.*, v. 31, n. 6, p.1637–1646.

Neitsch, S.L.; Arnold, J.G.; Kiniry, J.R.; Williams, J.R. 2005. **Soil and Water Assessment Tool - Theoretical Documentation**: Version 2005. Temple, Blackland Research Center, Texas Agricultural Experiment Station. 494 p.

Pellegrini, A. 2006. Sistemas de cultivo da cultura do fumo com ênfase às práticas de manejo e conservação do solo. 2006. 91 f. Dissertação (Mestrado em Ciência do Solo) - Universidade Federal de Santa Maria, Santa Maria.

Pellegrini, J.B.R.; Rheinheimer, D.R.; Gonçalves, C.S.; Copetti, A.C.C.; Bortoluzzi, E.C.; Tessier, D. 2006. Impacts of anthropic pressures on soil phosphorus availability, concentration, and phosphorus forms in sediments in a Southern Brazilian watershed**.** *J. Soils Sediments*, v. 10, n. 3, p. 1614-7480.

Quinton, J.N.; John, A.C.; Tim, M.H. 2001. The Selective Removal of Phosphorus from Soil: Is Event Size Important? *Journal of Environmental Quality*, v. 30, p. 538–545.

Ulrich, A.; Volk, M. 2009. Application of the Soil and Water Assessment Tool (SWAT) to predict the impact of alternative management practices on water quality and quantity. *Agricultural Water Management***,** v. 96, p. 1207–1217.

Uzeika, T., G. Merten, J.P.G. Minella, and M. Moro. 2012. Use of the SWAT model for hydro-sedimentologic simulation in a small rural watershed. *Brazilian J. Soil Sci.* 36(2):1-9.

Soil loss prediction using SWAT in a small ungaged catchment with Mediterranean climate and vines as the main land use

Ramos, M.C. (*)
Department of Environment and Soil Science. University of Lleida
Alcalde Rovira Roure 171, 25198 Lleida, Spain
cramos@macs.udl.es

Martínez-Casasnovas J.A.
Department of Environment and Soil Science. University of Lleida
Alcalde Rovira Roure 171, 25198 Lleida, Spain
j.martinez@macs.udl.cat

Abstract

Soil erosion is recognized as the major cause of land degradation in Mediterranean and semiarid environments. The present work shows the results of the application of SWAT (ArcSWAT 2009.93.5) to model soil erosion in a small ungaged catchment (46 ha) located in the Anoia-Penedés region (NE Spain). This area belongs to the Penedès Tertiary Depression, where unconsolidated materials (marls) outcrop. The main agricultural uses are rainfed vines, herbaceous crops (winter barley) and olive trees. The main data sources to run SWAT were the detailed Soil Map of Catalonia, a 5 m resolution DEM and land use / vegetation maps derived from orthophotos taken in 2010. The model was calibrated and validated using field data (soil water content and runoff samples) collected at different subbasins. The model was run for the period 2000-2012, which includes years with different climatic characteristics. Precipitation ranged between 329 mm and 785 mm, runoff rates ranged between 4 and 20% and average annual soil losses ranged between 2 and 14 Mg/ha, with clear differences between hydrological response units depending on soil characteristics and land management. The highest values correspond to areas located near the catchment outlet, where soils were more affected by land levelling operations.

Keywords: soil loss, runoff rates, vineyards, Mediterranean climate, small catchment.

Introduction

In Mediterranean areas, factors such as climate, topography, soil characteristics, land use change and intensive agricultural practices have turned soil erosion into the major cause of land degradation (Cerdà, 2009; García-Ruíz and López-Bermúdez, 2009). The Anoia-Penedès region, located Northeastern Spain, with main crop of vineyards, is a particular example of the effects of the intensive erosion processes recorded in the Mediterranean Spain (Martínez-Casasnovas et al., 2002; 2005). In this region, the coincidence of frequent high intensity rainfall events, high erodible soil parent materials (marls and unconsolidated sandstones) and the extensive vineyard cropping, conditioned by land use changes and abandonment of traditional soil conservation measures, have accelerated the erosion processes (Ramos and Martínez-Casasnovas 2009, 2010). In addition, vines cultivated in the area without soil cover due to water restrictions, is one of the land uses that more favor erosion processes (Kosmas et al., 2004).

In this area, erosion in vineyards has been analysed at plot scale. However, in order to have a wider view of the problem and to know the exact impact of that land use in soil losses the catchment scale should be analysed. According to several authors, the monitoring of erosion and water quality variables should be studied within the context of the characteristics and particularities of the broad area in which these activities take place (Zalidis et al., 2002), being best approached in small sized watersheds (0.5–2.0 km^2) (Casalí et al., 2008) as model areas to be later up-scaled to larger watersheds.

Different models have been used by many researchers to predict soil erosion and sediment transport, and to assess the impacts of land use, management practices and changes in land cover on water resource and non-point source pollution problems. The selection of the model depends on the final objective, the existing information to run and calibrate the model and on the uncertainty in interpreting the results. Among them, in this work the Soil and Water Assessment Tool (SWAT), widely used to predict the impact of management on water, sediment yield and agricultural chemical exportation in basins at different scales (Akhavan et al., 2010; Behera and Panda, 2006; Gitau et al., 2008; Gikas et al., 2006, Jayakrishnan et al., 2005; Lam et al., 2010; Lee et al., 2010; Roebeling et al., 2011). Nevertheless, there are few works in which SWAT has been applied to small agricultural basins (about 50-100 ha) with very detail input data.

In this respect, the aim of this research was to analyse the suitability of using SWAT for a small ungaged agricultural basin in the Mediterranean area, which due to soil and climate characteristics and land use and management, is prone to erosion. Runoff and erosion responses were modelled at basin scale, taking into account the effect of land use and soil properties on erosion processes in the different subbasins. Very detailed of soil information was used in this study. Given the lack of a gauging station in the basin, the model was calibrated using runoff and erosion samples and soil water content data measured in different subbasins, which also constitutes a novelty as SWAT calibration methodology.

Material and methods

Study area

The study area is located in the Anoia region, about 40 km northwest of Barcelona (1.769722 E, 41.53111 N, 340 m.a.s.l.). A small basin of 0.46 km2 was selected for this study (Figure 1). The main land use in the area is vineyards, which has a long tradition of vine cultivation under the Penedès Designation of Origin (DO). Other crops like olive trees, alfalfa, winter barley, winter pasture and ranges are also found in the basin. The rest of the land is occupied by urban areas and transportation routes (paved and un-paved roads).

The soils are on alluvial deposits from the Pleistocene, which cover a substratum of Miocene marls, sandstones and unconsolidated conglomerates. A high percentage of coarse elements of metamorphic origin are present. According to the soil map (1:25,000) of the Penedès region (DAR, 2008), the most frequent soils in the basin are classified as *Typic Xerorthents* and *Fluventic Haploxerepts*. The basin drains into a gully system, which is also a characteristic of the landscape of the region where the basin is located (Martínez-Casasnovas et al., 2009).

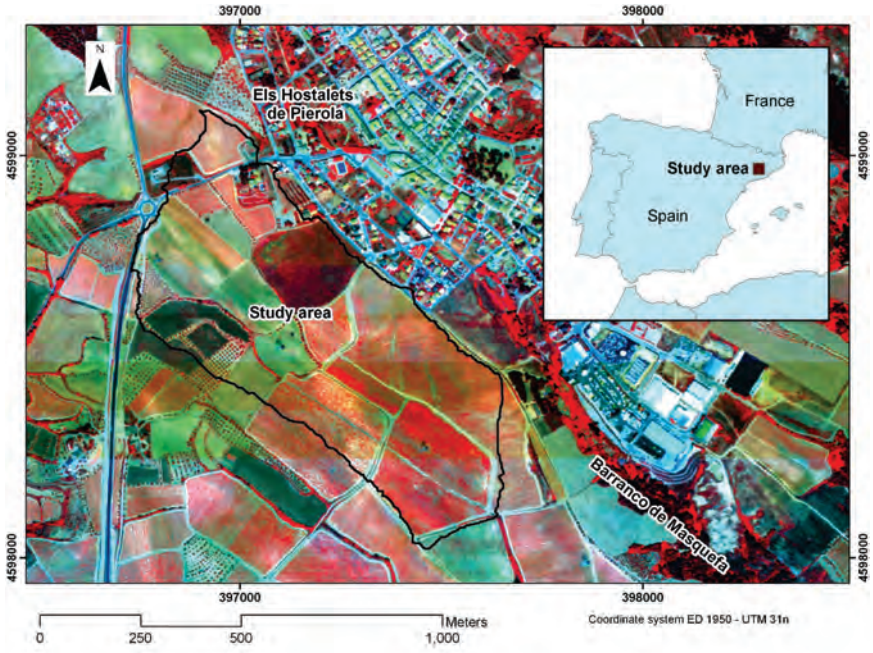

Figure 1. Location of the study area.

SWAT input data

Soil and topographic characteristics

A detailed scale soil map (1:25,000) (DAR 2008) was used as input data for the model. Additional top soil properties of, such as soil particle distribution, bulk density, organic carbon, water retention capacity at saturation -33 kPa and -1500 kPa and the infiltration capacity were obtained in 40 sample points of the basin. The selection of these points was

based on the multi-spectral response of soils in a false colour composite WorldView-2 image acquired in July 2010. The soil erodibility factor (K USLE factor) was also computed for each soil unit, as required by SWAT, using the equation proposed by Wischmeier and Smith (1971).

Table 1 shows the summary statistics of soil properties in the study basin. Most soils had loamy or loamy-sandy texture, with an average percentage of coarse elements ranging between 9.8 and 28.4% in the top horizon. The organic matter content was relatively low, ranging between 0.9 and 2.3%. The available water capacity ranged between 7.7 and 12.2 mm and the steady infiltration rate ranged between 8.0 and 29.5 mm h^{-1}. Some soils in the basin were very erodible, with K-factors up to 0.055 Mg h MJ-1mm^{-1} (ranging between 0.033 to 0.055). Soil depth ranged between 80 and 110 cm and all the soils sampled did not present redox depletions, indicating a good circulation of drainage water in the profile.

A 1m-resolution digital elevation model of the study area, generated from a low altitude photogrammetric aerial survey carried out in 2010, was also used. The definition of the SWAT hydrological response units (HRU) were done by considering the slope intervals of 0-2, 2-5, 5-10, 10-15 and > 15%. Thirty-four sub-basins and 1180 hydrological response units (HRU) were defined within the study basin. The average HRU extension was 1.88 ha.

Table 1. Summary statistics of soil properties of the most representative soils in the study basin: percentage in the basin, root depth, texture fraction (clay, silt, sand- USDA), coarse elements, bulk density (BD), available water capacity (AWC), electrical conductivity (EC); steady infiltration rate (StIR); K-erodibility USLE factor (K-factor), organic carbon (OC).

Soil	S1	S2	S5	S4	S5
Perc.Basin (%)	14.18	12.45	11.93	8.97	8.35
Root depth (cm)	800	1000	1670	1000	800
Clay (%)	20+2	13.4+7	20.1+7	20+7	19.3+3
Silt (%)	37+3	40+2	43.5+3	30+1	27.4+3
Sand (%)	43+1	41+10	36.4+10	50+7	53.3+9
Coarse elem. (%)	25+2	44+8	23.6+5	25+4	17.5+1
BD (kg m^{-3})	1586+73	1638+160	1350+22	1750+320	1900+310
AWC (mm)	10.8±0.6	13.7 ±0.5	10.8 ±1.1	9.6 ±1.0	8.0±0.5
EC (dS m^{-1})	0.14+0.01	0.10+0.01	0.14+0.01	0.10+0.01	0.16+0.01
StIR (mm h^{-1})	27.3+2.3	8.2+1.2	11.5+1.6	12.0+2.0	9.5+1.0
USLE K–factor (Mg h $MJ^{-1}mm^{-1}$)	0.43+0.08	0.48+0.07	0.42+0.07	0.38+0.06	0.38+0.05
OC (%)	0.70+0.30	0.41+0.18	0.90+0.2	0.81+0.13	0.75+0.12

Land use and crop characteristics

A land use map was created after ortho-rectification of 2010 aerial photos at 1:3,000 scale and field work. The main land use in the basin was vines, which occupied 62.87% of its surface area. Other crops present in the basin were: olive trees (4.79%), alfalfa (8.47%),

winter barley (9.45%), winter pasture (1.49%) and scrub (3.59%). The rest of the area, about 9.34%, were urban areas and (paved and un-paved) roads and tracks (Figure 2). Crop parameters were taken from the SWAT data base and updated with information existing for the study area for biomass P and N concentrations, crop fertilization and tillage operations for each land use.

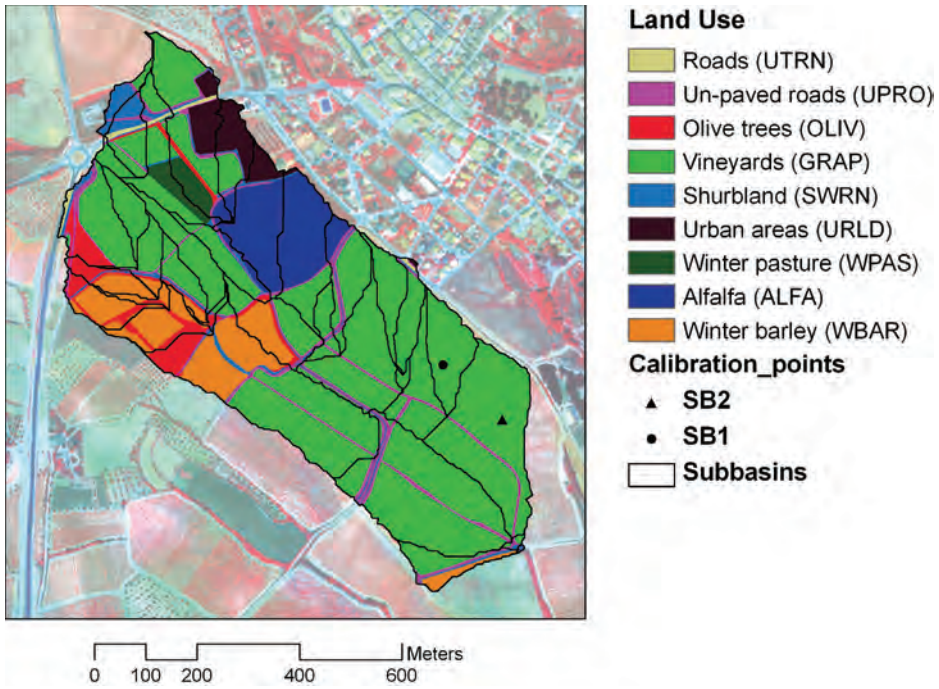

Figure 2. Land use and subbasins in the study basin.

Table 2 shows the values of the parameters used in the model. The curve number (CN2), the saturated hydraulic conductivity (SOL_K), and some parameters related to groundwater (GW_REVAP: Groundwater 'revap' coefficient; GW_DELAY: Groundwater delay (days) and REVAPMIN: Threshold depth of water in the shallow aquifer required for "revap" to occur were among the most sensible parameters. Additionally, the ESCO (Soil evaporation compensation factor) and the EPCO (Plant evaporation compensation factor) were also adjusted.

Climatic data

Daily climatic information was taken from the Els Hostalest de Pierola observatory, which belongs to the Servei Meteorològic de Catalunya (1.809 E; 41.5328 N, 316 m.a.s.l.). That observatory is located 2.5 km far away from the basin. The daily data, as well as the average values of a 15-year series (1998-2012) of temperatures (maximum and minimum), precipitation, solar radiation, relative humidity and wind velocity, were input to run the model. Additionally, precipitation was recorded in the basin at 1-min interval in order to know the detailed rainfall intensity. This information together with the steady infiltration rates were used to calculate runoff rates.

Model calibration and validation

A sensitivity analysis was conducted to identify and rank the parameters that affect the response of the model and the rate of change of its output with respect to changes in its inputs. This analysis was carried out using different series, covering different periods within the available data (1998-2009).

Calibration was carried out following a heuristic approach, adjusting the selected parameters, one parameter at a time, until the statistical calibration criteria were met. Calibration was carried out for the period May 1st, 2010 – April 30th, 2011, which included events with different characteristics (depth and intensity), as well as long dry periods and periods of high intensity rainfall.

The model was individually calibrated for two different subbasins SB1 and SB2 (Figure 2), but trying to fit the parameters in order to obtain the best results for both sub-basins considered together and at the same time. The control parameters were: crop evapotranspiration, soil water content, runoff rates and soil loss due to runoff. Evapotranspiration was estimated in the SWAT using the Hargreaves equation. As vineyards were the main land use in the basin, and particularly within the selected sub-basins, the evapotranspiration estimated by the model was compared with values obtained using the ETo obtained from Els Hostalets de Pierola meteorological station and the crop coefficients proposed by Allen et al. (1998). The ESCO (evaporation compensation factor) and EPCO (plant uptake compensation factor) coefficients were also adjusted to find the best fit between simulated and estimated evaporation data.

The soil water content data for profiles of the two sample sub-basins were acquired using soil moisture TFR probes (Decagon), which were installed at different depths (10-30, 30-50, 50-70 and 70-90 cm) in two sub-basins SB1 and SB2 (Figure 2). Measurements were recorded every 4h and then daily averaged. The probes were calibrated by comparison with soil water contents measured by gravimetry.

Runoff rates, calculated taking into account the steady infiltration rates, sealing and antecedent soil moisture, were estimated and compared with the surface runoff simulated by the model. Soil loss was estimated for the same events using the sediment concentration in runoff collected in the same subbasins.

Validation was carried out for the period May 1st 2011- May 15th 2012 using field measurements for soil water content, rainfall and runoff. Model performance in both cases, calibration and validation periods was defined based on three statistical methods: the Nash–Sutcliff efficiency (NSE; Nash and Sutcliffe, 1970), the percent bias (PBIAS, %; Gupta et al., 1999) and the ratio of the root mean square error to standard deviation (RSR).

Results

Table 2 shows the values of the parameters used in the model. The curve number (CN2), the saturated hydraulic conductivity (SOL_K), and some parameters related to groundwater (GW_REVAP: Groundwater 'revap' coefficient; GW_DELAY: Groundwater delay (days) and REVAPMIN: Threshold depth of water in the shallow aquifer required for "revap" to occur were among the most sensible parameters. Additionally, the ESCO (Soil evaporation compensation factor) and the EPCO (Plant evaporation compensation factor) were also adjusted.

Model sensibility, calibration and validation

Table 3 shows the statistics of calibration and validation for soil water, runoff and soil loss. For soil loss, during the calibration period, the RSR statistics were 0.488 and 0.677, respectively for SB1 and SB2; the PBIAS was -1.75 and 2.68% and the NSE was 0.687 for both sub-basins. The NSE was of the same order as those observed by Narasimhan et al. (2005), and the RSRs were similar to those observed by MinXing et al. (2010) for soil moisture analysis. For runoff rates the fits was slightly better for SB1 than for SB2 according to RSR, but not according to the other two statistics (PBIAS and NSE). For soil loss, however, the agreement between simulated and measured soil loss was better for SB2 than for SB1, according to RSR and NSE, but was poorer according to PBIAS.

Table 2. Final values of sensitive parameters used for modeling runoff and soil loss

Parameter Description	value
1- ESCO: Soil evaporation compensation factor	0.9
2- CN2 _SCS runoff curve number for moisture condition II	72-79 agric. 92-96 urban
3- EPCO Plant evaporation compensation factor	0.9
4- GW_REVAP Groundwater 'revap' coefficient	0.15
5- GW_DELAY Groundwater delay (days)	14
6- REVAPMIN Threshold depth of water in the shallow aquifer required for "revap" to occur (mm)	10
7- Sol_K Soil conductivity (mm h–1)	10
8- Ch_K2 Effective hydraulic conductivity in main channel alluvium (mm h–1)	0.045
9- CH_N Manning coefficient for channel	0.020
10-GWQMN Threshold depth of water in shallow aquifer required for return flow to occur (mm)	1000
11- Alpha_Bf Baseflow Alpha factor (days)	0.05

Following the criteria provided by Moriasi et al. (2007) for runoff and sediment, this first calibration analysis could be considered satisfactory, particularly considering that the analysis was carried out using daily data. Suitable runoff rates and reasonably good soil loss predictions were obtained for most situations, but less satisfactory results when extreme events or high intensity, short duration, rainfall events occur.

Table 3. Statistics of the comparisons between simulated and measured data during calibration and validation periods

	RSR	**PBIAS %**	**NSE**	**RSR**	**PBIAS %**	**NSE**
	calibration			validation		
Soil water SB1	0.488	-1.752	0.687	0.444	0.329	0.862
Soil water SB2	0.670	2.684	0.687	0.742	2.249	0.852
Runoff rates SB1	0.381	-16.333	0.885	0.528	-13.823	0.817
Runoff rates SB2	0.421	-16.200	0.637	0.384	-8.964	0.881
Soil loss SB1	0.517	-15.791	0.663	0.714	8.627	0.714
Soil loss SB2	0.139	-28.701	0.331	0.281	23.120	0.910

Soil loss and runoff losses under different rainfall patterns

The analysed period included years with different total amount of rainfall and different rainfall distributions throughout the year. Table 4 summaries the total precipitation recorded for the period 2000-2012 and the water and sediment yield predicted by the model for those years.

Table 4: summary of results obtained with the model during the period 2000-2012

Year	P (mm)	SurQ (mm)	LatQ (mm)	GwQ (mm)	Percol (mm)	ET (mm)	Water yield (mm)	Sed yield ($Mgha^{-1}$)
2000	491.2	28.4	4.0	30.2	85.2	372.0	64.0	1.28
2001	447.8	28.3	5.1	93.9	99.5	353.7	124.7	1.37
2002	612.6	82.6	6.3	126.7	160.5	412.6	202.9	6.56
2003	496.0	67.7	5.4	114.7	126.9	354.7	174.2	5.99
2004	785.5	84.2	6.2	129.2	116.7	603.8	175.2	5.55
2005	365.0	15.1	3.3	44.0	67.7	323.5	61.5	0.19
2006	329.8	60.1	3.2	68.9	62.2	303.6	129.1	4.41
2007	548.0	37.7	5.5	74.7	107.6	386.8	127.5	1.63
2008	751.5	112.2	7.1	152.7	207.7	424.2	274.1	7.54
2009	541.9	93.5	5.4	108.7	83.0	432.9	196.6	7.33
2010	729.4	105.9	7.4	159.0	191.2	447.1	271.6	13.9
2011	655.7	119.3	7.4	184.4	207.1	384.9	288.6	9.8
2012	510.7	40.62	5.77	98.33	133.59	331.6	168.47	1.63

Precipitation ranged between 329.8 mm and 785.5 mm. Runoff rates ranged between 4.2 and 21.5% of rainfall and represented between 21 and 55% of water yield. Due to soil characteristics a significant amount of rainfall infiltrate and moved as lateral flow, which represented about 50% of water yield, on average. This result was confirmed with soil moisture measurements at different points in the catchment and with subsurface water flow in a point close to the catchment outlet, where water flows during all year with a near constant rate. Sediment yield depended on rainfall amounts, ranging between less than 1 Mg ha^{-1} and up to 13.9 Mg ha^{-1}. These high erosion rates, in several years higher

than the soil tolerance limits (between 7 and 11 Mg ha^{-1}) proposed by different authors (Schertz, 1983, Centeri et al., 2001, Terrence et al., 2002), may be justified by the management practices used in the area, which include bare soil and frequent tillage throughout the crop cycle. Within the basin, however, differences may be found between subbasins due to the influence of soil properties and slope degree on parameters such as water runoff and sediment yield. Within the basin, the highest erosion rates were recorded near the outlet, where the slope degree was one of the highest and the infiltration capacity of the soils was the lowest.

Figure 3 shows the spatial variability of soil losses produced in the basin on average (average form 2000-2012), and for two contrasted years: a very wet year (2008) and a dry year (2006). It can be observed that the highest erosion rates were produced near the basin outlet. In that area, not only the slope was higher but it was the area where the basin had been severely disturbed by land leveling operations before vineyard establishment. Although on average in the basin, the erosion rates may be considered an in rank of moderate soil loss (5–10 Mg ha^{-1} yr^{-1}), in the areas near the outlet the it could be considered in the rank of high erosion (10–20 Mg ha^{-1} yr^{-1}), very high (20– 40 Mg ha^{-1} yr^{-1}) and severe (40–80 Mg ha^{-1} yr^{-1}).

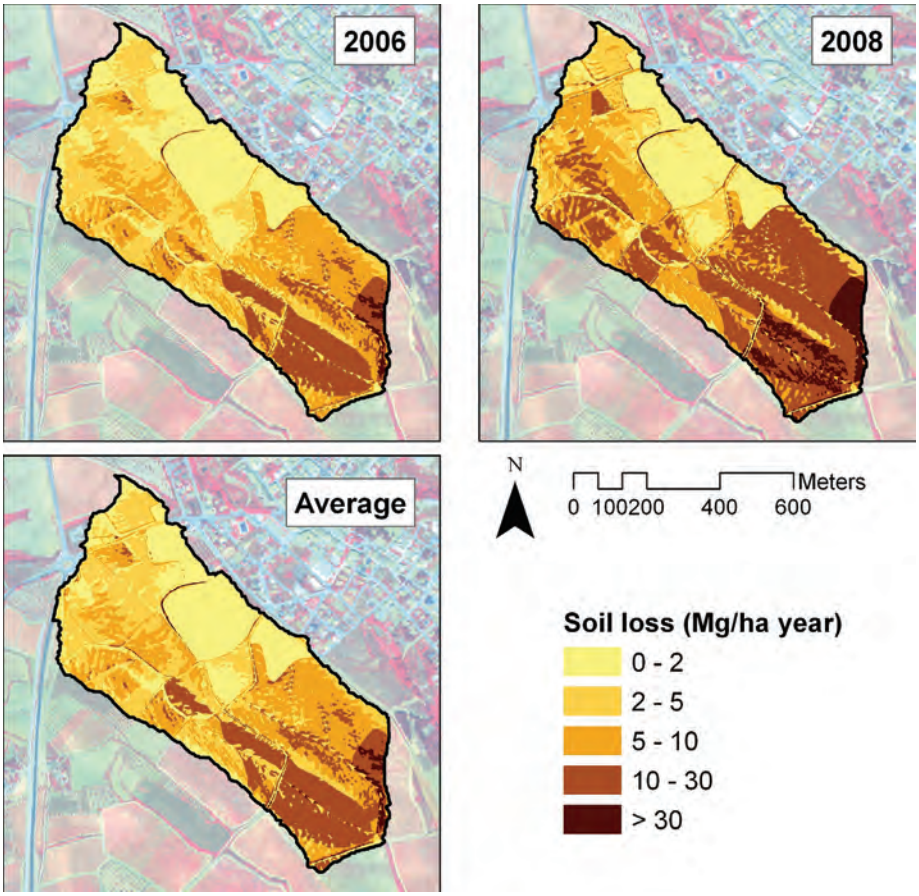

Figure 3. Average annual soil losses (2002-2012) and soil losses for two contrasted years: 2008 (very wet year) and 2006 (dry year).

Conclusions

The present work is a contribution to the application of SWAT in agricultural areas with Mediterranean climate. This application refers to the use of the model to predict soil and water losses in small ungaged basin with vines as the main land use. The use of soil moisture data and runoff and samples collected at different points within the basin allowed to adjust and calibrate the model to the study conditions. In addition, the detail information of soil allowed a better understanding of the processes occurring in the basin. At very detail scale of analysis, SWAT showed an agreement between measured and simulated soil water content. Runoff rates and soil losses predicted by the model were in agreement with the soil loss estimated by combining runoff rates and sediment concentration in runoff on average conditions, with PBIAS less or about 16% in the validation analysis for both runoff and soil loss in one the subbasin located at mid slope and up to 23% in the areas were erosion was the highest. The greatest differences existed when extreme rainfall events of high intensity and short duration occurred, which are not well detected in the daily scale analysis. This result also shows the high variability in soil and water losses that can occur in the basin, in several cases higher than the soil tolerance levels. These results point out the need of establishing some soil conservation measures in the basin, that could reduce soil erosion processes and contribute to increase available water for the crops.

Acknowledgements
This work is part of the research project AGL2009-08353 funded by the Spanish Ministry of Science and Innovation. We thank very much Dr. R. Srinivasan for his help in the model set up and the adaptation of different model parameters for a better fit to the study case, and to the Castell d'Age winery for their support to carry out the field experiments in its property.

References

Akhavan, S., J. Abedi-Koupai, S.F.Mousavi, M.Afyuni, S.S. Eslamian and K.C. Abbaspour, 2010. Application of SWAT model to investigate nitrate leaching in Hamadan-Bahar Watershed, Iran. *Agriculture, Ecosystems and Environment* 139 (4); 675-688

Allen R.G., L.S.Pereira, D. Raes and M. Smith. 1998. Crop evapotranspiration. Guidelines for computing crop water requirements. *FAO Irrigation and Drainage Paper*, nº. 56. FAO - Food and Agriculture Organization of the United Nations. Roma.

Behera, S. And R.K. Panda, 2006. Evaluation of management alternatives for an agricultural watershed in a sub-humid subtropical region using a physical process based model. *Agriculture, Ecosystems & Environment* 113 (1–4): 62–72.

Casali, J., R. Gastesi, J. Álvarez-Mozos, L.M. De Santisteban, J.D.V. Lersundi, R. Giménez, A. Larrañaga, M. Goñi, U. Agirre, M.A. Campo, J.J. López and M. Donézar. 2008. Runoff, erosion, and water quality of agricultural basins in central Navarre (Spain). *Agricultural Water Management* 95: 1111-1128

Centeri, C., R. Pataki, and A. Barczi. 2001. Soil erosion, soil loss tolerance and sustainability in Hungary. 3rd International Conference on Land Degradation and Meeting of the IUSS Subcommission C - Soil and Water Conservation September 17-21, 2001 - Rio de Janeiro.

Cerdà, A. 2009. Erosión y degradación del suelo agrícola en España. Publ. Universidad de Valencia. Valencia. España.

DAR, 2008. Mapa de Sòls (1:25.000) de l'àmbit geogràfic de la Denominació d'Origen Penedès. Departament d'Agricultura, Alimentació i Acció Rural, Generalitat de Catalunya, Vilafranca del Penedès-Lleida.

Favis-Mortlock D.T. and J. Boardman. 1995. Nonlinear responses of soil erosion to climate change: a modelling study on the UK South Downs. *Catena* 25: 365-387.

García-Ruíz, J.M. and F. López-Bermúdez. 2010. La erosión del suelo en España. Sociedad española de Geomorfología. Zaragoza. 441 pp

Gikas, G.D., T. Yiannakopoulou, and V.A. Tsihrintzis. 2006. Modeling of non-point source pollution in a Mediterranean drainage basin. *Environmental Modeling and Assessment* 11 (3): 219-233

Gitau, M.W., W.J. Gburek and P.L. Bishop. 2008. Use of the SWAT model to quantify water quality effects of agricultural BMPs at the farm-scale level. *Transactions of the ASABE* 51 (6): 1925-1936.

Gupta, H. V., S. Sorooshian and P.O. Yapo. 1999. Status of automatic calibration for hydrologic models: Comparison with multilevel expert calibration. *Journal of Hydrologic Engineering* 4(2): 135-143.

Jayakrishnan R., R. Srinivasan, C. Santhi and J.G. Arnold. 2005. Advances in the application of the SWAT model for water resources management. *Hydrological Processes 19* (3): 749–762.

Lam, Q.D., B. Schmalz and N. Fohrer. 2010. Modelling point and diffuse source pollution of nitrate in a rural lowland catchment using the SWAT model. *Agricultural Water Management* 97 (2): 317-325.

Lee, M., G. Park, M. Park, J. Park, J. Lee and S. Kim, S. 2010. Evaluation of non-point source pollution reduction by applying Best Management Practices using a SWATmodel and QuickBird high resolution satellite imagery. *Journal of Environmental Sciences* 22: 826–833.

Martínez-Casasnovas, J.A., M.C. Ramos and M. Ribes-Dasi. 2002. Soil erosion caused by

extreme rainfall events: Mapping and quantification in agricultural plots from very detailed digital elevation models. *Geoderma* 105, 125-140

Martínez-Casasnovas, J.A., M.C. Ramos and M. Ribes-Dasi 2005. On-site ephemeral gully impacts in vineyard fields: erosion, filling and economical implications. Catena 60, 129-146

Martínez-Casasnovas, J.A., M.C. Ramos and D.García-Hernández. 2009. Effects of land-use changes in vegetation cover and sidewall erosion in a gully head of the Penedès region (northeast Spain). *Earth Surface Processes and Landforms* 34: 1927-1937.

Moriasi, D. N., J. G. Arnold, M.W. Van Liew, R.L. Binger, R.D, Harmel and T.L. Veith, 2007. Model Evaluation Guidelines for Systematic Quantification of Accuracy in Watershed Simulations. *American Society of Agricultural and Biological Engineers*, 50(3): 885-900.

Nash, J.E. and J.E. Sutcliffe. 1970. River flow forecasting through conceptual models. Part 1. A discussion of principles. *Journal of Hydrology* 10 (3): 282–290.

Ramos, M.C. and J.A. Martínez-Casasnovas. 2010. Effects of field reorganisation on the spatial vairability of runoff and erosion rates in vineyards of Northeastern Spain. *Land Degradation and Development*, 21: 1-15

Ramos, M.C. and J.A. Martínez-Casasnovas. 2009. Erosivity of Precipitation Extremes and its Influence on Soil and Nutrient Losses in Vineyards of NE Spain. *Hydrological Processes*. 23: 225-234

Roebeling, P.C., J. Rocha, J.P. Nunes, T. Fidelis, H. Aves and S, Fonseca. 2012. Using the Soil and Water Assessment Tool to estimate Dissolved Inorganic Nitrogen water pollution abatement cost functions in Central Portugal. *Journal of Environmental Quality*. doi:10.2134/jeq2011.0400

Schertz, D.L. 1983. The basis for soil loss tolerances*. J. Soil Water Conservation*, 38 (1): 10–14

Toy, T,J., G. R. Foster and K.G. Renard. 2002 Soil Erosion: Processes, Prediction, Measurement, and Control. John Wiley and Sons, Inc New York.

Wischmeier, W.H., C.B. Johnson and B.V. Cross. 1971. A Soil erodibility nomograph for farmland and construction sites. Journal of Soil and Water Conservation, 26: 189-193

Deployment of SWAT-DEG as a Web Infrastructure Utilizing Cloud Computing for Stream Restoration

Jeffrey Kwon Ditty
Dept. Civil-Env. Eng., Colorado State University, Fort Collins, CO, United States

Dr. Peter Allen
Dept. Geology., Baylor University, Waco, TX, United States

Dr. Jeff Arnold
USDA-ARS., Temple, TX, United States

Dr. Michael White
USDA-ARS., Temple, TX, United States

Dr. Mazdak Arabi
Dept. Civil-Env. Eng., Colorado State University, Fort Collins, CO, United States

Abstract

This study aims to investigate the enhanced accessibility and scalability of the SWAT-DEG model deployed as a cloud service. Frequent monitoring of hydrologic processes and simulation modeling on short (i.e., sub-daily) time steps are essential tools for effective stream rehabilitation and restoration on first and second order streams with drainage areas less than 20 square kilometers. The SWAT-DEG model was developed to assess how changes in climate and land use beget changes in watershed processes such as runoff, sheet and rill erosion, channel geomorphology and sedimentation. Deployment of the model on a user-friendly and scalable web-platform enables a broader population of watershed planners and decision makers to account for urban development, climatic variability and change, and other human activities in the planning process. The environmental Risk Assessment and Management System (eRAMS) was used to facilitate collection and organization of geospatial data, scenario assessment and visualization, and uncertainty analysis. The platform, eRAMS, is operating system independent and deployable on desktop or mobile devices. Implications for application performance and resource requirements (CPU, disk, and network) resulting from multi-tier applications of SWAT-DEG as a cloud service are discussed.

Keywords: SWAT, watershed modeling, stream restoration, stream rehabilitation, scalability, accessibility, cloud, eRAMS, SWAT-DEG, channel stability

Introduction

River stabilization is a rapidly growing business, with an exponential increase of river restoration projects within the last decade of the United States. In fact, the United States spent on average > $1 billion a year for small and midsize projects alone (Bernhardt et al., 2005). High priority goals in river restoration projects are typically riparian management as shown by the national database stating that the top three project intents are water quality (27%), riparian management (26.5%), and bank stabilization (12%) (Bernhardt et al. 2007) (Fig 1). However, despite the increase in river restoration projects, appeasing the stakeholders to maintain and gather resources for a given project is incredibly hard and ultimately very expensive. (Kondolf et al., 2007).

Channel stability is a complicated subject and there is a lack of tools to assist both consulting engineers and stakeholders to a better understanding of river geomorphologic processes. Models such as SWAT-DEG can provide insight and visualizations of such processes. Recent advances in web-based deployment and cloud computing allows SWAT-DEG's users to maximize time and minimize resources spent on a given project. As a result, SWAT-DEG becomes more accessible and scalable.

Engineers spend countless hours battling software installation, version control, and computer administration privileges before analyzing or furthering any project endeavors. SWAT-DEG avoids this by utilizing the internet, through www.eRAMS.com as a host. SWAT-DEG is now globally accessible with the added bonus of an online GIS-style interface. Using the internet or using your desktop both consumes your physical computer's resources, which does not allow the user to maximize his/her time. Thus, SWAT-DEG utilizes Cloud Services Innovation Platform (CSIP) (Lloyd et al., 2012), via www.eRAMS.com, to enable parallel computing and to eliminate using your physical computer's resources.

SWAT-DEG

SWAT-DEG is a modified version of SWAT (Arnold et al., 1998) that simulates stream down-cutting and widening and allows analysis of flow duration curves and cumulative stream power (Figure 1) (Allen et al., 1999). SWAT-DEG allows three variables to vary: bankfull depth, width, and slope, under a continuous simulation of discharge over a long period of time (50+ years) (Allen et al., 2008). SWAT-DEG's role in assessing stability of urban streams and more information on SWAT-DEG's methodology is outlined in Allen and others (2008). Simulating channel's down-cutting and widening allows for preparation of future costs (grade control) or allows prescription of necessary setbacks from the river corridor to protect public and private infrastructure. In addition, the ability to predict changes in channel morphology allow stakeholders to illustrate potential future changes in the river which should enhance support for funding on river restoration/rehabilitation projects.

The flow duration curve uses historical data to determine the percent of time a stream discharge value has been met or exceeded. The flow duration curve can then be used to derive a load duration curve from which Total Maximum Daily Loads (TMDL) can be derived (EPA, 2007). The advantage of SWAT-DEG over regression based FDC's is it can assess changes in watershed land use and or climate and therefore be used to anticipate future flow characteristics in urbanizing areas which in turn impact the channel's effective discharge and hyporheic processes (SWAT-DEG models low flow utilizing baseflow recession analysis). The sub-daily

time-step allows modeling bed material transport processes that daily time-step flow durations cannot address on smaller watersheds.

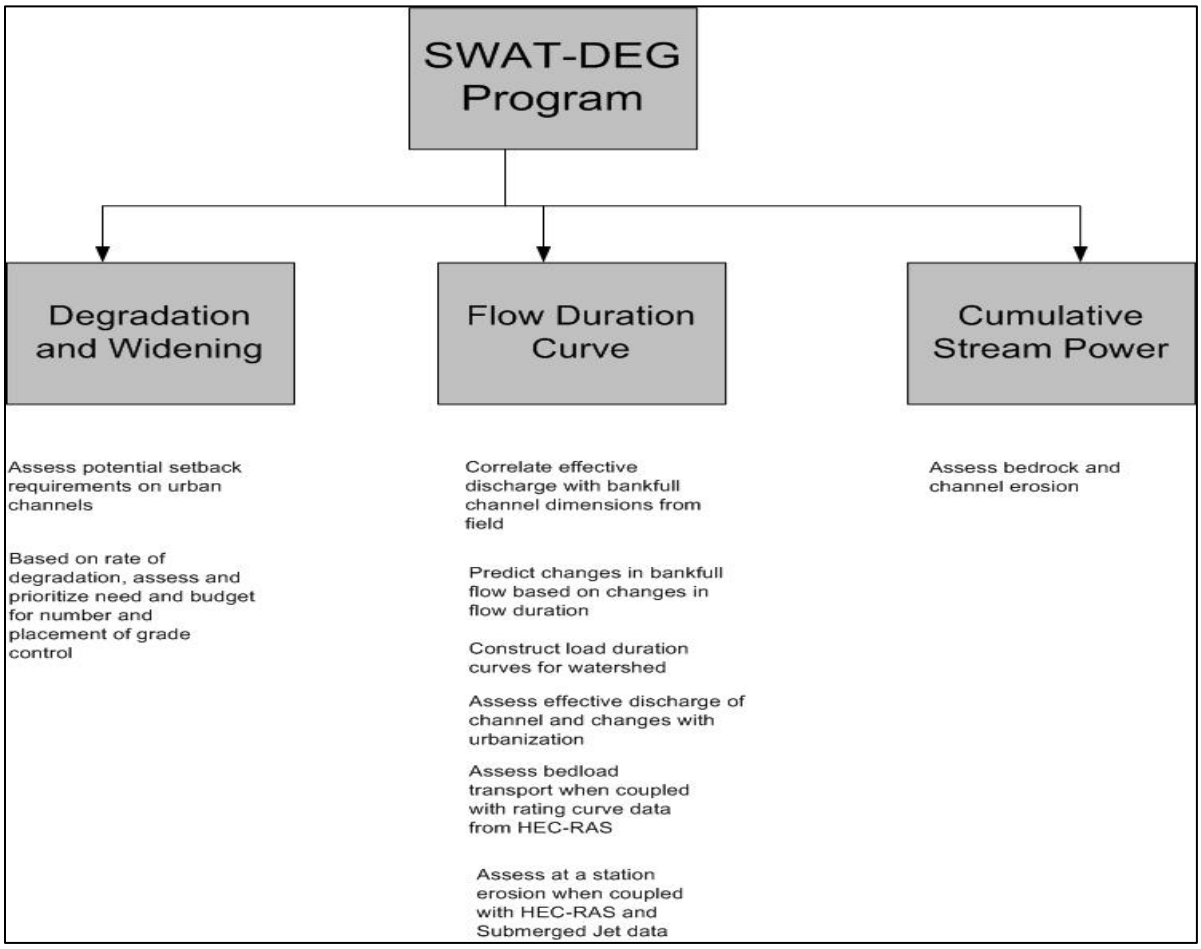

Figure 1: SWAT-DEG's output for stream assessment.

Web-based Deployment

Web-based implementation of SWAT-DEG provides benefits in several ways: 1.) enabling analysis with any device connected to the internet, 2.) minimizing desktop software, 3.) minimizing the time needed to gather input data, 4.) ability to demonstrate inputs and outputs to any stakeholder with internet access, 5.) provide a better comprehensive solution to the current project.

Any current browser (i.e. Firefox, Chrome, Safari) can access SWAT-DEG through the server Environmental Risk Analysis Management System (eRAMS) at www.eRAMS.com. Thus, the only software needed is a browser, and every web based device can utilize eRAMS' server. Furthering the user's benefits, eRAMS provides a centralized location for storing data, downloading data, and geospatial analysis (Figure 2). Downloadable databases include NCDC, USGS, SSURGO, STATSGO, STORET, and SNOTEL. Once the data is downloaded, the data can be stored for future reference, re-uploaded to eRAMS for use in different analytical models hosted by eRAMS, and manipulated via eRAMS' GIS interface.

Manipulation of GIS layers (raster, polyline, and polygon) and data extraction enhances SWAT-DEG's convenience to the users. After obtaining the results of SWAT-DEG, two other options are available that aid in project completion: scenario analysis and graphing capabilities.

After a project is established in SWAT-DEG, the user has the potential to manipulate the project to assess the impact of changes in climate and potential changes in the watershed's properties. As a result, SWAT-DEG's interface allows users to display the results in a readable and flexible format, via statistical analysis, timeseries, boxplots, and graphical analysis. If the outputs and graphing capabilities are not sufficient to make an informed decision, supplementary models, such as Complete Flow Analysis, Multi-Criteria Decision Analysis, Watershed Delineation Tool, Load Duration Curve, and Integrated Urban Water Management, are available on eRAMS.com. Thus, through the internet, the user has access to all the tools needed to deduce a solution that looks at both a broad and specific viewpoint upon the project. Unfortunately, running multiple applications consumes substantial central processing unit (CPU) resources; to circumvent this issue, eRAMS utilizes cloud computing via CSIP.

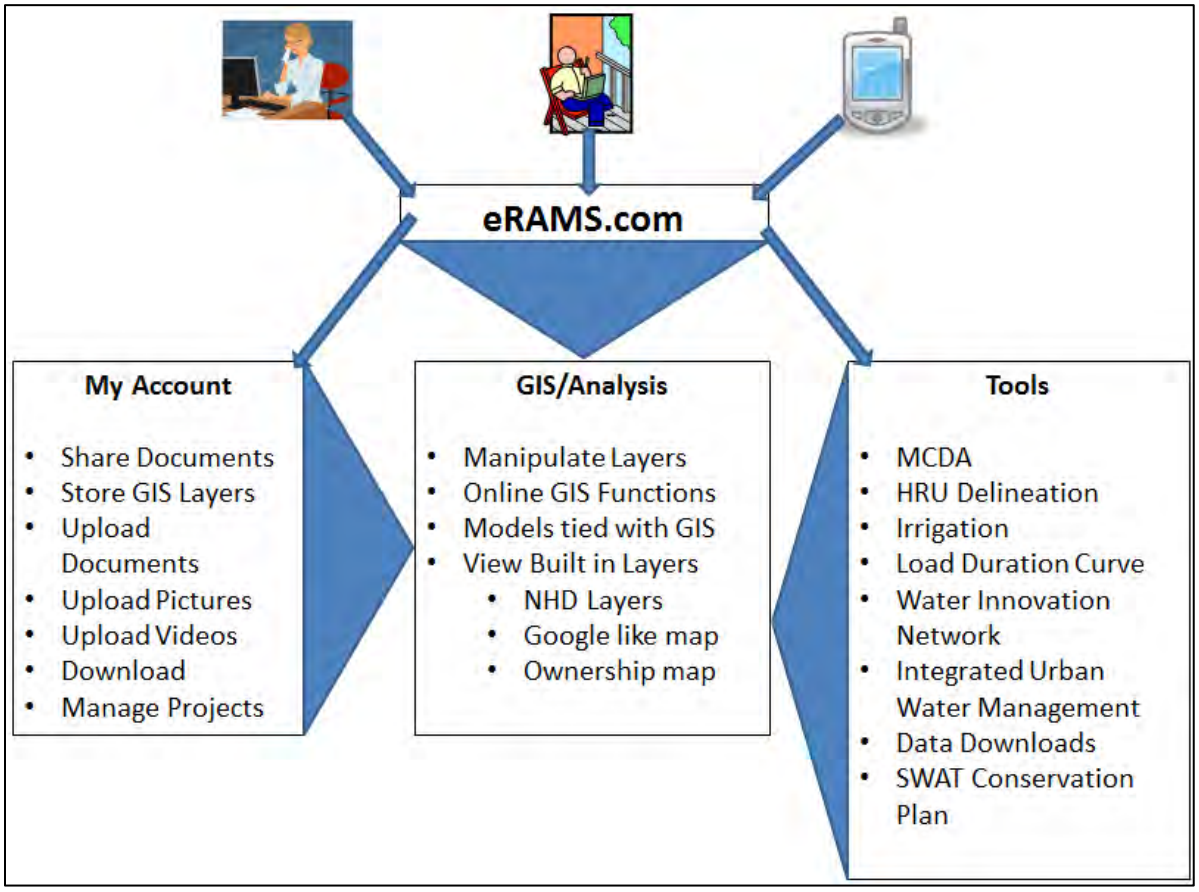

Figure 2: Flow Chart of Environmental Risk Analysis Management System

Cloud Deployment

Currently, most engineering models, such as SWAT-DEG, are run one at a time and run for one simulation at a time. Cloud computing enables parallel model runs and running multiple simulations without consuming much of the user's computer resources, relative to a desktop application (Figure 3). Cloud computing is a service oriented structure that enables models to

exist on a server created by a cluster of hardware in another location (Lloyd et al., 2012). SWAT-DEG and eRAMS utilize cloud computing through the infrastructure called Cloud Services Innovation Platform (CSIP) (Lloyd et al., 2012). CSIP takes inputs from the user and allocates all the model runs to different virtual machines (VM in Figure 3), on the eRAMS server, such that computation time is optimized. A virtual machine is essentially a virtual computer that read inputs, run the model, and returns outputs to the user. As such, all scenario runs and model iterations are on the eRAMS server rather than on a personal computer. When the model simulations are done, the user can use the interface to view and manipulate the results. In addition, if scenario analysis was utilized, the user can view and compare multiple scenarios against each other.

Time and resource constraints are greatly diminished by the use of cloud computing, via eRAMS. The user can run as many models as desired to discover unknown and uncertain properties of the current problem being analyzed. In addition, the user can use the results as instructive teaching materials for stakeholders or novice engineers to better understand river geomorphological processes.

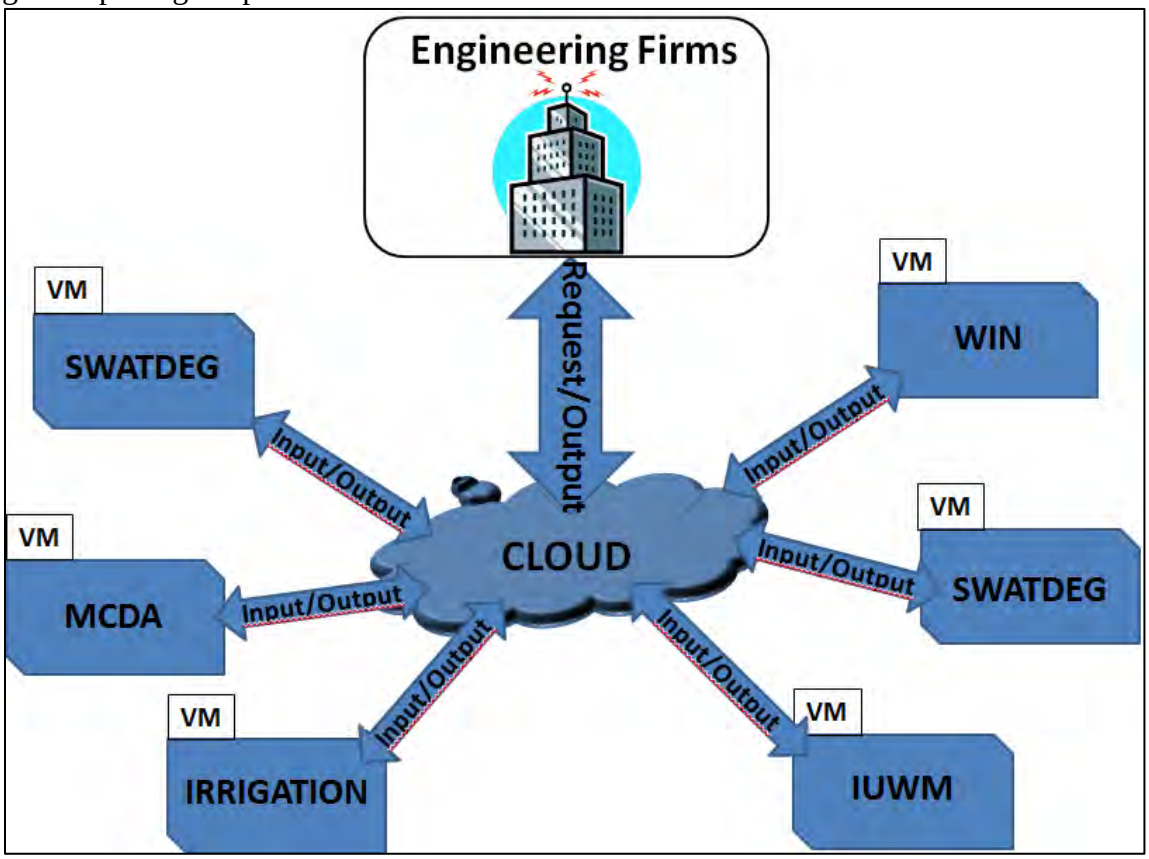

Figure 3: Cloud Services Innovation Platform (CSIP) interaction with a user. "VM" = Virtual Machine

Future of SWAT-DEG

SWAT-DEG will utilize CSIP, via eRAMS server, to decrease computational time for three modeling applications: 1.) running multiple deterministic runs, 2.) scenario analysis, 3.) uncertainty analysis for a given scenario (Figure 4).

Doing multiple deterministic runs or scenario analysis simply requires multiple input files, which are automatically generated by SWAT-DEG's interface. The only exception to automatic generation of input files is the input file containing climate data. After generating all necessary input files, SWAT-DEG will run in the background of the server while the user is free to do other work. After the user has established a scenario in SWAT-DEG, uncertainty analysis becomes an option.

Uncertainty analysis, via Monte Carlo Sampling Method, requires thousands of iterations to produce adequate results. Compounding the number of iterations needed is the amount of uncertain variables within channel stability analysis. The user chooses which parameters and their corresponding distribution to run uncertainty analysis on. SWAT-DEG automatically generates all the input files and sends them to CSIP. CSIP will now disperse the input files to different virtual machines such that the computational time is minimized. The same concept of dispersing simulations to different virtual machines can be translated to any model.

Any model, especially those that require a copious amount of runs or long computational times, can benefit from CSIP, via eRAMS. By deploying the models within CSIP the following benefits occur: 1.) minimization of the user's CPU resources, 2.) maximization of the user's time, 3.) maximization of simulations run. In addition, even if the benefits listed before are not applicable to a given model, the model should still exist in CSIP, since CSIP provides flexibility if the model's capabilities expands and there are no consequences for the user placing the model into CSIP.

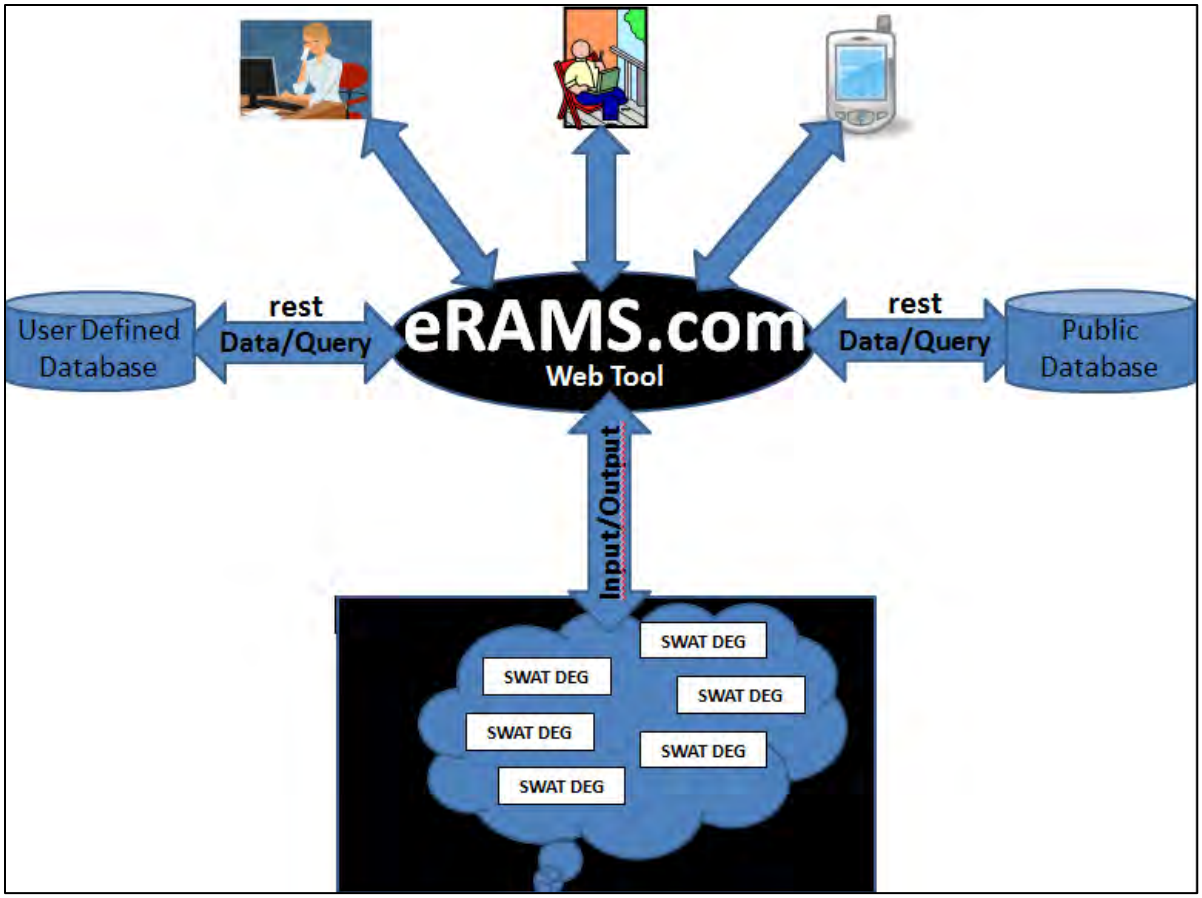

Figure 4: Interaction between CSIP, eRAMS, and SWAT-DEG

Conclusion

SWAT-DEG utilizes flow duration curves and simulation of widening and down-cutting to assist in channel stability evaluation. SWAT-DEG allows engineers and stakeholders to predict future costs, predict possible future events, teach river stability, and gain support and money for past, current, and future projects. SWAT-DEG, like any other model, usually requires installation and version control, but eRAMS eliminates both of these desktop limitations through CSIP. SWAT-DEG is now on the internet and is accessible to any user with internet access on any device. Model simulations require minimal use of the user's CPU resources. Thus, the web-based cloud deployment of SWAT-DEG frees the user's device for other needs.

Acknowledgements
This study was funded by the US Department of Agriculture-National Institute of Food and Agriculture (NIFA) grant number 2009-51130-06038.

References

Allen, P. M., Arnold, J. G. & Jakubowski, E. (1999) Prediction of stream channel erosion potential. *J. Environ. & EngngGeosci.* **5**, 339–351.

Allen P. M., Arnold J. G. & Skipwith W. (2008): Prediction of channel degradation rates in urbanizing watersheds, Hydrological Sciences Journal, 53:5, 1013-1029

Arnold, J.G., Srinivasan, R., Muttiah, R.S., Williams, J.R. 1998. Large area hydrologic modeling and assessment Part I Model development. *Journal of American Water Resources Association. (JAWRA),* 34(1): 73-89.

Bernhardt E. S., E. B. Sudduth, M. A. Palmer, J. D. Allan, J. L. Meyer, G. Alexander, et al. 2007. Restoring rivers one reach at a time: results from a survey of U.S. river restoration practitioners. Restoration Ecology 15:482–493. Christian-Smith, J. 2006. The politics

Bernhardt, E. S., M. A. Palmer, J. D. Allan, and the National River Restoration Science Synthesis Working Group (2005), Restoration of U.S. rivers: A national synthesis, Science, 308, 636 – 637.

EPA. 2007. An Approach for Using Load Duration Curves in the Development of TMDLs. Available at: http://water.epa.gov/lawsregs/lawsguidance/cwa/tmdl/techsupp.cfm. Accessed 23 June 2013.

Kondolf, G. M., Anderson, S., Lave, R., Pagano, L., Merenlender, A. and Bernhardt, E. S. (2007), Two Decades of River Restoration in California: What Can We Learn?. Restoration Ecology, 15: 516–523. doi: 10.1111/j.1526-100X.2007.00247.x

R. Seppelt, A.A. Voinov, S. Lange, D. Bankamp (Eds.) (2012): International Environmental Modelling and Software Society (iEMSs) 2012 International Congress on Environmental Modelling and Software. Managing Resources of a Limited Planet: Pathways and Visions under Uncertainty, Sixth Biennial Meeting, Leipzig, Germany. http://www.iemss.org/society/index.php/iemss-2012-proceedings. ISBN: 978-88-9035-742-8

Development of the SWAT-ICZ Model

Nikolaos P. Nikolaidis
School of Environmental Engineering, Technical University of Crete, University Campus, 73100 Chania, Greece, nikolaos.nikolaidis@enveng.tuc.gr

Johan Valstar
Deltares Soil and Groundwater Systems, Soil and Urban Groundwater, 3508 AL Utrecht, The Netherlands, Johan.Valstar@deltares.nl.

Edwin Rowe
Centre for Ecology and Hydrology, Environment Centre Wales, Bangor, LL57 2UW, UK, ecro@ceh.ac.uk.

Konstantia Moirogiorgou
School of Electrical and Computer Engineering, Technical University of Crete, University Campus, 73100 Chania, Greece, dina@display.tuc.gr.

Abstract

The 1D Integrated Critical Zone (1D-ICZ) Model links soil aggregate formation and soil structure to nutrient dynamics and biodiversity. The 1D-ICZ Model integrates models of: a) Flow and transport (Hydrus 1D); b) bioturbation; c) Chemical equilibrium, d) weathering (SAFE); e) C/N/P dynamics and soil structure, CAST; and f) Plant dynamics, PROSUM. The scientific advancement made through the development of the 1D-ICZ model is the rigorous simulation and quantification of the following soil functions: C, N and P sequestration in soils, simulated dynamically in relation to soil structure and organic matter protection; Biomass production, including effects of exudates and mycorrhizae on nutrient mobilisation and acquisition; C stocks in microorganisms, fungi and consumers, as an index of biodiversity; and Water transformations and filtration. To upscale the model to simulate catchments, we are using the hydrologic and geochemical model SWAT as a platform to incorporate the 1D-ICZ Model. Once SWAT has simulated the hydrologic cycle of the basin, water fluxes and storages from the soil and shallow aquifer for each Hydrologic Response Unit (HRU) are routed to the 1D-ICZ to simulate the nutrient and soil structure dynamics of the watershed. The SWAT-ICZ model can quantify the above soil functions at the catchment scale and will be used for Ecosystem Valuation analyses since it links inventory data to indicators representing critical soil functions.

Keywords: critical zone, soil functions, soil structure, watershed modeling.

Introduction

Soil structure has a strong influence on the physical, chemical and biological processes that take place within the soil. These processes have an influence on soil structure in return. Many of the feedbacks involved are described in literature and in more or less detailed process models, but the complex interactions among all the processes are rarely simulated.

The overarching SoilTrEC project research aim is the assessment of physical, geochemical and biological structure of soil from first principles. It is hypothesized that changes of soil parameters and soil functions can be quantified through process models which couple soil dynamics with soil structure, carbon (C) turnover processes and biodiversity. There is a particular focus on the development of soil aggregates. A further research hypothesis is that soil has a life cycle, meaning that it evolves from the parent material through different stages of development, modified by land management which result in the degradation of soil functions and the development of new soil from the regolith. Finally, it is assumed that the description of soil structure and processes provides a basis for quantifying soil ecosystem services within the soil life cycle, and that an economic valuation of these services is possible.

To test these hypotheses, a network of four European Critical Zone Observatories (CZOs) was formed to study soil processes and transformations from plot to catchment scale. A key conceptual advance of SoilTrEC is considering the entire life cycle of soil from soil formation to soil degradation that results finally in the loss of soil functions.

The 4 European CZOs represent key stages of soil development and degradation:

- The BigLink field station is located in the chronosequence of the Damma Glacier forefield in alpine Switzerland; the site is established to study the initial stages of soil development on crystalline bedrock;
- The Lysina Catchment in the Czech Republic with fairly productive soils managed for intensive forestry;
- The Fuchsenbigl Field Station in Austria as an agricultural research site with highly productive alluvial soils managed as arable land;
- The Koiliaris Catchment in Crete, a degraded Mediterranean region with heavily impacted soils during centuries through intensive grazing and farming, under severe risk of desertification.

The objective of this manuscript is to provide a brief description of the Integrated Critical Zone (ICZ) Model and outline the procedure that will be used for upscaling. The aim is to develop a tractable and defensible mathematical model that links soil aggregate formation and soil structure to nutrient dynamics and biodiversity. The 1D-ICZ Model is a combination of four sub-models:

- Flow, transport and Bioturbation model, HYDRUS
- Chemical equilibrium model and the SAFE weathering module
- C/N/P dynamics and structure model, CAST
- Carbon and nutrient elements in vegetation, PROSUM

Model Description

A brief description of the four sub-models included in the 1D-ICZ Model follows:

- **Flow, transport and bioturbation model, HYDRUS 1D -** The flow and transport model makes use of the model code Hydrus-1D (Šimunek et al, 2009).The model simulates the flow of water as well as heat and solute transport. A bioturbation model has been included, based on the procedure developed in the SoilGen model. Within a certain time step the model assumes that fractions of the solid and aqueous components are mixed within a soil layer to represent bioturbation by soil fauna.

- **Chemical equilibrium model and weathering, SAFE -** The chemical equilibrium model BRNS (Aquilera et al., 2005) was adapted to account for the effects of time-varying water saturation and exchange with the gas phase. The adapted code makes use of the SAFE chemical weathering module from ForSAFE (Wallman et al., 2005). The weathering components used within the weathering model are Ca^{2+}, Na^{+}, K^{+}, Mg^{2+}, Al^{3+}, H_4SiO_4, PO_4^{3-}. The chemical equilibrium constants used are obtained from PhreeqC (Parkhurst and Appelo, 1999; Krám et al., 1999). The following components are used in the model:
    - Aqueous phase: Ca^{2+}, Mg^{2+}, Na^{+}, K^{+}, H^{+}, Al^{3+}, Cl^{-}, SO_4^{2-}, HCO_3^{-}, OH^{-}, F^{-}, A^{3-} (organic anion), H_2CO_3, $CaCO_3$(l), $CaHCO_3^{+}$, $CaOH^{+}$, $CaSO_4$(l), $MgCO_3$, $MgHCO_3^{+}$, $MgOH^{+}$, $MgSO_4$, $NaSO_4^{-}$, $NaCO_3^{-}$, KSO_4^{-}, $Al(OH)^{2+}$, $Al(OH)_2^{+}$, $Al(OH)_3$, $Al(OH)_4^{-}$, AlF^{2+}, AlF_2^{+}, AlF_3, AlF_4^{-}, AlF_5^{2-}, $AlSO_4^{+}$, $Al(SO4)_2^{-}$, AlA, $Al(HA)^{+}$, HA^{2-}, H_2A^{-}, H_3A, NH_3 and NH_4^{+}
    - Cation exchange phase: $X\text{-}Ca^{2+}$, $X\text{-}Mg^{2+}$, $X\text{-}Na^{+}$, $X\text{-}K^{+}$, $X\text{-}Al^{3+}$, Surface–O^{-}, Surface-OH, Surface-OH_2^{+}, Surface-$OH_2SO_4^{-}$.
    - Solid phase: $CaCO_3$ (calcite), $CaSO_4$ (gipsum), $Al(OH)_3$ (Gibbsite)
    - Gaseous phase: CO_2 and NH_3

- **C/N/P dynamics and structure model, CAST -** The knowledge obtained from the review of current literature was synthesized to develop the conceptual model of soil critical zone functions (Nikolaidis and Bidoglio, 2013). In this conceptual framework, the transformations of organic matter have been linked with a dynamic model of soil aggregation/disaggregation, a simplified terrestrial ecology model that is comprised of mycorrhizal fungi, microorganisms (BIO pool), consumers and predators, and plant/root dynamics model. The representation of C pools with different turnover rates that is used in ROTH-C (Coleman and Jenkinson, 1999) was adapted to simulate the dynamics of C, N and P pools by using C:N:P ratios. The description of the CAST model has been presented in detail by Stamati et al., (2013). The HUM pool is enzymatically polymerized to produce light molecular weight organic nitrogen and phosphorous compounds which then are being mineralized to inorganic N and P. This model is driven by plant litter input and it is applicable to the top layer of the soil. Below the top layer, the input of OM is in the dissolved phase or obtained from root litter input and redistributed organic matter. The CAST model and a simplified mechanistic

N and P model were developed, based on current knowledge of the proposed mechanism in the relative scientific literature (Stamati et al., 2013; Pohlert et al., 2005, 2007).

- **Plant dynamics model, PROSUM -** PROSUM is a comparatively simple plant productivity module that was developed for inclusion in the 1D-ICZ model. The fixation of C by plants is a key process in soil formation. Plants affect soil in many ways, such as through the addition of leaf and root litter; by weathering, intercepting and recycling nutrient elements; by changing soil structure and water relations; and by providing energy for the soil microflora. Most commercial returns from land come directly or indirectly from plant products, and the management of vegetation has profound effects on soils. Thus a plant productivity module is an essential component of a model of soil processes and function that is usable for quantifying impacts on economic value. The PROSUM model is based on theoretical production ecology principles, and predicts the dynamics of key variables (e.g. above- and below-ground production of litter C and N; nutrient and water uptake) in response to key drivers (temperature; availability of light, water, CO_2 and the nutrient elements N, P, Ca, Mg and K; grazing and management events), for the wide range of vegetation types covered by the CZOs. Nutrient limitation essentially follows a Liebig minimum-element approach, but the model incorporates current understanding (e.g. Elser et al. 2007, **Rowe et al. 2008**) that plants avoid single-element limitation in part by manipulating nutrient availability. Mycorrhizal effects on nutrient acquisition are incorporated into PROSUM on the basis of soil volume explored, and root exudate fluxes are calculated for use in the weathering component of the 1D transport model.

All submodels are run by an overall main program. After initialization and reading the required input the main program runs the submodels sequentially using a mixed time-step algorithm. For the CAST, PROSUM, chemical weathering and bioturbation models, a fixed time-step of 1 month is used. The model of water and solute flow and transport uses a variable time step. At the start of each month, the amounts of water and nutrient elements in each layer that are available for plant growth are calculated within the flow and transport model. Chemical weathering is added to the nutrient fluxes, and then interactions with organic matter are calculated by CAST, which can result in net mineralization or immobilization. The resultant nutrient fluxes are considered to be available for plant growth. Next, PROSUM calculates nutrient uptake and fluxes of C and nutrients to the soil in surface litter, root litter and exudates. At the end of the PROSUM calculation, the production and consumption rates of water and all solutes during the month are known. Then, a number of variable time-steps for the flow and transport model is performed until the time of 1 month has been simulated. The last time-step of the flow and transport model is adapted as necessary. Solute production and consumption rates are multiplied by the current time-step size, and the water content and solute concentrations are updated accordingly. After each flow and transport model time-step, a chemical equilibrium model is run in order to determine the division of the chemical components between mobile (dissolved) and immobile (precipitated or adsorbed) phases. At the end of the month, the bioturbation model is run. Finally, the chemical concentrations are equilibrated again and the calculation continues with the next month.

In order to upscale the model to simulate basins, we evaluated various modelling platforms and decided to utilize the hydrologic and geochemical model SWAT as the platform that will

incorporate the 1D-ICZ Model (Neitsch et al., 2002; Arnold et al., 1998; Baffault and Benson, 2009; Debele et al., 2008). Once the SWAT model has simulated the hydrologic cycle of the basin, the flows in and out from all layers of the unsaturated zone for each Hydrologic Response Unit (HRU) of SWAT will be routed to the 1D-ICZ to simulate the nutrient and soil structure dynamics of the watershed.

Model Results

The developed 1D reactive transport model code was tested on a soil profile of 1 m length with model layers of 1 cm thick for a simulation period of 1 year. The soil profile was a homogeneous sandy clay loam. The van Genuchten parameters that describe the dependence of the water pressure, the water saturation and the hydraulic conductivity were obtained from the soil catalog of Hydrus-1D: residual soil water content is 0.1; saturated soil water content is 0.39; the saturated hydraulic conductivity is 0.3144 [m day^{-1}]; the pore connectivity parameter is 0.5. The parameters α and n in the soil water retention curve are 5.9 [m^{-1}] and 1.48 respectively. At the top of the soil profile the precipitation, potential evaporation and the temperature were prescribed as boundary conditions. The lower boundary condition was chosen as a free drainage boundary condition. Bioturbation was assumed for the upper 30 cm during the first month where 10% of the soil and solutes was mixed and redistributed**.**

Figure 1 presents the vertical distribution of the solute concentrations at various times during the simulation. The model simulated the water content, temperature, pH, 41 solute species, exchange reactions, weathering of K-feldspar and the solid phases of calcite, gypsum and gibbsite. A 1D reactive transport model was built and successfully applied on a simplified synthetic case study. The model code is flexible as it already combines a transport with a chemical equilibrium, weathering and bioturbation in one single model.

The PROSUM model was set up to simulate growth of a plantation of spruce, *Picea abies*, at the Lysina Critical Zone Observatory. Climatic data were obtained from the Czech Geological Survey (Anna Lamacova, pers. com.). Nitrogen and phosphorus availability were set to give half of the maximum growth without any nutrient limitation, and Ca, Mg and K were assumed not to limit growth. The model was calibrated by adjusting litterfall rates, to reproduce stocks of leaf, wood and litter C observed in 2008 in a 36 year old stand: 3.0 t leaf C ha^{-1}, 58.6 t wood C ha^{-1} and 6.1 t root C ha^{-1} (Figure 2a) . The model was broadly able to reproduce observed stocks of N (Figure 2b). The development over time of C pools in leaf, wood and root biomass as well as the distributions within the soil profile of roots and mycorrhizae, and of surface and below-ground litter inputs, were simulated. Simulated growth (i.e. carbon fixation) in a given month is set according to the most-limiting resource. In the Lysina simulation, growth was limited by temperature from November to April, by phosphorus availability from May to August, by water availability in September, and by light availability in October. The PROSUM model was designed to cover a wide range of vegetation types and management practices.

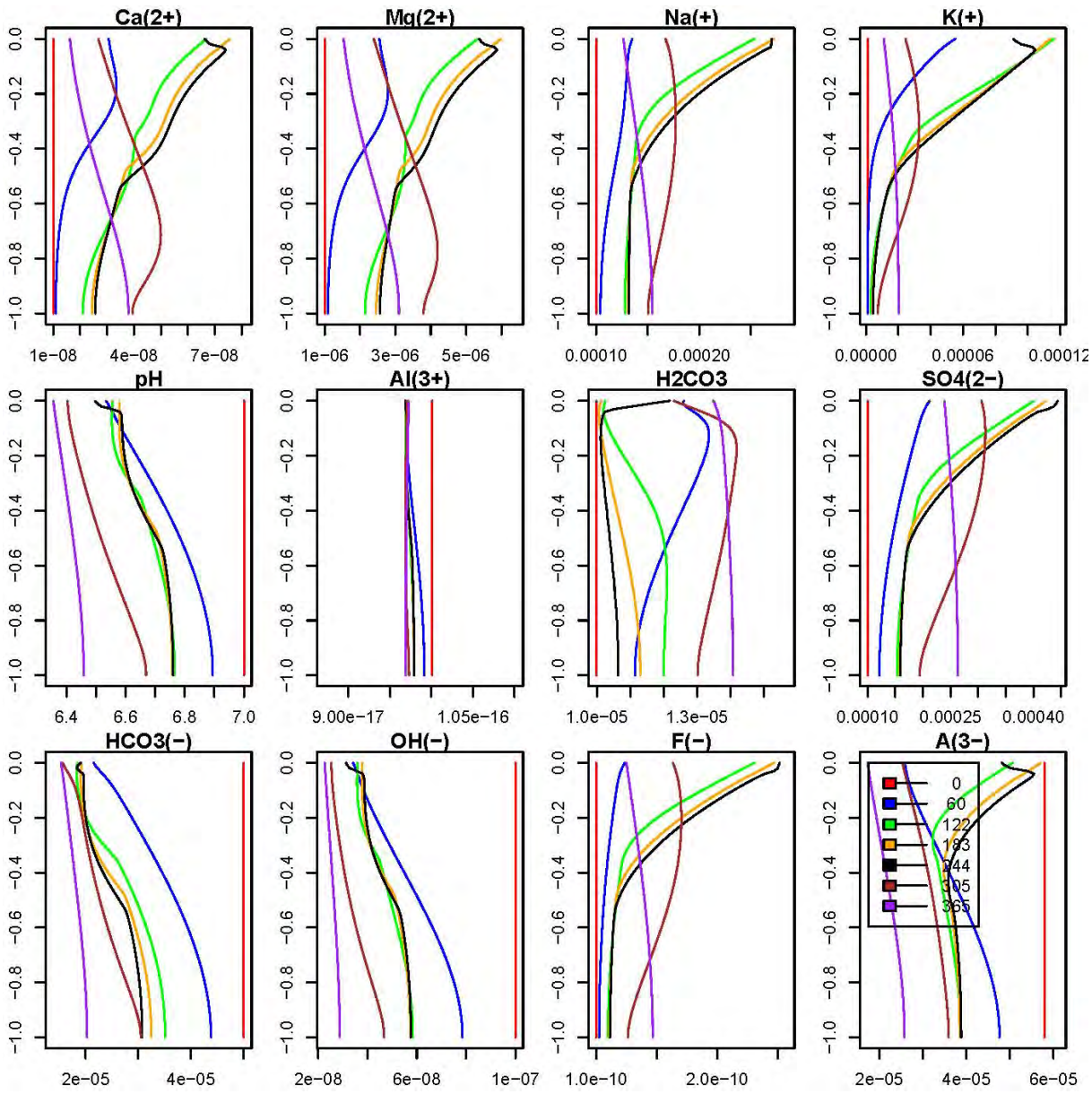

Figure 1. Solute concentration profiles as function of depth at various times.

The CAST model was used to simulate a change in a Greek agroecosystem from cultivated to set-aside conditions for 35 years and then a return to cultivation with carbon additions at 10% of the set aside rates. Figure 3 depicts the results of the simulation: a) the soil Water Stable Aggregate distribution; b) the soil organic carbon stock distribution in the various size aggregates. The CAST model was able to capture both water stable aggregate distribution and the carbon content fractionation very well.

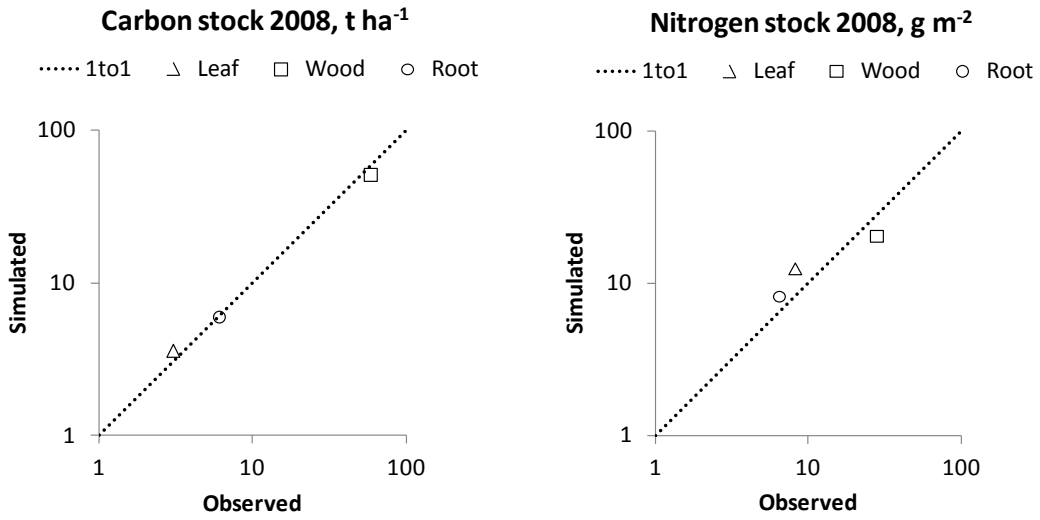

a) b)

Figure 2. Observed stocks in wood, leaf and root of: a) carbon, tonnes ha^{-1}; and b) nitrogen, g m^{-2}, in a *Picea abies* stand at Lysina CZO, 38 years after planting in 1972, versus stocks as simulated by the PROSUM model.

Litter fragmentation to coarse POM exhibited turnover times of 0.12 years in Greece. Litter fragmentation due to earthworms, nematodes and other small fauna is facilitated by coarser texture. The turnover time of fragmentation of coarse macro-aggregated POM was 3.5 years for the DPM pool and 17.7 years for the RPM pool. The turnover time for the litter and for non-aggregated, decomposition-resistant POM was 5.8 years, while macro-aggregation resulted in doubling the protection period (11.8 years).

Coarse decomposable plant material (DPM) contained in macro-aggregates turned over more than 3 times more slowly (0.6 years) than non-aggregated coarse DPM (0.2 years). The fine DPM within both macro and micro aggregates exhibited 2 times slower turnover (1.2 years) compared to the relative coarse macro-aggregated POM. The turnover time of the silt-clay related C (humus) of micro-aggregates within macro-aggregates (841.8 years) was 1.5 times higher than the silt-clay sized aggregates within macro-aggregates (570.3 years). Finally, the calibrated turnover of the biomass carbon pools was the same in all fractions and estimated to be 2.9 years.

The turnover time for macro-aggregation with no limiting factor was found to be 2.9 years. Similarly the micro-aggregation inside the macro-aggregates exhibited turnover time of 8.8 years. The macro-aggregates formed contained 30% C that was associated with the silt-clay fraction and 30% C associated with the micro-aggregate fraction. The formed micro-aggregates inside the macro-aggregates exhibited 23.4% fine POM content. The soil system reaches a maximum macro-aggregation after about 7 years. The limiting factor for macro-aggregation is the availability of the silt-clay fraction. The sum of C related with the macro-aggregate fraction and the free coarse POM is stabilized to a steady-state C content. Macro-aggregate disruption takes place after this period from January to April presenting a consistent seasonal pattern. Total SOC after this period increases due to the increase of micro-aggregates, indicating that maximum physical protection capacity for SOM is determined by the maximum micro-aggregation, which is in turn, determined by clay content and type. Macro-aggregate destruction takes place when

macro-aggregates contain lower than 0.15% DPM. The CAST model provided a rigorous simulation and quantification of C and N sequestration in soils in a dynamic way by relating it to soil structure and C/N protection.

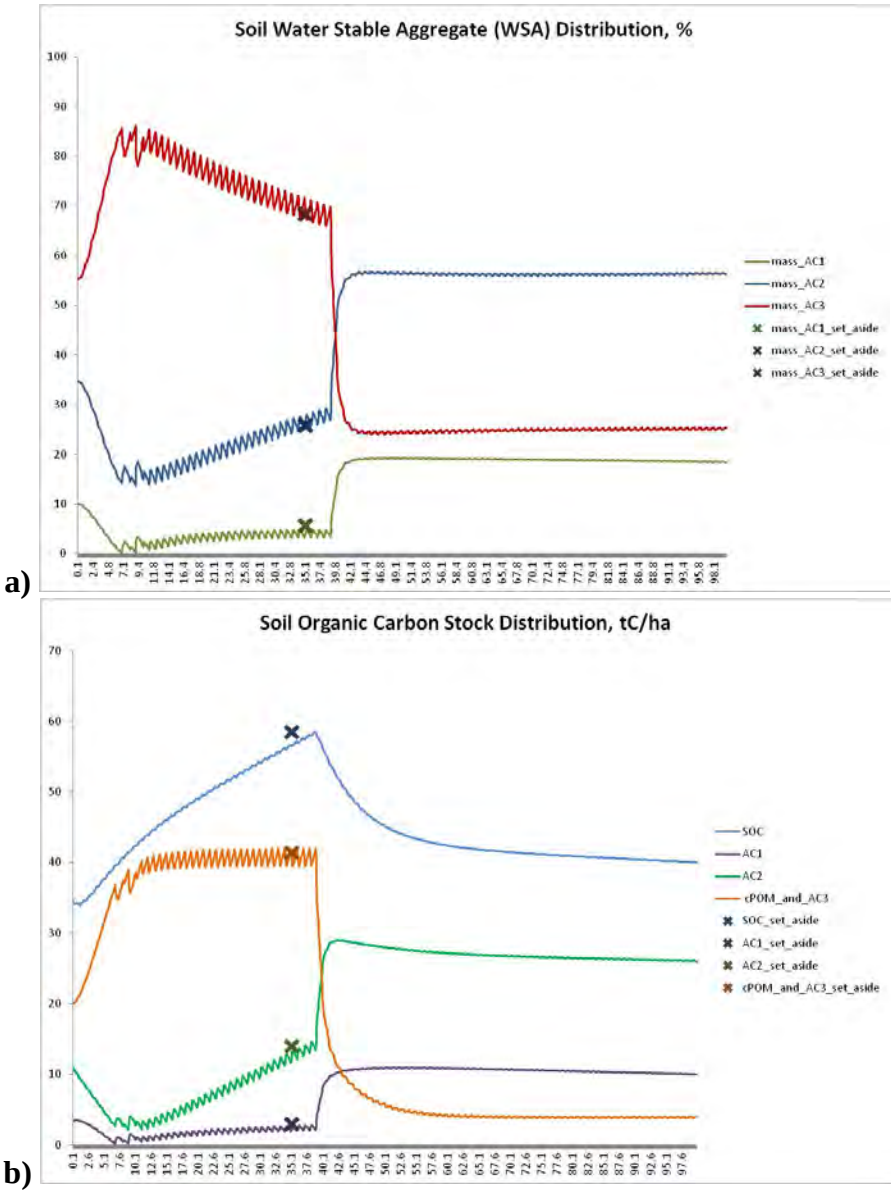

Figure 3. Simulation of a change in a Greek agroecosystem from cultivated to set-aside (a form of fallow) conditions for 40 years and then return to cultivation with carbon application at 10% of the set aside condition. The graphs depict: a) the soil Water Stable Aggregate distribution; b) the soil organic carbon stock distribution in the various size aggregates.

Conclusions

The component modules used within the 1D-ICZ model were each developed with the aim of addressing key processes that are necessary for an integrated analysis of soil function. The scientific advancement made through the development of the 1D-ICZ model is the rigorous simulation and quantification of the following soil functions and ecosystem services:

- C, N and P storage in soils, a fundamental soil function which is simulated dynamically, including relationships between soil structure and organic matter protection;
- Biomass production including effects of mycorrhizae and exudates on nutrient acquisition;
- Quantification of C in microorganisms, fungi and consumers, as an index of soil biodiversity; and
- Water transformations and filtration and simulation of the weathering of base cations / nutrient elements.

In order to upscale the model to basin scale, the hydrologic and geochemical model SWAT will be used as the platform that will incorporate the 1D-ICZ Model. The combination of the 1D-ICZ model with SWAT further extends capacity to simulate soil function and ecosystem services through quantifying:

- Erosion and sediment transport
- Water regulation in floods and droughts

The SWAT-ICZ model can be used to quantify the above soil functions and ecosystem services at the watershed scale. The model provides an integral component of soil Life Cycle Assessments and Ecosystem Valuation Analyses since it can link inventory data to midpoint indicators of soil functions and services.

References

Aguilera D., P. Jourabchi, C. Meile, C. Spiteri, and P. Regnier, 2005. A Knowledge-Based reactive transport approach for the simulation of biogeochemical dynamics in Earth systems. Geochemistry, Geophysics, Geosystems, 6, Q07012, doi:10.1029/2004GC000899.

Arnold, J. G., Srinivasan, R., Muttiah, R. S. and Williams, Jr., 1998. Large-area hydrologic modeling and assessment: Part I. Model development, Journal of American Water Resources Association, 34**,** 73–89

Baffaut, C. and Benson, V. W., 2009. Modeling flow and pollutant transport in a karst watershed with SWAT, Transactions of the ASABE, 52, 469-479.

Coleman, K., and Jenkinson, D.S., 1999. RothC-26.3 – a model for the turnover of carbon in soil – Model description and users guide, IACR Rothamsted, UK.

Debele, B., Srinivasan, R., Parlange, J-Yves, 2008. Hourly Analyses of hydrological and water quality simulations using the ESWAT Model, *Water Resources Manage*ment, 23, 303-324.

Elser, J.J., Bracken, M.E.S., Cleland, E.E., Gruner, D.S., Harpole, W.S., Hillebrand, H., et al., 2007. Global analysis of nitrogen and phosphorus limitation of primary producers in freshwater, marine and terrestrial ecosystems, Ecology Letters, 10, 1135-1142.

Krám, P. , R. C. Santore, C. T. Driscoll, J. D. Aber, and J. Hruška, 1999. Application of the forest–soil–water model (PnET-BGC:CHESS) to the Lysina catchment, Czech Republic, Ecological modeling 120, p. 9-30.

Neitsch, S.L., Arnold, J.G., Kinry, J.R., and Williams, J.R., 2002. Soil and Water Assessment Tool. Version 2000. Theoretical Documentation. USDA-ARS, Temple, TX.

Nikolaidis, N.P. and G. Bidoglio, 2013. Soil Organic Matter Dynamics and Structure, Sustainable Agriculture Reviews, 12, 175-196.

Parkhurst, D.L., and Appelo, C.A.J., 1999. User's guide to PhreeqC (version 2)— a computer program for speciation, batch-reaction, one-dimensional transport, and inverse geochemical calculations, USGS, Water-Resources Investigations Report 99-4259.

Pohlert, T., Huisman, J.A., Breuer, L., and Frede, H.-G., 2005. Evaluation of the soil nitrogen balance model in SWAT with lysimeter data. In: Srinivasan, R., Jacobs, J., Day, D., Abbaspour, K. (editors), Proceedings of the 3rd International SWAT Conference, Zurich, Switzerland, July 11–15, 2005, pp. 496–508.

Pohlert, T., Huisman, J.A., Breuer, L., and Frede, H.-G., 2007. Integration of a detailed biogeochemical model into SWAT for improved nitrogen predictions—Model development, sensitivity, and GLUE analysis, Ecological Modelling, 203, 215–228.

Rowe, E.C., Smart, S.M., Kennedy, V.H., Emmett, B.A., and Evans, C.D., 2008. Nitrogen deposition increases the acquisition of phosphorus and potassium by heather *Calluna vulgaris*. Environmental Pollution, 155, 201-207.

Šimůnek, J., M. Šejna, H. Saito, M. Sakai, and M. Th. van Genuchten, 2009. The HYDRUS-1D Software Package for Simulating the One-Dimensional Movement of Water, Heat, and Multiple Solutes in Variably-Saturated Media versison 4.08 , Department of Environmental Sciences, University of California Riverside.

Stamati F., N.P. Nikolaidis, S.A. Banwart and W.E. Blum, 2013. A Coupled Carbon, Aggregation, and Structure Turnover (CAST) Model for topsoils, Geoderma (in review).

Wallman, P., Svensson, M.G.E., Sverdrup, H., and Belyazid, S., 2005. ForSAFE - an integrated process-oriented forest model for long-term sustainability assessments. Forest Ecology and Management, 207, 19-36.

.

Application of Soil and Water Assessment Tool (SWAT) and Visual Modflow to delineate the water logging areas– A case study in Parts of Rupen Basin of Mehsana District, Gujarat, India.

Ms.Darshana Rawal
Research Assistant, CEPT University, University Road, Navragpura, Ahmedabad-380009
rawalnet@cept.ac.in

Ms. Anjana Vyas
Professor, CEPT University, University Road, Navragpura, Ahmedabad-380009
anjanavyas@cept.ac.in

Dr. S.S.Rao
Professor, CEPT University, University Road, Navragpura, Ahmedabad-380009
ssrao1742@gmail.com

Abstract

Assessment of ground water resources of an area which requires proper identification and mapping of geological structures, geomorphic features along with sound information regarding slope, drainage, lithology, soil as well as thickness of the weathered zones. GIS has been found to be one of the most powerful techniques in assessing the suitability of land based on the spatial variability of hydro geological parameters. GIS offers many tools to extract the information about the ground water prospect of an area by integrating information regarding geologic structures, geomorphology, soil, lithology, drainage, land use, vegetation etc.

Gujarat is the seventh largest state of India, situating in the Western part of the country is largely an arid state for most of its part. In the hard rock terrain of Aravalli, ground water is the only source of water in the northern part of the Gujarat. Due to the combination of hard rock areas and the perched water table conditions occurring due to the occurrence of clay at very shallow depths in area of the Dharoi Command (RBC) in Mahesana District of the Gujarat state particularly in Kheralu Vadnagar, Visnagar and Unjha Talukas have water logging conditions. The objective of this work is to understand the hydrogeology of the terrain and its influence in ground water recharge and then to develop an appropriate ground water recharge -forecast model using Visual Modflow and SWAT and recharge capacity of injection wells is estimated by in study area to recharge the water from water logged area to the lower aquifer.

Key Words : Ground Water Recharge, GIS, Geological Structures, Geomorphic

Introduction

Assessment of ground water resources of an area requires proper identification and mapping of geological structures, geomorphic features along with sound information regarding slope, drainage, lithology, soil as well as thickness of the weathered zones. Amongst the latest available technologies, the remote sensing technique has acquired the supreme position over the conventional methods in studying the hydrogeology due to its synoptic view, repetitive coverage, and high ratio of benefit to cost and availability of data in different wavelength ranges of the electromagnetic spectrum. Through digital image processing of the remotely sensed satellite images, the controlling features of ground water can be identified accurately and thus the terrain can be classified properly in terms of ground water potentiality and prosperity. Geographic Information System (GIS) has been found to be one of the most powerful techniques in assessing the suitability of land based on the spatial variability of hydro geological parameters. GIS offers many tools to extract the information about the ground water prospect of an area by integrating information regarding geologic structures, geomorphology, soil, lithology, drainage, land use, vegetation etc.

Gujarat is the seventh largest state of India, situating in the Western part of the country is largely an arid state for most of its part. In the mountainous hard rock terrain of Aravalli, ground water is the only source of water in the northern part of the Gujarat. A part of Northern command of Dharoi command area falls in hard rock areas while the lower and southern portion fall in alluvial areas. Due to the combination of hard rock areas and the perched water table conditions occurring due to the occurrence of clay at very shallow depths in area of the Dharoi Command (RBC) in Mahesana District of the Gujarat state particularly in Kheralu Vadnagar, Visnagar and Unjha Talukas have water logging conditions. The objective of this work is to understand the hydrogeology of the terrain and its influence in ground water recharge and then to develop an appropriate ground water recharge - forecast model using Visual Modflow and Soil and Water Assessment Tool (SWAT).

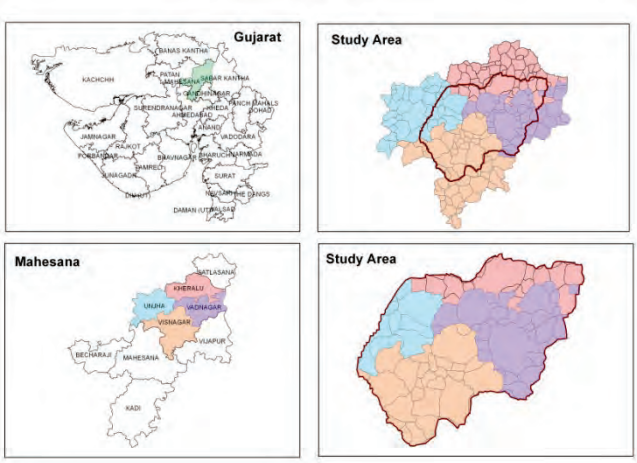

The study includes

- Delineation the aerial extent of the perched aquifer
- Study the geohydrological characteristics of perched and deeper aquifer system.
- Quantify the ground water withdrawal and recharge input potential of layered aquifer system.
- To develop a mathematical model of the area using Visual Modflow and SWAT

Physiography

The Study has a diverse landscape. It is characterized by hilly upland in the northeast, followed by piedmont zone with shallow alluvium and residual hills/inselbergs, and rolling to gently sloping vast Alluvial-Eolian plain.

The elevation in the Study ranges from less than 95 meters in the south-western part, and 194 meters above mean sea level (AMSL) in the north-eastern part. The master slope is towards southwest. The higher elevations in the study are attained by hills in the northwest. The Degital Elevation Model and the study area is shown below.

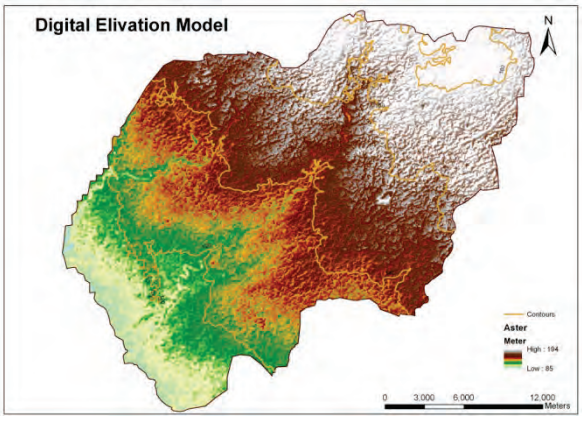

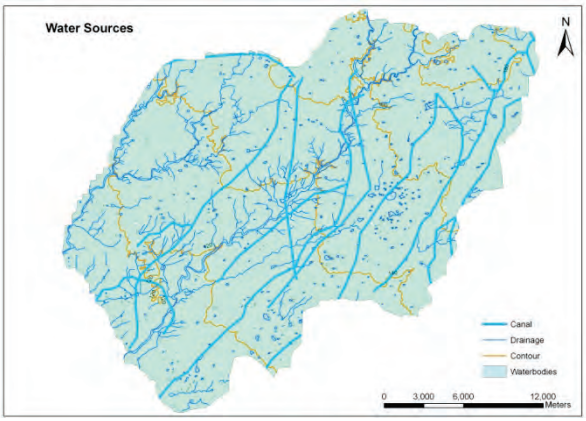

Major part of the Study area is underlain by post-Miocene alluvium and older sedimentary formations. These sediments mainly consist of fine to coarse-grained sand, gravel, silt, clay, clay stones, siltstones and grit. Thickness of alluvium gradually increases from piedmont zone in the northeast towards west and southwest. Maximum thickness of alluvium in the district is estimated to be about 550-600 m in the central part.

Occurrence and Movement of Groundwater

Ground water occurs both under phreatic and confined conditions in arenaceous horizons within sedimentary. The occurrence and movement of ground water is mainly controlled by

inter-granular pore spaces. Two major aquifer units identified within the explored depth have been described in detail in the “Aquifer Systems”.

Ground water is extensively developed by dug, dug-cum-bored and tube wells in areas underlain by alluvium. Depth of dug and dug-cum-bored wells ranges from 5 m to 65 m below ground water level whereas depth to water level, in general, varies from 10 to 20 m below ground water level. Deeper water table, between 20 and 32 m below ground water level, however, is observed in the central part, south of Saraswati river, and in the eastern part. In such areas, the dug section of the wells is generally dry and ground water is extracted directly from the bores and/or tube wells that generally tap deeper aquifers. Depth to water level in phreatic aquifer is shallow, less than 10 m, in command areas of Dharoi covering parts of Patan and Kheralu, Visnagar, Mahesana talukas. Also in entire south-western part, where ground water is saline, water levels are shallow. In such areas dug wells are rare and/or located in or vicinity of ponds. Ground water development using dug wells and/or shallow bore wells in phreatic aquifer is limited because of salinity in major part, deep water levels and limited saturated water column and/or meager yields in some areas also to some extent presence of high yielding deep aquifers. Such areas are confined and localized in parts of Kheralu. The yield of wells is generally low to moderate and ranges from 200 to 800 m3/day for 3 to 5 m drawdown.

The tube wells are the main groundwater withdrawal structures in the district and range in depth from 60 to 350 m. Shallow tube wells (<100 m) are restricted to the alluvial area in the northeast, mainly in parts of Kheralu and Vijapur talukas. In the central, south-western and southern parts, deep tube wells tap one or more aquifers. The depth to piezometric surface of deep confined aquifers ranges from near surface in the south-western part to more than 120 m bgl in the central part. The discharges of tube wells vary from 20 to 60 lps for 8 to 13 m of drawdown. The average yield of a 250 m deep tube well is around 20 lps. The transmissivity of deeper aquifer varies from 300 to more than 1200 m2/day. The panel diagram shown indicates the aquifer configuration in the area.

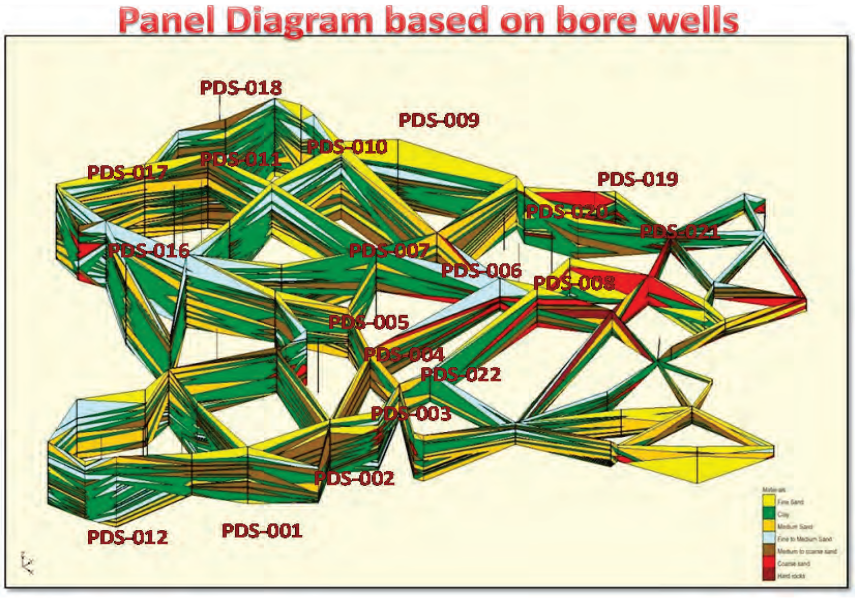

Soil and Water Assessment Tool (SWAT)

The SWAT Model is the latest software that is used to showcase the total water inflow and outflow from any watershed . It also indicates the sedimentation rates, the pollution rates on daily, monthly basis. But it requires very rigorous information on various parameters like Digital Elevation Model (DEM), Land use and land cover map and soil map along with daily rainfall, temperature, relative humidity, wind velocity etc. The SWAT is used to estimate the total water balance of the area including surface flow, groundwater flow and evapotranspiration and Visual modflow is used to estimate the quantity of groundwater, its direction and the likely area of water logging.

The study area includes a watershed consisting part of Rupen river basin, in Mehsan district, Gujarat, India, which is shown below. The watershed is used for SWAT model and the outer boundary is used for Groundwater model development using Visual Modflow. The variation is as per requirement of the study.

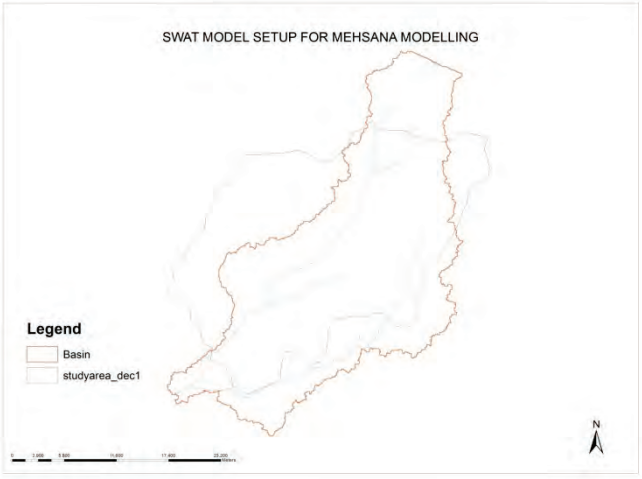

The results of SWAT analysis is shown below

The details are given below.

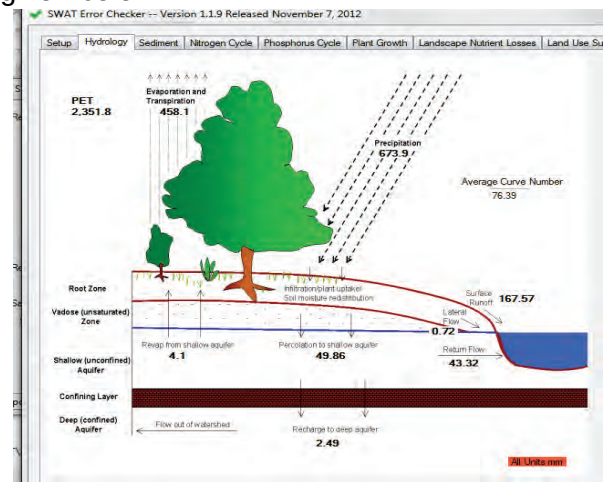

AVERAGE ANNUAL BASIN VALUES		
	mm	Percentage
PRECIP =	673.9	
SURFACE RUNOFF Q =	167.57	24.87
LATERAL SOIL Q =	0.72	0.11
GROUNDWATER (SHAL AQ) Q =	43.32	6.43
GROUNDWATER (DEEP AQ) Q =	0	0.00
REVAP (SHAL AQ => SOIL/PLANTS) =	4.1	0.61
DEEP AQ RECHARGE =	2.49	0.37
TOTAL AQ RECHARGE =	49.86	7.40
TOTAL WATER YLD =	211.6	31.40
PERCOLATION OUT OF SOIL =	49.87	7.40
ET =	458.1	
PET =	2351.8	
TOTAL SEDIMENT LOADING T/Ha=	0.911	

As seen from the above table, the groundwater recharge in the area is about 7.4 % of the total rainfall.

Groundwater Model

Considering average recharge factor from SWAT, the groundwater levels, aquifer parameters like conductivity and Specific yield in the area, and other boundary conditions, the groundwater movement, the inflow and out flow from various aquifers has been estimated and demarkated the water logged area from 0 to 5 m during different seasons using Visual Modflow under Non Steady State condition for 365 days running period with monthly recharge values with variable pumping rates starting from July 1 during Kharif, Rabi and summer. The results of the same are given below.

Behaviour of water table contours

The actual initial water table contours and estimated from the model are compared to see whether the model is working correctly. If they match, it can be safely assumed that the results would be reasonably accurate.

It is seen that the estimated and actual initial water levels are compare very well.

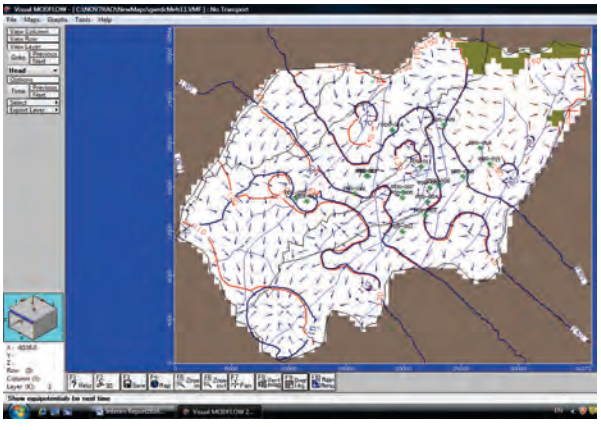

Figure : Actual initial water levels and predicted water levels

The model has been calibrated and it is found that the actual and observed water levels fall within the accepted levels of accuracy.

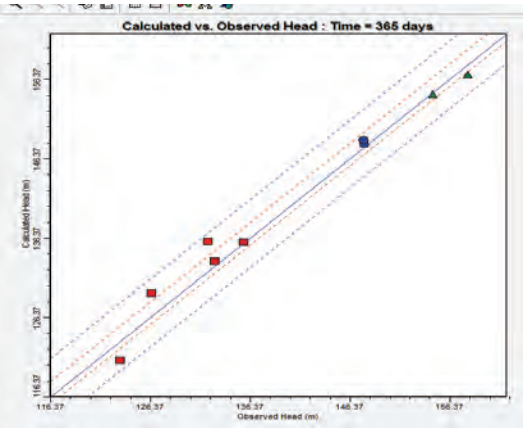

The inflow and out flow from different aquifers

The inflow and out flow from different aquifers is given below. It is seen that the second and third aquifer contribute to the total discharge in the area.There is no contribution for the deeper aquifer in the area.

Inflow	Outflow	Net flow
Zone 2 to 1 = 870520 m^3/day	Zone 1 to 2 = 855320 m^3/day	15200
Zone 3 to 1 = 432750 m^3/day	Zone 1 to 3 = 351860 m^3/day	80890
Zone 4 to 1 = 0 m^3/day	Zone 1 to 4 = 126.15 m^3/day	-126.15

(Zone 1- Unconfined aquifer, Zone 2- confined aq 1, Zone3- confined aqu3,

Zone 4, confined aq 4.)

Water Logging Conditions

In the South Western part of the study area, Flodding is taking place i.e, the water table elevation is more than the surface contours. This is mainly due to accumulated recharge in the area both by canal as well as downward groundwater flow. It also appears that the flow from out side the study area is also coming into the study area in these part causing the flood.

The water logged area is considered for different water levels 0 to 10 m, 0 to 7 m and 0 to 5 m mainly during Kharif (123 days). Accordingly the dewatering efforts can be made.

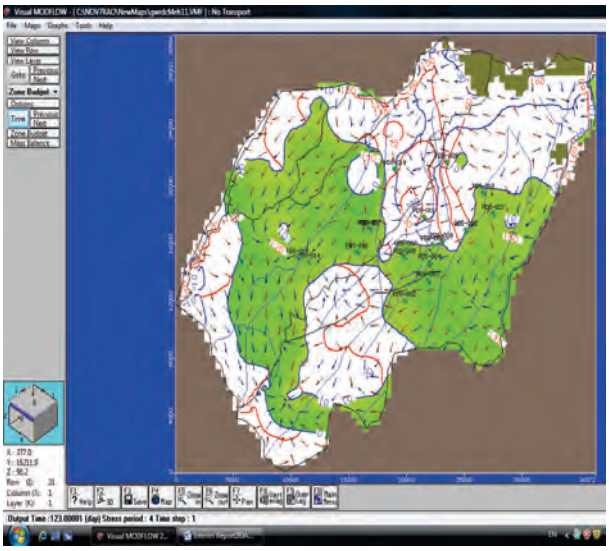

Figure 8 The water logged area from 0 to10

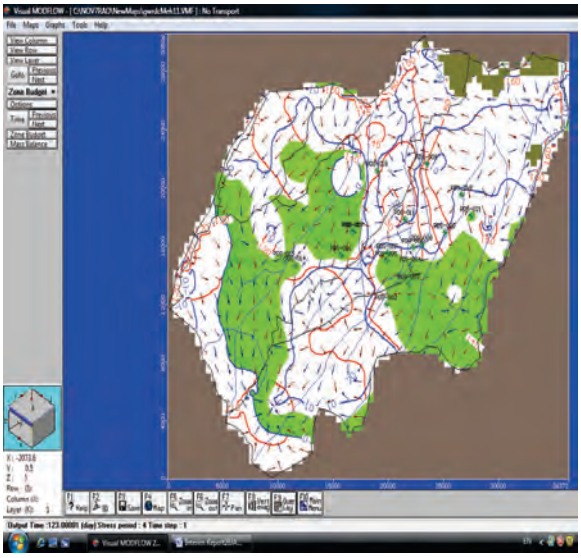

Figure 9 The water logged area from 0 to 7

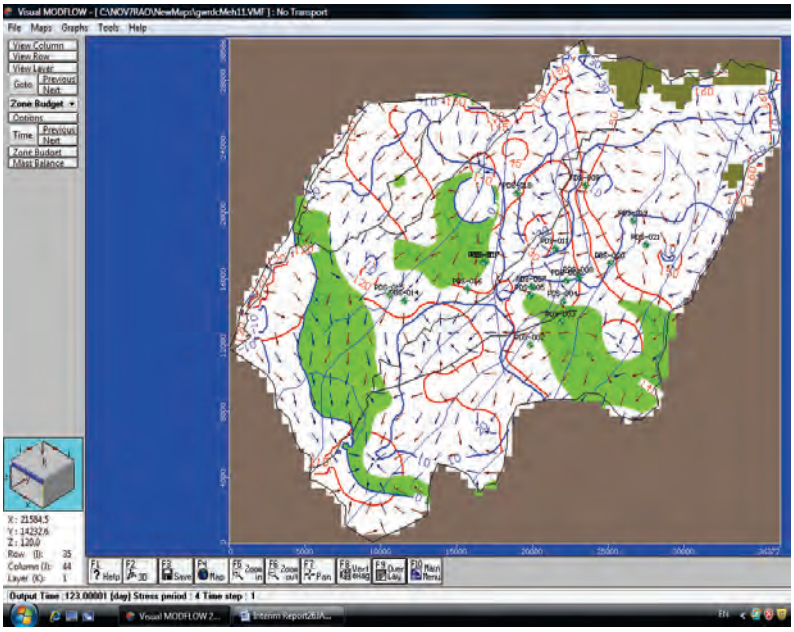

Figure 10 The water logged area from 0 to 5

Artificial Recharge in the water logging areas

Recharge from each well

The recharge from each well is considered based on the aquifer parameters and also the present depth of water level before recharge and after recharge. Considering dewatering upto a depth of 5 m, the recharge capacity of the wells in the area is about 2.34 lps which is about 202.27 m3 / day

Recharge Calculations

Water logging area for dewatering upto 5 m below ground level is(BGL) considered. About an area of 127 sq.km would be covered upto 5 m BGL. The recharge calculations for the same is given below.

Radius of influence of each well (r0- (m)	250	50 percent of 99 days of Rabi(50 days)	51533.29
Area of each well (sq.m) 3.14*r^2	196250	Total Recharge per year per sq.km-cum	125741.2
no of wells per sq.km	5	Total Recharge per year per sq.km-mcm	0.126
Recharge per sq.km per day (cum)	1030.666	Total Recharge area (sq.km)	127
Recharge per sq.km in monsoon (72 days)-cum	74207.94	Total No of wells	635
		Total Recharge (mcm)	80.01

Conclusions

The groundwater conditions in the study area is unique in the sense that on one side there exists the water logging conditions due to oversupply of water from canal and rainfall where very shallow aquifer thickness conditions exist, while in other neighbouring areas, the water table and piezometric levels are very deep. In this paper an attenpt is made to study the overall water availability due to rainfall using SWAT model and then the groundwater movement in different aquifers is assessed using Visual Modflow and arrive at a solution of artificially recharging the aquifers in the water logged areas. It is seen that about 80 Million cubic meters(mcm) water can be recharged in the area by reducing the water table to 5 m below ground level. The average capacity of the injection well is in the order of 2.34 lps (Liters per second)

Refernces

1. Sharma & Gupta (1987) have studied the flow of groundwater through different aquifers in Mehsana by tritium study.
2. Simmers, 1988) has indicated the reduction of specific yields due to decline in water levels
3. Rushton & Tiwari, (1989) have studied the Regional studies of the Mehsana alluvial aquifer regarding the vertical flows and arrived at the conclusion that the vertical flow through clay zones are the ultimate source of most of the water that is pumped from the tube wells and that the horizontal flows account for about 5 % of the abstraction.
4. Bradley & Phadtare (1989) has studied the aquifers of Mehsana in detail.
5. Rushton (1990)has reviewed the Methods of estimating the quantity of water leaving the soil zone towards the deeper aquifer in the Mehsana aquifer
6. M.V.Patel (1992) has developed a mathematical model for determination of aquifer parameters in alluvial areas with special reference to Rupen Basin, Mehsana.
7. P.K.Majumdar(2008) has also modelled the water logging conditions of parts of Rupen basin
8. Majumdar, P. K., Sekhar, M., Sridharan K., Mishra, G. C.(2008)has conducted Numerical simulation of groundwater flow with gradually increasing heterogeneity due to clogging.
9. N. B. KAVALANEKARA , S. C. SHARMA & K. R. RUSHTON, Dec 2009 have studied the over exploitation of groundwater resources in Mehsana.
10. Columbia Water Centre 2011has conducted surveys to confirm that the groundwater crisis in North Gujarat is severe and likely to get worse
11. S.D.Dhiman& A.K.Kesari have studied groundwater modelling for Mehsana aquifers.

Building a meteorological data set as input for the SWAT model in order to simulate the extreme flood event which occured in the municipality of São Luiz do Paraitinga, São Paulo, Brasil, between 31/12/2009-01/01/2010

Fernanda Viana Paiva Arguello
CCST/INPE, São José dos Campos-SP, fernanda.arguello@inpe.br; viana_fernanda@yahoo.com.br

Laura De Simone Borma
CCST/INPE, São José dos Campos-SP, laura.borma@inpe.br

Diogenes Salas Alves
CCST/INPE, São José dos Campos-SP, dalves@dpi.inpe.br

Suelen Trindade Roballo
CCST/INPE, São José dos Campos-SP, suelenroballo@gmail.com

Abstract

In recent years, Brazil has figured among the countries with highest frequency and intensity of damages caused by extreme events of floods and droughts. Worldwide increase in disaster occurrence has been attributed both to a change in environmental conditions (increase in frequency and intensity of extreme events) as well as an increase in the overall population, especially in places considered as "risk areas". A high number of floods has been reported for the Southern and Southeastern regions of the country in recent years. The Brazilian Atlas of Natural Disasters - São Paulo volume, identified the largest number of flash flood events in the last two decades within this state, which occurred mainly during the months of December, January and February. This article presents the partial results of a research which aims to investigate the causes and the short, medium and long-term consequences of an extreme flood event which occurred in the municipality of São Luiz do Paraitinga, São Paulo, Brazil, between Dec, 31 2009 and Jan, 01 2010. We will use the SWAT model in order to identify the causes of this event (i.e., a meteorological or hydrological extreme event). This article presents the steps followed in order to obtain the meteorological data set for use as an initial input data for the model. Due to the lack of observational weather data set with extensive time series for the study area, we conducted a joint assessment of the various available data sources, such as: in situ stations, satellite data, reanalysis products and interpolated data. The steps followed to build the meteorological data set are presented here.

Keywords: disasters; SWAT model, flash flood event, meteorological data set.

Introduction

In recent years, Brazil has figured among the countries with highest relative frequency and intensity of damages caused by natural disasters. According to Guha-Sapir et. al. (2012), a total of 101 countries were affected by 332 disasters in 2011. Among these, the Philippines, United States, China, India and Indonesia were the most affected, with 31% of the total events. In this classification, Brazil figured 7th in the number of events, recording 8 hydrological disasters in 2011.

At the national level, the records of Natural Disasters were published in the Brazilian Atlas of Natural Disaster, developed by the Centre for Disaster Studies and Research of the Federal University of Santa Catarina (UFSC) in partnership with the National Civil Defense (BRAZIL, 2011). According to this Atlas, the period from 1990 to 2010 recorded a total of 31,909 disasters across the Brazilian territory, with 8,671 in the first decade and 23,238 in the second decade. Of this total, Sudden Floods and Flooding accounted for 21% (6,771 records) of occurrences. The Brazilian Atlas of Natural Disasters also quantified the number of victims involved in hydrological disasters. Sudden Floods accounted for 29.6% of the 96,220,879 people affected in the country, and have caused the most deaths in the last two decades. With regard to the distribution of disasters in the country, BRAZIL (2011) identifies Sudden Floods as the largest number of records: 452 instances in two decades, equivalent to 54% of total disasters in São Paulo state, which occurred especially during the months of December, January and February.

A typical case of Sudden Flood occurred in São Luiz do Paraitinga (São Paulo state) during New Year's Eve 2009/2010, with many material losses - almost complete destruction of the historic center of the city and thousands rendered homeless. According to Dias et. al. (2011), this flood event was associated with a significant increase in the discharge of the Paraitinga river, which, according to the Brazilian Department of Water and Energy (DAEE, 2012), reached 1000m^3/s, a value associated with precipitation events of return time of about 300 years. Rainfall data collected at a nearby weather station (Núcleo Santa Virginia station) registered 77.8 mm of total rainfall in December 31 and 200.2 mm in January 1st, and a cumulative monthly value of 1011.8 mm. These precipitation values resulted in a flooding period of 4 days in the center of the municipality, during the first days of January 2010 (DAEE, 2012).

In this context, a PhD thesis study is conducted whose goal is to use the SWAT (Soil and Water Assessment Tool) model to investigate the causes and short, medium and long-term consequences of extreme flood event occurred in the municipality of São Luiz do Paraitinga, SP, in the beginning of January 2010. We consider the SWAT model as an important tool for the development of this research. However, the shortage of rainfall data in the study area can hinder the understanding and analysis of the causes associated with this extreme event.

The present study aims to describe the diverse datasets available for the study area, such as *in situ* stations, satellite data, reanalysis products and interpolation of data, as a source of complementary meteorological data suitable for input to the SWAT model. Follows a description of the different steps performed for the evaluation of this data set.

Methodology

Study Area

The study area covers the Paraitinga River Basin (Figure 1), with an area of 2413 km ², located between the coordinates 22°43' and 23°22' South latitude, and 44°39' and 45°29' West longitude, which is partially located in the municipality of São Luiz do Paraitinga, plus 9 other municipalities belonging to the Paraíba Valley, São Paulo, Brazil.

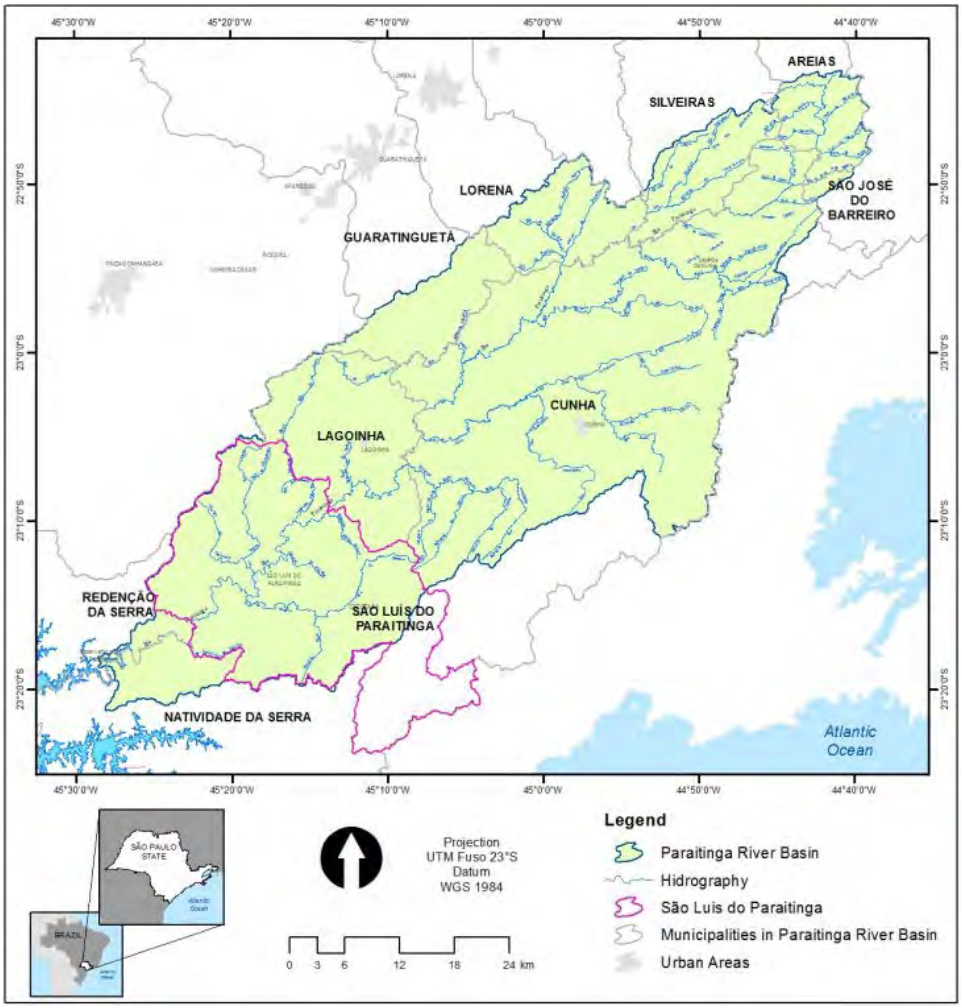

Figure 1 - Paraitinga River Basin (Arguello et al., 2013).

The confluence of the Paraitinga River with the Paraibuna River, where is currently located the reservoir of the Paraibuna hydroelectric plant, is the starting point of the Paraíba do Sul River, the main river in the southeast region of Brazil. The source of the Paraitinga River is located in the Serra do Mar, in the municipality of Areias, at about 1800 meters altitude.

The Paraitinga River Basin, inserted in the São Paulo stretch of the Paraíba Valley, consists partially of mountains and high altitude areas, which foster the formation of orographic

precipitation, influencing the distribution of precipitation in the region. According to Setzer (1966), the coastal plains experience precipitation events over 60mm in the driest month; in the region of the Paraíba do Sul River valley to the region of Queluz, rainfall has an annual variation between 1100mm and 1700mm, in the higher regions along the Paraíba do Sul River valley, total annual rainfall varies between 1300mm and 1700mm; between the escarpments of the Serra do Mar and the coastal plain, the driest month sees precipitation greater than 30mm; and in the higher points of the Serra do Mar and the Serra da Mantiqueira, rainfall varies between 1100mm and 1200mm annually.

Data acquisition

For the composition of the meteorological database, we conducted a survey of different meteorological data sources available for the study area and for the required period. We initially consulted the databases available observed by ANA (National Water Agency), DAEE (Department of Water and Power) and INMET (National Institute of Meteorology), presented in Table 1 (Arguello et al., 2013). The spatial distribution of these stations is shown in Figure 2.

Table 1. Availability of observational data.

Pluviometric stations	Source	Data Period	Location of the station relative to Paraitinga River Basin
E2-135	DAEE	1972-2010	Out
E2-132	DAEE	2000-2010	Inside
Ponte Alta	ANA	1971-2004	Out
São Luiz do Paraitinga	INMET	2007-2010	Limit
Meteorological Stations			
Campos de Jordão	INMET	1990-2010	Out
Taubaté	INMET	1990-2010	Out

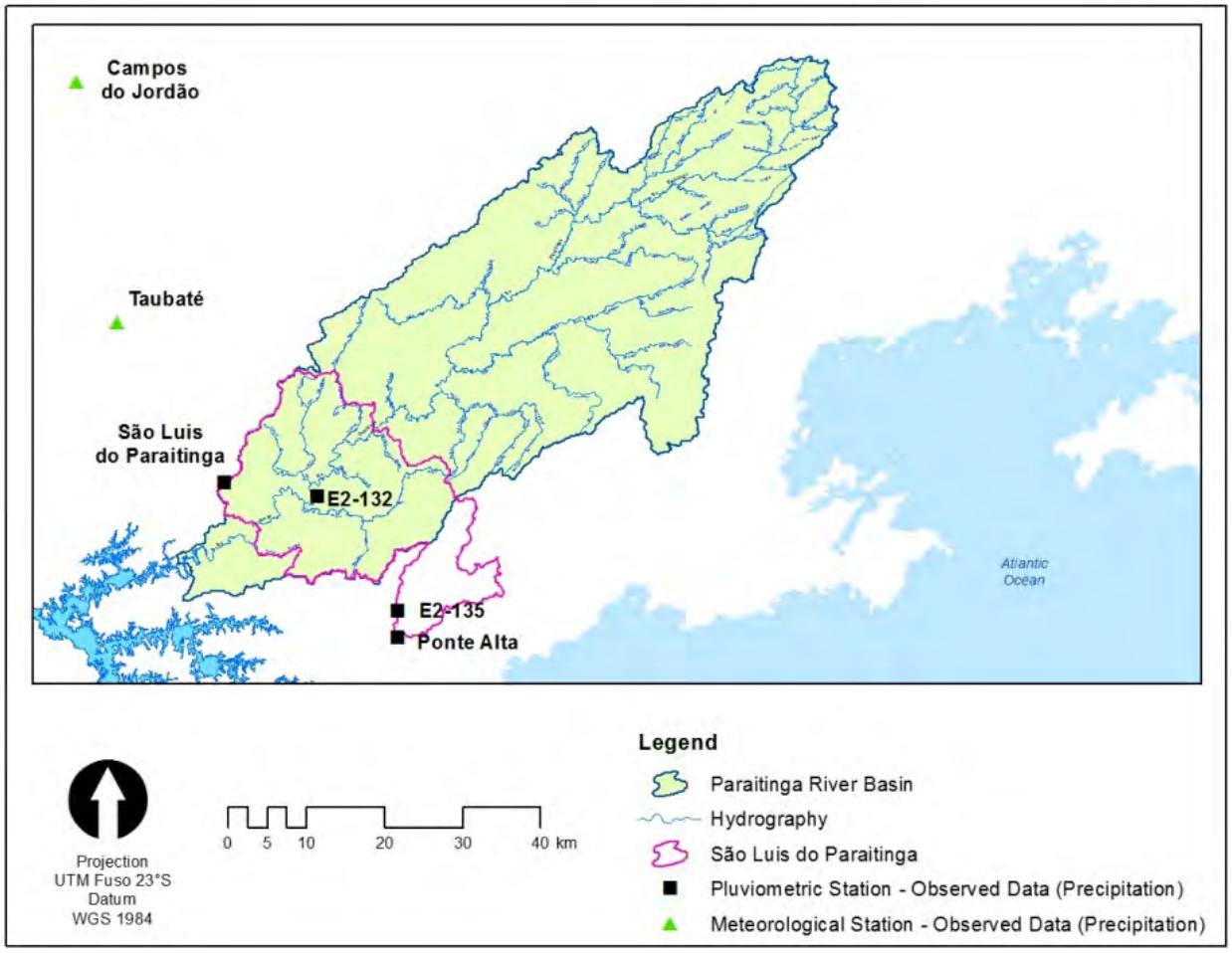

Figure 2-Spatial distribution of weather stations in the Paraitinga River Basin (Arguello et al., 2013).

For the 6 rainfall/weather stations presented in Table 1, we analyzed the data of 6 stations. Among these, 4 are classified as rainfall stations, providing only rainfall data and two weather stations (Campos de Jordão and Taubaté), which provided data for rainfall, temperature, humidity, evaporation, radiation, etc.

We also evaluated other types of data, such as data provided by the Global Precipitation Climatology Project (GPCP), which are obtained from estimates of satellite and surface station data-(Huffman et al. 1995; Huffman et al. 1997; Xie et al. 2003; Adler et al. 2003). GPCP data is available in a resolution of 2.5°x 2.5° latitude / longitude and can be obtained at http://www.esrl.noaa.gov/psd/data/gridded/data.gpcp.html.

Another source of data researched was the 3B42 satellite product from Tropical Rainfall Measuring Mission (TRMM). The TRMM project generates various products (estimates) obtained from the combination of instruments. The 3B42 product calibrates infrared (IR) data from the VIRS (Visible and Infrared Scanner) instrument, with precipitation estimates from TMI (Microwave Imager). The calibration parameters are applied to the IR daily data embedded in IR geosynchronous satellites. The estimates of the 3B42 algorithm are produced in three stages: 1) microwave-based precipitation estimates are calibrated with the parameters obtained from the

validation of PR x TMI found in the TCI (TRMM Combined Instruments) product, 2) precipitation estimates are created using the calibrated microwave IR precipitation, and 3) the IR and microwave estimates are combined. Estimates are available in grids of 0.25°x0.25° and temporal resolution of 3 hours, between the latitudes of 50ºN and 50ºS (Huffman et al., 2007).

The precipitation data obtained from the Hidroestimador, which uses data provided by the GOES (Geostationary Operational Environmental Satellites) infrared satellite from NOAA, in operation since 2002, were also evaluated in this study. This is an automatic method that uses an exponential empirical relationship between precipitation (estimated by radar) and the brightness temperature of the cloud tops generating precipitation rates in real time (Scofield, 2001; Scofield and Kuligowski, 2003; Saldanha et al. 2007). The Hidroestimador presents the best performance in the determination of precipitation from clouds with cold tops, considering the value of the brightness temperature of 241 K as the threshold for identifying precipitation. These data were provided by the Division of Environmental Satellite Center for Weather Forecasting and Climate Studies (CPTEC/INPE).

In addition to these data sources, we analyzed data interpolated by the Brazilian Research Network on Global Climate Change Network (Rede-Clima) from CPTEC/INPE. It uses available observational data from different stations in Brazil, which are interpolated by means of the inverse distance squared method, considering the effects of latitude and topography, which according to Lefevre et al. (2002) tend increase the accuracy of the interpolation.

Results

The scarcity of time series of rainfall and other meteorological variables, combined with the poor spatial distribution of the stations with observed data, highlighted the need for additional sources of meteorological data, presented above. However, the data provided by GPCP were discarded for this research, as due to their relatively coarse resolution of 2.5ºx2.5º, cover an area larger than the interest area. Besides, the monthly scale provided by this product is not suitable for studies of extremes events, like sudden floods. Also, the data provided by TRMM, with a resolution of 0.25ºx0.25º (˜ 25 km), despite being finer than the resolution of GPCP, is still not sufficiently refined to the space scale of interest in the present study.

Data obtained by Hidroestimador, whose resolution could be refined to a distance of 1 km, would attend the needs of this study. However, the region of São Luiz do Paraitinga is susceptible to the formation of orographic precipitation, which generally has very high precipitation rates and clouds with hot tops, making it impossible to estimate rainfall with the methodology applied in the Hidroestimador algorithm, preventing its use in this study. The limitations of the various data sources described above has led to the use of interpolated data from CPTEC/INPE, which will be used in complement to the results obtained from the observational station data, presented in Table 2 (Arguello et al., 2013).

Figure 3 presents the rainfall fields interpolated to 31, December, 2009 and 1st, January, 2010. These results were based on the interpolation data from a greater number of available stations, presented in Figure 4, allowing more cohesive rainfall input for the SWAT model.

Table 2. Maximum observed daily precipitation data.

	Maximum daily precipitation (mm)			
Pluviometric stations	**Period 2000-2010**	**Date of occurrence**	**31-01-2009**	**01-01-2010**
E2-135	205,5	26-01-2005	81,2	104,5
E2-132	90,0	12-02-2006	No data	No data
Ponte Alta	67,9	02-01-2001	No data	No data
São Luiz do Paraitinga	64,9	21-12-2008	11,0	56,0
Meteorological Stations				
Campos de Jordão	108,4	25-05-2005	44,4	45,4
Taubaté	121,2	24-11-2004	10,4	56,8

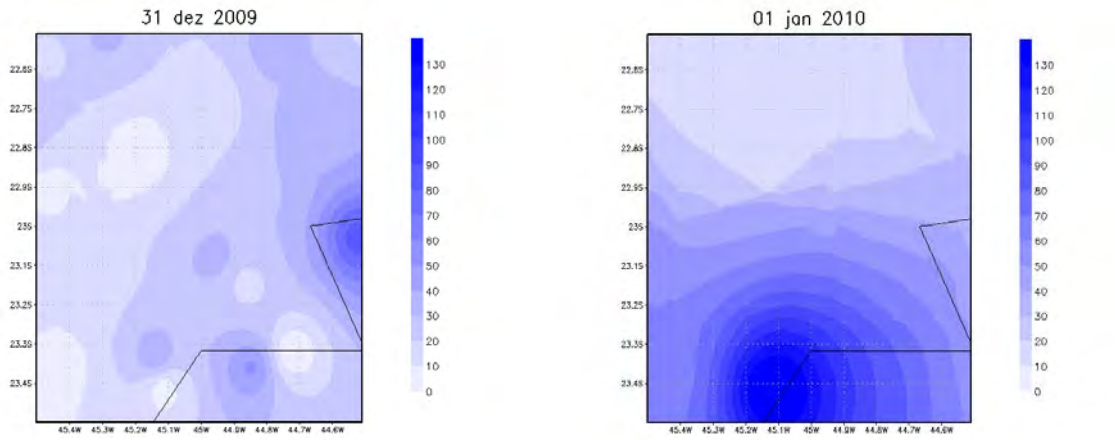

Figure 3- Results of interpolated precipitation data (Arguello et al., 2013). a) 31 december, 2009; b) 01 january 2010;

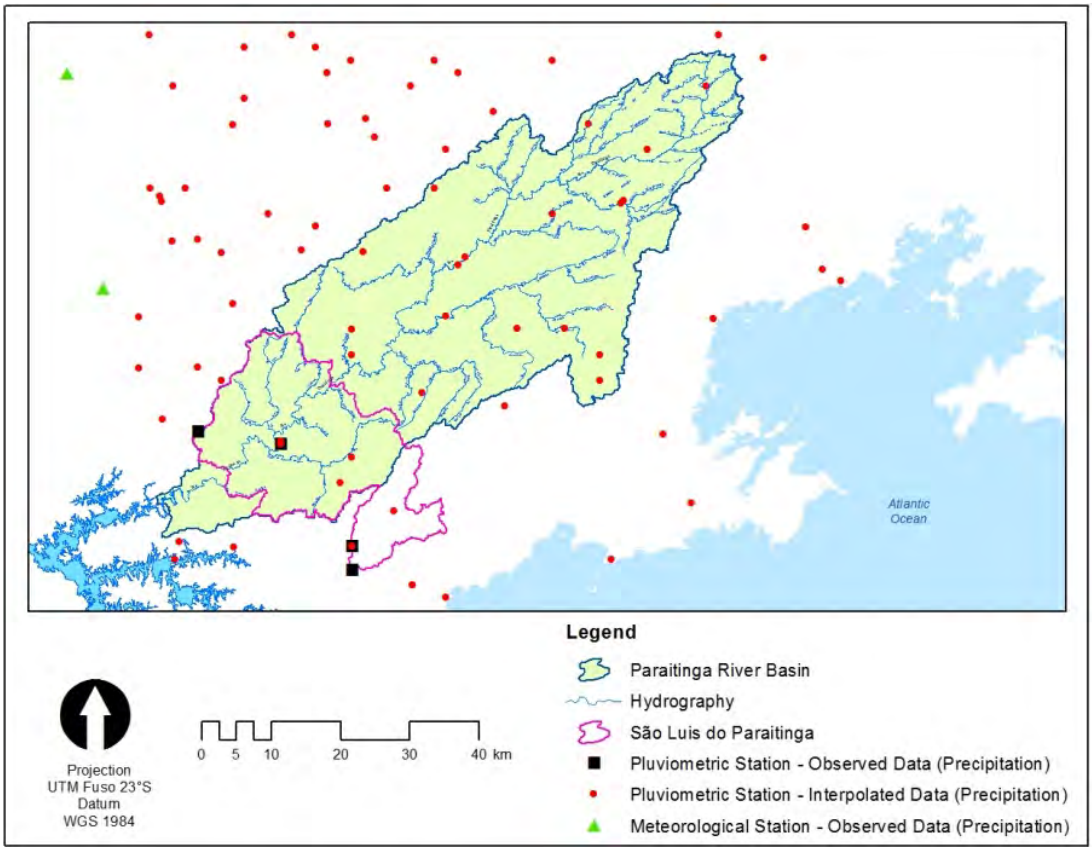

Figure 4 - Spatial distribution of stations with observed and interpolated data (Arguello et al., 2013).

Additionally, the numerous flaws in the historical series observed, for example, for a period of 15 days before and 15 days after the event (15/12/2009 to 15/01/2010 – Figure 5) could be complemented by interpolated data (Figure 6). This feature will be important for the calibration/validations steps in the SWAT model use.

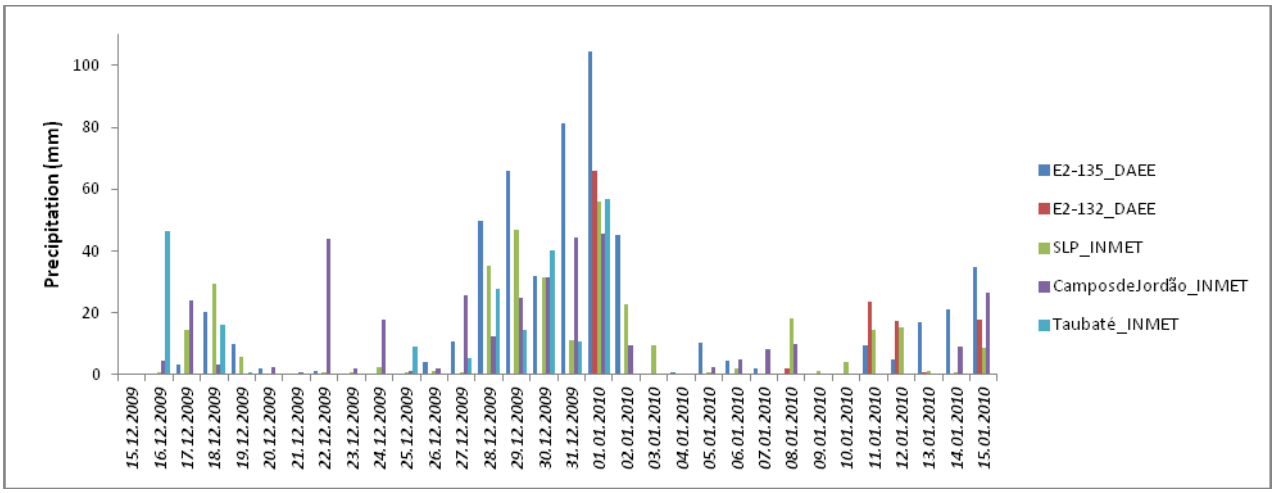

Figure 5 – Precipitation data obtained from in situ stations for the period of 15/12/2009 to 15/01/2010 (Arguello et al., 2013).

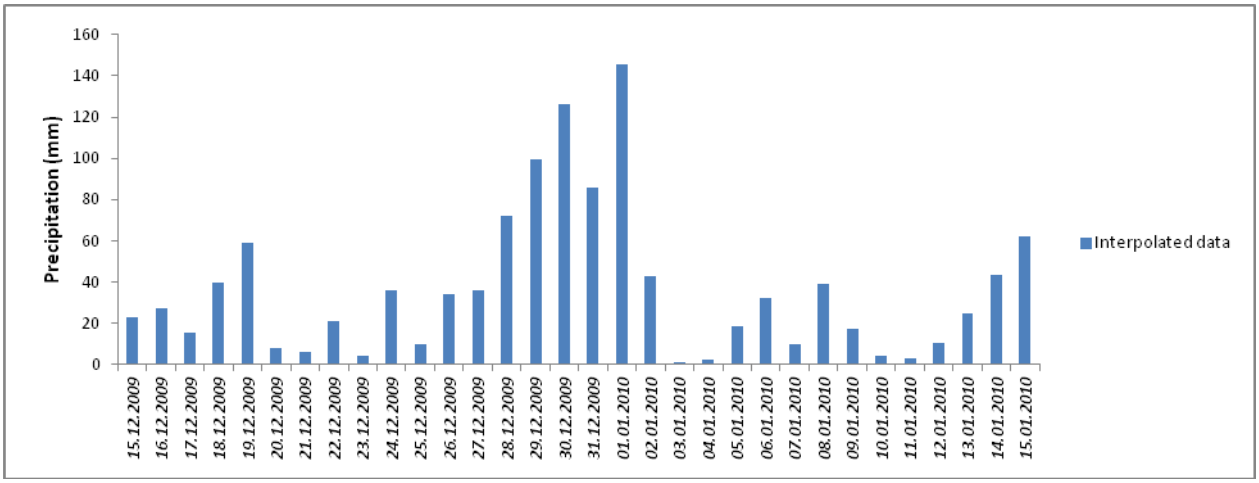

Figure 6 - Data availability of interpolated precipitation (Arguello et al., 2013).

The temporal distribution of stations with observed data was also complemented by interpolated data, to fill the gaps in the time series of stations with observed data for the period 1990 to 2010, exemplified in Figure 7.

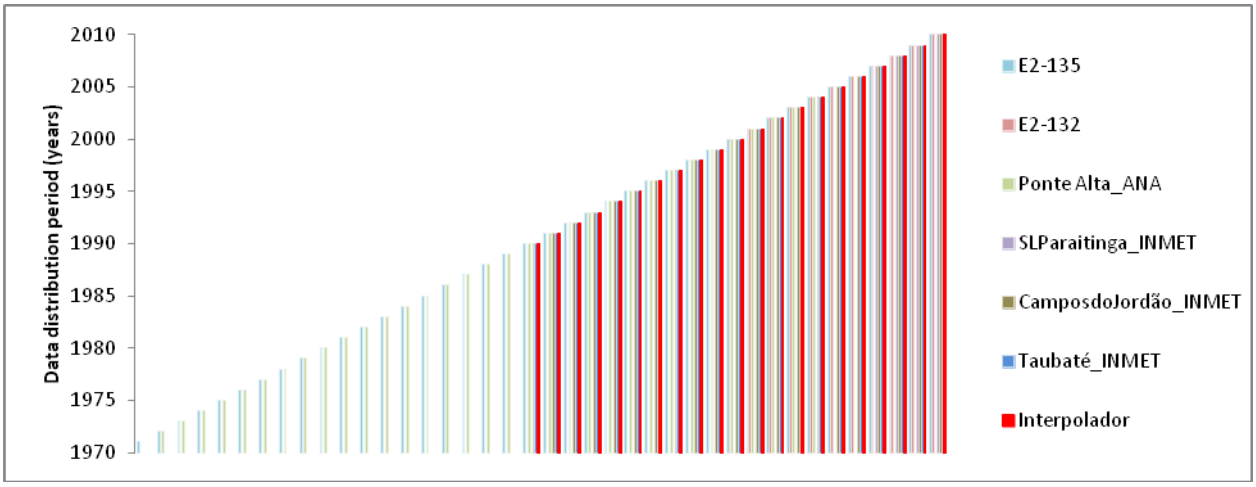

Figure 7 - Temporal distribution of stations with observed and interpolated data (Arguello et al., 2013).

For the following steps, we are going to validate the interpolated rainfall values with the values obtained from in situ stations. The same is being done to the other meteorological data, such as temperature, radiation, humidity, wind speed, etc.

Conclusion

This paper describes a part of a PhD research that aims to simulate the extreme flood event occurred in the city of São Luiz do Paraitinga, São Paulo, Brazil, in early January 2010.The shortage of meteorological stations in the study area to compose an input database for the SWAT model drove the evaluation of some possible weather data sources to supplement the precipitation database. However, the improper spatial resolution of the GPCP and TRMM data limit their use in the study area. Besides, the operating principle used for the Hidroestimador algorithm is not suitable to simulate orographic precipitations, which are the common type of precipitation which occurs at the Paraitinga River Basin. Thus, the rainfall data interpolated by CPTEC/INPE proved to be most suitable for simulation of the event of interest, with regard to issues of spatial and temporal scale. However, further steps will be carried out to calibrate these values.

Acknowledgements

The authors thank the organizers of the research and data made available by the responsible agencies ANA, INMET, DAEE CPTEC-INPE.

References

Journal article

Adler et al. 2003: The version-2 Global Precipitation Climatology Project (GPCP) Monthly Precipitation Analysis (1979-Present): *Journal of Hydrology, 1147-1167*.

Lefèvre, M., Remund, J., Albuisson, M., Wald, L., 2002. Study of effective distances for interpolation schemes in meteorology. *Geophysical Research Abstracts, 4, April 2002, EGS02-A-03429, European Geophysical Society, 2002*.

Huffman, G.J.; Adler, R.F.; Rudolf, B.; Schneider, U.; Keehn, P.R. (1995) – A Technique for Combining Satellite Data, Raingauge Analysis and Model Precipitation Information into Global Precipitation Estimates. *Journal of Climate, 8: 1284-1295*.

Huffman, G.J., R.F. Adler, D.T. Bolvin, G. Gu, E.J. Nelkin, K.P. Bowman, Y. Hong, E.F. Stocker, D.B. Wolff, 2007: The TRMM Multi-satellite Precipitation Analysis (TMPA): Quasi-Global, Multiyear, Combined-Sensor Precipitation Estimates at Fine Scale. *Journal of Hydrometeorology, v. 8, p. 38-55, 2007*.

Scofield, R.A. (2001). Comments on "A quantitative assessment of the NESDIS AutoEstimador". *Weather and Forecasting, v.16, pp. 277-278*.

Scofield, R.; Kuligowski, R. Status and outlook of operational satellite precipitation, algorithms for extreme events. *Weather and Forecasting, v.18, n.6, pp. 1037–1051. 2003*.

Xie, P.; J.E. Janowiak; P.A. Arkin; R. Adler; A. Gruber; R. Ferraro; G.H. Huffman; S. Curtis. GPCP Pentad Precipitation Analyses: An Experimental Dataset Based on Gauge Observations and Satellite Estimates. *Journal of Climate, v. 16, p. 2197-2214. 2003*.

Book

BRASIL. Ministério da Integração Nacional. *Atlas Brasileiro de Desastres Naturais, 1991 a 2010: volume Brasil*. Florianópolis: Centro Universitário de Estudos e Pesquisas Sobre Desastres/UFSC, 2011.

BRASIL. Ministério da Integração Nacional. *Atlas Brasileiro de Desastres Naturais, 1991 a 2010: volume São Paulo*. Florianópolis: Centro Universitário de Estudos e Pesquisas Sobre Desastres/UFSC, 2011.

DAEE-Departamento De Água E Energia Elétrica. *Plano Diretor de Macrodrenagem da bacia do Rio Paraitinga*.Volume1.Secretaria de Saneamento e Recursos Hídricos, 2012, 86 p.

Guha-Sapir, D.; Vas F.; Below, R.; Ponserre, S. *Annual Disaster Statistical Review 2011: The numbers and trends*. Brussels: CRED, 2012. 42p.

Setzer, J. *Atlas Climático e Ecológico do Estado de São Paulo*. Comissão Interestadual da Bacia Paraná-Uruguai, 1966. 61p.

Bulletin or Report

Huffman, G.J.; Adler R.F.; Arkin, P.; Chang, A.; Ferraro, R.; Gruber, A.; Janowiak, J.; McNab, A.; Rudolf, B.; Schneider, U. (1997) – The Global Precipitation Climatology Project (GPCP) Combined Precipitation Data Set. Bulletin of the American Meteorological Society, 78: 5-20.

Published Paper

Dias, N. W., Batista, G. T., Catelani, C. S. A enchente de São Luis do Paraitinga: evidências de sua dimensão obtidas a partir de dados orbitais. *In: XV Simpósio Brasileiro de Sensoriamento Remoto - SBSR, Anais XV Simpósio Brasileiro de Sensoriamento Remoto - SBSR, Curitiba, PR, Brasil, 30 de abril a 05 de maio de 2011, INPE p.1411*.

Saldanha, C. B.; Paz, A. R.; Allasia, D.; Collischonn, W E Barrera, D. Avaliação da chuva da hidroestimador para modelagem hidrológica na região da bacia do rio Grande. São Paulo. *IN: Anais do XVII Simpósio Brasileiro de Recursos Hídricos. 17p., 2007.*

Appendix or Nomenclature

ANA (National Water Agency)
DAEE (Department of Water and Power)
INMET (National Institute of Meteorology)

Arguello, F. V. P.; Borma, L. S.; Alves, D. S.; Roballo, S. T. Building a meteorological data set as input for the SWAT model in order to simulate the extreme flood event which occured in the municipality of São Luiz do Paraitinga, São Paulo, Brasil, between 31/12/2009-01/01/2010. Toulouse, France. *International SWAT Conference. 2013.*

Development of a soil database for applying SWAT model in a catchment of the Brazilian Savanna

Jorge Enoch Furquim Werneck Lima*
Embrapa Cerrados, Brazil, jorge.werneck-lima@embrapa.br

Euzebio Medrado da Silva
Embrapa Cerrados, Brazil, euzebio.medrado@gmail.com

Michael Strauch
Helmholtz Centre for Environmental Research - UFZ, Germany, michael.strauch@ufz.de

Carsten Lorz
Hochschule Weihenstephan Triesdorf - HSWT, Germany, carsten.lorz@hswt.de

Abstract

Knowledge about physical and hydraulic characteristics of soils is fundamental for the proper application of physically-based hydrological models with distributed parameters, such as the SWAT model (Soil and Water Assessment Tool). In Brazil, since 1999 the number of SWAT users and applications are increasing in an accelerated way. In the case of the Brazilian Savanna region (Cerrado biome), the first applications are very recent and, in general, generic soil database or pedotransfer functions, as well as the default data developed for other soil types and regions, were used. This study aimed to present a reference soil database for applying SWAT in catchments of the Brazilian Savanna. Based on soil samples and analyses, performed at least in triplicate, the following soil characteristics were measured: bulk density, soil-water retention curve, hydraulic conductivity, organic matter, and soil texture. Using soil data collected in 66 sites and three depths, most of them in the Upper Jardim Experimental River Basin, Federal District, Brazil, a conceptual model for introducing this data in SWAT was proposed, as well as a summary table showing the average and range for each of the soil parameters considered by the model. Seven representative soils commonly found in the Cerrado biome were covered by this study. Considering the soil data used in previous applications of the SWAT model in catchments of the region, the results of this study may represent a step forward to obtain more realistic hydrological models, with better physical basis.

Keywords: Hydrological modeling, soil database, model calibration, Brazil.

Introduction

Knowledge about physical and hydraulic characteristics of soils is fundamental for the proper application of physically-based hydrological models with distributed parameters (Romanowicz et al., 2005; Peschel et al., 2006; Geza e McCray, 2008), such as the SWAT model - Soil and Water Assessment Tool (Arnold et al., 1998; Arnold e Fohrer, 2005).

In Brazil, since 1999 the number of SWAT users and applications are increasing in an accelerated way in many regions (Garbossa et al., 2011). As of 2010, SWAT had not been used for the Cerrado biom, in particular the Brazilian Central Plateau region, as reported in the review of Garbossa et al. (2011). However, since 2011, the use of the SWAT model is rapidly advancing also in the Cerrado biome. Several studies were conducted for experimental watersheds in the Federal District – DF, Brazil (Silva, 2010; Strauch et al., 2011; Ferrigo et al., 2011; Minoti et al., 2011; Salles e Chaves, 2011; Strauch et al., 2012; Ferrigo et al., 2012; Strauch et al., 2013).

Hydrological data collection in experimental watersheds in the DFstartedmore intensively about a decade ago, producing water and sediment yield time series that can be used for evaluating various hydrological models including SWAT. Nevertheless, even though the DF is covered by a soil map at 1:100,000 scale (Embrapa, 1978; Reatto et al. 2004), which is a privilege compared to the rest of the country, the organization and availability of soil data are insufficient for an adequate use of hydrological models like SWAT. These limitations on soil data result in large model uncertainties, as described by Silva (2010) in a SWAT study focused on sensitivity and uncertainty analysis for the Descoberto river basin (DF). Minoti et al. (2011), who applied SWAT in the Bananal and the Gama watersheds (both in DF), also highlighted the difficulties in defining physical and hydrological characteristics of the soils of that region, mainly because they are extremely specific. Due to the lack of certain soil information, Strauch et al. (2011, 2012, 2013) were forced to use pedotransfer functions developed for other regions in order to estimate soil physical parameters needed for modeling the Pipiripau river basin (DF and Goiás State) using SWAT.

The very distinctive physical-hydric behavior of the Cerrado soils is evidenced. As an example, although Oxisols are generally rich in clay their permeability is unusually high due to the aggregation of clay minerals into pseudo-silt and pseudo-sand particles (Stoner et al., 1991; Yerima and Van Ranst, 2005). This soil behavior can be attributed to specific soils in tropical regions, but is totally different from in the behavior of soils in temperate regions, for which the SWAT model was designed. Therefore, the US reference soils provided in the (default) SWAT soil database is in general not applicable to Cerrado/tropical soils.

A further problem with the soil data required for proper SWAT model applications in basins of the Cerrado is the definition of ranges for each parameter, which represent key information in the calibration process, fundamental for the maintenance of the model physical basis.

This study aims to present a reference soil database for applying SWAT in catchments of the Brazilian Savanna, by providing initial parameters values and their ranges of variation.

Material and methods

Study area

Situated in the eastern part of the Federal District, between latitudes 15.71° and 15.86° S and longitudes 47.55° and 47.64° W, the Upper Jardim Experimental River Basin is within the central part of the Cerrado Biome continuous area (Figure 1).

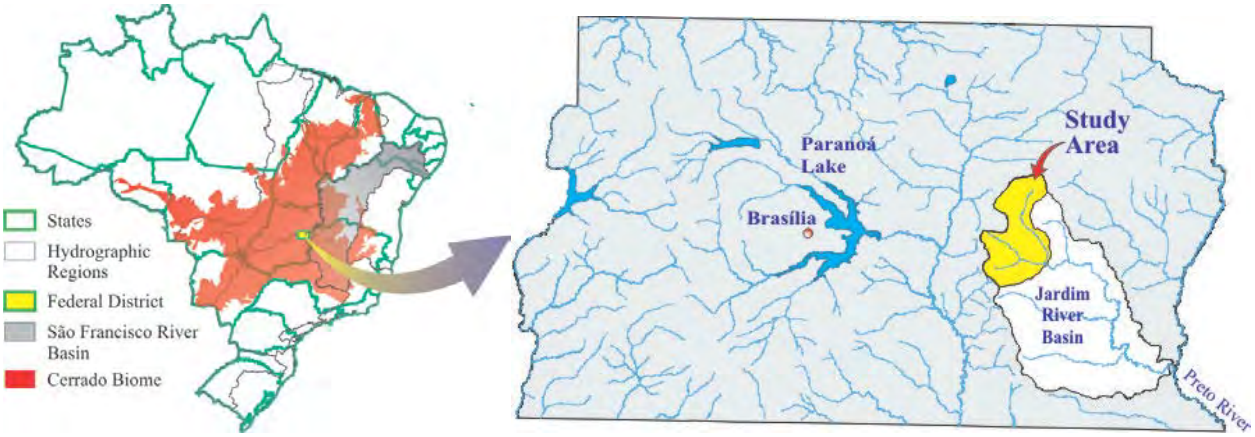

Figure 1 - Location of the Upper Jardim Experimental River Basin in relation to Brazil, the Brazilian hydrographic regions, the continuous area of the Cerrado and the Federal District.

With respect to large Brazilian hydrographic regions (CNRH, 2003), the Upper Jardim Experimental River Basin is inserted into the Hydrographic Region of the San Francisco River. The Jardim River is a tributary of the Preto River, which flows into the Paracatu River, an important contributor of the left bank of the São Francisco River.

The Upper Jardim Experimental River Basin has a total drainage area of 104.86 km ², divided into two main basins, the Estanislau stream (49.71 km²) and the Jardim River itself (55.15 km²).

The climate in the basin is typical for the Cerrado region, with two well defined seasons: a rainy summer and a dry winter. Following the classification of Köppen, the climate is of AW Tropical type.

76.38% of the Upper Jardim Basin are covered by Latosols (Oxisols), 16.68% by Cambisols, 2.54% by Plinthosol, 2.41% by Gleisoil, 2.09% by Quartzarenic Neosols, and 0.24% by Rock outcrops (Lima et al., 2007).

Situated within the main agricultural region of the Federal District, , land management is characterized by crop production (grain crops (soy, beans, maize, and sorghum), cotton, citrus, coffee, cassava and vegetables) as well as by poultry and cattle.

Data collection

Figure 2 shows the soil map (scale: 1:50,000) of the Upper Jardim Experimental River Basin (Reatto et al., 2000) as well as 56 sampling points used in this work.

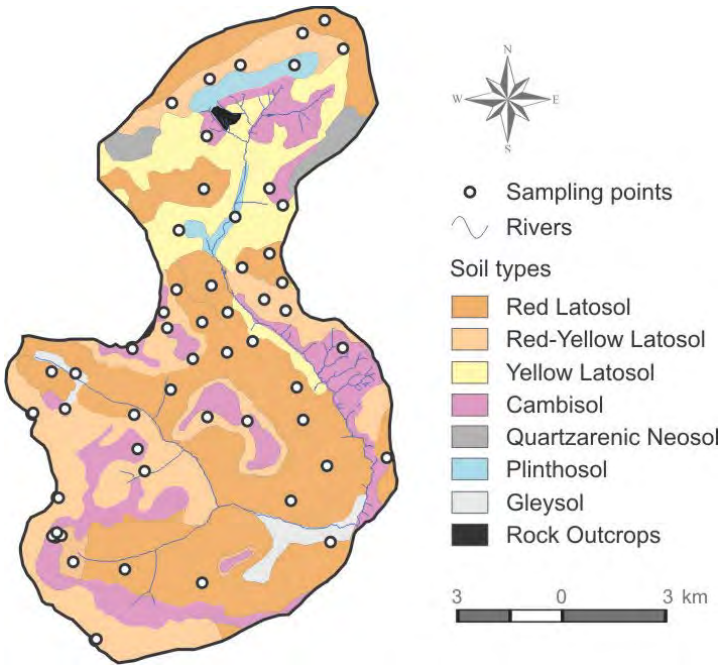

Figure 2 - Soil map (1:50,000) of the Upper Jardim Experimental River Basin (Reatto et al., 2000) with the location of 56 sampling points used in the present work.

22 points are located in Red Latosols (LV) areas; 19 in Red-Yellow Latosols (LVA); 10 in Cambisols (CX); two in Gleysols (GX); two in Plinthosols (FX); and one in Yellow Latosol (LA). For Quartzarenic Neosols (RQ), samples were collected at 12 sites outside the basin but also in the Federal District.

Each of the soil samples (core and disturbed samples) were collected at two depths (15 and 60 cm), and only the saturated hydraulic conductivity was measured in the water table level using piezometric wells installed at each point as shown in the map (Figure 2).

Soil texture was evaluated in triplicate using the sieving and the pipetting methods (Embrapa, 1997), whereas bulk density was measured in triplicate using the volumetric ring method (Embrapa, 1997).

The saturated hydraulic conductivity was determined using the constant head permeameter method (Klute, 1965) with six replicates per depth. The higher number of repetitions in the determination of this parameter was adopted because of its greater natural variability. The determination of saturated hydraulic conductivity in the water table level was achieved using the Slug Test (Hvorslev, 1951).

The soil water retention curves of each point were determined in the laboratory, in triplicate, using the centrifuge method as described by Reatto et al. (2008).

The available water content of the sampled soils was extracted from their soil water retention curves, considering the difference between soil moistures corresponding to the tensions of 10 and 1,500 kPa (Reichardt, 1988).

The content of organic matter was obtained in triplicate using the oxidation method and soil erodibility (K factor of USLE) was determined indirectly by means of the equation developed by Lima et al. (2007).

Data Analysis

Based on the collected data, we first defined a conceptual model to describe how the soil would be spatially represented in SWAT.

The results for each sample / repetition were organized in tables, generating averages, standard deviations and coefficients of variation for each data. With this, it was possible to either verify the data consistency,or alternatively (in some cases) to identify the need to redo the analysis.

After that, the data were organized to provide the following SWAT parameters, where most of the parameters are layer-specific:

- SNAM: Soil name
- NLAYERS: Number of layer on the soil (field information)
- HYDGRP: Soil Hydrologic Group (field information + Sartori et al., 2005)
- SOL_ZMX: Maximum rooting depth of soil profile (mm)

- SOL_Z: Depth of soil surface to bottom (mm)
- SOL_BD: Moist bulk density (g/cm^3)
- SOL_AWC: Available water capacity of the soil layer (mm/mm)
- SOL_K: Saturated hydraulic conductivity (mm/hr)
- SOL_CBN: Organic carbon content (%) (1,724 factor)
- CLAY: % Clay content
- SILT: % Silt content
- SAND: % Sand content
- ROCK: % Rock fragment content
- USLE_K: USLE equation soil erodibility (K) factor (t.m^2.hr/m^3.t.cm)

In addition to the average values, minimum and maximum values were organized to indicate the range of variation of each parameter considering the soil class and its respective layer.

Results and discussion

Figure 3 shows the conceptual model developed for representing and entering soil data in the SWAT model.

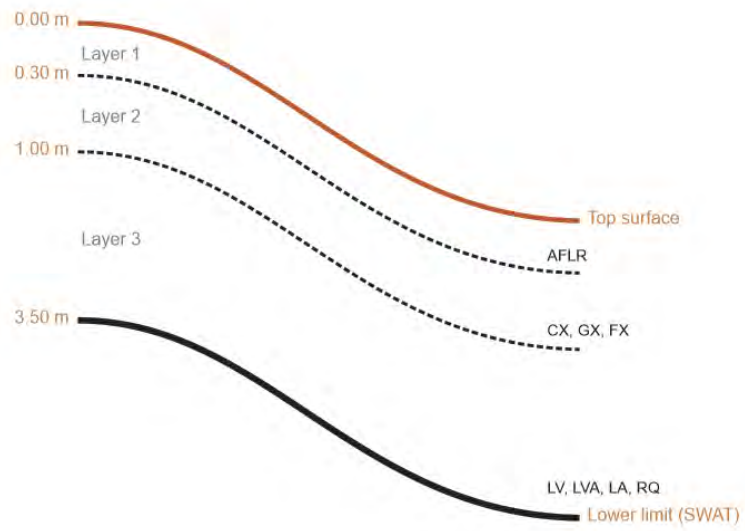

Figure 3 - Conceptual model for representation of soil layers in the model SWAT.

As shown in Figure 3, the representation of the conceptual model soil has three layers. The first layer goes from the terrain surface (0.00m) to 0.30m, the second from 0.30 to 1.00m and the

third, from 1.00 to 3.50 meters. It is noteworthy that the lower limit of 3.50m deep is an obstacle of the SWAT model in representing the reality of the Cerrado soils, especially in the case of Latosols, dominant in the biome and, in general, like in the Upper Jardim River Basin, with depths much greater than this. The acronyms in the right part of Figure 3 show the limit depth considered for each soil type.

The average, minimum and maximum values of the parameters for each soil layer and class are presented in Tables 1, 2 and 3, respectively.

Table 1 - Average values of the parameters per layer and soil class.

	SNAM	NLAYERS	HYDGRP	SOL_ZMX	SOL_Z1	SOL_BD1	SOL_AWC1	SOL_K1	SOL_CBN1	CLAY1	SILT1	SAND1	ROCK1	USLE_K1
Red Latosols	LV	3	A	300.00	300.00	0.90	0.12	612.20	1.67	53.93	28.37	12.94	0.00	0.018
Red-Yellow Latosols	LVA	3	A	300.00	300.00	0.94	0.11	1112.85	1.69	57.36	24.61	18.03	0.00	0.019
Yellow Latosol	LA	3	A	300.00	300.00	0.86	0.15	2602.59	1.65	58.81	21.75	19.44	0.00	0.017
Quartzarenic Neosols	RQ	3	A	300.00	300.00	1.30	0.08	281.26	0.60	30.10	9.65	60.25	0.00	0.031
Cambisols	CX	2	C	300.00	300.00	0.99	0.11	874.33	1.58	49.84	32.95	17.20	0.00	0.023
Gleysols	GX	2	D	300.00	300.00	0.87	0.13	494.44	2.56	51.59	28.54	19.86	0.00	0.021
Plinthosols	FX	2	D	300.00	300.00	1.09	0.14	553.78	1.14	37.97	21.91	40.13	0.00	0.030
Rock Outcrop	AFLR	1	D	300.00	300.00	2.62	0.01	0.01	0.01	0.00	0.00	0.01	99.99	0.001

	SNAM	NLAYERS	HYDGRP	SOL_ZMX	SOL_Z2	SOL_BD2	SOL_AWC2	SOL_K2	SOL_CBN2	CLAY2	SILT2	SAND2	ROCK2	USLE_K2
Red Latosols	LV	3	A	1000.00	1000.00	0.94	0.14	461.07	1.01	66.28	22.93	10.79	0.00	0.015
Red-Yellow Latosols	LVA	3	A	1000.00	1000.00	0.96	0.13	401.26	0.95	64.37	20.54	15.09	0.00	0.017
Yellow Latosol	LA	3	A	1000.00	1000.00	0.94	0.12	505.50	0.87	62.28	19.89	17.83	0.00	0.015
Quartzarenic Neosols	RQ	3	A	1000.00	1000.00	1.38	0.08	102.85	0.40	34.35	9.58	42.90	0.00	0.030
Cambisols	CX	2	C	1000.00	1000.00	1.00	0.16	262.52	0.72	49.16	34.31	16.53	0.00	0.023
Gleysols	GX	2	D	1000.00	1000.00	0.87	0.13	494.44	2.56	51.59	28.54	19.86	0.00	0.021
Plinthosols	FX	2	D	1000.00	1000.00	1.09	0.14	553.78	1.14	37.97	21.91	40.13	0.00	0.030

	SNAM	NLAYERS	HYDGRP	SOL_ZMX	SOL_Z3	SOL_BD3	SOL_AWC3	SOL_K3	SOL_CBN3	CLAY3	SILT3	SAND3	ROCK3	USLE_K3
Red Latosols	LV	3	A	2000.00	3500.00	0.94	0.14	142.32	1.01	66.28	22.93	10.79	0.00	0.015
Red-Yellow Latosols	LVA	3	A	2000.00	3500.00	0.96	0.13	230.05	0.95	64.37	20.54	15.09	0.00	0.017
Yellow Latosol	LA	3	A	2000.00	3500.00	0.94	0.12	186.92	0.87	62.28	19.89	17.83	0.00	0.015
Quartzarenic Neosols	RQ	3	A	2000.00	3500.00	1.38	0.08	102.85	0.40	34.35	9.58	42.90	0.00	0.030

Table 2 - Minimum values of the parameters per layer and soil class.

	SNAM	NLAYERS	HYDGRP	SOL_ZMX	SOL_Z1	SOL_BD1	SOL_AWC1	SOL_K1	SOL_CBN1	CLAY1	SILT1	SAND1	ROCK1	USLE_K1
Red Latosols	LV	3	A	300.00	300.00	0.83	0.10	34.21	0.96	40.97	18.57	5.92	0.00	0.014
Red-Yellow Latosols	LVA	3	A	300.00	300.00	0.83	0.07	342.36	0.71	40.70	9.22	4.98	0.00	0.014
Yellow Latosol	LA	3	A	300.00	300.00	0.83	0.13	2602.59	1.65	58.81	21.75	19.44	0.00	0.017
Quartzarenic Neosols	RQ	3	A	300.00	300.00	1.14	0.06	75.78	0.40	17.65	3.44	39.44	0.00	0.027
Cambisols	CX	2	C	300.00	300.00	0.88	0.09	342.32	0.92	35.12	23.83	10.40	0.00	0.015
Gleysols	GX	2	D	300.00	300.00	0.87	0.13	494.44	2.56	51.59	28.54	19.86	0.00	0.021
Plinthosols	FX	2	D	300.00	300.00	1.00	0.14	8.15	0.88	35.99	15.98	32.23	0.00	0.029
Rock Outcrop	AFLR	1	D	300.00	300.00	2.62	0.01	0.01	0.01	0.00	0.00	0.01	99.99	0.001

	SNAM	NLAYERS	HYDGRP	SOL_ZMX	SOL_Z2	SOL_BD2	SOL_AWC2	SOL_K2	SOL_CBN2	CLAY2	SILT2	SAND2	ROCK2	USLE_K2
Red Latosols	LV	3	A	1000.00	1000.00	0.88	0.08	177.48	0.65	57.11	13.86	4.93	0.00	0.014
Red-Yellow Latosols	LVA	3	A	1000.00	1000.00	0.86	0.09	49.34	0.65	47.31	7.61	3.84	0.00	0.014
Yellow Latosol	LA	3	A	1000.00	1000.00	0.94	0.12	505.50	0.87	62.28	19.89	17.83	0.00	0.015
Quartzarenic Neosols	RQ	3	A	1000.00	1000.00	1.24	0.07	13.05	0.31	18.63	2.79	34.02	0.00	0.026
Cambisols	CX	2	C	1000.00	1000.00	0.84	0.13	123.03	0.15	35.20	22.67	11.10	0.00	0.015
Gleysols	GX	2	D	1000.00	1000.00	0.87	0.13	494.44	2.56	51.59	28.54	19.86	0.00	0.021
Plinthosols	FX	2	D	1000.00	1000.00	1.00	0.14	8.15	0.88	35.99	15.98	32.23	0.00	0.029

	SNAM	NLAYERS	HYDGRP	SOL_ZMX	SOL_Z3	SOL_BD3	SOL_AWC3	SOL_K3	SOL_CBN3	CLAY3	SILT3	SAND3	ROCK3	USLE_K3
Red Latosols	LV	3	A	2000.00	3500.00	0.88	0.08	0.34	0.65	57.11	13.86	4.93	0.00	0.014
Red-Yellow Latosols	LVA	3	A	2000.00	3500.00	0.86	0.09	0.60	0.65	47.31	7.61	3.84	0.00	0.014
Yellow Latosol	LA	3	A	2000.00	3500.00	0.94	0.12	186.92	0.87	62.28	19.89	17.83	0.00	0.015
Quartzarenic Neosols	RQ	3	A	2000.00	3500.00	1.24	0.07	13.05	0.31	18.63	2.79	34.02	0.00	0.026

Table 3 - Maximum values of the parameters per layer and soil class.

	SNAM	NLAYERS	HYDGRP	SOL_ZMX	SOL_Z1	SOL_BD1	SOL_AWC1	SOL_K1	SOL_CBN1	CLAY1	SILT1	SAND1	ROCK1	USLE_K1
Red Latosols	LV	3	A	300.00	300.00	1.19	0.15	1310.33	2.65	70.79	37.80	37.78	0.00	0.028
Red-Yellow Latosols	LVA	3	A	300.00	300.00	1.16	0.16	2345.27	2.50	78.26	38.15	47.19	0.00	0.029
Yellow Latosol	LA	3	A	300.00	300.00	0.86	0.15	2602.59	1.65	58.81	21.75	19.44	0.00	0.017
Quartzarenic Neosols	RQ	3	A	300.00	300.00	1.40	0.09	763.70	0.96	42.78	23.03	78.90	0.00	0.033
Cambisols	CX	2	C	300.00	300.00	1.14	0.13	1436.40	1.77	64.61	51.72	29.66	0.00	0.031
Gleysols	GX	2	D	300.00	300.00	0.87	0.13	494.44	2.56	51.59	28.54	19.86	0.00	0.021
Plinthosols	FX	2	D	300.00	300.00	1.18	0.15	1099.40	1.41	39.95	27.83	48.03	0.00	0.031
Rock Outcrop	AFLR	1	D	300.00	300.00	2.62	0.01	0.01	0.01	0.00	0.00	0.01	99.99	0.001

	SNAM	NLAYERS	HYDGRP	SOL_ZMX	SOL_Z2	SOL_BD2	SOL_AWC2	SOL_K2	SOL_CBN2	CLAY2	SILT2	SAND2	ROCK2	USLE_K2
Red Latosols	LV	3	A	1000.00	1000.00	1.04	0.19	1324.30	1.45	75.54	34.21	25.83	0.00	0.018
Red-Yellow Latosols	LVA	3	A	1000.00	1000.00	1.14	0.18	839.63	1.31	85.16	32.58	43.70	0.00	0.025
Yellow Latosol	LA	3	A	1000.00	1000.00	0.94	0.12	505.50	0.87	62.28	19.89	17.83	0.00	0.015
Quartzarenic Neosols	RQ	3	A	1000.00	1000.00	1.50	0.09	235.70	0.52	44.51	23.56	77.86	0.00	0.032
Cambisols	CX	2	C	1000.00	1000.00	1.19	0.20	430.54	1.16	64.62	53.69	30.96	0.00	0.031
Gleysols	GX	2	D	1000.00	1000.00	0.87	0.13	494.44	2.56	51.59	28.54	19.86	0.00	0.021
Plinthosols	FX	2	D	1000.00	1000.00	1.18	0.15	1099.40	1.41	39.95	27.83	48.03	0.00	0.031

	SNAM	NLAYERS	HYDGRP	SOL_ZMX	SOL_Z3	SOL_BD3	SOL_AWC3	SOL_K3	SOL_CBN3	CLAY3	SILT3	SAND3	ROCK3	USLE_K3
Red Latosols	LV	3	A	1000.00	3500.00	1.04	0.19	1000.00	1.45	75.54	34.21	25.83	0.00	0.018
Red-Yellow Latosols	LVA	3	A	1000.00	3500.00	1.14	0.18	1000.00	1.31	85.16	32.58	43.70	0.00	0.025
Yellow Latosol	LA	3	A	1000.00	3500.00	0.94	0.12	186.92	0.87	62.28	19.89	17.83	0.00	0.015
Quartzarenic Neosols	RQ	3	A	1000.00	3500.00	1.50	0.09	235.70	0.52	44.51	23.56	77.86	0.00	0.032

The data shown in Table 1 are mean values for each parameter and soil layer which can be used as a reference for the initial values to be assigned in the molding process using SWAT. The data presented in Tables 2 and 3 (minimum and maximum values) represent the ranges for each parameter, which should be considered during the model calibration process in order to maintain the physical basis of the model.

The small number of samples collected in areas of Gleysol, Plinthosol, and Yellow Latosol represent an evident limitation of this study; however, it is remarkable that the first two soil classes usually occupy only a small percentage of the Brazilian Central Plateau area. In case of the Yellow Latosol, a possible solution is using the limits of variation established for other Latosols of the region as a reference.

Conclusion

The study provides reference values for defining layer-specific soil parameters in the Cerrado biome. Besides suggesting initial parameter values, we also presented physically meaningful parameter ranges, which can be used for model calibration. This should significantly increase the applicability and reliability of the SWAT model in order to support land and water resources management in the Cerrado biome.

Acknowledgements

The authors thank CNPq for funding the project SWAT-DF (CNPq No. 483410/2011-0).

References

Arnold, J.G., and N. Fohrer. 2005. SWAT2000: Current capabilities and research opportunities in applied watershed modeling. *Hydrol. Process*., 19:563-572.

Arnold, J.G., R. Srinivasan, R.S. Muttiah, and J.R. Williams. 1998. Large area hydrologic modeling and assessment. Part I: Model development. *J. Am. Water Res. Assoc*., 34:73-89.

EMBRAPA, 1978. Levantamento de reconhecimento dos solos do Distrito Federal. In: *Boletim Técnico* 53. Rio de Janeiro, p. 455.

EMBRAPA. Centro Nacional de Pesquisa de Solos. 1997. Manual de métodos de análise de solo. *Série Documentos* 1, 2.ed. Rio de Janeiro: Embrapa CNPS. 212p.

Ferrigo, S., R.T. Minoti, and S. Koide. 2011. Utilização do Modelo SWAT na estimativa da produção de sedimentos decorrentes de diferentes cenários de uso do solo na bacia do córrego Capão Comprido no Distrito Federal. In: *anais do XIX SBRH*, Maceió: ABRH, 2011.

Ferrigo, S.; R.T. Minoti, H. Roig, and S. Koide. 2012. Análise do modelo SWAT na simulação de produção de sedimentos quando calibrado unicamente para vazão em uma pequena bacia hidrográfica rural. In: *anais do X ENES*, Foz do Iguaçu: ABRH, 2012.

Garbossa, L.H.P., L.R.C. Vasconcelos, K.R. Lapa, E. Blainski, and A. Pinheiro. 2011. The use results of the Soil and Water Assessment Tool in Brazil: A review from 1999 until 2010. In: *International SWAT Conference & Workshops*. Toledo, Espanha. p. 1-27.

Geza, M., and J.E McCray. 2008. Effects of soil data resolution on SWAT model stream flow and water quality predictions. *Journal of Environmental Management* 88(3):393-406.

Hvorslev, M.J. 1951. Time lag and soil permeability in ground-water observations. Vicksburg, Miss.: U.S. Army Corps of Engineers, Waterways Experiment Station, *Bulletin* 36, 50p.

Klute, A. 1965. Laboratory measurements of hydraulic conductivity of saturated soil. In: Black et al. (ed.). *Methods of soil analysis*. Monograph 9, Madison: American Soc. of Agron. 253-261.

Lima, J.E.F.W., E.M. Silva, N.J. Eid, E.S. Martins, S. Koide, and A. Reatto. 2007. Desenvolvimento e verificação de métodos indiretos para a estimativa da erodibilidade dos solos da bacia experimental do alto rio Jardim, DF. *Revista Brasileira de Geomorfologia*, 8, p.21-34.

Minoti, R.T., S. Koide, and L.M. Liporoni. 2011. Estimativa das cargas de sedimentos e nutrientes em duas sub-bacias do lago Paranoá Brasília/DF. In: *Anais do XIX SBRH*. Maceió: ABRH, 2011.

Peschel, J.M., P.K. Haan, and R.E. Lacey. 2006. Influences of soil dataset resolution on hydrologic modeling. *Journal of the American Water Resources Association* 42(5):1371-1389.

Reatto, A., J.R. Correia, S.T. Spera, C.S. Chagas, E.S. Martins, J.P. Andahur, M.J.S. Godoy, and M.L.C.L. Assad. 2000. Levantamento semi-detalhado dos solos da bacia do rio Jardim-DF, escala 1:50,000. Planaltina: Embrapa Cerrados. 63p. CD ROM (*Boletim de pesquisa* nº 18).

Reatto, A., E.M. Silva, A. Bruand, E.S. Martins, and J.E.F.W. Lima. 2008. Validity of the centrifuge method for determining the water retention properties of soils. *Soil Science Society of America Journal*, 72, 1547-1553.

Reatto, A., E.S.Martins, M.F.R. Farias, A.V. Silva, and O.A.C Carvalho Jr. 2004. Mapa Pedológico Digital – SIG atualizado do Distrito Federal, escala 1:100,000 e uma síntese do texto explicativo. *Documentos*, Nº 120. EMBRAPA Cerrados, Distrito Federal.

Reichardt, K. 1988. Capacidade de campo. *Rev. Bras. de Ciência do Solo*, 12, 211-216.

Romanowicz, A.A., M. Vanclooster, M. Rounsevell, and I. La Junesse. 2005. Sensitivity of the SWAT model to the soil and land use data parameterization: A case study in the Thyle catchment, Belgium. *Ecological Modelling* 187(1):27-39.

Salles, L.A., and H.M.L. Chaves. 2011. Estudo da sensibilidade de variáveis sedimentológicas influentes no desempenho do modelo SWAT. In: Lima, J.E.F.W., and W.T.A. Lopes. (Org.). *Engenharia de Sedimentos: na busca de soluções para problemas de erosão e assoreamento*. Brasília: ABRH, v.1, p.345-364.

Sartori, A., F. Lombardi Neto, and A.M. Genovez. 2005. Classificação hidrológica de solos brasileiros para a estimativa da chuva excedente com o método do Serviço de Conservação do Solo dos Estados Unidos parte I: Classificação. *Rev. Bras. Rec. Hídr.*, v10, n4, p.5-18.

Silva, L.R.S. 2010. Análise de incertezas e avaliação dos fatores influentes no desempenho de modelos de simulação de bacias hidrográficas, 241f. *Tese* (Doutorado em Tecnologia Ambiental e Recursos Hídricos), Departamento de Engenharia Civil e Ambiental, UnB, Distrito Federal.

Stoner, E., E. Freitas Jr, J. Macedo, R.C.A. Mendes, I.M. Cardoso, R.F.Mabile, R.B. Bryant, and D.J. Lathwell. 1991. Physical constraints to root growth in savanna oxisols. Raleigh: NCSU, 28p. (*TropSoils Bulletin*, 91-01).

Strauch, M.; F.I. Bakker, A. Araujo, J.E.F.W. Lima, C. Lorz, and F.Makeschin. 2011. Assessing the hydrologic impact of conservation management practices for the Pipiripau River basin, Central Brazil, using SWAT. In: *Proceedings of the 12th International Specialized Conference on Watershed and River Basin Management*. Recife: IWA, 2011.

Strauch, M., C. Bernhofer, S. Koide, M. Volk, C. Lorz, and F. Makeschin. 2012. Using precipitation data ensemble for uncertainty analysis in SWAT streamflow simulation. *Journal of Hydrology* (Amsterdam), v. 414-415, p. 413-424.

Strauch, M., J.E.F.W. Lima, M. Volk, C. Lorz, and F.Makeschin. 2013. The impact of Best Management Practices on simulated streamflow and sediment load in a Central Brazilian catchment. *Journal of Environmental Management*, v. 1, p. 10.1016/j.jenvm-13, 2013.

Yerima, B.P.K.; Van Ranst, E. (2005) Introduction to Soil Science: Soils of the Tropics. 417p.

SWATShare – A portal for sharing, publishing, and running SWAT model using XSEDE resources

Venkatesh Merwade*

Associate Professor, School of Civil Engineering, Purdue University, West Lafayette IN 47907, USA. vmerwade@purdue.edu

Carol Song

Senior Research Scientist, Rosen Center for Advanced Computing, Purdue University, West Lafayette, IN 47907, USA.

Lan Zhao

Research Scientist, Rosen Center for Advanced Computing, Purdue University, West Lafayette, IN 47907, USA.

Shandian Zhe

Graduate Research Assistant, Rosen Center for Advanced Computing, Purdue University, West Lafayette, IN 47907, USA.

Mohammad Adnan Rajib

Graduate Research Assistant, School of Civil Engineering, Purdue University, West Lafayette IN 47907, USA

Abstract

Many hydrologic modelers around the world use SWAT to simulate hydrologic processes, water quality loadings and testing agricultural management scenarios. Once these tasks are complete including publication of results, the models generally are not published or made available to the public for further use and improvement. Although publication or sharing of models is not required for journal publications, sharing of models may open doors for new collaborations, and avoids duplication of efforts if other researchers are interested in simulating a particular watershed for which a model already exists. For researchers, who are interested in sharing models, there are limited avenues to publishing their models to the wider community. Towards filling this gap, a prototype cyberinfrastructure (CI), called SWATShare, is developed for publishing, sharing and running SWAT models in an interactive GIS-enabled web environment. SWATShare is a part of WaterHUB cyberinfrastructure developed at Purdue University to share water related data and models. Users can utilize SWATShare to publish or upload their own models, search and download existing SWAT models developed by others, run simulations including calibration using high performance resources provided by XSEDE, and visualize model outputs. This paper describes the infrastructure behind SWATShare and demonstrate the utility of SWATShare for collaborative research and education.

Keywords: SWATShare; WaterHUB; SWAT; XSEDE; cyberinfrastructure

Introduction

SWAT is a versatile tool that is used by many educators, researchers, watershed managers and decision makers to teach, conduct research, and make decisions related to watershed management. Because it is so versatile, how a SWAT model is used or applied varies from user to user. For example, a hydrologist may be more concerned about the accurate representation of watershed characteristics and processes to get the water balance right. On the other hand, a decision maker may be interested in getting final number on pollutant or nutrient loads without much attention to the technical details in the model. Regardless of the ultimate use of the model or its output, setting up a good SWAT model does involve significant amount of human and computational efforts. Thus, if a hydrologist spends all the needed efforts to set-up a SWAT model to simulate the hydrology of a watershed, the same model can become a starting point for a watershed manager, who may be interested in simulating the water quality for the same watershed. Similarly, a decision maker should be able to use the same model to look at the outputs and make decisions without spending time in creating a model that is already being created by someone else for the same watershed. A SWAT model can also serve as a great educational tool, if students can just look at model outputs from different watersheds, and develop or test hypothesis related land use, agricultural practices and climate change on watershed hydrology.

Significant advances have been made in the last two decades in the area of on computational resources, computing technology and the availability of digital data. Several initiatives are ongoing in to harness the power of these advances for hydrology including the CUAHSI HIS in the United States, OpenMI in Europe and xx in yy. Aligned with these initiatives which mainly deal with data access and integration of modeling systems, there is a need to also develop cyberinfrastructure that can integrated both data and models in a cyber environment. To address this need, a prototype cyberinfrastructure, called SWATShare, is developed specifically for the SWAT model. SWATShare provides the following functions for SWAT modelers and users:

1) Publication and sharing of SWAT models on the internet including input data and related output files with other researchers, educators and decision makers.
2) A cyber platform for executing SWAT models including sensitivity analysis and auto-calibration using the NSF XSEDE advanced computing resources (http://xsede.org).
3) A cyber platform for collaborating on research and other projects using a common SWAT model.
4) A cyber platform for students to use existing SWAT models to study about hydrology under different physical as well as climatic conditions.
5) A potential global repository of SWAT models that can be discovered through simple search involving geographic location and/or watershed name.

SWATShare is still in its infancy so the objective of this paper is to provide basic description of its functionality and the cyberinfrastructure architecture behind it so the tool becomes more visible to the SWAT community for use in the coming years.

SWATShare Interface

The SWATShare interface is a part of WaterHUB, which is based on Purdue University's HUBZero technology (McLennan et al., 2010). All functionalities of SWATShare are only accessible to WaterHUB members. Anyone with a valid email address can join WaterHUB at www.water-hub.org. The SWATShare interface enables searching of available SWAT models through geographic view of watersheds, uploading of SWAT models, editing of metadata information for uploaded SWAT models, running of uploaded SWAT models and output visualization. Each interface is described in detail in the following sections:

View

The main purpose of the *View* interface (Fig. 1) is to display all watershed models that are uploaded into the SWATShare interface. The models are displayed in the right panel in three groups: (i) *My Models*: models that are uploaded by the current user; (ii) *Shared Models*: models that are uploaded by other users, but are shared with all users; and (iii) *Other models*: models that are uploaded by other users but not shared. If a user clicks on a model in the list, the map view in the left panel will highlight the selected model and display its metadata as shown in Fig. 1.

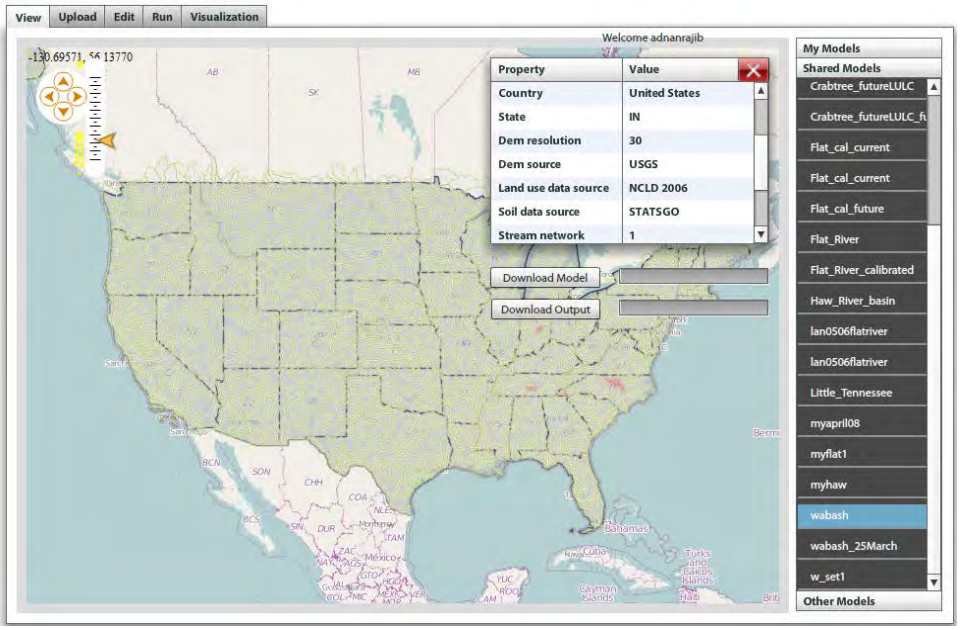

Figure 1. SWATShare view tab components

In the view tab, users can download their own model or a shared model and the associated output files by using the download buttons.

Upload

This interface (Fig. 2) allows a user to upload SWAT models into SWATShare interface by providing the key metadata associated with the model. A model is uploaded as a zip or tar file that includes the following files or folders from an ArcSWAT project (Fig. 3): (i) ESRI ArcMap document that is used for creating the input files using ArcSWAT; (ii) Project geodatabase. This will be the Microsoft Access Database (.mdb) file which will have the same name as the ArcMap

document but with an .mdb extension; (iii) SWAT2009 is the geodatabase available with ArcSWAT 2009. This usually remains in the 'swat' folder of the user's computer directory where the ArcSWAT is installed; and (iv) Watershed and Scenarios folders, RasterStore folder and its geodatabase. These are created automatically during an ArcSWAT project setup.

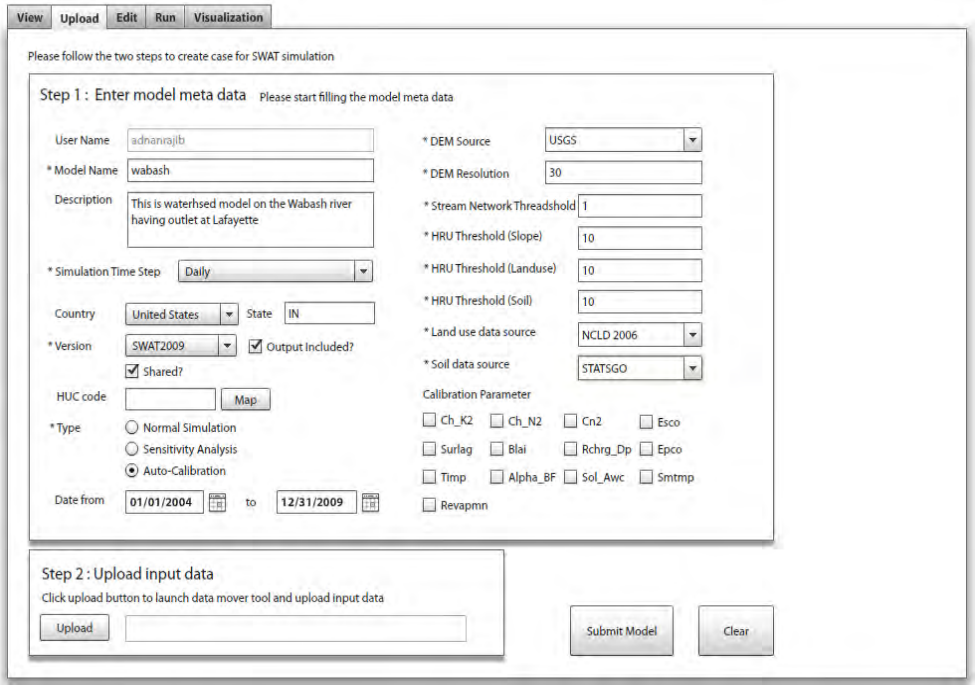

Figure 2. SWATShare Upload Interface with information filled for a model named wabash

Uploading of model into SWATShare involves a two-step procedure. In the first step, a user has to enter the metadata associated with the model including model name and description, simulation time-step (daily/monthly) and duration, DEM source and resolution, stream network threshold (%), slope, landuse and soil threshold (%) for HRU definition, landuse and soil data source, as well as the SWAT version being used. By default, the output included box is not checked, but if the output of the model is included in the upload, the user can check the 'Output Included' box. Similarly, if the user wants to share the model with others, the 'Shared' box should be checked. The default option for Model Type is 'Normal Simulation'; the other two options are 'Sensitivity Analysis' and 'Auto-calibration'. Users can check boxes for the parameters that are included in the sensitivity analysis or calibration depending on the option chosen as modeling 'Type'. However, these are just some of the common parameters listed as meta-information; the model actually can have other parameters incorporated into it. In the second step, the model is uploaded by clicking the 'Upload' button and browsing to the computer directory where the zip folder is located. The upload process is completed by selecting the "Submit Model" button.

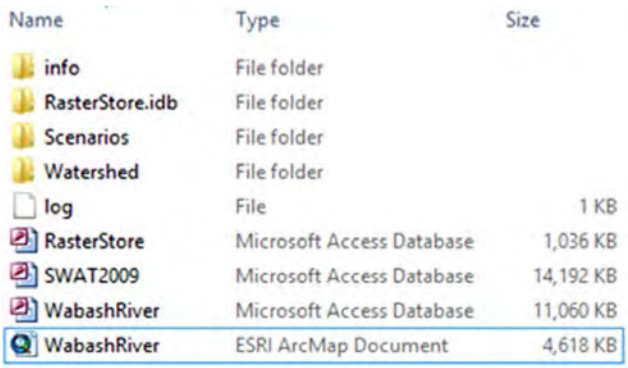

Figure 3. Typical components in a SWATShare model zip folder

Now, in order to produce a successful model execution in SWATShare, following key features has to be taken care of prior to uploading:

Appropriate Method-flag in file.cio: Depending on the type of the simulation selected during the upload, the interface uses the "ICLB" flag in the file.cio file to run a normal simulation (ICLB = 0) or sensitivity analysis (ICLB = 1) or auto-calibration (ICLB = 2). Currently ICLB = 3 (calibration with uncertainty analysis) and ICLB = 4 (re-run of a calibrated model with best parameter set) cases are not supported by SWATShare.

***Simulation Duration and Time-step*:** The information for simulation duration and time step should correspond to appropriate values in the file.cio file. Specifically, the file.cio contains this information using the following variables: (i) NBYR: number of years simulated, (ii) IYR: beginning year of simulation, (iii) IDAF: beginning julian day of simulation, and (iv) NYSKIP: number of years to skip output summarization. In SWATShare, the simulation duration should cover the whole period including NYSKIP. The simulation time step gets decided by the variable IPRINT (IPRINT = 0 for monthly, IPRINT = 1 for daily, and IPRINT = 2 for yearly simulation).

Default Simulation Folder: Input files needed to run a SWAT model are generally stored in the TxtInOut folder inside the "Default" folder within the Scenarios folder. However, if multiple TxtInOut folders exist within an ArcSWAT project, SWATShare uses the file.cio and other input files from the TxtInOut folder that is inside the Default folder. Other file.cio files are ignored.

***Setting up Auto-calibration and Sensitivity Analysis for New and Shared Models*:** In order to upload a SWAT model for auto-calibration run on SWATShare, a user must first run the auto-calibration using ArcSWAT by using a very small number of trials (e.g., maximum number of trials allowed before parameter optimization is terminated, MAXN = 10 or less). Simultaneously, all other input or output parameters such as the observed data, objective function, analysis location (a particular sub-basin), as well as the calibration parameters are defined within the ArcSWAT's auto-calibration dialogue box following Winchell et al. (2010). Out of three calibration methods in SWAT 2009, Only PARASOL should be selected so as to make the process compatible with the current version of SWATShare. Thus, a new folder called AutoCal gets created in the TxtInOut of the model's Default simulation. Running the auto-calibration in ArcSWAT with small MAXN will populate AutoCal with certain necessary files which were

initially absent in the TxtInOut during a normal simulation. Finally, the user has to modify the parasolin.dat inside the newly populated AutoCal folder by setting a higher MAXN value; thereby completing the model preparation for auto-calibration run in SWATShare.

The model preparation for sensitivity analysis is identical to the one described above for auto-calibration. In the case of sensitivity analysis, a folder named *Sensitivity* gets created instead of *AutoCal*, and there is no need to specify MAXN. Hence, a user has to set and initiate the sensitivity analysis in ArcSWAT and then manually terminate the program after few runs to enable the creation of necessary files inside the *Sensitivity* folder.

Edit

The *Edit* interface (Fig. 4) is similar to the Upload interface. However, this interface can only be used to update or replace information including the model file for an existing model in the system. When a model is selected in the right hand column, all the information related to the model will be displayed on the left hand side. If any changes are made, clicking the 'Change' button will save those changes. The 'Reset' button will restore the original information that was saved with the original model. The 'Delete' button will delete the selected model from SWATShare. Generally, a user can only edit or modify model owned by him or her (My Models). However, if a user is interested in using another shared model, that model needs to be first copied into the user's own account by using the "Copy Model to My Account" button on the right top corner, and giving it a different name.

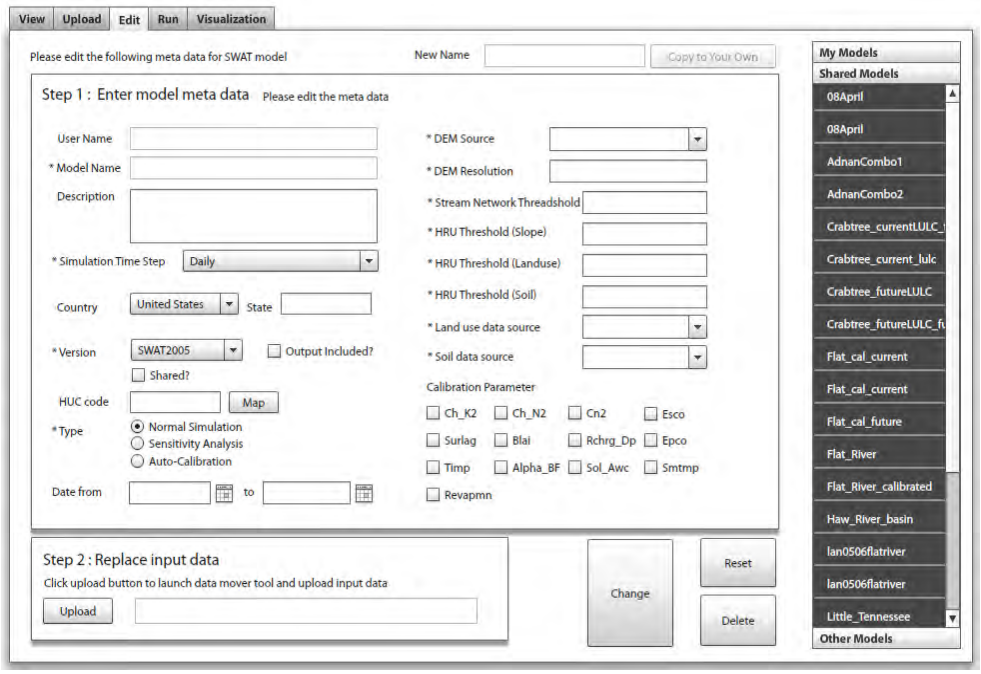

Figure 4. SWATShare Edit Interface

Run

The *Run* interface allows users to perform a regular SWAT simulation, sensitivity analysis, or auto-calibration depending on the option selected in 'Model Type' field while uploading the model, and as defined in the *file.cio*. A user can only run models from his or her account. Fig. 5 shows the *Run* tab with different possible job status. First, a model is selected from the list on the right panel. Clicking the 'Run' button will submit the model to run either on the Purdue Condor pool or one of the XSEDE clusters. Depending on the resource availability, the model run may start immediately or it may be dispatched in a job queue waiting to be executed on the cluster.

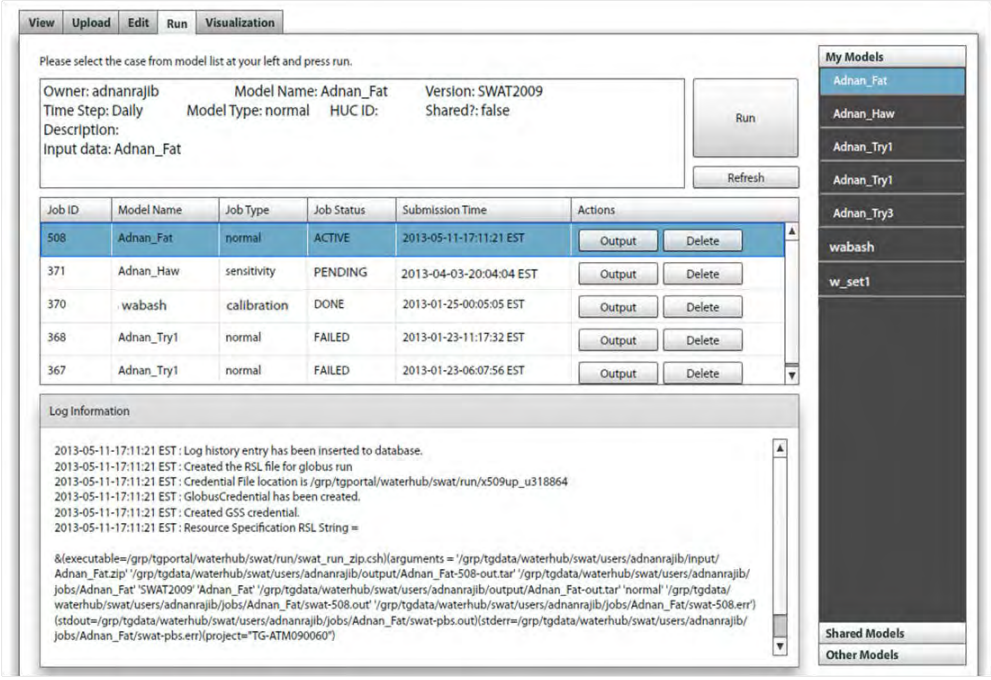

Figure 5. SWATShare Run Interface with Example of Different Job Statuses

Visualization

The *Visualization* interface can only be used for visualizing the results of a user's own models that have been executed successfully. If a user has several successfully run models in the account, any one of the models can be picked from the dropdown list on the top of the *Visualization* tab (Fig. 6).

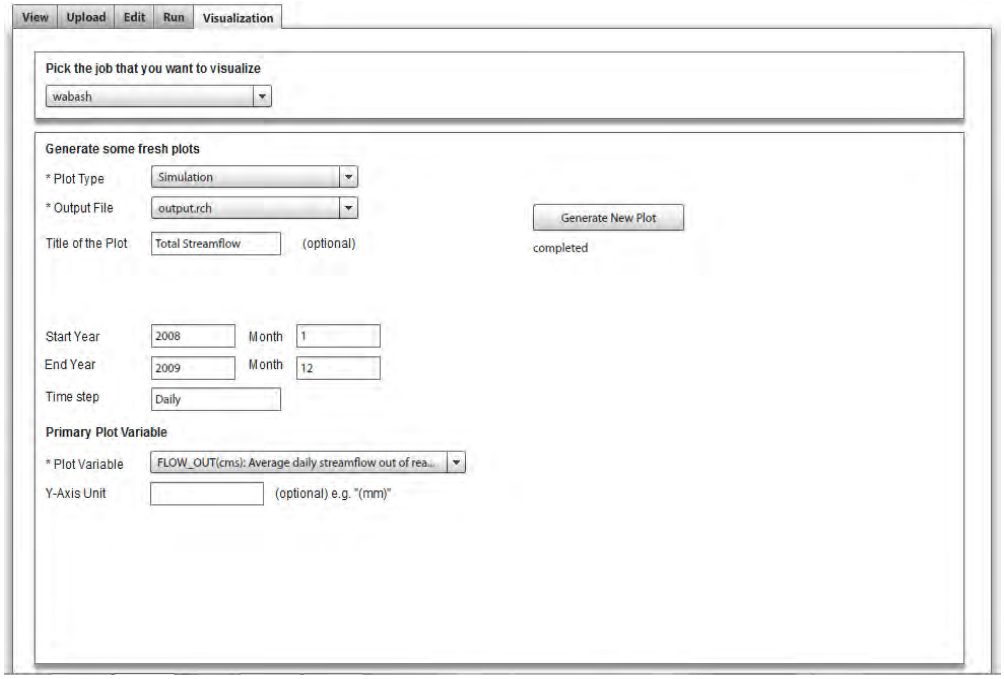

Figure 6. SWATShare Visualization Interface

The present version of SWATShare can be used to visualize results from three types of output files including: (i) output.std, (ii) output.sub and (iii) output.rch. Once a model and a particular output file is selected, users can then select then select one variable at a time to produce the visual plot as shown in Fig. 7. In case of output.rch and output.sub, all the plots correspond to the output at the watershed outlet.

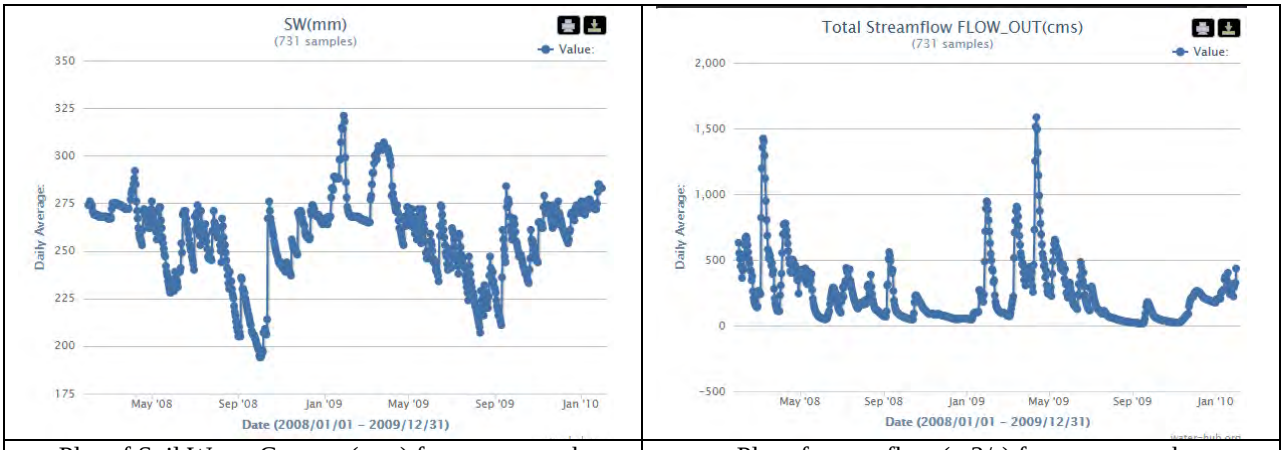

Plot of Soil Water Content (mm) from output.sub	Plot of streamflow (m3/s) from output.rch

Figure 7. Example plots (generated for only one year out of the 6 year simulation period)

SWATShare Architecture

SWATShare user interface is developed using FLEX, and it is deployed on WaterHUB, which is built using the HUBzero technology. The tool's access control defaults to the security layer provided by the HUBzero framework. A Tomcat web service is invoked to check authorization for all operations a user tries to perform. As described earlier, SWATShare supports five key functions for publishing, sharing, and executing a SWAT model. These functions include: View, Upload, Edit, Run and Visualize. The software architecture for SWATShare presented in Figure 8, and described below.

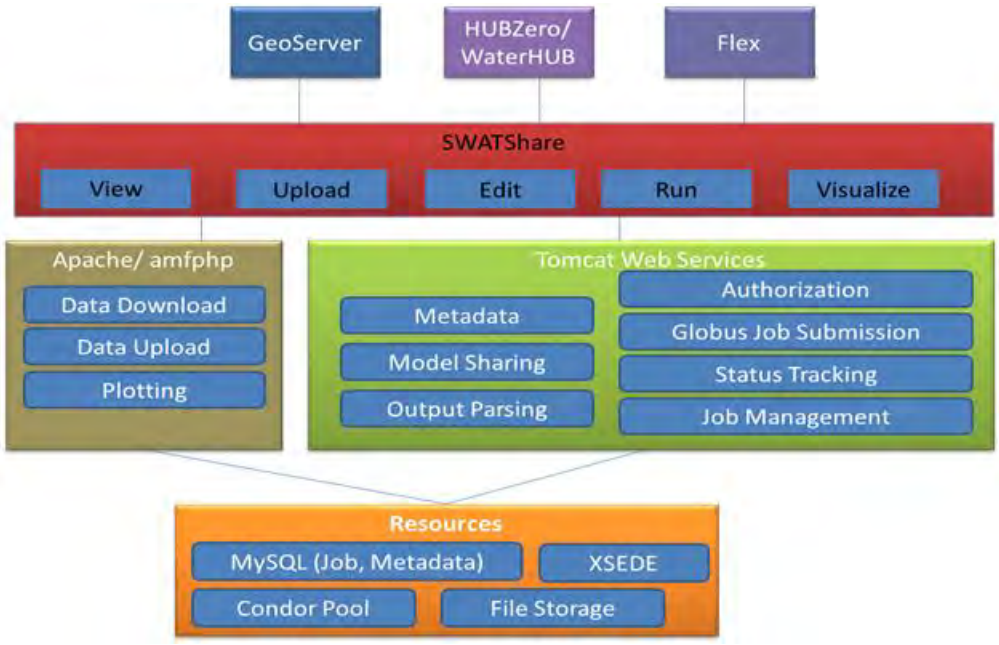

Figure 8. SWATShare Architecture

The view function uses Geoserver for rendering GIS layers and associated metadata so users can select an area to see if any model is available for the selected area. The metadata for available models is extracted from a MySQL database using tomcat web services. A user may also be able to download any shared model from the view interface using HTTP protocol via an Apache server.

The upload function enables a user to upload a SWAT model and its associated files in a compressed format (.zip or .tar). During this step a user provides necessary metadata such as the source of data used in creating the model, data resolution, and location, which is stored in the MySQL database. The actual upload of the data is enabled by using an Apache PHP service and the uploaded file is stored on a storage server. The edit interface is similar to the upload interface. A user can use this interface to edit metadata or change the input data for an existing model.

The run interface is used for running simulations of SWAT models. It invokes the tomcat web services to submit jobs to the Purdue Condor pool or an XSEDE resource, depending on the type of computation required, and to keep track of the simulation. All the outputs from the model are stored on the storage server. The run interface allows users to track the status of their jobs, access log files for debugging, and download the model output after a successful simulation.

Finally, the visualization interface enables a user to visualize plots of model results by selecting an appropriate output file, a variable of interest, and the time period. The plotting is enabled by extracting data from the model outputs using tomcat web services and then producing the plot using PHP.

Summary and Concluding Remarks

A cyberinfrastructure, called SWATShare, to publish, share and run SWAT models is presented in this paper. Such an infrastructure is expected to reduce the redundancy in creating multiple SWAT models for the same area, and at the same time encourage enhancement of existing models by incorporating modifications from multiple users with diverse modeling needs. Similarly, a common platform to share a versatile model such as SWAT will also enable new collaboration for watershed management and research. Besides research, SWATShare can also be used in teaching where students can run SWAT models for different watersheds to study the effect of landuse change, climate change and watershed management decisions on the overall watershed hydrology and ecology. Although the current view interface only displays models within the United States, SWAT model for any international watershed can be published and shared. A global map to view any existing SWAT model will be added to the view tab in the near future.

References

Arnold, J.G., Kiniry, J.R., Srinivasan, R., Williams, J.R., Haney, E.B. and Neitsch, S.L. (2011) Soil and Water Assessment Tool-Input/Output File Documentation Version 2009, Texas Water Resources Institute Technical Report No. 365, Texas A&M University System, College Station, TX, USA.

M. McLennan, R. Kennell, “HUBzero: A Platform for Dissemination and Collaboration in Computational Science and Engineering,” *Computing in Science and Engineering*, 12(2), pp. 48-52, March/April, 2010.

Winchell, M., Srinivasan, R., Di Luzio, M. and Arnold, J.G. (2010) ArcSWAT Interface of SWAT 2009 User’s Guide, Texas A&M University System, College Station, TX, USA.

The Impact of Climate Data Uncertainty on Calibration of the SWAT Model

Bahareh Kamali
Amirkabir University of Technology, Tehran, Iran, Kamali.civil@gmail.com
Swiss Federal Institute of Aquatic Science and Technology, Duebendorf, Switzeland

S. Jamshid Mousavi
Amirkabir University of Technology, Tehran, Iran, Kamali.civil@gmail.com

Karim Abbaspour
Swiss Federal Institute of Aquatic Science and Technology, Duebendorf, Switzeland

Hong Yang
Swiss Federal Institute of Aquatic Science and Technology, Duebendorf, Switzeland
Department of Environmental Science, University of Basel, Switzerland

Abstract

Successful application of hydrological models is highly dependent on the correctness of the climate data. Usually different sources of data are available for a single watershed, hence accounting for their uncertainty is an important issue which has often been neglected by modelers. In this paper, the impact of climate data was investigated in modeling the Karkheh River Basin (KRB) located in semiarid region of Iran. Using four sources of climate data, we constructed six data sets to be used in a SWAT model of the region. All sets were calibrated using the Sequential Uncertainty Fitting (SUFI-2) in the SWAT-CUP software and their performances were compared using simulated and observed discharges at 12 stations. The results showed that the quality of climate data was more important than the number of climate stations in our region. Besides, the climate data sets with approximately similar behavior in the whole watershed did not have similar performances at each individual outlet. As the final results for different climate data sets were quite different, we conclude that careful attention must be paid to the correctness of the climate data and its uncertainty should be considered in the hydrological models.

Keywords: Climate data uncertainty, Hydrologic Model, SWAT, Sufi-2, Calibration.

Introduction

The use of models to analyze the spatial hydrological characteristics of a watershed has helped management of water resource and is an indispensible tool for the analysis of climate change impacts. Successful applications of models depend on the correctness of the model inputs and the correct identification of the hydrological processes through model calibration. As uncertainty in the quantification of natural phenomena is unavoidable, model inputs such as climate, crop, and soil information, as well as the simplification of processes in the conceptual model introduce errors in the model outputs, which must be quantified.

Proper calibration of the parameters of a hydrological model faces many challenges due to different sources of uncertainties such as; model structure, input data, competence of search (optimization) algorithms, selection of objective functions or parameterization. While many studies have addressed the complexities in model structures (Farmer et al., 2003; Atkinson et al. 2002, 2003), optimization algorithms (Muttil and Liong, 2004; Blasone et al., 2007; Ndiritu, 2009) and parameterization (Refsgaard, 1997; Samanta and Mackay, 2009); few have paid attention on uncertainties stemmed from different sources of input data (Michaud and Sorooshian, 1994; sun et al, 2002) and incorporate them in the assessment of impact of future climate change on water resources.

Among different input data, precipitation and temperature are considered as critical variables for hydrologic modeling because they have high impact on the components of water budgets such as runoff, evaporation and infiltration (Guo et al., 2004; Beven, 2001, 2002; Boyle et al. 2001). Usually different sources of climate data recorded by different organizations and institute are available for a watershed. Selecting the appropriate data sets and considering their uncertainties in hydrologic models is an important issue which has been generally ignored in the literature and becomes the focus of attention in this paper.

In what follows, the Soil and Water Assessment Tool (SWAT) was used to simulate the Karkheh River Basin (KRB), the third largest watershed in Iran. Four sources of climate data were used to construct six data sets to feed into the model. Our strategy is to explore 1) Is it possible to explore dataset with highest performances? 2) If adding more climatological stations enhance the results of hydrological simulation and calibration? 3) Which of quantitative and qualitative levels of data are more significant for model calibration?

Materials and Tools

The SWAT Simulator

SWAT (Arnold et al, 1998) is a semi-distributed, time continues watershed simulator operating on the daily and sub-daily time step. The model has been developed to quantify the impact of land management practices in large and complex watersheds in two phases named; land hydrological cycle and routing hydrological cycle. SWAT's hydrological processes include simulation of surface runoff, percolation, lateral flow and flow from shallow aquifer to streams,

potential evapotranspiration, and snow melt and transmission loss. Spatial parameterization of SWAT is performed through dividing the watershed into subbasins.

The soil water balance equation is the basis of hydrologic modeling. Surface runoff is estimated by a modified Soil Conservation Service-Curve Number (SCS-CN) equation using daily precipitation data and soil hydrologic group, land use and land cover characteristics and antecedent soil moisture. A more detailed description of the model is given by Neitsch et al (2002). In this study; we have used ARC-SWAT 2009 (Winchell et al, 2009) where ArcGIS (Version 9.1) was used for project development.

Calibration and Uncertainty Analysis

Sensitivity analysis and calibration were performed in terms of monthly discharge values. The key parameters were identified through sensitivity analysis and the SUFI-2 (Abbaspour et al., 2007) algorithm in SWAT-CUP program. The algorithm maps all uncertainty on the parameter ranges and tries to capture most of the measured data within the 95% prediction uncertainty. The overall uncertainty in the output is quantified by the 95% prediction uncertainty (95 PPU) calculated at the 2.5 % and 97.5% levels of cumulative distribution of an output variable obtained through Latin hypercube sampling. We have used *br2* (Krause et al, 2005) criteria to compare the performance of simulated and observed discharge values.

Study Area and Data Preparation

The Karkhe River Basin (KRB) is located in the south western part of Iran with total area of about 50800 km^2 (Fig. 1). The catchment is the third largest basin in Iran. The climate of KRB is mainly semi-arid with large annual precipitation, ranging from 150 mm in south to 1000 mm in the upper karkheh. Nearly two thirds of the basin lie in the mountains (elevations between 1000 and 2500 m), and the surface and ground water resources are replenished from winter snow falls in the high Zagros ranges.

Data for modeling KRB was put together from different sources. Digital Elevation Model (DEM) was extracted from CGIAR-CSI consortium for spatial information with a spatial resolution of 90 meters (http://srtm.csi.cgiar.org/). The soil map for the study area was obtained from global soil map of the Food and Agricultural Organization (FAO) of the united nation. The land use map was obtained from USGS Global Land use Cover Characterization (GLCC) database.

Four sources of climate data were available. The first set (*Climate1*) with nine climate stations was obtained from Iranian Ministry of Energy. The second climate data (*Climate2*) with 23 stations were gotten from public Weather Service of Iranian Meteorological Organization (WSIMO). Climate Research Unit (CRU) data (*Climate3*) was the third source. The fourth set (*Climate4*) was from GFDL-ESM2M model. Based on $0.5^0 * 0.5^0$ resolutions, the 32 grid points obtained from the last two sources. The positions of all sources are depicted on Figure 1.

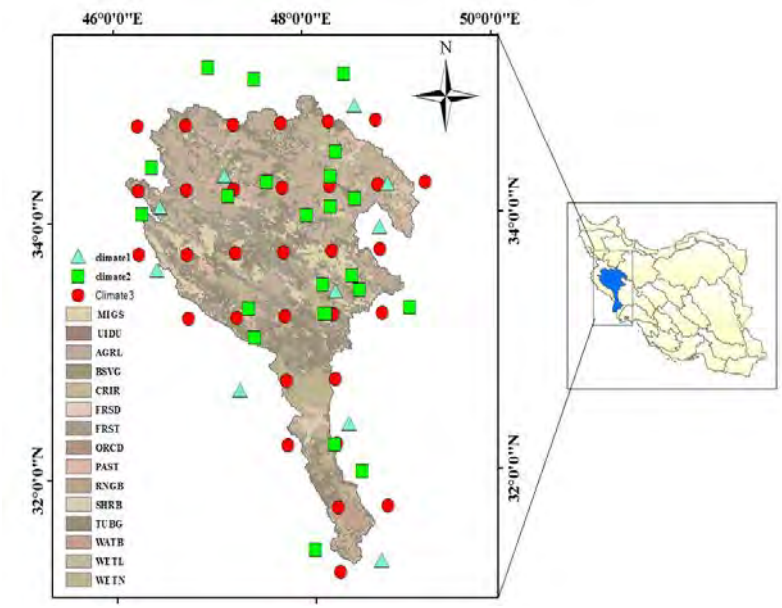

Figure 1. Locations of the Karkheh basin; land use classifications

Six different combinations of climate data (*DataSets 1-6*) were constructed. *DataSets 1-4* were constructed using *Climate1*, *Climate2*, *Climate3* and *Climate4* data sets respectively. In *DataSet 5*, we put together *Climate1* and *Climate2* (from local stations) to assess whether adding more climate stations would be helpful to enhance model calibration. In *DataSet 6*, we selected climate stations which were better representative of watershed characteristics in terms of simulating discharge values. To investigate the significance of input data, their performances of the six data sets were compared in term of simulating 12 discharge hydrographs.

Results

All six datasets were used to build SWAT model of study area and the results were compared both before and after calibration processes. The *br2* median, 25th, 75th percentiles and also the variability in 12 outlets for all six data sets were depicted in Figure 2. As shown, before calibration *DataSets 4* had the worst performance. *DataSets 1&3* have approximately equal median. While *br2* variations are higher in *DataSets 1*, the 75th percentile is also higher compared to *DataSets 3*. Comparison of *DataSets 1&2* showed that *Climate1* with even fewer numbers of stations had higher median, 25th and 75th percentiles; means the set is more suitable to represent climatological characteristic of watershed. This issue disclosed that more intense quantitative information does not necessarily improve model performances.

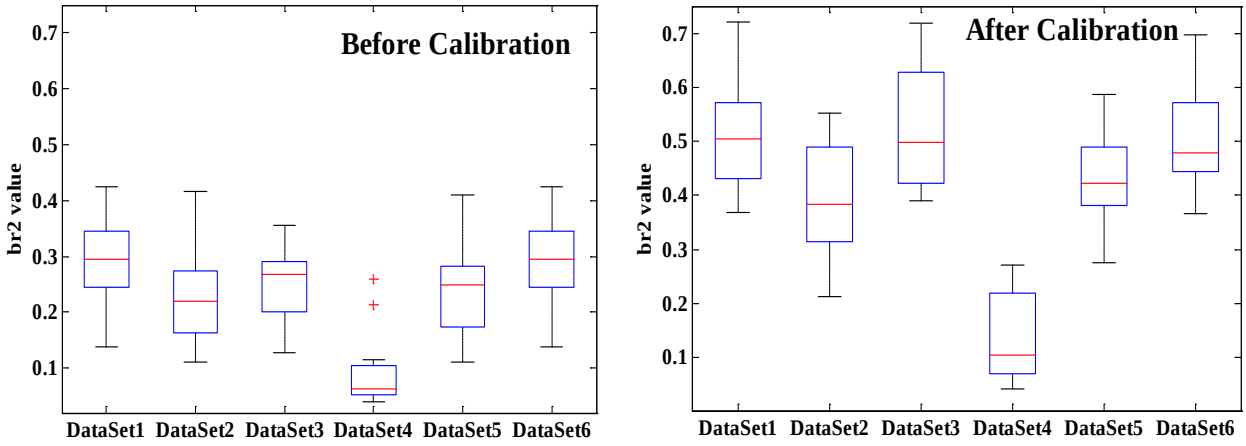

Figure 2. The performance of *Datasets 1-6* in discharge simulation before and after Calibration; (the red line shows the median and the box show the 25th and 75th percentiles)

An interesting point in comparing the criteria values of different outlets was that *DataSets 1* with higher median did not work well for the outlets located in upper region of watershed where *DataSets 2* had much better results. This means that in *climate2*, the climate stations located in upper regions of watershed were better representative of watershed characteristics. For this reason, in *DataSets 6* climate stations of *Climate1* located at the upper regions of basin were replaced with *Climate2* stations. In this data set the median, 25th and 75th percentiles were much improved.

All results of simulation before calibration showed that there are great variations in performances of different datasets in discharge simulations. It suggests that any hydrologic model should be evaluated in calibration steps before the results are assessed. In order to calibrate all input data sets using SUFI-2 algorithm, sensitivity analysis was performed to select the most sensitive parameters related to discharge values (White and Chaybey; 2005, and Abbaspour et al, 2007). The parameters are illustrated in Table 1.

Table 1. SWAT parameters included in calibration process

Parameter name	**Definition**	**Parameter name**	**Definition**
CN2.mgt	SCS runoff curve number	*GWQMN.gw*	Threshold depth of water in shallow aquifer required for return flow to occur (mm)
CH_N2.rte	Manning's n value for main channel	*OVN. hru*	Manning's n value for overland flow
CH_K2.rte	Hydraulic conductivity for main channel	*ESCO. hru*	Soil available water storage capacity (mm H_2
GW_REVAP.gw	Groundwater revap coefficient	*SOL_AWC.sol*	Soil Water availability

After calibration (Figure 2), while the *br2* for *DataSet 4* improved, it still had the worst performances compared with the others. *DataSets 1&3&6* performed better. So, from the 6 datasets, *DataSets 4* had worst performance. *DataSets 1, 3, 6* had highest and quit similar to each other performances. The remaining two sets were in between.

The behavior of three datasets (*DataSets 1&3&6)* in simulating three discharge hydrographs (Gurbaghestan, Hamidieh and Poldokhtar) with their corresponding *br2* values were depicted in Figure 3. As shown, the three datasets with similar mean *br2* showed different behavior in simulating discharge values. The sets with approximately similar *br2* values for the whole watershed did not show identical behavior in each individual outlet. *DataSet3* with *br2*=0.67 had the highest performances in Gurbaghestan station. In Hamidieh station, *DataSet1* outperformed the others and in Poldokhtar station, *DataSet7* performed better. Had

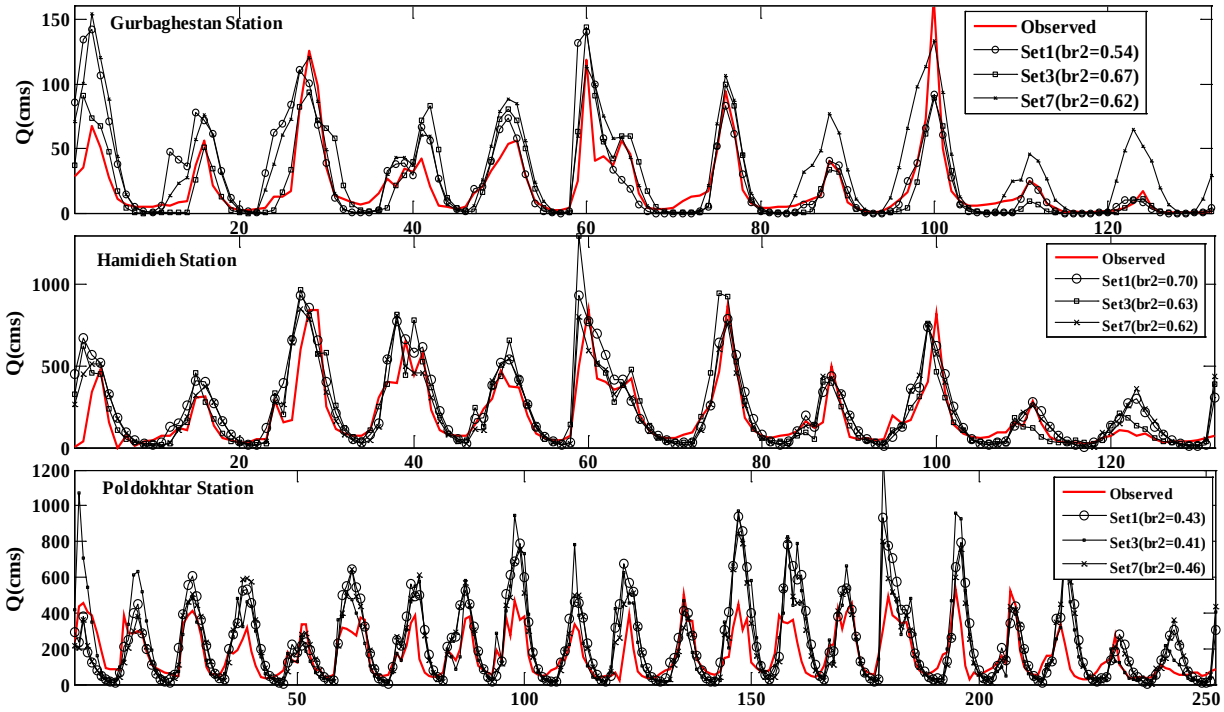

Figure 3. The simulated and observed hydrographs of three sets (*DataSets 1&3&6)* in three discharge stations

Conclusion

The importance of considering uncertainties stemmed from the sources of climate input data was discussed in simulation and calibration of the Karkheh river catchment model. Six combinations of data sets were constructed from four different sources of climate data and their performances were compared in terms of simulating observed discharges both before and after calibration. The results showed that adding more climate stations does not necessarily enhance the simulating performances. The qualitative nature of data is more crucial and should be more representative of

watershed characteristics. Assessing the performances of six datasets before and after calibration led to three sets with higher median *br2*. However, pursuing their behavior in simulating discharge stations showed that each set outperformed the others in terms of simulating some outlets. This revealed that there are uncertainties in the sources of input climate data which influences the simulation results. The corresponding uncertainties will then be emerged in terms of final adjusted parameters which will propagate in next management issues. Careful attention to uncertainties in the sources of climate data is needed for the modelers at the first stages of simulation in any water resources assessment using hydrological models.

References

Abbaspour, K. C. 2007. User Manual for SWAT-CUP, SWAT Calibration and Uncertainty Analysis Programs. *Swiss Federal Institute of Aquatic Science and Technology,* Eawag, Duebendorf, Switzerland. 93 pp.

Atkinson, S., R. A. Woods, and M. Sivapalan. 2002. Climate and landscape controls on water balance model complexity over changing time scales. *Water Resources Research* 38(12): 50.1–50.17

Atkinson, S., M. Sivapalan, R.A. Woods, and N.R. Viney. 2003. Dominant physical controls of hourly streamflow predictions and an examination of the role of spatial variability: Mahurangi catchment, New Zealand. *Advances in Water Resources* 26(3): 219–235.

Arnold, J. G., R. Srinivasan, R. S. Muttiah, and J. R. Williams, 1998. Large Area Hydrologic Modeling and Assessment Part I: Model Development. *Journal of the American Water Resources Association.* 34(1): 73-89

Blasone, R. S, H. Madsen, and D. Rosbjerg. 2007. Parameter estimation in distributed hydrological modeling: comparison of global and local optimization techniques, *Nordic Journal.* 38: 451-476

Beven, K. 2001. How far can we go in distributed hydrological modeling? *Hydrol. Earth Syst.* Sci., 5: 1–12.

Beven, K. 2002. Towards an alternative blueprint for a physically based digitally simulated hydrologic response modeling system, *Hydrol Process.* 16: 189–206.

Boyle, D. P. and H. V. Gupta, S. Sorooshian, V. Koren, Z. Zhang, and M. Smith. 2001. Toward improved streamflow forecast: value of semi-distributed modeling.*Water Resour. Res.,* 37: 2749–2759.

Farmer, D., M. Sivapalan, C. Jothityangkoon. 2003. Climate soil and vegetation controls upon the variability of the water balance in temperature and semi-arid landscapes. Downward approach to hydrologic prediction. *Water resource research* 39 (2).

Guo, J., X. Liang, and L. R. Leung. 2004. Impacts of different precipitation data sources on water budgets, *J. Hydrol.*, 298: 311–334.

Krause, D., B. P. Boyle, and F. Bäse. 2005. Comparison of different efficiency criteria for hydrological model assessment. *Adv. Geosci.* 89-97.

Muttil, N., S. Y. Liong. 2004**.** Superior exploration–exploitation balance in shuffled complex evolution, *Journal of Hydraulic Engineering.* 130: 1202-1205**.**

Michaud, J. D. and Sorooshian, S.. 1994. Effect of rainfall-sampling errors on simulations of desert 30 flash floods, *Water Resour. Res*. 30: 2765–2775.

Ndiritu J. G. 2009. Automatic calibration of the Pitman model using the shuffled complex evolution method. *Report to Water Research Commission School of Civil and Environmental Engineering*. KV 229/09, University of the Witwatersrand

Neitsch, S. L, J. G. Arnold, J. R. Kiniry, J. R. Williams, and K. W. King. 2002. Soil and water assessment tool. Theoretical documentation: Version 2000. TWRI TR-191. College Station, Texas: Texas Water Resources Institute.

Refsgaard J. Ch. 1997. Parameterisation, calibration and validation of distributed hydrological models. *Journal of Hydrology.* 198: 69-97.

Samanta, S, and D. S. Mackay. 2009. Flexible automated parameterization of hydrologic models using fuzzy logic. *Water Resource Research.* 39: 1-13.

Sun, H., P. S. Cornish, and T. M. Daniell. 2002. Spatial variability in hydrologic modeling using rainfall runo model and digital elevation model. *J. Hydrol. Eng.* 7: 404–412.

White, K. L, and I. Chaubey. 2005. Sensitivity analysis, calibration and validation for multisite and multi variable SWAT model. *Journal of the American Water Resources Association* 41(5): 1077-1089.

Winchell. M., R. D. Srinivasan, M. Lizo, and J. Arnold. 2009. ARC-SWAT Interface for SWAT 2009. User's guide. *Blackland Research Center, Texas Agricultural Experiment Station and Grassland*. Soil and Water Research Laboratory. USDA Agricultural research service. Temple, Tax.

Effects of Land-Cover Changes and other Remediations on Hydrology of Xinjiang River Sub-watershed, China

Ambika Khadka*
School of Forestry and Environmental Studies, Yale University, 195 Prospect Street, New Haven, CT-06511, USA. Khadka.ambi@gmail.com.

ChunFu
Research Center of Central China Economic Development, Nanchang University, Nanchang 330031, China

Muangmoe Myint
Mapping and Natural Resources Information Integration, Vaud La Brussus 1348, Switzerland

Chadwick Oliver
School of Forestry and Environmental Studies, Yale University, 195 Prospect Street, New Haven, CT-06511, USA

James Saiers
School of Forestry and Environmental Studies, Yale University, 195 Prospect Street, New Haven, CT-06511, USA

Abstract

To determine whether reforestation efforts in the denuded hills have significant impacts on hydrology in the Xinjiang River watershed, the authors examined eight land-cover scenarios to compare hydrologic responses and to provide a conceptual basis for restoration practices. The authors analyzed a 17-year time period using remote sensing to develop land-cover classification for the watershed. Climate, soil, and terrain data for the watershed were used as input in the SWAT (soil and water analysis tool) to quantify and compare the impacts on hydrologic processes. The model was calibrated to a two-year record of stream discharge measurements. The results show significant increase in forest-cover on hills (13%). However, the hydrological response is not very significant considering the changes in forest-cover, the surface runoff and percolation ratios only changed by 2% and 1% over time. Installment of earthen irrigation ponds in the outlets of sub-basin with maximum runoff had provided the most significant hydrologic improvements and could provide irrigation water to increase crop yield on remaining cropland. The study will provide information to the local government to aid decision-making in sustainable reforestation programs resulting in better hydrologic functioning for sustainable water resource management.

Key words: SWAT (Soil and Water Analysis Tool), hydrologic responses, surface runoff, percolation, reforestation efforts.

Introduction

China's massive reforestation plan, a program for re-conversion of farmland to forest called "Grain for Green" aimed at increasing perennial vegetation on cultivated land at slope of 25^{o} or more by 32 million ha by 2010 (Wei et al., 2008). Reforestation programs in southern China began back in the 1950's when degraded lands were reforested for timber production without environmental considerations (Zhou et al., 2002). Since 1975, increased awareness for environmental protection as well as the emergence of new markets for forest products promoted additional efforts at reforestation with the objectives of restoring degraded natural ecosystems (Zhou, et al., 2002). The devastating floods of 1981 and 1998 in the Yangtze River spurred hydrological research and motivated China to adopt a policy called the NFCP (Natural Forest Conservation Program) (Wei et al., 2008). The objectives of the NFCP include restoring natural forests in ecologically sensitive areas such as the headwaters of several large river basins (e.g. Yangtze and Yellow Rivers), planting trees for soil and water protection, increasing timber protection in forest plantations, banning excessive cutting, and maintaining multiple uses of forests (Sun et al., 2008).

In the 1980's after most of the existing vegetation was removed for firewood and industrial use, the area was called as the "red desert of southern China" (Zheng et al., 2008). These denuded hills were reforested in 1998 with species such as masson pine (*Pinusmassoniana*), slash pine (*Pinuselliottii*), China-fir (*Cunninghamialanceolata*), and eucalyptus (*Eucalyptus spp.*) (Jiang et al., 2003). These species were planted because of their ability to compete successfully on water-limited sites as well as their ability to hold soil in the hills. Despite high annual rainfall in southern China, surface and underground water resources are limited because of surface runoff during and following loss of high intensity rainfalls during the wet seasons, which cause problems of erosion, siltation, and flooding (Zhou et al., 2002).

The 2011 general forest survey by the department of forestry construction and ecology environment indicates that the total forestland area in Jiangxi Province has increased from 106,287 ha in 1999 to 107,202 ha in 2010 (Provincial Profile of Jiangxi Province, 2011). The increase in forestland is thought to be caused by the natural forest conservation and "returning farmland to forest" programs in the Yangtze River basin.

Study of forest and other land-cover changes within watershed is fundamental to a better understanding of watershed hydrology. Land-cover is characterized in part by the type of vegetation such as forest, agricultural crops, grass, open space, urban, or water. Vegetation type directly impacts the amount of evaporation, groundwater infiltration, and surface runoff that occur during and after precipitation events. Changes in land-cover alter both runoff behavior and the balance that exists between evaporation, groundwater recharge, and stream discharge with considerable effects for all water users (Sahin and Hall, 1996).

This study investigated the impacts of reforestation on hydrology of Xinjiang River Watershed using SWAT (soil and water analysis tool) (Neitsch et al., 2000) and remote sensing, with the following objectives: 1) to understand the effects of different land-cover and remediation scenarios on hydrology and the effects of vegetation on surface runoff in the hilly red soil region of southern China; 2) to assess the impact of different land-cover scenarios on surface runoff (quick flow) and delayed flow in the Xinjiang river sub-watershed; and 3) to provide a conceptual basis for restoration practices. To achieve these objectives, the authors conducted temporal and spatial assessments of land-cover changes and their impacts on hydrology by

quantifying the forest cover, surface runoff, percolation, and stream discharge. Study of the impacts of land use conversions on hydrological responses is essential for long-term planning of land-use/land-cover to protect water resources as well as to manage water availability (excess or scarce) in the watershed effectively.

Description of Study Area

The Xinjiang River drains a 6,168 km^2 watershed (Figure 1) within Jiangxi Province, which is located in southeastern China at 28.500° S and 117.500° E. The Xinjiang river watershed is the part of the bigger Poyang lake basin, which faces seasonal fluctuations in water volume. The red soil of the area is formed from arenaceous shale and is approximately 100 cm thick (Zhang et al., 2008). According to the Soil Taxonomy of China, this soil is classified as fine loamy, hyperthermic, and acidic UdicCambisols (Zheng et al., 2008). The watershed includes two major cities, Shangrao and Yintang of Jiangxi province and many rapidly growing city centers along the floodplains.

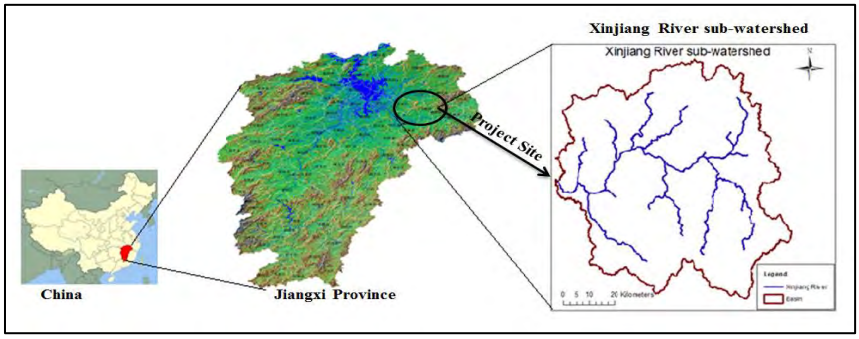

Figure 1. Project Area

Material and Methods

Remote Sensing

The four Landsat TM scenes were obtained from the USGS GLOVIS website (www.glovis.usgs.gov). Images were selected corresponding to a year (1992) before and a year (2009) after China's adoption of the NFCP. It was difficult to find cloudless images of the summer; so only dry season images were selected for classification. The Landsat scenes were pre-processed using ENVI 4.3 (ENVI, 2007). A maximum likelihood-supervised classification using user-specified training sites was performed on the two Landsat TM images. The land cover map from the 2000 land use survey by the Land Management Bureau of Jiangxi Province was also used as a control to find the logical training sites as verified with Google Earth. A land cover map with the following classes was derived: (1). Agriculture; (2). Bare soil/barren; (3). Dense Forest; (4). Dense Urban; (5). Floodplain; (6). New Forest (reforested area in the hills); (7). Paddy Field; (8). Rangeland; (9). Water; and (10). Wetland.

DEM (Digital Elevation Model)

The DEM of 30 m resolution was obtained from NASA's EOSDIS website (NASA, 2011). In mountainous areas, major variation in brightness values of pixels in the image can be found because of the presence of shadows, which might lead to erroneous land cover classifications (Yacouba et al., 2009). Therefore, the DEM (digital elevation model) was used as secondary data in the classification process to reduce the classification error and verify the presence and absence

of certain land-cover classes in some elevation zones. The DEM was also used in the SWAT for stream network and watershed delineation.

Soil Map and Weather Data

A soil data map with a resolution of 1:3,000,000 was obtained from a soil survey completed in 1990 by the Land Management Bureau of Jiangxi Province. The weather data (rainfall, temperature, wind speed, radiation, and solar radiation) from 15 stations around the study site for the period 2000-2010 was obtained from the NCEP (national centers for environmental predictions) (NCEP, 2012).

Hydrologic Modeling

The DEM, classified land cover maps, soil map, and weather data for the study area were used in the SWAT model to derive responses to hydrological parameters such as surface runoff, groundwater percolation, evapotranspiration, and stream discharge for the land cover of 1992 and 2009. SWAT is a physical-based model operating on a daily time step. The model divides the watershed into hydrological reference units with unique land cover, soil, and slope characteristics. Model parameters for land cover types were obtained from the earlier study on the same watershed using the concept of spatial proximity (Wang and Kalin, 2011).

The simulated flow from the SWAT model was calibrated against monthly discharge measurements made over a two-year period using SUFI2 automatic calibration. The calibration was performed by iteration and permutation of eight model parameters such as CN2.mgt, ALPHA_BF.gw, GW_DELAY.gw, GWQMN.gw, GW_REVAP.gw, ESCO.hru, CH_N2.rte, and CH_K2.rte. The model uncertainties were quantified by a measured P-factor, which is the percentage of measured data bracketed by the 95% prediction uncertainty (95PPU) (Abbaspour, 2007). An R-factor, the average thickness of the 95 PPU band divided by the standard deviation of the measured data, quantified the strength of a calibration/ uncertainty analysis. For the calibration period of 2009 to 2010, $R^2 = 0.87$, NS = 0.83, R-factor = 0.00 and P-factor = 0.50. The R-factor of 0 suggests that the simulation exactly corresponded to the observed discharge data therefore the calibration was strong. The obtained model efficiency was 0.74. The eight parameters estimated from the calibration were then used in predictive simulations of hydrology for various land-cover scenarios.

Land-cover Scenarios

The effects of land-cover changes on hydrology are derived from comparisons between the model results from the previous (1992) and current land-covers (2009) and the six other remediation scenarios.

1. Scenario 1 is the land-cover condition of the year 1992. It represents deforestation of natural broad-leaf forest in hills, barren and degraded land along the River (Figure 2, left).
2. Scenario 2 is the land-cover condition of year 2009. It represents reforestation of denuded hills and expansion of urban areas along river (Figure 2, right).
3. Scenario 3 is the land-cover condition when the reforestation in the hills is mechanical plantation of pine.
4. Scenario 4 is when 1-km riparian buffer strips are created along the main river as well as all tributaries. The buffer is afforested with broad leaf mixed forests.
5. Scenario 5 is when 78 km^2 of remaining floodplain is converted with broad leaf mixed

forest.

6. Scenario 6 is when 334 km^2 of remaining rangeland is converted to broad leaf mixed forest.
7. Scenario 7 is combination of scenario 5 and 6, when both the remaining floodplain and rangeland is converted to broad leaf mixed forest.
8. Scenario 8 is when a total area of 80,000 m^2 earthen irrigation ponds is installed in the outlet of sub-basins with maximum surface runoff. The thirteen sub-basins with slopes greater than 25% were hypothesized to have earthen irrigation ponds of various sizes to collect 60% of the precipitation during the flood months June and July for 60 days.

Results

Land-Cover Classification

Landsat TM imagery was used to quantify the changes and delineate land-cover over the 17-year period from 1992 to 2009. As shown in the table 1, different forest covers dominated more than 50% of watershed. The land cover change from 1992 to 2000 is static with small-scale changes in all classes except urban/impervious and dense forest areas. There is a continual conversion of new forest in 1992 to dense forest in 2009, which is consistent with what would be expected; the National Forest Conversion Program lasted from 1998 until 2009, in which time some of the new forest matured to become dense forest. The other land-cover such as paddy fields, urban/impervious areas and water bodies has increased over time at the expense of agricultural land, floodplains, and rangeland. The percentage increase in dense forest and urban area are 13% and 7% and the percentage decrease in agricultural land and floodplain are 7% and 3%.

Table 1. Land-cover changes in percentage from 1992 to 2009

Land cover	1992 area in km^2	1992 (%)	2009 area in km^2	2009 (%)	Percentage change
Agriculture	743	12.05	299	4.85	-7.20
Dense forest	1582	25.65	2396	38.85	13.20
Dense urban/ Impervious	484	7.85	934	15.14	7.29
Floodplain	228	3.70	78	1.27	-2.43
New forest	2131	34.55	1505	24.40	-10.12
Paddy field	482	7.82	574	9.31	1.49
Rangeland	485	7.86	334	5.41	-2.45
Water	32	0.52	47	0.77	0.25
Total	6168	100	6168	100	

Accuracy Assessment

A confusion matrix was created to check the accuracy of the land cover maps. The overall accuracy shows that our land classification accuracy was 81% and 91% for 1992 and 2009, respectively. The training classes were generated from the land use map (2000) obtained from Land Management Bureau of Jiangxi Province. These training classes were used as ground-truth information to evaluate the accuracy of classification maps.

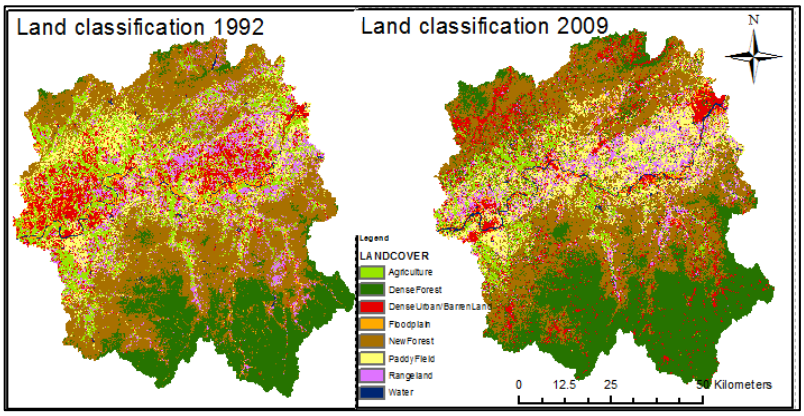

Figure 2. Land-cover classification map

Hydrology

Stream Discharge

Figure 3 shows the historical hydrograph and hyetograph for the study period (2003-2010). The rainfall and stream discharge amount have fluctuated over the period with an increasing trend from 2008 to 2010. There was an increasing trend of peak flow from 2008 to 2010. The year 2010 was the year that received continuous heavy rainfall from April through June, which inundated the region three times more than the annual average rainfall of previous years (Watts, 2010). According to Watts (2010), the area was hit by several flash floods following rain events throughout three months of heavy rain. The high stream discharge of the Xinjiang River might have been derived from its geologic location in the valley between two mountains. The high elevation gradient might have caused surface runoff and lateral flow to enter the river much faster than in gentle areas.

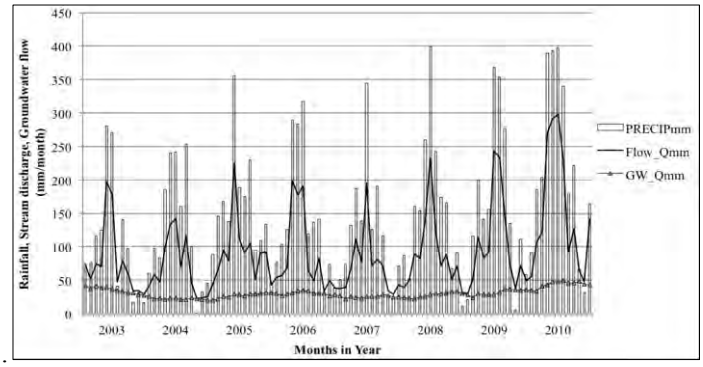

Figure 3. Historical hydrograph and hyetograph

Water Flow Components

Though the reforestation efforts in hills (Figure 5(b): scenario 2) have some impact on surface runoff (2%), the quick flow contribution to the River is almost the same. The quick flow in the month of June is as high as 248 mm for both scenarios 1 and 2, though surprisingly monoculture cultivation of pine in scenario 3 (Figure 4(c)) shows slight damping in the quick flow. However, a 1-km riparian buffer along the river showed highly dampened hydrograph (Figure 4(d): Scenario 4), the peak flow in the month of June was reduced by monthly average of 40 mm.

Scenarios 7 and 8(Figure 4 (e and f)) show a dampened curve of monthly average quick flow with corresponding increased monthly average delayed flow, suggesting more water availability for irrigation and stream discharge in dry season. The increasing curve of delayed flow for both the land-cover scenarios suggests lesser probability of immediate floods downstream during the wet season. Only about 40% of the precipitation in June and 33% in July becomes quick flow with scenario 8 (Figure 4(f)) compared to 53% in June and 44% in July with scenario 2.

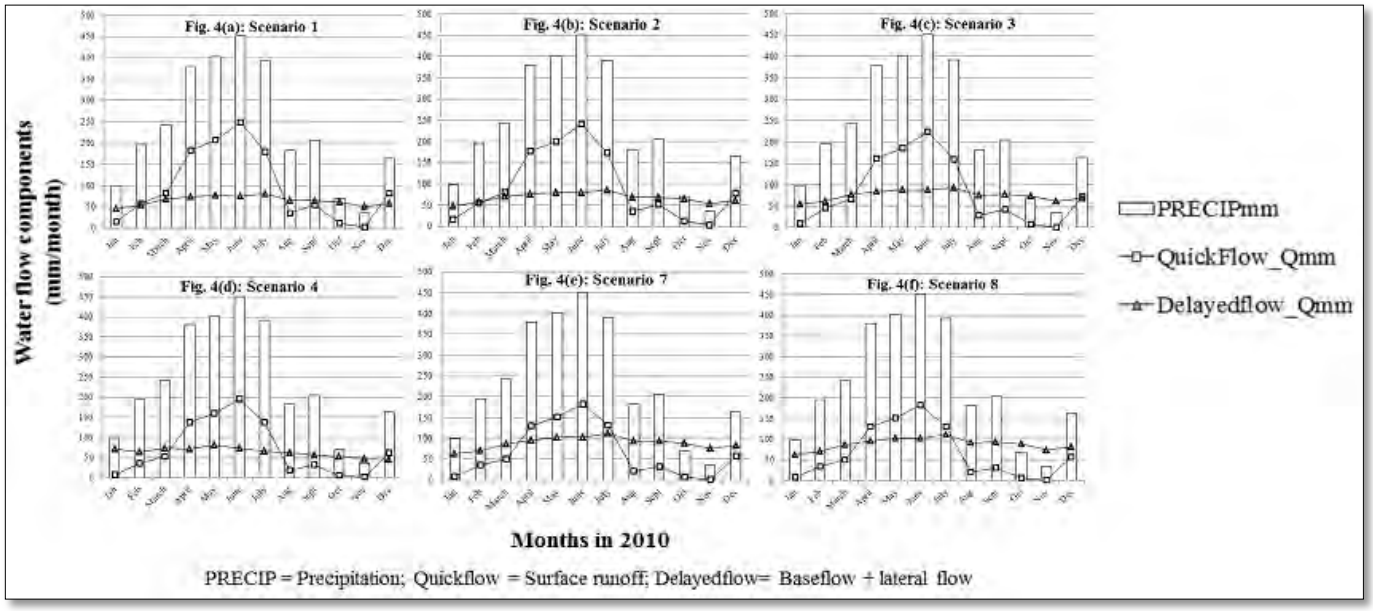

Figure 4. Water flow components for scenarios 1, 2, 3, 4, 7 and 8

Water Flux Components

Water fluxes components for land-cover scenarios 1 and 2 have no strong difference. The scenario 3 shows 3% decrease in surface runoff and 2% increase in percolation compared to scenario 2 (Figure 5 (b)). The effect of pine plantation on reduction of surface runoff is not very strong either. However, when scenario 4 (Figure 5 (c)) is taken into consideration, the surface runoff is reduced by 8% and replaced with increased percolation of 5% compared to scenario 2. With scenario 7 (Figure 5 (e), reforesting both remaining floodplain and rangelands with broad leaf mixed forest), there is 10% reduction in surface runoff as a result of 6% increase in percolation compared to scenario 2. The reduced surface runoff caused by increased percolation facilitated by vegetation.

The Xinjiang River sub-watershed is a hilly/mountainous watershed with 13 out of 31 sub-basins with slope greater than 25%. These steep basins contribute maximum surface runoff. In scenario 8 (Figure 5 (f)), 60% of the precipitation from these 13 sub-basins was collected during June and July for 60 days-the peak flood period in a total of 80,000 km^2 earthen irrigation ponds of various sizes within each sub-basin. The hydraulic conductivity through the bottom of the ponds was 0.5 mm/hr. The hypothetical installation of irrigation ponds reduced the surface runoff contribution by 60.9 mm in the month of June and overall there is 15% reduction in surface runoff and 8% increase in percolation compared to scenario 2.

The water fluxes components for eight land-cover scenarios are summarized as a form of hydrological indices in table 2. The average monthly runoff ratio varied across different land-cover scenarios. The ratio was highest (0.44) for scenario 1, which was the runoff condition in the study area before China adopted its reforestation policy. The ratio of base flows to total stream discharges has an increasing trend from land-cover scenario 1 to 8.The increased trend of base flow is caused by percolation aided by increased vegetation and flow reduction structures such as earthen ponds that reduce the amount of surface runoff. The ratio of evapotranspiration to precipitation is almost the same across all eight land-cover scenarios; however, the ratio of surface runoff to evapotranspiration has a decreasing trend from the land-cover scenarios 1 to 8.

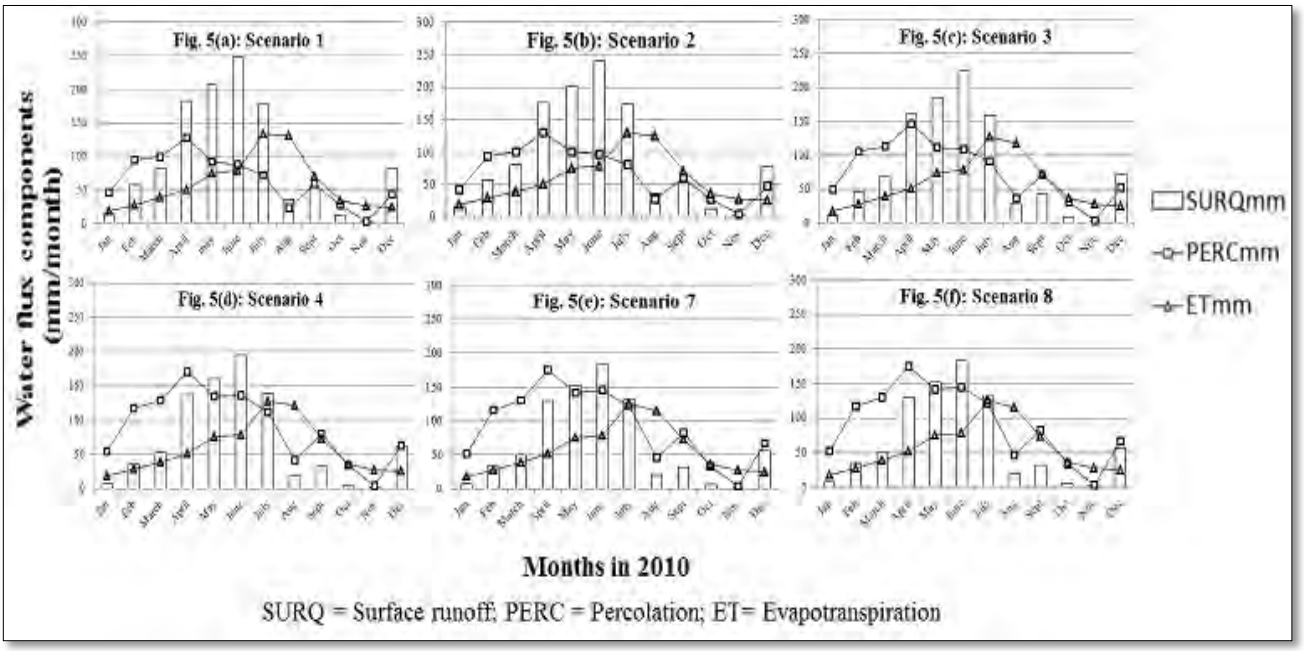

Figure 5. Water flux components for scenarios 1, 2, 3,4, 7 and 8.

Table 2. Hydrological indices for eight land-cover scenarios

Scenarios	SR/ Total flow	Perc/ Precip	Base flow/ Total flow	ET/Precip	SR/ ET	Deep recharge/Precip
Scenario 1	0.44	0.27	0.56	0.35	0.75	0.01
Scenario 2	0.42	0.28	0.58	0.35	0.74	0.01
Scenario 3	0.39	0.3	0.61	0.35	0.67	0.01
Scenario 4	0.34	0.33	0.66	0.35	0.57	0.02
Scenario 5	0.39	0.3	0.61	0.35	0.67	0.02
Scenario 6	0.36	0.33	0.64	0.33	0.68	0.02
Scenario 7	0.32	0.34	0.68	0.35	0.55	0.02
Scenario 8	0.27	0.36	0.73	0.35	0.46	0.02

Discussions

The Xinjiang River sub-watershed has undergone huge forest-cover changes from the original natural vegetation of dense mixed broad-leaf forests of *Castonopsis-Cinnamomum* and *Schima* species with shrubs and ground cover grasses on hills. Most of the natural forests have been heavily deforested and replaced by the scattered pines (*Pinusmassoniana*) and grasses with low nutritional value (Cheng-Fan, 1990). To assess the relative impacts on surface runoff, and percolation, land-cover of the years 1990 and 2009 as well as six other restoration scenarios were simulated with the post-reforestation period of pine plantations (2009-2011) treated as the time of calibration.

Although there is a 13% increase in forest-cover because of the Natural Forest Conversion and Grain to Green programs converted, the program's impacts on the hydrological process have not been very strong from 1992 to 2009. The program began after the 1998 Yangtze River floods, which the government blamed on loss of tree cover, although reduction in riparian buffers and soil infiltration capacity probably also had a major role. Most of the gains in forests resulted from the increase in trees such as pines, eucalyptus, and rubber, not recovery of natural forest. This change threatens ecosystem services, particularly watershed protection and biodiversity conservation. The reduction in runoff after 11 years of reforestation of denuded hills at the Xinjiang River watershed was 12mm. According to Bosch and Hawlett (1982), a 40 mm increase or decline in runoff per 10% change in forest cover should have yielded a 52 mm probable reduction when the 13% of the land surface was afforested. The reduction in runoff from mechanical cultivation of pine and eucalyptus in the hills for forest restoration is much less than expected from Bosch and Hawlett (1982) (Bosch and Hewlett, 1982). Pine plantations planted in hills to reduce flood risk downstream augmented or replaced with other restoration practices apparently reduce over land flow and increase subsurface flow. However, the percolated water on steep slopes moves rapidly through the soil and so does not reduce the flow very much.

Our study suggests that riparian buffer reforestation, restoration of floodplains, conversion of rangeland to mixed broad leaf forests, and installation of ponds have much higher hydrological impacts by lowering the monthly peak flow and thus reducing flash floods downstream. Our study suggests that large-scale watershed-based restoration efforts for hydrological functioning are more effective when focused on floodplains and gentle slopes; i.e. restoring rangelands on gentle slopes are more effective than highly forested hills. Forested riparian buffer strips of mixed broad leaf forests contribute to sustainable land management by reducing soil loss, improving water quality, and stabilizing riverbanks. Riparian buffer allows water to soak into the ground, thus reducing flash flooding and improving groundwater recharge (Patten, 1998). The riparian buffer strip of trees and shrubs also improves aesthetics and wildlife habitat.

The expanding population centers/ cities in China have directly affected riverside lands that once supported riparian ecosystems. Most of the city centers and town are founded along rivers because of ready water sources and transportation facilities. Runoff from hardened city centers is immediate and intense (Graf, 1988), sometime lowering riparian water tables as it causes downcutting in river channels, erosion, and floods. The Xinjiang River watershed is a highly diverse environment with mountains, valleys, plains; all play a role in creating opportunities for riparian ecosystems and restoration. The study has shown that a 1-km riparian buffer strip has a significant hydrological impact compared to the existing land-cover condition of 2009 when upland steep areas had been afforested.

In this study floodplain restoration is a hypothetical scenario, which involves re-establishment of the structures and function of an ecosystem by converting the remaining 78 km^2 of floodplain into a broad leaf mixed forest riparian area. This restoration scenario is 27 times more effective than scenario 2. Likewise the restoration scenario of converting the remaining 314 sq.km rangeland to broad leaf forest has a much larger impact on the hydrology than leaving the rangeland as it is (Sun et al., 2008). In the study of hydrological impacts of eucalyptus and indigenous species in southern China by Zhou (2003), the surface runoff coefficients for both mixed forest and eucalyptus forest decreased over the period 1981-1990, while the coefficient for rangeland showed no such trend.

Scenarios 1 through 7 yield fewer crops as they require loss of croplands and also require moving cities when we all understand that it is highly unlikely that people would move cities. However, scenario 8 looks highly promising as another alternative. The hills of the Xinjiang river sub-watershed are dissected and they drain quickly. The ongoing reforestation effort has been able to reduce the surface runoff from hills by a monthly average of only 2%. So the problem of flood and drought still exists. Our study suggests that watershed level water resource conservation in mountain/hilly watersheds can be met by building earthen irrigation ponds at the outlet of sub-basins where the maximum surface runoff originates to store surface runoff during the flood season. Building ponds in sub-basins with slopes greater than 25% and sub-basins generating high surface runoff proved very effective at holding water during flood season by reducing the flow rate and volume of water, allowing water to percolate and thus reducing immediate flow or quick flow - the major contributor of downstream flash flood. The enhanced percolation would increase soil water content. Since changes in base flow are driven by increases in soil water content, more water would probably be available for use during dry season. The pond water making the remaining areas more productive could compensate for the agriculture area lost to the ponds. The ponds would benefit water storage for irrigation; most of the paddy fields located on the alluvial plain beneath the ponds would be able to obtain more irrigation. The ponds can also be used for fish farming and pond peripheries can be used for forage crops (Cheng-Fan, 1990).

Conclusion

This paper has shown the hydrological impacts of land-cover changes and hypothetical restoration scenarios on reducing runoff and risk of flash floods downstream. The specific type of watershed restoration facilities such as 1-km riparian buffer strip of broad leaf mixed forests, conversion of remaining floodplain and rangeland to broad leaf mixed forest and earthen ponds in the outlet of sub-basins with maximum runoff along with existing pine plantation have a great bearing on localized hydrologic patterns. These three scenarios show hypothetical changes in land use changes within the watershed and have a range of potential benefits for downstream hydrologic functioning in the Xinjiang River watershed. Based on improved hydrologic functioning, scenario 8 yields the most significant improvements over a large extent of the watershed. Scenario 7 also yields significant hydrologic improvements. Scenario 4 yields a significant hydrologic improvement, however, it is the most expensive and is also difficult to implement. Therefore, based on our evaluation of hydrologic results, scenario 7 and 8 appears to be the most beneficial with respect to long-term hydrologic improvements in Xinjing River sub-watershed. Scenario 8 would be less disruptive to cities and could maintain the agricultural base within the basin.

Acknowledgments

We gratefully acknowledge funding received from Yale School of Forestry and Environmental Studies. The study would not have been possible without the help from Dr. HuaGuo and Dr. Qi S. Hu for sharing data from their previous published work in 2008 herein referred a lot. We are also grateful to the students of at Nanchang University, and Juijiang Hydrological Center for field assistance. Thanks also to Jing Ma for accompanying Ambika Khadka to field and Ellen Arnstein for helping edit this paper.

References

Wei X., G. Sun, S. Jiang, H. Zhou, and L. Dai. 2008. Forest-Streamflow Relationships in China: A 40-Year Retrospect. *JAWRA Journal of the American Water Resources Association, 44: 1076-1085.*

Zhou G.Y., J. D. Morris, J.H. Yan, Z.Y. Yu, and S.L. Peng. 2002. Hydrological impacts of reafforestation with eucalyptus and indigenous species: a case study in southern China. Forest Ecology and Management, 167: 209-222.

Sun G., S. Liu, Z. Zhang, and X. Wei. 2008. Forest hydrology in China: Introduction to the featured collection 1. JAWRA Journal of the American Water Resources Association 44 (5): 1073-1075.

Zheng H., F. Chen, Z. Ouyang, N. Tu, W. Xu, X. Wang, and Y. Tian. 2008. Impacts of reforestation approaches on runoff control in the hilly red soil region of Southern China. Journal of Hydrology, 365 (1): 174-184.

Jiang Z., S.Y. Zhang. 2003. China's plantation forests for sustainable wood supply and development, in Forestry 03. In 12th World Forestry Congress, Quebec.

Forestry Construction and Ecology Environment. 2011. Provincial Profile of Jiangxi Province, Jiangxi Province, China.

Sahin V., and M.J. Hall. 1996. The effects of afforestation and deforestation on water yields. Journal of Hydrology 178: 293-309.

Neitsch S.L., J.G. Arnold, J.R. Kiriry, R. Srinivasan, and J.R. Williams. 2000. Soil and Water Assessment Tool User's Manual Version 2000. Texas Water Resource Institute, College Station, Texas.

Guo H., Q. Hu, and T. Jiang. Annual and seasonal streamflow responses to climate and land-cover changes in the Poyang Lake basin. Journal of Hydrology 355: 106-122.

Zheng H., F. Chen, Z. Ouyang, N. Tu, W. Xu, H. Miao, and et al. 2008. Impacts of reforestation approaches on runoff control in the hilly red soil of Southern China. Journal of Hydrology 356: 174-184.

USGS. 2012. USGS Global Visualization Viewer (GloVis). EROS (Earth Resources Observation and Science Center). Available at http://www.glovis.usgs.gov.

ENVI. 2007. ENVI User's Guide, Version 4.3. ITT Visual Solutions, Boulder, Colorado, unpaginated (installation) CD-ROM, 2007.

NASA. 2011. EOSDIS (Earth Observing System Data and Information System) Version 10.70.05. Avialable at www.echo.nasa.gov/reverb.

Yacouba D., H. Guangdao, and W. Xingping. 2009. Assessment of land use cover changes using ndvi and dem in puer and simao counties, Yunnan Province, China. World Rural Observations 1 (2): 1-11.

NCEP (the National Centers for Environmental Predictions). 2012. CFSR (Climate Forecast System Reanalysis), Global Weather Data for SWAT. Available at www.globalweather.tamu.org.

Wang R., and L. Kalin. 2011. Modelling effects of landuse/ cover changes under limited data. Ecohydrology 4: 265-276.

Abbaspour K.C., J. Yang, I. Maximov, R. Siber, K. Bogner, J. Mieleitner, J. Zobrist, and R. Srinivasan. 2007. Modeling hydrology and water quality in the pre-alpine/ alpine Thur watershed using SWAT. Journal of Hydrology 333(2-4), 413-430.

Watts J. 2010. China devastated by floods. The Guardian 2013. Available at www.guardian.uk.co/world/2010.

Cheng-Fan X. 1990. Better land use and reclamation of red soil hilly region of southern China. Geo Journal 20 (4): 365-368.

Bosch J.M., and J.D. Hewlett. 1982. A review of catchment experiments to determine the effect of vegetation changes on water yield and evapotranspiration. Journal of hydrology 55 (1): 3-23.

Patten T. 1998. Riparian Ecosystems of semi-arid North America: Diversity and Human Impacts. Wetlands 18(4) 498-512.

W.L. Graf. 1988. *Fluvial Processes in Dryland Rivers*. New York, NY: Springer-Verlag.

Modeling flow and pesticide transport through surface water diversions in the California Central Valley

Lauren Padilla
Stone Environmental, Inc., Montpelier, Vermont, lpadilla@stone-env.com.

Michael Winchell
Stone Environmental, Inc., Montpelier, Vermont, mwinchell@stone-env.com.

Natalia Peranginangin
Syngenta Crop Protection, LLC, Greensboro, North Carolina,
natalia.peranginangin@syngenta.com.

Abstract

The watershed of the California Bay-Delta encompasses a large, complex network of engineered structures for flood control, irrigation, and drinking water; often transporting surface water to destinations hundreds of miles away. These diversions are substantial in magnitude, may be highly variable in time, and lack monthly or seasonal patterns. Accurately modeling surface water diversions including the simultaneous transport of nutrients and pesticide mass is critical to understanding the fate and transport of such chemicals and to better predict their concentrations throughout the watershed. Currently, the Soil and Water Assessment Tool (SWAT) model transfer scheme permits a constant daily transfer amount or a constant fraction of flow. Our work enhances the existing transfer operation by allowing daily or monthly time series of diverted flow rates to represent the appropriate temporal variability in transfers. Diverted pesticide mass is computed based on the ratio of diversion to overall flow rates. We use this modified scheme to model 9 daily-time-series and 24 monthly-time-series of flow and pesticide mass transfers throughout the Central Valley using California Department of Water Resources and U.S. Geological Survey data. This includes flood water spillage over weirs along the Sacramento River, and Sacramento and San Joaquin River water movement to federal and state pumping facilities that export up to half the total Delta inflow. Comparison with USGS gage data shows that the modified transfer scheme improves simulation of surface flow and mass concentrations in nearly every major reach in the watershed.

Keywords: SWAT, California Delta Model, Central Valley Model, diversions, transfers, flood control, pesticide

Introduction

The California Bay-Delta is an important estuary habitat as well as a major source of drinking water for the people of California. Within the Delta watershed lays the intensely-agricultural Central Valley region. Watershed-scale models of this region are needed to predict the concentrations of pesticides found in Delta water bodies for ecological risk assessments and regulatory decision making. However, the complex network of engineering controls on surface water flow in and around the Delta presents a challenge to accurately modeling flow rates and pesticide concentrations.

Engineering controls, like flood control structures, irrigation canals, and pumping plants can divert water hundreds of miles from its point of origin and even out of the watershed entirely. The volume of water diverted by these structures is substantial, for example, flood water spillage over weirs could be more than half the total flow above the weir. The magnitude of diversions may fluctuate daily and without following any particular temporal pattern.

The current version (2012, revision 589) of the Soil and Water Assessment Tool (SWAT) watershed model (Arnold, et al., 1998) has some capability for modeling diversions from the natural flow. One option allows the transfer of a constant volume of water into or out of a particular reach to be specified. A second option is to define a constant fraction of the natural flow to divert. A third option allows specification of a minimum flow rate to maintain in the reach. None of these options completely addresses the variable and unpredictable nature of many of the diversions in the Delta watershed.

This paper introduces a new transfer method for the SWAT model that processes monthly or daily diversion time-series to account for the temporal variability in flows through Central Valley and Delta control features. Along with the time-varying flows, a proportional amount of dissolved and suspended masses including pesticides, sediment, and nutrients, are also computed and transferred. The details of the implementation and use of the transfer method are explained in the next section. Following this, the method is applied to a SWAT model of the Delta watershed. Although this application focuses on pesticide transfer, it is illustrative of the broader capabilities of the new transfer method for additional masses transported through the watershed.

Time-Varying SWAT Transfer Scheme

The original SWAT transfer scheme was expanded to include the option to divert a time-varying portion of stream flow from one reach to another or out of the watershed entirely. The amount to transfer is specified by the modeler as daily or monthly time-series of diverted flow rates. The model's transfer routine is executed on a daily time-step. First, the routine verifies the source reach can supply the transferred amount to ensure remaining flow cannot become negative. If the flow rate of the source reach is smaller than the desired diversion flow rate, the diversion rate is limited to what the source can supply. Next, the routine calculates the ratio of diverted flow to total source flow before the diversion. This diversion ratio will always be less than or equal to one. Using this ratio, the routine calculates the amount of sediment, nutrients, pesticides, and other masses already suspended or dissolved in the reach that will be diverted to other parts of

the watershed. Assuming the amount of mass diverted is proportional to the flow volume diverted, the total mass is multiplied by the diversion ratio to get diverted mass. The mass remaining in the reach is updated by subtracting the diverted mass.

The transfer routine is executed after the in-stream processes and stream routing for each reach which effectively withdraws the transferred flow and mass from the bottom of the reach. This means that the amount removed from the reach is a function of whatever entered the reach via land processes or other inputs during the current time-step. The transferred flow and mass is added to its destination on the next time-step before routing. This effectively adds the flow and mass at the top of the reach where it will be joined by incoming mass from sources like runoff or spray drift to be included in stream processes and routing.

To activate the transfer scheme, the transfer command is called in the watershed configuration file (fig.fig). Each transfer command corresponds to an input file with a daily or monthly time-series of diversion flow rates that follows the same fixed format as point source input files. Note that all diversion flow rates in this input file must be negative. Additionally, there cannot be any missing data; gaps in observed flow data must be estimated. For short periods of time, missing data could be estimated by linear interpolation. Longer missing data periods could be filled in with data from years with similar seasonal rainfall amounts. The transfer scheme may be used along with other reach commands such as the daily or monthly point source commands, recday and recmon. The transfer command is issued after any additional flow or mass has been added from point sources. The transfer command has eleven input parameters occupying two rows of the fig.fig file. From left to right, the parameters are listed in Table 1.

Table 1 Transfer Parameters

Field	Description	Possible Values	Format
Row 1			
Field 1, spaces 1-10	Command name	"transfer"	I6
Field 2, spaces 11-16	Command code	Transfer=4	I6
Field 3, spaces 17-22	Source water body type	1=reach, 2=reservoir	I6
Field 4, spaces 23-28	Source reach number	1 to number of subbasins	I6
Field 5, spaces 29-34	Destination water body type	1=reach, 2=reservoir	I6
Field 6, spaces 35-40	Destination reach number	1 to number of subbasins, -9999 for outside watershed	I6
Field 7, spaces 41-46	Hydrograph number of source reach after route, before transfer (transfer type 4) OR flow amount transferred (transfer types 1-3)	1 to number of hydrograph ids (transfer type 4) OR flow fraction or volume (transfer types 1-3)	F6.3
Field 8, spaces 47-55	Transfer type	1=fraction, 2=minimum, 3=fixed,4=time-varying	I9
Field 9, spaces 56-58	Transfer identification number	Unique integer	I3
Row 2			
Field 1, spaces 11-14	Starting month of transfers[1]	1 to 12	I4
Field 2, spaces 15-18	Ending month of transfers[1]	1 to 12	I4
Field 3, spaces 19-22	Hydrograph number of source reach after transfer	1 to number of hydrograph ids	I4

1. Month is used to specify start and end period for transfers whether inputs are monthly or daily. Typically, for continuous time series spanning several years, starting month would be 1 and ending month would be 12.

The two excerpts from the watershed configuration file for the Delta SWAT model in Figure 1 demonstrate how to use the time-varying option of the modified transfer scheme. The top panel (A) is an example of commands for a headwater, reach 181, with daily diversions to reach 185. The recday command is called after routing to indicate the transfer amount is read from file 181p.dat and stored at hydrograph number 629. The add command sums the negative transfer amount with the route output flow stored at hydrograph number 628 to remove the transfer amount from the source reach. After the add command, the transfer command is called to complete the transfer by removing pesticide and other mass from the source reach and staging the flow and masses to be added to reach 185 on the next time step. The value of 4 in the second field indicates use of the time-varying option. Values of 1 in fields 3 and 5 mean the source and destination water bodies are of type reach. The unique identification number of 6 in field 9 means that this is the 6th transfer in the fig.fig file so far. Field 7, the hydrograph number for the routed flow before the transfer is made, is always the same as the hydrograph number for the route output (route field 3). Note that the decimal point in field 7 is required for the number to be read in properly because for the non-time-varying transfer types (transfer types 1-3), the expected value is a decimal amount transferred.

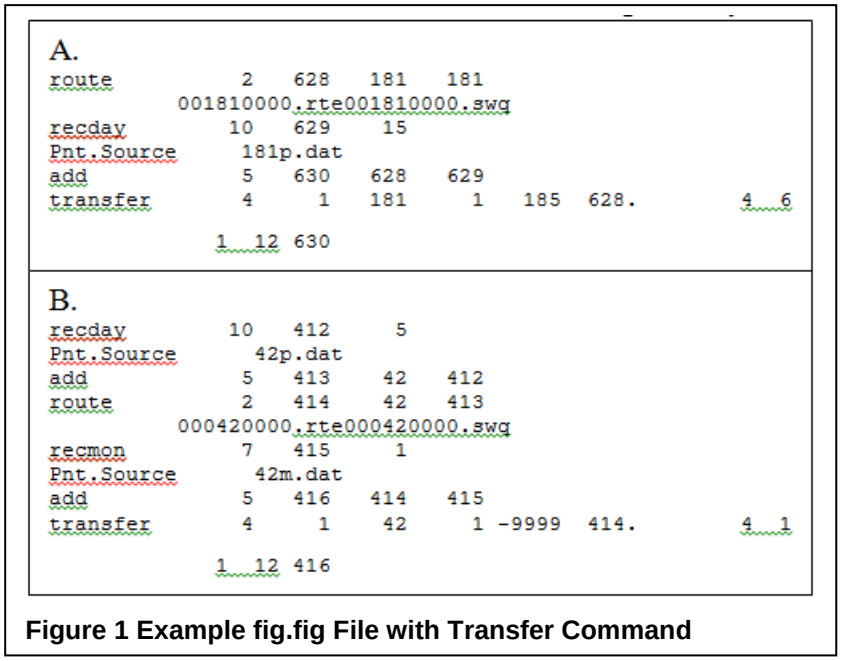

Figure 1 Example fig.fig File with Transfer Command

The bottom panel (B) of Figure 1 is an example of the watershed configuration file commands for a reach that also includes a daily point source input. Notice that the point source is summed with the current stream flow before routing while the monthly point source associated with the transfer occurs after routing. Also note that in this example, the diversion is directed to a destination outside of the watershed which is signaled by the use of -9999 in the destination field. There is currently no ArcSWAT capability for managing input file updates for transfers. However, a python script has been developed to automate fig.fig updates by reading in transfer parameters, inserting transfer commands in the correct positions, and shifting hydrograph numbers accordingly.

California Bay-Delta SWAT Model

The time-varying transfer scheme was applied to a SWAT model of the California Bay-Delta watershed. The Delta SWAT Model was developed as a tool to predict the magnitude and distribution of chemical concentrations in the water bodies flowing into the Delta-region, (see Delta boundary shown in Figure 2). The spatial extent of the model was designed to capture the

majority of the upstream historic pesticide use areas while keeping the model's computational complexity to a manageable level.

The full watershed extent as defined by the combined California Watershed Boundary Dataset (CA WBD) (USGS, 2012) hydrologic unit code (HUC) boundaries is shown in Figure 2 along with annual-average total historic use of agricultural, residential, and municipal pesticides by county in the period 2000-2011. The SWAT Model domain covered the fraction of the full watershed with past pesticide use on agricultural and developed land below water supply/flood control reservoirs in the foothills around the Central Valley. The reservoir outflows were modeled as point source inlets of freshwater at the perimeter of the modeled area using daily USGS observations. The 24 inlets, shown in Figure 3, account for 40% of the full watershed drainage area, significantly reducing the remaining watershed area to be modeled.

With the exception of the two southern most counties in the full watershed extent, the modeled area included the counties with the highest historic pesticide use. Most of Kings county and all of Tulare and Kern counties were excluded because these counties are only hydrologically connected to the Delta region when flood water, assumed to originate from the Kings River upstream of the heavy use areas, flows to the San Joaquin River at Mendota Pool (KRCD & KRWA, 2003).

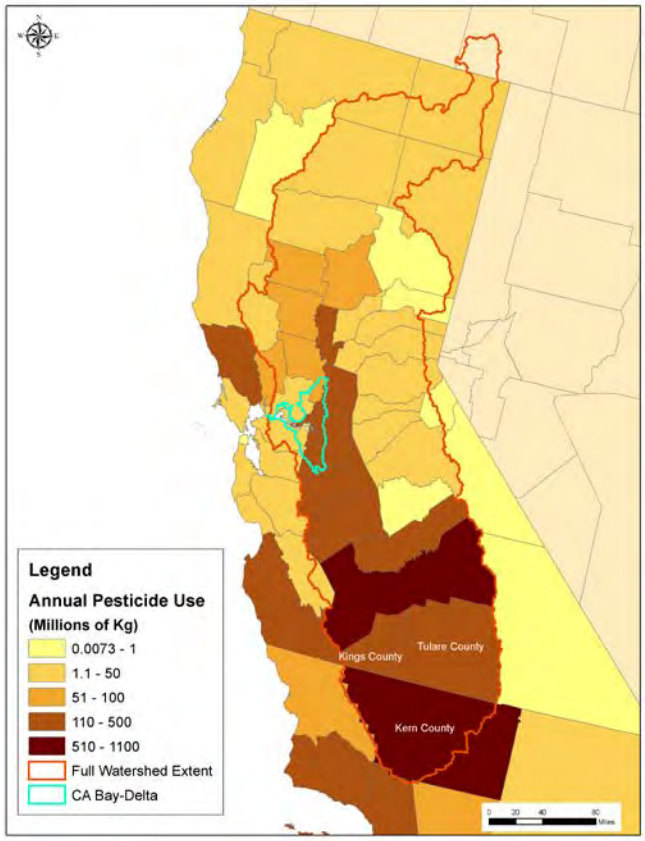

Figure 2 Historic Annual Pesticide Use by California County

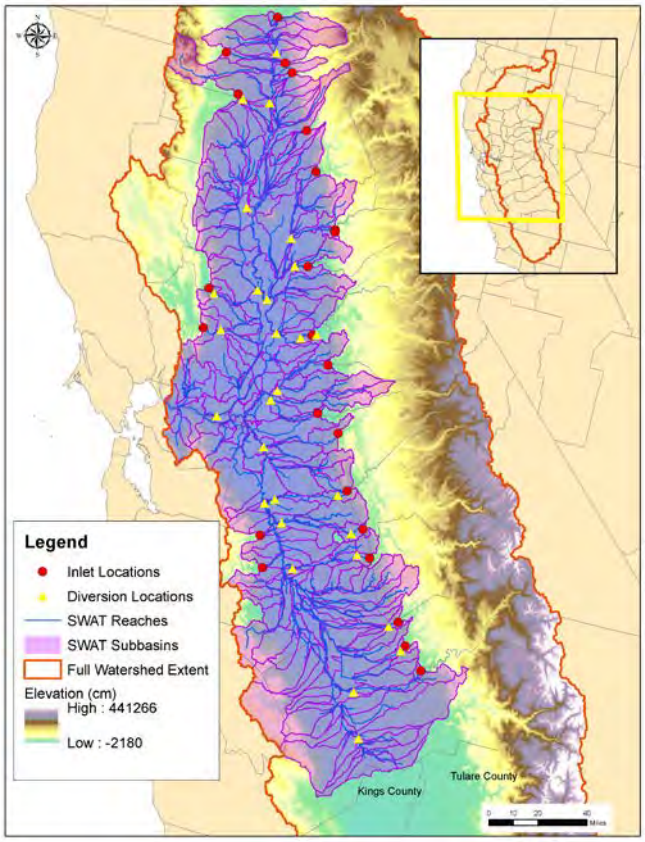

Figure 3 Delta SWAT Model

Using the 30m-resolution NHDPlus Version 2 hydrologically conditioned digital elevation map (Hydro-DEM) (McKay, et al., 2012), the modeled area was delineated into 344 subbasins ranging in area from 0.01 to 1000 km^2 with an average area of 140 km^2. The use of the Hydro-DEM led to subbasin boundaries that primarily followed the CA WBD 12-digit HUCs. The modeled area, subbasin boundaries and corresponding reaches, and point source inlet locations are shown in Figure 3.

The Model was further delineated into 37,000 hydrologic response units (HRUs), unique combinations of soil type, land use, and slope. The soils dataset was the 1:25,000-scale Soil Survey Geographic (SSURGO) database ((NRCS), 2012). The land use data was derived from five years of data from the 30m-resolution Cropland Data Layer (CDL) between 2006-2010. Eleven different generalized land use classes were created by grouping like CDL land uses and crop classes. Two slope classes were defined as 0-5, and 5-9999. Minor soil and slope classes within each subbasin were lumped together with the more dominant classes using a 5% threshold for each. This meant that for a given land use within a subbasin, the soil had to occupy a minimum of 5% of that land use area to be included as a distinct HRU. Similarly, for a given soil and land use within a subbasin, the slope class had to occupy a minimum of 5% of that soil and land use area to be included as a distinct HRU .

The model was simulated for the 30 year time period between 1981-2010 with daily precipitation and temperature data from the National Climatic Data Center Global Historical Climatology Network (NCDCa, 2012) and Integrated Surface Database (NCDCb, 2012) datasets and the California Irrigation Management Information System (DWR, 2012). The 51 and 48 weather stations with the most complete temperature and precipitation records, respectively, were used to capture the heterogeneity in weather across the large modeled watershed area.

Diversions

Three main diversion types were included in the Delta SWAT model: Spillage over flood control structures or weirs along the Sacramento River between Colusa and Sacramento, water exports to federal and state pumping facilities from Mokelumne, Old and Middle river channels inside the Delta, and irrigation diversions from major reaches throughout the watershed via canals

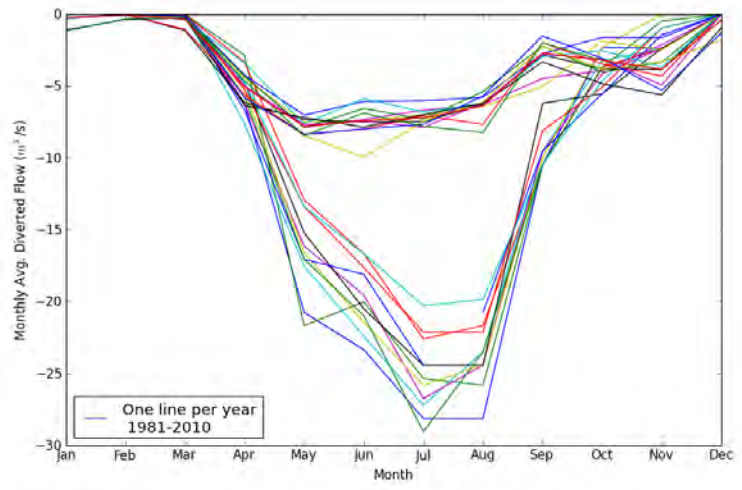

Figure 4 Monthly Average Colusa Basin Drain Diversions

and ditches. There were 33 diversions in total with 9 from daily-averaged U.S. Geological Survey gage data and 24 from monthly-averaged California Department of Water Resources data.

The monthly diversions were mainly related to irrigation; these are shown in Figure 3 as Diversion Locations. The monthly average irrigation diversions from the Colusa Basin Drain for each year, between 1981-2010, shown in Figure 4, exemplify the need for a time-varying transfer scheme. No single year of data would adequately represent the entire simulation period.

Daily flow data was used to model controlled flood flows along the Sacramento River. Daily gaged flow over Colusa, Moulton, and Tisdale weirs was transferred from the Sacramento River to Sutter Bypass and routed down the bypass until it re-joined the Sacramento near Fremont. Spillage at Fremont and Sacramento weirs was transferred to Yolo Bypass. All transferred water re-joined the main-stem Sacramento River by the time it reached Rio Vista. Weir locations are shown in Figure 5.

The export water leaving the Delta at the State Water Project and Central Valley Project facilities was also modeled using daily time-series. Water was drawn from the Sacramento River and San Joaquin River near the pumping plants at a ratio of three to one based on observations. The Sacramento export water was transferred and routed down the Mokelumne River at the Delta Cross-Channel. When the water joined the San Joaquin River, it was transferred again and routed in reverse through the Old and Middle Rivers, ultimately exiting the watershed to simulate removal at the pumps. The Middle River received 50% of the total export flow rate and 40% of the export rate moved up the Old River. The remaining 10% of the Delta export rate was withdrawn from the San Joaquin River near the entrance to the Contra Costa Canal. Points through which exports were routed are also shown in Figure 5.

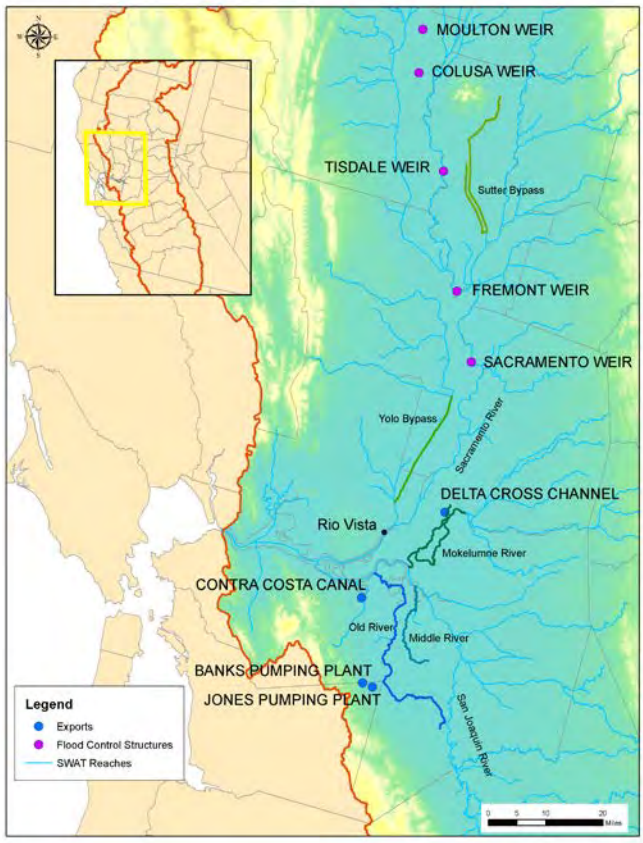

Figure 5 Delta SWAT Model Daily Transfer Locations

A comparison of the total flow rate for all Delta exports by pumping stations to the net Delta outflow, in Figure 6, shows that during non-peak times, the two flows are the same order of magnitude. This is further evidence that resolving the time-varying export flows is critical to model accuracy.

A complete listing of the daily time-series transfers related to flood control and Delta exports indicating the model identification number of the source and destination subbasins (where applicable) is provided in Table 2. All other diversions using monthly time-series, primarily related to irrigation, are listed in Table 3 and represented on the map in Figure 3. The substantial amount of surface water moved around the basin by engineering controls highlights the importance of accounting for transfers accurately in the Delta SWAT model.

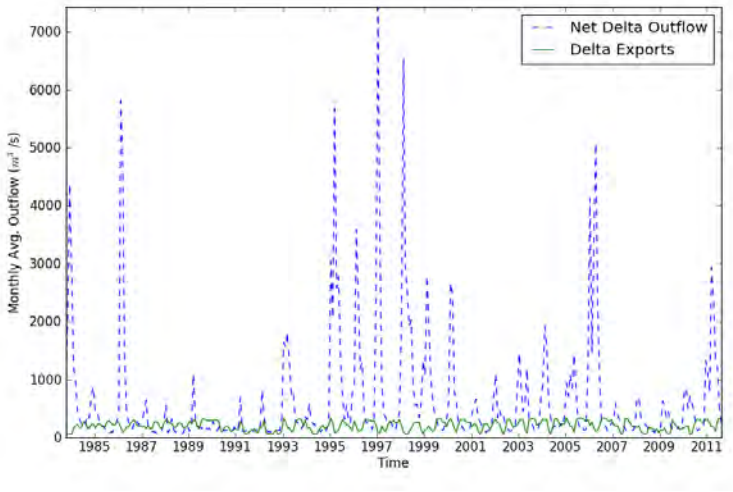

Figure 6 Comparison of Delta exports and net outflow

Table 2 Flood Control Transfers and Delta Exports

Description	Source Subbasin	Destination Subbasin
Flood Control transfers to Sutter Bypass	97	107
Fremont Weir spillage to Yolo Bypass	122	144
Sacramento Weir spillage to Yolo Bypass	138	146
Delta Cross Channel transfer from Sacramento to North Branch	174	181
Delta Cross Channel to South Mokelumne	181	185
South Mokelumne through little potato slough to San Joaquin River	185	193
CVP/SWP pumping from San Joaquin after Mokelumne	187	202
Contra-Costa Canal (CCC) exports	190	out of watershed
CVP/SWP pumping down Middle River	202	195

Table 3 Diversion Flow Rates by Subbasin

Subbasin	Average (m^3/s)	Maximum (m^3/s)	Minimum (m^3/s)
14	11	39	0
42	4	13	0
35	28	88	0
97	4	15	0
104	9	27	0
103	4	12	0
127	6	23	0
114	6	29	0
125	21	79	0
118	36	98	0
143	8	20	1
142	0	1	0
148	9	26	1
165	0	2	0
188	3	11	0
201	1	3	0
219	6	19	0
221	8	19	0
233	35	86	0
227	1	2	0
244	19	56	0
248	3	8	0
286	1	10	0
304	2	18	0
315	6	19	0
333	2	14	0
183	44	149	0

Results

The model was run both with and without the diversion scheme. A comparison of the two sets of results showed that transfers improved the prediction of both spatial and temporal aspects of the Delta hydrology and distribution of pesticides. One particular model area that saw improvement in the prediction of pesticide concentrations due to improved accounting of flow volumes in the reaches is shown in Figure 7. Without transfers, the natural flow down the Old and Middle rivers would carry higher mass flows from the San Joaquin County pesticide use area toward the San Joaquin River. With transfers, the effects of the Banks and Jones pumping facilities were modeled. Flow was directed away from the San Joaquin River, diluting chemical concentrations in the Old and Middle rivers, and ultimately exported from the watershed along with the carried chemical.

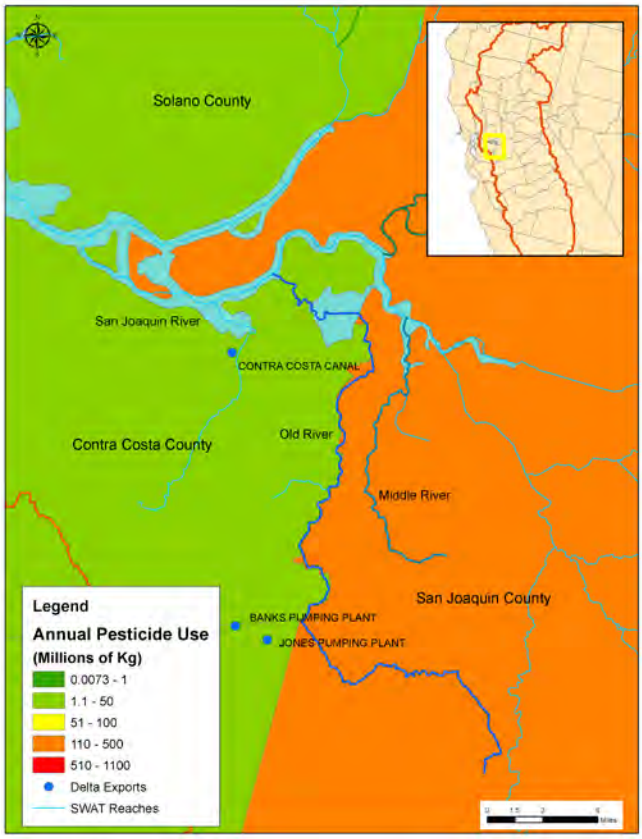

Figure 7 Old and Middle River Region

An example of improvement in the magnitude and timing of flow is shown for the Old River by comparison of 30 years of USGS observed data with modeled data in Figure 8. The model result for the Old River's natural outflow was orders of magnitude smaller than the flow drawn up the river toward the Banks and Jones plants. Whereas the result after applying the series of San Joaquin and Sacramento River diversions was a good approximation to the observed flow in most years between 1981-2010 with the exception of flood years 1995-1998 and 2006. During flood times San Joaquin overflow may be directed down the Old and Middle rivers, far exceeding the export flow rates. The model cannot simulate reaches with flow in two directions, so the peak flood flows were not captured.

The time-varying transfer scheme also significantly benefited flow calibration throughout the watershed. Recognizing and properly accounting for diversions before attempting calibration avoided overcompensating for model-observation discrepancies with gross parameter adjustments, saving time and leading to better calibration statistics. For example, in Figure 9, the results of model calibration against USGS data with and without transfers in place are shown for a segment of the Sacramento River downstream of the three major flood control structures. The Nash-Sutcliffe efficiency, percent bias, and ratio of root mean square error to observed standard deviation calibration metrics were all well within the ranges recommended in Moriasi, et al., 2007.

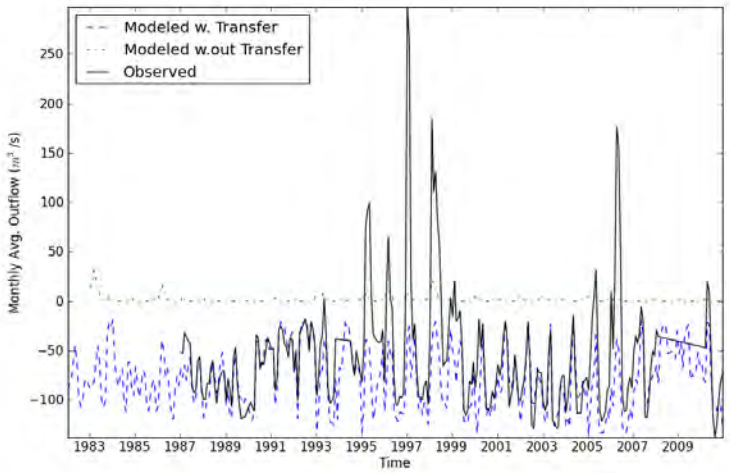

Figure 8 Comparison of modeled and observed Old River flow

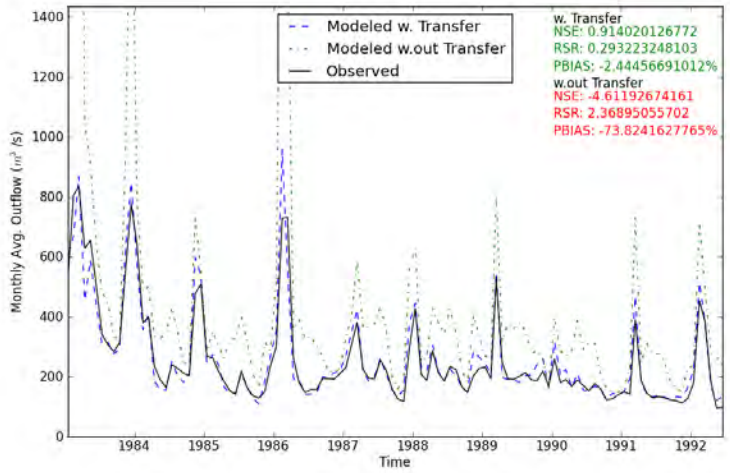

Figure 9 Comparison of modeled and observed flow at Sacramento River Below Wilkins

Conclusion

This paper introduced an expansion of the transfer scheme options in the SWAT model to account for daily and monthly variation in diversion flow rates. The scheme is implemented by adding transfer commands to the watershed configuration file and constructing input files with time-series of negative flow rates.

The time-varying transfer scheme was shown to improve spatial and temporal accuracy of model hydrology and consequently improve estimates of dissolved and suspended pesticide and other masses in the CA-Delta SWAT model. The scheme was particularly beneficial to this large-scale watershed model encompassing the California Central Valley due to the large number of engineering controls on surface water there. However, the technique depends on the availability of high quality flow observations. Several days to several months of missing data required the use of estimation techniques to build complete time-series for the Delta Model transfer inputs. Future work could involve the development of a more dynamic model for transfers to alleviate the need for complete data.

Acknowledgements
This project was supported by funding from Syngenta Crop Protection.

References

(DWR), California Department Water Resources. *California Irrigation Management Information System.* 2012.

(EPA), U.S. Environmental Protection Agency. "Analysis of CropLand Data Layer (CDL) for Use in Proximity Analysis for Registration Review Risk Assessments." Tech. rep., 2012.

(NCDC), National Climatic Data Center. *Global Historical Climatology Network Version 3.0.* 2012.

(NCDC), National Climatic Data Center. *Integrated Surface Database.* 2012.

(NRCS), Natural Resources Conservation Service. *Soil Survey Geographic Database.* 2012.

(USGS), United States Geological Survey. *National Hydrography Dataset Watershed Boundary Dataset.* 2012.

Arnold, J., R. Srinivasa, R. Muttiah, and J. Williams. "Large-area hydrologic modeling and assessment: Part I. Model development." *J. American Water Resource Assoc.* 34 (1998): 73-89.

KRCD, and KRWA. "The Kings River Handbook." Tech. rep., Kings River Conservation District; Kings River Water Association, 2003.

McKay, L., T. Bondelid, A. Rea, C. Johnston, R. Moore, and T. Dewald. "NHDPlus Version 2: User Guide." 2012.

Moriasi, D.N., J.G. Arnold, M.W. Van Liew, R.L. Bingner, R.D. Harmel, and T.L. Veith. "Model Evaluation Guidelines for Systematic Quantification of Accuracy in Watershed Simulations." *Transactions of the ASABE* 50 (2007): 885-900.

Temporal analysis of parameter sensitivity and model performance to improve the representation of hydrological processes in SWAT for a German lowland catchment

Björn Guse
Hydrology and Water Resources Management, Institute for Natural Resource Conservation, Christian-Albrechts-University of Kiel, Kiel, Germany, bguse@hydrology.uni-kiel.de

Dominik E. Reusser
Potsdam Institute for Climate Impact Research, Potsdam, Germany

Nicola Fohrer
Hydrology and Water Resources Management, Institute for Natural Resource Conservation, Christian-Albrechts-University of Kiel, Kiel, Germany

Abstract

A model evaluation for the whole discharge time series leads to an overall assessment of the model performance. However, temporal differences in the model performance, i.e. for different parts of the hydrograph, were not considered. Furthermore, model components which are the origin of the poor performance cannot be detected with classical model evaluation approaches.

In this study, the temporal dynamics of parameter sensitivity and model performance were investigated for the Treene lowland catchment in Northern Germany. A temporal sensitivity analysis was carried out to determine variations in the dominance of model parameters. Periods with poor performance were detected with an analysis of temporal variations in the values of different performance measures. By relating periods of poor model performance to the dominant parameters in these phases, the origin of these model errors can be identified.

The temporal analysis of the parameter sensitivity illustrates that the sensitivity varies within the discharge time series. The three groundwater parameters (GW_DELAY, ALPHA_BF, RCHRG_DP) dominate in peak and recession phases while the evaporation parameter ESCO is dominant in baseflow and resaturation phases. By temporally analyzing the model performance, three clusters which are characterized by different values of six performance measures were separated and related to different phases of hydrograph. The worst performance was found for the baseflow cluster.

Thus, the groundwater module was determined as the part of SWAT with the highest potential for model improvements. In this way, the proposed temporal diagnostic analyses improve the understanding of SWAT.

Keywords: temporal diagnostic analysis, sensitivity analysis, model performance

Introduction

Hydrological models can be seen as learning tools to obtain a better understanding of hydrological processes and their representation in models (Reusser et al., 2009). With diagnostic model analysis, the relationship between the model structure and the hydrologic behavior of a catchment can be investigated (Gupta et al., 2008). The goal of diagnostic analysis is to detect dominant hydrological processes and patterns. In a diagnostic model analyses several performance measures and a high temporal resolution are considered (Yilmaz et al., 2008). A high temporal resolved analysis provides results which cannot be detected when analyzing the whole time series (Wagener et al., 2003).
In this study, a joined temporal analysis of parameter sensitivity and model performance based on an approach of Reusser and Zehe (2011) are applied to the SWAT model (Arnold et al., 1998). The goal of this study is to improve the understanding of hydrological processes in the Treene lowland catchment and to detect dominant processes which are not adequately represented in SWAT (Guse et al., 2013).

Study area and data

This study was carried out in the Treene lowland catchment in Northern Germany. The hydrological station Treia was selected as catchment outlet resulting in catchment size of 481 km². Four climate stations from the STAR model dataset (Orlowsky et al., 2008) were used as input for SWAT. The Treene catchment is mainly covered by agricultural areas with low percentages of forest and urban area coverage (Fig. 1).

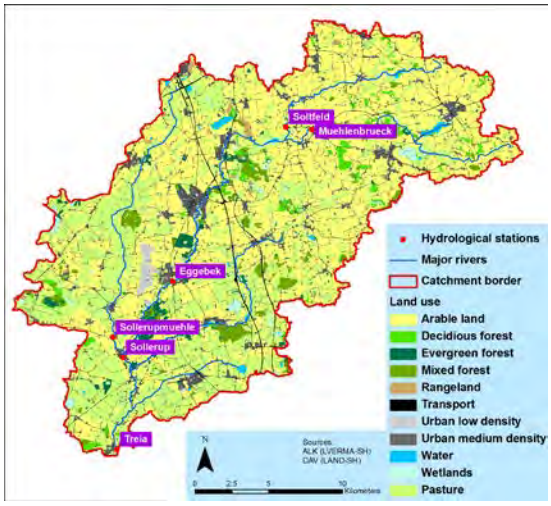

Fig. 1: Land use and hydrological stations in the Treene catchment (from Guse et al., 2013).

Model and methods

SWAT model parameters

Eight SWAT model parameters were selected for the temporal analyses. These parameters capture the major processes in the study catchment. The role of the eight parameters is shown in the SWAT model concept in Fig.2.

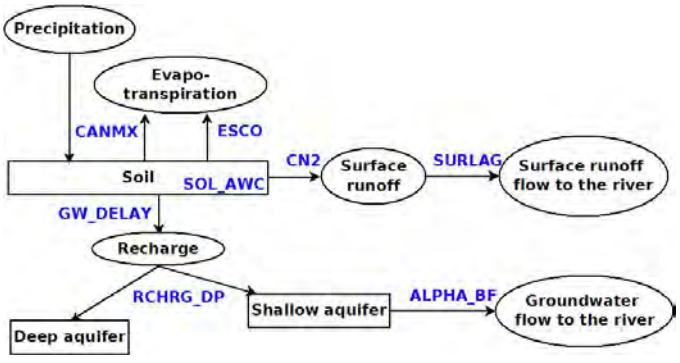

Fig. 2: SWAT flowchart. Storages are shown with boxes and processes with circles. Model parameters are highlighted in blue (from Guse et al., 2013).

Temporal diagnostic analyses

The temporal diagnostic analysis includes three steps as presented in Fig. 3.

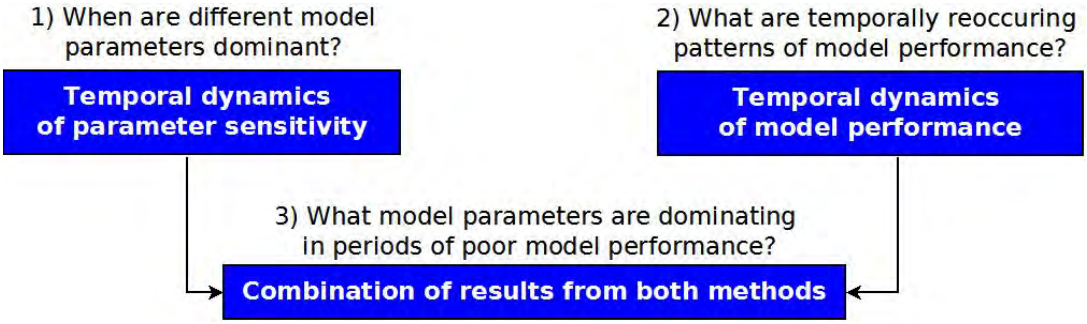

Fig. 3: Concept of the joined temporal model diagnostic analysis of parameter sensitivity and model performance (modified from Guse et al., 2013).

1. Temporal dynamic of model performance (TEDPAS)

Temporal variations of dominant model parameters were investigated by a temporal analysis of parameter sensitivity (TEDPAS) (Reusser et al., 2011). TEDPAS aims to detect dominant model parameters and thus differs from classical approaches of sensitivity analyses. A Fourier Amplitude Sensitivity Test (FAST) (Cukier et al., 1975) was used to estimate the first-order partial variance of each model parameter. Based on this, the dominant model parameters were estimated for each time step. For this analysis, the R-package FAST was used (Reusser, 2008).

2. Temporal dynamic of model performance

Time periods with good/poor model performance are detected by temporal analysis of model performance (Reusser et al., 2009). For this, a large set of performance measures was calculated with a moving window approach for each time step. The vectors of performance measures were classified by using Self-Organising Maps (SOM) and a fuzzy c-means clustering. Thus, temporal reoccurring patterns of typical model performance were obtained by using the R-package TIGER (Reusser, 2011).

3. Joined temporal analyses

Dominant parameters in periods of poor model performance are detected by a joined temporal analysis of both methods (Reusser and Zehe, 2011). For each cluster, all days were selected which have a fuzzy membership larger than 0.5. The parameter sensitivity was estimated separately for the four clusters (Guse et al., 2013).

Results

Temporal dynamic of parameter sensitivity

Fig. 4 shows the results of TEDPAS for the station Treia in four sub-plots for the different processes.

The surface runoff parameters CN2 and SURLAG are only rarely sensitive but have then a high sensitivity, especially in phases of high precipitation.

In contrast, the groundwater parameters GW_DELAY and ALPHA_BF are sensitive for longer periods. Whereas GW_DELAY dominates in recession phases, ALPHA_BF has a high sensitivity in recession and baseflow periods. RCHRG_DP is in particular sensitive under high flow conditions.

The evaporation parameter ESCO has its highest sensitivity in baseflow and resaturation phases.

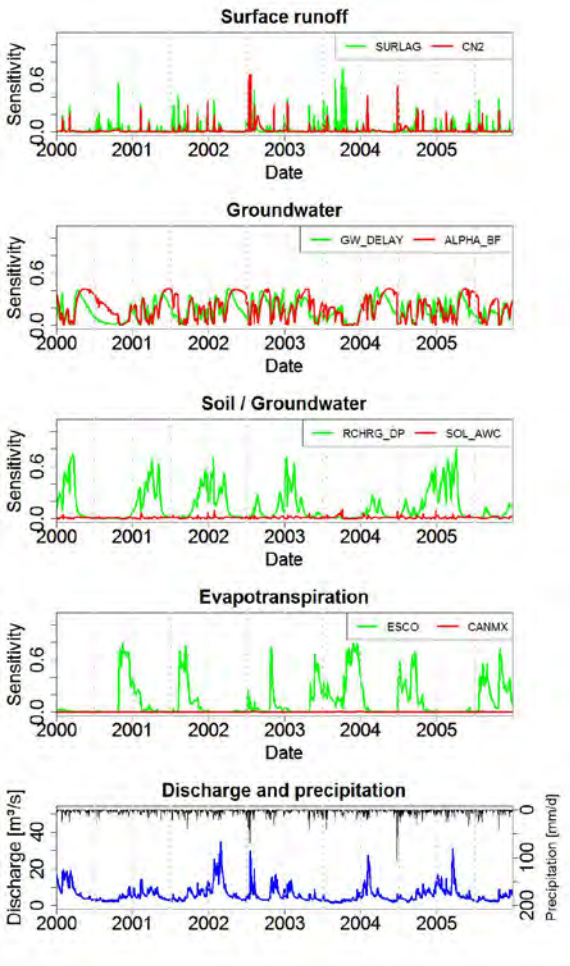

Fig. 4: Temporal dynamics of parameter sensitivity shown as first-order partial variance (modified from Guse et al., 2013).

Temporal dynamic of model performance

Three different clusters of typical model performance were distinguished. The normalized values of the performance measures vary between these three clusters (Fig. 5). These clusters are roughly related to the hydrograph phases and explained step-by-step as follows (Fig. 6).

Cluster A is related to discharge peaks. Whereas the peak dynamics are well performed (see in CE in Fig. 5), the measured discharge is underestimated (see PDIFF).

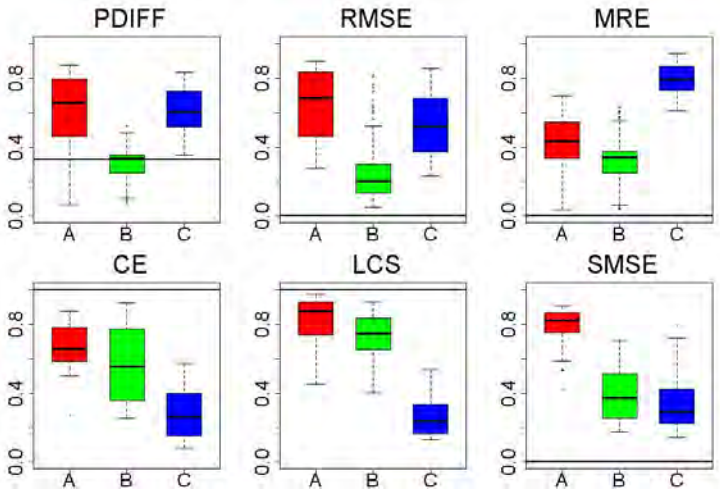

Fig. 5: Boxplots of performance measures different clusters (from Guse et al., 2013). PDIFF=peak difference, RMSE=root mean square error, MRE=mean relative error, CE=Nash-Sutcliffe Efficiency, LCS=Longest common sequence, SMSE=scaled mean square error.

Cluster B belongs to the recession phase. All six performance measures have good results for this cluster.

Cluster C is related to the long dry periods and the resaturation phase. These periods are characterized by an underestimation of the measured discharge time series (see PDIFF in Fig. 5). The discharge dynamic is not well reproduced (see LCS). There are high deviations between measured and modeled discharge time series (see MRE).

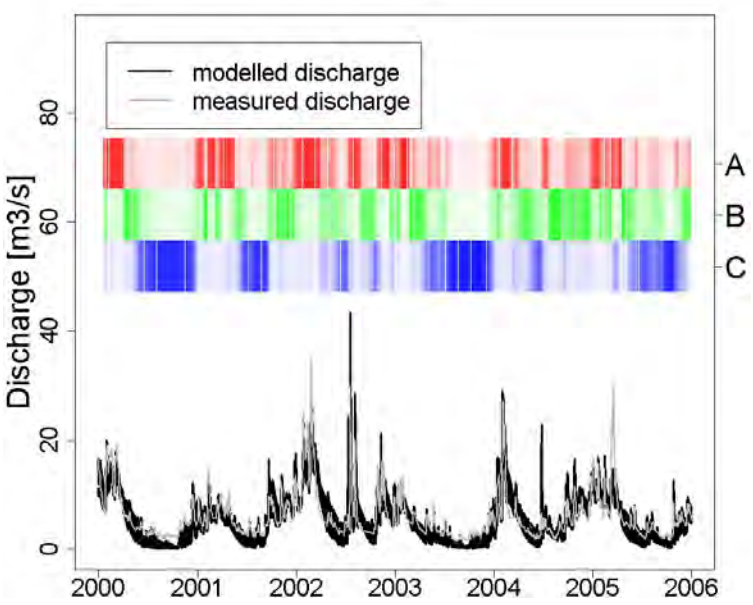

Fig. 6: Comparison of simulated and measured discharge time series. The contribution of the three clusters for each time step is emphasized by the colour intensity (from Guse et al., 2013).

Joined temporal analyses

The joined analysis of parameter sensitivity and model performance shows that the clusters A and B are dominated by the three groundwater parameters (ALPHA_BF, GW_DELAY, RCHRG_DP (Fig. 7). Cluster C is characterized by high sensitivities of ESCO, ALPHA_BF and GW_DELAY.

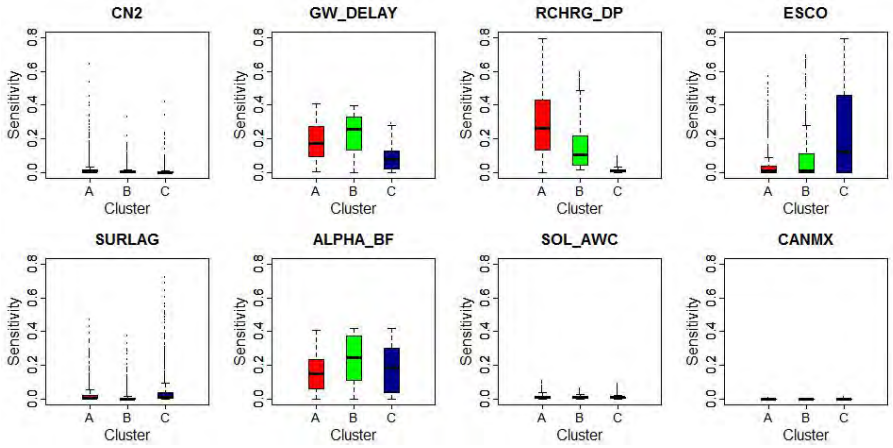

Fig. 7: Boxplots of temporal parameter sensitivities separately shown for all days with fuzzy memberships to a cluster of more than 0.5 (from Guse et al., 2013).

Conclusion

A joined temporal analysis of parameter sensitivity and model performance was applied to SWAT. The temporal dynamic of parameter sensitivity shows that the periods of high parameter sensitivity is related to the active phases of the corresponding process. Groundwater and evaporation are the dominant processes in the Treene lowland catchment. The six performance measures provide a representative characteristic of the model performance and support the use of several performance measures. The classification of the vectors of performance measures leads to three different clusters which represent three different phases of the hydrograph. The worst

performance was detected for the cluster C in which ESCO and ALPHA_BF are the dominant parameters.

Based on these results, we assumed that the concept of the groundwater module in SWAT is too strongly simplified for an application in lowlands and needs to be improved.

Acknowledgements
We thank Schleswig-Holstein Authority for National Parks, Coastal & Ocean Protection (LKN-SH), for the discharge data, the land survey office of Schleswig-Holstein for the digital elevation model and the land use map and the Land Schleswig-Holstein (LANU) for the river map (Digitales Anlagenverzeichnis). Furthermore, we thank the German Weather Service (DWD) for the climate data and the Potsdam Institute for Climate Impact Research (PIK) for the STAR data. This study is part of the IWRM-net project IMPACT and has been funded by the German Federal Ministry for Education and Research (BMBF) (grant number02WM1136). And this work was partially supported by the BMBF via its initiative Potsdam Research Cluster for Georisk Analysis, Environmental Change and Sustainability (PROGRESS).
We would like to thank the community of the open-source software R, which was used for the majority of the analysis.

References

Arnold J. G., R. Srinivasan, R. S. Muttiah and J. R. Williams. 1998. Large area hydrologic modeling and assessment part I: model development. *J. Am. Water Resour. A.* 34: 73–89.

Cukier R.I., J. H. Schaibly and K. E. Shuler. 1975. Study of sensitivity of coupled reaction systems to uncertainties in rate coefficients. 3. Analysis of approximations. *J. Chem. Phys.* 63(3): 1140–1149.

Gupta H.V., T. Wagener and Y. Liu. 2008. Reconciling theory with observations: elements of a diagnostic approach to model evaluation. *Hydrol. Process.* 22: 3802–3813.

Guse, B., D. E. Reusser and N. Fohrer. 2013. How to improve the representation of hydrological processes in SWAT for a lowland catchment – temporal analysis of parameter sensitivity and model performance. *Hydrol. Process.* doi: 10.1002/hyp.9777, in press.

Orlowsky B., F.-W. Gerstengarbe and P. C. Werner. 2008. A resampling scheme for regional climate simulations and its performance compared to a dynamical RCM. *Theor. Appl. Climatol.* 92: 209–223.

Reusser D. 2008. Implementation of the Fourier amplitude sensitivity test (FAST). R package 0.51.

Reusser D. 2011. Time series of grouped errors. R package 0.2.2.

Reusser D. E. and E. Zehe. 2011. Inferring model structural deficits by analyzing temporal dynamics of model performance and parameter sensitivity. *Water Resour. Res.* 47(7): W07550. doi:10.1029/2010WR009946.

Reusser D. E., T. Blume, B. Schaefli and E. Zehe. 2009. Analysing the temporal dynamics of model performance for hydrological models. *Hydrol. Earth Syst. Sci.* 13: 999–1018.

Reusser D. E., W. Buytaert and E. Zehe. 2011. Temporal dynamics of model parameter sensitivity for computationally expensive models with FAST (Fourier amplitude sensitivity test). *Water Resour Res.* 47(7): W07551. doi:10.1029/2010WR009947.

Wagener T., N. McIntyre, M. J. Lees, H. S. Wheater, H. V. Gupta. 2003. Towards reduced uncertainty in conceptual rainfall–runoff modelling: dynamic identifiability analysis. *Hydrol. Process.* 17: 455–476.

Yilmaz K. K., H. V. Gupta and T. Wagener. 2008. A process-based diagnostic approach to model evaluation: application to the NWS distributed hydrologic model. *Water Resour. Res.* 44: W09417. doi: 10.1029/2007WR006716.

Groundwater as the dominant control process to model recession and baseflow phases in lowland catchments

Matthias Pfannerstill
Christian-Albrechts-University of Kiel, Institute of Natural Resource Conservation, Department of Hydrology and Water Resources Management, Olshausenstr. 75, 24118 Kiel, Germany
mpfannerstill@hydrology.uni-kiel.de

Björn Guse, Dr.
Christian-Albrechts-University of Kiel, Institute of Natural Resource Conservation, Department of Hydrology and Water Resources Management, Olshausenstr. 75, 24118 Kiel, Germany

Nicola Fohrer, Prof. Dr.
Christian-Albrechts-University of Kiel, Institute of Natural Resource Conservation, Department of Hydrology and Water Resources Management, Olshausenstr. 75, 24118 Kiel, Germany

Abstract

The groundwater contribution to river discharge in North German lowlands is a key factor for a reasonable representation of the water balance, because of a strong interaction between near-surface groundwater and rivers. The winter season is characterized by high discharge conditions whereas the end-summer tends to distinctive low flow periods. Several studies revealed that the SWAT model may cause poor model performance for low flow periods, which are mainly controlled by groundwater. The reason could be the complexity of the processes in groundwater-dominated lowlands, which cannot be fully reproduced with one single contributing groundwater aquifer. Considering the non-linearity of the baseflow process, it is favourable to adapt the groundwater module of the SWAT model. In our investigations we divided the shallow aquifer to simulate a fast and a slow flow component of the groundwater and used the deep aquifer to account for water, which percolates into deep geologic formations. The new SWAT version leads to good prediction of the overall discharge especially for the recession limbs and the following low flow periods. This is reflected in the signature measures for the mid segment (PBIAS: -2.4% vs. -15:9%) and the low segment (PBIAS: 14.8% vs. 46:8%) of the flow duration curve.

Keywords: low flow, recession, groundwater, lowland, baseflow

Introduction

Hydrological models are used to address questions of water quality and water quantity in practice and science (Borah and Bera, 2003). For an integrated modeling of water and nutrients, the discharge components have to be represented with its connected processes as adequate as possible.

One important process in many lowlands is the groundwater interaction with the river. Shallow groundwater tables result in a groundwater flow, which is often the major contributor to stream flow (Gonzales et al., 2009; Schmalz et al., 2008a; Hattermann et al., 2004; Wittenberg, 2003). Describing complex interactions between groundwater storages and the resulting baseflow into the stream is an ambitious challenge. Nathan and McMahon (1990) revealed that baseflow is more a conceptual convenience than precise description of the natural processes. Numerical analyses of streamflow recessions showed, that a simple linear reservoir model does not represent the recession curve adequately (Fenicia et al., 2006). Many investigations concluded that an appropriate description of the base flow recession is not a single exponential function and thus there is a need of several storage reservoirs (Brandes et al., 2005).

The eco-hydrological Soil and Water Assessment Tool (SWAT, Arnold et al., 1998) has a wide range of application (Krysanova and Arnold, 2008; Gassman et al., 2007; Arnold and Fohrer, 2005), and was also used in several prior studies of the North German lowlands (Guse et al., 2013;Koch et al., 2013;Kiesel et al., 2010; Schmalz et al., 2008b). Several investigations with the SWAT model revealed limitations by modeling groundwater dominated discharge. Wu and Johnston (2007) found underestimated baseflow for dry years in a Great Lake watershed. Koch et al. (2013) reported that the baseflow and peak flows were constantly overestimated by the model. Additionally Watson et al. (2003) showed problems of baseflow recession rates, as the recession limb of the predicted discharge was much higher than the observed. Eckhardt (2008) concludes that it seems to be a short-coming of the model, that dry seasons cannot be reproduced satisfactorily with other discharge events.

Guse et al. (2013) proposed the modification of the SWAT groundwater module to enhance the process-based representation of low-flow periods. Luo et al. (2012) modified the groundwater module by activating groundwater contribution of the deep aquifer storage to the channel. Brandes et al. (2005) and Nathan and McMahon (1990) suggest multiple reservoirs to describe the recession as nonlinear process. Based on aforementioned suggestions, we extended the groundwater concept of the SWAT model to address following questions (Pfannerstill et al., 2013):

- How can nonlinearities of groundwater processes be emphasized in the existing SWAT model?
- Does the extension by additional storages and delay functions result in enhanced baseflow representation?

2.1 Study area

Our investigations took place in the Kielstau catchment, which is located within a lowland area of the federal state Schleswig-Holstein in Northern Germany. The catchment area is about 50 km^2 .The mean annual precipitation and temperature is 918.9 mm and 8.24 °C (DWD, 2012). Its landscape can be described as flat with rolling hills and depressions. The topography ranges between 27 m and 78 m above mean sea level. One important hydrological characteristic of the Kielstau catchment is the high fraction of drained agricultural area in the catchment, which is estimated to be 38% (Fohrer et al., 2007). Schmalz et al. (2008a) describe the dynamics of the near-surface groundwater at a riparian wetland as a dynamic interaction between groundwater and surface water. The near-surface groundwater is generally controlled by precipitation and, close to the river, also by river water level (Schmalz et al., 2008a).

2.2 The original and modified groundwater module of the SWAT model

In the SWAT model, soil water percolates into groundwater reservoirs which are divided into a shallow and a deep aquifer. The shallow aquifer represents an unconfined aquifer that may contribute to the channel. The deep aquifer is described as a confined aquifer, which does not contribute to the streamflow within the watershed but outside of the watershed. In this case the deep aquifer is considered as inactive, because water is lost from the system within the modeled catchment.

In our modification, the two storage concept of the original groundwater module was extended to emphasize the nonlinearity of the baseflow (Pfannerstill et al., 2013). Therefore a second aquifer is connected to the channel as proposed in Luo et al. (2012). The $SWAT_{3S}$ version (Pfannerstill et al., 2013) consists of three groundwater storages. The shallow groundwater storage is divided into two storages, which describe a fast shallow aquifer for fast responses of precipitation events and a slow shallow aquifer for the slow response of groundwater recharge. We assumed that a part of the groundwater does not contribute to the channel as the catchment of the Kielstau is relatively small with a size of 50 km^2. To realize this process of inactive groundwater contribution for small catchments, the assumption of the original SWAT model was taken up. A part of the groundwater recharge is routed to the deep aquifer, which is not connected to the channel and considered as inactive for contribution.

2.3 Model evaluation

Both model setups (original SWAT/$SWAT_{3S}$) were calibrated independently. Sets of model parameters were generated for calibration using the Latin Hypercube Sampling of the R-package FME (Soetaert and Petzoldt, 2010) for 5000 model runs. The generation of the parameter sets and the replacing of parameter values in the SWAT model input files were executed with the R environment (R Core Team, 2013). The model evaluation was done with the R-package hydroGOF (Zambrano-Bigiarini, 2012) and a simple reproduction of the flow duration curve (Smakhtin, 2001; Vogel and Fennessey, 1994). As proposed in Moriasi et al. (2007) the Nash-Sutcliffe efficiency (NSE, Nash and Sutcliffe, 1970) and the percent bias (PBIAS, e.g. Gupta et al., 1999) were used as performance measure of the modeled discharge. Due to disproportional weighting of high values in the NSE (Legates and McCabe, 1999]) and no existing sensitivity for systematic over- or underestimation (Krause et al., 2005), the performance measure was only used for high flow dynamics and temporal discharge dynamics evaluation. As the low-flow

periods are on focus, additional signature measures as proposed in Yilmaz et al. (2008) were used to calibrate the low-flow and mid-flow periods. These signature measures incorporate the PBIAS of the low flow with 90% of time flow equaled or exceeded (hereafter PBIASlow) and a PBIAS of the mid-flow (Yilmaz et al., 2008) with a range of 20% to 80% of time flow equaled or exceeded (hereafter PBIASmid).

3. Results

The calibration was evaluated for the hydrological years of 2003 – 2005 and 2009 – 2010. The two SWAT versions resulted in different hydrographs (Fig. 1). The original model tends to predict dry periods with days of no discharge and the recession limbs are overestimated. Referring to the late recession limb with following baseflow, $SWAT_{3S}$ predicts discharge which is visually at the level of the observed discharge. Additionally the extended groundwater module predicts much higher baseflow at dry periods than the two storage version of the original SWAT. Referring to the peaks of the discharge the two storage version simulates slightly higher peaks than the modified $SWAT_{3S}$.

The NSE indicates that $SWAT_{3S}$ and $SWAT_{orig}$ performed similar in predicting the discharge dynamics (NSE: 0.72 vs. 0.73). The PBIAS is near to the optimal measure value for both model versions ($SWAT_{3S}$: -4.4% and original SWAT: -6.3%). Referring to the prediction of the mid segment of the flow duration curve, $SWAT_{3S}$ produced less overestimation ($SWAT_{3S}$: -2.4% and original SWAT: -15.9%). Comparing the low flow segment of the FDC, differences become obvious. The original SWAT version predicts less discharge than observed (46.8%). The modified version predicts a difference of 14.8%.

4. Discussion

The results of this investigation show, that the original SWAT model with two groundwater storages is limited in reproducing the combination of recession and low flow periods. Because of the single groundwater reservoir for contribution to the discharge, it is challenging to reproduce all phases of the discharge. One single reservoir is not able to describe the fast flow and the slow flow component of the groundwater contribution exactly. In contrast, for the modified SWAT model $SWAT_{3S}$ with its two contributing storages it is much easier to reproduce the recession limb in combination with a good simulation of the baseflow. This refers to the model concept, which allows accounting for a fast flow component in the peak and recession phase mainly with the fast answer of the fast shallow aquifer. Additionally, the contributing slow shallow aquifer controls the baseflow with its delayed answer of groundwater recharge. A third control option for the baseflow is the loss to the deep aquifer which is especially important for small catchments. Considering the modified groundwater concept, our findings agree with Wittenberg (1999) who stated, that such approaches must result in better model performance since there are more parameters for calibration.

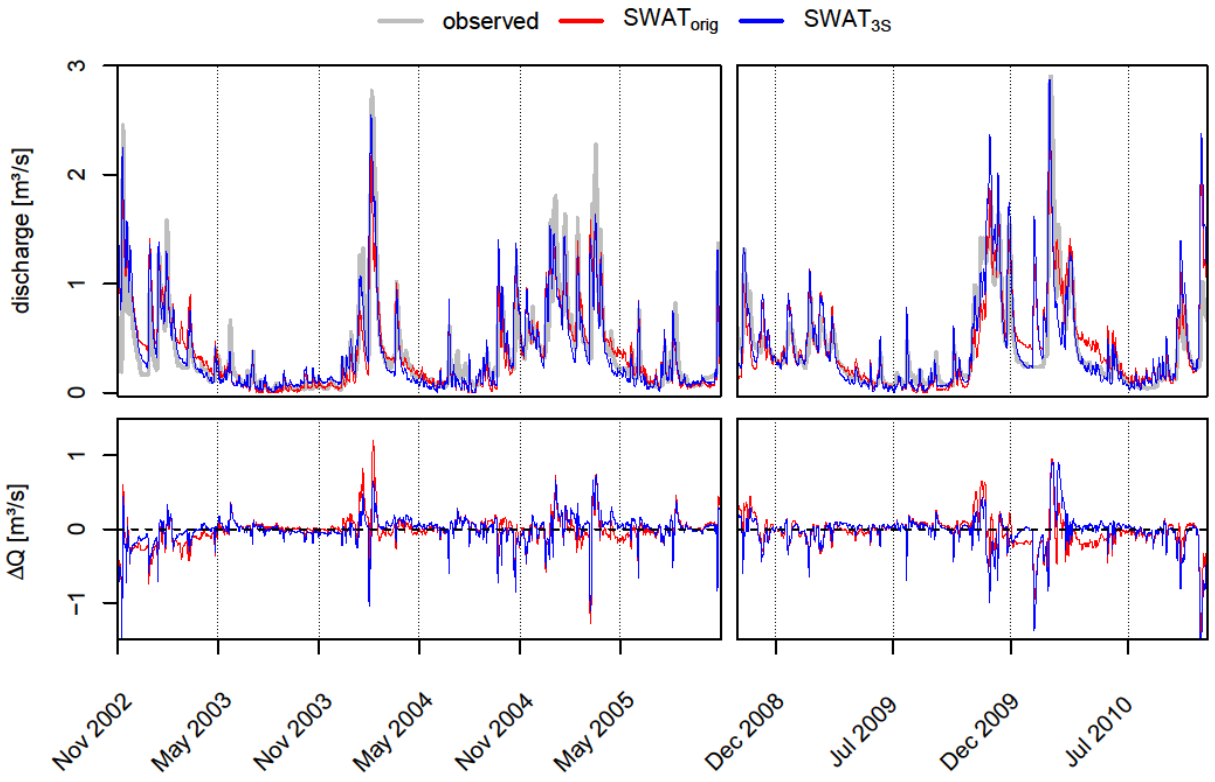

Figure 1: Observed and modeled (original and modified version) discharge for the calibration period of 2003 – 2005 and 2009 – 2010 (Pfannerstill et al., 2013).

Due to the modular structure of the groundwater model, it is possible to select the numbers of active groundwater storages. Consequently, the representation of the characteristic groundwater processes can be adapted to different catchments. Another advantage of the concept could be the possibility to model spatial heterogeneity of subcatchments due to the modular construction of the three storage concept. As the different aquifer types can be activated or inactivated, the extended groundwater concept enables more flexibility in groundwater modeling. Referring to spatial heterogeneity, groundwater aquifers can be activated and deactivated for each subcatchment individually which might lead to a better representation of spatial patterns in large catchments.

Despite of the promising results for the simulation of recession and baseflow phases with the modified version, the new concept has to be verified by field measurements. Is has to be kept in mind that representation of the groundwater processes are simplified and aggregated into a conceptual model. Field measurements should clarify if the extended groundwater concept is an acceptable simplification of the groundwater processes. Concerning the calibration process and the selection of best model runs, further research is needed to select model runs on the basis of a fair balanced consideration between the high flow, mid flow and low flow events with additional timing control.

5. Conclusion

In this paper we investigated if nonlinearities of groundwater processes can be emphasized in a modified SWAT model. Additional storages with time delay functions were implemented to reach an enhanced representation of the low flow periods. The shallow aquifer was separated into a fast and into a slow flow component. Additionally, a third aquifer was added to simulate groundwater flow out of the catchment. The results show, that the extended groundwater module leads to a calibration of recession limbs and ongoing low flow phases, which is more process-based. The calibration of the recession limb and the low flow in the original SWAT version was more or less a trade-off between these two discharge phases. With the process-based extension of the groundwater module, very good results of signature and performance measures were achieved with the new $SWAT_{3S}$.

The extended groundwater module was originally designed for small catchments where a certain part of the groundwater does not contribute to the discharge at the gauging station. Nonetheless this approach could be also a solution to integrate spatial heterogeneity of groundwater characteristics for catchments at larger scales. The groundwater contribution and recharge of subcatchments could be treated independently by activating/deactivating single aquifers.

Acknowlegdements

We thank the Government-Owned Company for Coastal Protection, National Parks and Ocean Protection (LKN-SH) of Schleswig-Holstein for the discharge data, the land survey office of Schleswig-Holstein for providing the digital elevation model and the rivernetwork, the German Weather Service (DWD) for the climate data and the Potsdam Institute for Climate Impact Research (PIK) for the STAR data. This project has been carried out with financial support of a scholarship for the first author by the German Environmental Foundation (DBU). We would like to thank the community of the open source software R, which was used for calibration of the SWAT model and following analysis.

References

Arnold, J. G., and N. Fohrer. 2005. Swat2000: Current capabilities and research opportunities in applied watershed modelling. Hydrological Processes, 19:563–572.

Arnold, J. G., R. Srinivasan, R. S. Muttiah, and J. R. Williams. 1998. Large area hydrologic modeling and assessment part I: Model development. Journal of the American Water Resources Association 34, 1:73–89.

Borah, D. K., and M. Bera. 2003. Watershed-scale hydrologic and nonpoint-source pollution models: Review of mathematical bases. Trans. ASAE 46, 6:1553–1566.

Brandes, D., J. G. Hoffmann, and J. T. Mangarillo. 2005. Base flow recession rates, low flows, and hydrologic features of small watersheds in Pennsylvania, USA. JAWRA Journal of the American Water Resources Association, 41(5):1177–1186.

DWD. 2012. Weather and climate data from the German Weather Service of the station Flensburg (1961-1990). Online climate data.

Eckhardt, K. 2008. A comparison of baseflow indices, which were calculated with seven different baseflow separation methods. Journal of hydrology, 352(1):168–173.

Fenicia, F., H. H. G. Savenije, P. Matgen, and L. Pfister. 2006. Is the groundwater reservoir linear? Learning from data in hydrological modelling. Hydrology and Earth System Sciences Discussions, 10(1):139–150.

Fohrer, N., A. Dietrich, O. Kolychalow, and U. Ulrich. 2013. Assessment of the environmental fate of the herbicides flufenacet and metazachlor with the SWAT model. Journal of Environmental Quality, 41:1-11.

Fohrer, N., B. Schmalz, F. Tavares, and J. Golon. 2007. Modelling the landscape water balance of mesoscale lowland catchments considering agricultural drainage systems. Hydrologie und Wasserbewirtschaftung/Hydrology and Water Resources Management-Germany, 51(4):164–169.

Gassman, P. W., M. R. Reyes, C. H. Green, and J. G. Arnold. 2007. The soil and water assessment tool: historical development, applications, and future research directions. Center for Agricultural and Rural Development, Iowa State University.

Gonzales, A. L., J. Nonner, J. Heijkers, and S. Uhlenbrook. 2009. Comparison of different base flow separation methods in a lowland catchment. Hydrology and Earth System Sciences, 13(11):2055.

Gupta, H. V., S. Sorooshian, and P. O. Yapo. 1999. Status of automatic calibration for hydrologic models: Comparison with multilevel expert calibration. Journal of Hydrologic Engineering, 4(2):135–143.

Guse, B., D. E. Reusser, and N. Fohrer. 2013. How to improve the representation of hydrological processes in SWAT for a lowland catchment - Temporal analysis of parameter sensitivity and model performance. Hydrological Processes, (in press), doi: 10.1002/hyp.9777.

Hattermann, F., V. Krysanova, F. Wechsung, and M. Wattenbach. 2004. Integrating groundwater dynamics in regional hydrological modelling. Environmental modelling & software, 19 (11):1039–1051.

Kiesel, J., N. Fohrer, B. Schmalz, and M. J. White. 2010. Incorporating landscape depressions and tile drainages of a northern German lowland catchment into a semi-distributed model. Hydrological Processes, 24(11):1472–1486.

Koch, S., A. Bauwe, and B. Lennartz. 2013. Application of the SWAT model for a tile-drained lowland catchment in North-Eastern Germany on subbasin scale. Water Resources Management, 27(3):791–805.

Krause, P., D. P. Boyle, and F. Bäse. 2005. Comparison of different efficiency criteria for hydrological model assessment. Advances in Geosciences, 5:89–97.

Krysanova, V., and J. G. Arnold. 2008. Advances in ecohydrological modelling with SWAT: a review. Hydrological Sciences Journal, 53(5):939–947.

Legates, D. R., and G. J. McCabe. 1999. Evaluating the use of goodness-of-fit measures in hydrologic and hydroclimatic model validation. Water Resources Research, 35:233–241.

Luo, Y., J. Arnold, P. Allen, and X. Chen. 2012. Baseflow simulation using SWAT model in an inland river basin in Tianshan Mountains, Northwest China. Hydrology and Earth System Sciences, 16(4):1259.

LVermA. 1995. Landesvermessungsamt Schleswig-Holstein Digitales Geländemodell für SchleswigHolstein. Quelle: TK25. Gitterweite 25 m x 25 m und TK50 Gitterweite 50 m x 50 m sowie ATKIS-DGM2-1 m x 1 m Gitterweite und DGM 5 m x 5 m Gitterweite, abgeleitet aus LiDAR-Daten.

Moriasi, D. N., J. G. Arnold, M. W. Van Liew, R. L. Bingner, R. D. Harmel, and T. L. Veith. 2007. Model evaluation guidelines for systematic quantification of accuracy in watershed simulations. Transactions of the ASABE, 50:885–900.

Nash, J. E., and J. V. Sutcliffe. 1970. River flow forecasting through conceptual models: Part 1 a discussion of principles. Journal of Hydrology, 10:282–290.

Nathan, R. J., and T. A. McMahon. 1990. Evaluation of automated techniques for base flow and recession analyses. Water Resources Research, 26(7):1465–1473, 1990.

Orlowsky, B., F. W. Gerstengarbe, and P. C. Werner. 2008. A resampling scheme for regional climate simulations and its performance compared to a dynamical RCM. Theoretical and Applied Climatology, 92(3):209–223.

Pfannerstill, M., B. Guse, and N. Fohrer. 2013. A multi-storage groundwater concept for the SWAT model to emphasize nonlinear groundwater dynamics in lowland catchments. Hydrological processes, doi: 10.1002/hyp.10062

R Core Team. 2013. R: A language and environment for statistical computing. Vienna, Austria: R foundation for statistical computing.

Schmalz, B., P. Springer, and N. Fohrer. 2008a. Interactions between near-surface groundwater and surface water in a drained riparian wetland. In Proceedings of International Union of Geodesy and Geophysics XXIV General Assemble" A New Focus on Integrated Analysis of Groundwater/Surface Water Systems", Perugia, Italy, 11-13 July 2007., pages 21–29. IAHS Press.

Schmalz, B., F. Tavares, and N. Fohrer. 2008b. Modelling hydrological processes in mesoscale lowland river basins with SWAT: capabilities and challenges. Hydrological sciences journal, 53(5):989–1000.

Smakhtin, V. U. 2001. Low flow hydrology: a review. Journal of hydrology, 240(3):147–186.

Soetaert, K., and T. Petzoldt. 2010. Inverse modelling, sensitivity and monte carlo analysis in R using package FME. Journal of Statistical Software, 33:1–28.

Vogel, R. M., and N. M. Fennessey. 1994. Flow-duration curves. I: New interpretation and confidence intervals. Journal of Water Resources Planning and Management, 120(4):485–504.

Watson, B. M., S. Selvalingam, and M. Ghafouri. 2003. Evaluation of SWAT for modeling the water balance of the Woady Yaloak River catchment, Victoria. MODSIM 2003 : International Congress on Modelling and Simulation, Jupiters Hotel and Casino, 14-17 July 2003 : integrative modelling of biophysical, social and economic systems for resource management solutions : proceedings, 2003:01–01.

Wittenberg, H. 2003. Effects of season and man-made changes on baseflow and flow recession: case studies. Hydrological Processes, 17(11):2113–2123.

Wittenberg, H. 1999. Baseflow recession and recharge as nonlinear storage processes. Hydrological Processes, 13(5):715–726.

Wu, K., and C. A. Johnston. 2007. Hydrologic response to climatic variability in a Great Lakes Watershed: A case study with the SWAT model. Journal of Hydrology, 337(1):187–199.

Yilmaz, K. K., H. V. Gupta, and T. Wagener. 2008. A process-based diagnostic approach to model evaluation: Application to the NWS distributed hydrologicmodel. Water Resour. Res, 44(9):W09417.

Zambrano-Bigiarini, M. 2012. hydrotsm: Time series management, analysis and interpolation for hydrological modelling. R package version 0.3-3.

Modeling water resources in Black Sea Basin

Elham Rouholahnejad
Eawag, Swiss Federal Institute of Aquatic Science and Technology, Ueberlandstrasse 133, 8600 Duebendorf, Switzerland.

ETH Zürich Institute of Terrestrial Ecosystem, Universitätstr. 16, 8092 Zürich, Switzerland.

Karim C. Abbaspour
Eawag, Swiss Federal Institute of Aquatic Science and Technology, Ueberlandstrasse 133, 8600 Duebendorf, Switzerland.

Anthony Lehmann
University of Geneva, Climatic Change and Climate Impacts, 7 Route de Drize, CH-1227 Carouge, Switzerland.

Abstract

Increasing water demand and conflict of interest presents a huge water management challenge in the Black Sea Basin (BSB). An integrated management of water is being sought, which requires a new level of consideration where water bodies are to be viewed in the context of the whole river system and managed as a unit within their basins. A frequently advocated approach is to have adequate knowledge of temporal and spatial variability of the fresh water availability and water quality in the basin. To achieve this, we used the program Soil and Water Assessment Tool (SWAT) to model the hydrology of the BSB with an area of 2.3 million km^2. The hydrological model of the BSB was calibrated, validated, and sensitivity and uncertainty analysis were performed to assess the goodness of modeling results using the Sequential Uncertainty Fitting program (SUFI-2). River discharges were used for model calibration. Grid technology was successfully tested for such a large model to improve calibration computation time by more than an order of magnitude. We calculated all components of water cycle using the calibrated hydrological model. In this paper we particularly discuss the challenges of building a large-scale model in fine spatial and temporal detail and show the strengths and pitfalls of such modeling tasks.

Keywords: Hydrology, Large scale, Calibration, Uncertainty, SWAT, SUFI-2, Grid computing.

Introduction

The Black Sea Basin (BSB) is internationally recognized for its ecologically unsustainable development and inadequate resource management leading to severe environmental, social and economical problems. The Black Sea itself is also affected by severe environmental degradation. In 1995, it was rated of being of the highest concern in five out of seven environmental categories, making it the worst of any of the European seas [Stanners and Boudreau 1995]. A frequently advocated approach to tackle the existing problems is to have adequate knowledge of temporal and spatial variability of the fresh water availability and water quality [UNEP, 2006].

Previous researches, which addressed water quantity and water quality in the BSB include WaterGAP2 [Alcamo et al., 2003; Döll et al., 2003] which is a global model for water availability and water use. The model focuses on the global hydrology at grid scale (30 arc min) considering 3,565 major basins in the world with the drainage areas greater than 2500 km^2. The model was initially used to estimate the water availability and demand and provides relatively limited water cycle-related components. In WaterGAP3 [Aus der Beek et al., 2012], a regional version of the WaterGAP2, the hydrological fluxes draining into Mediterranean and Black Sea were modeled with improved spatial resolution (5 arc min), snow melt, and water use. However, results using WaterGAP3 and WaterGAP2 are not significantly different in the BSB [Aus der Beek et al., 2012]. Furthermore, discharges of water and nutrient to the Mediterranean and Black Sea are reported in a study by Ludwig et al. [2009] for major rivers.

To help answering some of the above-stated problems, EnviroGrids project (Building Capacity for a Black Sea Basin Observation and Assessment System supporting Sustainable Development) was defined in the 7th European Union framework, to build capacities in the Black Sea region to gather, store, distribute, analyze, visualize and disseminate crucial information on past, present and future water states. As part of the EnviroGrids, the general goal of this study is to build a hydrological model of the Black Sea Basin. This model was used to estimate all components of water resources at the sub-basin level on a monthly time step. We explicitly quantified blue water flow (river discharge plus deep aquifer recharge), green water flow (evapotranspiration), green water storage (soil moisture), and river discharge among other water cycle components. Furthermore, the hydrologic model is calibrated and validated with sensitivity and uncertainty analyses.

To achieve the objectives of this research, we used the program Soil and Water Assessment Tool (SWAT) [Arnold, et al., 1998] to set up the hydrological model and the Sequential Uncertainty Fitting program SUFI-2 [Abbaspour et al., 2004, 2007] as a sensitivity analysis, multi-site calibration, and uncertainty analysis tool. SUFI-2 lends itself easily to parallelization, and is capable of analyzing a large number of parameters and measured data simultaneously. Parallelization and building of a distributed grid system for running SUFI-2 are described by Rouholahnejad et al. [2012] and Gorgan et al. [2012].

Figure 1. Black Sea Basin study area, major rivers basins, and measured stations of climate, discharge.

Methodology

Study area

The Black Sea is located between the continents of Europe and Asia. It is connected to the Atlantic Ocean via the Mediterranean Sea. The Black Sea Basin with the total area of around 2.3 million km^2 which is five times the surface of the Black Sea, is located between 38^o and 56^o north latitude and 8^o to 46^o east longitude and includes entirely or partially 23 European and Asian countries (Austria, Belarus, Bosnia, Bulgaria, Croatia, Czech Republic, Georgia, Germany, Hungary, Moldova, Montenegro, Romania, Russia, Serbia, Slovakia, Slovenia, Turkey, Ukraine, Italy, Switzerland, Poland, Albania and Macedonia) (Figure 1).

Some of Europe's longest and largest rivers flow into the Black Sea, including the Danube, the Dnieper, the Southern Bug, the Dniester and the Don (Figure 1). The area is inhabited by a total population of around 160 million people [BSEI, 2005] while the greatest sources of diffuse pollution are agricultural and households not connected to sewer systems. Areas of high precipitation (> 3000 mm y^{-1}) are in the west, and areas of low precipitation (< 190 mm y^{-1}) are in the north and east [Tockner et al., 2009]. The dominant landuse in the basin is agricultural with 65% of coverage according to MODIS Land Cover [NASA, 2001] (Figure 2).

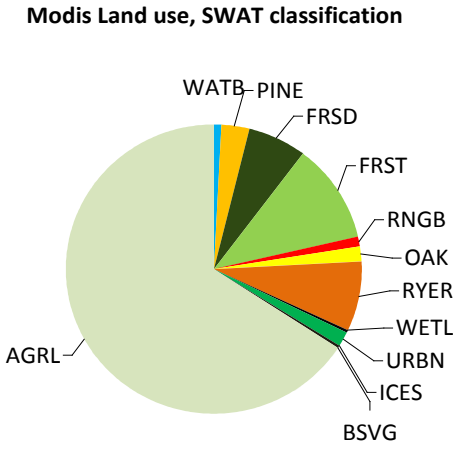

Figure 2. Share of Agricultural land in Black Sea Basin among other landuses, 65 %.

Model inputs and model set up

In this study, the Black Sea Basin was subdivided into 12982 subbasins and 89202 HRUs. Watershed parameterization and model inputs were derived using the Arc SWAT Interface [Winchell et al., 2007]. Using SWAT 2009, a single daily simulation runs for the period of 1970–2006 took 42 on a 64 bit laptop with 2.7 GHz processors, 4 cores, 8 GB of RAM and Windows7 operating system. The basic data sets required fro model development:

(i) Digital elevation model (DEM), by SRTM at 90 meter resolution [Jarvis et al, 2008].

(ii) Digital stream network, by European Catchments and RIvers Network System [ECRINS, 2012] at 30 meter resolution. The ECRINS river map was corrected in the areas where there was a mismatch with DEM to correct flow direction (Figure 3).

(iii) Soil map, was obtained from FAO global soil map [FAO, 1995]. It provides data for 5000 soil types in two layers (0–30 cm and 30–100 cm depth) at 5 km.

(iv) MODIS landuse maps, produced and maintained by the NASA Land Processes Distributed Active Archive Center (LP DAAC) at the USGS/Earth Resources Observation and Science Center (EROS) at spatial resolution of 500 m [NASA, 2001].

(v) Climate data, was taken from Climate Research Units [CRU, 2008; Mitchell and Jones, 2005] at 0.5 ^{o} resolution. 5 elevation bands was used in each subbasin to adjust temperature (-6^{o} km^{-1}) and precipitation (1 mm km^{-1}). The daily global solar radiation data was obtained from 6,110 virtual stations at 0.5^{o} resolution [Weedon et al., 2011].

(vi) River discharge for model calibration and validation was obtained from Global Runoff Data Center [GRDC, 2011], National Institute of Hydrology and Water Management (INHGA) and Danube Delta National Institute for Research and Development (DDNI) in Romania, and Turkish Ministry of Forest and Water Affairs (MEF) for 1970–2008.

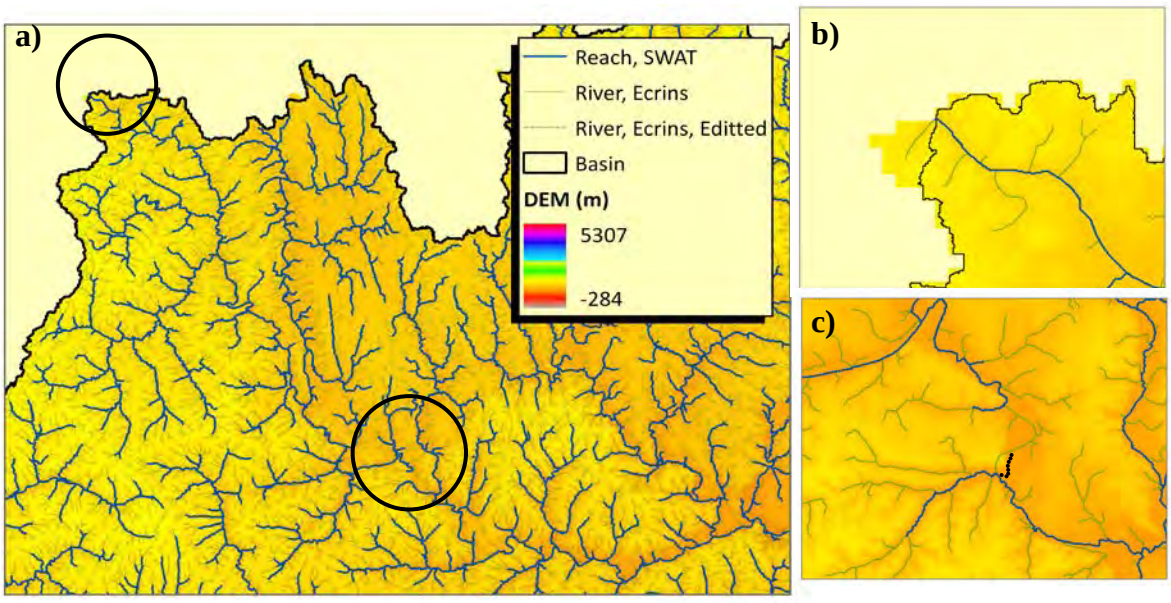

Figure 3. Reach delineated by SWAT (dark blue line) is disconnected (c) and flowing out of the watershed (b) due to incorrect digital river map given to model (light blue line) that passes the highly elevated area (light yellow color) (c). The digital river map is corrected (black dash line in C).

Model calibration

The Sequential Uncertainty Fitting algorithm (SUFI-2) [Abbaspour et al., 2004; Abbaspour et al., 2007] was used for calibration and uncertainty analysis for water quantity, water quality, and crop yields. Initially, a set of meaningful parameter ranges are assigned to calibrating parameters based on literature, knowledge of site processes, and sensitivity analyses. In SUFI2 algorithm all uncertainties (parameter, conceptual model, input, etc.) are mapped onto the

parameter ranges, which are calibrated to bracket most of the measured data in the 95% prediction uncertainty [Abbaspour *et al*., 2007]. The overall uncertainty in the output is quantified by the 95% prediction uncertainty (95PPU) calculated at the 2.5% and 97.5% levels of the cumulative distribution of an output variable obtained through Latin hypercube sampling. Two indices are used to quantify the goodness of calibration/uncertainty performance: the *P-factor*, which is the percentage of data bracketed by the 95PPU band, and the *R-factor*, which is the average width of the band divided by the standard deviation of the corresponding measured variable. Ideally, we would like to bracket most of the measured data within the 95PPU band (P-factor→1) while having the narrowest band (R-factor→0). We used the following efficiency criterion for discharge [Krause et al., 2005]:

$$g = |b|\, R^2 \quad \text{for} \quad |b| \le 1 \qquad (1)$$

$$g = |b|^{-1}\, R^2 \quad \text{for} \quad |b| > 1 \qquad (2)$$

where R^2 is the coefficient of determination and b is the slope of the regression line between the simulated and measured data. For multiple outlets and attributes, the objective function Φ was expressed as:

$$\Phi = \frac{1}{n}\left(\sum_{i=1}^{n} w_i g_i\right) \qquad (3)$$

where n is the number of discharge outlets w's are weights, and g is efficiency criteria for discharge. The efficiency criteria g vary between 0 and 1 where 1 indicates a perfect match. The best simulation is considered the one with the highest Φ value.

Results and discussion

Calibration and uncertainty analysis

A broad set of parameters were initially derived from Lenhart et al. [2002]; van Griensven et al. [2006]; Holvoet et al. [2005]; Abbaspour et al. [2007]; Ruget et al. [2002]; Wang et al. [2005], and Faramarzi et al. [2009]. Then a sensitivity analysis was performed to identify the key parameters across BSB, which led to selection of 24 parameters integrally related to stream flow. Although the initial parameter ranges were as wide as physically meaningful, some outlets were still completely outside of the 95PPU range. These outlets would obviously not benefit from parameter calibration alone. In the BING map, we observed the outlets and the surrounding areas. In some cases, we found that outlets were positioned on a wrong rive (Figure 4a,b). As SWAT connects each measured outlet to the nearest rivers, any errors in the coordinates of outlets can cause a wrong placement of the outlets. This perhaps leads to the biggest calibration problem. As shown in Figure 4b the outlet is placed on a tributary of the Danube called Tamis in Serbia. The black dash-line near the x-axis (Figure 4c) is simulated river discharge before correcting the location, and the red line shows the simulated discharge after correcting the location.

Other major problems result from an outlet being positioned downstream of a reservoir. Clearly the dynamics of such outlets depend on the management of the reservoir and not natural processes. Other problematic situations may arise when outlets are in a highly populated or agricultural region where water management and water transfers are large (Figure 5a,b) or glaciers (Figure 5c). In these situations also, SWAT cannot be expected to produce proper results unless proper cautions are taken during calibration. These include converting outlets to inlets, weighing those outlets under the influence of management less in the objective function, or removing the outlets downstream of reservoirs from the calibration process.

(a) **(b)**

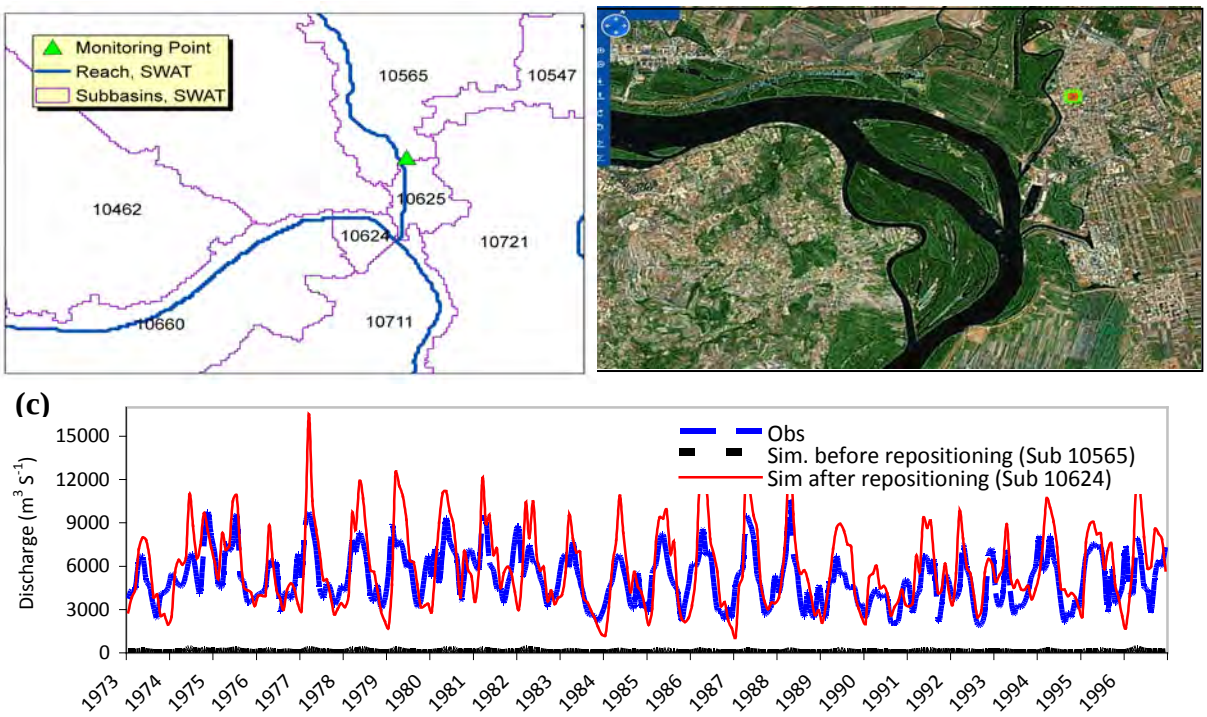

Figure 4. Example of a wrong positioning of the outlets due to errors in the reported coordinates of the measurement stations.

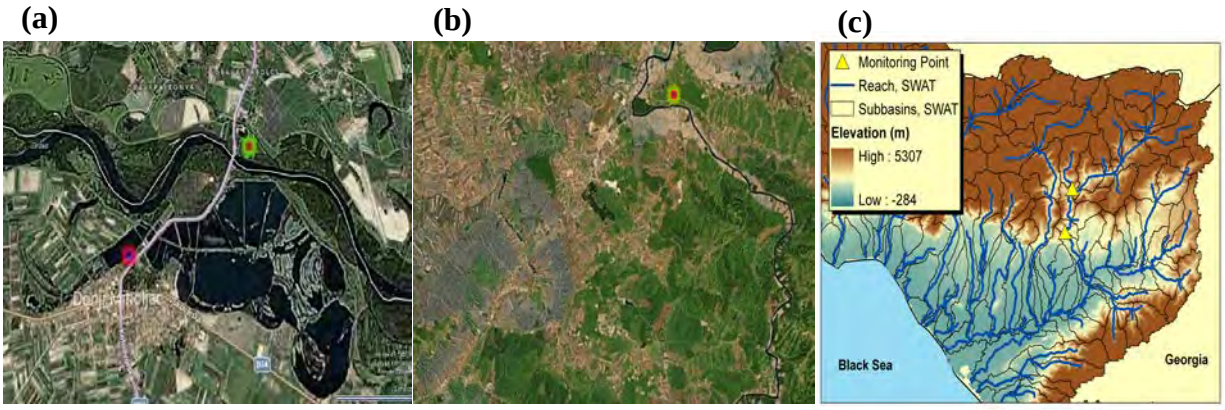

Figure 5. Examples of highly irrigation water infrastructure (a), highly agricultural areas (b), and glaciers (c).

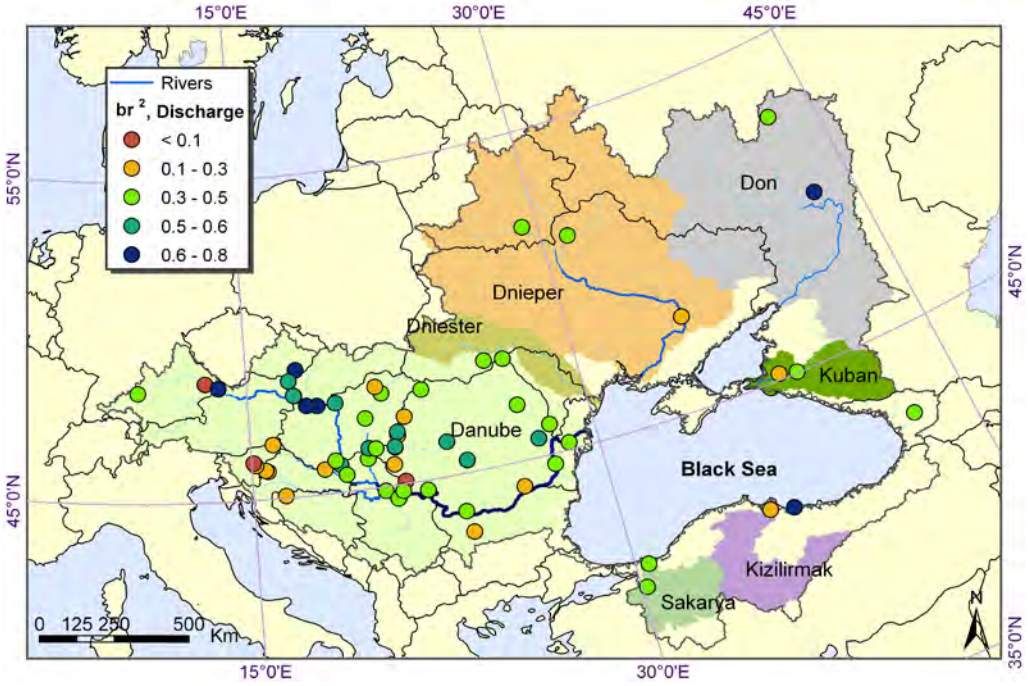

Figure 6. Comparison of observed and simulated discharge in the BSB using the objective function bR^2. Also shown are the six large river basins of Danube, Dnieper, Don, Kuban, Kizilirmak, and Sakarya.

After initial corrections, the model was parameterized to account for the differences between simulation and observation in terms of temporal shifts in diagrams, higher/lower peaks and higher/lower base flows. Parameterization refers to regionalization of parameters tailored to achieve the best response from the simulation program and individual outlets. The respective parameters to solve above mentioned problems are: overland flow (HRU_SLP), Manning's roughness coefficient (ON_N), flow length (SLSUBBSN), deep percolation loss (GWQMN), groundwater revap coefficient (GW_REVAP), threshold depth of water in shallow aquifer (REVAPMN), curve number (CN2), soil available water storage capacity (SOL_AWC), and soil evaporation compensation factor (ESCO).

A few calibration iterations are then carried out seeking to reach an optimal *P-factor* and *R-factor* until a further improvement in the objective function is not found. The calibration runs were made using the gridded gSWAT [Gorgan, et al., 2012; Rouholahnejad, 2012]. Eventually, we were left with 63. The final calibration results for all outlets range from very good to poor (Figure 6). The bR^2 statistic for discharge outlets range from 0.2 to 0.8. The time series example (Figure 7) for a discharge station on Prypiat river draining to Danieper in Belarus shows very good results in both calibration and validation periods.

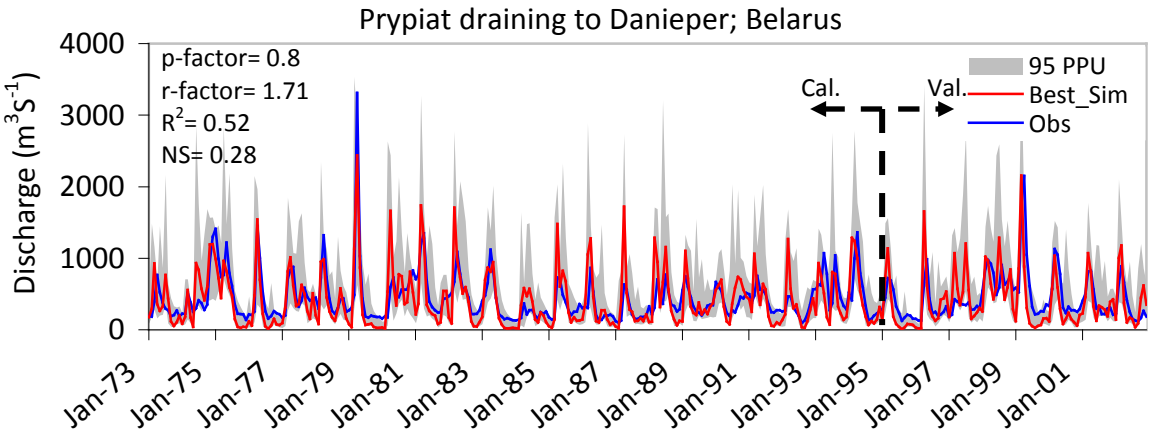

Figure 7. Comparison of simulated and observed discharges at Prypiat river for calibration and validation periods. The shaded region is 95% prediction uncertainty band. The best model simulation is in red line.

Quantification of water resources

To highlight the importance of uncertainty analysis, the upper and lower bounds of the 95% prediction uncertainties for the green water flow is depicted in Figure 8. Also shown are special distributions of long term annual average of blue water and green water storage at subbasin level for the period of 1973-2006 (Figure 9).

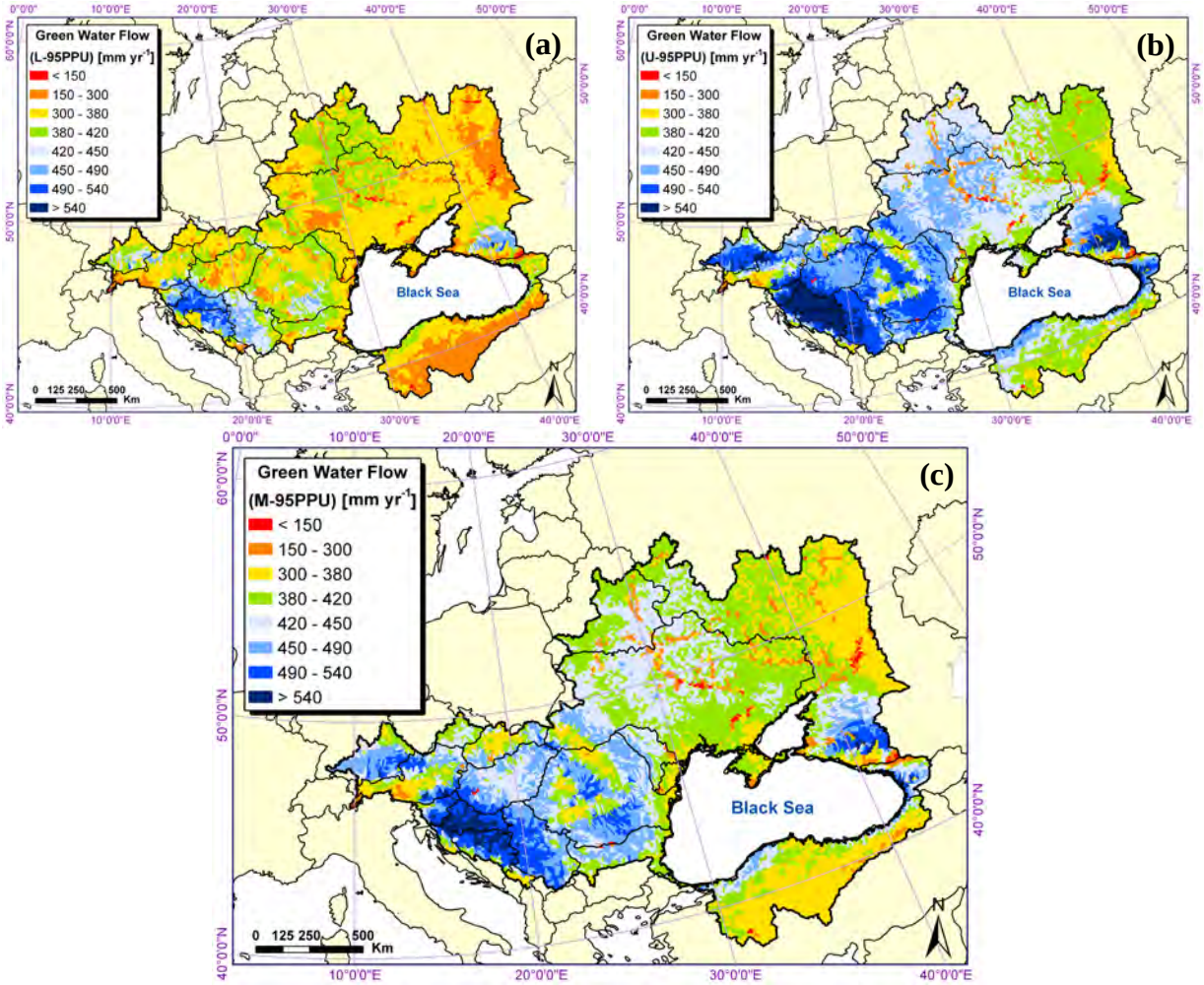

Figure 8. Annual averages of green water flow at 12982 modelled subbasins of BSB expressed as: (a) lower (L95), (b) upper (U95), and (c) median (M95) of the 95% prediction uncertainty for the period of 1973-2006.

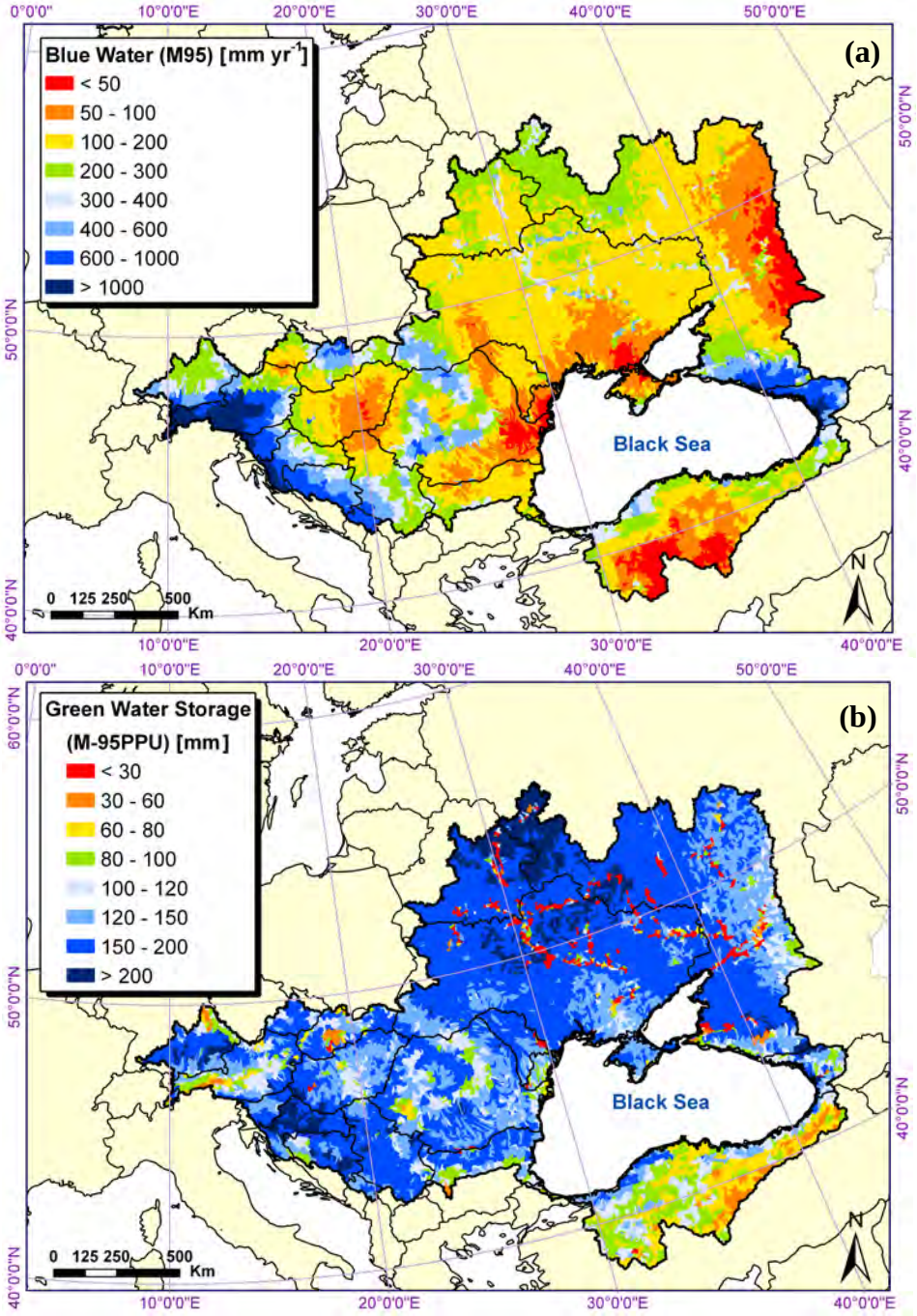

Figure 9. Annual averages of blue water (a), and green water storage (b) at 12982 modelled subbasins of BSB expressed as median (M95) of the 95% prediction uncertainty range calculated for the period of 1973-2006.

Conclusion

In this work we show that with the current technology it is possible to build a high-resolution large-scale model and successfully calibrate and validate the model. There are several pitfalls, which have to be addressed and checked by the analyst such as: correctness of the flow direction, correct placement of the outlets, and correct parameterization of the model. Use of a grid technology is indispensible for running such models. Many new additions in the SWAT-CUP help with the above considerations. The current study provides the basis for further research on landuse and climate change impacts on water resources in Black Sea Basin. More confidence in the model result could be achieved if there were more discharge and water quality observations.

Acknowledgment
This project has been funded by the European Commission's Seventh Research Framework through the enviroGRIDS project (Grant Agreement n 226740). The authors are especially grateful to Dr. Srinivasan from Texas A&M University and Prof. Dr. Rainer Schulin from ETH Zurich University for their valuable comments and discussions for this work.

References

Abbaspour, K. C., C. A. Johnson, and M. Th. van Genuchten (2004), Estimating Uncertain Flow and Transport Parameters Using a Sequential Uncertainty Fitting Procedure, J. Vadouse Zone, 3 (4), 1340-1352.

Abbaspour, K. C., J. Yang, I. Maximov, R. Siber, K. Bogner, J. Mieleitner, J. Zobrist, and R. Srinivasan (2007), Modelling hydrology and water quality in the pre-Alpine/Alpine Thur watershed using SWAT. J. Hydrology, 333, 413-430, doi: http://dx.doi.org/10.1016/j.jhydrol.2006.09.014.

Alcamo, J., P. Döll, T. Henrichs, F. Kaspar, B. Lehner, T. Rösch, and S. Siebert (2003), Development and testing of the WaterGAP 2 global model of water use and availability, Hydrological Sciences Journal, 48(3), 317-338.

Arnold, J. G., R. Srinivasan., R. S. Muttiah., and J. R. Williams (1998), Large area hydrologic modeling and assessment part I: model development. Journal of American Water Resources Association, 34 (1), 73-89.

Aus der Beek, T., L. Menzel, R. Rietbroek, L. Fenoglio-Marc, S. Grayekd, M. Becker, J. Kusche, and E. V. Stanev (2012), Modeling the water resources of the Black and Mediterranean Sea river basins and their impact on regional mass changes, J. Geodynamics, 59–60, 157–167.

Black Sea Investment Facility (BSEI) (2005), 'Review of the Black Sea Environmental Protection Activities. General review', Black Sea Investment Facility.

Climatic Research Unit (CRU) (2008), CRU Time Series (TS) high resolution gridded datasets, University of East Anglia Climatic Research Unit (CRU), NCAS British Atmospheric Data Centre, Available from: http://badc.nerc.ac.uk/view/badc.nerc.ac.uk__ATOM__dataent_1256223773328276.

Döll, P., F. Kaspar, and B. Lehner (2003), A global hydrological model for deriving water availability indicators: model tuning and validation, J. Hydrology, 270 (1-2), 105-134.

EEA Catchments and Rivers Network System (ECRINS) v1.1 (2012), Rationales, building and improving for widening uses to Water Accounts and WISE applications, Luxembourg: Publications Office of the European Union, ISBN *978-92-9213-320-7*, ISSN *1725-2237*, doi:10.2800/51667.

Faramarzi, M., K. C. Abbaspour, R. Schulin, and H. Yang (2009), Modelling blue and green water resources availability in Iran, J. Hydrol. Process., 23, 486–501, doi: 10.1002/hyp.7160.

Food and Agricultural Organization (FAO) (1995), The digital soil map of the world and derived soil properties, CD-ROM, Version 3.5, Rome, Italy.

Global Runoff Data Centre (GRDC) (2011), Long-Term Mean Monthly Discharges and Annual Characteristics of GRDC Station / Global Runoff Data Centre. Koblenz, Germany: Federal Institute of Hydrology (BfG), http://grdc.bafg.de.

Gorgan, D., V. Bacu, D. Mihon, D. Rodila, K. Abbaspour, and E. Rouholahnejad (2012), Grid based calibration of SWAT hydrological models, J. Nat. Hazards Earth Syst. Sci., 12, 2411–2423, doi:10.5194/nhess-12-2411-20.

Holvoet, K., A. van Griensven, P. Seuntjens, and P. A. Vanrolleghem (2005), Sensitivity analysis for hydrology and pesticide supply towards the river in SWAT, J. Phys. Chem. Earth, 30, 518–526, doi:10.1016/j.pce.2005.07.006.

Jarvis, A., H. I. Reuter, A. Nelson, and E. Guevara (2008), Hole-filled SRTM for the globe Version 4, Data access: The CGIAR-CSI SRTM 90m Database: http://srtm.csi.cgiar.org.

Krause P., D. P. Boyle,and F. Bäse (2005), Comparison of different efficiency criteria for hydrological model assessment, J. Advanced Geosciences, 5, 89–97.

Lenhart, T., K. Eckhardt, N. Fohrer, and H. G. Frede (2002), Comparison of two different approaches of sensitivity analysis, J. Phys. Chem. Earth, 27, 645–654.

Ludwig, W., E. Dumont, M. Meybeck, and S. Heussner (2009), River discharges of water and nutrients to the Mediterranean and Black Sea: Major drivers for ecosystem changes during past and future decades?, J. Progress in Oceanography, 80, 199-217.

NASA (2001), Land Processes Distributed Active Archive Center (LP DAAC), ASTER L1B, USGS/Earth Resources Observation and Science (EROS) Center, Sioux Falls, South Dakota, Data access: http://lpdaac.usgs.gov.

Rouholahnejada, E., K. C. Abbaspour, M. Vejdani, R. Srinivasan, R. Schulin, and A. Lehmann (2012), A parallelization framework for calibration of hydrological models, J. Environmental Modelling & Software, 31, 28–36, doi:http://dx.doi.org/10.1016/j.envsoft.2011.12.001.

Ruget, F., N. Brisson, R. Delecolle, and R. Faivre (2002), Sensitivity analysis of a crop simulation model, STICS, in order to choose the main parameters to be estimated, J. Agronomie, 22, 133–158.

Stanners, D. and P. Bourdeau (1995), "Europe's Environment: The Dobris Assessment," European Environment Agency Task Force, European Environment Agency, Copenhagen, Denmark.

Tockner, K., U. Uehlinger, and C. T. Robinson (2009), Rivers of Europe, Academic Press, ISBN: *978-0-12-369449-2*.

United Nation Environment Program (UNEP) (2006), Africa Environment Outlook 2, Our environment, our wealth. Division of early warning and assessment, Nairobi, Kenya.

van Griensven, A., T. Meixner, S. Grunwald, T. Bishop, A. Diluzio, and R. Srinivasan (2006), A global sensitivity analysis tool for the parameters of multi-variable catchment models, J. Hydrol., 324, 10–23, doi:10.1016/j.jhydrol.2005.09.008.

Wang, X., X. He, J. R. Williams, R. C. Izaurralde, and J. D. Atwood (2005), Sensitivity and uncertainty analyses of crop yields and soil organic carbon simulated with EPIC, American Society of Agricultural Engineers (ASAE), 48, 1041–1054.

Weedon, G. P., S. Gomes, P. Viterbo, W. J. Shuttleworth, E. Blyth, H. Österle, J. C. Adam, N. Bellouin, O. Bouche, and M. Best (2011), Creation of the WATCH Forcing Data and Its Use to Assess Global and Regional Reference Crop Evaporation over Land during the Twentieth Century, J. Water and Global change (WATCH), Special Collection, 823-848.

Winchell, M., R. Srinivasan, M. Di Luzio, and J. G. Arnold (2007), Arc-SWAT interface for SWAT2005 - User's guide, Blackland Research Center, Texas Agricultural Experiment Station and Grassland, Soil and Water Research Laboratory, USDA Agricultural Research Service, Temple,Tex.

swat.tamu.edu/conferences/2013

We would like to thank the following conference sponsors: